UNIVERSIDAD DE LA REPÚBLICA
FACULTAD DE INGENIERÍA

A Differential Game Theory Approach to DC-DC Buck Converter Control

TESIS PRESENTADA A LA FACULTAD DE INGENIERÍA DE LA
UNIVERSIDAD DE LA REPÚBLICA POR

Alejandro Pascual

EN CUMPLIMIENTO PARCIAL DE LOS REQUERIMIENTOS
PARA LA OBTENCIÓN DEL TÍTULO DE
MAGISTER EN INGENIERÍA ELÉCTRICA.

DIRECTORES DE TESIS
Dr. Gabriel Eirea .... Universidad de la República
Dr. Enrique Ferreira .... Universidad Católica del Uruguay

TRIBUNAL
Prof. Rafael Canetti .... Universidad de la República
Prof. Eleonora Catsigeras .... Universidad de la República
Prof. Martin Ordonez ..... University of British Columbia, Canadá

DIRECTOR ACADÉMICO
Dr. Gabriel Eirea .... Universidad de la República

Montevideo
lunes 7 septiembre, 2015

A Differential Game Theory Approach to DC-DC Buck Converter Control, Alejandro Pascual

Esta tesis fue preparada en LaTeX usando la clase iietesis (v1.0).
Contiene un total de 302 páginas.
Compilada el lunes 7 septiembre, 2015.
http://iie.fing.edu.uy/

Esta página ha sido intencionalmente dejada en blanco.

Agradecimientos

En las siguientes líneas quiero agradecer a las personas e instituciones que han hecho posible que esta tesis exista.

A mi esposa y a mi hija, que le dan sentido a mis esfuerzos, especialmente al volcado en este trabajo. Gracias por ayudarme a perseguir mi vocación tolerando mis ausencias. Este es un imperfecto tributo dedicado a ustedes, mis dos amores, Yania y Angelina.

A la memoria de mis padres, por todo lo que me dieron, por acompañarme.

A mis tutores, Gabriel Eirea y Enrique Ferreira, que confiando en mí me dieron libertad para explorar caminos nuevos, pero salvándome de perder el rumbo. Cada uno, en su momento y desde su especialidad, me brindó generosamente su tiempo y experiencia para guiarme a través de este difícil y disfrutable posgrado académico. El compromiso con que se embarcaron en esta actividad para mi es invalorable.

A los miembros del tribunal, Rafael Canetti, Eleonora Catsigeras, y Martin Ordonez por haber aceptado leer esta tesis. A Rafael Canetti (nuevamente) quien ofició de director académico temporalmente y siempre me animó a persistir, aun en los momentos de peor rendimiento. Además, hace ya bastante tiempo, me introdujo a la teoría de control entusiasmándome definitivamente por esta disciplina.

A Federico La Rocca (Director de Posgrados de Ingeniería Eléctrica) y Álvaro Giusto (Jefe del Departamento de Sistemas y Control del IIE) por su inmensa paciencia para con mis tiempos.

A la memoria de Jorge Lewowicz por haber compartido tan generosamente su contagiosa pasión por la matemática. A Elvio Accinelli gracias a quien conocí la teoría de juegos. A Pierre Bernhard y Valery Patsko quienes vía e-mail sugirieron literatura introductoria a la teoría de juegos diferenciales. A Anne Beuter y Jacques Henry quienes, durante los meses que supervisaron mi trabajo en el marco de una beca INRIA, afianzaron mi confianza para emprender trabajo de tipo académico.

A mi jefe Enrique Munné (Jefe de la Unidad Aseguramiento de Redes y Sistemas de Información de ANTEL) por la flexibilidad y horas autorizadas para llevar adelante este trabajo. A Gonzalo Escuder y Sergio Louro por su respaldo gerencial.

A ANTEL y su programa de patrocinio a tesis de posgrado. A Alicia Cuba, Pablo Menoni, Diego Durán, y Andrés Lucas por su involucramiento en este programa en relación a mi trabajo. A los compañeros del CEyD de ANTEL por el apoyo logístico. A la SCAPA-IIE, la Secretaría del IIE, y la Bedelía de Posgrados.

A los compañeros de ANTEL y del IIE que me animaron: Juan Sturzenegger, Enrique Munné, Rodolfo Grosso, Roberto Fleitas, Alfredo Rodríguez, Fernando Barizo, Ricardo Álvarez, Michel Hakas, Andrés Alcarraz, Linder Reyes, Eduardo Máscolo, Miguel Barreto, Federico Davoine, entre otros. A mis amigos de siempre.

Esta página ha sido intencionalmente dejada en blanco.

Para Yania y Angelina.

Esta página ha sido intencionalmente dejada en blanco.

Resumen

Esta tesis aborda el problema de controlar un convertidor sincrónico tipo buck genérico frente a perturbaciones impredecibles, y posiblemente discontinuas, pero acotadas de la corriente de carga. El problema se plantea en forma canónica como un conflicto dinámico entre el controlador automático encargado de la regulación del voltaje de salida y un perturbador hipotético. En particular, el conflicto es visto como un juego de persecución-evasión en distancia. Aplicando métodos clásicos de la teoría de juegos diferenciales, el juego es completamente resuelto identificando tres casos cualitativamente distintos que pueden ocurrir dependiendo de si el valor de un parámetro derivado positivo es menor, igual, o mayor que uno. La solución del juego provee estrategias óptimas para el controlador y para el perturbador que pueden ser utilizadas, respectivamente, para implementar control ante el peor caso y para realizar pruebas de referencia (aplicables a cualquier método de control). Además, de la topografía de la función valor del juego, se obtiene información cualitativa y cuantitativa acerca de los límites físicos inherentes al control de convertidores tipo buck, permitiendo la optimización del filtro LC con respecto al desempeño de la regulación en las primeras etapas de diseño, aun antes de haber finalmente elegido un método de control.

Esta página ha sido intencionalmente dejada en blanco.

Abstract

This thesis deals with the problem of controlling a generic synchronous buck converter against unpredictable, and possibly discontinuous, but bounded load disturbances. The problem is canonically framed as a dynamical conflict between the automatic controller in charge of the output voltage regulation and an hypothetical disturber. In particular, the conflict is regarded as a pursuit-evasion game in distance. Applying classical methods of differential game theory, the game is completely solved identifing three qualitative different cases that can take place depending on how a positive derived parameter value compares to unity. The game's solution provides optimal strategies for the controller and the disturber which can be used, respectively, for worst-case-aware control and benchmark testing (of any control method). Furthermore, from the topography of the game's value function, qualitative and quantitative information about the physical limits of buck converter control is gained, allowing for early design stage optimization of the converter's LC filter towards regulation performance, regardless of the control method that might finally be selected.

Esta página ha sido intencionalmente dejada en blanco.

Contents

Contents

Contents

Chapter 1

Introduction

Power electronics is concerned with the process and control of electrical power using electronic devices [1, 2]. It is a discipline of electrical engineering which is expected to play an increasingly significant role in the 21st century, as motivations to improve energy efficiency become more prominent [3]. Rough estimations indicate that 15–20 % of electrical power consumption can be saved by extensive application of power electronics [4].

A typical goal of power electronics is to efficiently convert electrical power from one form to another for convenient utilisation. Power converters are usually classified as follows according to the type of input and output, either alternating current (AC) or direct current (DC): DC-DC, DC-AC, AC-AC, and AC-DC.

DC to DC (DC-DC) converters can be classified into *switched-mode* or *linear*. Switched-mode converters are more efficient than their linear counterparts because, by design principle, their active components are not operated in linear regions. In switched-mode DC-DC converters, ideally lossless voltage or current conversion is achieved by controlled electronic connection and disconnection of the source to an appropriate intermediate storage device, so that the energy is transferred from the source to the load at the required voltage or current level.

Switched-mode DC-DC converters are widely used in modern electronic equipments and the market for them is expanding [5]. They find application in powering systems of: digital cameras, navigation systems, smart phones, tablets, notebooks, personal computers, medical and telecommunications equipments, light-emitting diode (LED) based lighting systems, industrial and military equipment, transportation, etc.

The focus of this thesis is on exploring some of the theoretical limits of *control* of a particular switched-mode DC-DC converter known as *buck*, also called *step-down* because its primary function is to step-down an input voltage to properly power a load at a lower output voltage. More specifically, the *synchronous* buck converter, characterized by the fact that the connection and disconnection of the voltage source is accomplished by a pair of electronic switches that operate synchronously.

Along with the boost and the buck-boost (the former used to step-up the input voltage, the later used to flexibly either step-down or step-up the input voltage as dynamically required) the buck converter topology is one of the most

common in DC powering systems. For example, buck converters lie at the heart of: motherboard-integrated voltage regulator modules (VRMs) designed to power high-speed digital integrated circuits (ICs) such as central processing units (CPUs), graphics processor units (GPUs) and memories, switched-mode power supplies (SMPSs) for personal computers, and point of load (POL) converters found in large distributed power systems (DPSs) such as those required by data centers and telecommunications buildings.

To meet the voltage required by the load to work properly, almost always a feedback controller becomes indispensable to regulate the converter's output voltage against input voltage and load current variations (i.e., disturbances), and against excessive sensitivity with respect to the converter's circuit element values. Generally desired features of a regulated converter are: stability, fast transient response with low overshoot to large signal disturbances, small steady-state error, and robustness. Voltage regulation performance, if not the factor of highest concern, is usually considered a crucial factor in buck converter design, among others such as overall efficiency, cost, size, and weight. For instance, the industry of VRM requires stringent regulation, because high-efficient modern microprocessors demand to be powered at very low and accurate voltage levels, even during large and fast transients of the supplied current [6].

Therefore, control theory is obviously relevant to buck converter design in particular, and to power electronics in general. Simultaneously, the switching character of power electronics poses interesting problems to control theory [7–9] that sometimes transcend the academic world. In fact, the continuously broadening scope of power electronics applications that require accurate power conversion to enhance efficiency under dynamic conditions, has stimulated the economically justifiable adoption of non-linear control methods currently implemented in actual commercial devices. In this scenario of rich interactions between the control and power electronics communities, among others, new control methods and refinements of old ones are frequently being proposed, often targeted to very specific applications. The still evolving situation in the niche of buck converter control is, in this respect, representative for the area of power electronics concerned with DC-DC power conversion.

In this thesis, the control of the synchronous buck converter is approached from the perspective of differential game theory in order to explore the theoretical limits of disturbance rejection that *any* controller shall face if put in charge of the output voltage regulation, specifically with respect to load current bounded variations. As a by product, a control method, that infimizes the largest error that a load current disturbance might cause, is proposed. The synchronous topology is preferred over the asynchronous one for the simple reason that its switching dynamics is more easily framed in the context of differential game theory, since it is entirely externally driven by the controller. By contrast, in the asynchronous topology, the autonomous switchings that take place due to the presence of free-wheeling diode complicate the intended approach.

Without aiming to cover the vast literature on DC-DC converter control, the following two sections are intended to briefly overview some common and some

novel approaches applicable to DC-DC converters in general, and buck converters in particular. Next, the motivation for proposing the differential game theory approach is presented, along with a description of the contributions of the present work. The last section describes the organization of this thesis, chapter by chapter.

1.1. Common approaches to DC-DC converter control

1.1.1. Conventional constant frequency pulse width modulation

The most conventional approach to buck converter control is by means of constant frequency (CF) pulse-width modulation (PWM) which is accomplished as follows. At the input stage, the electronic switches of the converter are driven so as to generate a rectangular voltage signal, of fixed period and adjustable duty cycle, from the voltage source. At the output stage, the rectangular signal is low-pass filtered by an inductor-capacitor (LC) filter to provide a regulated DC voltage to the load. Regulation is achieved by varying the duty cycle of the square wave, as necessary.

A well-established modelling tool known as *averaging* [1, 10] followed by conventional *small-signal linearization*, allow to come up with a small-signal linear model of the converter's dynamics under PWM excitation. It is by virtue of this modelling approach that buck converter control can be dealt with using classical control design methods, being the loop-shaping in the frequency-domain the prevalent one [11]. In practice, usually an analogous proportional-integral-derivative (PID) controller, or a close variant, [1] is used as the feedback controller to meet the required steady-state and transient voltage-regulation performance with acceptable stability margins.

Two control schemes are commonly used: voltage-mode control (VMC) and current-mode control (CMC), also called current-programmed control (CPC). The former involves a single feedback loop directly from the converter's output voltage or from the sensing point of an output voltage divider. The later involves, in addition, a second feedback loop from the converter's inductor current (usually sensed indirectly). In the *peak* type of CMC, the compensator is placed in the voltage loop to set the reference of the current loop, which generates the PWM signal by comparison between the current reference and the sensed current. Each scheme has its advantages and disadvantages. The small-signal control-to-output transfer function for CMC has the advantage that it is of first order, while it is of second order for VMC. CMC provides faster dynamic response at a given switching frequency than VMC [12], but is more prompt to noise susceptibility and sub-harmonic oscillations instability [13]. Of particular importance in the implementation of the basic *peak* type of CMC scheme is the addition of a ramp to the sensed current, in order to avoid a well-known instability triggered by duty cycles greater than 0.5, regardless the particular converter topology [1]. The *average* type of CMC solves the instability problem but adds a compensator, complicating the overall design.

Even though conventional, the PWM-based control approach just sketched has some well known limitations inherent to its conception geared towards the

application of linear control theory.

Averaging poses an upper limit to the regulator bandwidth which is already limited by the technological limits of switching efficiency [14]. That is to say, the gain crossover frequency of the feedback loop should be as high as possible to handle fast transients but must be kept sufficiently below the switching frequency so as to allow confidence in the averaged model. In addition, the switching frequency cannot be selected arbitrarily high because switching losses increase proportionally to switching frequency. Rules of thumb recommend that the unitary bandwidth feedback loop should not exceed one-tenth [2] to one-sixth of the switching frequency. Pushing the converter frequency response beyond these upper bounds results in poor filtering of the intended DC output voltage, and excites high-frequency unmodeled dynamics thereby compromising stability.

Small-signal analysis dismisses non-linear dynamics that in general persists after averaging [15]. Thereby, the large-signal transient performance of the controlled converter cannot be transparently handled during design. For example, the common practice of making the ramp slope of the sawtooth carrier signal (used to generate the PWM signal by comparison with the modulating signal) proportional to the input voltage is a feed-forward technique intended to alleviate one of the shortcomings of small-signal linearisation. Furthermore, and more seriously, small-signal analysis cannot predict global instabilities that can actually take place [16, 17].

1.1.2. Hysteretic control

In its most simple form, *hysteretic control*, consists in driving the converter's switches by comparison of the error voltage (difference between reference and output) against two symmetric hysteresis thresholds around zero. By contrast with a PWM-based controller, an hysteretic (also called *hysteresis* or *bang-bang*) controller does not require external timing and feedback compensation. As for CF-PWM controllers, either the VMC or the CMC scheme may be adopted for hysteretic controllers, however the former is more widely used.

The architectural simplicity of hysteretic control has long ago been appreciated, motivating the use of non-linear analysis to study its associated steady-state and transient characteristics [18–20].

Hysteretic control is the simplest form of *rippple-based control*, an approach characterized by the fact that the switching action is more or less directly driven by the amplitude of the converter's output ripple voltage. Rippple-based controllers are appreciated because of their fast response to large-signal transient perturbations. However, their most simple forms lack a clearly defined switching frequency, are noise-sensitive, perform mediocrely in DC regulation, and incline to fast-scale instability [21]. Although improvements have been developed to overcome these limitations, they all come at the cost of departing from the simplicity of the original conception.

1.2. Novel approaches to DC-DC converter control

1.2.1. Sliding mode control

Switched-mode DC-DC converters achieve power conversion by controlled switchings that modify the topology of a linear network topology. Therefore, they belong to the class of variable structure system (VSS) [22]. These systems are naturally prompted to be controlled by a non-linear control method known as sliding mode (SM) control that relies on a state-feedback discontinuous law to achieve the control goal. The feedback law is designed so that the system's state is guided towards a desired point in state-space from every possible initial state.

For systems with a single discrete two-valued variable $\sigma \in \{0,1\}$ as input and a state-space representation of the form $\dot{\boldsymbol{x}} = \boldsymbol{f}(\boldsymbol{x}, \sigma)$, the design of a SM controller involves the careful selection of a single *switching surface* $\{\boldsymbol{x} \ : \ S(\boldsymbol{x}) = 0\}$ in the system's state-space $\mathbb{R}^n$ such that three fundamental conditions hold: hitting, existence, and stability. The switching surface is used to define a state-feedback discontinuous law as follows:

$$\sigma(\boldsymbol{x}) = \begin{cases} 1 & \text{if } S(\boldsymbol{x}) > 0, \\ 0 & \text{if } S(\boldsymbol{x}) < 0. \end{cases} \tag{1.1}$$

The *hitting* condition requires that under the previous feedback law every state-space trajectory $t \mapsto \boldsymbol{x}(t)$ can be proved to hit the switching surface in finite time regardless the initial state $\boldsymbol{x}(0)$. The *existence* condition requires that

$$\lim_{S \to 0} S\dot{S} < 0 \tag{1.2}$$

so that for $\boldsymbol{x}$ close to $\{\boldsymbol{x} \ : \ S(\boldsymbol{x}) = 0\}$ the feedback law makes $\dot{\boldsymbol{x}}$ point to the switching surface, either if $\boldsymbol{x} \in \{\boldsymbol{x} \ : \ S(\boldsymbol{x}) < 0\}$ or $\boldsymbol{x} \in \{\boldsymbol{x} \ : \ S(\boldsymbol{x}) > 0\}$. Once the state hits the switching surface, the existence condition allows to conceive an ideal *sliding motion* of the state through the switching surface, caused by infinitely fast switching between the two possible input values. The system is then said to have entered into a *sliding mode*. The sliding motion must verify the invariance condition $\dot{S}(t) = \langle \boldsymbol{\nabla} S(\boldsymbol{x}(t)), \boldsymbol{f}(\boldsymbol{x}(t), \sigma_{\text{eq}}(t)) \rangle = 0$, where σ_{eq} is though of as an *equivalent control* for the infinitely fast switching action. Assuming that $\sigma_{\text{eq}}(t)$ can be solved out from the invariance condition, the *stability* condition requires that the ideal sliding dynamics, expressed as $\dot{\boldsymbol{x}} = \boldsymbol{f}(\boldsymbol{x}, \sigma_{\text{eq}}(t))$, has the desired point in state-space as its unique asymptotically stable equilibrium point. For systems with more than a scalar controllable input, the same idea is generalized defining a switching surface per input, giving rise to multiple sliding modes.

An ideally infinite switching frequency required to sustain a sliding mode is impracticable. Imperfections of the actual devices of the controlled system such as small delays, dead zones and hysteresis, preclude a state-feedback discontinuous law like (1.1) to sustain an ideal sliding motion. At most, a close approximation is attained by means of a high-frequency switching, known as *chattering*, limited only by the unmodelled limitations of the devices. Chattering is usually undesirable from a practical point of view since may cause excessive switching losses, wear,

and noise. For this reason, hysteresis is usually introduced in the implementation of SM controllers. A state-feedback law such as (1.1) is actually implemented as

$$\sigma\left(\boldsymbol{x}\right) = \begin{cases} 1 & \text{if } S\left(\boldsymbol{x}\right) > \delta, \\ 0 & \text{if } S\left(\boldsymbol{x}\right) < -\delta, \end{cases} \tag{1.3}$$

where δ is an arbitrarily small value. If $S\left(\boldsymbol{x}\right) \in [-\delta, \delta]$, the last value assigned to σ by (1.3) is held constant. Usually, δ is selected so as to achieve an acceptable approximation of the sliding motion without incurring into excessively high-frequency switching.

For switched-mode DC-DC power conversion applications, SM control is an attractive approach that, exploiting the geometric aspects of the regulation problems, provides an analysis and design methodology which is intuitively clear, mathematically feasible, and devoid of approximations [23]. As substitutes of conventional PWM controllers designed to perform satisfactorily only around a specific operating point, SM controllers are promising and therefore have stimulated a lot of research [24].

However, despite their well known advantages such as stability, robustness against parameter value variations, fast rejection of line and load disturbances, flexibility in design and relatively easy implementation; SM controllers are seldom used in the industry of power electronics [25]. There exists reluctance to adopt a control method based on variable high-frequency switching, because of the power losses and electromagnetic interference that it entails. Even though the variable frequency problem can be alleviated by the introduction of a constant ramp or timing function directly into the controller, or by including some forms of adaptive hysteresis; in any case the resulting controller is relatively complex and the switching frequency cannot be made absolutely constant [26].

In addition, it appears that there exists a lack of understanding of the design principle of SM controllers by power-supply engineers who, chiefly, need strong practical evidence to support the worthiness of applying the SM approach [27].

1.2.2. Boundary control

Boundary control may be thought of as a generalization of sliding mode control concepts [28], in the sense that a boundary in the system's state-space does not necessarily needs to exhibit sliding behaviour to be useful. It is a geometric-based approach to analysis and control that relies on the acquaintance with the phase-space picture of the system's dynamics, for each of its constituent structures in case of a VSS. Relevant design concerns, such as large-signal stability and dynamic response performance, can be addressed by this approach [29], often fairly transparently since sate-space representations of prevalent DC-DC converters are low-dimensional [23].

Boundary control has been successfully applied for actual buck converter control using either first or second order switching surfaces (SSs) [30], the later resulting in faster dynamical response. Further efforts to enhance the transient behaviour of boundary control gave rise to more involved SS. For example, minimum-

time transient response SS, derived from open-form solutions obtained by applying model-predictive minimum-time control (MTC), have been successfully implemented as digitalized raster images [31, 32].

However, maybe the most notable feature of the geometric-based approach is that it enhances the understanding of the dynamical behaviour of switched converters. The geometric domain provides an inherently bounded representation of the system's dynamics, as opposed to the time and frequency domains, which reveals the physical limits to large-signal stability and dynamic response performance, that any control strategy must face [33–35]. High-performance regulation can be attained by pushing control towards these limits. For instance, in [36] a natural unloaded SS was proposed to achieve time-optimal transient behaviour and no overshoot during start-up for any buck converter, by means of normalized analysis of natural trajectories in the state-space. The same approach has been extended to boost [37], and buck-boost converters [38], to discover the corresponding natural switching surfaces (NSSs) that achieve the desired steady state regime in only one switching action for start-up and large load disturbances, while exhibiting no overshoot and time-optimal response.

Deeper understanding of the physical limits proves valuable even to conventional CF-PWM operation, desirable in most noise-sensitive applications. In [39] switching surfaces derived from the analysis of an averaged generic large-signal model have been proved useful to enhance the dynamic response of CF-PWM-driven buck, boost, and buck-boost converters, by means of a circular centric-based controller. Similarly, in [40] the transient behaviour of a current-mode-controlled buck converter is improved by the introduction of geometric-based control in the voltage loop.

1.2.3. Digital control

In the past, medium to low power switched-mode DC-DC converters, were usually controlled using analog techniques, because digital components were too slow, expensive, and inefficient. However, recent advances in digital very-large-scale integration (VLSI) technology have made of digital control a very attractive option for power conversion regulation and management [41].

Digital control offers several advantages over analog control. Overall, it enhances regulation performance of the converter's primary feedback loop by enabling the implementation of complex non-linear control methods and auto-tuning mechanisms, while reducing the number of external passive components. Therefore, it is an implementation methodology rather than an specific control method. In fact, each control method already commented can be implemented digitally. For example, in [42] two auto-tuning techniques are proposed for a PID-based CF digital pulse-width modulation (DPWM) controller. In [43] hysteretic-based control is implemented digitally. In [44] the flexibility of digital control is explored in connection with multi-phase VRM control.

Another advantage of digital control over analog control is that it is intrinsically less sensitive to component and temperature variations. Furthermore, the digital

technique naturally accommodates modular complex architectures that allow the introduction of secondary functions such as programming, protection, monitoring, data storage, and communication, all beyond the capabilities of analog systems and central to intelligent power management.

The proposals for exploiting the advantages of digital control are numerous. In particular, as pointed out in [45] digital control enables the implementation of hybrid control. An hybrid controller is a switching control architecture in which a supervisor runs the logic necessary to select a proper controller at every instant of time from a bank of available controllers. Using this approach an hybrid digital adaptive (HDA) controller is proposed in [45] that behaves as a conventional CF DPWM controller in the vicinity of steady state, but during step-load transients it turns into a linear SS-based controller whose slope is selected based on capacitor and inductor current estimates, so that near-time-optimal transient responses can be obtained.

The same idea of decoupling between large and small deviations was previously used in [46] to propose a simple linear-non-linear control (LnLC) control method that forces saturation of the duty cycle of a conventional CF-PWM controller whenever the absolute voltage error exceeds certain threshold, thereby reducing the recovery time from step-load transients in comparison with standard linear control.

1.3. Motivation for a new approach

As it was briefly exposed before, DC-DC converter control is an intense area of research where new control methods are regularly being proposed, being the buck converter topology typically the first to be tested.

Often, new control methods are successfully validated on actual prototypes against step-shaped disturbances departing from the desired point of operation (see, for instance, [46, 47]). However, this kind of analysis does not encompass the full variety of possible arbitrarily-shaped large-signal disturbances and initial conditions that may compromise regulation performance. In addition, the large-signal stability analysis of a non-linearly-controlled converter is not easy. In [48], for example, the stability issue in connection to the LnLC method proposed in [46] is addressed by means of the approximate describing function procedure. Nevertheless, the question of whether a novel control method can fulfil the control requirement for which is intended even in the worst case, in general remains unanswered.

If buck converter designers were empowered with analytic or numerical tools to play the role of devil's advocate, they would be able to rigorously proof their designs against *every* possible disturbance and initial condition. These tools are provided by differential game theory.

1.4. Description of the present work

Much in the spirit of [34], this thesis aims at contributing to the understanding of the physical limits of synchronous buck converter control, specifically with respect to its ability to keeping within bounds the under-and overshoots caused by large and infinitely fast load current transients. Close attention to this aspect of the transient response is motivated by the VRM design target application, which requires the regulated voltage error to be kept within the bounds of a very tight tolerance band.

The selected approach to explore these limits was that of the worst-case analysis, for which differential game theory [49] provides an unbeatable framework, since it allows to place the controller's actions on equal footing with the uncontrollable disturbing actions, i.e., load and line variations.

A concrete result of this work is a formulation, under quite general assumptions, of a synchronous buck converter control problem with respect to a tolerance band, framed as a *canonical* dynamical conflict between the controller (who acts on the converter's ideal switch) and the disturber (who acts on line voltage and load current). This canonical form admits a geometrical interpretation as a planar kinematic conflict, which contributes to the intuitive understanding of the dynamic behaviour of any buck converter under the influence of independent actions performed by the controller and the disturber.

Two natural interpretations of the conflict are presented. One, in which both decision making agents, i.e., players, struggle for the supremum of the absolute regulation error over an infinite time horizon, the controller seeking to infimize it and the disturber seeking the opposite. The other, in which both players struggle for the time remaining before the absolute error exceeds the bounds stated by the tolerance band, the controller seeking to supremize it and the disturber seeking the opposite. Both interpretations are consolidated into canonical differential games, the former named a game in *distance*, the later a game in *time*, following the same taxonomy used in [50], with respect to Pierre Bernhard's "second order servomechanism problem", from where the key concept of *oriented* distance was borrowed.

The other concrete result of this work is the analytical solution of the aforementioned canonical game in distance. Regrettably, however, under the assumption that the disturber acts *only* on the load current while leaving the line voltage constant. This cut down in generality, introduced only to enable a way of figuring out a solution, deserves further work to endow the proposed approach its full potential. From the canonical solution of the game in distance, optimal state-feedback strategies are derived for both players, thereby opening up the possibility of carrying out not only optimal worst-case-based control, but also optimal worst-case-based load disturb; the last alternative being useful to benchmark control methods.

On the whole, what appears to be the most fruitful contribution of this work is the qualitative and quantitative information that can be obtained from the topography of the value function associated to the canonical game in distance. The

general shape adopted by the family of nested sup-level sets of this function can be associated with the suitability of the converter's parameter values with respect to the fulfilment of the voltage regulation requirement, given the bounds of load current excursion, regardless of the control method. Furthermore, this *suitability* can be quantified by finding the global maximum of this function, which is tied to a worst-case absolute error over an infinite time horizon that is unavoidable regardless of the merits of the controller in charge. Hence, the impact that the selection of the LC filter's component will have on the regulation performance can be addressed visually with a contour plot, and quantitatively with a figure of merit, in an early design stage, before having decided yet the ultimate control method.

In general, differential games are not easy to solve analytically, even if low-dimensional. The planar "homicidal chaufeur game", stated by Rufus Isaacs [49] and completely analytically solved by Antony Merz [51], suffices as a convincing example. However, numerical methods are being developed, which in particular for the two-dimensional case provide a clear visual insight into the conflictive dynamics in case (see, for instance, [52]). In this thesis the numerical approach was not followed because the benefits of the classical analytical way [49] looked accessible, at least leaving out the line disturbance, and because numerical methods intended to solve differential games and the quite different underlying theories sustaining them [53–55] are beyond the scope of this work. Nevertheless, we believe that applied differential game theory, eased by numerical methods if necessary, can shed a lot of light about the typically low-dimensional problems stated by DC-DC converter control, specially if these are formulated in a canonical dimensionless way. Hopefully, this work will contribute in this direction.

1.5. Thesis overview

This dissertation is organized as follows.

- *Chapter 1* presents the problem of buck converter control, its relevance, and some of the approaches to tackle it. It also describes the approach proposed in this thesis and the motivation behind it. Finally, the organization of the whole document is sketched.

- *Chapter 2* introduces differential game theory. Its scope, key concepts, and classical methods are overviewed to provide the rudiments necessary to deal with the buck converter control problem.

- *Chapter 3* precisely models the buck converter control problem as a pursuit-evasion conflict which accepts two natural interpretations: either as game in distance or as game in time. A canonical form of the conflict is developed, under quite general assumptions, by means of normalization of the defining parameters and a carefully chosen state-space transformation. The resulting canonical form allows to treat every buck converter control problem consistently as a pursuit-evasion conflict and provides valuable insight about its

dynamics because it can be geometrically interpreted as a simple kinematic conflict in the plane.

- *Chapter 4* develops basic technical results about the canonical buck converter conflict's dynamics.

- *Chapter 5* solves the canonical buck converter game in distance, relying on the results of Chapter 4. Three qualitatively different cases are discovered in the parameter-space of the game, each case related to how a normalized derived parameter compares to unity.

- *Chapter 6* proposes practical applications of the solution found in Chapter 5. Numerical simulations are reported to support the feasibility of the proposals.

- *Chapter 7* enumerates the main conclusions of this thesis and suggested future work.

Esta página ha sido intencionalmente dejada en blanco.

Chapter 2

Introduction to differential game theory

In this chapter, differential game theory is briefly introduced to provide a minimal theoretical framework to address the buck converter control problem that was qualitatively introduced in Chapter 1 and that will be precisely formulated in Chapter 3.

An illuminating introduction to differential games is Rufus Isaacs' pioneering work [49], where main concepts are introduced and several low-dimensional, but interesting, differential games are partially or completely solved. While solving these games, Isaacs found the prominent role played by *singular surfaces*, which are manifolds in the state space across which the backward solution procedure, derived from Isaacs' "tenet of transition", fails because the value function is discontinuous or not differentiable. The presence of these surfaces hamper what would otherwise be a routine solution procedure. After Isaacs, other researchers continued studying the variety richness of singular surfaces mainly by studying specific differential games examples (see, for example, [56, 57]). These early developments of two-player deterministic zero-sum differential game theory, consolidated into what is now known as *Isaacs-Breakwell theory*.

In Subsection 2.2.7, some of the most up-to-date developments of differential game theory are anecdotally cited, in connection with the difficulties that arise in the area of existence theory, concerned with the refinements of the concepts of *strategy* and *value function*. These developments allow to build differential game theory on solid ground. However, in the following chapters, none of them is applied to the application at hands. Indeed, the reformulation of the buck converter control problem in the realm of one of these modern developments has been postponed for future work. In the present work, the problem is addressed à la Isaacs-Breakwell.

What follows only introduces the most elementary concepts of Isaacs-Breakwell theory, closely following [58, Ch. 1], [59, Ch. 1, 8], [60], and [49], with convenient adaptations to fix vocabulary and notation. For a thorough coverage of this classical stage of differential game theory, refer to [60] and [61]. For a more recent overview of dynamic non-cooperative game theory, which is a broader subject, refer to [59].

2.1. What is a pursuit-evasion differential game?

The theory of differential games was born in the early 1950s with the work of its acknowledged father Rufus Isaacs in the United States of America (USA). Contemporary scientists working in related problems were Bellman in the USA and Pontryagin in the Soviet Union (for an historical survey see, for instance, [62]). The main motivation at that time was the study of military problems, in particular pursuit-evasion problems, i.e., the study of pursuit and evasion between two objects moving according to simple kinematic laws. Indeed, most of the problems studied by Isaacs in [49] are of this kind, e.g., "the homicidal chaufeur" game [49, 51] is about a circle (a "car") that moves in a plane, with constant magnitude of its linear velocity and lower bounded radius of turn, pursuing a slower point (a "pedestrian") that steers in the same plane by choosing his direction of travel at each instant.

Pure pursuit-evasion problems can be viewed, from a more general modelling perspective, as particular cases of dynamic struggles in which two players (a "pursuer" and an "evader") have antagonist goals with respect to the state's temporal evolution of a deterministic system that is under their (partial) control. According to this perspective, a pursuit-evasion differential game, as will be described soon, not necessarily models actual pursuit and evasion.

In the late 1960s extensions to many-players (i.e., not just a pursuer and an evader) nonzero-sum (i.e., non-antagonistic) differential (i.e., in continuous time) games were subsumed in what is called dynamic non-cooperative game theory, so nowadays differential game theory has a broader scope than it had when Isaacs published his book titled "Differential Games: A Mathematical Theory with Applications to Warfare and Pursuit" [49]. The kind of problems studied by Isaacs are referred to as pursuit-evasion games in [59], intending that they are differential games of a special subclass. Following this terminology, we next give a description of pursuit-evasion differential game that is suited for the application-oriented purpose of this thesis. The reader is referred to [59] for a more general and rigorous definition as a particular case of a dynamic non-cooperative game.

A *pursuit-evasion differential game* is given by a state equation, a target set, and a pay-off functional. These three components, delineated in the following paragraphs, comprise a (pursuit-evasion differential) *game* as it is understood in the literature. Often, particular instances of the first two components will be referred to as the defining components of a (pursuit-evasion differential) *conflict*, intentionally leaving unspecified the pay-off functional. This use of the term conflict is not standard, but is adopted here for convenience to name the common underlying structure of different but related games.

The *state equation (SE)* is an ordinary differential equation of the form

$$\frac{\mathrm{d}\boldsymbol{x}}{\mathrm{d}t}(t) = \boldsymbol{f}\left(\boldsymbol{x}\left(t\right), \boldsymbol{\phi}\left(t\right), \boldsymbol{\psi}\left(t\right)\right) \tag{2.1}$$

that describes a *dynamical system*. The evolution of the system's *state*, $\boldsymbol{x}\left(t\right) \in \mathbb{R}^n$, with respect to *time*, $t \in \mathbb{R}$, is influenced by two *players* who control the system's *inputs*, $\boldsymbol{\phi}$ and $\boldsymbol{\psi}$. At each instant of time t, one player, called the pursuer (P), chooses $\boldsymbol{\phi}\left(t\right) \in \boldsymbol{\Phi}$; and the other player, called the evader (E), chooses $\boldsymbol{\psi}\left(t\right) \in \boldsymbol{\Psi}$;

where $\boldsymbol{\Phi}$ and $\boldsymbol{\Psi}$, the *control sets*, are non-empty compact and convex subsets of $\mathbb{R}^{m_P}$ and $\mathbb{R}^{m_E}$, respectively, being m_P and m_E positive integers. The SE is characterized by: i) both control sets, and ii) its right-hand side (RHS) function, $\boldsymbol{f} : \mathbb{R}^n \times \mathbb{R}^{m_P} \times \mathbb{R}^{m_E} \to \mathbb{R}^n$, which is assumed to be continuous, and continuously differentiable with respect to its first argument. Under this assumption, for every *play* $(\boldsymbol{x_0}, \boldsymbol{\phi}, \boldsymbol{\psi})$, comprising an *initial state* $\boldsymbol{x_0} \in \mathbb{R}^n$ and a pair of *open loop control functions* $(\boldsymbol{\phi} : [0, +\infty) \to \boldsymbol{\Phi}, \boldsymbol{\psi} : [0, +\infty) \to \boldsymbol{\Psi})$; the state equation (2.1) has an unique continuous *solution*[1] $\boldsymbol{x}^{\boldsymbol{f}}_{\boldsymbol{x_0}, \boldsymbol{\phi}, \boldsymbol{\psi}} : [0, +\infty) \to \mathbb{R}^n$ through $\boldsymbol{x_0}$, i.e., verifying $\boldsymbol{x}^{\boldsymbol{f}}_{\boldsymbol{x_0}, \boldsymbol{\phi}, \boldsymbol{\psi}}(0) = \boldsymbol{x_0}$, provided the open loop control functions, $\boldsymbol{\phi}$ and $\boldsymbol{\psi}$, are *piecewise continuous*[2]. These solutions are also called *(state-space) trajectories*.

The *target set (TS)*, $\boldsymbol{\mathscr{T}}$, is a non-empty closed subset of $\mathbb{R}^n$ such that its boundary consists of a finite number of smooth (n-1)-dimensional surfaces. Its complement, $\boldsymbol{\mathscr{E}} = \mathbb{R}^n \setminus \boldsymbol{\mathscr{T}}$, is called the *playing set (PS)*.

The *pay-off functional (PF)* is a function $(\boldsymbol{x_0}, \boldsymbol{\phi}, \boldsymbol{\psi}) \mapsto \mathcal{P}_{\boldsymbol{f}, \boldsymbol{\mathscr{T}}}(\boldsymbol{x_0}, \boldsymbol{\phi}, \boldsymbol{\psi}) \in \overline{\mathbb{R}}$ that encodes each player's aim by assigning an element of $\overline{\mathbb{R}} = [-\infty, +\infty]$, the *extended real number line*[3], to every possible play, since it is understood that P aims to infimize it and E aims to supremize it (over a domain that will be sketched in Section 2.2). In the following subsections some typical forms of the PF are introduced.

2.1.1. Games of degree and games of kind

For a conflict, given by a SE of the form (2.1) (whose RHS is given by a function $\boldsymbol{f}$) and a TS denoted $\boldsymbol{\mathscr{T}}$, consider a PF defined by

$$\mathcal{P}^{\text{time}}_{\boldsymbol{f}, \boldsymbol{\mathscr{T}}}(\boldsymbol{x_0}, \boldsymbol{\phi}, \boldsymbol{\psi}) \triangleq \begin{cases} \inf \mathscr{I}_{\boldsymbol{f}, \boldsymbol{\mathscr{T}}}(\boldsymbol{x_0}, \boldsymbol{\phi}, \boldsymbol{\psi}) & \text{if } \mathscr{I}_{\boldsymbol{f}, \boldsymbol{\mathscr{T}}}(\boldsymbol{x_0}, \boldsymbol{\phi}, \boldsymbol{\psi}) \neq \emptyset, \\ +\infty & \text{otherwise,} \end{cases}$$

for every play $(\boldsymbol{x_0}, \boldsymbol{\phi}, \boldsymbol{\psi})$, where $\mathscr{I}_{\boldsymbol{f}, \boldsymbol{\mathscr{T}}}(\boldsymbol{x_0}, \boldsymbol{\phi}, \boldsymbol{\psi})$ is the following set of time instants:

$$\mathscr{I}_{\boldsymbol{f}, \boldsymbol{\mathscr{T}}}(\boldsymbol{x_0}, \boldsymbol{\phi}, \boldsymbol{\psi}) \triangleq \left\{ t \geq 0 \ : \ \boldsymbol{x}^{\boldsymbol{f}}_{\boldsymbol{x_0}, \boldsymbol{\phi}, \boldsymbol{\psi}}(t) \in \boldsymbol{\mathscr{T}} \right\}.$$

The *capture time* (also called *final time*), $\mathcal{P}^{\text{time}}_{\boldsymbol{f}, \boldsymbol{\mathscr{T}}}(\boldsymbol{x_0}, \boldsymbol{\phi}, \boldsymbol{\psi})$, is the first instant of time for which $\boldsymbol{x}^{\boldsymbol{f}}_{\boldsymbol{x_0}, \boldsymbol{\phi}, \boldsymbol{\psi}}(t)$ belongs to $\boldsymbol{\mathscr{T}}$ if it ever reaches it, otherwise it is defined as $+\infty$. In case $\mathcal{P}^{\text{time}}_{\boldsymbol{f}, \boldsymbol{\mathscr{T}}}(\boldsymbol{x_0}, \boldsymbol{\phi}, \boldsymbol{\psi}) < +\infty$, it is said that P *captures* E (or that the play *terminates*) at $\mathcal{P}^{\text{time}}_{\boldsymbol{f}, \boldsymbol{\mathscr{T}}}(\boldsymbol{x_0}, \boldsymbol{\phi}, \boldsymbol{\psi})$; otherwise it is said that E *escapes* from P (or that the play *does not terminate*). These terms are figurative, since the game may not necessarily be the model of a struggle between an actual pursuer and evader.

The form of the functional $\mathcal{P}^{\text{time}}_{\boldsymbol{f}, \boldsymbol{\mathscr{T}}}$, as just defined, is natural in the formulation of pursuit-evasion games. Indeed, this form of PF is the most commonly found in

---

[1]Solution in the extended sense of verifying (2.1) *almost everywhere*.

[2]A *piecewise continuous* function is continuous on every finite interval of time, except possibly at finitely many points in each such finite interval where it has *jump discontinuities*. A more general set-up would haver required *Lebesgue measurable* open loop control functions.

[3]More precisely, the *affinely extended real number system*: $\overline{\mathbb{R}} \triangleq \{-\infty\} \cup \mathbb{R} \cup \{+\infty\}$.

the literature on pursuit-evasion games. However, other forms are possible. For the same SE and TS, consider an alternative PF defined by

$$\mathcal{P}_{\boldsymbol{f},\mathscr{T}}^{\mathrm{dist_o}}\left(\boldsymbol{x_0},\boldsymbol{\phi},\boldsymbol{\psi}\right) \triangleq \begin{cases} \inf \mathscr{D}_{\boldsymbol{f},\mathscr{T}}\left(\boldsymbol{x_0},\boldsymbol{\phi},\boldsymbol{\psi}\right) & \text{if } \mathscr{D}_{\boldsymbol{f},\mathscr{T}}\left(\boldsymbol{x_0},\boldsymbol{\phi},\boldsymbol{\psi}\right) \text{ has a lower bound,} \\ -\infty & \text{otherwise.} \end{cases}$$

for every play $\left(\boldsymbol{x_0},\boldsymbol{\phi},\boldsymbol{\psi}\right)$, where $\mathscr{D}_{\boldsymbol{f},\mathscr{T}}\left(\boldsymbol{x_0},\boldsymbol{\phi},\boldsymbol{\psi}\right)$ is the following set:

$$\mathscr{D}_{\boldsymbol{f},\mathscr{T}}\left(\boldsymbol{x_0},\boldsymbol{\phi},\boldsymbol{\psi}\right) \triangleq \left\{ \mathrm{dist_o}\left(\boldsymbol{x}_{\boldsymbol{x_0},\boldsymbol{\phi},\boldsymbol{\psi}}^{\boldsymbol{f}}\left(t\right),\mathscr{T}\right) \ : \ t \geq 0 \right\},$$

being $\mathrm{dist_o} : \mathbb{R}^n \times 2^{\mathbb{R}^n} \setminus \{\emptyset\} \to \mathbb{R}$, the *oriented distance* function defined by

$$\mathrm{dist_o}\left(\boldsymbol{x},\mathscr{X}\right) \triangleq \begin{cases} +\mathrm{dist}\left(\boldsymbol{x},\mathscr{X}\right) & \text{if } \boldsymbol{x} \in \mathscr{X}^{\complement}, \\ -\mathrm{dist}\left(\boldsymbol{x},\mathscr{X}^{\complement}\right) & \text{if } \boldsymbol{x} \in \mathscr{X}, \end{cases}$$

where $\mathscr{X}^{\complement} \triangleq \mathbb{R}^n \setminus \mathscr{X}$, and $\mathrm{dist}\left(\boldsymbol{x},\mathscr{X}\right) \triangleq \inf_{\boldsymbol{y} \in \mathscr{X}} \|\boldsymbol{x}-\boldsymbol{y}\|$ for every $\boldsymbol{x} \in \mathbb{R}^n$ and every non-empty subset $\mathscr{X}$ of $\mathbb{R}^n$.

Suppose that every play $\left(\boldsymbol{x_0},\boldsymbol{\phi},\boldsymbol{\psi}\right)$ is allowed to continue even beyond capture time (in case capture occurs), thereby letting the state go out from the PS ($\mathscr{E}$) into the TS ($\mathscr{T}$). If $\mathcal{P}_{\boldsymbol{f},\mathscr{T}}^{\mathrm{time}}\left(\boldsymbol{x_0},\boldsymbol{\phi},\boldsymbol{\psi}\right) < +\infty$, P captures E at capture time $\mathcal{P}_{\boldsymbol{f},\mathscr{T}}^{\mathrm{time}}\left(\boldsymbol{x_0},\boldsymbol{\phi},\boldsymbol{\psi}\right)$ and $\mathcal{P}_{\boldsymbol{f},\mathscr{T}}^{\mathrm{dist_o}}\left(\boldsymbol{x_0},\boldsymbol{\phi},\boldsymbol{\psi}\right) \leq 0$. Complementary, if $\mathcal{P}_{\boldsymbol{f},\mathscr{T}}^{\mathrm{time}}\left(\boldsymbol{x_0},\boldsymbol{\phi},\boldsymbol{\psi}\right) = +\infty$, E escapes from P and $\mathcal{P}_{\boldsymbol{f},\mathscr{T}}^{\mathrm{dist_o}}\left(\boldsymbol{x_0},\boldsymbol{\phi},\boldsymbol{\psi}\right) > 0$. From E's viewpoint, with $\mathcal{P}_{\boldsymbol{f},\mathscr{T}}^{\mathrm{time}}$ as PF, the struggle is about the lapse of time available before being captured; while with $\mathcal{P}_{\boldsymbol{f},\mathscr{T}}^{\mathrm{dist_o}}$ as PF, the struggle is about the worst state proximity (resp. incursion) to (resp. into) the TS.

Following the terminology used in [50], a pursuit-evasion game is called a game *in time* if its PF is of the form $\mathcal{P}_{\boldsymbol{f},\mathscr{T}}^{\mathrm{time}}$, while it is called a game *in distance* if its PF is of the form $\mathcal{P}_{\boldsymbol{f},\mathscr{T}}^{\mathrm{dist_o}}$. Games in time and games in distance are instances of what Isaacs called games *of degree* in which the range of the PF is continuum, to distinguish them from what he called games *of kind* in which the range of the PF is discrete. Narrowing this concept slightly, a pursuit-evasion game will be referred to as a game *of kind*, only if its PF has the following form:

$$\mathcal{P}_{\boldsymbol{f},\mathscr{T}}^{\mathrm{kind}}\left(\boldsymbol{x_0},\boldsymbol{\phi},\boldsymbol{\psi}\right) \triangleq \begin{cases} -1 & \text{if } \mathscr{J}_{\boldsymbol{f},\mathscr{T}}\left(\boldsymbol{x_0},\boldsymbol{\phi},\boldsymbol{\psi}\right) \neq \emptyset, \\ +1 & \text{otherwise.} \end{cases}$$

Accordingly, from E's viewpoint, in a game of kind the struggle is only about being able to escape or not.

2.1.2. The standard form of the pay-off functional

Other forms of PF may be defined; the following *standard form* is typical in the literature on differential games:

$$\mathcal{P}_{\boldsymbol{f},\mathscr{T}}^{\mathrm{std}}\left(\boldsymbol{x_0},\boldsymbol{\phi},\boldsymbol{\psi}\right) \triangleq$$
$$\begin{cases} \int_0^{t_{\mathrm{cap}}} G\left(\boldsymbol{x}_{\boldsymbol{x_0},\boldsymbol{\phi},\boldsymbol{\psi}}^{\boldsymbol{f}}\left(t\right),\boldsymbol{\phi}\left(t\right),\boldsymbol{\psi}\left(t\right)\right) \mathrm{d}t + H\left(\boldsymbol{x}_{\boldsymbol{x_0},\boldsymbol{\phi},\boldsymbol{\psi}}^{\boldsymbol{f}}\left(t_{\mathrm{cap}}\right)\right) & \text{if } \mathscr{J}_{\boldsymbol{f},\mathscr{T}}\left(\boldsymbol{x_0},\boldsymbol{\phi},\boldsymbol{\psi}\right) \neq \emptyset, \\ +\infty & \text{otherwise.} \end{cases}$$

(2.2)

where $t_{\text{cap}} \triangleq \mathcal{P}_{\boldsymbol{f},\mathcal{T}}^{\text{time}}(\boldsymbol{x_0},\boldsymbol{\phi},\boldsymbol{\psi})$ is capture time (finite because $\mathcal{J}_{\boldsymbol{f},\mathcal{T}}(\boldsymbol{x_0},\boldsymbol{\phi},\boldsymbol{\psi}) \neq \emptyset$), and the functions $G : \mathbb{R}^n \times \boldsymbol{\Phi} \times \boldsymbol{\Psi} \to \mathbb{R}$ (the *running cost function*) and $H : \mathbb{R}^n \to \mathbb{R}$ (the *terminal cost function*), not both of them null, are smooth. If $H \equiv 0$ the game is said to have *integral pay-off*, while if $G \equiv 0$ the game is said to have *terminal pay-off*.

Note that, in the definition of $\mathcal{P}_{\boldsymbol{f},\mathcal{T}}^{\text{std}}$, preference for termination is arbitrarily assigned to P, but it could be assigned to E defining $\mathcal{P}_{\boldsymbol{f},\mathcal{T}}^{\text{std}}(\boldsymbol{x_0},\boldsymbol{\phi},\boldsymbol{\psi}) \triangleq -\infty$ in case $\mathcal{J}_{\boldsymbol{f},\mathcal{T}}(\boldsymbol{x_0},\boldsymbol{\phi},\boldsymbol{\psi}) = \emptyset$. The former option, is typically adopted so that if $G \equiv 1$ and $H \equiv 0$, $\mathcal{P}_{\boldsymbol{f},\mathcal{T}}^{\text{std}} = \mathcal{P}_{\boldsymbol{f},\mathcal{T}}^{\text{time}}$, i.e., the game is a game in time (as defined before) in which P considers any finite value of $\mathcal{P}_{\boldsymbol{f},\mathcal{T}}^{\text{time}}(\boldsymbol{x_0},\boldsymbol{\phi},\boldsymbol{\psi})$ preferable to $\mathcal{P}_{\boldsymbol{f},\mathcal{T}}^{\text{time}}(\boldsymbol{x_0},\boldsymbol{\phi},\boldsymbol{\psi}) = +\infty$.

2.2. Basic concepts to build a theory

In this section some basic concepts involved in study of pursuit-evasion differential games are introduced. For this porpouse, references [58, Ch. 1] and [59] are closely followed. The first one, to outline a purposely naive approximation to the difficult endeavour of building a rigours pursuit-evasion differential game theory. The second one, to evidence some essential results on non-cooperative two-player zero-sum games, not necessarily pursuit-evasion differential games.

From now on, up to the end of this chapter, consider a fixed (but generic) prototype pursuit-evasion game $\mathcal{G}$, given by the following state equation (SE), target set (TS), and pay-off functional (PF):

$$\mathcal{G} \begin{cases} \text{SE}: & \frac{\text{d}\boldsymbol{x}}{\text{d}t}(t) = \boldsymbol{f}(\boldsymbol{x}(t),\boldsymbol{\phi}(t),\boldsymbol{\psi}(t)), \\ \text{TS}: & \mathcal{T} \subset \mathbb{R}^n, \\ \text{PF}: & (\boldsymbol{x_0},\boldsymbol{\phi},\boldsymbol{\psi}) \mapsto \mathcal{P}_{\boldsymbol{f},\mathcal{T}}(\boldsymbol{x_0},\boldsymbol{\phi},\boldsymbol{\psi}), \end{cases} \tag{2.3}$$

This game acquires sense only if the available information on which each player can base his instantaneous control decisions is declared explicitly, i.e., if the *information structure* [59] of the game is given. In connection with this, it is assumed that at every instant of time, each player *perfectly* knows the current time t and the current state $\boldsymbol{x}(t)$. Moreover, it is rational for a player not to underestimate his opponent, and thus decide his current control action based *solely* on the current time and the current state, i.e., not making ungrounded predictions about his opponent current or future control actions (Isaacs discuss this point thoroughly in the first chapters of [49]). If both players put in practice this rationality, the game is said to have a *feedback* information structure [59].

2.2.1. Strategies

A *strategy*, or more precisely a *feedback strategy*, for P is a function

$$\tilde{\boldsymbol{\phi}} : [0,+\infty) \times \mathbb{R}^n \to \boldsymbol{\Phi} \tag{2.4}$$

that dictates P how to choose his control action $\boldsymbol{\phi}(t) = \tilde{\boldsymbol{\phi}}(t,\boldsymbol{x}(t))$, as a function of the current time t and the current state $\boldsymbol{x}(t)$. Likewise, a strategy for E is a

function $\tilde{\boldsymbol{\psi}} : [0, +\infty) \times \mathbb{R}^n \to \boldsymbol{\Psi}$ that dictates E how to choose his control action $\boldsymbol{\psi}(t) = \tilde{\boldsymbol{\psi}}(t, \boldsymbol{x}(t))$, as a function of the current time t and the current state $\boldsymbol{x}(t)$.

Although, this is the strategy concept employed throughout this thesis, note that it is quite naive. As pointed out in [58], given an initial state $\boldsymbol{x_0} \in \mathbb{R}^n$, and two arbitrary strategies $\tilde{\boldsymbol{\phi}} : [0, +\infty) \times \mathbb{R}^n \to \boldsymbol{\Phi}$ and $\tilde{\boldsymbol{\psi}} : [0, +\infty) \times \mathbb{R}^n \to \boldsymbol{\Psi}$; the initial value problem

$$\begin{cases} \frac{\mathrm{d}\boldsymbol{x}}{\mathrm{d}t}(t) = \boldsymbol{f}\left(\boldsymbol{x}(t), \tilde{\boldsymbol{\phi}}(t, \boldsymbol{x}(t)), \tilde{\boldsymbol{\psi}}(t, \boldsymbol{x}(t))\right), & t \geq 0, \\ \boldsymbol{x}(0) = \boldsymbol{x_0}, \end{cases} \tag{2.5}$$

(that results from plugging the strategies into the SE) does not necessarily has a solution, and if it has one it may not be unique. This difficulty asks for a restriction[4] on the sets of strategies that can be chosen by the players.

Literally following [58, Ch. 1] (where a first attempt to formalize an useful notion of strategy is developed), a pair $\left(\tilde{\Phi}, \tilde{\Psi}\right)$ of sets of strategies is called *admissible* if the following conditions are satisfied.

- All strategies of the form $\tilde{\boldsymbol{\phi}}(\cdot, \boldsymbol{x}) = \boldsymbol{\phi}(\cdot)$, where $\boldsymbol{x} \in \mathbb{R}^n$ and $\boldsymbol{\phi} : [0, +\infty) \to \boldsymbol{\Phi}$ is a piecewise continuous open loop control functions for P, belong to $\tilde{\Phi}$. Analogously for E's open loop control functions and $\tilde{\Psi}$.

- For every $\left(\boldsymbol{x_0}, \tilde{\boldsymbol{\phi}}, \tilde{\boldsymbol{\psi}}\right)$, such that $\boldsymbol{x_0} \in \mathbb{R}^n$ and $\left(\tilde{\boldsymbol{\phi}}, \tilde{\boldsymbol{\psi}}\right) \in \left(\tilde{\Phi}, \tilde{\Psi}\right)$, the initial value problem (2.5) has an unique solution.

- If $\tilde{\boldsymbol{\phi}}_{\boldsymbol{1}}, \tilde{\boldsymbol{\phi}}_{\boldsymbol{2}} \in \tilde{\Phi}$, then for every $\tau > 0$, the strategy defined by

$$\tilde{\boldsymbol{\phi}}_{\boldsymbol{3}}(t, \boldsymbol{x}) \triangleq \begin{cases} \tilde{\boldsymbol{\phi}}_{\boldsymbol{1}}(t, \boldsymbol{x}) & \text{if } t \in [0, \tau] \\ \tilde{\boldsymbol{\phi}}_{\boldsymbol{2}}(t, \boldsymbol{x}) & \text{otherwise} \end{cases} \quad \forall \boldsymbol{x} \in \mathbb{R}^n,$$

  also belongs $\tilde{\Phi}$. Symmetrically for $\tilde{\Psi}$.

- If $\tilde{\boldsymbol{\phi}} \in \tilde{\Phi}$, then for every $\tau > 0$ the strategy defined by

$$\tilde{\boldsymbol{\phi}}_{\boldsymbol{1}}(t, \boldsymbol{x}) \triangleq \tilde{\boldsymbol{\phi}}(t + \tau, \boldsymbol{x}) \quad \forall \boldsymbol{x} \in \mathbb{R}^n,$$

  also belongs $\tilde{\Phi}$. Symmetrically for $\tilde{\Psi}$.

From now on up to the end this chapter, consider a given admissible pair $\left(\tilde{\Phi}, \tilde{\Psi}\right)$ of sets of strategies. For every triplet $\left(\boldsymbol{x_0}, \tilde{\boldsymbol{\phi}}, \tilde{\boldsymbol{\psi}}\right)$, such that $\boldsymbol{x_0} \in \mathbb{R}^n$, $\tilde{\boldsymbol{\phi}} \in \tilde{\Phi}$ and $\tilde{\boldsymbol{\psi}} \in \tilde{\Psi}$, let $\boldsymbol{x}^{\boldsymbol{f}}_{\boldsymbol{x_0}, \tilde{\boldsymbol{\phi}}, \tilde{\boldsymbol{\psi}}} : [0, +\infty) \to \mathbb{R}^n$ be the unique solution of (2.5). The existence and uniqueness of $\boldsymbol{x}^{\boldsymbol{f}}_{\boldsymbol{x_0}, \tilde{\boldsymbol{\phi}}, \tilde{\boldsymbol{\psi}}}$ allows to define the *cost function of the (pursuit-evasion) game in normal form* [59] as the functional

$$\left(\boldsymbol{x_0}, \tilde{\boldsymbol{\phi}}, \tilde{\boldsymbol{\psi}}\right) \mapsto \tilde{\mathcal{P}}_{\boldsymbol{f}, \mathscr{T}}\left(\boldsymbol{x_0}, \tilde{\boldsymbol{\phi}}, \tilde{\boldsymbol{\psi}}\right) \triangleq \mathcal{P}_{\boldsymbol{f}, \mathscr{T}}\left(\boldsymbol{x_0}, \boldsymbol{\phi}, \boldsymbol{\psi}\right),$$

---

[4]For example, feedback strategies could be required to be piecewise continuous in t and Lipschitz-continuous in $\boldsymbol{x}$. However, such a restriction appears to be unrealistic in pursuit-evasion games. In [59], after discussing this issue, the authors conclude that "non-Lipschitz strategies cannot easily be put into a rigorous mathematical framework".

where $\phi : [0, +\infty) \to \boldsymbol{\Phi}$ and $\psi : [0, +\infty) \to \boldsymbol{\Psi}$ are *realizations* [60] (also called *open-loop representations* [59]) of strategies $\tilde{\phi}$ and $\tilde{\psi}$, respectively, defined by

$$\phi(t) \triangleq \tilde{\phi}\left(t, \boldsymbol{x}^{\boldsymbol{f}}_{\boldsymbol{x_0}, \tilde{\phi}, \tilde{\psi}}(t)\right),$$
$$\psi(t) \triangleq \tilde{\psi}\left(t, \boldsymbol{x}^{\boldsymbol{f}}_{\boldsymbol{x_0}, \tilde{\phi}, \tilde{\psi}}(t)\right),$$

for every $t \geq 0$. Notice that $\tilde{\mathcal{P}}_{\boldsymbol{f}, \mathscr{T}} : \tilde{\Phi} \times \tilde{\Psi} \to \overline{\overline{\mathbb{R}}}$ is well defined, because the existence and uniqueness of $\boldsymbol{x}^{\boldsymbol{f}}_{\boldsymbol{x_0}, \tilde{\phi}, \tilde{\psi}}$ (as a solution of (2.5)) permit the construction of the realizations (i.e., open loop control functions derived from the strategies and the SE) needed to evaluate $\mathcal{P}_{\boldsymbol{f}, \mathscr{T}}$.

The triplet $(\boldsymbol{x_0}, \boldsymbol{\phi}, \boldsymbol{\psi})$, that results (as just described) from P's adoption of strategy $\tilde{\phi}$ and E's adoption of strategy $\tilde{\psi}$, is a *play* of the game, since the realizations $\boldsymbol{\phi}$ and $\boldsymbol{\psi}$ are (actually) open-loop control functions. Overloading the use of this word, sometimes the triplet $\left(\boldsymbol{x_0}, \tilde{\phi}, \tilde{\psi}\right)$ will also be referred to as a *play* of the game, understanding that the aforementioned procedure to synthesise realizations of the adopted strategies is possible. Moreover, it will be said that $\tilde{\mathcal{P}}_{\boldsymbol{f}, \mathscr{T}}\left(\boldsymbol{x_0}, \tilde{\phi}, \tilde{\psi}\right)$ is the *outcome* that corresponds to the play $\left(\boldsymbol{x_0}, \tilde{\phi}, \tilde{\psi}\right)$.

2.2.2. Upper and lower value functions

Equipped with a cost function of the game in normal form, $\tilde{\mathcal{P}}_{\boldsymbol{f}, \mathscr{T}}$, it is straightforward to define upper and lower value functions [58, Ch. 1]. The *upper value function* $\overline{\mathcal{V}}$ is defined as

$$\boldsymbol{x} \mapsto \overline{\mathcal{V}}(\boldsymbol{x}) = \inf_{\tilde{\phi} \in \tilde{\Phi}} \sup_{\tilde{\psi} \in \tilde{\Psi}} \tilde{\mathcal{P}}_{\boldsymbol{f}, \mathscr{T}}\left(\boldsymbol{x}, \tilde{\phi}, \tilde{\psi}\right) \tag{2.6}$$

for every $\boldsymbol{x} \in \mathbb{R}^n$, and the *lower value function* $\underline{\mathcal{V}}$ is defined as

$$\boldsymbol{x} \mapsto \underline{\mathcal{V}}(\boldsymbol{x}) = \sup_{\tilde{\psi} \in \tilde{\Psi}} \inf_{\tilde{\phi} \in \tilde{\Phi}} \tilde{\mathcal{P}}_{\boldsymbol{f}, \mathscr{T}}\left(\boldsymbol{x}, \tilde{\phi}, \tilde{\psi}\right) \tag{2.7}$$

for every $\boldsymbol{x} \in \mathbb{R}^n$.

It is obvious that

$$\inf_{\tilde{\phi} \in \tilde{\Phi}} \tilde{\mathcal{P}}_{\boldsymbol{f}, \mathscr{T}}\left(\boldsymbol{x}, \tilde{\phi}, \tilde{\psi}_{\boldsymbol{0}}\right) \leq \tilde{\mathcal{P}}_{\boldsymbol{f}, \mathscr{T}}\left(\boldsymbol{x}, \tilde{\phi}_{\boldsymbol{0}}, \tilde{\psi}_{\boldsymbol{0}}\right) \leq \sup_{\tilde{\psi} \in \tilde{\Psi}} \tilde{\mathcal{P}}_{\boldsymbol{f}, \mathscr{T}}\left(\boldsymbol{x}, \tilde{\phi}_{\boldsymbol{0}}, \tilde{\psi}\right),$$

for every $\boldsymbol{x} \in \mathbb{R}^n$, every $\tilde{\phi}_{\boldsymbol{0}} \in \tilde{\Phi}$ and every $\tilde{\psi}_{\boldsymbol{0}} \in \tilde{\Psi}$. So,

$$\inf_{\tilde{\phi} \in \tilde{\Phi}} \tilde{\mathcal{P}}_{\boldsymbol{f}, \mathscr{T}}\left(\boldsymbol{x}, \tilde{\phi}, \tilde{\psi}_{\boldsymbol{0}}\right) \leq \sup_{\tilde{\psi} \in \tilde{\Psi}} \tilde{\mathcal{P}}_{\boldsymbol{f}, \mathscr{T}}\left(\boldsymbol{x}, \tilde{\phi}_{\boldsymbol{0}}, \tilde{\psi}\right) \quad \forall \boldsymbol{x} \in \mathbb{R}^n, \ \forall \tilde{\phi}_{\boldsymbol{0}} \in \tilde{\Phi}, \ \forall \tilde{\psi}_{\boldsymbol{0}} \in \tilde{\Psi}.$$

Application of $\sup_{\tilde{\psi}_{\boldsymbol{0}} \in \tilde{\Psi}}$ and $\inf_{\tilde{\phi}_{\boldsymbol{0}} \in \tilde{\Phi}}$, furnish:

$$\underline{\mathcal{V}}(\boldsymbol{x}) = \sup_{\tilde{\psi}_{\boldsymbol{0}} \in \tilde{\Psi}} \inf_{\tilde{\phi} \in \tilde{\Phi}} \tilde{\mathcal{P}}_{\boldsymbol{f}, \mathscr{T}}\left(\boldsymbol{x}, \tilde{\phi}, \tilde{\psi}_{\boldsymbol{0}}\right) \leq \inf_{\tilde{\phi}_{\boldsymbol{0}} \in \tilde{\Phi}} \sup_{\tilde{\psi} \in \tilde{\Psi}} \tilde{\mathcal{P}}_{\boldsymbol{f}, \mathscr{T}}\left(\boldsymbol{x}, \tilde{\phi}_{\boldsymbol{0}}, \tilde{\psi}\right) = \overline{\mathcal{V}}(\boldsymbol{x}) \quad \forall \boldsymbol{x} \in \mathbb{R}^n.$$

Hence $\underline{\mathcal{V}} \leq \overline{\mathcal{V}}$, in accordance with the names given to these two functions.

2.2.3. Security strategies

Conceptually, a security strategy [59, Ch. 2] models a conservative mode of play of a player against any (rational or irrational) behaviour of the other player.

A strategy $\tilde{\boldsymbol{\phi}}^* \in \tilde{\Phi}$ is called a *security strategy for* P if

$$\sup_{\tilde{\boldsymbol{\psi}} \in \tilde{\Psi}} \tilde{\mathcal{P}}_{\boldsymbol{f},\mathscr{T}} \left(\boldsymbol{x}, \tilde{\boldsymbol{\phi}}^*, \tilde{\boldsymbol{\psi}} \right) = \overline{\mathcal{V}}\left(\boldsymbol{x} \right)$$

for every $\boldsymbol{x} \in \mathbb{R}^n$. In a like manner, a strategy $\tilde{\boldsymbol{\psi}}^* \in \tilde{\Psi}$ is called a *security strategy for* E if

$$\inf_{\tilde{\boldsymbol{\phi}} \in \tilde{\Phi}} \tilde{\mathcal{P}}_{\boldsymbol{f},\mathscr{T}} \left(\boldsymbol{x}, \tilde{\boldsymbol{\phi}}, \tilde{\boldsymbol{\psi}}^* \right) = \underline{\mathcal{V}}\left(\boldsymbol{x} \right)$$

for every $\boldsymbol{x} \in \mathbb{R}^n$.

Security is understood in the following *worst-case* sense. Fix a generic initial state $\boldsymbol{x} \in \mathbb{R}^n$. For P (the infimizer), $\tilde{\boldsymbol{\phi}}^*$ is a security strategy because it renders him an outcome $\tilde{\mathcal{P}}_{\boldsymbol{f},\mathscr{T}} \left(\boldsymbol{x}, \tilde{\boldsymbol{\phi}}^*, \tilde{\boldsymbol{\psi}} \right)$ that is *at most* $\overline{\mathcal{V}}\left(\boldsymbol{x} \right)$, depending on E's strategy $\tilde{\boldsymbol{\psi}}$. For E (the supremizer), $\tilde{\boldsymbol{\psi}}^*$ is a security strategy because it renders him a outcome $\tilde{\mathcal{P}}_{\boldsymbol{f},\mathscr{T}} \left(\boldsymbol{x}, \tilde{\boldsymbol{\phi}}, \tilde{\boldsymbol{\psi}}^* \right)$ that is *at least* $\underline{\mathcal{V}}\left(\boldsymbol{x} \right)$, depending on P's strategy $\tilde{\boldsymbol{\phi}}$.

2.2.4. Value function

If functions $\overline{\mathcal{V}}$ and $\underline{\mathcal{V}}$ are equal, i.e., if the *inf* and *sup* operations in (2.7) or (2.6) commute, then the function $\mathcal{V} \triangleq \overline{\mathcal{V}} = \underline{\mathcal{V}}$ is called the *value function (VF)*, or just the *value*, of the (pursuit-evasion) game [58, Ch. 1]. In this case, if $\left(\tilde{\boldsymbol{\phi}}^*, \tilde{\boldsymbol{\psi}}^* \right) \in \tilde{\Phi} \times \tilde{\Psi}$ is a (somehow known) *ordered security strategy pair* (i.e., $\tilde{\boldsymbol{\phi}}^*$ and $\tilde{\boldsymbol{\psi}}^*$ are security strategies for P and E, respectively); it follows (by definition of security strategy) that

$$\sup_{\tilde{\boldsymbol{\psi}}_{\boldsymbol{0}} \in \tilde{\Psi}} \tilde{\mathcal{P}}_{\boldsymbol{f},\mathscr{T}} \left(\boldsymbol{x}, \tilde{\boldsymbol{\phi}}^*, \tilde{\boldsymbol{\psi}}_{\boldsymbol{0}} \right) = \overline{\mathcal{V}}\left(\boldsymbol{x} \right) = \mathcal{V}\left(\boldsymbol{x} \right) = \underline{\mathcal{V}}\left(\boldsymbol{x} \right) = \inf_{\tilde{\boldsymbol{\phi}}_{\boldsymbol{0}} \in \tilde{\Phi}} \tilde{\mathcal{P}}_{\boldsymbol{f},\mathscr{T}} \left(\boldsymbol{x}, \tilde{\boldsymbol{\phi}}_{\boldsymbol{0}}, \tilde{\boldsymbol{\psi}}^* \right), \quad (2.8)$$

for every $\boldsymbol{x} \in \mathbb{R}^n$. In addition, since $\tilde{\mathcal{P}}_{\boldsymbol{f},\mathscr{T}} \left(\boldsymbol{x}, \tilde{\boldsymbol{\phi}}^*, \tilde{\boldsymbol{\psi}} \right) \leq \sup_{\tilde{\boldsymbol{\psi}}_{\boldsymbol{0}} \in \tilde{\Psi}} \tilde{\mathcal{P}}_{\boldsymbol{f},\mathscr{T}} \left(\boldsymbol{x}, \tilde{\boldsymbol{\phi}}^*, \tilde{\boldsymbol{\psi}}_{\boldsymbol{0}} \right)$ for every $\tilde{\boldsymbol{\psi}} \in \tilde{\Psi}$ and $\inf_{\tilde{\boldsymbol{\phi}}_{\boldsymbol{0}} \in \tilde{\Phi}} \tilde{\mathcal{P}}_{\boldsymbol{f},\mathscr{T}} \left(\boldsymbol{x}, \tilde{\boldsymbol{\phi}}_{\boldsymbol{0}}, \tilde{\boldsymbol{\psi}}^* \right) \leq \tilde{\mathcal{P}}_{\boldsymbol{f},\mathscr{T}} \left(\boldsymbol{x}, \tilde{\boldsymbol{\phi}}, \tilde{\boldsymbol{\psi}}^* \right)$ for every $\tilde{\boldsymbol{\phi}} \in \tilde{\Phi}$; it must be

$$\tilde{\mathcal{P}}_{\boldsymbol{f},\mathscr{T}} \left(\boldsymbol{x}, \tilde{\boldsymbol{\phi}}^*, \tilde{\boldsymbol{\psi}} \right) \leq \mathcal{V}\left(\boldsymbol{x} \right) \leq \tilde{\mathcal{P}}_{\boldsymbol{f},\mathscr{T}} \left(\boldsymbol{x}, \tilde{\boldsymbol{\phi}}, \tilde{\boldsymbol{\psi}}^* \right) \quad \forall \boldsymbol{x} \in \mathbb{R}^n, \, \forall \tilde{\boldsymbol{\phi}} \in \tilde{\Phi}, \, \forall \tilde{\boldsymbol{\psi}} \in \tilde{\Psi}. \quad (2.9)$$

In particular, for $\tilde{\boldsymbol{\phi}} = \tilde{\boldsymbol{\phi}}^*$ and $\tilde{\boldsymbol{\psi}} = \tilde{\boldsymbol{\psi}}^*$, $\tilde{\mathcal{P}}_{\boldsymbol{f},\mathscr{T}} \left(\boldsymbol{x}, \tilde{\boldsymbol{\phi}}^*, \tilde{\boldsymbol{\psi}}^* \right) \leq \mathcal{V}\left(\boldsymbol{x} \right) \leq \tilde{\mathcal{P}}_{\boldsymbol{f},\mathscr{T}} \left(\boldsymbol{x}, \tilde{\boldsymbol{\phi}}^*, \tilde{\boldsymbol{\psi}}^* \right)$, and consequently (2.9) can be rewritten as

$$\tilde{\mathcal{P}}_{\boldsymbol{f},\mathscr{T}} \left(\boldsymbol{x}, \tilde{\boldsymbol{\phi}}^*, \tilde{\boldsymbol{\psi}} \right) \leq \tilde{\mathcal{P}}_{\boldsymbol{f},\mathscr{T}} \left(\boldsymbol{x}, \tilde{\boldsymbol{\phi}}^*, \tilde{\boldsymbol{\psi}}^* \right) \leq \tilde{\mathcal{P}}_{\boldsymbol{f},\mathscr{T}} \left(\boldsymbol{x}, \tilde{\boldsymbol{\phi}}, \tilde{\boldsymbol{\psi}}^* \right) \quad \forall \boldsymbol{x} \in \mathbb{R}^n, \, \forall \tilde{\boldsymbol{\phi}} \in \tilde{\Phi}, \forall \tilde{\boldsymbol{\psi}} \in \tilde{\Psi},$$
$$(2.10)$$

where $\tilde{\mathcal{P}}_{\boldsymbol{f},\mathscr{T}} \left(\boldsymbol{x}, \tilde{\boldsymbol{\phi}}^*, \tilde{\boldsymbol{\psi}}^* \right) = \mathcal{V}\left(\boldsymbol{x} \right) = \overline{\mathcal{V}}\left(\boldsymbol{x} \right) = \underline{\mathcal{V}}\left(\boldsymbol{x} \right)$. This motivates the following definition.

2.2.5. Saddle-point equilibriums

A strategy pair $\left(\tilde{\boldsymbol{\phi}}^*, \tilde{\boldsymbol{\psi}}^*\right) \in \left(\tilde{\Phi}, \tilde{\Psi}\right)$ is called a *saddle-point equilibrium* (and $\tilde{\boldsymbol{\phi}}^*$ and $\tilde{\boldsymbol{\psi}}^*$ are called *saddle-point strategies*) if it verifies the *saddle inequalities*:

$$\tilde{\mathcal{P}}_{\boldsymbol{f}, \mathscr{T}}\left(\boldsymbol{x}, \tilde{\boldsymbol{\phi}}^*, \tilde{\boldsymbol{\psi}}\right) \leq \tilde{\mathcal{P}}_{\boldsymbol{f}, \mathscr{T}}\left(\boldsymbol{x}, \tilde{\boldsymbol{\phi}}^*, \tilde{\boldsymbol{\psi}}^*\right) \leq \tilde{\mathcal{P}}_{\boldsymbol{f}, \mathscr{T}}\left(\boldsymbol{x}, \tilde{\boldsymbol{\phi}}, \tilde{\boldsymbol{\psi}}^*\right) \quad \forall \boldsymbol{x} \in \mathbb{R}^n, \forall \tilde{\boldsymbol{\phi}} \in \tilde{\Phi}, \forall \tilde{\boldsymbol{\psi}} \in \tilde{\Psi}.$$
$$(2.11)$$

Note that at the end of the previous subsection it was proved that if functions $\overline{\mathcal{V}}$ and $\underline{\mathcal{V}}$ are equal, every ordered security startegy pair is a saddle-point equilibrium.

The next proposition, adapted from [59, Ch. 2], states that the set of saddle-point equilibrium strategy pairs is not larger than the set of ordered security strategy pairs.

Proposition 2.2.1. *Every saddle-point equilibrium strategy pair is a security strategy pair.*

Proof. Let $\left(\tilde{\boldsymbol{\phi}}^*, \tilde{\boldsymbol{\psi}}^*\right)$ be saddle-point equilibrium strategy pair. From (2.11), supremizing over $\tilde{\boldsymbol{\psi}} \in \tilde{\Psi}$ the leftmost expression and comparing to the rightmost expression results:

$$\sup_{\tilde{\boldsymbol{\psi}} \in \tilde{\Psi}} \tilde{\mathcal{P}}_{\boldsymbol{f}, \mathscr{T}}\left(\boldsymbol{x}, \tilde{\boldsymbol{\phi}}^*, \tilde{\boldsymbol{\psi}}\right) \leq \tilde{\mathcal{P}}_{\boldsymbol{f}, \mathscr{T}}\left(\boldsymbol{x}, \tilde{\boldsymbol{\phi}}, \tilde{\boldsymbol{\psi}}^*\right) \leq \sup_{\tilde{\boldsymbol{\psi}} \in \tilde{\Psi}} \tilde{\mathcal{P}}_{\boldsymbol{f}, \mathscr{T}}\left(\boldsymbol{x}, \tilde{\boldsymbol{\phi}}, \tilde{\boldsymbol{\psi}}\right) \quad \forall \boldsymbol{x} \in \mathbb{R}^n, \forall \tilde{\boldsymbol{\phi}} \in \tilde{\Phi},$$

where the introduced right inequality is trivial. Now, from these last inequalities, infimizing the rightmost expression and comparing it to the leftmost expression,

$$\sup_{\tilde{\boldsymbol{\psi}} \in \tilde{\Psi}} \tilde{\mathcal{P}}_{\boldsymbol{f}, \mathscr{T}}\left(\boldsymbol{x}, \tilde{\boldsymbol{\phi}}^*, \tilde{\boldsymbol{\psi}}\right) \leq \inf_{\tilde{\boldsymbol{\phi}} \in \tilde{\Phi}} \sup_{\tilde{\boldsymbol{\psi}} \in \tilde{\Psi}} \tilde{\mathcal{P}}_{\boldsymbol{f}, \mathscr{T}}\left(\boldsymbol{x}, \tilde{\boldsymbol{\phi}}, \tilde{\boldsymbol{\psi}}\right) = \overline{\mathcal{V}}\left(\boldsymbol{x}\right) \quad \forall \boldsymbol{x} \in \mathbb{R}^n.$$

Moreover, since $\overline{\mathcal{V}}\left(\boldsymbol{x}\right) = \inf_{\tilde{\boldsymbol{\phi}} \in \tilde{\Phi}} \sup_{\tilde{\boldsymbol{\psi}} \in \tilde{\Psi}} \tilde{\mathcal{P}}_{\boldsymbol{f}, \mathscr{T}}\left(\boldsymbol{x}, \tilde{\boldsymbol{\phi}}, \tilde{\boldsymbol{\psi}}\right) \leq \sup_{\tilde{\boldsymbol{\psi}} \in \tilde{\Psi}} \tilde{\mathcal{P}}_{\boldsymbol{f}, \mathscr{T}}\left(\boldsymbol{x}, \tilde{\boldsymbol{\phi}}^*, \tilde{\boldsymbol{\psi}}\right),$

$$\overline{\mathcal{V}}\left(\boldsymbol{x}\right) \leq \sup_{\tilde{\boldsymbol{\psi}} \in \tilde{\Psi}} \tilde{\mathcal{P}}_{\boldsymbol{f}, \mathscr{T}}\left(\boldsymbol{x}, \tilde{\boldsymbol{\phi}}^*, \tilde{\boldsymbol{\psi}}\right) \leq \overline{\mathcal{V}}\left(\boldsymbol{x}\right) \quad \forall \boldsymbol{x} \in \mathbb{R}^n,$$

proving that $\tilde{\boldsymbol{\phi}}^*$ is a security strategy for P. Analogously, it can be shown that $\tilde{\boldsymbol{\psi}}^*$ is a security strategy for E. $\square$

The next proposition states that the existence of a saddle-point equilibrium guarantees the existence of a VF.

Proposition 2.2.2. *If $\left(\tilde{\boldsymbol{\phi}}^*, \tilde{\boldsymbol{\psi}}^*\right)$ is a saddle-point equilibrium strategy pair, then $\underline{\mathcal{V}}\left(\boldsymbol{x}\right) = \tilde{\mathcal{P}}_{\boldsymbol{f}, \mathscr{T}}\left(\boldsymbol{x}, \tilde{\boldsymbol{\phi}}^*, \tilde{\boldsymbol{\psi}}^*\right) = \overline{\mathcal{V}}\left(\boldsymbol{x}\right)$ for every $\boldsymbol{x} \in \mathbb{R}^n$.*

Proof. From (2.11), supremizing over $\tilde{\boldsymbol{\psi}} \in \tilde{\Psi}$ the leftmost expression:

$$\sup_{\tilde{\boldsymbol{\psi}} \in \tilde{\Psi}} \tilde{\mathcal{P}}_{\boldsymbol{f}, \mathscr{T}}\left(\boldsymbol{x}, \tilde{\boldsymbol{\phi}}^*, \tilde{\boldsymbol{\psi}}\right) \leq \tilde{\mathcal{P}}_{\boldsymbol{f}, \mathscr{T}}\left(\boldsymbol{x}, \tilde{\boldsymbol{\phi}}^*, \tilde{\boldsymbol{\psi}}^*\right) \quad \forall \boldsymbol{x} \in \mathbb{R}^n. \tag{2.12}$$

Similarly, from (2.11), infimizing over $\tilde{\boldsymbol{\phi}} \in \tilde{\Phi}$ the rightmost expression:

$$\tilde{\mathcal{P}}_{\boldsymbol{f}, \mathscr{T}}\left(\boldsymbol{x}, \tilde{\boldsymbol{\phi}}^*, \tilde{\boldsymbol{\psi}}^*\right) \leq \inf_{\tilde{\boldsymbol{\phi}} \in \tilde{\Phi}} \tilde{\mathcal{P}}_{\boldsymbol{f}, \mathscr{T}}\left(\boldsymbol{x}, \tilde{\boldsymbol{\phi}}, \tilde{\boldsymbol{\psi}}^*\right) \quad \forall \boldsymbol{x} \in \mathbb{R}^n. \tag{2.13}$$

21

By Proposition 2.2.1, $\tilde{\phi}^*$ is a security strategy for P, so the leftmost expression in (2.12) equals $\overline{\mathcal{V}}(\boldsymbol{x})$. Also by Proposition 2.2.1, $\tilde{\psi}^*$ is a security strategy for E, so the rightmost expression in (2.13) equals $\underline{\mathcal{V}}(\boldsymbol{x})$. These two facts imply that

$$\overline{\mathcal{V}}(\boldsymbol{x}) \leq \tilde{\mathcal{P}}_{\boldsymbol{f},\mathscr{T}}\left(\boldsymbol{x},\tilde{\phi}^*,\tilde{\psi}^*\right) \leq \underline{\mathcal{V}}(\boldsymbol{x}) \quad \forall \boldsymbol{x} \in \mathbb{R}^n, \tag{2.14}$$

but, as it has been noticed before, $\underline{\mathcal{V}}(\boldsymbol{x}) \leq \overline{\mathcal{V}}(\boldsymbol{x})$ must hold for every $\boldsymbol{x} \in \mathbb{R}^n$ (by definition of $\underline{\mathcal{V}}$ and $\overline{\mathcal{V}}$); so consequently

$$\underline{\mathcal{V}}(\boldsymbol{x}) = \tilde{\mathcal{P}}_{\boldsymbol{f},\mathscr{T}}\left(\boldsymbol{x},\tilde{\phi}^*,\tilde{\psi}^*\right) = \overline{\mathcal{V}}(\boldsymbol{x}) \quad \forall \boldsymbol{x} \in \mathbb{R}^n. \tag{2.15}$$

$\square$

The next proposition, adapted from [59, Ch. 2], states a feature of saddle-point strategies known as their *ordered interchangeability* property. It means that in case of multiple saddle-point equilibriums, each player does not have to guess the particular saddle-point strategy his opponent will adopt, since all such strategies are in equilibrium and yield the same outcome.

Proposition 2.2.3. *If $\left(\tilde{\phi}_1^*,\tilde{\psi}_1^*\right)$ and $\left(\tilde{\phi}_2^*,\tilde{\psi}_2^*\right)$ are a saddle-point equilibriums, then $\left(\tilde{\phi}_1^*,\tilde{\psi}_2^*\right)$ and $\left(\tilde{\phi}_2^*,\tilde{\psi}_1^*\right)$ are also saddle-point equilibriums and, for each $\boldsymbol{x} \in \mathbb{R}^n$, they all yield the same outcome $\mathcal{V}(\boldsymbol{x})$.*

Proof. The pairs $\left(\tilde{\phi}_1^*,\tilde{\psi}_1^*\right)$ and $\left(\tilde{\phi}_2^*,\tilde{\psi}_2^*\right)$ are saddle-point equilibriums, so

$$\tilde{\mathcal{P}}_{\boldsymbol{f},\mathscr{T}}\left(\boldsymbol{x},\tilde{\phi}_1^*,\tilde{\psi}\right) \leq \tilde{\mathcal{P}}_{\boldsymbol{f},\mathscr{T}}\left(\boldsymbol{x},\tilde{\phi}_1^*,\tilde{\psi}_1^*\right) \leq \tilde{\mathcal{P}}_{\boldsymbol{f},\mathscr{T}}\left(\boldsymbol{x},\tilde{\phi},\tilde{\psi}_1^*\right) \quad \forall \boldsymbol{x} \in \mathbb{R}^n, \forall \tilde{\phi} \in \tilde{\Phi}, \forall \tilde{\psi} \in \tilde{\Psi}, \tag{2.16}$$

$$\tilde{\mathcal{P}}_{\boldsymbol{f},\mathscr{T}}\left(\boldsymbol{x},\tilde{\phi}_2^*,\tilde{\psi}\right) \leq \tilde{\mathcal{P}}_{\boldsymbol{f},\mathscr{T}}\left(\boldsymbol{x},\tilde{\phi}_2^*,\tilde{\psi}_2^*\right) \leq \tilde{\mathcal{P}}_{\boldsymbol{f},\mathscr{T}}\left(\boldsymbol{x},\tilde{\phi},\tilde{\psi}_2^*\right) \quad \forall \boldsymbol{x} \in \mathbb{R}^n, \forall \tilde{\phi} \in \tilde{\Phi}, \forall \tilde{\psi} \in \tilde{\Psi}. \tag{2.17}$$

Choosing $\tilde{\psi} = \tilde{\psi}_2^*$ in (2.16) and $\tilde{\phi} = \tilde{\phi}_1^*$ in (2.17),

$$\tilde{\mathcal{P}}_{\boldsymbol{f},\mathscr{T}}\left(\boldsymbol{x},\tilde{\phi}_2^*,\tilde{\psi}\right) \leq \tilde{\mathcal{P}}_{\boldsymbol{f},\mathscr{T}}\left(\boldsymbol{x},\tilde{\phi}_2^*,\tilde{\psi}_2^*\right) \leq \tilde{\mathcal{P}}_{\boldsymbol{f},\mathscr{T}}\left(\boldsymbol{x},\tilde{\phi}_1^*,\tilde{\psi}_2^*\right)$$
$$\leq \tilde{\mathcal{P}}_{\boldsymbol{f},\mathscr{T}}\left(\boldsymbol{x},\tilde{\phi}_1^*,\tilde{\psi}_1^*\right) \leq \tilde{\mathcal{P}}_{\boldsymbol{f},\mathscr{T}}\left(\boldsymbol{x},\tilde{\phi},\tilde{\psi}_1^*\right) \quad \forall \boldsymbol{x} \in \mathbb{R}^n, \forall \tilde{\phi} \in \tilde{\Phi}, \forall \tilde{\psi} \in \tilde{\Psi}, \tag{2.18}$$

where $\tilde{\mathcal{P}}_{\boldsymbol{f},\mathscr{T}}\left(\boldsymbol{x},\tilde{\phi}_1^*,\tilde{\psi}_2^*\right) = \mathcal{V}(\boldsymbol{x})$, because, by Proposition 2.2.2, $\tilde{\mathcal{P}}_{\boldsymbol{f},\mathscr{T}}\left(\boldsymbol{x},\tilde{\phi}_1^*,\tilde{\psi}_1^*\right) = \mathcal{V}(\boldsymbol{x})$ and $\tilde{\mathcal{P}}_{\boldsymbol{f},\mathscr{T}}\left(\boldsymbol{x},\tilde{\phi}_2^*,\tilde{\psi}_2^*\right) = \mathcal{V}(\boldsymbol{x})$.

Choosing $\tilde{\phi} = \tilde{\phi}_2^*$ in (2.16) and $\tilde{\psi} = \tilde{\psi}_1^*$ in (2.17),

$$\tilde{\mathcal{P}}_{\boldsymbol{f},\mathscr{T}}\left(\boldsymbol{x},\tilde{\phi}_1^*,\tilde{\psi}\right) \leq \tilde{\mathcal{P}}_{\boldsymbol{f},\mathscr{T}}\left(\boldsymbol{x},\tilde{\phi}_1^*,\tilde{\psi}_1^*\right) \leq \tilde{\mathcal{P}}_{\boldsymbol{f},\mathscr{T}}\left(\boldsymbol{x},\tilde{\phi}_2^*,\tilde{\psi}_1^*\right)$$
$$\leq \tilde{\mathcal{P}}_{\boldsymbol{f},\mathscr{T}}\left(\boldsymbol{x},\tilde{\phi}_2^*,\tilde{\psi}_2^*\right) \leq \tilde{\mathcal{P}}_{\boldsymbol{f},\mathscr{T}}\left(\boldsymbol{x},\tilde{\phi},\tilde{\psi}_2^*\right) \quad \forall \boldsymbol{x} \in \mathbb{R}^n, \forall \tilde{\phi} \in \tilde{\Phi}, \forall \tilde{\psi} \in \tilde{\Psi}, \tag{2.19}$$

where $\tilde{\mathcal{P}}_{\boldsymbol{f},\mathscr{T}}\left(\boldsymbol{x},\tilde{\phi}_2^*,\tilde{\psi}_1^*\right) = \mathcal{V}(\boldsymbol{x})$, because, by Proposition 2.2.2, $\tilde{\mathcal{P}}_{\boldsymbol{f},\mathscr{T}}\left(\boldsymbol{x},\tilde{\phi}_1^*,\tilde{\psi}_1^*\right) = \mathcal{V}(\boldsymbol{x})$ and $\tilde{\mathcal{P}}_{\boldsymbol{f},\mathscr{T}}\left(\boldsymbol{x},\tilde{\phi}_2^*,\tilde{\psi}_2^*\right) = \mathcal{V}(\boldsymbol{x})$.

Consequently, (2.18) and (2.19) can be rewritten as

$$\tilde{\mathcal{P}}_{\boldsymbol{f},\mathscr{T}}\left(\boldsymbol{x},\tilde{\phi}_2^*,\tilde{\psi}\right) \leq \tilde{\mathcal{P}}_{\boldsymbol{f},\mathscr{T}}\left(\boldsymbol{x},\tilde{\phi}_2^*,\tilde{\psi}_1^*\right) \leq \tilde{\mathcal{P}}_{\boldsymbol{f},\mathscr{T}}\left(\boldsymbol{x},\tilde{\phi},\tilde{\psi}_1^*\right),$$

$$\tilde{\mathcal{P}}_{\boldsymbol{f},\mathscr{T}}\left(\boldsymbol{x},\tilde{\phi}_1^*,\tilde{\psi}\right) \leq \tilde{\mathcal{P}}_{\boldsymbol{f},\mathscr{T}}\left(\boldsymbol{x},\tilde{\phi}_1^*,\tilde{\psi}_2^*\right) \leq \tilde{\mathcal{P}}_{\boldsymbol{f},\mathscr{T}}\left(\boldsymbol{x},\tilde{\phi},\tilde{\psi}_2^*\right),$$

respectively. $\square$

Consequently, it makes sense for P to decide to adopt a saddle-point strategy, if it exists. Firstly, because as a security strategy it guarantees him an outcome that is at most equal to the evaluation of $\mathcal{V}$ at the initial state. Secondly, because the saddle inequalities verified by his saddle-point strategy guarantee him that he will not have reasons to regret his decision, once he knows the strategy adopted by his opponent. An analogous argument for the rationality of adopting a saddle-point strategy, applies for E.

For these reasons, the saddle-point strategies are also called *optimal* strategies. In accordance, a trajectory in the state space $\boldsymbol{x}^{\boldsymbol{f}}_{\boldsymbol{x_0},\tilde{\phi}^*,\tilde{\psi}^*} : [0,+\infty) \to \mathbb{R}^n$, that corresponds to a play $\left(\boldsymbol{x_0}, \tilde{\phi}^*, \tilde{\psi}^*\right)$ starting at $\boldsymbol{x_0} \in \mathbb{R}^n$ for which optimal strategies $\tilde{\phi}^* \in \tilde{\Phi}$ and $\tilde{\psi}^* \in \tilde{\Psi}$ have been adopted by both players, is called *optimal trajectory* or *optimal path.*

2.2.6. ϵ-saddle-points

As stated by Proposition 2.2.2, the existence of a saddle-point equilibrium of a game implies the existence of its VF. By contrast, the existence of the VF of a game, does not necessarily imply the existence of a (pure) saddle-point equilibrium; it, however, implies the existence of an ϵ-saddle-point defined as follows.

For a given $\epsilon \geq 0$, a pair $\left(\tilde{\phi}^{*\epsilon}, \tilde{\psi}^{*\epsilon}\right) \in \left(\tilde{\Phi}, \tilde{\Psi}\right)$ is called an ϵ-*saddle-point* if

$$\tilde{\mathcal{P}}_{\boldsymbol{f},\mathscr{T}}\left(\boldsymbol{x}, \tilde{\phi}^{*\epsilon}, \tilde{\psi}\right) - \epsilon \leq \tilde{\mathcal{P}}_{\boldsymbol{f},\mathscr{T}}\left(\boldsymbol{x}, \tilde{\phi}^{*\epsilon}, \tilde{\psi}^{*\epsilon}\right) \leq \tilde{\mathcal{P}}_{\boldsymbol{f},\mathscr{T}}\left(\boldsymbol{x}, \tilde{\phi}, \tilde{\psi}^{*\epsilon}\right) + \epsilon$$
$$\forall \boldsymbol{x} \in \mathbb{R}^n, \forall \tilde{\phi} \in \tilde{\Phi}, \ \forall \tilde{\psi} \in \tilde{\Psi}. \quad (2.20)$$

For the particular case $\epsilon = 0$, the pair $\left(\tilde{\phi}^{*\epsilon}, \tilde{\psi}^{*\epsilon}\right)$ is said to be simply a *saddle-point.*

The following result, transcribed literally from [59, Ch. 2], holds in connection with this relaxed version of the concept of equilibrium.

Theorem 2.2.1. *A two-player zero-sum (infinite) game has a finite value if, and only if, for every $\epsilon > 0$, an ϵ-saddle-point exists.*

Proof. See proof of Theorem 4.1 in [59, Ch. 4]. □

The word *infinite* between parentheses in the statement of Theorem 2.2.1 refers to the fact that at least one of the players is allowed to choose among an infinite number of strategies available to him. In the rare case in which both sets of strategies $\tilde{\Phi}$ and $\tilde{\Psi}$ were finite, the existence of a value would guarantee the existence of a *pure* saddle-point equilibrium, as it is shown in [59, Ch. 2] in the context of matrix games.

2.2.7. Criticism of the outlined theory

The problem with the just delineated approach to the central concepts of *strategy* and *value* is that "upper and lower value functions *a priori* depend on the admissible sets of strategies" $\left(\tilde{\Phi}, \tilde{\Psi}\right)$, as pointed out by Cardaliaguet in [58].

"In fact, with this definition of value function, the existence of a value is completely open." concludes Cardaliaguet before abandoning this approach.

Isaacs [49] already noticed this problem and heuristically dealt with it introducing K-*strategies* (the K due to Samuel Karlin for proposing them). The key point of this notion of strategy is that, by definition, the realization of a K-strategy is a piecewise constant function of time. For each player, the selection of the discontinuity instants is part of the act of choosing a K-strategy. Thereby, when both K-strategies are plugged into the SE, an obviously integrable differential equation arises which has an unique solution. The definition of value function proceeds by ranging the sup and inf operations over the player's classes of K-strategies. Isaacs explains, however, that "in general, the K-*strategies* will not yield optimal strategies but only ϵ-optimal strategies, that is, strategies that will attain within ϵ of the Value (this being done, it would seem, by increasing the fineness of the temporal subdivision)." [49].

Diverse approaches to the concept of strategy and value have been proposed since 1965, when Isaacs published [49]. For example, Friedman's theory (in which the game is approximated by a lower and an upper δ-approximation model) [63], the theory of minimax solutions [64], the theory of viscosity solutions [65], and the theory of viability [66]; are all possible, but quite different, approaches to build a mathematically rigorous pursuit-evasion game theory.

Despite the diversity of theoretical frameworks currently available, in this thesis just Isaacs' classical methods are used to obtain immediate practical results for the engineering problem at hands, postponing for future work a reformulation of the same problem in a modern theoretical framework. For instance, in [50], Bernhard's "second order servomechanism problem" is precisely formulated in terms of *VREK-strategies* [5] and the corresponding value function is obtained as a *viscosity solution* of the corresponding Hamilton-Jacobi-Isaacs equation. An analogous formulation of the power-electronics control problem that motivates this work in the same theoretical framework, would clearly enrich the results presented here. However, a pondered selection of one the aforementioned frameworks and its in-depth study are still pending duties.

2.3. An assumption about the pay-off functional

From the next section on, up to the end of this chapter, it is assumed that the PF of the prototype pursuit-evasion differential game (2.3) is of a particular form, namely the standard form (2.2), i.e., $\mathcal{P}_{\boldsymbol{f},\mathscr{T}} = \mathcal{P}^{\mathrm{std}}_{\boldsymbol{f},\mathscr{T}}$.

Why are PFs of the form $\mathcal{P}^{\mathrm{kind}}_{\boldsymbol{f},\mathscr{T}}$, $\mathcal{P}^{\mathrm{time}}_{\boldsymbol{f},\mathscr{T}}$, and $\mathcal{P}^{\mathrm{disto}}_{\boldsymbol{f},\mathscr{T}}$, left out of consideration? The reason for dropping games of kind is that they can always be turned into games of degree by reformulating them as games in time (with $\mathcal{P}^{\mathrm{time}}_{\boldsymbol{f},\mathscr{T}}$ as the PF instead of $\mathcal{P}^{\mathrm{kind}}_{\boldsymbol{f},\mathscr{T}}$). All that has to be done to view the reformulated game as game of kind is to make $\mathcal{P}^{\mathrm{time}}_{\boldsymbol{f},\mathscr{T}}(\boldsymbol{x_0},\boldsymbol{\phi},\boldsymbol{\psi}) < +\infty$ correspond to $\mathcal{P}^{\mathrm{kind}}_{\boldsymbol{f},\mathscr{T}}(\boldsymbol{x_0},\boldsymbol{\phi},\boldsymbol{\psi}) = -1$, and make $\mathcal{P}^{\mathrm{time}}_{\boldsymbol{f},\mathscr{T}}(\boldsymbol{x_0},\boldsymbol{\phi},\boldsymbol{\psi}) = +\infty$ correspond to $\mathcal{P}^{\mathrm{kind}}_{\boldsymbol{f},\mathscr{T}}(\boldsymbol{x_0},\boldsymbol{\phi},\boldsymbol{\psi}) = +1$, for any

---

[5]VREK for Varaiya, Roxin, Elliott and Kalton.

play $(\boldsymbol{x_0}, \boldsymbol{\phi}, \boldsymbol{\psi})$. In turn, as already noted, every game in time can be put as a game with standard PF (with unitary running cost and null terminal cost).

A different treatment is needed for a game in distance, since a PF of the form $\mathcal{P}_{\boldsymbol{f}, \mathcal{T}}^{\mathrm{dist_o}}$ can not in general be reduced to the standard form. In [67], the VF of a generic game in distance (as defined in Subsection 2.1.1) is obtained as the viscosity upper-envelope solution of a variational inequality, under quite general assumptions. However, having avoided the theory of viscosity solutions, Isaacs' hint [49, Ch. 2, Sec. 4] to deal with PFs of the form

$$\inf_{t \geq 0} K\left(\boldsymbol{x}_{\boldsymbol{x_0}, \boldsymbol{\phi}, \boldsymbol{\psi}}^{\boldsymbol{f}}(t)\right)$$

(where $K : \mathbb{R}^n \to \mathbb{R}$ is any smooth function) is resorted next.

Let $\mathscr{E}_{\boldsymbol{1}}$ be that subset of $\mathbb{R}^n$ in which E can cause $K(\boldsymbol{x})$ to increase whatever P may do, i.e.,

$$\mathscr{E}_{\boldsymbol{1}} \triangleq \left\{ \boldsymbol{x} \in \mathbb{R}^n \; : \; \sup_{\boldsymbol{\psi} \in \boldsymbol{\Psi}} \inf_{\boldsymbol{\phi} \in \boldsymbol{\Phi}} \langle \boldsymbol{\nabla} K(\boldsymbol{x}), \boldsymbol{f}(\boldsymbol{x}, \boldsymbol{\phi}, \boldsymbol{\psi}) \rangle > 0 \right\}$$

where $\langle \cdot, \cdot \rangle$ is the standard inner product on $\mathbb{R}^n$. Let $\mathscr{T}_{\boldsymbol{1}} \triangleq \mathbb{R}^n \setminus \mathscr{E}_{\boldsymbol{1}}$. It is clear that if an infimum of K occurs at all during the course of a play, against optimal opposition from E, it will occur on $\partial \mathscr{T}_{\boldsymbol{1}}$. Thus, matters are reduced to a game with (terminal) pay-off of the form (2.2) with $G \equiv 0$ and $H \equiv K$. Nevertheless, Isaacs warns that in certain cases P can achieve the optimal outcome only by causing the state to enter $\mathscr{E}_{\boldsymbol{1}}$ and leave it again. In such cases the proposed reduction presents some difficulties and must be handled with care.

A concrete exemplification of how to apply these ideas is deferred to Chapter 5, where the game in distance associated to the buck converter control problem is addressed. This game in distance is actually the main object of study of this thesis.

2.4. The solution concept

This and the following two sections of this chapter closely follow [60, Ch. 3-4].

The *solution* of the prototypical pursuit-evasion differential game $\mathcal{G}$, specified by (2.3), is a quintet $\left(\mathscr{E}_{\mathbf{C}}, \mathscr{E}_{\mathbf{E}}, \tilde{\boldsymbol{\phi}}^*, \tilde{\boldsymbol{\psi}}^*, \mathcal{V} \right)$ characterized by the following properties.

1. The sets $\mathscr{E}_{\mathbf{C}}$ and $\mathscr{E}_{\mathbf{E}}$, called the *capture set (CS)* and the *escape set (ES)*, respectively, are subsets of $\mathscr{E}$, the playing set (PS); such that $\mathscr{E}_{\mathbf{C}} \cap \mathscr{E}_{\mathbf{E}} = \emptyset$ and $\mathscr{E}_{\mathbf{C}} \cup \mathscr{E}_{\mathbf{E}} = \mathscr{E}$.

2. The strategy $\tilde{\boldsymbol{\phi}}^* \in \tilde{\Phi}$ is a strategy that, if adopted by P, guarantees him capture of E for every play $\left(\boldsymbol{x}, \tilde{\boldsymbol{\phi}}^*, \tilde{\boldsymbol{\psi}} \right)$ with $\boldsymbol{x} \in \mathscr{E}_{\mathbf{C}}$ and $\tilde{\boldsymbol{\psi}} \in \tilde{\Psi}$. The strategy $\tilde{\boldsymbol{\psi}}^* \in \tilde{\Psi}$ is a strategy that, if adopted by E, guarantees him escape from P for every play $\left(\boldsymbol{x}, \tilde{\boldsymbol{\phi}}, \tilde{\boldsymbol{\psi}}^* \right)$ with $\boldsymbol{x} \in \mathscr{E}_{\mathbf{E}}$ and $\tilde{\boldsymbol{\phi}} \in \tilde{\Phi}$.

3. The VF of the game $\mathcal{V}$ is required to verify

$$\begin{cases} \mathcal{V}(\boldsymbol{x}) = \tilde{\mathcal{P}}_{\boldsymbol{f},\mathscr{T}}\left(\boldsymbol{x}, \tilde{\phi}^*, \tilde{\psi}^*\right), \\ \tilde{\mathcal{P}}_{\boldsymbol{f},\mathscr{T}}\left(\boldsymbol{x}, \tilde{\phi}^*, \tilde{\psi}\right) \leq \tilde{\mathcal{P}}_{\boldsymbol{f},\mathscr{T}}\left(\boldsymbol{x}, \tilde{\phi}^*, \tilde{\psi}^*\right) \leq \tilde{\mathcal{P}}_{\boldsymbol{f},\mathscr{T}}\left(\boldsymbol{x}, \tilde{\phi}, \tilde{\psi}^*\right) \quad \forall \tilde{\phi} \in \tilde{\Phi},\ \forall \tilde{\psi} \in \tilde{\Psi}, \end{cases} \tag{2.21}$$

for every $\boldsymbol{x} \in \mathscr{E}_{\mathbf{C}}$. In accordance with the general set-up delineated in Section 2.2, the inequalities in (2.21) are called *saddle inequalities*.

2.5. Semipermeable surfaces

Let $\mathscr{S} = \{\boldsymbol{x} \in \mathbb{R}^n\ :\ D(\boldsymbol{x}) = 0\}$ be a *smooth* surface given implicitly by a scalar function D. Let $\hat{\boldsymbol{n}}(\boldsymbol{x}) \triangleq \frac{\boldsymbol{\nabla} D(\boldsymbol{x})}{\|\boldsymbol{\nabla} D(\boldsymbol{x})\|}$ be the (unit) *normal* vector to $\mathscr{S}$ at $\boldsymbol{x} \in \mathscr{S}$ (a generic point of the surface). The point $\boldsymbol{x}$ can be approached from the two sides of the surface $\mathscr{S}$.

Without loss of generality, assume that E prefers the side of the surface that corresponds to the *positive* sense of the normal $\hat{\boldsymbol{n}}(\boldsymbol{x})$ and, accordingly, call this side the *E-side*. Similarly, assume that P prefers the side of the surface that corresponds to the *negative* sense of the normal $\hat{\boldsymbol{n}}(\boldsymbol{x})$ and, accordingly, call this side the *P-side*.

Suppose that, at $\boldsymbol{x} \in \mathscr{S}$, there exists a control $\boldsymbol{\psi}^* \in \boldsymbol{\Psi}$ such that

$$\langle \boldsymbol{f}(\boldsymbol{x}, \boldsymbol{\phi}, \boldsymbol{\psi}^*), \hat{\boldsymbol{n}}(\boldsymbol{x}) \rangle \geq 0 \quad \forall \boldsymbol{\phi} \in \boldsymbol{\Phi}.$$

Likewise, suppose that, at $\boldsymbol{x} \in \mathscr{S}$, there exists a control $\boldsymbol{\phi}^* \in \boldsymbol{\Phi}$ such that

$$\langle \boldsymbol{f}(\boldsymbol{x}, \boldsymbol{\phi}^*, \boldsymbol{\psi}), \hat{\boldsymbol{n}}(\boldsymbol{x}) \rangle \leq 0 \quad \forall \boldsymbol{\psi} \in \boldsymbol{\Psi}.$$

If both $\boldsymbol{\psi}^*$ and $\boldsymbol{\phi}^*$ exist, then

$$\langle \boldsymbol{f}(\boldsymbol{x}, \boldsymbol{\phi}^*, \boldsymbol{\psi}), \hat{\boldsymbol{n}}(\boldsymbol{x}) \rangle \leq \langle \boldsymbol{f}(\boldsymbol{x}, \boldsymbol{\phi}^*, \boldsymbol{\psi}^*), \hat{\boldsymbol{n}}(\boldsymbol{x}) \rangle = 0 \leq \langle \boldsymbol{f}(\boldsymbol{x}, \boldsymbol{\phi}, \boldsymbol{\psi}^*), \hat{\boldsymbol{n}}(\boldsymbol{x}) \rangle$$
$$\forall \boldsymbol{\phi} \in \boldsymbol{\Phi},\ \forall \boldsymbol{\psi} \in \boldsymbol{\Psi} \quad (2.22)$$

which means that, obviating tangential penetrations of $\mathscr{S}$, at $\boldsymbol{x} \in \mathscr{S}$, P can prevent the state from crossing the surface $\mathscr{S}$ from the P-side to the E-side, and, at the same time, E can prevent the state from crossing the surface $\mathscr{S}$ from the E-side to the P-side. In this case, the surface $\mathscr{S}$ is said to be *semi-permeable at* $\boldsymbol{x}$.

If, for every $\boldsymbol{x} \in \mathscr{S}$, controls $\boldsymbol{\psi}^*$ and $\boldsymbol{\phi}^*$ exist (not necessarily unique) such that (2.22) holds, the surface $\mathscr{S}$ is said to be a *semipermeable surface*. If, at each $\boldsymbol{x} \in \mathscr{S}$ one of such controls is picked out for each player, candidate strategies $\boldsymbol{x} \mapsto \tilde{\phi}^*(\boldsymbol{x})$ and $\boldsymbol{x} \mapsto \tilde{\psi}^*(\boldsymbol{x})$ can be constructed and plugged into the SE to yield

$$\frac{\mathrm{d}\boldsymbol{x}}{\mathrm{d}t} = \boldsymbol{f}\left(\boldsymbol{x}, \tilde{\phi}^*(\boldsymbol{x}), \tilde{\psi}^*(\boldsymbol{x})\right). \tag{2.23}$$

If, for every initial condition $\boldsymbol{x_0} \in \mathscr{S}$, an unique solution of (2.23) exists through $\boldsymbol{x_0}$, then the trajectories initiating in $\mathscr{S}$ do not leave the surface for $t > 0$.

Observe that if $\mathscr{S}$ is a semipermeable surface for a pursuit-evasion game, then it is also a semipermeable surface for every other pursuit-evasion game with the same SE, i.e., the property of semipermeability does not depend on the TS nor on the PF.

Observe also that if the condition

$$\inf_{\boldsymbol{\phi}\in\boldsymbol{\Phi}} \sup_{\boldsymbol{\psi}\in\boldsymbol{\Psi}} \langle \boldsymbol{p}, \boldsymbol{f}\left(\boldsymbol{x}, \boldsymbol{\phi}, \boldsymbol{\psi}\right)\rangle = \sup_{\boldsymbol{\psi}\in\boldsymbol{\Psi}} \inf_{\boldsymbol{\phi}\in\boldsymbol{\Phi}} \langle \boldsymbol{p}, \boldsymbol{f}\left(\boldsymbol{x}, \boldsymbol{\phi}, \boldsymbol{\psi}\right)\rangle \quad \forall\,(\boldsymbol{x},\boldsymbol{p})\in\mathbb{R}^n\times\mathbb{R}^n \quad (2.24)$$

holds, then (2.22) is equivalent to

$$\inf_{\boldsymbol{\phi}\in\boldsymbol{\Phi}} \sup_{\boldsymbol{\psi}\in\boldsymbol{\Psi}} \langle \hat{\boldsymbol{n}}\left(\boldsymbol{x}\right), \boldsymbol{f}\left(\boldsymbol{x}, \boldsymbol{\phi}, \boldsymbol{\psi}\right)\rangle = 0. \quad (2.25)$$

Indeed, reasoning along the same lines as in Proposition 2.2.2, it can be proved that the existence of $\boldsymbol{\phi}^*\in\boldsymbol{\Phi}$ and $\boldsymbol{\psi}^*\in\boldsymbol{\Psi}$ satisfying (2.22) implies

$$\inf_{\boldsymbol{\phi}\in\boldsymbol{\Phi}} \sup_{\boldsymbol{\psi}\in\boldsymbol{\Psi}} \langle \hat{\boldsymbol{n}}\left(\boldsymbol{x}\right), \boldsymbol{f}\left(\boldsymbol{x}, \boldsymbol{\phi}, \boldsymbol{\psi}\right)\rangle = \sup_{\boldsymbol{\psi}\in\boldsymbol{\Psi}} \inf_{\boldsymbol{\phi}\in\boldsymbol{\Phi}} \langle \hat{\boldsymbol{n}}\left(\boldsymbol{x}\right), \boldsymbol{f}\left(\boldsymbol{x}, \boldsymbol{\phi}, \boldsymbol{\psi}\right)\rangle = 0.$$

Reciprocally, if (2.24) holds, reasoning along the same lines as in Subsection 2.2.4, the saddle inequalities (2.22) can be derived from (2.25). Note, however, that the inf-sup problem in the left-hand side (LHS) of (2.25) is defined on a pair of (non-empty compact and convex) *control sets* while the inf-sup problem involved in Subsection 2.2.4 and Subsection 2.2.5 is defined on a pair of *admissible sets of strategies*.

2.6. Isaacs' equation

The concept of *solution* of a pursuit-evasion game, as introduced in Section 2.4 for the prototype game $\mathcal{G}$ (formulated by (2.3)) with standard PF, relies on *global* objects like *plays*. For example, every play $\left(\boldsymbol{x}, \tilde{\boldsymbol{\phi}}^*, \tilde{\boldsymbol{\psi}}\right)$ with $\boldsymbol{x}\in\mathbb{R}^n$ and $\tilde{\boldsymbol{\psi}}\in\tilde{\Psi}$, must be considered to evaluate the cost function of the game in normal form $\tilde{\mathcal{P}}_{\boldsymbol{f},\mathscr{T}}$ and check if the leftmost of the saddle inequalities in (2.21) is satisfied or not. These objects are not easy to work with in order to construct *candidate solutions* for the game.

The VF, if it exists, may be continuously differentiable in some *regions*[6] of $\mathbb{R}^n$. Such regions are called *regular* regions and the points belonging to them are called *regular* points. The Isaacs' equation, which can be regarded as an extension of *Hamilton–Jacobi–Bellman equation* from the theory of optimal control to the theory of pursuit-evasion games, is a *necessary* condition that the VF has to satisfy at every regular point of the state space. Isaacs [49] introduces this equation in two different ways: analytically invoking his "tenet of transition"[7], and geometrically heavily relaying on the concept of semipermeable surface.

Isaacs also devised a verification theorem that, under certain *sufficient* conditions, allows to affirm that a certain *candidate solution* is actually a solution of the

---

[6]A *region* of $\mathbb{R}^n$ is a non-empty, connected, and *open*, subset of $\mathbb{R}^n$

[7]Which turns out to be a two-player extension of Bellman's "principle of optimality".

game in the global sense of section Section 2.4. The enunciation of this theorem is stated Section 2.7.

2.6.1. The Hamiltonian function

The *Hamiltonian function* [60] of the game is a function $\mathcal{H} : \mathbb{R}^n \times \mathbb{R}^n \times \boldsymbol{\Phi} \times \boldsymbol{\Psi} \to \mathbb{R}$ defined by

$$\mathcal{H}\left(\boldsymbol{x}, \boldsymbol{p}, \boldsymbol{\phi}, \boldsymbol{\psi}\right) \triangleq \left\langle \boldsymbol{p}, \boldsymbol{f}\left(\boldsymbol{x}, \boldsymbol{\phi}, \boldsymbol{\psi}\right) \right\rangle + G\left(\boldsymbol{x}, \boldsymbol{\phi}, \boldsymbol{\psi}\right),$$

for every $\left(\boldsymbol{x}, \boldsymbol{p}, \boldsymbol{\phi}, \boldsymbol{\psi}\right) \in \mathbb{R}^n \times \mathbb{R}^n \times \boldsymbol{\Phi} \times \boldsymbol{\Psi}$, where $G : \mathbb{R}^n \times \boldsymbol{\Phi} \times \boldsymbol{\Psi} \to \mathbb{R}$ is the running cost function as introduced in (2.2).

2.6.2. The Isaacs' condition

The *Isaacs' condition* [59] is said to hold if

$$\inf_{\boldsymbol{\phi} \in \boldsymbol{\Phi}} \sup_{\boldsymbol{\psi} \in \boldsymbol{\Psi}} \mathcal{H}\left(\boldsymbol{x}, \boldsymbol{p}, \boldsymbol{\phi}, \boldsymbol{\psi}\right) = \sup_{\boldsymbol{\psi} \in \boldsymbol{\Psi}} \inf_{\boldsymbol{\phi} \in \boldsymbol{\Phi}} \mathcal{H}\left(\boldsymbol{x}, \boldsymbol{p}, \boldsymbol{\phi}, \boldsymbol{\psi}\right) \quad \forall \left(\boldsymbol{x}, \boldsymbol{p}\right) \in \mathbb{R}^n \times \mathbb{R}^n. \quad (2.26)$$

From now on, it is assumed that the Isaacs' condition hold for the prototype pursuit-evasion differential game $\boldsymbol{\mathcal{G}}$ formulated by (2.3).

2.6.3. Isaacs' equation

If the value function $\mathcal{V}$ exists, it must satisfy *Isaacs' equation*:

$$\inf_{\boldsymbol{\phi} \in \boldsymbol{\Phi}} \sup_{\boldsymbol{\psi} \in \boldsymbol{\Psi}} \mathcal{H}\left(\boldsymbol{x}, \boldsymbol{\nabla}\mathcal{V}\left(\boldsymbol{x}\right), \boldsymbol{\phi}, \boldsymbol{\psi}\right) = \sup_{\boldsymbol{\psi} \in \boldsymbol{\Psi}} \inf_{\boldsymbol{\phi} \in \boldsymbol{\Phi}} \mathcal{H}\left(\boldsymbol{x}, \boldsymbol{\nabla}\mathcal{V}\left(\boldsymbol{x}\right), \boldsymbol{\phi}, \boldsymbol{\psi}\right) = 0, \quad (2.27)$$

in regular regions (i.e., where $\mathcal{V}$ is finite and continuously differentiable). In (2.27) it is made explicit that the order of the inf and sup operations is irrelevant as a consequence of the assumption that the Isaacs' condition (2.26) holds[8]. Note, however, that the order of the inf and sup may be crucial at points where $\mathcal{V}$ is *not* continuously differentiable, as emphasized in [59]. An alternative formulation of Isaacs' equation in terms of *local saddle inequalities* is the following:

$$\mathcal{H}\left(\boldsymbol{x}, \boldsymbol{\nabla}\mathcal{V}\left(\boldsymbol{x}\right), \boldsymbol{\phi}^*, \boldsymbol{\psi}\right) \leq \mathcal{H}\left(\boldsymbol{x}, \boldsymbol{\nabla}\mathcal{V}\left(\boldsymbol{x}\right), \boldsymbol{\phi}^*, \boldsymbol{\psi}^*\right) = 0 \leq \mathcal{H}\left(\boldsymbol{x}, \boldsymbol{\nabla}\mathcal{V}\left(\boldsymbol{x}\right), \boldsymbol{\phi}, \boldsymbol{\psi}^*\right)$$
$$\forall \boldsymbol{\phi} \in \boldsymbol{\Phi},\ \forall \boldsymbol{\psi} \in \boldsymbol{\Psi}, \quad (2.28)$$

which is equivalent to

$$\inf_{\boldsymbol{\phi} \in \boldsymbol{\Phi}} \sup_{\boldsymbol{\psi} \in \boldsymbol{\Psi}} \mathcal{H}\left(\boldsymbol{x}, \boldsymbol{\nabla}\mathcal{V}\left(\boldsymbol{x}\right), \boldsymbol{\phi}, \boldsymbol{\psi}\right) = 0, \quad (2.29)$$

under the assumption that Isaac's condition (2.26) holds.

---

[8]Sometimes the interchangeability of inf and sup operations as stated in (2.27) is also referred to as *Isaacs' condition*, even though (2.27) is a weaker condition than (2.26).

Following Isaacs' terminology, both (2.28) and (2.29) will be indistinctly referred to as Isaacs' main equation in its first form (ME$_1$). It may be regarded as

$$\inf_{\phi \in \Phi} \sup_{\psi \in \Psi} \mathcal{H}\left(\boldsymbol{x}, \boldsymbol{p}, \boldsymbol{\phi}, \boldsymbol{\psi}\right) = 0, \tag{2.30}$$

where $\boldsymbol{p}$ subsumes $\boldsymbol{\nabla}\mathcal{V}\left(\boldsymbol{x}\right)$ as a particular case. If *functions* $\left(\boldsymbol{x}, \boldsymbol{p}\right) \mapsto \boldsymbol{\phi}^{*}\left(\boldsymbol{x}, \boldsymbol{p}\right)$ and $\left(\boldsymbol{x}, \boldsymbol{p}\right) \mapsto \boldsymbol{\psi}^{*}\left(\boldsymbol{x}, \boldsymbol{p}\right)$ can be judiciously defined such that $\left(\boldsymbol{\phi}^{*}\left(\boldsymbol{x}, \boldsymbol{p}\right), \boldsymbol{\psi}^{*}\left(\boldsymbol{x}, \boldsymbol{p}\right)\right)$ solves the $\left(\boldsymbol{x}, \boldsymbol{p}\right)$-parametrized family of inf-sup point-wise problems stated in the LHS of (2.30), then (2.29) may be rewritten as Isaacs' main equation in its second form (ME$_2$):

$$\mathcal{H}\left(\boldsymbol{x}, \boldsymbol{\nabla}\mathcal{V}\left(\boldsymbol{x}\right), \boldsymbol{\phi}^{*}\left(\boldsymbol{x}, \boldsymbol{\nabla}\mathcal{V}\left(\boldsymbol{x}\right)\right), \boldsymbol{\psi}^{*}\left(\boldsymbol{x}, \boldsymbol{\nabla}\mathcal{V}\left(\boldsymbol{x}\right)\right)\right) = 0. \tag{2.31}$$

The following two sub-subsections are intended to provide a geometric derivation of Isaacs' equation.

2.6.3.1. Reduction to a game with terminal pay-off functional

The PF of the prototype pursuit-evasion differential game $\boldsymbol{\mathcal{G}}$, specified by (2.3), was previously assumed to be of the *standard* form (2.2). However, if found convenient, it can be reduced to a game with *terminal* PF by means of a well known state space augmentation technique.

The augmented game $\boldsymbol{\mathcal{G}_{aug}}$ is conceived from $\boldsymbol{\mathcal{G}}$ as follows:

$$\boldsymbol{\mathcal{G}_{aug}} \begin{cases} \text{SE}: & \frac{\mathrm{d}\boldsymbol{x_{aug}}}{\mathrm{d}t}\left(t\right) = \frac{\mathrm{d}}{\mathrm{d}t}\begin{bmatrix} \boldsymbol{x} \\ x_{n+1} \end{bmatrix}\left(t\right) = \begin{bmatrix} \boldsymbol{f}\left(\boldsymbol{x}\left(t\right), \boldsymbol{\phi}\left(t\right), \boldsymbol{\psi}\left(t\right)\right) \\ G\left(\boldsymbol{x}\left(t\right), \boldsymbol{\phi}\left(t\right), \boldsymbol{\psi}\left(t\right)\right) \end{bmatrix}, \\ \text{TS}: & \boldsymbol{\mathcal{T}_{aug}} \triangleq \boldsymbol{\mathcal{T}} \times \mathbb{R} \subset \mathbb{R}^{n+1}, \\ \text{PF}: & \left(\begin{bmatrix} \boldsymbol{x_0} \\ 0 \end{bmatrix}, \boldsymbol{\phi}, \boldsymbol{\psi}\right) \mapsto \mathcal{P}_{\boldsymbol{f}, \boldsymbol{\mathcal{T}}}^{\mathrm{aug}}\left(\begin{bmatrix} \boldsymbol{x_0} \\ 0 \end{bmatrix}, \boldsymbol{\phi}, \boldsymbol{\psi}\right), \end{cases} \tag{2.32}$$

where $\mathcal{P}_{\boldsymbol{f}, \boldsymbol{\mathcal{T}}}^{\mathrm{aug}}$ is a PF *of the form* (2.2), with G_{aug} and H_{aug} in place of G and H, respectively, being $G_{\mathrm{aug}} \equiv 0$ and H_{aug} defined such that

$$H_{\mathrm{aug}}\left(\begin{bmatrix} \boldsymbol{x} \\ x_{n+1} \end{bmatrix}\right) = H\left(\boldsymbol{x}\right) + x_{n+1}$$

for every $\begin{bmatrix} \boldsymbol{x} \\ x_{n+1} \end{bmatrix} \in \mathbb{R}^{n+1}$.

2.6.3.2. Geometrical derivation of Isaacs' equation

Assume, without loss of generality, that $\boldsymbol{\mathcal{G}}$ is such that it has terminal PF, i.e., its running cost G is identically null. Accordingly, $\mathcal{V}\left(\boldsymbol{x}\right)$ equals the outcome $H\left(\boldsymbol{x}_{\boldsymbol{x}, \tilde{\phi}^{*}, \tilde{\psi}^{*}}^{\boldsymbol{f}}\left(t_{\mathrm{cap}}\right)\right)$ that results from optimal play by both players, for a play whose initial state is $\boldsymbol{x} \in \boldsymbol{\mathcal{E}_C} \subset \boldsymbol{\mathcal{E}}$ and that terminates at capture time $t_{\mathrm{cap}} = \tilde{\mathcal{P}}_{\boldsymbol{f}, \boldsymbol{\mathcal{T}}}^{\mathrm{time}}\left(\boldsymbol{x_0}, \tilde{\phi}^{*}, \tilde{\psi}^{*}\right)$ (finite because $\boldsymbol{x} \in \boldsymbol{\mathcal{E}_C}$).

Suppose that in a region of $\boldsymbol{\mathcal{E}_C}$, the value function $\mathcal{V}$ is continuously differentiable and non-constant. Every level surface of $\mathcal{V}$ in such region must be necessarily

semipermeable; otherwise, either P could not prevent the state from going into the side of the surface with higher value of $\mathcal{V}$, or E could not prevent the state from going into the side of the surface with lower value of $\mathcal{V}$. More precisely:

$$\langle \boldsymbol{f}\left(\boldsymbol{x}, \boldsymbol{\phi}^*, \boldsymbol{\psi}\right), \boldsymbol{\nabla}\mathcal{V}\left(\boldsymbol{x}\right)\rangle \leq \langle \boldsymbol{f}\left(\boldsymbol{x}, \boldsymbol{\phi}^*, \boldsymbol{\psi}^*\right), \boldsymbol{\nabla}\mathcal{V}\left(\boldsymbol{x}\right)\rangle = 0 \leq \langle \boldsymbol{f}\left(\boldsymbol{x}, \boldsymbol{\phi}, \boldsymbol{\psi}^*\right), \boldsymbol{\nabla}\mathcal{V}\left(\boldsymbol{x}\right)\rangle$$
$$\forall \boldsymbol{\phi} \in \boldsymbol{\Phi}, \ \forall \boldsymbol{\psi} \in \boldsymbol{\Psi}.$$

Assuming that (2.24) holds, which is Isaacs' condition (2.26) for the (current) $G \equiv 0$ case, the above semipermeability condition can be equivalently stated as

$$\inf_{\boldsymbol{\phi} \in \boldsymbol{\Phi}} \sup_{\boldsymbol{\psi} \in \boldsymbol{\Psi}} \langle \boldsymbol{\nabla}\mathcal{V}\left(\boldsymbol{x}\right), \boldsymbol{f}\left(\boldsymbol{x}, \boldsymbol{\phi}, \boldsymbol{\psi}\right)\rangle = 0. \tag{2.33}$$

as it was argued at the end of (2.5). This last expression is Isaacs' main equation in its first form for the the terminal PF case.

If it was the case that the terminal PF considered here had resulted from augmenting the state space of a n-dimensional game with a standard PF given by (2.2), then (2.33) could be rewritten as

$$\inf_{\boldsymbol{\phi} \in \boldsymbol{\Phi}} \sup_{\boldsymbol{\psi} \in \boldsymbol{\Psi}} \left\{\langle \boldsymbol{\nabla}\mathcal{V}\left(\boldsymbol{x}\right), \boldsymbol{f}\left(\boldsymbol{x}, \boldsymbol{\phi}, \boldsymbol{\psi}\right)\rangle + G\left(\boldsymbol{x}, \boldsymbol{\phi}, \boldsymbol{\psi}\right)\right\} = 0. \tag{2.34}$$

in terms of the functions $\mathcal{V}$ and $\boldsymbol{f}$ related to the original game, because the *distinct* functions $\mathcal{V}$ and $\boldsymbol{f}$ related to the augmented game would satisfy $\frac{\partial \mathcal{V}}{\partial x_{n+1}} = 1$ and $\langle \hat{\boldsymbol{e}}_{\boldsymbol{n+1}}, \boldsymbol{f}\left(\boldsymbol{x}, \boldsymbol{\phi}, \boldsymbol{\psi}\right)\rangle = G\left(\boldsymbol{x}, \boldsymbol{\phi}, \boldsymbol{\psi}\right)$, where $\hat{\boldsymbol{e}}_{\boldsymbol{n+1}}$ is the $(n+1)$-th canonical unit vector of $\mathbb{R}^{n+1}$. The equation (2.34) is Isaacs' main equation in its first form for the standard PF case.

2.7. The verification theorem

The following verification theorem (VT) (adapted from [59, Ch. 8]) states *sufficient* conditions for the existence of a VF and a pair of saddle-point strategies. It links the solution of a pursuit-evasion differential game with the solution of a partial differential equation (Isaacs' equation) with appropriate boundary conditions.

Theorem 2.7.1 (Verification theorem)**.** *Consider the pursuit-evasion differential game $\mathcal{G}$, specified in (2.3) by means of a SE, a TS, and a PF, $\mathcal{P}_{\boldsymbol{f}, \mathscr{T}} = \mathcal{P}^{\mathrm{std}}_{\boldsymbol{f}, \mathscr{T}}$, of the standard form (2.2) with running cost G and terminal cost H. Assume that the Isaacs' condition (2.26) holds for $\mathcal{G}$.*

If a candidate solution $\left(\mathscr{E}_{\mathbf{C}}, \mathscr{E}_{\mathbf{E}}, \tilde{\phi}^*, \tilde{\psi}^*, \mathcal{V}\right)$ for $\mathcal{G}$ is known to satisfy only the first two properties that a valid solution must verify (see Section 2.4), and

1. *$\mathcal{V}$ is continuously differentiable and satisfies (2.28) in $\mathscr{E}_{\mathbf{C}}$,*

2. *$\mathcal{V}\left(\boldsymbol{x}\right) = H\left(\boldsymbol{x}\right)$ on $\partial\mathscr{T}$, and*

3. $\tilde{\phi}^*$ and $\tilde{\psi}^*$ are of the form $(t, \boldsymbol{x}) \mapsto \tilde{\phi}^* (t, \boldsymbol{x}) = \phi^* (\boldsymbol{x}, \boldsymbol{\nabla} \mathcal{V} (\boldsymbol{x}))$ and $(t, \boldsymbol{x}) \mapsto \tilde{\psi}^* (t, \boldsymbol{x}) = \psi^* (\boldsymbol{x}, \boldsymbol{\nabla} \mathcal{V} (\boldsymbol{x}))$, respectively, where $(\boldsymbol{x}, \boldsymbol{p}) \mapsto \phi^* (\boldsymbol{x}, \boldsymbol{p})$ and $(\boldsymbol{x}, \boldsymbol{p}) \mapsto \psi^* (\boldsymbol{x}, \boldsymbol{p})$ are two (not necessarily unique functions) such that $(\phi^* (\boldsymbol{x}, \boldsymbol{p}), \psi^* (\boldsymbol{x}, \boldsymbol{p}))$ solves the LHS of (2.30);

then, $\left(\mathscr{E}_{\mathbf{C}}, \mathscr{E}_{\mathbf{E}}, \tilde{\phi}^*, \tilde{\psi}^*, \mathcal{V} \right)$ is a valid solution of $\boldsymbol{\mathcal{G}}$.

Proof. The third and last property of a valid solution of $\boldsymbol{\mathcal{G}}$ needs to be proved, i.e.,

$$
\begin{cases}
\mathcal{V} (\boldsymbol{x_0}) = \tilde{\mathcal{P}}_{\boldsymbol{f}, \mathscr{T}} \left(\boldsymbol{x_0}, \tilde{\phi}^*, \tilde{\psi}^* \right), \\
\tilde{\mathcal{P}}_{\boldsymbol{f}, \mathscr{T}} \left(\boldsymbol{x_0}, \tilde{\phi}^*, \tilde{\psi} \right) \leq \tilde{\mathcal{P}}_{\boldsymbol{f}, \mathscr{T}} \left(\boldsymbol{x_0}, \tilde{\phi}^*, \tilde{\psi}^* \right) \leq \tilde{\mathcal{P}}_{\boldsymbol{f}, \mathscr{T}} \left(\boldsymbol{x_0}, \tilde{\phi}, \tilde{\psi}^* \right) & \forall \tilde{\phi} \in \tilde{\Phi}, \; \forall \tilde{\psi} \in \tilde{\Psi},
\end{cases}
\tag{2.35}
$$

for every $\boldsymbol{x_0} \in \mathscr{E}_{\mathbf{C}}$.

Consider a play $\left(\boldsymbol{x_0}, \tilde{\phi}^*, \tilde{\psi} \right)$ whose initial state $\boldsymbol{x_0}$ belongs to $\mathscr{E}_{\mathbf{C}}$. Such a a play must necessary terminate at some $t_{\mathrm{cap}} > 0$. Integrating the Hamiltonian function along the play's trajectory $t \mapsto \boldsymbol{x} (t) = \boldsymbol{x}^{\boldsymbol{f}}_{\boldsymbol{x_0}, \tilde{\phi}^*, \tilde{\psi}} (t)$:

$$
\int_0^{t_{\mathrm{cap}}} \mathcal{H} \left(\boldsymbol{x} (t), \boldsymbol{\nabla} \mathcal{V} (\boldsymbol{x} (t)), \tilde{\phi}^* (t, \boldsymbol{x} (t)), \tilde{\psi} (t, \boldsymbol{x} (t)) \right) \, \mathrm{d}t
$$

$$
= \int_0^{t_{\mathrm{cap}}} \left\langle \boldsymbol{\nabla} \mathcal{V} (\boldsymbol{x} (t)), \boldsymbol{f} \left(\boldsymbol{x} (t), \tilde{\phi}^* (t, \boldsymbol{x} (t)), \tilde{\psi} (t, \boldsymbol{x} (t)) \right) \right\rangle \, \mathrm{d}t
$$

$$
+ \int_0^{t_{\mathrm{cap}}} G \left(\boldsymbol{x} (t), \tilde{\phi}^* (t, \boldsymbol{x} (t)), \tilde{\psi} (t, \boldsymbol{x} (t)) \right) \, \mathrm{d}t
$$

$$
= \int_0^{t_{\mathrm{cap}}} \left\langle \boldsymbol{\nabla} \mathcal{V} (\boldsymbol{x} (t)), \frac{\mathrm{d}}{\mathrm{d}t} \boldsymbol{x} (t) \right\rangle \, \mathrm{d}t + \int_0^{t_{\mathrm{cap}}} G \left(\boldsymbol{x} (t), \tilde{\phi}^* (t, \boldsymbol{x} (t)), \tilde{\psi} (t, \boldsymbol{x} (t)) \right) \, \mathrm{d}t
$$

$$
= \underbrace{\mathcal{V} (\boldsymbol{x} (t_{\mathrm{cap}}))}_{H(\boldsymbol{x}(t_{\mathrm{cap}}))} - \mathcal{V} (\boldsymbol{x_0}) + \int_0^{t_{\mathrm{cap}}} G \left(\boldsymbol{x} (t), \tilde{\phi}^* (t, \boldsymbol{x} (t)), \tilde{\psi} (t, \boldsymbol{x} (t)) \right) \, \mathrm{d}t
$$

$$
= \tilde{\mathcal{P}}_{\boldsymbol{f}, \mathscr{T}} \left(\boldsymbol{x_0}, \tilde{\phi}^*, \tilde{\psi} \right) - \mathcal{V} (\boldsymbol{x_0}) \leq 0 \quad (2.36)
$$

where the last inequality results from recognizing that

$$
\int_0^{t_{\mathrm{cap}}} \mathcal{H} \left(\boldsymbol{x} (t), \boldsymbol{\nabla} \mathcal{V} (\boldsymbol{x} (t)), \tilde{\phi}^* (t, \boldsymbol{x} (t)), \tilde{\psi} (t, \boldsymbol{x} (t)) \right) \, \mathrm{d}t \leq 0
$$

because $\mathcal{H} \left(\boldsymbol{x} (t), \boldsymbol{\nabla} \mathcal{V} (\boldsymbol{x} (t)), \underbrace{\tilde{\phi}^* (t, \boldsymbol{x} (t))}_{\phi^*(\boldsymbol{x}(t), \boldsymbol{\nabla}\mathcal{V}(\boldsymbol{x}(t)))}, \tilde{\psi} (t, \boldsymbol{x} (t)) \right) \leq 0$ for $t \in (0, t_{\mathrm{cap}})$.

Now consider a play $\left(\boldsymbol{x_0}, \tilde{\phi}, \tilde{\psi}^* \right)$ whose initial state $\boldsymbol{x_0}$ belongs to $\mathscr{E}_{\mathbf{C}}$. Similarly, if $\left(\boldsymbol{x_0}, \tilde{\phi}, \tilde{\psi}^* \right)$ terminates at some (other) $t_{\mathrm{cap}} > 0$:

$$
\int_0^{t_{\mathrm{cap}}} \mathcal{H} \left(\boldsymbol{x} (t), \boldsymbol{\nabla} \mathcal{V} (\boldsymbol{x} (t)), \tilde{\phi} (t, \boldsymbol{x} (t)), \tilde{\psi}^* (t, \boldsymbol{x} (t)) \right) \, \mathrm{d}t
$$

$$
= \tilde{\mathcal{P}}_{\boldsymbol{f}, \mathscr{T}} \left(\boldsymbol{x_0}, \tilde{\phi}, \tilde{\psi}^* \right) - \mathcal{V} (\boldsymbol{x_0}) \geq 0. \quad (2.37)
$$

From inequalities (2.36) and (2.37), follows (2.35). For plays $\left(\boldsymbol{x_0}, \tilde{\phi}, \tilde{\psi}^* \right)$ that do not terminate, (2.35) still holds because $\tilde{\mathcal{P}}_{\boldsymbol{f}, \mathscr{T}} \left(\boldsymbol{x_0}, \tilde{\phi}, \tilde{\psi}^* \right) = +\infty$. $\qquad \square$

2.8. The retrograde path equations

The Theorem 2.7.1 presupposes that $\mathcal{V}$ is known. However, such function is not known right at the outset. All that is known is that, in regular regions, it must satisfy Isaacs' equation, which reads as ME_2, i.e.,

$$\mathcal{H}\left(\boldsymbol{x}, \boldsymbol{\nabla}\mathcal{V}\left(\boldsymbol{x}\right), \boldsymbol{\phi}^*\left(\boldsymbol{x}, \boldsymbol{\nabla}\mathcal{V}\left(\boldsymbol{x}\right)\right), \boldsymbol{\psi}^*\left(\boldsymbol{x}, \boldsymbol{\nabla}\mathcal{V}\left(\boldsymbol{x}\right)\right)\right) = 0, \qquad (2.38)$$

after a concrete selection of functions $\left(\boldsymbol{x}, \boldsymbol{p}\right) \mapsto \boldsymbol{\phi}^*\left(\boldsymbol{x}, \boldsymbol{p}\right)$ and $\left(\boldsymbol{x}, \boldsymbol{p}\right) \mapsto \boldsymbol{\psi}^*\left(\boldsymbol{x}, \boldsymbol{p}\right)$, such that $\left(\boldsymbol{\phi}^*\left(\boldsymbol{x}, \boldsymbol{p}\right), \boldsymbol{\psi}^*\left(\boldsymbol{x}, \boldsymbol{p}\right)\right)$ solves the LHS of (2.30), has been done. Recalling the definition of the Hamiltonian function, the partial differential equation (2.38), which has $\mathcal{V}$ as unknown, can be rewritten as

$$\left\langle \boldsymbol{\nabla}\mathcal{V}\left(\boldsymbol{x}\right), \boldsymbol{f}\left(\boldsymbol{x}, \boldsymbol{\phi}^*\left(\boldsymbol{x}, \boldsymbol{\nabla}\mathcal{V}\left(\boldsymbol{x}\right)\right), \boldsymbol{\psi}^*\left(\boldsymbol{x}, \boldsymbol{\nabla}\mathcal{V}\left(\boldsymbol{x}\right)\right)\right)\right\rangle$$
$$+ G\left(\boldsymbol{x}, \boldsymbol{\phi}^*\left(\boldsymbol{x}, \boldsymbol{\nabla}\mathcal{V}\left(\boldsymbol{x}\right)\right), \boldsymbol{\psi}^*\left(\boldsymbol{x}, \boldsymbol{\nabla}\mathcal{V}\left(\boldsymbol{x}\right)\right)\right) = 0,$$

or equivalently, alleviating notation, as $\left\langle \boldsymbol{\nabla}\mathcal{V}, \boldsymbol{f}\right\rangle + G = 0$. Developing the inner product:

$$\sum_{i=1}^{n} \frac{\partial \mathcal{V}}{\partial x_i} f_i + G = 0. \qquad (2.39)$$

Suppose that $\mathcal{V}$ is twice continuously differentiable. Differentiation of (2.39) with respect to x_k, i.e., the k-th component of $\boldsymbol{x}$, yields

$$\sum_{i=1}^{n} \frac{\partial \mathcal{V}}{\partial x_k \partial x_i} f_i + \sum_{i=1}^{n} \frac{\partial \mathcal{V}}{\partial x_i} \left(\frac{\partial f_i}{\partial x_k} + \sum_{j=1}^{m_P} \frac{\partial f_i}{\partial \phi_j} \frac{\partial \phi_j^*}{\partial x_k} + \sum_{j=1}^{m_E} \frac{\partial f_i}{\partial \psi_j} \frac{\partial \psi_j^*}{\partial x_k} \right)$$
$$+ \frac{\partial G}{\partial x_k} + \sum_{j=1}^{m_P} \frac{\partial G}{\partial \phi_j} \frac{\partial \phi_j^*}{\partial x_k} + \sum_{j=1}^{m_E} \frac{\partial G}{\partial \psi_j} \frac{\partial \psi_j^*}{\partial x_k} = 0,$$

where $\frac{\partial \mathcal{V}}{\partial x_k \partial x_i} = \frac{\partial \mathcal{V}}{\partial x_i \partial x_k}$. Rearranging terms:

$$\sum_{i=1}^{n} \frac{\partial \mathcal{V}}{\partial x_i \partial x_k} f_i + \sum_{i=1}^{n} \frac{\partial \mathcal{V}}{\partial x_i} \frac{\partial f_i}{\partial x_k} + \frac{\partial G}{\partial x_k}$$
$$+ \sum_{j=1}^{m_P} \frac{\partial}{\partial \phi_j} \left(\sum_{i=1}^{n} \frac{\partial \mathcal{V}}{\partial x_i} f_i + G \right) \frac{\partial \phi_j^*}{\partial x_k} + \sum_{j=1}^{m_E} \frac{\partial}{\partial \psi_j} \left(\sum_{i=1}^{n} \frac{\partial \mathcal{V}}{\partial x_i} f_i + G \right) \frac{\partial \psi_j^*}{\partial x_k} = 0.$$

Each ϕ_j is bounded. The infimizing ϕ_j^* occurs either in the interior of the bounding interval or at one of its endpoints. In the former case, the factor $\frac{\partial}{\partial \phi_j}\left(\sum_{i=1}^{n} \frac{\partial \mathcal{V}}{\partial x_i} f_i + G\right)$ is zero; in the later case, the factor $\frac{\partial \phi_j^*}{\partial x_k}$ is zero. In any case, the product of these two factors is zero, and, accordingly, $\sum_{j=1}^{m_P} \frac{\partial}{\partial \phi_j}\left(\sum_{i=1}^{n} \frac{\partial \mathcal{V}}{\partial x_i} f_i + G\right) \frac{\partial \phi_j^*}{\partial x_k} = 0$. Analogously, $\sum_{j=1}^{m_E} \frac{\partial}{\partial \psi_j}\left(\sum_{i=1}^{n} \frac{\partial \mathcal{V}}{\partial x_i} f_i + G\right) \frac{\partial \psi_j^*}{\partial x_k} = 0$. Moreover, $\sum_{i=1}^{n} \frac{\partial \mathcal{V}}{\partial x_i \partial x_k} f_i = \frac{\partial}{\partial x_i}\left(\frac{\partial \mathcal{V}}{\partial x_k}\right)\dot{x}_i^* = \frac{\mathrm{d}}{\mathrm{d}t}\left(\frac{\partial \mathcal{V}}{\partial x_k}\right)$, being $t \mapsto \boldsymbol{x}^*\left(t\right)$ the state space trajectory that results from P and E playing strategies $\left(t, \boldsymbol{x}\right) \mapsto \tilde{\boldsymbol{\phi}}^*\left(t, \boldsymbol{x}\right) = \boldsymbol{\phi}^*\left(\boldsymbol{x}, \boldsymbol{\nabla}\mathcal{V}\left(\boldsymbol{x}\right)\right)$ and

$(t, \boldsymbol{x}) \mapsto \tilde{\boldsymbol{\psi}}^* (t, \boldsymbol{x}) = \boldsymbol{\psi}^* (\boldsymbol{x}, \boldsymbol{\nabla} \mathcal{V} (\boldsymbol{x}))$, respectively. Hence, for each $k \in \{1, \ldots, n\}$:

$$\frac{\mathrm{d}}{\mathrm{d}t} \left(\frac{\partial \mathcal{V}}{\partial x_k} \right) = - \left(\sum_{i=1}^{n} \frac{\partial \mathcal{V}}{\partial x_i} \frac{\partial f_i}{\partial x_k} + \frac{\partial G}{\partial x_k} \right),$$

where the opposite of the formal derivative of the Hamiltonian function with respect to x_k is recognized in the RHS. Accordingly, introducing the *co-state* $\boldsymbol{p}(t) \triangleq \boldsymbol{\nabla} \mathcal{V} (\boldsymbol{x}^* (t))$, the n scalar equations (2.8) can be expressed in a single vectorial equation as:

$$\frac{\mathrm{d}\boldsymbol{p}}{\mathrm{d}t} (t) = -\frac{\partial \mathcal{H}}{\partial \boldsymbol{x}} (\boldsymbol{x}^* (t), \boldsymbol{p}(t), \boldsymbol{\phi}^* (\boldsymbol{x}^* (t), \boldsymbol{p}(t)), \boldsymbol{\psi}^* (\boldsymbol{x}^* (t), \boldsymbol{p}(t))). \qquad (2.40)$$

In addition, $\boldsymbol{x}^*$ must satisfy the vectorial SE

$$\frac{\mathrm{d}\boldsymbol{x}^*}{\mathrm{d}t} (t) = \boldsymbol{f} (\boldsymbol{x}^* (t), \boldsymbol{\phi}^* (\boldsymbol{x}^* (t), \boldsymbol{p}(t)), \boldsymbol{\psi}^* (\boldsymbol{x}^* (t), \boldsymbol{p}(t))),$$

which can be written as

$$\frac{\mathrm{d}\boldsymbol{x}^*}{\mathrm{d}t} (t) = \frac{\partial \mathcal{H}}{\partial \boldsymbol{p}} (\boldsymbol{x}^* (t), \boldsymbol{p}(t), \boldsymbol{\phi}^* (\boldsymbol{x}^* (t), \boldsymbol{p}(t)), \boldsymbol{\psi}^* (\boldsymbol{x}^* (t), \boldsymbol{p}(t))). \qquad (2.41)$$

The *Hamiltonian system*

$$\begin{cases} \frac{\mathrm{d}\boldsymbol{x}^*}{\mathrm{d}t} (t) = \frac{\partial \mathcal{H}}{\partial \boldsymbol{p}} (\boldsymbol{x}^* (t), \boldsymbol{p}(t), \boldsymbol{\phi}^* (\boldsymbol{x}^* (t), \boldsymbol{p}(t)), \boldsymbol{\psi}^* (\boldsymbol{x}^* (t), \boldsymbol{p}(t))) \\ \frac{\mathrm{d}\boldsymbol{p}}{\mathrm{d}t} (t) = -\frac{\partial \mathcal{H}}{\partial \boldsymbol{x}} (\boldsymbol{x}^* (t), \boldsymbol{p}(t), \boldsymbol{\phi}^* (\boldsymbol{x}^* (t), \boldsymbol{p}(t)), \boldsymbol{\psi}^* (\boldsymbol{x}^* (t), \boldsymbol{p}(t))) \end{cases}, \qquad (2.42)$$

that results from collecting (2.40) and (2.41), is a system of $2n$ scalar ordinary differential equations, also called *characteristic equations* of ME_2. Solutions of ME_2 can be built from the integral curves of (2.42). This solution method, which reduces the solution of a partial differential equation to the solution of a system of ordinary differential equations is known as the *method of characteristics.*

The solutions of the Hamiltonian system are usually found integrating (2.42) backwards in time from $\partial \mathcal{T}$ into $\mathcal{E}$, because all that is known at the outset of the game problem in connection with the boundary conditions of ME_2 is that every terminating optimal play must terminate on $\partial \mathcal{T}$ where $\mathcal{V} = H$. For this reason, it is convenient to introduce *retrogressive time* τ such that $\frac{\mathrm{d}\tau}{\mathrm{d}t} = -1$, and to rewrite (2.42) as

$$\begin{cases} \frac{\mathrm{d}\boldsymbol{x}^*}{\mathrm{d}\tau} (\tau) = -\frac{\partial \mathcal{H}}{\partial \boldsymbol{p}} (\boldsymbol{x}^* (\tau), \boldsymbol{p}(\tau), \boldsymbol{\phi}^* (\boldsymbol{x}^* (\tau), \boldsymbol{p}(\tau)), \boldsymbol{\psi}^* (\boldsymbol{x}^* (\tau), \boldsymbol{p}(\tau))) \\ \frac{\mathrm{d}\boldsymbol{p}}{\mathrm{d}\tau} (\tau) = \frac{\partial \mathcal{H}}{\partial \boldsymbol{x}} (\boldsymbol{x}^* (\tau), \boldsymbol{p}(\tau), \boldsymbol{\phi}^* (\boldsymbol{x}^* (\tau), \boldsymbol{p}(\tau)), \boldsymbol{\psi}^* (\boldsymbol{x}^* (\tau), \boldsymbol{p}(\tau))) \end{cases}. \qquad (2.43)$$

The $2n$ scalar ordinary differential equations subsumed in (2.43) are called retrograde path equations (RPE) by Isaacs. Each *a priori* feasible initial condition $(\boldsymbol{x}|_{\tau=0}, \boldsymbol{p}|_{\tau=0})$ (in retrogressive sense) needed for carrying out an integration of (2.43) is obtained from

$$\begin{cases} \boldsymbol{x}^*|_{\tau=0} \in \mathcal{UP}, \\ \boldsymbol{p}|_{\tau=0} = \boldsymbol{\nabla} \mathcal{V} (\boldsymbol{x}^*|_{\tau=0}), \\ \mathcal{V} (\boldsymbol{x}) = H (\boldsymbol{x}) \text{ and } \mathcal{H} (\boldsymbol{x}, \boldsymbol{\nabla} \mathcal{V} (\boldsymbol{x}), \boldsymbol{\phi}^* (\boldsymbol{x}, \boldsymbol{\nabla} \mathcal{V} (\boldsymbol{x})), \boldsymbol{\psi}^* (\boldsymbol{x}, \boldsymbol{\nabla} \mathcal{V} (\boldsymbol{x}))) = 0 \text{ if } \boldsymbol{x} \in \partial \mathcal{T}, \end{cases}$$

where $\mathscr{U}\mathscr{P}$, the usable part (UP) of $\partial\mathscr{T}$, is the set defined as

$$\mathscr{U}\mathscr{P} \triangleq \left\{ \boldsymbol{x} \in \partial\mathscr{T} \; : \; \inf_{\boldsymbol{\phi}\in\boldsymbol{\Phi}} \sup_{\boldsymbol{\psi}\in\boldsymbol{\Psi}} \langle \hat{\boldsymbol{n}}\left(\boldsymbol{x}\right), \boldsymbol{f}\left(\boldsymbol{x}, \boldsymbol{\phi}, \boldsymbol{\psi}\right) \rangle \leq 0 \right\},$$

being $\hat{\boldsymbol{n}}\left(\boldsymbol{x}\right)$ the normal vector to $\partial\mathscr{T}$, at $\boldsymbol{x} \in \partial\mathscr{T}$. Observe that at points of $\mathscr{E}$ very near $\partial\mathscr{T} \setminus \mathscr{U}\mathscr{P}$, E can prevent immediate termination, because he can force the state velocity vector to point back into $\mathscr{E}$, regardless P's control action. For this reason, only $\mathscr{U}\mathscr{P} \subset \partial\mathscr{T}$ is usable to fix initial conditions (in the retrogressive sense) to integrate the RPE.

2.9.   Singular surfaces

When solving pursuit-evasion games it is almost always assumed that the PS is divided into a number of mutually disjoint regions, where the VF is continuously differentiable. The boundaries of these regions are called singular surfaces. In [59] a slightly more general definition is adopted: a *singular surface* is a manifold on which

1. the values taken by the equilibrium strategies are not uniquely determined from Isaacs' equation, or

2. the VF is not continuously differentiable, or

3. the VF function is discontinuous.

Unfortunately, the integration of the RPE fails when reaching a singular surface and, trickily, in most cases the failure is not evident. An exception, is the *switching surface* (also called *transition surface*) which clearly manifests itself during the integration of the RPE by occurrence of the first condition enumerated above. Other known singular surfaces across which the VF is continuous are: the *dispersal*, *equivocal*, *universal*, *focal*, and *switching envelope* surfaces. A singular surface across which the VF is discontinuous is the *barrier*. If the ES is not empty, the semipermeable surface that separates the CS from the ES, in the PS, is a barrier.

Optimal trajectories, do not cross barriers but may cross or follow, other singular surfaces. In this respect, it must be noted that, the initial conditions for the integration of the RPE may be specified at any other surface other than the UP of the boundary of the TS, if an appropriate *junction condition* for the VF can be established therein. Accordingly, even if the state space is partitioned by singular surfaces, the method of characteristics is still the fundamental tool for solving the game in the regular regions. *Generalized characteristics* of first order partial differential equations were developed by Melikyan [68] to extend the method of characteristics so as to overcome the presence of singular surfaces, but the investigation of this generalization is much beyond the scope of this work.

"In conclusion, the crucial problem in the construction of the value function is to locate the singular surfaces, but hitherto this problem

has not been solved in a systematic way. On the other hand, once a particular V has been constructed, which is continuously differentiable in each of a finite number of mutually disjoint regions of the state space, some conditions (known as "junction conditions") exist to check whether the V(x) obtained is really the value function or not. Since these conditions are not yet very well understood, we do not treat them here; but for some discussion on this topic the reader is referred to Bernhard (1977)." (T. Başar and G. J. Olsder 1999, 447–448 [59])

The reference cited by Başar and Olsder is reference [61].

2.10. Concluding remarks

Pursuit-evasion differential games are models of common dynamic conflicts between two players that evolve in continuous time, such as actual pursuit of an evader by a pursuer. Within these conflicts, each player would ask himself how to make the best possible decisions taking into account that his opponent is doing the same. Although quite natural, these questions are not trivial. The theory of differential games was born out of trying to answer these questions, motivated by military combat problems.

Fusing game theory and optimal control theory, Rufus Isaacs, the acknowledged father of differential game theory, setted up the basis of a new theory which transcends both, with applications in many areas including engineering, economics, military, biology, and social science.

Differential game theory is actually subsumed in what is mainly called theory of dynamic games. Nevertheless, it is still a subject of active research often carried out within involved mathematical frameworks which differ significantly among each other, both in origin and nature.

In this chapter, just the most fundamental concepts of the classical part of differential game theory, known as Isaacs-Breakwell theory, have been introduced. These early theoretical developments are highly problem-solving oriented, and therefore, both accessible and appropriate for the practical goal of this thesis, which is devoted to a concrete game problem.

However, the treatment of singular surfaces, a major part or Isaacs-Breakwell theory which is far from trivial and fundamental to the solution method, has not been presented here. Instead, the emphasis of this chapter was put on making precise, as far as possible, what is meant by solving a pursuit-evasion game, a notion without with the rest of this work would be meaningless.

Esta página ha sido intencionalmente dejada en blanco.

Chapter 3

Model of the buck converter controller's struggle against disturbances

In this chapter the buck converter control problem, introduced in Chapter 1, is precisely formulated in the realm of differential game theory.

In Section 3.1 the selected model for the buck converter is presented and the requirements on its controller are stated. The control problem is next framed, in Section 3.2, as a pursuit-evasion differential *conflict*, in the technical sense given to the word in Chapter 2, i.e., as the common structure underneath two related pursuit-evasion *games* that may be naturally considered in connection with the control problem: a game *in distance* and a game *in time*. All the assumptions made about the conflict are listed throughout Sections 3.1–3.3.

The rest of the chapter is devoted to the canonization of the conflict and to the furnishing of a geometric interpretation of it.

3.1. The buck converter control problem

Consider the circuit diagram depicted in Figure 3.1. It is a simplified model of a DC-DC *buck* converter, also called *step-down* converter. A series arrangement of an ideal inductor L and an ideal resistance R_L, and a series arrangement of
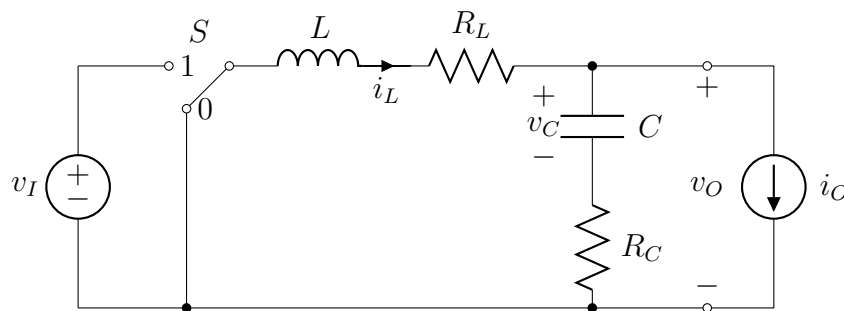
Figure 3.1: Circuit diagram of the buck converter model.

Figure 3.2: Equivalent circuit diagram of the buck converter model.

an ideal capacitor C and an ideal resistance R_C, model the converter's inductor and capacitor, respectively. Resistances R_L and R_C, are usually referred to as the parasitic equivalent series resistance (ESR) of the converter's inductor and capacitor, respectively. Naturally, it is assumed that

$$L, R_L, C, R_C > 0. \tag{A1}$$

An input voltage v_I is supplied to the converter in order to step it down to a lower voltage, suitable to feed a load which is modelled by an ideal current source i_O.

A switch S is driven by the automatic controller in charge of the converter's output voltage control. Let σ be a switching action variable such that: $\sigma = 0$ if the switch is in position 0, while $\sigma = 1$ if the switch is in position 1 (see labelled positions in Figure 3.1). Despite its discrete nature, for convenience of analysis, σ is allowed to take values in a continuum between its only two realistic values, i.e.,

$$\sigma \in [0, 1]. \tag{3.1}$$

As will be seen, this carries no loss of applicability of the results reported in the following chapters. In Figure 3.2, an equivalent circuit diagram is shown, where the joint effect of the input voltage and the switching action is modelled by a an ideal voltage source $v_I \sigma$.

The input signals i_O and v_I are considered as unpredictable *disturbances* such that

$$I_{O\min} \leq i_O \leq I_{O\max}, \tag{3.2}$$

$$V_{I\min} \leq v_I \leq V_{I\max}, \tag{3.3}$$

where the constant bounds, $I_{O\min}$, $I_{O\max}$, $V_{I\min}$ and $V_{I\max}$, are supposed to satisfy

$$0 \leq I_{O\min} < I_{O\max}, \tag{A2}$$

$$0 < V_{I\min} \leq V_{I\max}. \tag{A3}$$

Let i_L be the current through the inductor and let v_C be the voltage across the capacitor. Applying circuit element laws and Kirchhoff's circuit laws, it readily

follows that the dynamics of the converter is ruled by

$$L\frac{\mathrm{d}i_L}{\mathrm{d}t} = \sigma v_I - R_L i_L - v_C - R_C\left(i_L - i_O\right), \tag{3.4}$$

$$C\frac{\mathrm{d}v_C}{\mathrm{d}t} = i_L - i_O, \tag{3.5}$$

where t denotes time. The output voltage of the converter v_O, supplied to the load, is

$$v_O \triangleq R_C\left(i_L - i_O\right) + v_C. \tag{3.6}$$

Let $\hat{\boldsymbol{e}}_1 \triangleq \begin{bmatrix}1 & 0\end{bmatrix}^\top$ and $\hat{\boldsymbol{e}}_2 \triangleq \begin{bmatrix}0 & 1\end{bmatrix}^\top$ denote the canonical unit vectors of $\mathbb{R}^2$. Choosing $\boldsymbol{y} \triangleq i_L\hat{\boldsymbol{e}}_1 + v_C\hat{\boldsymbol{e}}_2$ as the state variable, σ and $\boldsymbol{v} \triangleq i_O\hat{\boldsymbol{e}}_1 + v_I\hat{\boldsymbol{e}}_2$ as the input variables, and v_O as the output variable, Equations (3.4), (3.5) and (3.6) can be rewritten as the following *state space representation* for the converter's model:

$$\frac{\mathrm{d}\boldsymbol{y}}{\mathrm{d}t} = \boldsymbol{A}'\boldsymbol{y} + \boldsymbol{B}'\boldsymbol{S}\left(\sigma\right)\boldsymbol{v}, \tag{3.7}$$

$$v_O = \boldsymbol{l}^\top\boldsymbol{y} + \left(\hat{\boldsymbol{e}}_2 - \boldsymbol{l}\right)^\top\boldsymbol{v},$$

where

$$\boldsymbol{A}' \triangleq \begin{bmatrix} -\frac{R_L+R_C}{L} & -\frac{1}{L} \\ \frac{1}{C} & 0 \end{bmatrix}, \quad \boldsymbol{B}' \triangleq \begin{bmatrix} \frac{R_C}{L} & \frac{1}{L} \\ -\frac{1}{C} & 0 \end{bmatrix}, \quad \text{and} \quad \boldsymbol{l} \triangleq \begin{bmatrix} R_C \\ 1 \end{bmatrix} \tag{3.8}$$

are constant matrices, while

$$\boldsymbol{S}\left(\sigma\right) = \begin{bmatrix} 1 & 0 \\ 0 & \sigma \end{bmatrix}$$

depends on σ.

The output voltage is required to closely track a reference voltage v_R defined by

$$v_R \triangleq V_{LL0} - R_{LL}i_O, \tag{3.9}$$

where V_{LL0} and R_{LL} are constant parameters of a given *load line* specification such that

$$V_{LL0} > 0, \quad R_{LL} \geq 0. \tag{A4}$$

The *(tracking) error e* is defined as

$$e \triangleq v_R - v_O = V_{LL0} - \boldsymbol{l}^\top\boldsymbol{y} + \left(R_C - R_{LL}\right)i_O.$$

The maximum permissible departure from perfect tracking is established by a given error tolerance E, such that

$$E > 0, \tag{A5}$$

by means of the following requirement: $|e| < E$, which is equivalent to

$$v_R - E < v_O < v_R + E. \tag{3.10}$$

In (3.10), the left inequality prevents against under-voltage across the load, whereas the right inequality prevents against over-voltage across the load. Accordingly, the
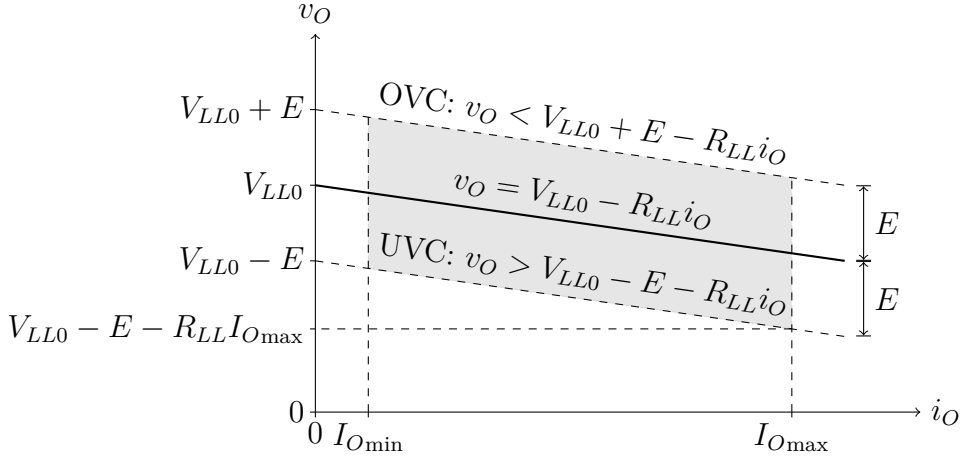
Figure 3.3: The output voltage of the converter v_O, is required to remain within a $\pm E$-tolerance band of a reference load line specification (given by parameters $V_{LL0} > 0$ and $R_{LL} \geq 0$) for every load current i_O, in the loading range ($0 \leq I_{O\min} \leq i_O \leq I_{O\max} > 0$). The upper boundary of the tolerance band corresponds to an over-voltage constraint (OVC) and its lower boundary corresponds to an under-voltage constraint (UVC). It is assumed that $V_{LL0} - E - R_{LL}I_{O\max} > 0$.

left one will be referred to as the under-voltage constraint (UVC) and the right one will be referred to as the over-voltage constraint (OVC). In terms of $\boldsymbol{y}$ and i_O, the requirement (3.10) can be restated as

$$ - E \underset{\text{OVC}}{<} \underbrace{V_{LL0} - \boldsymbol{l}^\top \boldsymbol{y} + (R_C - R_{LL})\, i_O}_{e} \underset{\text{UVC}}{<} E, \tag{3.11} $$

for every instant of time. Loosely stated, the control problem consists of finding a control law for σ capable of fulfilling (3.11) for every $t \geq 0$, under arbitrary changes in i_O and v_I, constrained by (3.2) and (3.3). In the following section, this statement is made precise by describing the control problem as a pursuit-evasion conflict in the realm of differential game theory.

It is assumed that

$$ V_{LL0} - E - R_{LL}I_{O\max} > 0, \tag{A6} $$

so that, even at maximum load current, the lower bound for the required output voltage is still positive (see Figure 3.3). Note that if the requirement (3.10) is fulfilled, the electrical power flows from the converter to the load (because $v_O i_O \geq 0$) and becomes zero if and only if $i_O = 0$ (because $v_O > 0$).

3.2. The buck converter control problem as a pursuit-evasion conflict

The buck converter is supposed to be operated by two *players*: a "malicious" agent, which will be referred to as the pursuer (P), who controls input $\boldsymbol{v}$; and a

3.2. The buck converter control problem as a pursuit-evasion conflict

"benevolent" automatic controller, which will be referred to as the evader (E), who controls input σ.

Both control signals, $\boldsymbol{v}$ and σ, are assumed to be bounded (as already stated by (3.1), (3.2) and (3.3)) but not necessarily continuous; in fact, they are assumed to be *piecewise continuous* functions of time. In this set up, for every $\boldsymbol{y_0} \in \mathbb{R}^2$, every piecewise continuous function $\boldsymbol{v} : [0, +\infty) \to [I_{O\min}, I_{O\max}] \times [V_{I\min}, V_{I\max}]$ and every piecewise continuous function $\sigma : [0, +\infty) \to [0, 1]$; the non-homogeneous linear ordinary differential equation (3.7), has an unique *continuous* solution $\boldsymbol{y_{y_0, v, \sigma}} : [0, +\infty) \to \mathbb{R}^2$, such that $\boldsymbol{y_{y_0, v, \sigma}}(0) = \boldsymbol{y_0}$, given by

$$\boldsymbol{y_{y_0, v, \sigma}}(t) = \mathrm{e}^{\boldsymbol{A}' t} \boldsymbol{y_0} + \int_0^t \mathrm{e}^{\boldsymbol{A}'(t-s)} \boldsymbol{B}' \boldsymbol{S}(\sigma(s)) \boldsymbol{v}(s) \, \mathrm{d}s$$

(see, for instance, [69]). Therefore, in (3.11), the term $\boldsymbol{l}^\top \boldsymbol{y}$ is a continuous function of time, while the term $(R_C - R_{LL}) i_O$ may be a discontinuous function of time if $R_C \neq R_{LL}$. The point is that whereas $\boldsymbol{l}^\top \boldsymbol{y}$ can not change instantaneously, the error e can, if the *resistance mismatch R_M* defined as

$$R_M \triangleq R_C - R_{LL},$$

is not equal to zero. It makes sense, then, to define the *(instantaneous) worst-case error at state $\boldsymbol{y} \in \mathbb{R}^2$* as

$$\mathrm{e}^{\mathrm{wc}}(\boldsymbol{y}) \triangleq V_{LL0} - \boldsymbol{l}^\top \boldsymbol{y} + R_M \, \mathrm{i}_\mathrm{O}^{\mathrm{wc}}(\boldsymbol{y}) \tag{3.12}$$

where $\mathrm{i}_\mathrm{O}^{\mathrm{wc}}(\boldsymbol{y})$, is a not necessarily unique *(instantaneous) worst-case load at state $\boldsymbol{y}$*, such that

$$\mathrm{i}_\mathrm{O}^{\mathrm{wc}}(\boldsymbol{y}) \in \underset{i_O \in [I_{O\min}, I_{O\max}]}{\arg\max} \left| V_{LL0} - \boldsymbol{l}^\top \boldsymbol{y} + R_M i_O \right|. \tag{3.13}$$

In accordance, the *(instantaneous) worst-case output voltage at state $\boldsymbol{y}$* is defined as:

$$\mathrm{v}_\mathrm{O}^{\mathrm{wc}}(\boldsymbol{y}) \triangleq v_R - \mathrm{e}^{\mathrm{wc}}(\boldsymbol{y}). \tag{3.14}$$

Since E wants to ensure (3.11) for every $t \geq 0$, whatever P does, he must keep the state in the set

$$\mathscr{E}' \triangleq \left\{ \boldsymbol{y} \in \mathbb{R}^2 \; : \; -E \underset{\mathrm{ROVC}}{<} \mathrm{e}^{\mathrm{wc}}(\boldsymbol{y}) \underset{\mathrm{RUVC}}{<} E \right\},$$

where ROVC and RUVC are acronym labels for robust over-voltage constraint and robust under-voltage constraint, respectively. The set $\mathscr{E}'$ is called the playing set (PS). It is the set where E wants the state to remain in. Its complement,

$$\mathscr{T}' \triangleq \mathbb{R}^2 \setminus \mathscr{E}', \tag{3.15}$$

is called the target set (TS). It is the set where P wants the state to reach.

3.2.1. Geometric characterization of the playing set

Define V and D by

$$V \triangleq V_{LL0} + R_M \frac{I_{O\min} + I_{O\max}}{2}, \quad D \triangleq E - |R_M| \frac{I_{O\max} - I_{O\min}}{2},$$

and let $\mathrm{sgn}^+ : \mathbb{R} \to \{-1, 1\}$ be a variation of the sign function defined by

$$\mathrm{sgn}^+(x) \triangleq \begin{cases} 1 & \text{if } x \geq 0, \\ -1 & \text{if } x < 0. \end{cases}$$

Proposition 3.2.1. *For every state $\boldsymbol{y} \in \mathbb{R}^2$, the worst-case error at $\boldsymbol{y}$ is*

$$\mathrm{e}^{\mathrm{wc}}(\boldsymbol{y}) = \left(\left| V - \boldsymbol{l}^\top \boldsymbol{y} \right| + |R_M| \frac{I_{O\max} - I_{O\min}}{2} \right) \mathrm{sgn}^+ \left(V - \boldsymbol{l}^\top \boldsymbol{y} \right), \qquad (3.16)$$

and a worst-case load at $\boldsymbol{y}$, that can instantaneously attain it, is

$$\mathrm{i}_O^{\mathrm{wc}}(\boldsymbol{y}) = \frac{I_{O\min} + I_{O\max}}{2} + \mathrm{sgn}^+(R_M)\,\mathrm{sgn}^+ \left(V - \boldsymbol{l}^\top \boldsymbol{y} \right) \frac{I_{O\max} - I_{O\min}}{2}. \qquad (3.17)$$

Proof. For every $\boldsymbol{y} \in \mathbb{R}^2$, $\mathrm{i}_O^{\mathrm{wc}}(\boldsymbol{y}) \in \arg\max_{i_O \in [I_{O\min}, I_{O\max}]} \left| V_{LL0} - \boldsymbol{l}^\top \boldsymbol{y} + R_M i_O \right|$. Parametrizing all possible arguments of this optimization problem as

$$i_O = \frac{I_{O\min} + I_{O\max}}{2} + \phi \frac{I_{O\max} - I_{O\min}}{2} \quad \text{with} \quad \phi \in [-1, 1],$$

it can be stated that

$$\mathrm{i}_O^{\mathrm{wc}}(\boldsymbol{y}) = \frac{I_{O\min} + I_{O\max}}{2} + \phi^* \frac{I_{O\max} - I_{O\min}}{2}, \qquad (3.18)$$

where $\phi^* \in \arg\max_{\phi \in [-1,1]} \left| R_M \frac{I_{O\max} - I_{O\min}}{2} \phi + V_{LL0} + R_M \frac{I_{O\min} + I_{O\max}}{2} - \boldsymbol{l}^\top \boldsymbol{y} \right|$. Recall that, by definition, $V = V_{LL0} + R_M \frac{I_{O\min} + I_{O\max}}{2}$, and, to simplify notation, define: $P \triangleq R_M \frac{I_{O\max} - I_{O\min}}{2}$ and $Q \triangleq V - \boldsymbol{l}^\top \boldsymbol{y}$. With the introduced notation,

$$\phi^* \in \arg\max_{\phi \in [-1,1]} |P\phi + Q|.$$

For every $m, n \in \mathbb{R}$, check that

$$\arg\max_{\phi \in [-1,1]} |m\phi + n| = \begin{cases} \{1\} & \text{if } mn > 0, \\ \{-1\} & \text{if } mn < 0, \\ \{-1, 1\} & \text{if } m \neq 0 \text{ and } n = 0, \\ [-1, 1] & \text{if } m = 0; \end{cases}$$

and note that $\mathrm{sgn}^+(m)\,\mathrm{sgn}^+(n) \in \arg\max_{\phi \in [-1,1]} |m\phi + n|$. Hence, in particular, setting $m = P$ and $n = Q$,

$$\phi^* = \mathrm{sgn}^+(P)\,\mathrm{sgn}^+(Q) = \mathrm{sgn}^+(R_M)\,\mathrm{sgn}^+ \left(V - \boldsymbol{l}^\top \boldsymbol{y} \right)$$

turns out to be an admissible maximizer to substitute in (3.18), in order to choose a value for $\mathrm{i}_O^{\mathrm{wc}}(\boldsymbol{y})$. The resulting value is

$$\mathrm{i}_O^{\mathrm{wc}}(\boldsymbol{y}) = \frac{I_{O\min} + I_{O\max}}{2} + \mathrm{sgn}^+(R_M)\,\mathrm{sgn}^+\left(V - \boldsymbol{l}^\top \boldsymbol{y}\right)\frac{I_{O\max} - I_{O\min}}{2}. \quad (3.19)$$

By definition, $\mathrm{e}^{\mathrm{wc}}(\boldsymbol{y}) = V_{LL0} - \boldsymbol{l}^\top \boldsymbol{y} + R_M\,\mathrm{i}_O^{\mathrm{wc}}(\boldsymbol{y})$. Substitution of (3.19) yields

$$\mathrm{e}^{\mathrm{wc}}(\boldsymbol{y}) =$$

$$V_{LL0} - \boldsymbol{l}^\top \boldsymbol{y} + R_M\left(\frac{I_{O\min} + I_{O\max}}{2} + \mathrm{sgn}^+(R_M)\,\mathrm{sgn}^+\left(V - \boldsymbol{l}^\top \boldsymbol{y}\right)\frac{I_{O\max} - I_{O\min}}{2}\right) =$$

$$V - \boldsymbol{l}^\top \boldsymbol{y} + R_M\left(\mathrm{sgn}^+(R_M)\,\mathrm{sgn}^+\left(V - \boldsymbol{l}^\top \boldsymbol{y}\right)\frac{I_{O\max} - I_{O\min}}{2}\right) =$$

$$\left(\left|V - \boldsymbol{l}^\top \boldsymbol{y}\right| + |R_M|\frac{I_{O\max} - I_{O\min}}{2}\right)\mathrm{sgn}^+\left(V - \boldsymbol{l}^\top \boldsymbol{y}\right).$$

$\square$

Corollary 3.2.1.

$$\mathcal{E}' = \left\{\boldsymbol{y} \in \mathbb{R}^2 \ : \ V - D \underset{RUVC}{<} \boldsymbol{l}^\top \boldsymbol{y} \underset{ROVC}{<} V + D\right\} = \left\{\boldsymbol{y} \in \mathbb{R}^2 \ : \ \left|\boldsymbol{l}^\top \boldsymbol{y} - V\right| < D\right\}$$

Proof. For every $\boldsymbol{y} \in \mathbb{R}^2$, $\boldsymbol{y} \in \mathcal{E}'$ if and only if $-E \underset{ROVC}{<} \mathrm{e}^{\mathrm{wc}}(\boldsymbol{y}) \underset{RUVC}{<} E$, being $\mathrm{e}^{\mathrm{wc}}(\boldsymbol{y}) = \left(\left|V - \boldsymbol{l}^\top \boldsymbol{y}\right| + |R_M|\frac{I_{O\max} - I_{O\min}}{2}\right)\mathrm{sgn}^+\left(V - \boldsymbol{l}^\top \boldsymbol{y}\right)$ as proved in the previous proposition.

If $V - \boldsymbol{l}^\top \boldsymbol{y} \geq 0$, ROVC is automatically satisfied, whereas RUVC requires: $V - \boldsymbol{l}^\top \boldsymbol{y} < E - |R_M|\frac{I_{O\max} - I_{O\min}}{2} = D$. If $V - \boldsymbol{l}^\top \boldsymbol{y} < 0$, RUVC is automatically satisfied, whereas ROVC requires: $-D = -\left(E - |R_M|\frac{I_{O\max} - I_{O\min}}{2}\right) < V - \boldsymbol{l}^\top \boldsymbol{y}$.

Consequently, $\boldsymbol{y} \in \mathcal{E}'$ if and only if $\left|\boldsymbol{l}^\top \boldsymbol{y} - V\right| < D$. $\square$

From the previous corollary, it is clear that in order to avoid the case in which $\mathcal{E}' = \emptyset$ (extremely unfortunate for E), it must be assumed that

$$D = E - |R_C - R_{LL}|\frac{I_{O\max} - I_{O\min}}{2} > 0. \quad (A7)$$

Recalling the definitions of V, D, and R_M, it can be easily checked that

$$V - D - R_C I_{O\max} = \begin{cases} V_{LL0} - E - R_{LL}I_{O\max} & \text{if } R_M > 0, \\ V_{LL0} - E - R_{LL}I_{O\min} + R_C\left(I_{O\min} - I_{O\max}\right) & \text{if } R_M < 0, \\ V_{LL0} - E - R_C I_{O\max} & \text{if } R_M = 0, \end{cases}$$

$$= \begin{cases} V_{LL0} - E - R_{LL}I_{O\max} & \text{if } R_M > 0, \\ V_{LL0} - E - R_{LL}I_{O\max} - R_M\left(I_{O\max} - I_{O\min}\right) & \text{if } R_M < 0, \\ V_{LL0} - E - R_{LL}I_{O\max} & \text{if } R_M = 0, \end{cases}$$

consequently, by assumptions (A6), (A1), (A2), and (A4), the following inequality must hold:
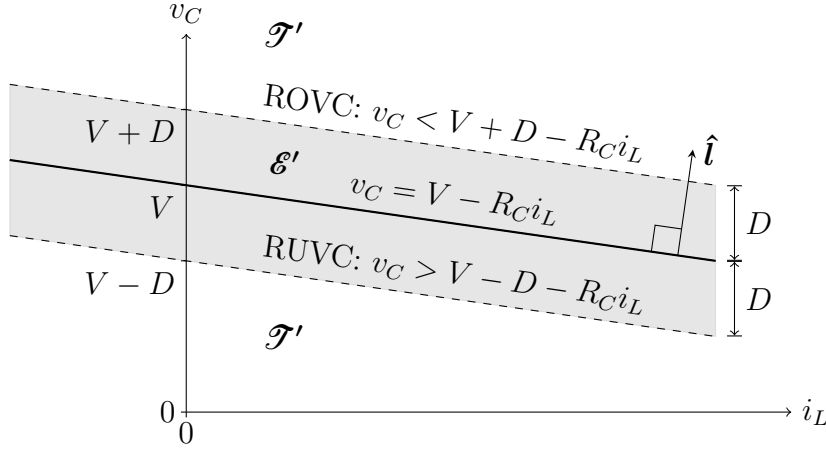
$$V - D - R_C I_{O\max} > 0. \quad (3.20)$$

Figure 3.4: The playing set (PS) $\mathscr{E}'$ is an unbounded open band in the state space, delimited by two straight lines: $R_C i_L + v_C = V + D$ (the ROVC) and $R_C i_L + v_C = V - D$ (the RUVC), where $V > D > 0$. This band is perpendicular to the unit vector $\hat{\boldsymbol{l}} = \frac{1}{\sqrt{R_C{}^2+1}}\begin{bmatrix} R_C & 1 \end{bmatrix}^\top$. The target set (TS) is $\mathscr{T}' = \mathbb{R}^2 \setminus \mathscr{E}'$.

In addition,

$$V > D > 0, \tag{3.21}$$

since $R_C I_{O\max} > 0$ by (A1)–(A2), and $D > 0$ by (A7).

Geometrically, $\mathscr{E}'$, the PS, is an unbounded open band delimited by two straight lines:

$$\left\{ \boldsymbol{y} \in \mathbb{R}^2 \ : \ \langle \boldsymbol{y}, \hat{\boldsymbol{l}} \rangle = \frac{V}{\|\boldsymbol{l}\|} + \frac{D}{\|\boldsymbol{l}\|} \right\},$$

$$\left\{ \boldsymbol{y} \in \mathbb{R}^2 \ : \ \langle \boldsymbol{y}, \hat{\boldsymbol{l}} \rangle = \frac{V}{\|\boldsymbol{l}\|} - \frac{D}{\|\boldsymbol{l}\|} \right\};$$

where $\hat{\boldsymbol{l}} \triangleq \frac{\boldsymbol{l}}{\|\boldsymbol{l}\|} = \frac{1}{\sqrt{R_C{}^2+1}}\begin{bmatrix} R_C & 1 \end{bmatrix}^\top$ is a unit vector perpendicular to the band, and $\langle \cdot, \cdot \rangle$ is the standard inner product on $\mathbb{R}^2$, defined by $\langle \boldsymbol{y_1}, \boldsymbol{y_2} \rangle \triangleq \boldsymbol{y_1}^\top \boldsymbol{y_2}$ for every $\boldsymbol{y_1}, \boldsymbol{y_2} \in \mathbb{R}^2$. This band is illustrated in Figure 3.4. Observe that $\boldsymbol{0} \notin \mathscr{E}'$, because (3.21) holds.

3.2.2. The relation between the worst-case error and the oriented distance to the target set

Recall, from Chapter 2, that the *oriented distance* function $\mathrm{dist_o} : \mathbb{R}^2 \times 2^{\mathbb{R}^2} \setminus \{\emptyset\} \to \mathbb{R}$ between a point and a non-empty subset of $\mathbb{R}^2$ is defined by

$$\mathrm{dist_o}\left(\boldsymbol{x}, \mathscr{X}\right) \triangleq \begin{cases} +\mathrm{dist}\left(\boldsymbol{x}, \mathscr{X}\right) & \text{if } \boldsymbol{x} \in \mathscr{X}^{\complement}, \\ -\mathrm{dist}\left(\boldsymbol{x}, \mathscr{X}^{\complement}\right) & \text{if } \boldsymbol{x} \in \mathscr{X}, \end{cases}$$

for every $\boldsymbol{x} \in \mathbb{R}^2$ and every $\mathscr{X}$ such that $\emptyset \neq \mathscr{X} \subset \mathbb{R}^2$. Having characterized the PS geometrically, it is a simple matter to find the oriented distance function to its complement (the TS):

$$\text{dist}_{\text{o}}\left(\boldsymbol{y}, \mathscr{T}'\right) = \frac{D}{||\boldsymbol{l}||} - \left|\left\langle \boldsymbol{y} - \frac{V}{||\boldsymbol{l}||}\hat{\boldsymbol{l}}, \hat{\boldsymbol{l}} \right\rangle\right| = \frac{1}{||\boldsymbol{l}||}\left(D - \left|V - \boldsymbol{l}^\top \boldsymbol{y}\right|\right). \qquad (3.22)$$

Note that, the term $\left|V - \boldsymbol{l}^\top \boldsymbol{y}\right|$ in (3.22) is given by proposition 3.2.1 (after taking absolute value of $\text{e}^{\text{wc}}\left(\boldsymbol{y}\right)$):

$$\left|V - \boldsymbol{l}^\top \boldsymbol{y}\right| = |\text{e}^{\text{wc}}\left(\boldsymbol{y}\right)| - |R_M|\frac{I_{O\max} - I_{O\min}}{2}. \qquad (3.23)$$

Hence, $\text{dist}_{\text{o}}\left(\boldsymbol{y}, \mathscr{T}'\right) = \frac{1}{||\boldsymbol{l}||}\left(D - |\text{e}^{\text{wc}}\left(\boldsymbol{y}\right)| + |R_M|\frac{I_{O\max}-I_{O\min}}{2}\right)$, where, by definition, $D = E - |R_M|\frac{I_{O\max}-I_{O\min}}{2}$. Cancellation of $|R_M|\frac{I_{O\max}-I_{O\min}}{2}$ yields

$$\text{dist}_{\text{o}}\left(\boldsymbol{y}, \mathscr{T}'\right) = \frac{1}{||\boldsymbol{l}||}\left(E - |\text{e}^{\text{wc}}\left(\boldsymbol{y}\right)|\right). \qquad (3.24)$$

This last equality endows the concept of oriented distance to $\mathscr{T}'$ with physical significance in terms of the (state-dependent) worst-case error (as defined by (3.12)–(3.13)), the error tolerance E, and the factor $||\boldsymbol{l}|| = \sqrt{R_C^2 + 1}$. Moreover, it makes clear that maximization of $\text{dist}_{\text{o}}\left(\cdot, \mathscr{T}'\right)$ is equivalent to minimization of $|\text{e}^{\text{wc}}\left(\cdot\right)|$.

Observe, however, that even for points $\boldsymbol{y}$ on the line $\left\{\boldsymbol{y} \in \mathbb{R}^2 : \boldsymbol{l}^\top \boldsymbol{y} = V\right\}$ (where the oriented distance to $\mathscr{T}'$ is maximum), the quantity $|\text{e}^{\text{wc}}\left(\boldsymbol{y}\right)|$ is *not* equal to zero in general. Actually, it follows from (3.23) that

$$|\text{e}^{\text{wc}}\left(\boldsymbol{y}\right)| = |R_M|\frac{I_{O\max} - I_{O\min}}{2} \quad \text{if} \quad \boldsymbol{l}^\top \boldsymbol{y} = V. \qquad (3.25)$$

Therefore, the absolute value of the worst-case error is *uniform* and *positive* (except if $R_M = 0$) along the axis $\left\{\boldsymbol{y} \in \mathbb{R}^2 : \boldsymbol{l}^\top \boldsymbol{y} = V\right\}$ of the band $\mathscr{E}'$ (see Figure 3.4). The distance $\frac{D}{||\boldsymbol{l}||} = \frac{D}{\sqrt{R_C^2+1}}$ between this axis and $\mathscr{T}'$, is $\frac{1}{\sqrt{R_C^2+1}}$ times the difference $D = E - |R_M|\frac{I_{O\max}-I_{O\min}}{2}$ (which was assumed to be positive by (A7)).

In summary, the difference $E - |\text{e}^{\text{wc}}\left(\boldsymbol{y}\right)|$, between the error tolerance and the *(instantaneous) absolute worst-case error at state* $\boldsymbol{y} = \begin{bmatrix} i_L & v_C \end{bmatrix} \in \mathbb{R}^2$ is proportional to the oriented distance $\text{dist}_{\text{o}}\left(\boldsymbol{y}, \mathscr{T}'\right)$ between the state $\boldsymbol{y}$ and the target set $\mathscr{T}'$, being $\sqrt{R_C^2 + 1}$ the coefficient of proportionality, i.e.,

$$E - |\text{e}^{\text{wc}}\left(\boldsymbol{y}\right)| = \sqrt{R_C^2 + 1}\,\text{dist}_{\text{o}}\left(\boldsymbol{y}, \mathscr{T}'\right). \qquad (3.26)$$

The *(instantaneous) absolute worst-case error function*

$$\boldsymbol{y} \mapsto |\text{e}^{\text{wc}}\left(\boldsymbol{y}\right)| = \left|V_{LL0} + R_M\frac{I_{O\min} + I_{O\max}}{2} - R_C i_L - v_C\right| + |R_M|\frac{I_{O\max} - I_{O\min}}{2}, \qquad (3.27)$$

has a minimum positive value equal to $|R_M| \frac{I_{O\max} - I_{O\min}}{2}$, along the line

$$\left\{ \begin{bmatrix} i_L, v_C \end{bmatrix}^\top \in \mathbb{R}^2 \; : \; R_C i_L + v_C = V_{LL0} + R_M \frac{I_{O\min} + I_{O\max}}{2} \right\} \qquad (3.28)$$

(which vanishes only if the mismatch $R_M = R_C - R_{LL}$ is zero), and is constant along straight lines parallel to (3.28). Assumption (A7) prevents the playing set $\mathscr{E}' = \left\{ \boldsymbol{y} \in \mathbb{R}^2 \; : \; E - |\mathrm{e}^{\mathrm{wc}}(\boldsymbol{y})| > 0 \right\}$ from being empty.

3.2.3. The conflict and its two related games

So far, a pursuit-evasion differential *game* has not been properly formulated yet, but the two components needed to pose a pursuit-evasion *conflict* have already been introduced, namely a state equation (SE) (differential equation (3.7)) and a target set (TS) (set definition (3.15)). Let $\mathcal{C}'$ denote this *(realistic) buck converter (pursuit-evasion) conflict*:

$$\mathcal{C}' \left\{ \begin{array}{rll} \text{SE}: & \frac{\mathrm{d}\boldsymbol{y}}{\mathrm{d}t} = \boldsymbol{f}'(\boldsymbol{y}, \boldsymbol{v}, \sigma) & \triangleq \boldsymbol{A}'\boldsymbol{y} + \boldsymbol{B}'\boldsymbol{S}(\sigma)\boldsymbol{v}, \\ \text{TS}: & \mathscr{T}' = & \left\{ \boldsymbol{y} \in \mathbb{R}^2 \; : \; |\boldsymbol{l}^\top \boldsymbol{y} - V| \geq D \right\}, \end{array} \right. \qquad (3.29)$$

where $\boldsymbol{f}'$ is introduced just to denote the right-hand side the SE, being its first argument the state, its second argument P's control, and its third argument E's control. This conflict formulation will be referred to as *realistic* to distinguish it from the *canonical* formulation that will be derived in Section 3.4.

In order to formulate a pursuit-evasion differential *game*, as defined in Chapter 2, a pay-off functional (PF) must be introduced to make precise both players' (antagonistic) aims. Two alternative PFs may be naturally considered to accompany (3.29); one gives rise to a *game in distance* $\mathcal{G}_{\mathbf{dist}}'$ and the other one gives rise to a *game in time* $\mathcal{G}_{\mathbf{time}}'$. With the notation introduced in Chapter 2, these two games are unambiguously given by:

$$\mathcal{G}_{\mathbf{dist}}' \left\{ \begin{array}{l} \mathcal{C}', \\ \text{PF}: \quad (\boldsymbol{y_0}, \boldsymbol{v}, \sigma) \mapsto \mathcal{P}_{\boldsymbol{f}', \mathscr{T}'}^{\mathrm{dist_o}}(\boldsymbol{y_0}, \boldsymbol{v}, \sigma) = \inf \left\{ \mathrm{dist_o}\left(\boldsymbol{y}_{\boldsymbol{y_0}, v, \sigma}^{\boldsymbol{f}'}(t), \mathscr{T}' \right) \; : \; t \geq 0 \right\}, \end{array} \right.$$

$$\mathcal{G}_{\mathbf{time}}' \left\{ \begin{array}{l} \mathcal{C}', \\ \text{PF}: \quad (\boldsymbol{y_0}, \boldsymbol{v}, \sigma) \mapsto \mathcal{P}_{\boldsymbol{f}', \mathscr{T}'}^{\mathrm{time}}(\boldsymbol{y_0}, \boldsymbol{v}, \sigma) = \inf \left\{ t \geq 0 \; : \; \boldsymbol{y}_{\boldsymbol{y_0}, v, \sigma}^{\boldsymbol{f}'}(t) \in \mathscr{T}' \right\}; \end{array} \right.$$

where it is understood that $\mathcal{P}_{\boldsymbol{f}', \mathscr{T}'}^{\mathrm{dist_o}}(\boldsymbol{y_0}, \boldsymbol{v}, \sigma) = -\infty$ if $\left\{ \mathrm{dist_o}\left(\boldsymbol{y}_{\boldsymbol{y_0}, v, \sigma}^{\boldsymbol{f}'}(t), \mathscr{T}' \right) \; : \; t \geq 0 \right\}$ is not bounded below, and $\mathcal{P}_{\boldsymbol{f}', \mathscr{T}'}^{\mathrm{time}}(\boldsymbol{y_0}, \boldsymbol{v}, \sigma) = +\infty$ if $\left\{ t \geq 0 \; : \; \boldsymbol{y}_{\boldsymbol{y_0}, v, \sigma}^{\boldsymbol{f}'}(t) \in \mathscr{T}' \right\}$ is empty.

3.2.4. Physical interpretation of the game in distance

Note that, by virtue of (3.26) which relates the functions $\text{dist}_\text{o}\left(\cdot, \mathscr{T}'\right)$ and $\left|\mathrm{e}^{\mathrm{wc}}\left(\cdot\right)\right|$, the game $\boldsymbol{\mathcal{G}_\mathbf{dist}}'$ may be also expressed as

$$\boldsymbol{\mathcal{G}_\mathbf{dist}}' \begin{cases} \boldsymbol{\mathcal{C}}', \\ \mathrm{PF}: \quad (\boldsymbol{y_0}, \boldsymbol{v}, \sigma) \mapsto \mathcal{P}_{\boldsymbol{f}', \mathscr{T}'}^{\text{dist}_\text{o}}(\boldsymbol{y_0}, \boldsymbol{v}, \sigma) = \inf\left\{ \frac{E - \left|\mathrm{e}^{\mathrm{wc}}\left(\boldsymbol{y}_{\boldsymbol{y_0}, v, \sigma}^{\boldsymbol{f}'}(t)\right)\right|}{\sqrt{R_C^2 + 1}} \; : \; t \geq 0 \right\}, \end{cases}$$
(3.30)

which is equivalent to

$$\boldsymbol{\mathcal{G}_{-|\boldsymbol{e}^\mathbf{wc}|}}' \begin{cases} \boldsymbol{\mathcal{C}}', \\ \mathrm{PF}: \quad (\boldsymbol{y_0}, \boldsymbol{v}, \sigma) \mapsto \mathcal{P}_{\boldsymbol{f}', \mathscr{T}'}^{-|\mathrm{e}^{\mathrm{wc}}|}(\boldsymbol{y_0}, \boldsymbol{v}, \sigma) = \inf\left\{ -\left|\mathrm{e}^{\mathrm{wc}}\left(\boldsymbol{y}_{\boldsymbol{y_0}, v, \sigma}^{\boldsymbol{f}'}(t)\right)\right| \; : \; t \geq 0 \right\}, \end{cases}$$

because their PFs are related by

$$\sqrt{R_C^2 + 1}\; \mathcal{P}_{\boldsymbol{f}', \mathscr{T}'}^{\text{dist}_\text{o}}(\boldsymbol{y_0}, \boldsymbol{v}, \sigma) = E + \mathcal{P}_{\boldsymbol{f}', \mathscr{T}'}^{-|\mathrm{e}^{\mathrm{wc}}|}(\boldsymbol{y_0}, \boldsymbol{v}, \sigma)$$
(3.31)

for every play $(\boldsymbol{y_0}, \boldsymbol{v}, \sigma)$, where $\sqrt{R_C^2 + 1}$ is clearly positive. Accordingly, the games $\boldsymbol{\mathcal{G}_\mathbf{dist}}'$ and $\boldsymbol{\mathcal{G}_{-|\boldsymbol{e}^\mathbf{wc}|}}'$ share the same optimal strategies, and their VFs (let them be $\mathcal{V}_{\text{dist}_\text{o}}$ and $\mathcal{V}_{-|\mathrm{e}^{\mathrm{wc}}|}$, respectively) relate as their respective PFs, i.e.,

$$\sqrt{R_C^2 + 1}\; \mathcal{V}_{\text{dist}_\text{o}}(\boldsymbol{y_0}) = E + \mathcal{V}_{-|\mathrm{e}^{\mathrm{wc}}|}(\boldsymbol{y_0}),$$
(3.32)

for every $\boldsymbol{y_0} \in \mathbb{R}^2$.

Observe that while both in (3.31) and (3.32) the two factors involved in the left-hand side lack a physical meaning, the sum of the right-hand side has a clear physical meaning, namely: for every initial state $\boldsymbol{y_0}$, the signed difference (in a voltage unit such as volts) between the error tolerance and the absolute value of the worst-case error along *a whole* play $(\boldsymbol{y_0}, \boldsymbol{v}, \sigma)$ in case of (3.31), and along *the whole* play that results from P and E putting into practice their *optimal* strategies in case of (3.32).

Just to emphasise the above interpretation in a slightly different (more natural) way, suppose we abandon the until now respected criterion that assigns P the role of the infimizer and E the role of the supremizer. Suppouse P becomes the supremizer and E the infimizer in a new game defined as

$$\boldsymbol{\mathcal{G}_{|\boldsymbol{e}^\mathbf{wc}|}}' \begin{cases} \boldsymbol{\mathcal{C}}', \\ \mathrm{PF}: \quad (\boldsymbol{y_0}, \boldsymbol{v}, \sigma) \mapsto \mathcal{P}_{\boldsymbol{f}', \mathscr{T}'}^{|\mathrm{e}^{\mathrm{wc}}|}(\boldsymbol{y_0}, \boldsymbol{v}, \sigma) = \inf\left\{ \left|\mathrm{e}^{\mathrm{wc}}\left(\boldsymbol{y}_{\boldsymbol{y_0}, v, \sigma}^{\boldsymbol{f}'}(t)\right)\right| \; : \; t \geq 0 \right\}. \end{cases}$$
(3.33)

whose VF is named $\mathcal{V}_{|\mathrm{e}^{\mathrm{wc}}|}$. In agreement with the above statements, $\mathcal{V}_{|\mathrm{e}^{\mathrm{wc}}|}$ relates to $\mathcal{V}_{\text{dist}_\text{o}}$ by

$$\sqrt{R_C^2 + 1}\; \mathcal{V}_{\text{dist}_\text{o}}(\boldsymbol{y_0}) = E - \mathcal{V}_{|\mathrm{e}^{\mathrm{wc}}|}(\boldsymbol{y_0}),$$
(3.34)

for every $\boldsymbol{y_0} \in \mathbb{R}^2$. This last expression, makes clear the significance that $\mathcal{V}_{\text{dist}_\text{o}}$ (the VF of $\boldsymbol{\mathcal{G}_\mathbf{dist}}'$) has, by relating it to $\mathcal{V}_{|\mathrm{e}^{\mathrm{wc}}|}$ which is the VF of the game $\boldsymbol{\mathcal{G}_{|\boldsymbol{e}^\mathbf{wc}|}}'$ in which E struggles to infimize the worst-case error (which depends only on the system's state) over an infinite time horizon, while P struggles to supremize it.

Parameter	Description	Unit
L	inductance of the converter's inductor	H
R_L	parasitic ESR of the converter's inductor	Ω
C	capacitance of the converter's capacitor	F
R_C	parasitic ESR of the converter's capacitor	Ω
$I_{O\min}$	minimum load current	A
$I_{O\max}$	maximum load current	A
$V_{I\min}$	minimum input voltage	V
$V_{I\max}$	maximum input voltage	V
V_{LL0}	reference voltage for open circuit load	V
R_{LL}	characteristic load line resistance	Ω
E	error tolerance	V

Table 3.1: List of (realistic) parameters that define a buck converter conflict.

3.3. Further assumptions

The pursuit-evasion conflict just described is completely characterized by eleven independent parameters listed in Table 3.1. In order to limit the analysis scope of this thesis to the region of interest in the parameter space, the following non-trivial assumptions on time constants are introduced, in addition to the natural general assumptions (A1)–(A7):

$$\frac{\sqrt{LC}}{2} < \frac{L}{R_L + R_C}, \tag{A8}$$

$$R_C C < \sqrt{LC}. \tag{A9}$$

Assumption (A8) is equivalent to require that the L-C filter is designed to be under-damped, which is the usual case. Assumption (A9) states that the parasite time constant $R_C C$ is lower than the L-C filter time constant, which is also the usual case.

Note that assumption (A9) could have been equivalently stated as an inequality for impedances, $R_C < \sqrt{\frac{L}{C}}$, or as an inequality for other time constants, $R_C C < \frac{L}{R_C}$, since

$$R_C C < \sqrt{LC} \iff R_C < \sqrt{\frac{L}{C}} \iff R_C{}^2 < \frac{L}{C} \iff R_C C < \frac{L}{R_C}. \tag{A9'}$$

3.4. A canonical formulation of the conflict

In this section it is shown that, under assumptions (A1)–(A9), the buck converter conflict can be put in a *canonical form*, characterized by seven dimensionless real parameters, in which the SE and the PS turn out to acquire quite simple forms.

The canonical form results from following Hirsch and Smale's [70] approach to ordinary differential equations. In particular, by transforming the state space by means of a suitably chosen affine transformation (interpreted geometrically in Appendix A) and by normalizing time and P's control.

3.4.1. State space transformation

Let ω_n, ζ, R and λ be defined as follows:

$$\omega_n \triangleq \frac{1}{\sqrt{LC}}, \quad \zeta \triangleq \frac{1}{2\omega_n}\left(\frac{R_L + R_C}{L}\right), \quad R \triangleq \sqrt{\frac{L}{C}}, \quad \lambda \triangleq \frac{R_C}{R}. \tag{3.35}$$

Assumptions (A1) and (A8) imply that

$$0 < \zeta < 1. \tag{3.36}$$

Likewise, assumptions (A1) and (A9) imply that

$$0 < \lambda < 1. \tag{3.37}$$

Since $R_L = (2\zeta - \lambda)R$, assumption (A1) requires that

$$\lambda < 2\zeta. \tag{3.38}$$

Matrices $\boldsymbol{A}'$ and $\boldsymbol{B}'$, defined in (3.8), can be expressed as $\boldsymbol{A}' = \begin{bmatrix} -2\zeta\omega_n & -\frac{\omega_n}{R} \\ R\omega_n & 0 \end{bmatrix}$ and $\boldsymbol{B}' = \begin{bmatrix} \lambda\omega_n & \frac{\omega_n}{R} \\ -R\omega_n & 0 \end{bmatrix}$. The eigenvalues of $\boldsymbol{A}'$ are the roots of the characteristic polynomial

$$p_{\boldsymbol{A}'}(s) \triangleq s^2 + 2\zeta\omega_n s + \omega_n^2,$$

whose roots are $-\zeta\omega_n \pm \mathrm{j}\omega_d$, being

$$\omega_d \triangleq \sqrt{1 - \zeta^2}\,\omega_n.$$

Let $\boldsymbol{h} : \mathbb{R}^2 \to \mathbb{R}^2$ such that

$$\boldsymbol{h}\left(\cdot\right) \triangleq \boldsymbol{P}\left(D \cdot + V\hat{\boldsymbol{e}}_2\right), \tag{3.39}$$

where $\boldsymbol{P} \triangleq \frac{\sqrt{1-\zeta^2}}{(\zeta-\lambda)^2 + 1 - \zeta^2}\frac{1}{R}\begin{bmatrix} 1 & -\frac{\zeta-\lambda}{\sqrt{1-\zeta^2}} \\ -\lambda R & \frac{(1-\zeta\lambda)}{\sqrt{1-\zeta^2}}R \end{bmatrix}$. $\boldsymbol{P}$ is invertible because $\det \boldsymbol{P} = \frac{\sqrt{1-\zeta^2}}{(\zeta-\lambda)^2 + 1 - \zeta^2}\frac{1}{R} > 0$. Therefore, $\boldsymbol{h}$ is invertible and

$$\boldsymbol{x} \triangleq \boldsymbol{h}^{-1}\left(\boldsymbol{y}\right) = \frac{1}{D}\left(\boldsymbol{P}^{-1}\boldsymbol{y} - V\hat{\boldsymbol{e}}_2\right) \tag{3.40}$$

can be introduced as a new state variable. Substitution of

$$\boldsymbol{y} = \boldsymbol{h}\left(\boldsymbol{x}\right) = \boldsymbol{P}\left(D\boldsymbol{x} + V\hat{\boldsymbol{e}}_2\right) \tag{3.41}$$

in the SE of (3.29) followed by left-multiplication by matrix $\boldsymbol{P}^{-1}$ yields

$$\frac{\mathrm{d}\left(D\boldsymbol{x}\right)}{\mathrm{d}t} = \boldsymbol{J}\left(D\boldsymbol{x}\right) + \boldsymbol{P}^{-1}\boldsymbol{B}'\boldsymbol{S}\left(\sigma\right)\boldsymbol{v} + V\boldsymbol{J}\hat{\boldsymbol{e}}_{\boldsymbol{2}}. \tag{3.42}$$

where $\boldsymbol{J} = \boldsymbol{P}^{-1}\boldsymbol{A}'\boldsymbol{P} = \omega_d \begin{bmatrix} -\dfrac{\zeta}{\sqrt{1-\zeta^2}} & -1 \\ 1 & -\dfrac{\zeta}{\sqrt{1-\zeta^2}} \end{bmatrix}$, $\boldsymbol{P}^{-1}\boldsymbol{B}' = \omega_d \begin{bmatrix} -\dfrac{\zeta\left(1+\lambda^2\right)-2\lambda}{1-\zeta^2}R & \dfrac{1-\zeta\lambda}{1-\zeta^2} \\ -\dfrac{1-\lambda^2}{\sqrt{1-\zeta^2}}R & \dfrac{\lambda}{\sqrt{1-\zeta^2}} \end{bmatrix}$.

Observe that the ordinary differential equation (3.42) rules the temporal evolution of $D\boldsymbol{x}$, whose two components have the dimension of voltage, but the components of $\boldsymbol{x} = \boldsymbol{h}^{-1}\left(\boldsymbol{y}\right)$ are dimensionless.

To find out how the PS, $\mathscr{E}'$, is transformed through $\boldsymbol{h}^{-1}$ observe that

$$\boldsymbol{y} \in \mathscr{E}' \iff \left|\boldsymbol{l}^{\top}\boldsymbol{y} - V\right| < D \iff \left|\boldsymbol{l}^{\top}\boldsymbol{P}\left(D\boldsymbol{x} + V\hat{\boldsymbol{e}}_{\boldsymbol{2}}\right) - V\right| < D$$

$$\iff \left|\hat{\boldsymbol{e}}_{\boldsymbol{2}}^{\top}\left(D\boldsymbol{x} + V\hat{\boldsymbol{e}}_{\boldsymbol{2}}\right) - V\right| < D \iff \left|D\hat{\boldsymbol{e}}_{\boldsymbol{2}}^{\top}\boldsymbol{x}\right| < D \iff \left|\hat{\boldsymbol{e}}_{\boldsymbol{2}}^{\top}\boldsymbol{x}\right| < 1, \quad (3.43)$$

where it was used that $\boldsymbol{l}^{\top} = \begin{bmatrix} R_C & 1 \end{bmatrix} = \begin{bmatrix} \lambda R & 1 \end{bmatrix}$ and $\boldsymbol{l}^{\top}\boldsymbol{P} = \hat{\boldsymbol{e}}_{\boldsymbol{2}}^{\top}$ as can be easily checked. Defining

$$\mathscr{E} \triangleq \left\{\boldsymbol{x} \in \mathbb{R}^2 \;:\; \left|\langle\hat{\boldsymbol{e}}_{\boldsymbol{2}}, \boldsymbol{x}\rangle\right| < 1\right\},$$

the chain of double implications (3.43) proves that $\boldsymbol{h}^{-1}\left(\mathscr{E}'\right) = \mathscr{E}$. Likewise, $\boldsymbol{h}^{-1}\left(\mathscr{T}'\right) = \mathscr{T}$, where

$$\mathscr{T} \triangleq \mathbb{R}^2 \setminus \mathscr{E} = \left\{\boldsymbol{x} \in \mathbb{R}^2 \;:\; \left|\langle\hat{\boldsymbol{e}}_{\boldsymbol{2}}, \boldsymbol{x}\rangle\right| \geq 1\right\}.$$

Note that $\boldsymbol{J} = \boldsymbol{P}^{-1}\boldsymbol{A}'\boldsymbol{P}$ is the *real Jordan form* [70] of $\boldsymbol{A}'$, obtained by the *similarity transformation matrix* $\boldsymbol{P}$. The first and second columns of $\boldsymbol{P}$ are, respectively, the imaginary part and the real part of an eigenvector $\boldsymbol{w}^{+}$ of $\boldsymbol{A}'$ that corresponds to the eigenvalue $\zeta\omega_n + \mathrm{j}\omega_d$. Every eigenvector $\boldsymbol{w}_z^{+} = z\boldsymbol{w}^{+}$ of the same eigenspace, such that $z \in \mathbb{C} \setminus \{0\}$, would have yielded the same real Jordan form $\boldsymbol{J}$ through a similarity transformation matrix $\boldsymbol{P}_z$ defined as $\boldsymbol{P}_z = \begin{bmatrix} \Im\boldsymbol{w}_z^{+} & \Re\boldsymbol{w}_z^{+} \end{bmatrix}$; but, only for $z = 1$, the property $\boldsymbol{l}^{\top}\boldsymbol{P}_z = \hat{\boldsymbol{e}}_{\boldsymbol{2}}^{\top}$ used in 3.43, would have been preserved.

The only "other" real Jordan form of $\boldsymbol{A}'$ that could have been considered is $\boldsymbol{J}^{\top}$. It could have been obtained by any similarity transformation matrix constructed as just described, but derived from the other eigenspace (the one that corresponds to the eigenvalue $\zeta\omega_n - \mathrm{j}\omega_d$). The inconvenience of these similarity transformation matrices is that, unlike matrices $\boldsymbol{P}_z$, they all have negative determinant; so, if they were used in place of $\boldsymbol{P}$ in (3.39), they would define orientation reversing transformations $\boldsymbol{y} \mapsto \boldsymbol{x} \triangleq \boldsymbol{h}^{-1}\left(\boldsymbol{y}\right)$ of $\mathbb{R}^2$. From the two alternatives, the orientation preserving one was selected.

3.4.2. Pursuer's control normalization

Defining

$$\boldsymbol{N} \triangleq \begin{bmatrix} I_{O\max} & 0 \\ 0 & V_{I\max} \end{bmatrix}, \quad i_o^{\triangledown} \triangleq I_{O\min} / I_{O\max}, \quad v_i^{\triangledown} \triangleq V_{I\min} / V_{I\max},$$

and a new control variable for the pursuer,

$$\boldsymbol{u} \triangleq \begin{bmatrix} i_o \\ v_i \end{bmatrix} = \boldsymbol{N}^{-1} \boldsymbol{v} = \begin{bmatrix} i_O/I_{O\max} \\ v_I/V_{I\max} \end{bmatrix},$$

(3.42) becomes

$$\frac{\mathrm{d}\,(D\boldsymbol{x})}{\mathrm{d}t} = \boldsymbol{J}\,(D\boldsymbol{x}) + \boldsymbol{P}^{-1}\boldsymbol{B}'\boldsymbol{N}\boldsymbol{S}\,(\sigma)\,\boldsymbol{u} + V\boldsymbol{J}\hat{\boldsymbol{e}_2}, \qquad (3.44)$$

because $\boldsymbol{v} = \boldsymbol{N}\boldsymbol{u}$ and $\boldsymbol{S}\,(\sigma)\,\boldsymbol{N} = \boldsymbol{N}\boldsymbol{S}\,(\sigma)$. The new parameters $i_o^{\triangledown}$ and $v_i^{\triangledown}$ satisfy

$$0 \le i_o^{\triangledown} < 1, \qquad (3.45)$$

$$0 < v_i^{\triangledown} \le 1, \qquad (3.46)$$

because of assumptions (A2) and (A3).

Dividing by $V_{I\max}$, (3.44) becomes

$$\frac{\mathrm{d}\,(\delta\boldsymbol{x})}{\mathrm{d}t} = \boldsymbol{J}\,(\delta\boldsymbol{x}) + \frac{1}{V_{I\max}}\boldsymbol{P}^{-1}\boldsymbol{B}'\boldsymbol{N}\boldsymbol{S}\,(\sigma)\,\boldsymbol{u} + \nu\boldsymbol{J}\hat{\boldsymbol{e}_2}, \qquad (3.47)$$

where

$$\nu \triangleq \frac{V}{V_{I\max}}, \quad \delta \triangleq \frac{D}{V_{I\max}},$$

being $V_{I\max} > 0$ by (A3). Note, for future reference, that

$$\delta > 0 \qquad (3.48)$$

because of (A7).

3.4.3. Time normalization

Introducing *normalized time* as

$$\mathfrak{t} \triangleq \omega_d t,$$

and dividing both sides of (3.47) by $\omega_d \delta$, it turns to

$$\frac{\mathrm{d}\boldsymbol{x}}{\mathrm{d}\mathfrak{t}} = \underbrace{\frac{1}{\omega_d}\boldsymbol{J}}_{\boldsymbol{A}}\boldsymbol{x} + \underbrace{\frac{1}{\omega_d\delta V_{I\max}}\boldsymbol{P}^{-1}\boldsymbol{B}'\boldsymbol{N}}_{\boldsymbol{B}}\boldsymbol{S}\,(\sigma)\,\boldsymbol{u} + \underbrace{\frac{\nu}{\delta}\frac{1}{\omega_d}\boldsymbol{J}\hat{\boldsymbol{e}_2}}_{\boldsymbol{c}},$$

where new matrices $\boldsymbol{A}$, $\boldsymbol{B}$, and a new vector $\boldsymbol{c}$ were introduced. Denoting

$$\rho \triangleq \frac{I_{O\max}}{V_{I\max}}R,$$

matrix $\boldsymbol{B}$ can be expressed as $\boldsymbol{B} = \frac{1}{\omega_d\delta V_{I\max}}\boldsymbol{P}^{-1}\boldsymbol{B}'\boldsymbol{N} = \frac{1}{\delta}\begin{bmatrix} -\frac{\zeta(1+\lambda^2)-2\lambda}{1-\zeta^2}\rho & \frac{1-\zeta\lambda}{1-\zeta^2} \\ -\frac{1-\lambda^2}{\sqrt{1-\zeta^2}}\rho & \frac{\lambda}{\sqrt{1-\zeta^2}} \end{bmatrix}$.

Clearly, from assumptions (A1)–(A3):

$$\rho > 0. \qquad (3.49)$$

Notice also that

$$\nu - \delta - \lambda\rho > 0 \qquad (3.50)$$

because $(\nu - \delta - \lambda\rho)\,V_{I\max} = V - D - R_C I_{O\max} > 0$ by (3.20).

3.4.4. The proposed canonical form

In conclusion, every buck converter conflict (3.29) can be put in the following *canonical form*:

$$\mathcal{C} \begin{cases} \text{SE}: & \frac{\mathrm{d}\boldsymbol{x}}{\mathrm{d}t} = \boldsymbol{f}\left(\boldsymbol{x}, \boldsymbol{u}, \sigma\right) \quad \triangleq \quad \boldsymbol{A}\boldsymbol{x} + \boldsymbol{B}\boldsymbol{S}\left(\sigma\right)\boldsymbol{u} + \boldsymbol{c}, \\ \text{TS}: & \qquad\qquad\qquad \mathscr{T} \;\; = \;\; \left\{\boldsymbol{x} \in \mathbb{R}^2 \;:\; |\langle \hat{\boldsymbol{e}}_2, \boldsymbol{x}\rangle| \geq 1\right\}; \end{cases} \tag{3.51}$$

where

$$\boldsymbol{A} \triangleq \begin{bmatrix} -\frac{\zeta}{\sqrt{1-\zeta^2}} & -1 \\ 1 & -\frac{\zeta}{\sqrt{1-\zeta^2}} \end{bmatrix}, \; \boldsymbol{B} \triangleq \frac{1}{\delta}\begin{bmatrix} -\frac{1+\lambda^2}{1-\zeta^2}\left(\zeta - \frac{2\lambda}{1+\lambda^2}\right)\rho & \frac{1-\zeta\lambda}{1-\zeta^2} \\ -\frac{1-\lambda^2}{\sqrt{1-\zeta^2}}\rho & \frac{\lambda}{\sqrt{1-\zeta^2}} \end{bmatrix}, \; \boldsymbol{c} \triangleq \frac{\nu}{\delta}\begin{bmatrix} -1 \\ -\frac{\zeta}{\sqrt{1-\zeta^2}} \end{bmatrix},$$

$$\boldsymbol{S}\left(\sigma\right) = \begin{bmatrix} 1 & 0 \\ 0 & \sigma \end{bmatrix}, \quad \boldsymbol{u} = \begin{bmatrix} i_o \\ v_i \end{bmatrix}, \quad i_o^\triangledown \leq i_o \leq 1, \quad v_i^\triangledown \leq v_i \leq 1, \quad 0 \leq \sigma \leq 1.$$

The new function $\boldsymbol{f}$, introduced in (3.51), denotes the right-hand side the SE, being its first argument the state, its second argument P's control, and its third argument E's control.

The canonical form is given by seven dimensionless real parameters, derived from the eleven realistic parameters listed in Table 3.1, as it is detailed in Table 3.2. The seven parameters that characterize the canonical form will be referred to as *canonical parameters* and they must satisfy the following *necessary* conditions

$$0 < \zeta, \lambda < 1, \qquad \lambda < 2\zeta, \tag{3.52}$$

$$0 \leq i_o^\triangledown < 1, \quad 0 < v_i^\triangledown \leq 1, \tag{3.53}$$

$$\delta, \rho > 0, \qquad \nu > \delta + \lambda\rho, \tag{3.54}$$

derived from assumptions (A1)–(A9), as already noted in (3.36), (3.37), (3.38), (3.45), (3.46), (3.48), (3.49), and (3.50). According to (3.52)–(3.54), the canonical form parameter space is strictly included in the half-space $\nu > 0$. This parameter space, is not bounded, however its intersection with every hyperplane of constant ν *is* bounded. Moreover, recalling that $\nu = V_{I\max}{}^{-1}\left(V_{LL0} + R_M\frac{I_{O\min}+I_{O\max}}{2}\right)$, it is clear that a reasonable upper bound for ν can be established if it were necessary to explore a *bounded* parameter space under assumptions (A1)–(A9). This would be the case if, for example, optimal parameters (in some sense) were being searched.

It must be emphasised that this canonical form is proposed just as a *convention* to parametrize the collection of all possible instances of buck converter conflicts. However, other conventions may be used. In a deep sense, what only deserves to be called *canonical* is the *real Jordan form*, $\boldsymbol{J}$, of $\boldsymbol{A}'$.

Just for completeness, notice that as a result of the conflict canonization $\mathcal{C}' \rightsquigarrow \mathcal{C}$, the accompanying games, $\boldsymbol{\mathcal{G}_{dist}}'$ and $\boldsymbol{\mathcal{G}_{time}}'$, need consistent canonizations, $\boldsymbol{\mathcal{G}_{dist}}' \rightsquigarrow \boldsymbol{\mathcal{G}_{dist}}$ and $\boldsymbol{\mathcal{G}_{time}}' \rightsquigarrow \boldsymbol{\mathcal{G}_{time}}$, into natural reformulations:

$$\boldsymbol{\mathcal{G}_{dist}} \begin{cases} \mathcal{C}, \\ \text{PF}: \quad (\boldsymbol{x_0}, \boldsymbol{u}, \sigma) \mapsto \mathcal{P}_{\boldsymbol{f}, \mathscr{T}}^{\text{dist}_o}(\boldsymbol{x_0}, \boldsymbol{u}, \sigma) = \inf\left\{\text{dist}_o\left(\boldsymbol{x}_{\boldsymbol{x_0}, \boldsymbol{u}, \sigma}^{\boldsymbol{f}}(\mathfrak{t}), \mathscr{T}\right) \;:\; \mathfrak{t} \geq 0\right\}, \end{cases}$$

$$\boldsymbol{\mathcal{G}_{time}} \begin{cases} \mathcal{C}, \\ \text{PF}: \quad (\boldsymbol{x_0}, \boldsymbol{u}, \sigma) \mapsto \mathcal{P}_{\boldsymbol{f}, \mathscr{T}}^{\text{time}}(\boldsymbol{x_0}, \boldsymbol{u}, \sigma) = \inf\left\{\mathfrak{t} \geq 0 \;:\; \boldsymbol{x}_{\boldsymbol{x_0}, \boldsymbol{u}, \sigma}^{\boldsymbol{f}}(\mathfrak{t}) \in \mathscr{T}\right\}. \end{cases}$$

Parameter	Definition	Range
ζ	$\frac{1}{2}\left(R_L + R_C\right)\big/\sqrt{\frac{L}{C}}$	$\frac{\lambda}{2} < \zeta < 1$
λ	$R_C\big/\sqrt{\frac{L}{C}}$	$0 < \lambda < \min\{1, 2\zeta\}$
ρ	$\sqrt{\frac{L}{C}}\Big/\left(\frac{V_{I\max}}{I_{O\max}}\right)$	$0 < \rho < \frac{\nu - \delta}{\lambda}$
ν	$\left(V_{LL0} + \left(R_C - R_{LL}\right)\frac{I_{O\min}+I_{O\max}}{2}\right)\big/V_{I\max}$	$\nu > \delta + \lambda\rho$
δ	$\left(E - \lvert R_C - R_{LL}\rvert \frac{I_{O\max}-I_{O\min}}{2}\right)\big/V_{I\max}$	$0 < \delta < \nu - \lambda\rho$
$i_o^{\triangledown}$	$I_{O\min}\big/I_{O\max}$	$0 \le i_o^{\triangledown} < 1$
$v_i^{\triangledown}$	$V_{I\min}\big/V_{I\max}$	$0 < v_i^{\triangledown} \le 1$

Table 3.2: If assumptions (A1)–(A9) hold for a *(realistic) buck converter conflict*, then it can be reduced to a *canonical form* characterized by the seven dimensionless *canonical parameters* defined in this table.

3.4.5. From the canonical form back to a realistic form

Given known values for the *seven* canonical parameters (ζ, λ, ρ, ν, δ, $i_o^{\triangledown}$, and $v_i^{\triangledown}$) that verify the necessary conditions (3.52)–(3.54), there is no unique way of obtaining values for the *eleven* realistic parameters (L, R_L, C, R_C, $I_{O\min}$, $I_{O\max}$, $V_{I\min}$, $V_{I\max}$, V_{LL0}, R_{LL} and E). A way to do so, is to choose values for

$$I_{O\max}, \quad V_{I\max}, \quad \omega_n = \frac{1}{\sqrt{LC}}, \quad \text{and} \quad R_M = R_C - R_{LL};$$

such that

$$I_{O\max}, V_{I\max}, \omega_n > 0, \tag{3.55}$$

$$\nu V_{I\max} - R_M \frac{1 + i_o^{\triangledown}}{2} I_{O\max} > 0, \tag{3.56}$$

$$\lambda\rho \frac{V_{I\max}}{I_{O\max}} - R_M \ge 0, \tag{3.57}$$

$$(\nu - \delta - \lambda\rho)\, V_{I\max} + R_M \left(1 - i_o^{\triangledown}\right) I_{O\max} > 0 \quad \text{if } R_M < 0; \tag{3.58}$$

and calculate each realistic parameter as dictated by Table 3.3. The inequalities (3.56) and (3.57) must hold in order to obtain $V_{LL0} > 0$ and $R_{LL} \ge 0$, respectively, as required by assumption (A4). If R_M is chosen negative, the inequality (3.58) must also hold in order to guarantee $V_{LL0} - E - R_{LL}I_{O\max} > 0$, as required by assumption (A6); but if $R_M > 0$, the necessary condition $\nu - \delta - \lambda\rho > 0$ is sufficient to guarantee $V_{LL0} - E - R_{LL}I_{O\max} > 0$, since (according to Table 3.3):

$$V_{LL0} - E - R_{LL}I_{O\max} = (\nu - \delta - \lambda\rho)\, V_{I\max} - \left(\lvert R_M\rvert - R_M\right)\frac{1 - i_o^{\triangledown}}{2} I_{O\max}.$$

The necessary conditions (3.52)–(3.54) in conjunction with (3.55)–(3.58) are *sufficient* conditions to comply with assumptions (A1)–(A9), as can be easily checked.

Observe that if the necessary conditions (3.52)–(3.54) hold and (3.55) hold, then (3.56)–(3.58) also hold for R_M sufficiently small.

Realistic parameter	Synthesised as
L	$(\rho/\omega_n)\,(V_{I\max}/I_{O\max})$
R_L	$(2\zeta - \lambda)\,\rho\,(V_{I\max}/I_{O\max})$
C	$(\omega_n\rho)^{-1}\,(I_{O\max}/V_{I\max})$
R_C	$\lambda\rho\,(V_{I\max}/I_{O\max})$
$I_{O\min}$	$i_o^\triangledown I_{O\max}$
$I_{O\max}$	$I_{O\max}$
$V_{I\min}$	$v_i^\triangledown V_{I\max}$
$V_{I\max}$	$V_{I\max}$
V_{LL0}	$\nu V_{I\max} - R_M I_{O\max}\left(1 + i_o^\triangledown\right)/2$
R_{LL}	$\lambda\rho\,(V_{I\max}/I_{O\max}) - R_M$
E	$\delta V_{I\max} + |R_M|\,I_{O\max}\left(1 - i_o^\triangledown\right)/2$

Table 3.3: Synthesis of a 11-tuple of *realistic parameters* values from a given 7-tuple of *canonical parameters* values $(\zeta, \lambda, \rho, \nu, \delta, i_o^\triangledown, v_i^\triangledown)$ and a choice of values for $I_{O\max}$, $V_{I\max}$, $\omega_n = 1/\sqrt{LC}$ and $R_M = R_C - R_{LL}$.

3.4.6. Geometric parameters

To end this section about the canonical formulation of the buck converter conflict, a new set of derived parameters is introduced.

Let α and β be defined by

$$\alpha \triangleq \operatorname{Arctan}\left(\frac{\zeta}{\sqrt{1-\zeta^2}}\right), \quad \beta \triangleq \operatorname{Arctan}\left(\frac{\zeta-\lambda}{\sqrt{1-\zeta^2}}\right), \tag{3.59}$$

where Arctan is the *principal value function* of the arctangent relation, so that $\alpha, \beta \in \left(-\frac{\pi}{2}, \frac{\pi}{2}\right)$. These two angles depend only on L, R_L, C and R_C as it is shown in figure Figure 3.5. Let also δ_0, δ_1 and δ_2 be defined by

$$\delta_0 \triangleq \frac{\nu}{\delta},$$

$$\delta_1 \triangleq \frac{\rho}{\delta}\frac{1-\zeta^2+(\zeta-\lambda)^2}{\sqrt{1-\zeta^2}} = \frac{\rho}{\delta}\frac{\cos\alpha}{\cos^2\beta},$$

$$\delta_2 \triangleq \frac{1}{\delta}\frac{\sqrt{1-\zeta^2+(\zeta-\lambda)^2}}{\sqrt{1-\zeta^2}} = \frac{1}{\delta}\frac{1}{\cos\beta}.$$

The previous five definitions define a map

$$\left(\zeta, \lambda, \rho, \nu, \delta, i_o^\triangledown, v_i^\triangledown\right) \mapsto \left(\alpha, \beta, \delta_0, \delta_1, \delta_2, i_o^\triangledown, v_i^\triangledown\right) \tag{3.60}$$

on the parameter space of the canonical form. The parameters defined by this map will be referred to as the *geometric parameters* of the conflict (for reasons that will become apparent soon) and are summarized in Table 3.4. Since this map
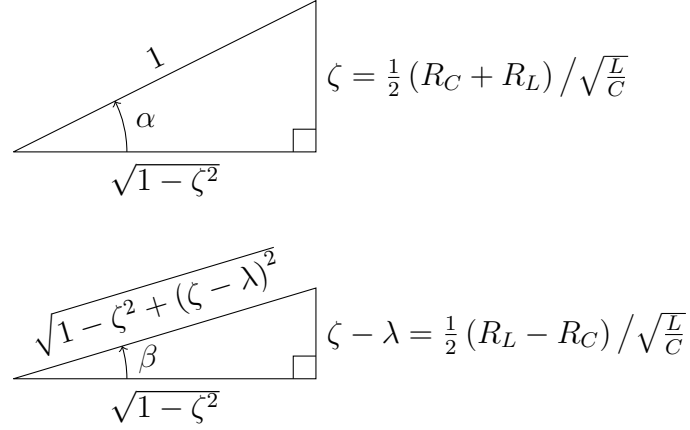
Figure 3.5: Geometric definition of angles α and β.

Geometrical parameter	Definition
α	$\mathrm{Arctan}\left(\frac{\zeta}{\sqrt{1-\zeta^2}}\right)$
β	$\mathrm{Arctan}\left(\frac{\zeta-\lambda}{\sqrt{1-\zeta^2}}\right)$
δ_0	ν/δ
δ_1	$(\rho/\delta)\,\frac{1-\zeta^2+(\zeta-\lambda)^2}{\sqrt{1-\zeta^2}}$
δ_2	$(1/\delta)\,\frac{\sqrt{1-\zeta^2+(\zeta-\lambda)^2}}{\sqrt{1-\zeta^2}}$
i_o^∇	i_o^∇
v_i^∇	v_i^∇

Table 3.4: Definitions of the *geometrical parameters* of a buck conflict. The function Arctan that appears in the table is the *principal value function* of the arctangent relation.

is invertible (see Table 3.5), it is clear that any *realistic buck converter conflict*, once reduced to its *canonical from*, can be characterized equally well by its *canonical parameters* or by its *geometrical parameters*. The only geometric parameter that can take a non-positive value is β, in case $R_L \leq R_C$. The rest of the geometric parameters are positive by definition.

As the canonical parameters, the geometric parameters are not all independent. Indeed, they must satisfy

$$0 < \alpha < \frac{\pi}{2}, \quad -\alpha < \beta < \alpha, \qquad\qquad \tan\alpha - \tan\beta < \sec\alpha, \quad (3.61)$$

$$\delta_1, \delta_2 > 0, \quad \delta_0 > 1 + (\tan\alpha - \tan\beta)\,\delta_1\cos^2\beta, \qquad\qquad (3.62)$$

$$0 \leq i_o^\nabla < 1, \quad 0 < v_i^\nabla \leq 1. \qquad\qquad (3.63)$$

so that if they are converted into canonical parameters (as detailed in Table 3.5),

Canonical parameter	Expression in terms of geometrical parameters
ζ	$\sin \alpha$
λ	$\cos \alpha \left(\tan \alpha - \tan \beta \right)$
ρ	$\left(\delta_1/\delta_2 \right) \left(\frac{\cos \beta}{\cos \alpha} \right)$
ν	$\left(\delta_0/\delta_2 \right) \left(\frac{1}{\cos \beta} \right)$
δ	$\left(1/\delta_2 \right) \left(\frac{1}{\cos \beta} \right)$
$i_o^{\triangledown}$	$i_o^{\triangledown}$
$v_i^{\triangledown}$	$v_i^{\triangledown}$

Table 3.5: Conversion from *geometric parameters* to *canonical parameters*.

the necessary conditions (3.52)–(3.54) are fulfilled. In particular, the inequalities (3.61) are consequence of (3.52) and definitions (3.59) for α and β (see Figure 3.5); and in (3.62) the inequality $\delta_0 > 1 + \left(\tan \alpha - \tan \beta \right) \delta_1 \cos^2 \beta$ results from requiring $\frac{\nu}{\delta} > 1 + \frac{\lambda \rho}{\delta}$ as imposed by (3.54). Accordingly, observe that $\delta_0 = \frac{\nu}{\delta} > 1$.

3.5. Geometric interpretation of the canonical conflict

The canonical form derived in the previous section not only reduces the dimension of the original parameter space, but it also formulates the conflict in a way amenable to geometric reasoning. In order to exploit this, using a succinct mathematical language, the standard representation of complex numbers as points of the Euclidean plane will be employed. However, we take Ahlfors' [71] point of view that conclusions in analysis should be derived from the properties of real numbers, and not from the axioms of geometry, thereby relieving us from the exigencies of rigor in connection with geometric considerations.

To follow this approach to plane geometry, described by Zwikker [72] as "the geometrical interpretation of identities in complex numbers", in this section the canonical conflict is reformulated in the complex plane. Before doing this, some basic facts about complex analysis are recalled to fix notation.

3.5.1. Identification of the Euclidean plane with the set of complex numbers

Throughout this thesis, almost standard notation of *complex analysis* is used (see, for instance, [71] for a thorough treatment of this branch of mathematical analysis). The set of all complex numbers, the *complex plane*, is denoted $\mathbb{C}$. For every element $z = \xi + j\eta$ in $\mathbb{C}$ (where $\xi, \eta \in \mathbb{R}$ and where j is the *imaginary unit*) the *real part* of z, ξ, is denoted $\Re z$; the *imaginary part* of z, η, is denoted $\Im z$; and the *complex conjugate* of z, $\xi - j\eta$, is denoted $\bar{z}$. The *absolute value* of z is $|z| \triangleq \sqrt{z\bar{z}} = \sqrt{\xi^2 + \eta^2}$ (it is understood that all square roots of positive numbers

are taken with the positive sign).

The *exponential function* $z \mapsto e^z$ can be characterized in a variety of equivalent ways. Typically, it is defined in $\mathbb{C}$ by $e^z \triangleq \sum_{n=0}^{\infty} \frac{z^n}{n!}$, after having proved the convergence of the series for every $z \in \mathbb{C}$. Equipped with the exponential function, the *trigonometric functions* are defined by $\cos z \triangleq \frac{e^{jz} + e^{-jz}}{2}$ and $\sin z \triangleq \frac{e^{jz} - e^{-jz}}{2}$, and Euler's formula, $e^{jz} = \cos z + j \sin z$, can be inferred.

For every $z \in \mathbb{C} \setminus \{0\}$, a *logarithm* of z, denoted $\log z$, is any complex number of the set $\{w \in \mathbb{C} : e^w = z\}$. The *principal logarithm* of z, denoted $\operatorname{Log} z$, is the unique element of the set whose imaginary part lies in the interval $(-\pi, \pi]$. The *principal argument* of z, denoted $\operatorname{Arg} z$, is the imaginary part of $\operatorname{Log} z$, and an *argument* of z, denoted $\arg z$, is the imaginary part of any logarithm of z.

To go back and forth between $\mathbb{R}^2$ and $\mathbb{C}$, consider the function $\operatorname{cplx} : \mathbb{R}^2 \to \mathbb{C}$ defined by $\operatorname{cplx}(\boldsymbol{x}) \triangleq \langle \boldsymbol{x}, \hat{\boldsymbol{e}}_{\boldsymbol{1}} \rangle + j \langle \boldsymbol{x}, \hat{\boldsymbol{e}}_{\boldsymbol{2}} \rangle$ for every $\boldsymbol{x} \in \mathbb{R}^2$. It has an inverse function $\operatorname{cplx}^{-1} : \mathbb{C} \to \mathbb{R}^2$ given by $\operatorname{cplx}^{-1}(z) = (\Re z) \hat{\boldsymbol{e}}_{\boldsymbol{1}} + (\Im z) \hat{\boldsymbol{e}}_{\boldsymbol{2}}$ for every $z \in \mathbb{C}$. Note that

$$\forall \boldsymbol{x}_{\boldsymbol{1}}, \boldsymbol{x}_{\boldsymbol{2}} \in \mathbb{R}^2 \qquad \operatorname{cplx}(\boldsymbol{x}_{\boldsymbol{1}} + \boldsymbol{x}_{\boldsymbol{2}}) = \operatorname{cplx}(\boldsymbol{x}_{\boldsymbol{1}}) + \operatorname{cplx}(\boldsymbol{x}_{\boldsymbol{2}}), \qquad (3.64)$$

$$\forall \boldsymbol{x} \in \mathbb{R}^2, \forall \mu \in \mathbb{R} \qquad \operatorname{cplx}(\mu \boldsymbol{x}) = \mu \operatorname{cplx}(\boldsymbol{x}), \qquad (3.65)$$

$$\forall \boldsymbol{x}_{\boldsymbol{1}}, \boldsymbol{x}_{\boldsymbol{2}} \in \mathbb{R}^2 \qquad \langle \boldsymbol{x}_{\boldsymbol{1}}, \boldsymbol{x}_{\boldsymbol{2}} \rangle = \Re \langle \operatorname{cplx}(\boldsymbol{x}_{\boldsymbol{1}}), \operatorname{cplx}(\boldsymbol{x}_{\boldsymbol{2}}) \rangle_{\mathrm{c}}, \qquad (3.66)$$

where $\langle \cdot, \cdot \rangle_{\mathrm{c}}$ is the standard inner product on the *complex* vector space $\mathbb{C}$, defined by $\langle z_1, z_2 \rangle_{\mathrm{c}} \triangleq \overline{z_1} z_2$ for every $z_1, z_2 \in \mathbb{C}$.

The properties (3.64)–(3.66) show that the bijection cplx, is an *isomorphism of Euclidean spaces* [73], since it is an isomorphism of the underlying vector spaces (the *real* vector space $\mathbb{R}^2$ endowed with the standard inner product $\langle \cdot, \cdot \rangle$ and the *real* vector space $\mathbb{C}$ endowed with the inner product $\Re \langle \cdot, \cdot \rangle_{\mathrm{c}}$) that preserves the inner product.

The identification $\mathbb{R}^2 \simeq \mathbb{C}$, provided by cplx, is the standard one used in applications of complex analysis to analytic plane geometry (see, for instance, [74], [75], [72]). Concretely, given a plane endowed with a *Cartesian coordinate system*, each complex number $z \in \mathbb{C}$ is *interpreted* geometrically as the point of coordinates $(\Re z, \Im z)$. In addition, z may also be interpreted as the *(geometric) vector* pointing from the origin of the Cartesian coordinate system to the aforementioned point. As usual, all geometric vectors which can be obtained from each other by translations are identified.

We adopt the convention that whenever the geometric interpretation of a complex number needs to be appealed, both its point representation and its vector representation are denoted by the same lower-case Latin letter that denotes the complex number. Greek letters are reserved to denote real numbers, exclusively.

The reason for preferring complex numbers over elements of $\mathbb{R}^2$ to do analytic geometry, lies in the fact that multiplication is well defined for complex numbers while it is not for pairs of real numbers. Actually, $\mathbb{C}$ is a *field*, while $\mathbb{R}^2$ is not.

$$x \xrightarrow{\ \boldsymbol{T}_{\xi,\eta}\,(\cdot)\ } \boldsymbol{A}_{\xi,\eta}\boldsymbol{x}$$

$$\downarrow \mathrm{cplx}\,(\cdot) \qquad\qquad \downarrow \mathrm{cplx}\,(\cdot)$$

$$z \xrightarrow[\ (\xi + \mathrm{j}\eta)\cdot\ ]{} (\xi + \mathrm{j}\eta)\, z$$

Figure 3.6: The linear planar transformation $\boldsymbol{T}_{\xi,\eta} : \mathbb{R}^2 \to \mathbb{R}^2$, whose matrix in the canonical basis of $\mathbb{R}^2$ is $\boldsymbol{A}_{\xi,\eta}$, corresponds to multiplication by $\xi + \mathrm{j}\eta$, under the identification $\mathbb{R}^2 \simeq \mathbb{C}$ established by the isomorphism $\mathrm{cplx} : \mathbb{R}^2 \to \mathbb{C}$ between both real vector spaces.

3.5.1.1.   Roto-homothety transformations

As will be soon recognized, it is relevant to our application to consider a linear planar operator $\boldsymbol{T}_{\xi,\eta} : \mathbb{R}^2 \to \mathbb{R}^2$ defined by $\boldsymbol{T}_{\xi,\eta}\,(\boldsymbol{x}) = \boldsymbol{A}_{\xi,\eta}\boldsymbol{x}$, for every $\boldsymbol{x} \in \mathbb{R}^2$, such that

$$\boldsymbol{A}_{\xi,\eta} = \begin{bmatrix} \xi & -\eta \\ \eta & \xi \end{bmatrix} \tag{3.67}$$

where $\xi, \eta \in \mathbb{R}$ and $\eta \neq 0$. Under the identification $\mathbb{R}^2 \simeq \mathbb{C}$, established by cplx, the application of the operator $\boldsymbol{T}_{\xi,\eta}$ to each element $\boldsymbol{x}$ of $\mathbb{R}^2$, corresponds to multiplication of $z \triangleq \mathrm{cplx}\,(\boldsymbol{x})$ by $\xi + \mathrm{j}\eta$ in $\mathbb{C}$ (as pointed out in [70, Ch. 3]), because

$$\begin{aligned}
\mathrm{cplx}\,(\boldsymbol{A}_{\xi,\eta}\boldsymbol{x}) &= \xi\,\langle \boldsymbol{x}, \hat{\boldsymbol{e}}_1 \rangle - \eta\,\langle \boldsymbol{x}, \hat{\boldsymbol{e}}_2 \rangle + \mathrm{j}\,(\eta\,\langle \boldsymbol{x}, \hat{\boldsymbol{e}}_1 \rangle + \xi\,\langle \boldsymbol{x}, \hat{\boldsymbol{e}}_2 \rangle) \\
&= (\xi + \mathrm{j}\eta)\,(\langle \boldsymbol{x}, \hat{\boldsymbol{e}}_1 \rangle + \mathrm{j}\,\langle \boldsymbol{x}, \hat{\boldsymbol{e}}_2 \rangle) = (\xi + \mathrm{j}\eta)\,\mathrm{cplx}\,(\boldsymbol{x}) \\
&= (\xi + \mathrm{j}\eta)\,z,
\end{aligned}$$

for every $\boldsymbol{x} \in \mathbb{R}^2$. This is illustrated by the commutative diagram shown in Figure 3.6.

Reminding the geometrical interpretation of complex multiplication (see, for instance, [71]) and identifying it with the action of $\boldsymbol{T}_{\xi,\eta}$ on $\mathbb{R}^2$, it follows that $\boldsymbol{T}_{\xi,\eta}$ can be interpreted as a rotation of angle $\mathrm{Arg}\,(\xi + \mathrm{j}\eta)$ around the origin followed or preceded by an homothety of ratio $|\xi + \mathrm{j}\eta|$ with centre at origin.

3.5.1.2.   Dot and cross product of complex numbers

For every $z_1, z_2 \in \mathbb{C}$, let

$$z_1 \odot z_2 \triangleq \frac{\overline{z_1}z_2 + z_1\overline{z_2}}{2} = \Re\langle z_1, z_2 \rangle_{\mathrm{c}} = \Re\,(\overline{z_1}z_2) = |z_1|\,|z_2|\cos\,(\mathrm{Arg}\,z_2 - \mathrm{Arg}\,z_1),$$

$$z_1 \otimes z_2 \triangleq \frac{\overline{z_1}z_2 - z_1\overline{z_2}}{2\mathrm{j}} = \Im\langle z_1, z_2 \rangle_{\mathrm{c}} = \Im\,(\overline{z_1}z_2) = |z_1|\,|z_2|\sin\,(\mathrm{Arg}\,z_2 - \mathrm{Arg}\,z_1).$$

The products $z_1 \odot z_2$ and $z_1 \otimes z_2$ will be referred to as the *dot product* and *cross product*, respectively, of z_1 and z_2.

Observe that if $\boldsymbol{x_1}, \boldsymbol{x_2} \in \mathbb{R}^2$ and $z_1 = \mathrm{cplx}\,(\boldsymbol{x_1})$, $z_2 = \mathrm{cplx}\,(\boldsymbol{x_2})$; then

$$z_1 \odot z_2 = \langle \boldsymbol{x_1}, \boldsymbol{x_2} \rangle = \boldsymbol{x_1}^\top \boldsymbol{x_2},$$

$$z_1 \otimes z_2 = \det \begin{bmatrix} \boldsymbol{x_1} & \boldsymbol{x_2} \end{bmatrix} = \det \begin{bmatrix} \langle \boldsymbol{x_1}, \hat{\boldsymbol{e}}_1 \rangle & \langle \boldsymbol{x_2}, \hat{\boldsymbol{e}}_1 \rangle \\ \langle \boldsymbol{x_1}, \hat{\boldsymbol{e}}_2 \rangle & \langle \boldsymbol{x_2}, \hat{\boldsymbol{e}}_2 \rangle \end{bmatrix};$$

i.e., $\odot$ codifies the standard inner product (also called dot product) in $\mathbb{R}^2$, and $\otimes$ resembles the cross product (also called vector product) in $\mathbb{R}^3$.

3.5.2. Reformulation of the canonical conflict in the complex plane

3.5.2.1. The target set

Recall that the TS of the buck converter conflict in its canonical form (3.51) is $\boldsymbol{\mathscr{T}} = \{ \boldsymbol{x} \in \mathbb{R}^2 \ : \ |\langle \hat{\boldsymbol{e}}_2, \boldsymbol{x} \rangle| \geq 1 \}$. Clearly, if $\mathbb{R}^2 \simeq \mathbb{C}$, by means of the isomorphism $\mathrm{cplx} : \mathbb{R}^2 \to \mathbb{C}$, it is natural to define

$$\mathscr{T} \triangleq \mathrm{cplx}\,(\boldsymbol{\mathscr{T}}) = \{ z \in \mathbb{C} \ : \ |\Im z| \geq 1 \}$$

as the TS in a complex plane reformulation of the conflict, and its complement

$$\mathscr{E} \triangleq \mathrm{cplx}\,(\boldsymbol{\mathscr{E}}) = \{ z \in \mathbb{C} \ : \ |\Im z| < 1 \}$$

as the PS.

3.5.2.2. The state equation

According to (3.51), the SE of the buck converter conflict in its canonical form is

$$\frac{\mathrm{d}\boldsymbol{x}}{\mathrm{d}t} = \boldsymbol{f}\,(\boldsymbol{x}, \boldsymbol{u}, \sigma) = \boldsymbol{A}\boldsymbol{x} + \boldsymbol{B}\boldsymbol{S}\,(\sigma)\,\boldsymbol{u} + \boldsymbol{c}. \tag{3.68}$$

Defining $\boldsymbol{q} : ([i_o^\triangledown, 1] \times [v_i^\triangledown, 1]) \times [0, 1] \to \mathbb{R}^2$ such that

$$\boldsymbol{q}\,(\boldsymbol{u}, \sigma) \triangleq -\boldsymbol{A}^{-1}\,(\boldsymbol{B}\boldsymbol{S}\,(\sigma)\,\boldsymbol{u} + \boldsymbol{c})\,, \tag{3.69}$$

the differential equation (3.68) can be rewritten as

$$\frac{\mathrm{d}\boldsymbol{x}}{\mathrm{d}t} = \boldsymbol{f}\,(\boldsymbol{x}, \boldsymbol{u}, \sigma) = \boldsymbol{A}\,(\boldsymbol{x} - \boldsymbol{q}\,(\boldsymbol{u}, \sigma))\,. \tag{3.70}$$

Let $\boldsymbol{b_1} \triangleq \boldsymbol{B}\hat{\boldsymbol{e}}_1$ and $\boldsymbol{b_2} \triangleq \boldsymbol{B}\hat{\boldsymbol{e}}_2$ be the first and second columns of matrix $\boldsymbol{B}$, respectively. For every $\boldsymbol{u} = [i_o, v_i]^\top \in [i_o^\triangledown, 1] \times [v_i^\triangledown, 1]$ and every $\sigma \in [0, 1]$, (3.69) can be expressed as

$$\boldsymbol{q}(\boldsymbol{u}, \sigma) = -\boldsymbol{A}^{-1}\boldsymbol{c} - \boldsymbol{A}^{-1}\boldsymbol{B}\boldsymbol{S}\,(\sigma)\,\boldsymbol{u} = -\boldsymbol{A}^{-1}\boldsymbol{c} - \boldsymbol{A}^{-1}\boldsymbol{B} \begin{bmatrix} 1 & 0 \\ 0 & \sigma \end{bmatrix} \begin{bmatrix} i_o \\ v_i \end{bmatrix} =$$

$$= -\boldsymbol{A}^{-1}\boldsymbol{c} - \boldsymbol{A}^{-1}\boldsymbol{b_1}i_o - \boldsymbol{A}^{-1}\boldsymbol{b_2}v_i\sigma,$$

59

where

$$-\boldsymbol{A}^{-1}\boldsymbol{c} = -\delta_0\hat{\boldsymbol{e}}_{\boldsymbol{2}},$$
$$-\boldsymbol{A}^{-1}\boldsymbol{b_1} = \delta_1\left(\cos 2\beta\hat{\boldsymbol{e}}_{\boldsymbol{1}} - \sin 2\beta\hat{\boldsymbol{e}}_{\boldsymbol{2}}\right),$$
$$-\boldsymbol{A}^{-1}\boldsymbol{b_2} = \delta_2\left(\sin \beta\hat{\boldsymbol{e}}_{\boldsymbol{1}} + \cos \beta\hat{\boldsymbol{e}}_{\boldsymbol{2}}\right),$$

as can be checked retrieving the definitions of Subsection 3.4.6.

Define sets

$$U \triangleq [i_o^\triangledown, 1] + \mathrm{j}\,[v_i^\triangledown, 1] = \left\{i_o + \mathrm{j}v_i \in \mathbb{C} \;:\; i_o^\triangledown \leq i_o \leq 1, \; v_i^\triangledown \leq v_i \leq 1\right\},$$
$$\boldsymbol{\Sigma} \triangleq [0,1] = \left\{\sigma \in \mathbb{R} \;:\; 0 \leq \sigma \leq 1\right\};$$

and functions $\mathsf{q} : U \times \boldsymbol{\Sigma} \to \mathbb{C}$, $f : \mathbb{C} \times U \times \boldsymbol{\Sigma} \to \mathbb{C}$, such that

$$\mathsf{q}\left(u, \sigma\right) \triangleq -\mathrm{j}\delta_0 + \delta_1\mathrm{e}^{-\mathrm{j}2\beta}\Re u + \delta_2\mathrm{e}^{\mathrm{j}\left(\frac{\pi}{2}-\beta\right)}\sigma\Im u,$$
$$f\left(z, u, \sigma\right) \triangleq k\left(z - \mathsf{q}\left(u, \sigma\right)\right).$$

Note that $\boldsymbol{A} = \begin{bmatrix} -\kappa & -1 \\ 1 & -\kappa \end{bmatrix}$, where

$$\kappa \triangleq \frac{\zeta}{\sqrt{1-\zeta^2}} = \tan\alpha,$$

so $\boldsymbol{A}$ has the form (3.67) (with $\xi = -\kappa$ and $\eta = 1$). Identifying the action of $\boldsymbol{x} \mapsto \boldsymbol{A}\boldsymbol{x}$ on $\mathbb{R}^2$ with multiplication by

$$k \triangleq -\kappa + \mathrm{j}$$

in $\mathbb{C}$, the state equation (3.70) can be treated as a single scalar equation

$$\dot{z} = f\left(z, u, \sigma\right) = k\left(z - \mathsf{q}\left(u, \sigma\right)\right), \tag{3.71}$$

where $z = \mathrm{cplx}\left(\boldsymbol{x}\right)$ and Newton's dot notation denotes derivation with respect to normalized time t.

The control signals $\mathsf{t} \mapsto \boldsymbol{v} = i_O\hat{\boldsymbol{e}}_{\boldsymbol{1}} + v_I\hat{\boldsymbol{e}}_{\boldsymbol{2}}$ and $\mathsf{t} \mapsto \sigma$ were assumed to be piecewise continuous in Section 3.2, so $\mathsf{t} \mapsto u = \frac{i_O}{I_{O\max}} + \mathrm{j}\frac{v_I}{V_{I\max}} = i_o + \mathrm{j}v_i$ and $\mathsf{t} \mapsto \sigma$ are piecewise continuous in (3.71). This guarantees, for every $z_0 \in \mathbb{C}$, the existence of an unique continuous solution

$$z_{z_0,u,\sigma}^f\left(\mathsf{t}\right) = \mathrm{e}^{k\mathsf{t}}z_0 - k\int_0^{\mathsf{t}}\mathrm{e}^{k(\mathsf{t}-s)}\mathsf{q}\left(u\left(s\right), \sigma\left(s\right)\right)\,\mathrm{d}s \tag{3.72}$$

of (3.71), such that $z_{z_0,u,\sigma}\left(0\right) = z_0$.

Observe that if u and σ are constant, then $\mathsf{q}\left(u, \sigma\right)$ is constant and (3.72) is the parametrization of a *logarithmic spiral* [72] with centre at $q \triangleq \mathsf{q}\left(u, \sigma\right)$:

$$z_{z_0,u,\sigma}^f\left(\mathsf{t}\right) = q + \mathrm{e}^{k\mathsf{t}}\left(z_0 - q\right) = q + \mathrm{e}^{-\kappa\mathsf{t}}\mathrm{e}^{\mathrm{j}\mathsf{t}}\left(z_0 - q\right).$$

The angle $\mathrm{Arg}\,\frac{\dot{z}}{z-q} = \mathrm{Arg}\,k = \frac{\pi}{2} + \alpha$, between the spiral's tangent, $\dot{z}$, at any of its points, z, and the radius vector, $z - q$; is constant (as it can be directly inferred

from the differential equation (3.71)). For this reason, this kind of spiral is also called *equiangular spiral*. Since $\Re k = -\kappa < 0$, a point moving along the spiral approaches its centre as time increases, and since $\Im k = 1 > 0$ it does so spinning counter-clockwise.

Of course, $\mathsf{q}(u, \sigma)$ needs not be constant, however, *instantaneously*, players P and E can be thought as disputing the position of the centre of an α-*equiangular spiral*, that drives the state evolution (see Figures 3.7 and 3.8). The possible *instantaneous centres* are confined to the set

$$
\begin{aligned}
\mathsf{q}(U, \boldsymbol{\Sigma}) &= \{\mathsf{q}(u, \sigma) \; : \; u \in U, \sigma \in \boldsymbol{\Sigma}\} \\
&= \left\{-\mathrm{j}\delta_0 + \delta_1 \mathrm{e}^{-\mathrm{j}2\beta} i_o + \delta_2 \mathrm{e}^{\mathrm{j}\left(\frac{\pi}{2}-\beta\right)} \sigma v_i \; : \; i_o^{\triangledown} \leq i_o \leq 1, \; v_i^{\triangledown} \leq v_i \leq 1, \; 0 \leq \sigma \leq 1\right\}.
\end{aligned}
$$

This set is a parallelogram in the complex plane (see Figures 3.7 and 3.8) with sides of lengths δ_1 and δ_2, parallel to $\mathrm{e}^{-\mathrm{j}2\beta}$ and $\mathrm{e}^{\mathrm{j}\left(\frac{\pi}{2}-\alpha\right)}$, respectively, whose vertices are:

$$
\begin{aligned}
a &\triangleq -\mathrm{j}\delta_0 + i_o^{\triangledown}\delta_1 \mathrm{e}^{-\mathrm{j}2\beta} &, \\
b &\triangleq -\mathrm{j}\delta_0 + \delta_1 \mathrm{e}^{-\mathrm{j}2\beta} &, \\
c' &\triangleq -\mathrm{j}\delta_0 + \delta_1 \mathrm{e}^{-\mathrm{j}2\beta} + \delta_2 \mathrm{e}^{\mathrm{j}\left(\frac{\pi}{2}-\beta\right)}, \\
d' &\triangleq -\mathrm{j}\delta_0 + i_o^{\triangledown}\delta_1 \mathrm{e}^{-\mathrm{j}2\beta} + \delta_2 \mathrm{e}^{\mathrm{j}\left(\frac{\pi}{2}-\beta\right)}.
\end{aligned}
$$

If v_i is held constant at $v_i = v_i^{\triangledown}$, the possible instantaneous centres are confined to a (smaller) parallelogram

$$
\begin{aligned}
\mathsf{q}\left([i_o^{\triangledown}, 1] + \mathrm{j}v_i^{\triangledown}, \boldsymbol{\Sigma}\right) &= \left\{\mathsf{q}(u, \sigma) \; : \; u \in [i_o^{\triangledown}, 1] + \mathrm{j}v_i^{\triangledown}, \sigma \in [0, 1]\right\} \\
&= \left\{-\mathrm{j}\delta_0 + \delta_1 \mathrm{e}^{-\mathrm{j}2\beta} i_o + \delta_2 \mathrm{e}^{\mathrm{j}\left(\frac{\pi}{2}-\beta\right)} \sigma v_i^{\triangledown} \; : \; i_o^{\triangledown} \leq i_o \leq 1, \; 0 \leq \sigma \leq 1\right\},
\end{aligned}
$$

included in $\mathsf{q}(U, \boldsymbol{\Sigma})$, whose vertices are:

$$
\begin{aligned}
a &= -\mathrm{j}\delta_0 + i_o^{\triangledown}\delta_1 \mathrm{e}^{-\mathrm{j}2\beta} &, \\
b &= -\mathrm{j}\delta_0 + \delta_1 \mathrm{e}^{-\mathrm{j}2\beta} &, \\
c &\triangleq -\mathrm{j}\delta_0 + \delta_1 \mathrm{e}^{-\mathrm{j}2\beta} + v_i^{\triangledown}\delta_2 \mathrm{e}^{\mathrm{j}\left(\frac{\pi}{2}-\beta\right)}, \\
d &\triangleq -\mathrm{j}\delta_0 + i_o^{\triangledown}\delta_1 \mathrm{e}^{-\mathrm{j}2\beta} + v_i^{\triangledown}\delta_2 \mathrm{e}^{\mathrm{j}\left(\frac{\pi}{2}-\beta\right)}.
\end{aligned}
$$

Both parallel parallelograms, $\mathsf{q}(U, \boldsymbol{\Sigma})$ and $\mathsf{q}\left([i_o^{\triangledown}, 1] + \mathrm{j}v_i^{\triangledown}, \boldsymbol{\Sigma}\right)$, have a side in common (the one joining vertices a and b) and coincidence if and only if $v_i^{\triangledown} = 1$ (i.e., $V_{I\min} = V_{I\max}$ in the realistic formulation of the conflict).

The points just defined (listed in Table 3.6 for future reference), will be referred to as *anchor points*. Together with angle α, they represent just another way of characterizing a buck converter conflict, once it has been reduced to its canonical form, however not as minimal as a 7-tuple of canonical parameters (Subsection 3.4.4) or a 7-tuple of geometric parameters (Subsection 3.4.6). Observe that

$$
\begin{aligned}
\mu_1 &\triangleq |b - a| = |c - d| = |c' - d'| = \left(1 - i_o^{\triangledown}\right)\delta_1 \\
\mu_2 &\triangleq |d - a| = |c - b| = v_i^{\triangledown}\delta_2 \\
&\quad |d' - d| = |c' - c| = \delta_2\left(1 - v_i^{\triangledown}\right),
\end{aligned}
$$

Anchor point	Definition
a	$-\mathrm{j}\delta_0 + i_o^\triangledown \delta_1 \mathrm{e}^{-\mathrm{j}2\beta}$
b	$-\mathrm{j}\delta_0 + \delta_1 \mathrm{e}^{-\mathrm{j}2\beta}$
c	$-\mathrm{j}\delta_0 + \delta_1 \mathrm{e}^{-\mathrm{j}2\beta} + v_i^\triangledown \delta_2 \mathrm{e}^{\mathrm{j}\left(\frac{\pi}{2}-\beta\right)}$
d	$-\mathrm{j}\delta_0 + i_o^\triangledown \delta_1 \mathrm{e}^{-\mathrm{j}2\beta} + v_i^\triangledown \delta_2 \mathrm{e}^{\mathrm{j}\left(\frac{\pi}{2}-\beta\right)}$
c'	$-\mathrm{j}\delta_0 + \delta_1 \mathrm{e}^{-\mathrm{j}2\beta} + \delta_2 \mathrm{e}^{\mathrm{j}\left(\frac{\pi}{2}-\beta\right)}$
d'	$-\mathrm{j}\delta_0 + i_o^\triangledown \delta_1 \mathrm{e}^{-\mathrm{j}2\beta} + \delta_2 \mathrm{e}^{\mathrm{j}\left(\frac{\pi}{2}-\beta\right)}$

Table 3.6: *Anchor points* of the canonical conflict in terms of its geometric parameters.

where μ_1 and μ_2 are defined as the side lengths of the parallelogram $\mathsf{q}\left([i_o^\triangledown, 1] + \mathrm{j}v_i^\triangledown, \mathbf{\Sigma}\right)$ (see Figures 3.7 and 3.8).

3.5.2.3. The conflict in the complex plane

In conclusion, under assumptions (A1)–(A9), every buck converter conflict $\mathcal{C}'$ (3.29), can be put in the following simple form

$$\mathcal{C}\begin{cases} \text{SE}: & \frac{\mathrm{d}z}{\mathrm{d}t} = f\left(z, u, \sigma\right) = k\left(z - \mathsf{q}\left(u, \sigma\right)\right), \\ \text{TS}: & \mathscr{T} = \left\{z \in \mathbb{C} \ : \ |\Im z| \geq 1\right\}; \end{cases} \tag{3.73}$$

where $[0, +\infty) \ni \mathsf{t} \mapsto u\left(\mathsf{t}\right) \in U = \{i_o + \mathrm{j}v_i \in \mathbb{C} \ : \ i_o^\triangledown \leq i_o \leq 1, \ v_i^\triangledown \leq v_i \leq 1\}$ and $[0, +\infty) \ni \mathsf{t} \mapsto \sigma\left(\mathsf{t}\right) \in \mathbf{\Sigma} = \{\sigma \in \mathbb{R} \ : \ 0 \leq \sigma \leq 1\}$ are P's and E's control functions, respectively, $k = -\kappa + \mathrm{j}$, $\kappa > 0$, and $\mathsf{q}: U \times \mathbf{\Sigma} \to \mathbb{C}$ is such that

$$\mathsf{q}\left(u, \sigma\right) = -\mathrm{j}\delta_0 + \delta_1 \mathrm{e}^{-\mathrm{j}2\beta}\Re u + \delta_2 \mathrm{e}^{\mathrm{j}\left(\frac{\pi}{2}-\beta\right)}\sigma\Im u.$$

The conflict $\mathcal{C}$ is just the translation of the canonical formulation $\mathcal{C}$ (see (3.51)) from $\mathbb{R}^2$ to $\mathbb{C}$, by means of the standard identification $\mathbb{R}^2 \simeq \mathbb{C}$. The sets U and $\mathbf{\Sigma}$, are P's and E's control sets, respectively.

The conflict reformulation process $\mathcal{C}' \rightsquigarrow \mathcal{C} \rightsquigarrow \mathcal{C}$, demands consistent reformulation processes, $\mathcal{G_{dist}}' \rightsquigarrow \mathcal{G_{dist}} \rightsquigarrow \mathcal{G}_{\text{dist}}$ and $\mathcal{G_{time}}' \rightsquigarrow \mathcal{G_{time}} \rightsquigarrow \mathcal{G}_{\text{time}}$, of the accompanying games, to end with:

$$\mathcal{G}_{\text{dist}}\begin{cases} \mathcal{C}, \\ \text{PF}: & \left(z_0, u, \sigma\right) \mapsto \mathcal{P}_{f, \mathscr{T}}^{\text{dist}_{\mathrm{o}}}\left(z_0, u, \sigma\right) \triangleq \inf\left\{\mathrm{d}_{\mathrm{o}}\left(z_{z_0, u, \sigma}^f\left(\mathsf{t}\right), \mathscr{T}\right) \ : \ \mathsf{t} \geq 0\right\}, \end{cases} \tag{3.74}$$

$$\mathcal{G}_{\text{time}}\begin{cases} \mathcal{C}, \\ \text{PF}: & \left(z_0, u, \sigma\right) \mapsto \mathcal{P}_{f, \mathscr{T}}^{\text{time}}\left(z_0, u, \sigma\right) \triangleq \inf\left\{\mathsf{t} \geq 0 \ : \ z_{z_0, u, \sigma}^f\left(\mathsf{t}\right) \in \mathscr{T}\right\}. \end{cases}$$

The function $\mathrm{d}_{\mathrm{o}}: \mathbb{C} \times 2^{\mathbb{C}} \setminus \{\emptyset\} \to \mathbb{R}$ is an oriented distance function that takes the place of $\text{dist}_{\mathrm{o}}: \mathbb{R}^2 \times 2^{\mathbb{R}^2} \setminus \{\emptyset\} \to \mathbb{R}$ as a consequence of the reformulation of the game in distance from $\mathbb{R}^2$ to $\mathbb{C}$. It is naturally defined by

$$\mathrm{d}_{\mathrm{o}}\left(z, \mathscr{W}\right) \triangleq \begin{cases} +\mathrm{d}\left(z, \mathscr{W}\right) & \text{if } z \in \mathscr{W}^{\complement}, \\ -\mathrm{d}\left(z, \mathscr{W}^{\complement}\right) & \text{if } z \in \mathscr{W}; \end{cases}$$

where $\mathscr{W}^{\complement} = \mathbb{C} \setminus \mathscr{W}$, and $\mathrm{d}\,(z, \mathscr{W}) \triangleq \inf_{w \in \mathscr{W}} |z - w|$ for every $z \in \mathbb{C}$ and every non-empty subset $\mathscr{W}$ of $\mathbb{C}$.

It is understood that $\mathcal{P}_{f,\mathscr{T}}^{\mathrm{dist_o}}(z_0, u, \sigma) = -\infty$ if $\left\{ \mathrm{d_o}\left(z_{z_0,u,\sigma}^f(\mathfrak{t}), \mathscr{T}\right) \ : \ \mathfrak{t} \geq 0 \right\}$ is not bounded below, and $\mathcal{P}_{f,\mathscr{T}}^{\mathrm{time}}(z_0, u, \sigma) = +\infty$ if $\left\{\mathfrak{t} \geq 0 \ : \ z_{z_0,u,\sigma}^f(\mathfrak{t}) \in \mathscr{T}\right\}$ is empty; as has been understood for the analogous previous forms of the PFs.

Finally, notice that the oriented distance (in $\mathbb{R}^2$) to the target set $\mathscr{T}'$ (of the original conflict (3.29)) relates to the oriented distance (in $\mathbb{C}$) to the target set $\mathscr{T}$ (of the canonical conflict (3.73)), as follows:

$$\sqrt{R_C^2 + 1}\ \mathrm{dist_o}\,(\boldsymbol{y}, \mathscr{T}') = D\,\mathrm{d_o}\,(z, \mathscr{T}) \tag{3.75}$$

where $z = \begin{bmatrix} 1 & \mathrm{j} \end{bmatrix} \boldsymbol{x} = \langle \boldsymbol{x}, \hat{\boldsymbol{e}}_1 \rangle + \mathrm{j}\langle \boldsymbol{x}, \hat{\boldsymbol{e}}_2 \rangle$ and $\boldsymbol{x} = \boldsymbol{h}^{-1}(\boldsymbol{y}) = \frac{1}{D}\left(\boldsymbol{P}^{-1}\boldsymbol{y} - V\hat{\boldsymbol{e}}_2\right)$, for every $\boldsymbol{y} \in \mathbb{R}^2$. To prove (3.75), substitute $\boldsymbol{y} = \boldsymbol{h}(\boldsymbol{x}) = \boldsymbol{P}\,(D\boldsymbol{x} + V\hat{\boldsymbol{e}}_2)$ into (3.22) to obtain

$$
\begin{aligned}
\mathrm{dist_o}\,(\boldsymbol{y}, \mathscr{T}') &= \frac{1}{||\boldsymbol{l}||}\left(D - \left|V - \boldsymbol{l}^\top \boldsymbol{P}\,(D\boldsymbol{x} + V\hat{\boldsymbol{e}}_2)\right|\right) \\
&= \frac{1}{||\boldsymbol{l}||}\left(D - \left|V - \hat{\boldsymbol{e}}_2^\top (D\boldsymbol{x} + V\hat{\boldsymbol{e}}_2)\right|\right) \\
&= \frac{D}{||\boldsymbol{l}||}\left(1 - |\langle \boldsymbol{x}, \hat{\boldsymbol{e}}_2 \rangle|\right) = \frac{D}{||\boldsymbol{l}||}\left(1 - |\Im z|\right) \\
&= \frac{D}{\sqrt{R_C^2 + 1}}\mathrm{d_o}\,(z, \mathscr{T})\,,
\end{aligned}
$$

where $\boldsymbol{l}^\top = \begin{bmatrix} R_C & 1 \end{bmatrix} = \begin{bmatrix} \lambda R & 1 \end{bmatrix}$, $\boldsymbol{l}^\top \boldsymbol{P} = \hat{\boldsymbol{e}}_2^\top$, and $\mathrm{d_o}\,(z, \mathscr{T}) = 1 - |\Im z|$ were used.

The VF of the original game in distance $\boldsymbol{\mathcal{G}_{\mathrm{dist}}}'$ (formulated in (3.30)) has been already denoted $\mathcal{V}_{\mathrm{dist_o}}$. Let $\mathcal{V}_{\mathrm{d_o}}$ be the VF of the canonical game in distance $\mathcal{G}_{\mathrm{dist}}$ (formulated in the complex plane by (3.74)). According to (3.75), $\mathcal{V}_{\mathrm{dist_o}}$ and $\mathcal{V}_{\mathrm{d_o}}$ must be related by

$$\sqrt{R_C^2 + 1}\ \mathcal{V}_{\mathrm{dist_o}}(\boldsymbol{y}) = D\,\mathcal{V}_{\mathrm{d_o}}(z) \tag{3.76}$$

where $z = \begin{bmatrix} 1 & \mathrm{j} \end{bmatrix} \boldsymbol{x} = \langle \boldsymbol{x}, \hat{\boldsymbol{e}}_1 \rangle + \mathrm{j}\langle \boldsymbol{x}, \hat{\boldsymbol{e}}_2 \rangle$ and $\boldsymbol{x} = \boldsymbol{h}^{-1}(\boldsymbol{y}) = \frac{1}{D}\left(\boldsymbol{P}^{-1}\boldsymbol{y} - V\hat{\boldsymbol{e}}_2\right)$, for every $\boldsymbol{y} \in \mathbb{R}^2$. In addition, from (3.34) and (3.76), $\mathcal{V}_{\mathrm{d_o}}$ can be expressed as

$$D\,\mathcal{V}_{\mathrm{d_o}}(z) = E - \mathcal{V}_{|\mathrm{e^{wc}}|}(\boldsymbol{y}) \tag{3.77}$$

where $\mathcal{V}_{|\mathrm{e^{wc}}|}$ is the VF of the the game $\boldsymbol{\mathcal{G}_{|e^{wc}|}}'$, formulated in (3.33) with P as the supremizer and E as the infimizer. Similarly, from (3.26) and (3.75),

$$D\,\mathrm{d_o}\,(z, \mathscr{T}) = E - |\mathrm{e^{wc}}\,(\boldsymbol{y})|\,. \tag{3.78}$$

3.6. Concluding remarks

Under quite general assumptions, every buck converter control problem, as formulated in this chapter, can be framed in a canonical way as a dynamical
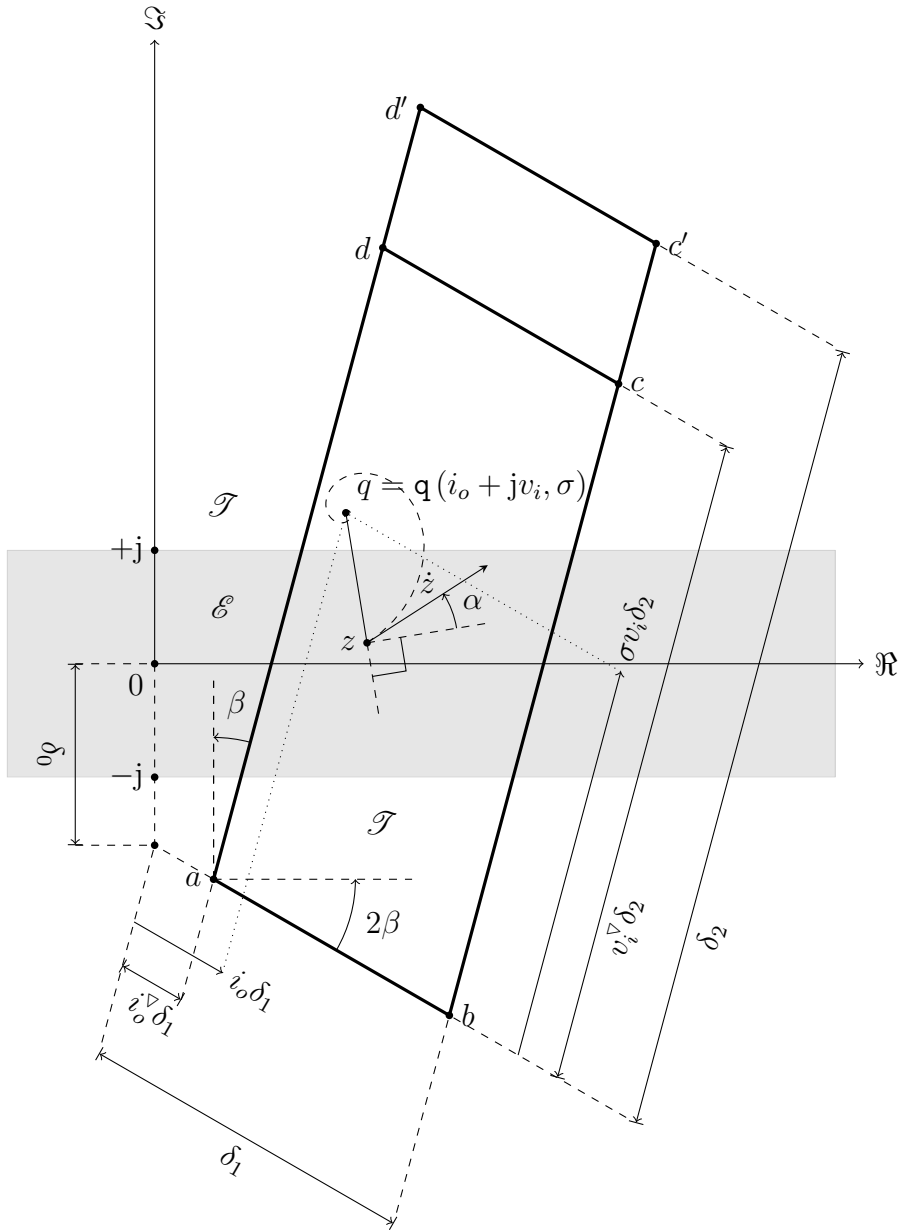
Figure 3.7: Geometric interpretation of the canonical conflict. The conflict is given by seven geometrical parameters: three distances (δ_0, δ_1, δ_2), two less-than-one scaling factors ($i_o^\triangledown$, $v_i^\triangledown$) and two angles (α and β). All these parameters, except for α, determine the fixed *anchor points*: $a, b, c, d, c', d' \in \mathbb{C}$. The playing set is $\mathscr{E} = \{z \in \mathbb{C} : |\Im z| < 1\}$. The target set is $\mathscr{T} = \mathbb{C} \setminus \mathscr{E}$. Instantaneously, the state z moves in the state space following an α-equiangular spiral with centre at $q = \mathsf{q}(i_o + \mathrm{j}v_i, \sigma) = -\mathrm{j}\delta_0 + i_o\delta_1\mathrm{e}^{-\mathrm{j}2\beta} + \sigma v_i\delta_2\mathrm{e}^{\mathrm{j}(\frac{\pi}{2}-\alpha)}$ in the convex hull of $\{a, b, c', d'\}$. The pursuer's control variable is: $u = i_o + \mathrm{j}v_i$, with $i_o \in [i_o^\triangledown, 1]$ and $v_i \in [v_i^\triangledown, 1]$. The evader's control variable is $\sigma \in [0, 1]$. For the case represented in the figure, $\operatorname{sgn}\beta > 0$. Recall that $\operatorname{sgn}\beta = \operatorname{sgn}2\beta = \operatorname{sgn}(R_L - R_C)$ and $\beta = \operatorname{Arg}\frac{\mathrm{j}}{d-a}$
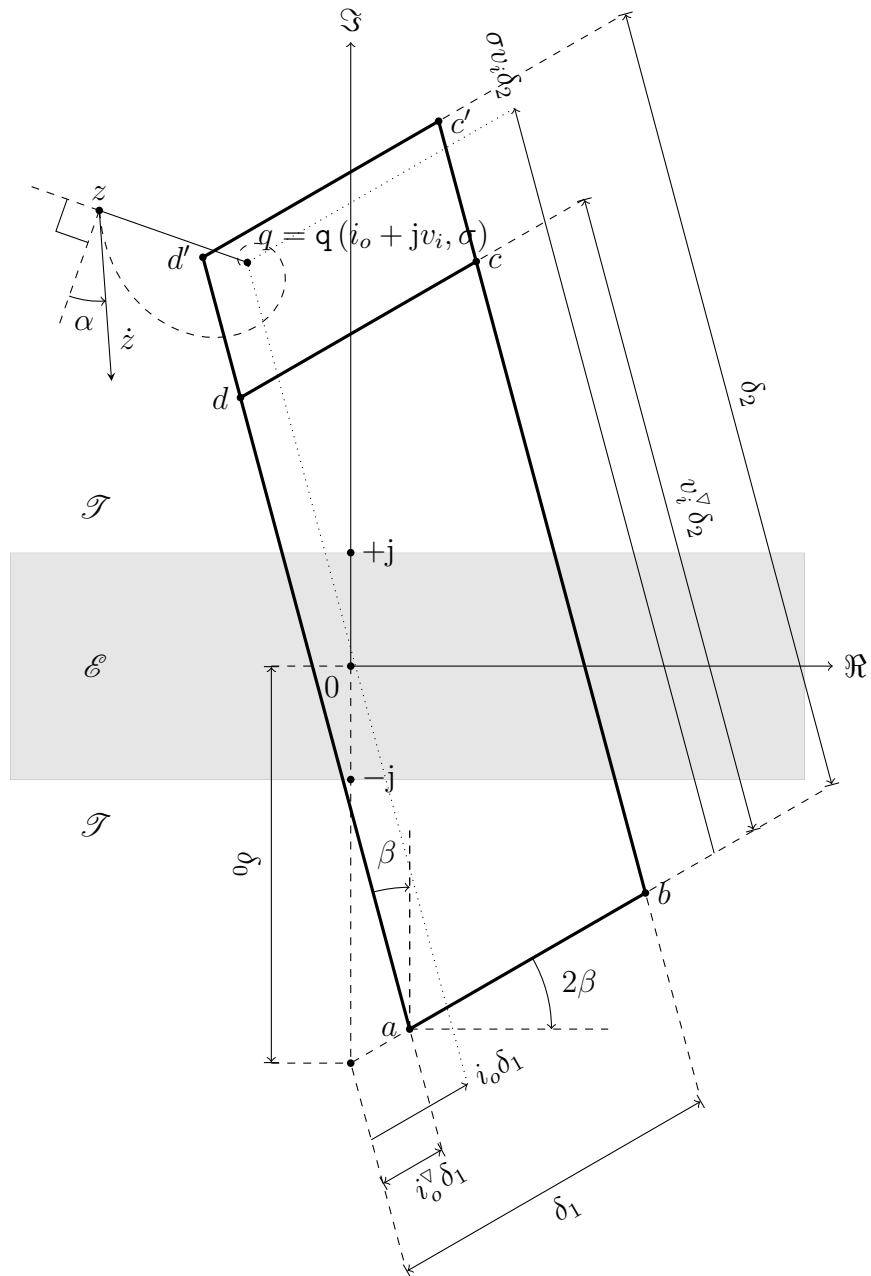
Figure 3.8: Geometric interpretation of the canonical conflict for a case in which $\operatorname{sgn}\beta < 0$. Recall that $\operatorname{sgn}\beta = \operatorname{sgn}2\beta = \operatorname{sgn}(R_L - R_C)$ and $\beta = \operatorname{Arg}\frac{\mathrm{j}}{d-a}$.

conflict between the converter's controller and an hypothetical disturber that acts on the load current and the line voltage.

The canonization, achieved by normalization of the realistic parameters and by transformation of the original state-space, allows to deal with the buck converter problem in a general and consistent way in the realm of differential game theory.

The resulting canonical formulation admits a simple geometric interpretation as a kinematic conflict in the complex plane.

Chapter 4

The conflict's dynamics

4.1. Introduction

The main purpose of this chapter is to prove a few facts about the dynamics of the buck converter conflict, presented in Chapter 3. These facts will be used, in the following chapter, to solve the game in distance associated to the conflict. Hopefully, the concentration of rather technical results herein, will ease the reading of the following chapter which is the main matter of this thesis.

Another purpose of this chapter is to introduce the notation that will be freely used in the following chapter to communicate geometrical ideas sustained by the algebra of complex numbers.

4.2. Definitions and notation

In this section the formulation of the conflict is very briefly reviewed and some notation needed for this and the following chapter is introduced.

4.2.1. Recapitulation of the conflict's formulation

For ease of reference, recall from Chapter 3, that every buck converter conflict can be formulated as a state equation (SE) and a target set (TS) in the complex plane, as follows:

$$\mathcal{C} \begin{cases} \text{SE}: & \frac{\mathrm{d}z}{\mathrm{d}t} = f(z, u, \sigma), \\ \text{TS}: & \mathscr{T} \triangleq \{z \in \mathbb{C} \ : \ |\Im z| \ge 1\}; \end{cases} \tag{4.1}$$

where $f : \mathbb{C} \times U \times \boldsymbol{\Sigma} \to \mathbb{C}$ is defined by

$$f(z, u, \sigma) \triangleq F(z, \mathsf{q}(u, \sigma)),$$

being $F : \mathbb{C} \times \mathbb{C} \to \mathbb{C}$ such that $F(z, q) \triangleq k(z - q)$ and $\mathsf{q} : U \times \boldsymbol{\Sigma} \to \mathbb{C}$ such that $\mathsf{q}(u, \sigma) \triangleq -\mathsf{j}\delta_0 + \delta_1 \mathrm{e}^{-\mathsf{j}2\beta}\Re u + \delta_2 \mathrm{e}^{\mathsf{j}\left(\frac{\pi}{2} - \beta\right)}\sigma\Im u$, where

$$U \triangleq \left\{ i_o + \mathsf{j}v_i \in \mathbb{C} \; : \; i_o^\triangledown \le i_o \le 1, \; v_i^\triangledown \le v_i \le 1 \right\},$$
$$\boldsymbol{\Sigma} \triangleq \left\{ \sigma \in \mathbb{R} \; : \; 0 \le \sigma \le 1 \right\},$$
$$k \triangleq -\kappa + \mathsf{j}, \quad \kappa \triangleq \tan\alpha.$$

Seven real parameters, introduced in Subsection 3.4.6 as *geometric parameters*, characterize the *conflict* $\mathcal{C}$, namely: α, β, δ_0, δ_1, δ_2, $i_o^\triangledown$, and $v_i^\triangledown$. They must satisfy the following inequalities which are derived from modelling assumptions:

$$0 < \alpha < \frac{\pi}{2}, \quad -\alpha < \beta < \alpha, \qquad\qquad\qquad \tan\alpha - \tan\beta < \sec\alpha, \quad (4.2)$$
$$\delta_1, \delta_2 > 0, \quad \delta_0 > 1 + (\tan\alpha - \tan\beta)\,\delta_1 \cos^2\beta, \qquad\qquad (4.3)$$
$$0 \le i_o^\triangledown < 1, \quad 0 < v_i^\triangledown \le 1. \qquad\qquad\qquad\qquad\qquad\qquad (4.4)$$

In (4.1), the SE specifies the *dynamics* of $\mathcal{C}$. It models a buck converter *system* whose *inputs* are: a disturbance action, $u = i_o + \mathsf{j}v_i$, controlled by the pursuer (P); and a switching action, σ, controlled by the evader (E). The real part of the disturbance action, $\Re u = i_o$, is the normalized load current drained from the converter, while its imaginary part, $\Im u = v_i$, is the normalized input voltage supplied to the converter. The SE rules the temporal evolution of the system's state, $z \in \mathbb{C}$, with respect to normalized time t. The other object, present in the formulation of the conflict $\mathcal{C}$, is the TS, which is an essential component of the *game* to be treated in the following chapter but irrelevant for this chapter concerned solely with the conflict's dynamics.

Since it will not be necessary to further refer to the *canonical parameters* (defined in Subsection 3.4.4), hereafter the symbols ζ, λ, ρ, ν, and δ are released from the meaning they had in Chapter 3. By contrast, the symbols $i_o^\triangledown$ and $v_i^\triangledown$ (which are canonical parameters, but also geometrical parameters) retain their meaning.

The *anchor points* a, b, c, d, c', and d', introduced in Subsection 3.5.2 in terms of the geometric parameters, also retain their meaning (see Table 3.6).

4.2.2. Introducing notation to describe subsets of $\mathbb{C}$

For every subset $\mathscr{W}$ of $\mathbb{C}$, the *complement* of $\mathscr{W}$, which is $\mathbb{C} \setminus \mathscr{W}$, is denoted $\mathscr{W}^\complement$. The union of $\mathscr{W}$ and its *boundary* $\partial\mathscr{W}$, is the *closure* of $\mathscr{W}$ which is denoted $\mathrm{cl}(\mathscr{W})$. The *interior* of $\mathscr{W}$, which is $\left(\mathrm{cl}\left(\mathscr{W}^\complement\right)\right)^\complement$, is denoted $\mathrm{int}(\mathscr{W})$. The *convex hull* of $\mathscr{W}$, i.e., the intersection of all *convex* sets that include $\mathscr{W}$, is denoted $\mathrm{conv}(\mathscr{W})$. If $\mathscr{W} \ne \emptyset$, its *diameter*, denoted $\mathrm{diam}(\mathscr{W})$, is $\sup\left\{|w_1 - w_2| \; : \; w_1, w_2 \in \mathscr{Q}\right\}$ (possibly infinite), and the *distance* from a point $z \in \mathbb{C}$ to the set $\mathscr{W}$, denoted $\mathrm{d}(z, \mathscr{W})$, is $\inf_{w \in \mathscr{W}} |z - w|$. If in addition $\mathscr{W}' \ne \emptyset$, the distance from $\mathscr{W}$ to $\mathscr{W}'$, denoted $\mathrm{d}(\mathscr{W}, \mathscr{W}')$, is $\inf_{w \in \mathscr{W}, w' \in \mathscr{W}'} |w - w'|$.

For example, $\mathrm{conv}(\{a, b, c', d'\})$ can be checked to be a parallelogram in the complex plane that coincides with the image of the function $\mathsf{q} : U \times \boldsymbol{\Sigma} \to \mathbb{C}$, denoted $\mathsf{q}(U, \boldsymbol{\Sigma})$.

Given an ordered pair $(z_1, z_2) \in \mathbb{C} \times \mathbb{C}$ such that $z_1 \neq z_2$, the (*oriented*) *half-plane*, *line*, *ray*, and *line segment* determined by the pair (z_1, z_2) are respectively defined as:

$$\mathscr{H}_{z_1, z_2} \triangleq \left\{ z \in \mathbb{C} \ : \ (z_2 - z_1) \otimes (z - z_1) > 0 \right\},$$

$$\overleftrightarrow{z_1 z_2} \triangleq \left\{ z \in \mathbb{C} \ : \ \frac{z - z_1}{z_2 - z_1} \in \mathbb{R} \right\},$$

$$\overrightarrow{z_1 z_2} \triangleq \left\{ z \in \mathbb{C} \ : \ \frac{z - z_1}{z_2 - z_1} \in [0, +\infty) \right\},$$

$$\underline{z_1 z_1} \triangleq \left\{ z \in \mathbb{C} \ : \ \frac{z - z_1}{z_2 - z_1} \in [0, 1] \right\} = \mathrm{conv}\left(\{z_1, z_2\}\right).$$

If $\theta \in \left(-\frac{\pi}{2}, \frac{\pi}{2}\right)$ and $o, z_0 \in \mathbb{C}$, such that $o \neq z_0$, the set

$$\left\{ z - o = \mathrm{e}^{(-\tan\theta + \mathrm{j})\lambda}\left(z_0 - o\right) \ : \ \lambda \in \mathbb{R} \right\}$$

is a *θ-equiangular spiral* centred at $o \in \mathbb{C}$ through z_0. If $\theta \in \left(-\frac{\pi}{2}, 0\right)$, it *expands* in the counter-clockwise direction; if $\theta \in \left(0, \frac{\pi}{2}\right)$, it *shirnks* in the counter-clockwise direction; and if $\theta = 0$, it is a *circumference* through z_0 centred at o.

The remaining part of this subsection is devoted to introduce the notation that will be used hereafter to describe subsets of the complex plane intimately related to the dynamics of the conflict.

As it was already mentioned at the end of the previous chapter, while both players keep their control actions constant, the state traverses an arc of an α-equiangular spiral in the state-space, so this kind of curve and the possible sets delimited by it play a central role in the conflict's dynamics. To efficiently describe these subsets of the complex plane, a *level set method* is introduced next which is supported by a pair of parameter-dependent real-valued complex-variable functions closely related to the pair $\left(|\cdot|, \mathrm{Arg}\left(\cdot\right)\right)$. Before defining each of these two functions, a calculation technique that will be used to calculate their real gradients is briefly introduced next.

4.2.2.1. Wirtinger calculus

Consider a non-constant purely real-valued function $\mathcal{U} : \mathscr{R} \to \mathbb{R}$ defined in a region $\mathscr{R}$ of the complex plane (i.e., in an open connected non-empty subset of $\mathbb{C}$). Let $z = \xi + \mathrm{j}\eta \in \mathscr{R}$, such that $\xi, \eta \in \mathbb{R}$, be the independent variable of $\mathcal{U}$.

Such a function $\mathcal{U}$ does not satisfy the *Cauchy-Riemann equations* in $\mathscr{R}$. If it did, it would be true that

$$\forall z \in \mathscr{R}, \qquad \frac{\partial}{\partial \xi}\Re\mathcal{U} = \frac{\partial}{\partial \eta}\Im\mathcal{U}, \quad \frac{\partial}{\partial \eta}\Re\mathcal{U} = -\frac{\partial}{\partial \xi}\Im\mathcal{U};$$

but this is false because $\Im\mathcal{U}(z) = 0$ and $\Re\mathcal{U}(z) = \mathcal{U}(z)$, for every $z \in \mathscr{R}$. Consequently, $\mathcal{U}$ is not *complex-differentiable* at every $z \in \mathscr{R}$. However, if $\mathcal{U}$ is *real-differentiable* [76] at every $z \in \mathscr{R}$, partial derivatives $\frac{\partial \mathcal{U}}{\partial \xi}(z)$ and $\frac{\partial \mathcal{U}}{\partial \eta}(z)$ exist $\forall z \in \mathscr{R}$; and borrowing from *Wirtinger calculus* [76] the formal equalities

$$\frac{\partial}{\partial z} = \frac{1}{2}\left(\frac{\partial}{\partial \xi} - \mathrm{j}\frac{\partial}{\partial \eta}\right), \qquad \frac{\partial}{\partial \overline{z}} = \frac{1}{2}\left(\frac{\partial}{\partial \xi} + \mathrm{j}\frac{\partial}{\partial \eta}\right),$$

between operators, the real gradient information can be obtained directly within the complex variables framework [77]. Concretely, introducing the notation,

$$\partial \triangleq \frac{\partial}{\partial z}, \qquad \overline{\partial} \triangleq \frac{\partial}{\partial \overline{z}},$$

to derive with respect to z and $\overline{z}$, as if they were independent variables; the gradient of the (underlying) function $\begin{bmatrix} \xi & \eta \end{bmatrix}^\top \mapsto \mathcal{U}(\xi + \mathrm{j}\eta)$, can be computed, at $\begin{bmatrix} \xi_0 & \eta_0 \end{bmatrix}^\top$, as

$$\begin{bmatrix} \Re(2\partial \mathcal{U}(z_0)) \\ -\Im(2\partial \mathcal{U}(z_0)) \end{bmatrix} = \begin{bmatrix} \Re(2\overline{\partial}\mathcal{U}(z_0)) \\ \Im(2\overline{\partial}\mathcal{U}(z_0)) \end{bmatrix},$$

where $z_0 = \xi_0 + \mathrm{j}\eta_0$, for every $\begin{bmatrix} \xi_0 & \eta_0 \end{bmatrix}^\top \in \left\{ \begin{bmatrix} \xi & \eta \end{bmatrix}^\top \in \mathbb{R}^2 \ : \ \xi + \mathrm{j}\eta \in \mathscr{R} \right\}$. To facilitate the identification with the vector calculus notation used in Chapter 2, let

$$\nabla \triangleq 2\overline{\partial}.$$

Note, however, that $\boldsymbol{\nabla}$ (bold type) is reserved to be applied to real-valued functions defined on $\mathbb{R}^n$ instead of $\mathbb{C}$.

With the above notation, if $\mathcal{U} : \mathscr{R} \to \mathbb{R}$ is a real-valued complex variable function that is real-differentiable in $\mathscr{R}$, its *real gradient* at $z_0 = \xi_0 + \mathrm{j}\eta_0 \in \mathscr{R}$ is defined as

$$\nabla \mathcal{U}(z_0).$$

4.2.2.2. A customized argument function

Given $o, v \in \mathbb{C}$, such that $v \neq 0$, define $\mathcal{A}_o^v : \mathbb{C} \setminus \{o\} \to (-\pi, \pi]$ such that

$$\mathcal{A}_o^v(z) \triangleq \operatorname{Arg} \frac{z-o}{v} = \Im \operatorname{Log} \frac{z-o}{v} = \frac{1}{2\mathrm{j}} \left(\operatorname{Log} \frac{z-o}{v} - \overline{\operatorname{Log} \frac{z-o}{v}} \right),$$

$$= \begin{cases} \frac{1}{2\mathrm{j}} \left(\operatorname{Log} \frac{z-o}{v} - \operatorname{Log} \frac{\overline{z}-\overline{o}}{\overline{v}} \right), & \text{if } z \notin \{o - \rho v \ : \ \rho > 0\}, \\ \frac{1}{2\mathrm{j}} \left(\operatorname{Log} \frac{z-o}{v} - \operatorname{Log} \frac{\overline{z}-\overline{o}}{\overline{v}} + \mathrm{j}2\pi \right) & \text{if } z \in \{o - \rho v \ : \ \rho > 0\}; \end{cases} \tag{4.5}$$

where $\operatorname{Arg} : \mathbb{C} \setminus \{0\} \to (-\pi, \pi]$ is the principal argument function, and $\operatorname{Log} : \mathbb{C} \setminus \{0\} \to \{z \in \mathbb{C} \ : \ -\pi < \Im z \leq \pi\}$ is the principal logarithm function. Observe that $\mathcal{A}_o^v$ is discontinuous in $\{o - \rho v \ : \ \rho > 0\}$, but it is continuous in the following region of $\mathbb{C}$:

$$\mathscr{R}_o^v \triangleq \mathbb{C} \setminus \{o - \rho v \ : \ \rho \geq 0\}.$$

The distinction between two different cases becomes necessary after the last equality in (4.5) because for every $w \in \mathbb{C}$ such that $\operatorname{Arg} w = \pi$, the equality $\overline{\operatorname{Log} w} = \operatorname{Log} \overline{w}$ does not hold. Indeed, if $\operatorname{Arg} w = \pi$, then $\overline{\operatorname{Log} w} = \overline{\ln|w| + \mathrm{j}\pi} = \ln|w| - \mathrm{j}\pi = \ln|w| + \mathrm{j}\pi - \mathrm{j}2\pi = \operatorname{Log} \overline{w} - \mathrm{j}2\pi \neq \operatorname{Log} \overline{w}$.

Since $\mathcal{A}_o^v(z)$ has been purposely expressed in terms of z and $\overline{z}$ in (4.5), Wirtinger calculus can be applied to readily obtain

$$\nabla \mathcal{A}_o^v(z) = 2\overline{\partial}\mathcal{A}_o^v(z) = \frac{1}{\mathrm{j}} \left(-\frac{\overline{v}}{\overline{z}-\overline{o}} \right) \frac{1}{\overline{v}} = \mathrm{j}\frac{z-o}{|z-o|^2}, \tag{4.6}$$

for every $z \in \mathscr{R}_o^v$.

For every $\theta \in (-\pi, \pi]$, verify that $\{z \in \mathbb{C} \setminus \{o\} \;:\; \mathcal{A}_o^v(z) = \theta\}$ coincides with $\left\{ o + \rho e^{j\theta} \frac{v}{|v|} \;:\; \rho > 0 \right\}$, i.e., every θ-level set of $\mathcal{A}_o^v$ is a ray with endpoint at o and orientation given by $e^{j\theta} \frac{v}{|v|}$.

For every subset I of $(-\pi, \pi]$, let

$$\mathscr{A}_{o,I}^v \triangleq \{z \in \mathbb{C} \setminus \{o\} \;:\; \mathcal{A}_o^v(z) \in I\}.$$

Clearly, if I is a subinterval of $(-\pi, \pi]$, the set $\mathscr{A}_{o,I}^v$ is just the sector of the complex plane, of amplitude $\sup \{|\theta_1 - \theta_2| \;:\; \theta_1, \theta_2 \in I\}$ and vertex at o, that is obtained by union of the rays $\left\{ o + \rho e^{j\theta} \frac{v}{|v|} \;:\; \rho > 0 \right\}$ such that $\theta \in I$, i.e.,

$$\mathscr{A}_{o,I}^v = \left\{ o + \rho e^{j\theta} \frac{v}{|v|} \;:\; \rho > 0 \;\wedge\; \theta \in I \right\}.$$

4.2.2.3. A customized modulus function

Given $o, v \in \mathbb{C}$, such that $v \neq 0$, another non-constant purely real-valued function, derived from $\mathcal{A}_o^v$, that will be proved to be useful is $\mathcal{M}_o^v : \mathbb{C} \to [0, \infty)$, defined by

$$\mathcal{M}_o^v(z) \triangleq \begin{cases} \left| e^{-k\mathcal{A}_o^v(z)}(z - o) \right| = e^{\kappa \mathcal{A}_o^v(z)} \sqrt{(z - o)(\overline{z} - \overline{o})} & \text{if } z \neq o, \\ 0 & \text{otherwise,} \end{cases}$$

where $\sqrt{\cdot}$ is the principal value of the square root, and $k = -\kappa + j$ being $\kappa = \tan \alpha$. Notice that $\mathcal{M}_o^v(z) > 0$, for every $z \in \mathbb{C} \setminus \{o\}$, and $\mathcal{M}_o^v(z) = 0$ if and only if $z = o$. Furthermore, $\mathcal{M}_o^v$ is continuous and real-differentiable in the region $\mathscr{R}_o^v = \mathbb{C} \setminus \{o - \rho v \;:\; \rho \geq 0\}$.

Again, taking advantage of Wirtinger calculus,

$$\nabla \mathcal{M}_o^v(z) = 2 \overline{\partial} \mathcal{M}_o^v(z)$$

$$= 2 e^{\kappa \mathcal{A}_o^v(z)} \left(\kappa \overline{\partial} \mathcal{A}_o^v(z) \sqrt{(z - o)(\overline{z} - \overline{o})} + \frac{z - o}{2\sqrt{(z - o)(\overline{z} - \overline{o})}} \right)$$

$$= 2 e^{\kappa \mathcal{A}_o^v(z)} \left(\kappa \frac{j}{2} \frac{z - o}{|z - o|^2} \sqrt{(z - o)\overline{(z - o)}} + \frac{z - o}{2\sqrt{(z - o)\overline{(z - o)}}} \right)$$

$$= e^{\kappa \mathcal{A}_o^v(z)} (1 + j\kappa) \frac{z - o}{|z - o|} = e^{\kappa \mathcal{A}_o^v(z)} (-jk) \frac{z - o}{|z - o|} \tag{4.7}$$

for every $z \in \mathscr{R}_o^v$.

For every $\rho \in [0, \infty)$, verify that the set

$$\mathscr{L}_o^v(\rho) \triangleq \{z \in \mathbb{C} \;:\; \mathcal{M}_o^v(z) = \rho\}$$

coincides with $\left\{ o + \rho \frac{v}{|v|} e^{(-\tan \alpha + j)\theta} \;:\; \theta \in (-\pi, \pi] \right\}$, i.e., every ρ-level set of $\mathcal{M}_o^v$ is an arc, of amplitude 2π, of an α-equiangular spiral centred at o, except for the

71
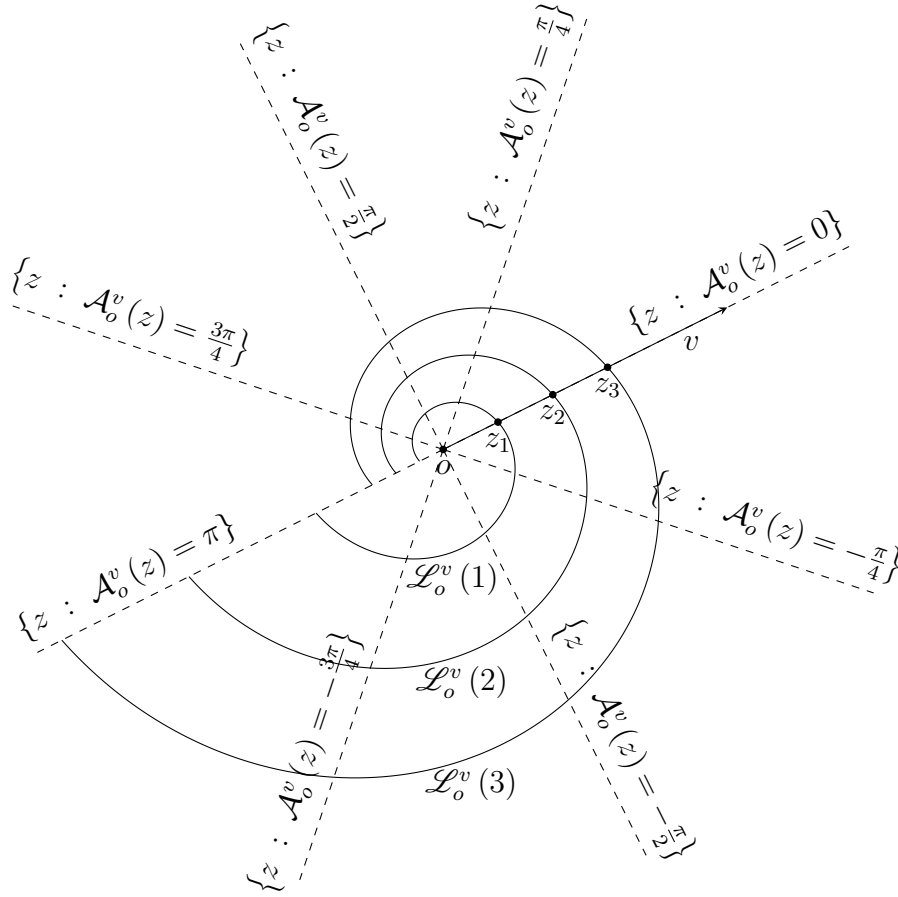
Figure 4.1: Contour diagrams of the functions $\mathcal{M}_o^v : \mathbb{C} \to \mathbb{R}$ (continuous level curves: $\mathscr{L}_o^v(1)$, $\mathscr{L}_o^v(2)$, and $\mathscr{L}_o^v(3)$) and $\mathcal{A}_o^v : \mathbb{C} \to \mathbb{R}$ (dashed level curves). For every $\rho > 0$, let $z_\rho \triangleq o + \rho \frac{v}{|v|}$ and $\mathscr{L}_o^v(\rho) \triangleq \{z \in \mathbb{C} \; : \; \mathcal{M}_o^v(z) = \rho\}$. The level curves $\mathscr{L}_o^v(1)$, $\mathscr{L}_o^v(2)$, and $\mathscr{L}_o^v(3)$, shown in the figure, are arcs of α-equiangular spirals which correspond to the functional values 1, 2, and 3, respectively.

case $\rho = 0$ in which the ρ-level set of $\mathcal{M}_o^v$ degenerates into the singleton $\{o\}$ (see Figure 4.1).

In addition, for every subset I of $(-\pi, \pi]$ let

$$\mathscr{S}_{o,I}^v(\rho) \triangleq \mathscr{L}_o^v(\rho) \cap \mathscr{A}_{o,I}^v = \{z \; : \; \mathcal{M}_o^v(z) = \rho \; \wedge \; \mathcal{A}_o^v(z) \in I\}$$
$$= \left\{o + \rho \frac{v}{|v|} e^{(-\tan\alpha + \mathrm{j})\theta} \; : \; \theta \in I\right\}.$$

Clearly, $\mathscr{S}_{o,I}^v(\rho)$ is an arc of spiral, of amplitude $\sup\{|\theta_2 - \theta_1| \; : \; \theta_2, \theta_1 \in I\}$, included in $\mathscr{L}_o^v(\rho)$.

4.3. Some observations on the system's dynamics

4.3.1. The state equation interpreted geometrically

Coming back to the actual subject of this chapter, reconsider the conflict's formulation as detailed in Subsection 4.2.1. In particular, after scrutinizing the definitions of functions $\mathsf{q} : U \times \boldsymbol{\Sigma} \to \mathbb{C}$ and $F : \mathbb{C} \times \mathbb{C} \to \mathbb{C}$, it is readily realized that the SE in (4.1) has the following form:

$$\dot{z} = f\left(z, u, \sigma\right) = k\left(z - \mathsf{q}\left(z, u, \sigma\right)\right),$$

where $k = -\kappa + \mathsf{j}$ (being $\kappa = \tan\alpha > 0$) and $\mathsf{q}\left(u, \sigma\right) \triangleq -\mathsf{j}\delta_0 + \delta_1 \mathrm{e}^{-\mathsf{j}2\beta}\Re u + \delta_2 \mathrm{e}^{\mathsf{j}\left(\frac{\pi}{2} - \beta\right)}\sigma\Im u$. The players' control functions, $u : [0, +\infty) \to U$ for P and $\sigma : [0, +\infty) \to \boldsymbol{\Sigma}$ for E, take values in

$$U = \left\{i_o + \mathsf{j}v_i \in \mathbb{C} \ : \ i_o^\triangledown \leq i_o \leq 1, \ v_i^\triangledown \leq v_i \leq 1\right\} \quad \text{and} \quad \boldsymbol{\Sigma} = [0, 1],$$

respectively.

The function $\mathsf{q} : U \times \boldsymbol{\Sigma} \to \mathbb{C}$ blends together both system's inputs, u and σ, into a single *compound input* $q \triangleq \mathsf{q}\left(u, \sigma\right)$. The instantaneous value $q\left(\mathsf{t}\right)$, at current time t, may be interpreted as the *instantaneous centre* (introduced in Subsubsection 3.5.2.3) of the α-equiangular spiral, through the current state $z\left(\mathsf{t}\right)$, that would be traversed by the system's state thereupon, if both players decided to keep their controls constant in their current values, $u\left(\mathsf{t}\right)$ and $\sigma\left(\mathsf{t}\right)$, for all future instants. Otherwise stated, the SE

$$\dot{z} = F\left(z, q\right) = k\left(z - q\right) = \sqrt{1 + \kappa^2}\mathrm{e}^{\mathsf{j}\left(\frac{\pi}{2} + \alpha\right)}\left(z - q\right) = \frac{\mathrm{e}^{\mathsf{j}\left(\frac{\pi}{2} + \alpha\right)}}{\cos\alpha}\left(z - q\right)$$

may be regarded point-wisely, and consequently, for every *state* $z \in \mathbb{C}$ and every *compound control action* $q \in \mathsf{q}\left(U, \boldsymbol{\Sigma}\right)$, the *velocity vector* $F\left(z, q\right) = k\left(z - q\right) \in \mathbb{C}$ acquires a clear geometrical interpretation (see Figures 3.7 and 3.8).

4.3.1.1. A notational issue

The aforementioned *point-wise* interpretation of the SE, which is in natural accordance with its *functional* interpretation, is freely exploited throughout this text, whenever necessary, at the cost of notational abuse, i.e., u, σ, $q = \mathsf{q}\left(u, \sigma\right)$ and z may be either *functions* of time or *function values*, depending on the context.

However, when (for the sake of clarity) it is found convenient to distinguish the compound control *function q* from the compound control *action q at a certain instant*, the upper-case letter Q will be used to denote the former.

4.3.1.2. Generalization of the possible compound control actions to an arbitrary set $\mathscr{Q}$

Sometimes, to examine all the possible state's velocity vectors $F\left(z, q\right)$ at a fixed state $z \in \mathbb{C}$, it is convenient to imagine the compound control action q restricted

to belong to a certain non-empty compact subset $\mathscr{Q}$ of the complex plane, not necessarily equal to the parallelogram $\mathsf{q}\,(U, \boldsymbol{\Sigma}) = \mathrm{conv}\,(\{a, b, c', d'\})$. The flexibility of considering an *arbitrary* set $\mathscr{Q} \subset \mathbb{C}$, instead of $\mathsf{q}\,(U, \boldsymbol{\Sigma})$, as the set of all possible compound control actions q, simplifies the exposition that follows. This is the reason why, in Subsection 4.2.1, the function F was defined on $\mathbb{C} \times \mathbb{C}$ and not on $\mathbb{C} \times \mathsf{q}\,(U, \boldsymbol{\Sigma})$. However, it must be remarked, that in any actual case (which respects the conflict's model), it must necessarily be true that $q \in \mathscr{Q} \subseteq \mathsf{q}\,(U, \boldsymbol{\Sigma}) \subset \mathbb{C}$, as exemplified in Figures 3.7 and 3.8.

4.3.1.3. Vectograms

Given $z \in \mathbb{C}$ and $\mathscr{Q} \subset \mathbb{C}$, a *$\mathscr{Q}$-vectogram at z* is defined as the set $F\,(z, \mathscr{Q})$.

Note that the $\mathsf{q}\,(u_0, \boldsymbol{\Sigma})$-vectogram at z is the set $F\,(z, \mathsf{q}\,(u_0, \boldsymbol{\Sigma}))$ of all the alternative velocity vectors allowed to be chosen by E, with the system's state at z, *once* P has irrevocably decided to apply $u_0 \in U$ as his control action. Symmetrically, the $\mathsf{q}\,(U, \sigma_0)$-vectogram at z is the set $F\,(z, \mathsf{q}\,(U, \sigma_0))$ of all alternative velocity vectors allowed to be chosen by P, with the system's state at z, *once* E has irrevocably decided to apply $\sigma_0 \in \boldsymbol{\Sigma}$ as his control action.

4.3.2. State-space trajectories in closed form

With the above considerations in mind, conceive the following initial value problem

$$\begin{cases} \frac{\mathrm{d}z}{\mathrm{d}\mathsf{t}} = F\,(z, Q)\,, \\ z\,(0) = z_0, \end{cases} \tag{4.8}$$

where $z_0 \in \mathbb{C}$ is a given initial value, $Q : [0, +\infty) \to \mathscr{Q}$ is a prescribed piecewise continuous function, and $\mathscr{Q}$ is a non-empty compact subset of $\mathbb{C}$.

The solution $z_{z_0, Q}^F : [0, +\infty) \to \mathbb{C}$ of this initial value problem, is given by

$$z_{z_0, Q}^F\,(\mathsf{t}) = e^{k\mathsf{t}} z_0 - k \int_0^{\mathsf{t}} e^{k(\mathsf{t} - s)} Q\,(s)\;\mathrm{d}s. \tag{4.9}$$

If $\mathscr{Q} \subseteq \mathsf{q}\,(U, \boldsymbol{\Sigma})$, the conflict's model formulation (detailed in Subsection 4.2.1) is respected and, consequently, the expression (4.9) gives, *in closed form*, the state-space trajectory ruled by the SE in (4.1), through $z\,(0) = z_0$, in the particular case in which the control functions $u : [0, +\infty) \to U$ and $\sigma : [0, +\infty) \to \boldsymbol{\Sigma}$ are such that $\mathsf{q}\,(u\,(\mathsf{t})\,, \sigma\,(\mathsf{t})) = Q\,(\mathsf{t})$ for every $\mathsf{t} \geq 0$.

Note that setting the initial time equal to zero in (4.8) carries no loss of generality, due to the system's obvious *time invariance*.

4.3.3. The distant vector field approximation

As a first example of the insight provided by the geometrical interpretation of the SE, the *distant vector field* is commented next. Consider a non-empty compact set $\mathscr{Q} \subset \mathbb{C}$, a fixed point $q_0 \in \mathscr{Q}$, and an arbitrary point z such that $|z - q_0| \gg \mathrm{diam}\,(\mathscr{Q})$ (see Figure 4.2). For every such z which belongs to the exterior of a
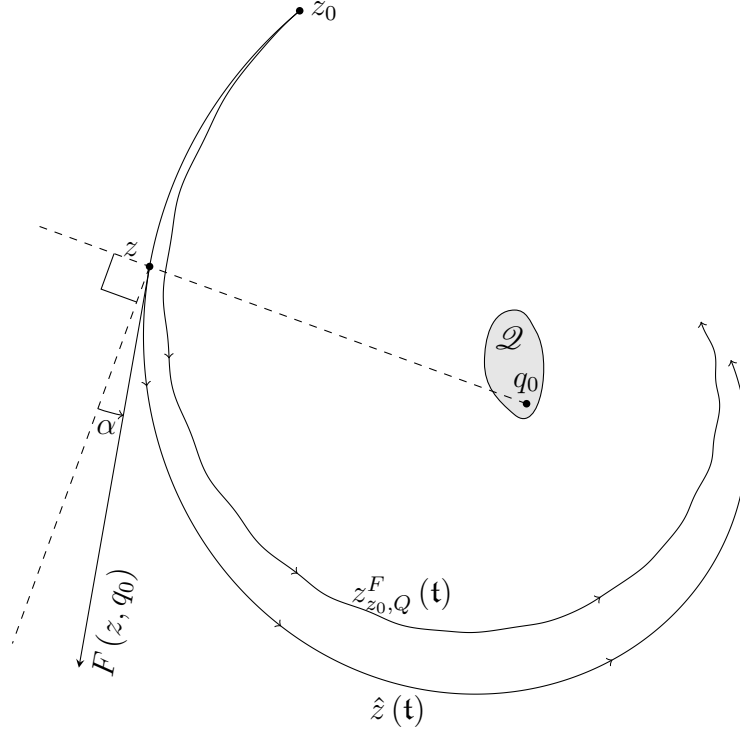
Figure 4.2: For $z \gg \operatorname{diam}(\mathcal{Q})$, the dynamics of the conflict can be approximated by $\dot{z} \approx k\,(z - q_0)$, where q_0 is an arbitrary fixed point of $\mathcal{Q}$. Consequently, for $z_0 \gg \operatorname{diam}(\mathcal{Q})$ and $\mathfrak{t} \in [0, \mathfrak{t}_1]$, the approximation $z_{z_0,Q}^{F}(\mathfrak{t}) \approx \hat{z}(\mathfrak{t}) \triangleq q_0 + \mathrm{e}^{k\mathfrak{t}}\,(z_0 - q_0)$ holds if $\mathfrak{t}_1$ is sufficiently small.

sufficiently large circle centred at q_0, the velocity vector can be approximated as follows:

$$F\,(z, q) = k\,(z - q) = k\,(z - q_0 + q_0 - q) \approx k\,(z - q_0)\,.$$

This means that the influence of the players' control actions u and σ, blended into q, on the velocity vector $f\,(z, u, \sigma) = F\,(z, q)$ is negligibly small if the current state z is sufficiently far away from $\mathcal{Q}$. Accordingly, the solution of (4.8), through an initial state z_0 sufficiently distant from $\mathcal{Q}$, may be approximated by

$$z_{z_0,Q}^{F}(\mathfrak{t}) \approx \hat{z}(\mathfrak{t}) \triangleq q_0 + \mathrm{e}^{k\mathfrak{t}}\,(z_0 - q_0)\,,$$

at least for $\mathfrak{t} \in [0, \mathfrak{t}_1]$ being $\mathfrak{t}_1$ sufficiently small, whatever input function Q is consolidated as the result of both players' continuum decision making process (see Figure 4.2).

4.3.4. The angular transmission property

As a second example of the intuition that can be gained from the geometrical interpretation of the SE, consider three points $z, q, q' \in \mathbb{C}$ such that $z \notin \{q, q'\}$. It

is immediate that

$$\mathrm{Arg}\,\frac{F\left(z,q'\right)}{F\left(z,q\right)} = \mathrm{Arg}\,\frac{k\left(z-q'\right)}{k\left(z-q\right)} = \mathrm{Arg}\,\frac{z-q'}{z-q} = \mathrm{Arg}\,\frac{q'-z}{q-z},$$

which can be interpreted as follows: the relative orientation between the velocity vectors $F\left(z,q'\right)$ and $F\left(z,q\right)$ is the same as the relative orientation between the vectors $q'-z$ and $q-z$ and (see Figure 4.3). Otherwise stated, the angular change $\mathrm{Arg}\,\frac{z-q'}{z-q}$ caused by moving q to q' is *"transmitted"* to the velocity vector, based at z, that changes from $F\left(z,q\right)$ to $F\left(z,q'\right)$.

Now let $z,q,q' \in \mathbb{C}$ without restrictions. Note that

$$\begin{aligned} F\left(z,q\right) \otimes F\left(z,q'\right) &= \Im\left(\overline{k\left(z-q\right)}k\left(z-q'\right)\right) = \Im\left(|k|^2\overline{\left(z-q\right)}\left(z-q'\right)\right) \\ &= |k|^2\Im\left(\overline{\left(q-z\right)}\left(q'-z\right)\right) \\ &= |k|^2\left(q-z\right) \otimes \left(q'-z\right) \end{aligned}$$

and that the projection of $F\left(z,q'\right)$ along $\mathrm{j}F\left(z,q\right)$ is positive if and only if q' belongs to the half-plane $\{w \in \mathbb{C} \; : \; \left(q-z\right) \otimes \left(w-z\right) > 0\}$, because

$$\left(\mathrm{j}F\left(z,q\right)\right) \odot F\left(z,q'\right) = F\left(z,q\right) \otimes F\left(z,q'\right) = |k|^2\left(q-z\right) \otimes \left(q'-z\right). \qquad (4.10)$$

The leftmost equality in this last expression holds because

$$\begin{aligned} \left(\mathrm{j}w_1\right) \odot w_2 = \Re\left(\overline{\mathrm{j}w_1}w_2\right) &= \frac{-\mathrm{j}\overline{w_1}w_2 + \mathrm{j}w_1\overline{w_2}}{2} = \frac{\overline{w_1}w_2 - w_1\overline{w_2}}{2\mathrm{j}} = \Im\left(\overline{w_1}w_2\right) \\ &= w_1 \otimes w_2, \qquad\qquad\qquad\qquad\qquad\qquad\qquad\qquad (4.11) \end{aligned}$$

for every $w_1,w_2 \in \mathbb{C}$.

4.3.5. Four special supporting half-planes of $\mathscr{Q}$

In general, the sign of the real part of the state velocity vector $F\left(z,q\right) = k\left(z-q\right)$, at $z \in \mathbb{C}$, depends on the compound control action $q \in \mathscr{Q}$. However, there are certain regions in $\mathbb{C} \setminus \mathscr{Q}$ where the sign of $\Re F\left(z,q\right)$ is independent of q and thereby independent of both player's control actions. In a like manner, there exist analogous regions in connection with the the sign of $\Im F\left(z,q\right)$. It is next shown that these regions are four supporting half-planes of $\mathscr{Q}$ whose boundaries are directed along $\overline{k}$ and $\mathrm{j}\overline{k}$.

Let $\mathscr{Q}$ be a non-empty compact subset of $\mathbb{C}$, such as the one represented by the curved shape in Figure 4.4. Consider the following sets:

$$\begin{aligned} R^+ &\triangleq \{z \in \mathbb{C} \; : \; \Re F\left(z,q\right) > 0 \quad \forall q \in \mathscr{Q}\} = \{z \in \mathbb{C} \; : \; +1 \odot F\left(z,q\right) > 0 \quad \forall q \in \mathscr{Q}\}, \\ R^- &\triangleq \{z \in \mathbb{C} \; : \; \Re F\left(z,q\right) < 0 \quad \forall q \in \mathscr{Q}\} = \{z \in \mathbb{C} \; : \; -1 \odot F\left(z,q\right) > 0 \quad \forall q \in \mathscr{Q}\}, \\ I^+ &\triangleq \{z \in \mathbb{C} \; : \; \Im F\left(z,q\right) > 0 \quad \forall q \in \mathscr{Q}\} = \{z \in \mathbb{C} \; : \; +\mathrm{j} \odot F\left(z,q\right) > 0 \quad \forall q \in \mathscr{Q}\}, \\ I^- &\triangleq \{z \in \mathbb{C} \; : \; \Im F\left(z,q\right) < 0 \quad \forall q \in \mathscr{Q}\} = \{z \in \mathbb{C} \; : \; -\mathrm{j} \odot F\left(z,q\right) > 0 \quad \forall q \in \mathscr{Q}\}. \end{aligned}$$
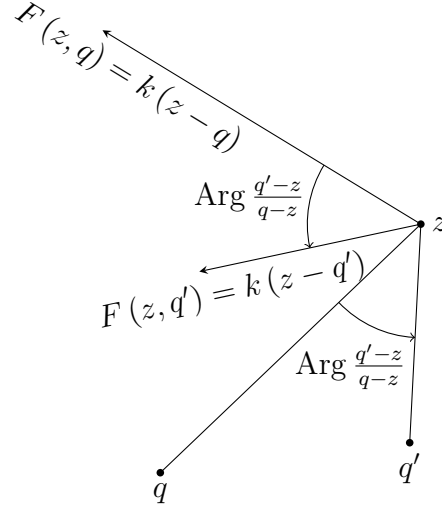
Figure 4.3: Let $z, q, q' \in \mathbb{C}$ such that $z \notin \{q, q'\}$. The relative orientation between vectors $F(z, q)$ and $F(z, q')$ is the same as the relative orientation between vectors $q' - z$ and $q - z$.

The above four sets may be expressed alternatively as

$$R^+ = \left\{ z \in \mathbb{C} \ : \ \left(\mathrm{j}\overline{k}\right) \otimes (z - q) < 0 \quad \forall q \in \mathscr{Q} \right\},$$
$$R^- = \left\{ z \in \mathbb{C} \ : \ \left(\mathrm{j}\overline{k}\right) \otimes (z - q) > 0 \quad \forall q \in \mathscr{Q} \right\},$$
$$I^+ = \left\{ z \in \mathbb{C} \ : \ \overline{k} \otimes (z - q) > 0 \quad \forall q \in \mathscr{Q} \right\},$$
$$I^- = \left\{ z \in \mathbb{C} \ : \ \overline{k} \otimes (z - q) < 0 \quad \forall q \in \mathscr{Q} \right\};$$

since $\pm 1 \odot F(z, q) = \mp \mathrm{j}^2 \odot (k(z - q)) = \mp \left(\mathrm{j}\left(\mathrm{j}\overline{k}\right)\right) \odot (z - q) = \mp \left(\mathrm{j}\overline{k}\right) \otimes (z - q)$ and $\pm \mathrm{j} \odot F(z, q) = \pm \mathrm{j} \odot (k(z - q)) = \pm \left(\mathrm{j}\overline{k}\right) \odot (z - q) = \pm \overline{k} \otimes (z - q)$.

The last expressions for the sets R^+ and R^- make apparent that they are disjoint supporting half-planes of the bounded set $\mathscr{Q}$. Moreover, the parallel boundaries of these two half-planes are directed along $\mathrm{j}\overline{k}$. Analogous observations apply for I^+ an I^-.

In Figure 4.4, the sets R^+, R^-, I^+, and I^- are represented by the overlapping shaded half-planes that lie in $\mathscr{Q}^{\complement}$. Each of these four half-planes is a supporting half-plane of $\mathscr{Q}$. The boundaries of R^+ and R^- are directed along $\mathrm{j}\overline{k}$ while the boundaries of I^+ and I^- are directed along $\overline{k}$. For the example of the figure: $\alpha = \frac{\pi}{6}$ (recall that $k = -\kappa + \mathrm{j}$ where $\kappa = \tan \alpha$).

4.3.6. A relevant particular case: $\mathscr{Q}$ is a line segment

This whole subsection focus on the particular case in which the compound system's input q is restricted to take values in an arbitrary fixed closed segment of the complex plane. The relevance of this particular case is justified next. However, the reader must be aware that the results presented in this subsection will only
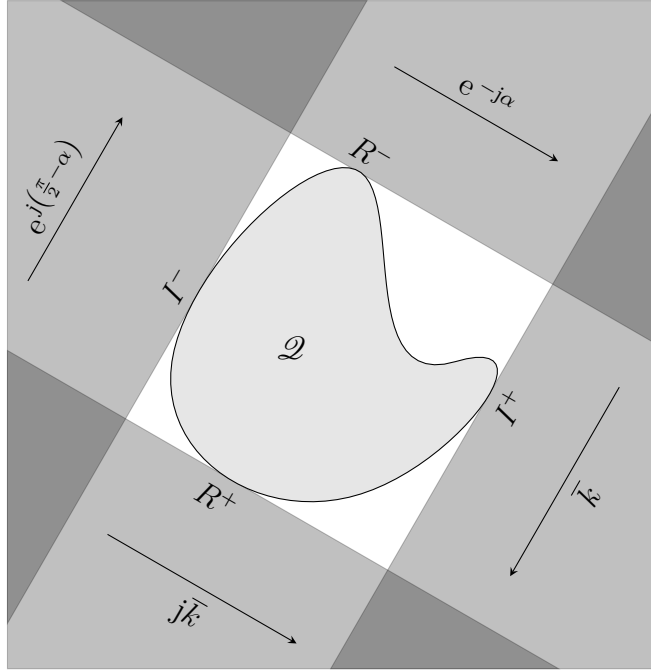
Figure 4.4: The sets R^+, R^-, I^+, and I^- are open supporting half-planes of $\mathscr{Q}$.

become meaningful within the context of solving the conflict's game in distance (Chapter 5).

4.3.6.1. Justification

As it was already mentioned, the compound input q depends on each player's input, u and σ, as prescribed by $\mathsf{q} : U \times \mathbf{\Sigma} \to \mathbb{C}$, which is defined by

$$\mathsf{q}(u, \sigma) \triangleq -\mathrm{j}\delta_0 + \delta_1 \mathrm{e}^{-\mathrm{j}2\beta}\Re u + \delta_2 \mathrm{e}^{\mathrm{j}\left(\frac{\pi}{2}-\beta\right)}\sigma\Im u,$$

being $U \triangleq \{i_o + \mathrm{j}v_i \in \mathbb{C} \ : \ i_o^\triangledown \leq i_o \leq 1, \ v_i^\triangledown \leq v_i \leq 1\}$ and $\mathbf{\Sigma} \triangleq [0,1]$ (see Figures 3.7 and 3.8).

Observe that if P decides to keep u constant with a value $u_0 = i_{o0} + \mathrm{j}v_{i0} \in U$, he forces q to take values in the line segment

$$\mathsf{q}(u_0, \mathbf{\Sigma}) = \left\{ -\mathrm{j}\delta_0 + \delta_1 \mathrm{e}^{-\mathrm{j}2\beta}i_{o0} + \delta_2 \mathrm{e}^{\mathrm{j}\left(\frac{\pi}{2}-\beta\right)}\sigma v_{i0} \ : \ \sigma \in [0,1] \right\}.$$

If E decides to keep σ constant with a value $\sigma_0 \in \mathbf{\Sigma}$, the set

$$\mathsf{q}(U, \sigma_0) = \left\{ -\mathrm{j}\delta_0 + \delta_1 \mathrm{e}^{-\mathrm{j}2\beta}i_o + \delta_2 \mathrm{e}^{\mathrm{j}\left(\frac{\pi}{2}-\beta\right)}\sigma_0 v_i \ : \ i_o \in \left[i_o^\triangledown, 1\right], \ v_i \in \left[v_i^\triangledown, 1\right] \right\}.$$

where he forces q to take values, is a parallelogram in general (included in the larger parallelogram $\mathsf{q}(U, \mathbf{\Sigma})$), but it reduces to a line segment if $\sigma_0 = 0$ or $v_i^\triangledown = 1$. Accordingly, it is not completely devoid of interest the analysis of the conflict's
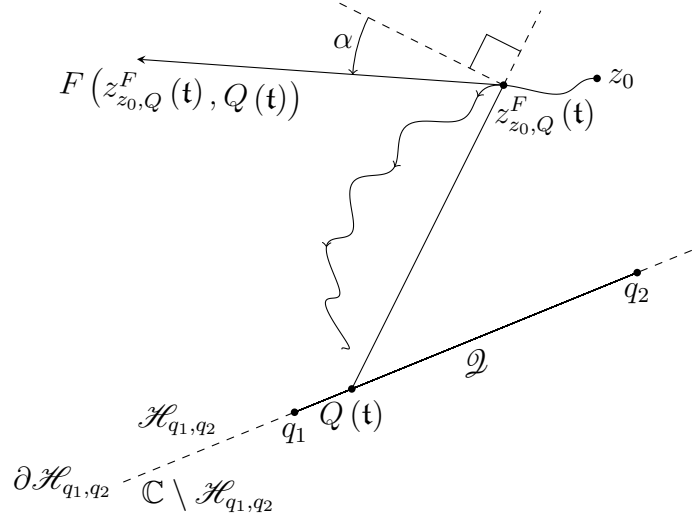
Figure 4.5: Given two fixed points $q_1, q_2 \in \mathbb{C}$, such that $q_1 \neq q_2$, consider the initial value problem, with initial value $z_0 \in \mathscr{H}_{q_1,q_2} = \{z \in \mathbb{C} : (q_2 - q_1) \otimes (z - q_1) > 0\}$, under the assumption that the piecewise-continuous compound input function $Q : [0, +\infty) \to \mathscr{Q}$ is such that $\mathscr{Q} = \operatorname{conv}(\{q_1, q_2\})$.

dynamics in the particular case in which the possible values of the compound input q are restricted to vary piecewise-continuously in a *fixed line segment* of the complex plane. In fact, the understanding of this particular case will allow to explain (in the following chapter) why, for certain region in the parameter space of the conflict, the value function (VF) of the game in distance is constant over some subset of the state space.

Because of the reasons just given, the rest of this subsection is devoted to analyse the initial value problem (4.8) under the following two assumptions: i) the set $\mathscr{Q}$ (the non-empty compact co-domain of the piecewise continuous compound input function Q) is a closed line segment, i.e., $\mathscr{Q} = \underline{q_1 q_2}$, being $q_1, q_2 \in \mathbb{C}$ two fixed points such that $q_1 \neq q_2$; ii) the initial condition of (4.8) is assumed to lie in the oriented half-plane $\mathscr{H}_{q_1,q_2} = \{z \in \mathbb{C} : (q_2 - q_1) \otimes (z - q_1) > 0\}$ (see figure Figure 4.5). Under these assumptions, it will be shown that the solution $z_{z_0,Q}^F$, of (4.8), is such that $z_{z_0,Q}^F(\mathsf{t})$ must come arbitrarily close to the line $\partial \mathscr{H}_{q_1,q_2} = \overleftrightarrow{q_1 q_2}$, in finite time. In addition, sufficient conditions on z_0, for assuring that there exists a finite time $\mathsf{t}_1 > 0$, such that $z_{z_0,Q}^F(\mathsf{t}_1) \in \partial \mathscr{H}_{q_1,q_2}$, will be further investigated.

4.3.6.2. Some possible state-space trajectories when $\mathscr{Q}$ is a line segment

Let $q_1, q_2 \in \mathbb{C}$, such that $q_1 \neq q_2$, be the endpoints points of a fixed line segment $\mathscr{Q} = \underline{q_1 q_2}$. For an initial state $z_0 \in \mathscr{H}_{q_1,q_2}$ sufficiently distant from $\mathscr{Q}$, it is foreseeable that there must exist some finite t_1 such that $z_{z_0,Q}^F(\mathsf{t}_1) \in \partial \mathscr{H}_{q_1,q_2}$, because the trajectory emanating from z_0 approximately spirals around $\mathscr{Q}$ (see Figure 4.2), which in this case coincides with the segment $\underline{q_1 q_2}$. However, for an
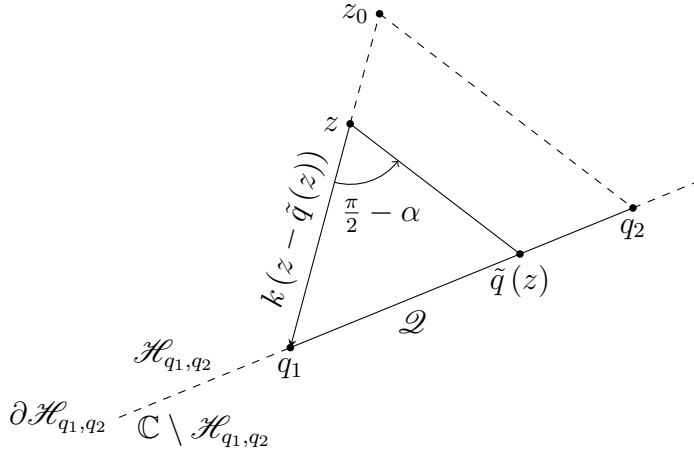
Figure 4.6: Given q_1 and $z_0 \in \mathbb{C} \setminus \{q_1\}$, the feedback law $\tilde{q} : \mathbb{C} \to \mathbb{C}$ such that $\tilde{q}(z) \triangleq q_1 + \left(1 + k^{-1}\right)(z - q_1)$, achieves $F(z, \tilde{q}(z)) = -k(z - \tilde{q}(z)) = -(z - q_1)$ for every $z \in \mathbb{C}$. In addition, the particular definition $q_2 \triangleq \tilde{q}(z_0)$, makes $\tilde{q}(z)$ belong to $\mathscr{Q} \triangleq \mathrm{conv}\left(\{q_1, q_2\}\right)$ for every $z \in \mathrm{conv}\left(\{q_1, z_0\}\right)$, and z_0 belong to $\mathscr{H}_{q_1, q_2} = \{z \in \mathbb{C} : (q_2 - q_1) \otimes (z - q_1) > 0\}$. If $\tilde{q}$ is put into practice, the resulting state-space trajectory, from z_0, tends to $q_1 \in \partial \mathscr{H}_{q_1, q_2}$ as $t \to +\infty$, but it never intersects $\partial \mathscr{H}_{q_1, q_2}$.

initial state z_0 close to $\mathscr{Q}$, such t_1 may not exist.

For example, let q_1 be a fixed point of the complex plane and suppose that both players agree to implement a state feedback law $\tilde{q} : \mathbb{C} \to \mathbb{C}$, given by

$$\tilde{q}(z) = q_1 + \left(1 + k^{-1}\right)(z - q_1), \tag{4.12}$$

for the compound input q. Accordingly, the SE of the feedback system is

$$\dot{z} = F(z, \tilde{q}(z)) = k(z - \tilde{q}(z)) = -(z - q_1),$$

and the resulting trajectory that departs from a given initial state $z_0 \in \mathbb{C} \setminus \{q_1\}$ is $z(t) = q_1 + e^{-t}(z_0 - q_1)$, for every $t \geq 0$. Let $q_2 \triangleq \tilde{q}(z_0) = q_1 + (1 + k^{-1})(z_0 - q_1)$. Note that, for every $t \geq 0$,

$$\begin{aligned}
\tilde{q}(z(t)) &= q_1 + \left(1 + k^{-1}\right) e^{-t}(z_0 - q_1) \\
&= q_1 + e^{-t}(q_2 - q_1) \in \underline{q_1 q_2} = \mathrm{conv}\left(\{q_1, q_2\}\right), \\
(q_2 - q_1) \otimes (z(t) - q_1) &= (q_2 - q_1) \otimes e^{-t}(z_0 - q_1) \\
&= e^{-t} \Im\left(\overline{(1 + k^{-1})(z_0 - q_1)}(z_0 - q_1)\right) \\
&= e^{-t} |z_0 - q_1|^2 \Im\left(\frac{1 - \kappa + j}{1 + \kappa^2}\right) > 0,
\end{aligned}$$

i.e., for every $t \geq 0$, the action $\tilde{q}(z(t))$ belongs to the segment $\mathscr{Q} \triangleq \underline{q_1 q_2}$ and the state $z(t)$ belongs a the half-plane $\mathscr{H}_{q_1, q_2} = \{w \in \mathbb{C} : (q_2 - q_1) \otimes (w - q_1) > 0\}$. Hence, if $\tilde{q}(z(\cdot))$ is now used to synthesise an open loop compound input function $Q : [0, \infty) \to \mathscr{Q}$, defined by $Q(t) = q_1 + e^{-t}(q_2 - q_1)$, the resulting trajectory
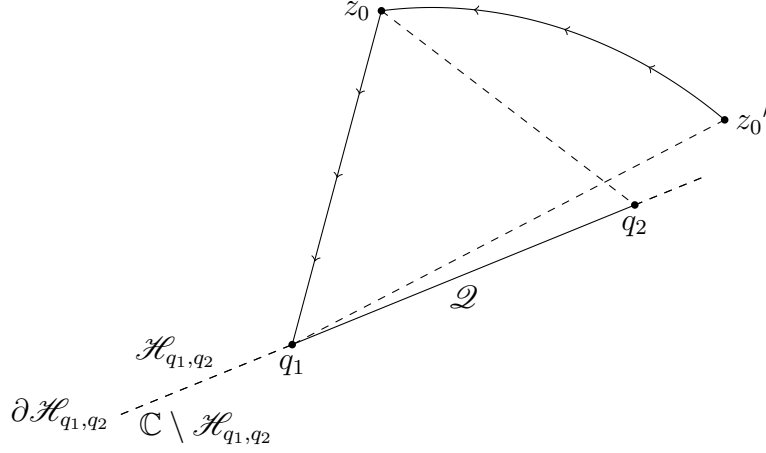
Figure 4.7: An example in which the distance from the state to the boundary of $\mathscr{H}_{q_1,q_2}$ does not decrease monotonously.

$z^F_{z_0,Q}\left([0,\infty)\right)$ is an example of a state temporal evolution, from $z_0 \in \mathscr{H}_{q_1,q_2}$, that does not reach $\partial\mathscr{H}_{q_1,q_2}$. Indeed, $\mathrm{d}\left(z^F_{z_0,Q}(\mathfrak{t}),\partial\mathscr{H}_{q_1,q_2}\right) = \frac{q_2-q_1}{|q_2-q_1|} \otimes (z(\mathfrak{t})-q_1) > 0$, for every $\mathfrak{t} > 0$. The geometrical interpretation of this example, in which $\mathrm{d}\left(z^F_{z_0,Q}(\cdot),\partial\mathscr{H}_{q_1,q_2}\right)$ is monotonously decreasing, is facilitated by Figure 4.6. However, in general, $\mathrm{d}\left(z^F_{z_0,Q}(\cdot),\partial\mathscr{H}_{q_1,q_2}\right)$ is not necessarily monotonously decreasing.

For example, keeping z_0, $\mathscr{Q} = q_1q_2$, and $Q:[0,\infty) \to \mathscr{Q}$ as before, let $\Theta \triangleq \frac{9}{10}\mathrm{Arg}\left(\frac{1}{1+k^{-1}}\right) = \frac{9}{10}\mathrm{Arg}\left(\frac{z_0-q_1}{q_2-q_1}\right)$, $z_0' \triangleq q_1 + (z_0-q_1)\,\mathrm{e}^{-k\Theta}$ and $Q':[0,+\infty) \to \mathscr{Q}$ such that

$$Q'(\mathfrak{t}) = \begin{cases} q_1 & \text{if } \mathfrak{t}\in[0,\Theta), \\ Q(\mathfrak{t}-\Theta) & \text{if } \mathfrak{t}\in[\Theta,+\infty). \end{cases}$$

The trajectory $z^F_{z_0',Q'}\left([0,+\infty)\right)$, from z_0', that results from applying input Q' is represented graphically in figure Figure 4.7. Clearly, in this case, $\mathrm{d}\left(z^F_{z_0',Q'}(\cdot),\partial\mathscr{H}_{q_1,q_2}\right)$ is *not* monotonously decreasing.

4.3.6.3. The state must approach the line that includes segment $\mathscr{Q}$

The previous examples have in common that sooner or later the state comes arbitrarily close to the straight line $\partial\mathscr{H}_{q_1,q_2}$ that includes the segment q_1q_1 where the compound input (instantaneous centre of the guiding α-equiangular spiral) is allowed to vary. This rather intuitive result is stated rigorously by the first proposition that follows. Before, a lemma that will be useful to conceive Lyapunov-like functions defined in $\mathscr{H}_{q_1,q_2}$ is presented next.

Lemma 4.3.1. *Let $o,v,q \in \mathbb{C}$ such that $v \neq 0$.*
For every $z \in \mathscr{R}^v_o = \mathbb{C} \setminus \{o - \rho v \ : \ \rho \geq 0\}$,

$$\nabla\mathcal{M}^v_o(z) \odot F(z,q) = -\frac{(1+\kappa^2)\,\mathrm{e}^{\kappa\mathcal{A}^v_o(z)}}{|z-o|}\,(o-z)\otimes(q-z).$$

81

Proof. The real gradient of $\mathcal{M}_o^v : \mathbb{C} \to [0,\infty)$ at $z \in \mathcal{R}_o^v = \mathbb{C} \setminus \{o - \rho v \ : \ \rho \geq 0\}$ was already calculated in (4.7) as

$$\nabla \mathcal{M}_o^v (z) = \frac{e^{\kappa \mathcal{A}_o^v(z)}}{|z - o|} (-\mathrm{j}) \, k \, (z - o). \tag{4.13}$$

Since $F : \mathbb{C} \times \mathbb{C} \to \mathbb{C}$ was defined such that $F (z_1, z_2) \triangleq k (z_1 - z_2)$, the expression (4.13) may be rewritten as

$$\nabla \mathcal{M}_o^v (z) = \frac{e^{\kappa \mathcal{A}_o^v(z)}}{|z - o|} (-\mathrm{j}) \, F (z, o). \tag{4.14}$$

Accordingly,

$$\begin{aligned}
\nabla \mathcal{M}_o^v (z) \odot F (z, q) &= -\frac{e^{\kappa \mathcal{A}_o^v(z)}}{|z - o|} (\mathrm{j} F (z, o)) \odot F (z, q) \\
&= -\frac{e^{\kappa \mathcal{A}_o^v(z)}}{|z - o|} |k|^2 (o - z) \otimes (q - z),
\end{aligned} \tag{4.15}$$

where the last equality results from the application of (4.10) with o in place of q and q in place of q'. Since $|k|^2 = 1 + \kappa^2$, there is nothing else to prove. $\qquad\square$

In Figure 4.8, the previous lemma is interpreted geometrically for the particular case in which $q \in \{w = o + \rho v \ : \ \rho \in \mathbb{R}\}$. Observe that the $\{o + \rho v \ : \ \rho < 0\}$-vectogram (resp. $\{o + \rho v \ : \ \rho > 0\}$-vectogram) at z is such that $\mathcal{M}_o^v (z)$ is lead to *decrease* (resp. *increase*), for every $z \in \{w \ : \ (w - o) \otimes v > 0\}$. This observation is exploited in the proofs of two propositions that follow.

Proposition 4.3.1. *Let $q_1, q_2 \in \mathbb{C}$ such that $q_1 \neq q_2$ and*

$$\mathcal{H}_{q_1,q_2} = \{z \in \mathbb{C} \ : \ (q_2 - q_1) \otimes (z - q_1) > 0\}.$$

Consider the initial value problem (4.8), with $z_0 \in \mathcal{H}_{q_1,q_2}$ and $Q : [0, +\infty) \to \mathcal{Q}$ piecewise continuous, being $\mathcal{Q} = \underline{q_1 q_2} = \{z \in \mathbb{C} \ : \ \frac{z - q_1}{q_2 - q_1} \in [0, 1]\}$. If its solution, $z_{z_0,Q}^F : [0, +\infty) \to \mathbb{C}$, is such that $z_{z_0,Q}^F (\mathsf{t}) \in \mathcal{H}_{q_1,q_2}$ for every $\mathsf{t} \geq 0$; then, for every $\epsilon > 0$, there exists a finite $\mathsf{t}_1 > 0$ such that

$$\mathrm{d} \left(z_{z_0,Q}^F (\mathsf{t}_1), \partial \mathcal{H}_{q_1,q_2} \right) < \epsilon. \tag{4.16}$$

Proof. Let δ be an arbitrary real positive constant. Define $v \triangleq \frac{q_1 - q_2}{|q_1 - q_2|}$ and $o \triangleq q_1 + \delta v$ (see Figure 4.9). Observe that

$$\begin{aligned}
v \otimes (o - z) &= v \otimes (q_1 + \delta v - z) = v \otimes (q_1 - z) = (-v) \otimes (z - q_1) \\
&= \frac{q_2 - q_1}{|q_2 - q_1|} \otimes (z - q_1) = \mathrm{d} (z, \partial \mathcal{H}_{q_1,q_2}) > 0.
\end{aligned} \tag{4.17}$$

for every $z \in \mathcal{H}_{q_1,q_2} \{z \in \mathbb{C} \ : \ (q_2 - q_1) \otimes (z - q_1) > 0\}$.

$$\{w \in \mathbb{C} \ : \ \mathcal{M}_o^v(w) = \mathcal{M}_o^v(z)\}$$
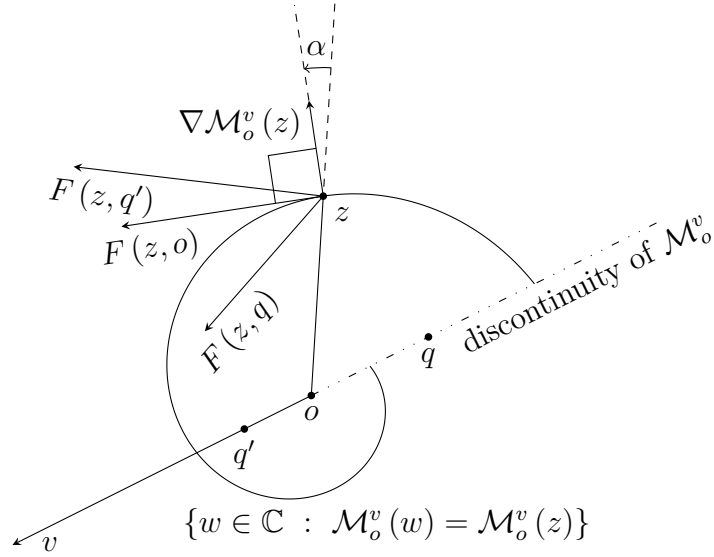
Figure 4.8: Geometrical interpretation of Lemma 4.3.1 for the particular case in which $q \in \{w = o + \rho v \ : \ \rho \in \mathbb{R}\}$. Let $o, v \in \mathbb{C}$ such that $v \neq 0$; for every $z \in \{w \ : \ (w - o) \otimes v > 0\}$ the velocity vector $F(z, q)$, based at z, points to a direction such that $\mathcal{M}_o^v(z) = \left|e^{-k\mathcal{A}_o^v(z)}(z - o)\right|$ is lead to *decrease* (resp. *increase*), whatever point $q \in \{o + \rho v \ : \ \rho < 0\}$ (resp. $q' \in \{o + \rho v \ : \ \rho > 0\}$) is selected as the instantaneous centre of the α-equiangular guiding spiral.

Let $q \in \mathscr{Q} = \underline{q_1 q_2} = \left\{z \in \mathbb{C} \ : \ \frac{z - q_1}{q_2 - q_1} \in [0, 1]\right\}$. By Lemma 4.3.1,

$$\nabla \mathcal{M}_o^v(z) \odot F(z, q) = -\frac{\left(1 + \kappa^2\right) e^{\kappa \mathcal{A}_o^v(z)}}{|z - o|} (o - z) \otimes (q - z),$$

for every $z \in \mathscr{R}_o^v = \mathbb{C} \setminus \{o - \rho v \ : \ \rho \geq 0\}$, where the factor $(q - z)$ is

$$q - z = q_1 + \frac{q - q_1}{q_2 - q_1}(q_2 - q_1) - z = o - \delta v - \frac{q - q_1}{q_2 - q_1}(q_1 - q_2) - z$$

$$= o - \delta v - \frac{q - q_1}{q_2 - q_1}|q_1 - q_2| v - z =$$

$$= (o - z) - \left(\delta + \frac{q - q_1}{q_2 - q_1}|q_1 - q_2|\right) v. \tag{4.18}$$

Hence,

$$\nabla \mathcal{M}_o^v(z) \odot F(z, q) = \frac{\left(1 + \kappa^2\right) e^{\kappa \mathcal{A}_o^v(z)}}{|z - o|}\left(\delta + \frac{q - q_1}{q_2 - q_1}|q_1 - q_2|\right)(o - z) \otimes v$$

$$= -\frac{\left(1 + \kappa^2\right) e^{\kappa \mathcal{A}_o^v(z)}}{|z - o|}\left(\delta + \frac{q - q_1}{q_2 - q_1}|q_1 - q_2|\right) v \otimes (o - z).$$

In this last expression $\frac{q - q_1}{q_2 - q_1} \in [0, 1]$ (because $q \in \mathscr{Q}$) and $v \otimes (o - z) > 0$ for every $z \in \mathscr{H}_{q_1, q_2}$ (as already noted in (4.17)). Consequently,

$$\forall z \in \mathscr{H}_{q_1, q_2}, \ \forall q \in \mathscr{Q}, \qquad \nabla \mathcal{M}_o^v(z) \odot F(z, q) < 0. \tag{4.19}$$
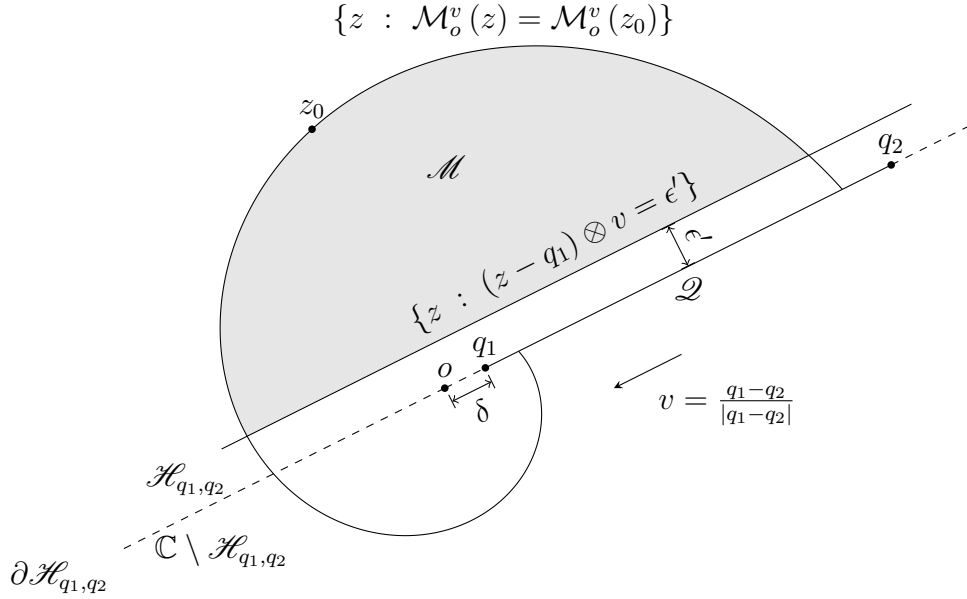
Figure 4.9: The set $\mathscr{M} \triangleq \{z \in \mathscr{H} \; : \; \mathcal{M}_o^v(z) \leq \mathcal{M}_o^v(z_0) \; \wedge \; (z - q_1) \otimes v \geq \epsilon'\}$ referred to in the proof of Proposition 4.3.1.

Fix the initial value $z_0 \in \mathscr{H}_{q_1,q_2}$, of the initial value problem (4.8). Given any $\epsilon > 0$, let ϵ' be a real positive number, such that $\epsilon' < \min\{\epsilon, (z_0 - q_1) \otimes v\}$, and consider the compact set

$$\mathscr{M} \triangleq \{z \in \mathscr{H}_{q_1,q_2} \; : \; \mathcal{M}_o^v(z) \leq \mathcal{M}_o^v(z_0) \; \wedge \; (z - q_1) \otimes v \geq \epsilon'\} \subset \mathscr{H}_{q_1,q_2}.$$

Check that $z_0 \in \mathscr{M}$ (see Figure 4.9). Let

$$m \triangleq -\max\{\nabla\mathcal{M}_o^v(z) \odot F(z, q) \; : \; z \in \mathscr{M} \; \wedge \; q \in \mathscr{Q}\}.$$

The real number m is positive, because of (4.19).

Consider the (unique) continuous solution $z_{z_0,Q}^F : [0, \infty) \to \mathbb{C}$ of the initial value problem (4.8). By hypothesis, $z_{z_0,Q}^F(\mathfrak{t}) \in \mathscr{H}_{q_1,q_2}$, for every $\mathfrak{t} \geq 0$. Define $H \triangleq \mathcal{M}_o^v \circ z_{z_0,Q}^F$, which is a continuous function, whose time derivative is

$$\dot{H}(\mathfrak{t}) = \nabla\mathcal{M}_o^v\left(z_{z_0,Q}^F(\mathfrak{t})\right) \odot F\left(z_{z_0,Q}^F(\mathfrak{t}), Q(\mathfrak{t})\right)$$

at every instant of time $\mathfrak{t} > 0$ at which Q is continuous. By (4.19), it can be stated that

$$\forall \mathfrak{t} > 0, \quad \dot{H}(\mathfrak{t}) < 0,$$

which means that H is a monotonously decreasing function of time. Therefore

$$\forall \mathfrak{t} > 0, \quad H(\mathfrak{t}) = \mathcal{M}_o^v\left(z_{z_0,Q}^F(\mathfrak{t})\right) < \mathcal{M}_o^v(z_0). \tag{4.20}$$

Suppose, by absurd, that $z_{z_0,Q}^F(\mathfrak{t}) \in \mathscr{M}$ for every $\mathfrak{t} > 0$. Since

$$\forall \mathfrak{t} > 0, \quad \dot{H}(\mathfrak{t}) \leq -m < 0,$$

integration between 0 and $\mathfrak{t} \geq 0$ leads to

$$\forall \mathfrak{t} \geq 0, \quad H\left(\mathfrak{t}\right) - H\left(0\right) \leq -m\mathfrak{t},$$

or equivalently

$$\forall \mathfrak{t} \geq 0, \quad \mathcal{M}_o^v\left(z_{z_0,Q}^F\left(\mathfrak{t}\right)\right) = H\left(\mathfrak{t}\right) \leq H\left(0\right) - m\mathfrak{t}, \tag{4.21}$$

from where it can be inferred that $\lim_{\mathfrak{t} \to +\infty} \mathcal{M}_o^v\left(z_{z_0,Q}^F\left(\mathfrak{t}\right)\right) = -\infty$; but, this is absurd because $\mathcal{M}_o^v\left(z\right) > 0$ for every $z \in \mathscr{H}_{q_1,q_2} \supset \mathscr{M}$. In conclusion, there exists an instant $\mathfrak{t}_1 > 0$, such that $z_{z_0,Q}^F\left(\mathfrak{t}_1\right) \notin \mathscr{M}$; but since (4.20) must hold, it must be

$$\left(z_{z_0,Q}^F\left(\mathfrak{t}_1\right) - q_1\right) \otimes v < \epsilon'. \tag{4.22}$$

Recalling from (4.17) that $\mathrm{d}\left(z, \partial \mathscr{H}_{q_1,q_2}\right) = \left(z - q_1\right) \otimes v$, for every $z \in \mathscr{H}_{q_1,q_2}$, and remembering that $\epsilon' < \epsilon$; the thesis of the proposition follows immediately. $\qquad \square$

4.3.6.4. The state bounded by the level sets of two Lyapunov-like functions

The just preceding proposition states that the state must approach the straight line $\partial \mathscr{H}_{q_1,q_2}$ that includes the segment $\mathscr{Q} = \underline{q_1 q_2}$ where the compound input takes values, but it does not inform about *how* does the approach take place. The following proposition bounds the possible state-space trajectories by two arcs of α-equiangular spirals through the initial condition $z_0 \in \mathscr{H}_{q_1,q_2}$: one whose centre is at q_1 and another whose centre is at q_2. The former is a subset of a level-set of a Lyapunov-like function which is monotonically *decreasing* along state-space trajectories included in $\mathrm{cl}\left(\mathscr{H}_{q_1,q_2}\right)$, and the later is a subset of a level-set of a Lyapunov-like function which is monotonically *increasing* along state-space trajectories included $\mathrm{cl}\left(\mathscr{H}_{q_1,q_2}\right)$.

Proposition 4.3.2. *Let $q_1, q_2 \in \mathbb{C}$ such that $q_1 \neq q_2$ and*

$$\mathscr{H}_{q_1,q_2} = \left\{z \in \mathbb{C} \; : \; \left(q_2 - q_1\right) \otimes \left(z - q_1\right) > 0\right\}. \tag{4.23}$$

Consider the solution $z_{z_0,Q}^F : [0, +\infty) \to \mathbb{C}$ of initial value problem (4.8), with $z_0 \in \mathscr{H}_{q_1,q_2}$ and $Q : [0, +\infty) \to \mathscr{Q}$ piecewise continuous, being $\mathscr{Q} = \underline{q_1 q_2} = \left\{z \in \mathbb{C} \; : \; \frac{z - q_1}{q_2 - q_1} \in [0, 1]\right\}$.
If $\mathfrak{t}_1 = \sup\left\{\mathfrak{t} \in [0, +\infty) \; : \; z_{z_0,Q}^F\left(\mathfrak{t}\right) \in \mathrm{cl}\left(\mathscr{H}_{q_1,q_2}\right)\right\}$ (possibly infinite), the functions $\mathfrak{t} \mapsto \mathcal{M}_{q_1}^{q_1 - q_2}\left(z_{z_0,Q}^F\left(\mathfrak{t}\right)\right)$ and $\mathfrak{t} \mapsto \mathcal{M}_{q_2}^{q_1 - q_2}\left(z_{z_0,Q}^F\left(\mathfrak{t}\right)\right)$ are monotonously decreasing and monotonously increasing, respectively, in the interval $(0, \mathfrak{t}_1)$. Accordingly,

$$z_{z_0,Q}^F\left(\mathfrak{t}\right) \in \mathscr{D}_{q_1,q_2}\left(z_0\right), \quad \forall \mathfrak{t} \in [0, \mathfrak{t}_1],$$

where,

$$\mathscr{D}_{q_1,q_2}\left(z_0\right) = \left\{z \in \mathbb{C} \; : \; \mathcal{M}_{q_1}^{q_1 - q_2}\left(z\right) \leq \mathcal{M}_{q_1}^{q_1 - q_2}\left(z_0\right) \; \wedge \; \mathcal{M}_{q_2}^{q_1 - q_2}\left(z\right) \geq \mathcal{M}_{q_2}^{q_1 - q_2}\left(z_0\right)\right\}.$$

Proof. To prove the proposition, it suffices to prove that

Chapter 4. The conflict's dynamics

(i) $\nabla \mathcal{M}_{q_1}^v(z) \odot F(z,q) \leq 0$ for every $q \in \mathscr{Q}$ and every $z \in \mathrm{cl}\left(\mathscr{H}_{q_1,q_2}\right)$,

(ii) $\nabla \mathcal{M}_{q_2}^v(z) \odot F(z,q) \geq 0$ for every $q \in \mathscr{Q}$ and every $z \in \mathrm{cl}\left(\mathscr{H}_{q_1,q_2}\right)$,

where $v = q_1 - q_2$. Let

$$z \in \mathrm{cl}\left(\mathscr{H}_{q_1,q_2}\right) = \{z \in \mathbb{C} \ : \ (q_1 - z) \otimes (q_2 - q_1) \geq 0\}$$
$$= \{z \in \mathbb{C} \ : \ (q_2 - z) \otimes (q_1 - q_2) \leq 0\},$$

and

$$q \in \mathscr{Q} = \underline{q_1 q_2} = \left\{z \in \mathbb{C} \ : \ \frac{z - q_1}{q_2 - q_1} \in [0,1]\right\}$$
$$= \left\{z \in \mathbb{C} \ : \ \frac{z - q_2}{q_1 - q_2} \in [0,1]\right\}.$$

By Lemma 4.3.1,

$$\nabla \mathcal{M}_o^v(z) \odot F(z,q) = -\frac{\left(1 + \kappa^2\right) \mathrm{e}^{\kappa \mathcal{A}_o^v(z)}}{|z - o|}\, (o - z) \otimes (q - z),$$

for every $z \in \mathscr{R}_o^v = \mathbb{C} \setminus \{o - \rho v \ : \ \rho \geq 0\}$, where o may stand for q_1 or q_2 as needed.

For the case $o = q_1$, the factor $(q - z)$ may be expanded as

$$q - z = (q_1 - z) + \frac{q - q_1}{q_2 - q_1}\,(q_2 - q_1), \tag{4.24}$$

and consequently

$$\nabla \mathcal{M}_{q_1}^v(z) \odot F(z,q) = -\frac{\left(1+\kappa^2\right)\mathrm{e}^{\kappa \mathcal{A}_{q_1}^v(z)}}{|z - q_1|}\,(q_1 - z) \otimes \left(\frac{q - q_1}{q_2 - q_1}\,(q_2 - q_1)\right)$$
$$= -\frac{\left(1+\kappa^2\right)\mathrm{e}^{\kappa \mathcal{A}_{q_1}^v(z)}}{|z - q_1|}\left(\frac{q - q_1}{q_2 - q_1}\right)(q_1 - z) \otimes (q_2 - q_1),$$

where $\frac{q - q_1}{q_2 - q_1} \in [0,1]$ (because $q \in \mathscr{Q}$) and $(q_1 - z) \otimes (q_2 - q_1) \geq 0$ (because $z \in \mathrm{cl}\left(\mathscr{H}_{q_1,q_2}\right)$). Hence, $\nabla \mathcal{M}_{q_1}^v(z) \odot F(z,q) \leq 0$.

For the case $o = q_2$, the factor $(q - z)$ may be expanded as

$$q - z = (q_2 - z) + \frac{q - q_2}{q_1 - q_2}\,(q_1 - q_2), \tag{4.25}$$

and consequently

$$\nabla \mathcal{M}_{q_2}^v(z) \odot F(z,q) = -\frac{\left(1+\kappa^2\right)\mathrm{e}^{\kappa \mathcal{A}_{q_2}^v(z)}}{|z - q_2|}\,(q_2 - z) \otimes \left(\frac{q - q_2}{q_1 - q_2}\,(q_1 - q_2)\right)$$
$$= -\frac{\left(1+\kappa^2\right)\mathrm{e}^{\kappa \mathcal{A}_{q_2}^v(z)}}{|z - q_2|}\left(\frac{q - q_2}{q_1 - q_2}\right)(q_2 - z) \otimes (q_1 - q_2),$$

where $\frac{q - q_2}{q_1 - q_2} \in [0,1]$ (because $q \in \mathscr{Q}$) and $(q_2 - z) \otimes (q_1 - q_2) \leq 0$ (because $z \in \mathrm{cl}\left(\mathscr{H}_{q_1,q_2}\right)$). Hence, $\nabla \mathcal{M}_{q_2}^v(z) \odot F(z,q) \geq 0$. $\square$
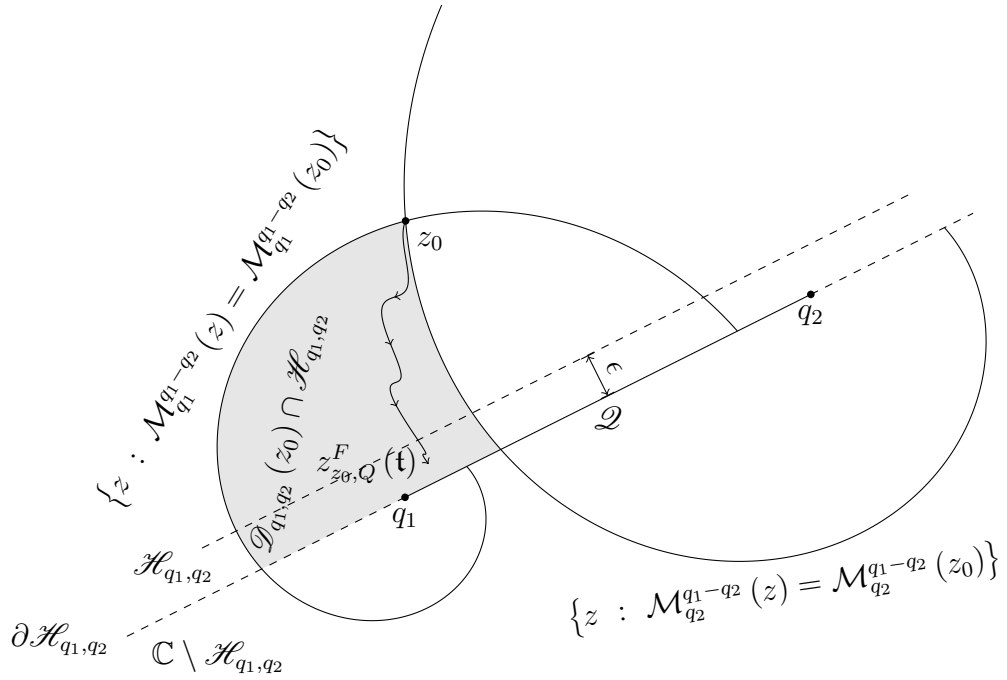
Figure 4.10: Geometric interpretation of Propositions 4.3.1 and 4.3.2. By Proposition 4.3.1, the state must come closer than an arbitrary $\epsilon > 0$ to $\partial\mathscr{H}_{q_1,q_2}$, in finite time. By Proposition 4.3.2, as long as the state remains in $\mathrm{cl}\left(\mathscr{H}_{q_1,q_2}\right)$, it must belong to the set $\mathscr{D}_{q_1,q_2}\left(z_0\right) = \left\{z \in \mathbb{C} \ : \ \mathcal{M}_{q_1}^{q_1-q_2}\left(z\right) \leq \mathcal{M}_{q_1}^{q_1-q_2}\left(z_0\right) \ \wedge \ \mathcal{M}_{q_2}^{q_1-q_2}\left(z\right) \geq \mathcal{M}_{q_2}^{q_1-q_2}\left(z_0\right)\right\}$.

Remark 1. The above proposition states that as long as the state remains in $\mathrm{cl}\left(\mathscr{H}_{q_1,q_2}\right)$, it must belong to the set

$$\mathscr{D}_{q_1,q_2}\left(z_0\right) \triangleq \left\{z \in \mathbb{C} \ : \ \mathcal{M}_{q_1}^{q_1-q_2}\left(z\right) \leq \mathcal{M}_{q_1}^{q_1-q_2}\left(z_0\right) \ \wedge \ \mathcal{M}_{q_2}^{q_1-q_2}\left(z\right) \geq \mathcal{M}_{q_2}^{q_1-q_2}\left(z_0\right)\right\}.$$

where $z_0 \in \mathscr{H}_{q_1,q_2}$ is the initial condition. In addition, by Proposition 4.3.1 it is already known that the state must come closer to $\partial\mathscr{H}_{q_1,q_2}$ than an arbitrary $\epsilon > 0$, in finite time. Both facts are graphically represented in Figure 4.10.

4.3.6.5. Escape form compact sets

It was already commented that for regions in space very distant from the bounded set $\mathscr{Q}$ (where the compound input takes values) the state approximately spirals around $\mathscr{Q}$ in the counter-clockwise direction. The following propositions examines, for the case in which $\mathscr{Q}$ is a line segment, how close to $\mathscr{Q}$ can the state still be considered to be approximately spiralling around $\mathscr{Q}$.

Proposition 4.3.3. *Let* $q_1, q_2 \in \mathbb{C}$ *such that* $q_1 \neq q_2$. *Let also:*

$$\mathscr{H}_{q_1,q_2} = \left\{z \in \mathbb{C} \ : \ \left(q_2 - q_1\right) \otimes \left(z - q_1\right) > 0\right\},$$
$$\mathscr{C}_{q_1,q_2} = \left\{z \in \mathbb{C} \ : \ |z - o| \leq |l|\right\},$$
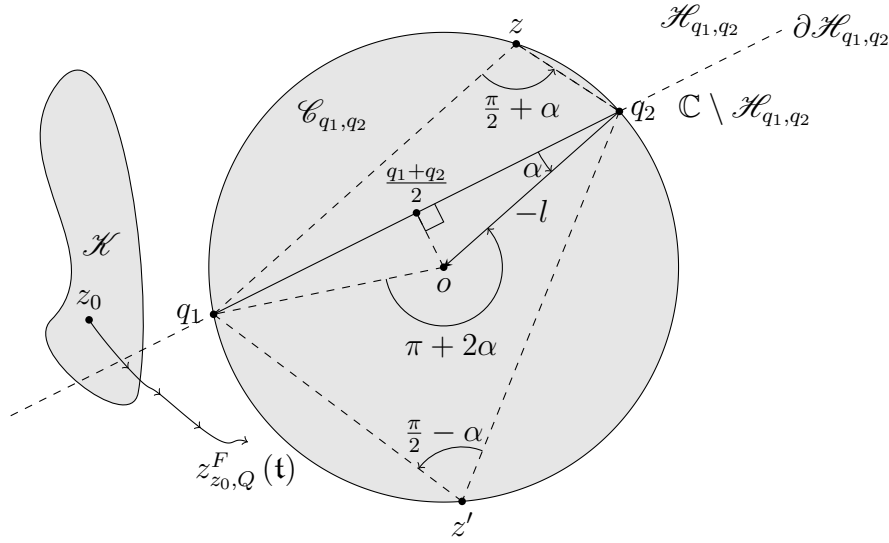
Figure 4.11: Auxiliary figure for Proposition 4.3.3.

where $l \triangleq -\mathrm{j}k\frac{q_2-q_1}{2}$ and $o \triangleq q_2 - l$ (see Figure 4.11).

Suppose $\mathscr{K}$ is a non-empty compact connected subset of $\mathbb{C}$, included in the region $\mathscr{R}_{q_2}^{q_1-q_2} = \mathbb{C} \setminus \{q_2 - \rho(q_1 - q_2) \ : \ \rho \geq 0\}$, such that $\mathscr{K} \cap \mathscr{C}_{q_1,q_2} = \emptyset$ (see Figure 4.11).

Consider the initial value problem (4.8), with $z_0 \in \mathscr{H}_{q_1,q_2}$ and $Q : [0,+\infty) \to \mathscr{Q}$ piecewise continuous, being $\mathscr{Q} = \underline{q_1 q_2} = \left\{z \in \mathbb{C} \ : \ \frac{z-q_1}{q_2-q_1} \in [0,1]\right\}$. Its solution, $z_{z_0,Q}^{F} : [0,+\infty) \to \mathbb{C}$, is such that $z_{z_0,Q}^{F}(\mathfrak{t})$ escapes from $\mathscr{K}$ in finite time:

$$\mathfrak{t}_1 = \sup\left\{\mathfrak{t} \in [0,+\infty) \ : \ z_{z_0,Q}^{F}(\mathfrak{t}) \in \mathscr{K}\right\} < +\infty.$$

Moreover, $\mathfrak{t} \mapsto \mathcal{A}_{q_2}^{q_1-q_2}\left(z_{z_0,Q}^{F}(\mathfrak{t})\right)$ is strictly monotonously increasing in $(0, \mathfrak{t}_2)$, where $\mathfrak{t}_2 = \sup\left\{\mathfrak{t} \in [0,+\infty) \ : \ z_{z_0,Q}^{F}(\mathfrak{t}) \in \mathscr{R}_{q_2}^{q_1-q_2} \setminus \mathscr{C}_{q_1,q_2}\right\}$ is greater than $\mathfrak{t}_1$.

Before delving into the proof of this proposition, observe that, by construction of circle $\mathscr{C}_{q_1,q_2}$ (as defined in the statement of the proposition), the arc $\partial\mathscr{C}_{q_1,q_2} \cap \mathscr{H}_{q_1,q_2}$ is the set of points in $\mathscr{H}_{q_1,q_2}$ from where the segment $\underline{q_1 q_2}$ "is seen" with an angle equal to $\frac{\pi}{2} + \alpha$ (see Figure 4.11). Furthermore, for every $z \in \mathscr{R}_{q_2}^{q_1-q_2} \setminus \mathscr{C}_{q_1,q_2}$, the velocity vector $F(z,q)$, based at z, points to a direction such that $\mathcal{A}_{q_2}^{q_1-q_2}(z) = \operatorname{Arg}\frac{z-q_2}{q_1-q_2}$ is lead to *increase*, whatever point $q \in \underline{q_1 q_2}$ is selected as the instantaneous centre of the α-equiangular guiding spiral (see Figure 4.12). The algebraic version of this geometrical observation is a key point for the following proof.

Proof. For each $z \in \mathscr{R}_{q_2}^{q_1-q_2} = \mathbb{C} \setminus \{q_2 - \rho(q_1 - q_2) \ : \ \rho \geq 0\}$ and each $\xi \in [0,1]$, consider the scalar product

$$\nabla\mathcal{A}_{q_2}^{q_1-q_2}(z) \odot F(z, \mathfrak{q}(\xi)) = \Re\left(\overline{\nabla\mathcal{A}_{q_2}^{q_1-q_2}(z)}k(z - \mathfrak{q}(\xi))\right), \qquad (4.26)$$
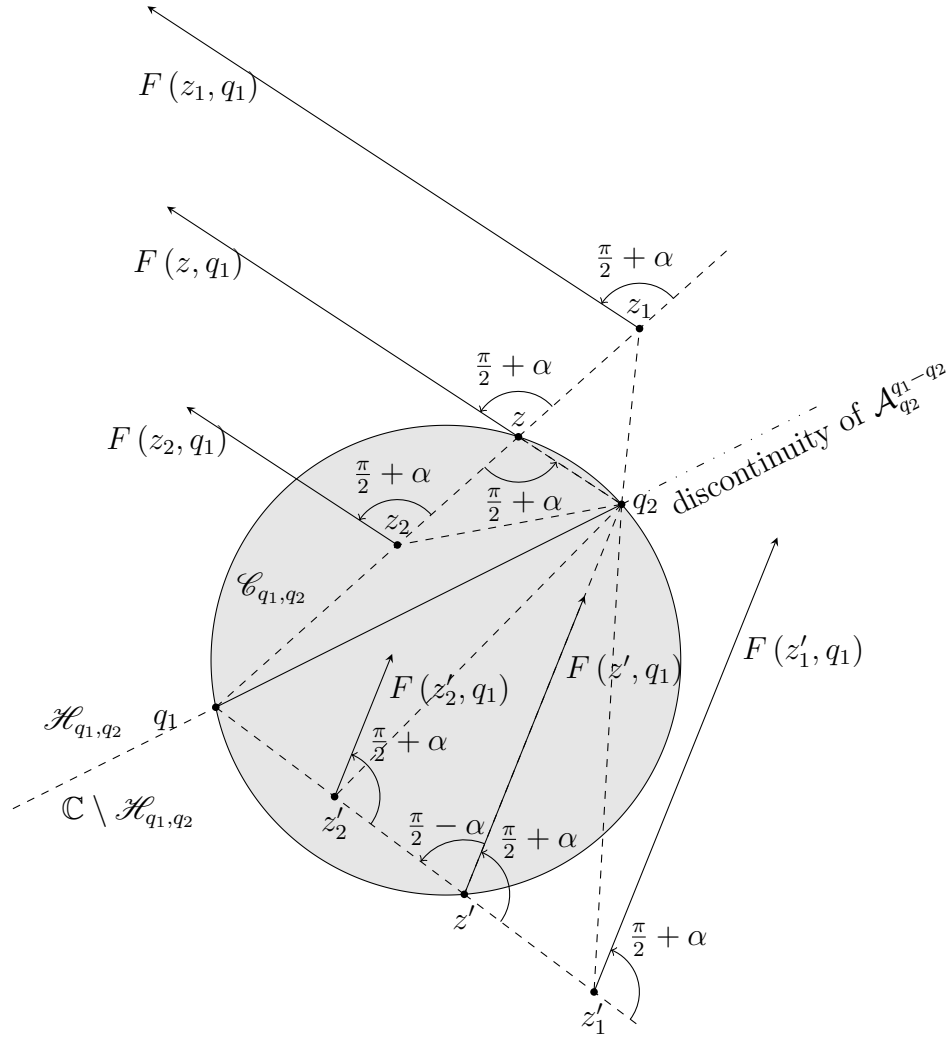
Figure 4.12: Key point for the proof of Proposition 4.3.3: for every $z \in \mathscr{R}^{q_1-q_2}_{q_2} \setminus \mathscr{C}_{q_1,q_2}$, the velocity vector $F(z,q)$, based at z, points to a direction such that $\mathcal{A}^{q_1-q_2}_{q_2}(z) = \mathrm{Arg}\, \frac{z-q_2}{q_1-q_2}$ is lead to *increase*, whatever point $q \in \mathrm{conv}(\{q_1,q_2\})$ is selected as the instantaneous centre of the α-equiangular guiding spiral. The set $\mathscr{R}^{q_1-q_2}_{q_2} \setminus \mathscr{C}_{q_1,q_2}$ is just the region $\mathbb{C} \setminus (\mathscr{C}_{q_1,q_2} \cup \{q_2 - \rho(q_1-q_2) : \rho \geq 0\})$, i.e., the whole complex plane except for circle $\mathscr{C}_{q_1,q_2}$ and the ray where $\mathcal{A}^{q_1-q_2}_{q_2}$ is discontinuous.

where $\mathfrak{q} : [0,1] \to \mathscr{Q}$ is defined such that $\mathfrak{q}(\xi) \triangleq q_1 + \xi(q_2 - q_1)$. Recall of (4.6) furnish the following expression for the factor $\overline{\nabla \mathcal{A}_{q_2}^{q_1 - q_2}(z)}k$ in (4.26)

$$\overline{\nabla \mathcal{A}_{q_2}^{q_1 - q_2}(z)}k = -j\frac{\overline{z - q_2}}{|z - q_2|^2}k = -jk\frac{1}{z - q_2}. \tag{4.27}$$

The remaining factor in (4.26) is

$$(z - \mathfrak{q}(\xi)) = z - q_1 - \xi(q_2 - q_1) = z - q_2 + q_2 - q_1 - \xi(q_2 - q_1)$$
$$= z - q_2 + (1 - \xi)(q_2 - q_1). \tag{4.28}$$

Making use of (4.27) and (4.28), the scalar product (4.26) may be written as

$$\nabla \mathcal{A}_{q_2}^{q_1 - q_2}(z) \odot F(z, \mathfrak{q}(\xi)) = \Re\left(-jk\left(1 + (1 - \xi)\frac{q_2 - q_1}{z - q_2}\right)\right)$$
$$= \Re\left(-jk - jk(1 - \xi)\frac{q_2 - q_1}{z - q_2}\right)$$
$$= \Re(-jk) + \Re\left(-jk(1 - \xi)\frac{q_2 - q_1}{z - q_2}\right).$$

Since $\Re(-jk) = \Re(1 + j\kappa) = 1$,

$$\nabla \mathcal{A}_{q_2}^{q_1 - q_2}(z) \odot F(z, \mathfrak{q}(\xi)) = 1 + (1 - \xi)\Re\left(-jk\frac{q_2 - q_1}{z - q_2}\right).$$

Define $\mathscr{C}'$ as the following set:

$$\mathscr{C}' \triangleq \left\{z \in \mathscr{R}_{q_2}^{q_1 - q_2} \ : \ \exists\xi \in [0,1], \quad \nabla \mathcal{A}_{q_2}^{q_1 - q_2}(z) \odot F(z, \mathfrak{q}(\xi)) \leq 0\right\}.$$

A point $z \in \mathscr{R}_{q_2}^{q_1 - q_2}$ belongs to $\mathscr{C}'$, if and only if there exists an $\xi \in [0,1]$ such that

$$1 + (1 - \xi)\Re\left(-jk\frac{q_2 - q_1}{z - q_2}\right) \leq 0.$$

For $\xi = 1$, the inequality (4.3.6.5) does not hold for every $z \in \mathscr{R}_{q_2}^{q_1 - q_2}$. Therefore, a point $z \in \mathscr{R}_{q_2}^{q_1 - q_2}$ belongs to $\mathscr{C}'$, if and only if there exists an $\xi \in [0,1)$ such that

$$\Re\left(-jk\frac{q_2 - q_1}{z - q_2}\right) \leq -\frac{1}{1 - \xi},$$

i.e., if and only if

$$\Re\left(-jk\frac{q_2 - q_1}{z - q_2}\right) \leq \max\left\{-\frac{1}{1 - \xi} \ : \ \xi \in [0,1)\right\} = -1.$$

So, $\mathscr{C}' = \left\{z \in \mathscr{R}_{q_2}^{q_1 - q_2} \ : \ \Re\left(-jk\frac{q_2 - q_1}{z - q_2}\right) \leq -1\right\}$. Note that

$$\Re\left(-jk\frac{q_2 - q_1}{z - q_2}\right) = \frac{1}{2}\left(-jk\frac{q_2 - q_1}{z - q_2} + j\overline{k}\frac{\overline{q_2 - q_1}}{\overline{z - q_2}}\right)$$
$$= \frac{-jk\frac{q_2 - q_1}{2}(\overline{z} - \overline{q_2}) + j\overline{k}\frac{\overline{q_2 - q_1}}{2}(z - q_2)}{|z - q_2|^2}$$
$$= \frac{l(\overline{z} - \overline{q_2}) + \overline{l}(z - q_2)}{|z - q_2|^2},$$

where $l = -\mathrm{j}k\frac{q_2-q_1}{2}$ as defined in the statement of the proposition. Rearranging the condition of belonging to the set $\mathscr{C}'$, it can be stated that

$$\mathscr{C}' = \left\{ z \in \mathscr{R}_{q_2}^{q_1-q_2} \ : \ (z-q_2)(\overline{z}-\overline{q_2}) + l(\overline{z}-\overline{q_2}) + \overline{l}(z-q_2) \leq 0 \right\}.$$

Check that

$$(z-q_2)(\overline{z}-\overline{q_2}) + l(\overline{z}-\overline{q_2}) + \overline{l}(z-q_2) = z\overline{z} - \overline{o}z - o\overline{z} + q_2\overline{q_2} - \overline{q_2}l - q_2\overline{l},$$

where $o = q_2 - l$ as defined in the statement of the proposition. The RHS of this last equality can be rewritten as

$$
\begin{aligned}
z\overline{z} - \overline{o}z - o\overline{z} + q_2\overline{q_2} - \overline{q_2}l - q_2\overline{l} + l\overline{l} - l\overline{l} &= z\overline{z} - \overline{o}z - o\overline{z} + (q_2 - l)\left(\overline{q_2} - \overline{l}\right) - l\overline{l}, \\
&= z\overline{z} - \overline{o}z - o\overline{z} + o\overline{o} - l\overline{l} \\
&= (z-o)(\overline{z}-\overline{o}) - l\overline{l} \\
&= |z-o|^2 - |l|^2.
\end{aligned}
$$

Thus,

$$\mathscr{C}' = \left\{ z \in \mathscr{R}_{q_2}^{q_1-q_2} \ : \ |z-o| \leq |l| \right\} = \mathscr{C}_{q_1,q_2} \setminus \left\{ q_2 - \rho(q_1 - q_2) \ : \ \rho \geq 0 \right\},$$

i.e., $\mathscr{C}'$ coincides with the circle defined in the enunciation of the proposition, except for the ray $\{q_2 - \rho(q_1 - q_2) \ : \ \rho \geq 0\}$ where $\mathcal{A}_{q_2}^{q_1-q_2}$ is discontinuous. Check that $\mathscr{C}_{q_1,q_2} \cap \{q_2 - \rho(q_1 - q_2) \ : \ \rho \geq 0\} = \{q_2\}$, to conclude that $\mathscr{C}' = \mathscr{C}_{q_1,q_2} \setminus \{q_2\}$, and therefore

$$\mathscr{C}' \triangleq \left\{ z \in \mathscr{R}_{q_2}^{q_1-q_2} \ : \ \exists \xi \in [0,1], \quad \nabla\mathcal{A}_{q_2}^{q_1-q_2}(z) \odot F(z, \mathfrak{q}(\xi)) \leq 0 \right\} = \mathscr{C}_{q_1,q_2} \setminus \{q_2\}.$$

Consequently,

$$\forall z \in \mathscr{R}_{q_2}^{q_1-q_2} \setminus (\mathscr{C}_{q_1,q_2} \setminus \{q_2\}), \quad \forall \xi \in [0,1], \qquad \nabla\mathcal{A}_{q_2}^{q_1-q_2}(z) \odot F(z, \mathfrak{q}(\xi)) > 0,$$

and, since $q_2 \notin \mathscr{R}_{q_2}^{q_1-q_2} = \mathbb{C} \setminus \{q_2 - \rho(q_1 - q_2) \ : \ \rho \geq 0\}$,

$$\forall z \in \mathscr{R}_{q_2}^{q_1-q_2} \setminus \mathscr{C}_{q_1,q_2}, \quad \forall \xi \in [0,1], \qquad \nabla\mathcal{A}_{q_2}^{q_1-q_2}(z) \odot F(z, \mathfrak{q}(\xi)) > 0. \qquad (4.29)$$

Let

$$
\begin{aligned}
M &\triangleq \max\left\{ \mathcal{A}_{q_2}^{q_1-q_2}(z) \ : \ z \in \mathscr{K} \right\}, \\
m &\triangleq \min\left\{ \nabla\mathcal{A}_{q_2}^{q_1-q_2}(z) \odot F(z, \mathfrak{q}(\xi)) \ : \ z \in \mathscr{K} \ \wedge \ \xi \in [0,1] \right\}.
\end{aligned}
$$

By hypothesis, $\mathscr{K} \subset \mathscr{R}_{q_2}^{q_1-q_2} \setminus \mathscr{C}_{q_1,q_2}$, so (4.29) guarantees that $m > 0$.

Consider the unique and continuous solution $z_{z_0,Q}^F : [0,\infty) \to \mathbb{C}$ of the initial value problem (4.8). Suppose, by absurd, that $z_{z_0,Q}^F(\mathfrak{t}) \in \mathscr{K}$, for every $\mathfrak{t} > 0$, i.e., $\left\{ \mathfrak{t} \in [0,+\infty) \ : \ z_{z_0,Q}^F(\mathfrak{t}) \in \mathscr{K} \right\}$ is unbounded above. Define $H \triangleq \mathcal{A}_{q_2}^{q_1-q_2} \circ z_{z_0,Q}^F$, which is a continuous function, whose time derivative satisfies

$$\dot{H}(\mathfrak{t}) = \nabla\mathcal{A}_{q_2}^{q_1-q_2}\left(z_{z_0,Q}^F(\mathfrak{t})\right) \odot F\left(z_{z_0,Q}^F(\mathfrak{t}), Q(\mathfrak{t})\right) \geq m > 0. \qquad (4.30)$$

at every instant of time $t > 0$ at which $Q : [0, +\infty) \to \mathscr{Q}$ is continuous. Integration between 0 and $t \geq 0$ leads to

$$\forall t \geq 0, \quad H(t) - H(0) \geq mt,$$

or equivalently

$$\forall t \geq 0, \quad \mathcal{A}_{q_2}^{q_1 - q_2}\left(z_{z_0,Q}^F(t)\right) = H(t) \geq H(0) + mt, \tag{4.31}$$

from where it can be inferred that $\lim_{t \to +\infty} \mathcal{A}_{q_2}^{q_1 - q_2}\left(z_{z_0,Q}^F(t)\right) = +\infty$; but, this is absurd because, since $z_{z_0,Q}^F(t) \in \mathscr{K}$ for every $t \geq 0$, it must be $\mathcal{A}_{q_2}^{q_1 - q_2}\left(z_{z_0,Q}^F(t)\right) \leq M$ for every $t \geq 0$.

In conclusion, $\left\{ t \in [0, +\infty) \ : \ z_{z_0,Q}^F(t) \in \mathscr{K} \right\}$ must be bounded above. Accordingly, there exists $t_1 = \sup\left\{ t \in [0, +\infty) \ : \ z_{z_0,Q}^F(t) \in \mathscr{K} \right\} < +\infty$.

Observe that as long as $z_{z_0,Q}^F(t) \in \mathscr{R}_{q_2}^{q_1 - q_2} \setminus \mathscr{C}_{q_1,q_2}$, if Q is continuous at t, the proposition (4.29) guarantees that

$$\dot{H}(t) = \nabla \mathcal{A}_{q_2}^{q_1 - q_2}\left(z_{z_0,Q}^F(t)\right) \odot F\left(z_{z_0,Q}^F(t), Q(t)\right) > 0.$$

Therefore, $H = \mathcal{A}_{q_2}^{q_1 - q_2} \circ z_{z_0,Q}^F$ is strictly monotonously increasing in $(0, t_2)$, where $t_2 = \sup\left\{ t \in [0, +\infty) \ : \ z_{z_0,Q}^F(t) \in \mathscr{R}_{q_2}^{q_1 - q_2} \setminus \mathscr{C}_{q_1,q_2} \right\}$ is necessarily greater than t_1 because $\mathscr{K}$ and $\mathscr{C}_{q_1,q_2}$ are two disconnected non-empty compact sets and $z_{z_0,Q}^F$ is continuous. $\qquad \square$

4.3.6.6. Sufficient conditions to reach a ray

The following corollary provides sufficient conditions on the initial state in $\mathscr{H}_{q_1,q_2}$, for assuring that the state finally reaches a ray, with endpoint at q_2, in finite time. It follows from a particular choice for the compact set $\mathscr{K}$ of Proposition 4.3.3.

Corollary 4.3.1. *Let $q_1, q_2 \in \mathbb{C}$ such that $q_1 \neq q_2$. Let also:*

$$\mathscr{H}_{q_1,q_2} = \left\{ z \in \mathbb{C} \ : \ (q_2 - q_1) \otimes (z - q_1) > 0 \right\},$$
$$\mathscr{C}_{q_1,q_2} = \left\{ z \in \mathbb{C} \ : \ \left| z - \left(q_2 + jk\frac{q_2 - q_1}{2} \right) \right| \leq \left| k\frac{q_2 - q_1}{2} \right| \right\}.$$

Consider the initial value problem (4.8), with $z_0 \in \mathscr{H}_{q_1,q_2}$ and $Q : [0, +\infty) \to \mathscr{Q}$ piecewise continuous, being $\mathscr{Q} = \underline{q_1 q_2} = \left\{ z \in \mathbb{C} \ : \ \frac{z - q_1}{q_2 - q_1} \in [0, 1] \right\}$. Let $z_{z_0,Q}^F : [0, +\infty) \to \mathbb{C}$ be its solution. Fix $\theta \in \left[0, -\mathcal{A}_{q_2}^{q_1 - q_2}(z_0) \right)$ and let:

$$\mathscr{R}_{q_2}^{q_1 - q_2} = \mathbb{C} \setminus \left\{ q_2 - \rho(q_1 - q_2) \ : \ \rho \geq 0 \right\}$$
$$\mathscr{D}_{q_1,q_2}(z_0) = \left\{ z \in \mathbb{C} \ : \ \mathcal{M}_{q_1}^{q_1 - q_2}(z) \leq \mathcal{M}_{q_1}^{q_1 - q_2}(z_0) \ \wedge \ \mathcal{M}_{q_2}^{q_1 - q_2}(z) \geq \mathcal{M}_{q_2}^{q_1 - q_2}(z_0) \right\},$$
$$\mathscr{K}_{q_1,q_2}^{\theta}(z_0) = \mathscr{D}_{q_1,q_2}(z_0) \cap \left\{ z \in \mathscr{R}_{q_2}^{q_1 - q_2} \ : \ -\pi < \mathcal{A}_{q_2}^{q_1 - q_2}(z) \leq -\theta \right\},$$

as represented in Figure 4.13.

If $\mathscr{K}_{q_1,q_2}^{\theta}(z_0) \cap \mathscr{C}_{q_1,q_2} = \emptyset$, the solution $z_{z_0,Q}^F : [0, +\infty) \to \mathbb{C}$ is such that $z_{z_0,Q}^F(t)$ escapes from $\mathscr{K}_{q_1,q_2}^{\theta}(z_0)$ in finite time:

$$t_1 = \sup\left\{ t \in [0, +\infty) \ : \ z_{z_0,Q}^F(t) \in \mathscr{K}_{q_1,q_2}^{\theta} \right\} < +\infty.$$

Moreover,
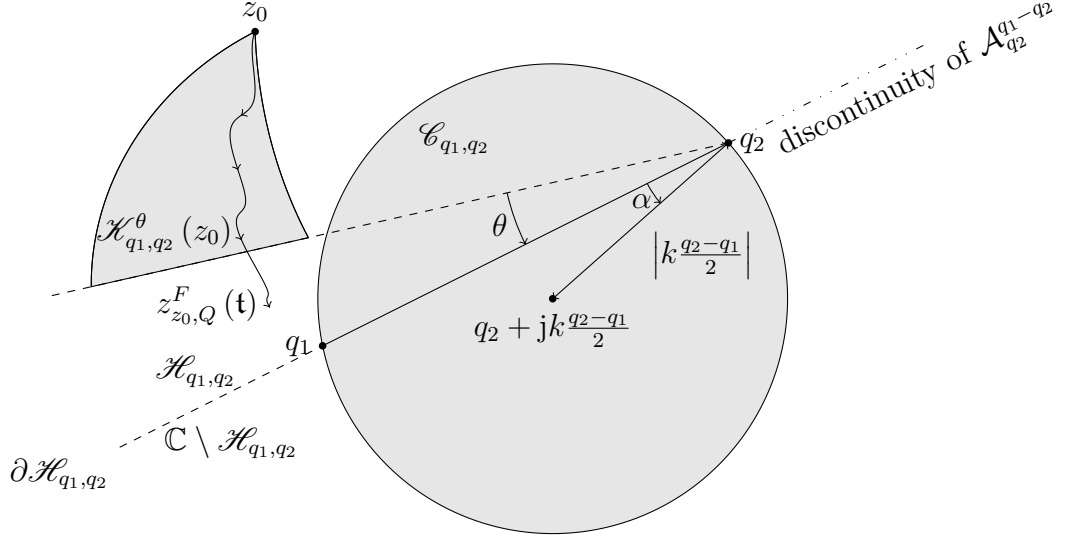
Figure 4.13: Auxiliary figure for .

1. $z_{z_0,Q}^F(\mathsf{t}) \in \mathscr{K}_{q_1,q_2}^\theta(z_0), \quad \forall \mathsf{t} \in [0, \mathsf{t}_1]$;

2. $\mathcal{A}_{q2}^{q_1-q_2}\left(z_{z_0,Q}^F(\mathsf{t}_1)\right) = -\theta$;

3. $\mathscr{K}_{q_1,q_2}^\theta(z_0) \setminus \{z_0\} \subset \{z \in \mathbb{C} \ : \ (z_0 - q_2) \otimes (z - q_2) > 0\}$.

Proof. By Proposition [4.3.3], there exists

$$\mathsf{t}_1 = \sup\left\{\mathsf{t} \in [0, +\infty) \ : \ z_{z_0,Q}^F(\mathsf{t}) \in \mathscr{K}_{q_1,q_2}^\theta(z_0)\right\} < +\infty.$$

Also, by Proposition [4.3.3], $\mathsf{t} \mapsto \mathcal{A}_{q2}^{q_1-q_2}\left(z_{z_0,Q}^F(\mathsf{t})\right)$ is *strictly* monotonously increasing in $(0, \mathsf{t}_2)$, where $\mathsf{t}_2 = \sup\left\{\mathsf{t} \in [0, +\infty) \ : \ z_{z_0,Q}^F(\mathsf{t}) \in \mathscr{R}_{q2}^{q_1-q_2} \setminus \mathscr{C}_{q_1,q_2}\right\}$ is greater than t_1. Use Proposition [4.3.2] to conclude that the continuous trajectory $\mathsf{t} \mapsto z_{z_0,Q}^F(\mathsf{t})$ is such that $z_{z_0,Q}^F(\mathsf{t})$ remains in $\mathscr{K}_{q_1,q_2}^\theta(z_0)$ while $\mathsf{t} \in [0, \mathsf{t}_1]$ and it leaves $\mathscr{K}_{q_1,q_2}^\theta(z_0)$, at $\mathsf{t} = \mathsf{t}_1$, by crossing

$$\mathscr{D}_{q_1,q_2}(z_0) \cap \left\{z \in \mathscr{R}_{q2}^{q_1-q_2} \ : \ \mathcal{A}_{q2}^{q_1-q_2}(z) = -\theta\right\} \subset \partial\mathscr{K}_{q_1,q_2}^\theta(z_0).$$

The last statement, $\mathscr{K}_{q_1,q_2}^\theta(z_0) \setminus \{z_0\} \subset \{z \in \mathbb{C} \ : \ (z_0 - q_2) \otimes (z - q_2) > 0\}$, follows directly from the fact that $\mathsf{t} \mapsto \mathcal{A}_{q2}^{q_1-q_2}\left(z_{z_0,Q}^F(\mathsf{t})\right)$ is *strictly* monotonously increasing in $(0, \mathsf{t}_2)$. $\qquad\square$

Remark 2. Note that for the case $\theta = 0$, the Corollary [4.3.1] gives sufficient conditions on the initial state in $\mathscr{H}_{q_1,q_2}$ for assuring that the state finally reaches $\partial\mathscr{H}_{q_1,q_2}$ at some finite time.

Remark 3. Check that if $z_0 \in \mathscr{H}_{q_1,q_2}$, $\theta \in \left[0, -\mathcal{A}_{q2}^{q_1-q_2}(z_0)\right)$ and $\mathcal{M}_{q2}^{q_1-q_2}(z_0) > |q_1 - q_2|$; the condition $\mathscr{K}_{q_1,q_2}^\theta(z_0) \cap \mathscr{C}_{q_1,q_2} = \emptyset$, required by Corollary [4.3.1], necessarily holds.

4.3.6.7. Switching dwell time

The next proposition may be a applied to examine a situation in which E's control set $\Sigma = [0,1]$ is replaced by the discrete set $\{0,1\}$ and a *dwell time* $\mathsf{t}_{\mathrm{dw}} > 0$ must elapse between every two consecutive discontinuities of every E's control function $\mathsf{t} \mapsto \sigma(\mathsf{t}) \in \{0,1\}$. Under such hypothesises, consider for example a case such that P selects a constant control action $u_0 \in U$ for which $\mathsf{q}(u_0,0) = q_1$ and $\mathsf{q}(u_0,1) = q_2$. For such a case, it is a fact that E cannot prevent the state from getting into $\mathbb{C} \setminus \mathscr{H}_{q_1,q_2}$ whatever the initial state in $\mathscr{H}_{q_1,q_2}$ is, and it follows logically from the next proposition. This contrasts with the state-space trajectories represented in Figures 4.6 and 4.7 included in $\mathscr{H}_{q_1,q_2}$ which never reach $\partial \mathscr{H}_{q_1,q_2}$. Actually, the next proposition shows that if in Figures 4.6 and 4.7 was E the only player in control of the compound input taking values in $\{q_1,q_2\}$, the represented trajectories would have been possible only at the cost of *infinitely fast* switching between both endpoints of $\underline{q_1 q_2}$, if $\Sigma = [0,1]$ is replaced by the discrete set $\{0,1\}$.

Proposition 4.3.4. *Let $q_1, q_2 \in \mathbb{C}$ such that $q_1 \neq q_2$ and*

$$\mathscr{H}_{q_1,q_2} = \{z \in \mathbb{C} \ : \ (q_2 - q_1) \otimes (z - q_1) > 0\}.$$

Consider the solution, $z_{z_0,Q}^F : [0,+\infty) \to \mathbb{C}$, of the initial value problem (4.8), with $z_0 \in \mathscr{H}_{q_1,q_2}$ and $Q : [0,+\infty) \to \mathscr{Q}$ piecewise continuous, being $\mathscr{Q} = \{q_1,q_2\}$.

If there exists a $\mathsf{t}_{\mathrm{dw}} > 0$ such that $\mathsf{t}_{i+1} - \mathsf{t}_i > \mathsf{t}_{\mathrm{dw}}$ for every pair $(\mathsf{t}_i, \mathsf{t}_{i+1})$ of consecutive time instants at which Q is discontinuous, then there exists a finite time $\mathsf{t}_f > 0$ such that $z_{z_0,Q}^F(\mathsf{t}_f) \in \mathbb{C} \setminus \mathscr{H}_{q_1,q_2}$.

Proof. Let

$$\mathscr{R}_{q_2}^{q_1-q_2} = \mathbb{C} \setminus \{q_2 - \rho(q_1 - q_2) \ : \ \rho \geq 0\},$$
$$\mathscr{D}_{q_1,q_2}(z_0) = \left\{z \in \mathbb{C} \ : \ \mathcal{M}_{q_1}^{q_1-q_2}(z) \leq \mathcal{M}_{q_1}^{q_1-q_2}(z_0) \ \wedge \ \mathcal{M}_{q_2}^{q_1-q_2}(z) \geq \mathcal{M}_{q_2}^{q_1-q_2}(z_0)\right\},$$

and $q \in \{q_1, q_2\}$. By Lemma 4.3.1,

$$\nabla \mathcal{M}_{q_2}^{q_1-q_2}(z) \odot F(z,q) = -\frac{\left(1+\kappa^2\right) \mathrm{e}^{\kappa \mathcal{A}_{q_2}^{q_1-q_2}(z)}}{|z - q_2|}(q_2 - z) \otimes (q - z),$$

for every $z \in \mathscr{K}_{q_1,q_2}^\theta \subset \mathscr{R}_{q_2}^{q_1-q_2} = \mathbb{C} \setminus \{q_2 - \rho(q_1 - q_2) \ : \ \rho \geq 0\}$. Expanding $(q - z)$ as

$$q - z = (q_2 - z) + \frac{q - q_2}{q_1 - q_2}(q_1 - q_2),$$

the previous dot product can be rewritten as

$$\nabla \mathcal{M}_{q_2}^{q_1-q_2}(z) \odot F(z,q) = -\frac{\left(1+\kappa^2\right) \mathrm{e}^{\kappa \mathcal{A}_{q_2}^{q_1-q_2}(z)}}{|z - q_2|}\left(\frac{q - q_2}{q_1 - q_2}\right)(q_2 - z) \otimes (q_1 - q_2),$$

where $\frac{q - q_2}{q_1 - q_2} \in \{0,1\}$ (because $q \in \{q_1, q_2\}$) and $(q_2 - z) \otimes (q_1 - q_2) < 0$ if $z \in \mathscr{H}_{q_1,q_2}$. Hence:

$$\forall z \in \mathscr{H}_{q_1,q_2}, \quad \nabla \mathcal{M}_{q_2}^{q_1-q_2}(z) \odot F(z,q) \begin{cases} > 0 & \text{if } q = q_1, \\ = 0 & \text{if } q = q_2; \end{cases} \tag{4.32}$$

$$\forall z \in \mathscr{H}_{q_1,q_2}, \quad \nabla \mathcal{M}_{q_2}^{q_1-q_2}(z) \odot F(z,q_1) \to 0 \iff \mathcal{A}_{q_2}^{q_1-q_2}(z) \to 0. \tag{4.33}$$

The function $t \mapsto Q(t)$ is piecewise constant and takes only two possible values: q_1 and q_2. The function $t \mapsto z_{z_0,Q}^F(t)$ is continuous. During the time intervals in which $Q(t) = q_1$ (resp. $Q(t) = q_2$), the state $z_{z_0,Q}^F(t)$ spirals counter-clockwise around q_1 (resp. q_2) with unitary angular speed. Therefore, t_{dw} must be less than π and $Q(t)$ cannot remain constant for intervals of length larger or equal than π, if there is any chance for $z_{z_0,Q}^F(t)$ to remain in $\mathscr{H}_{q_1,q_2}$ for every $t \geq 0$. Suppose this is the case, i.e., $t_{dw} < \pi$ and in every time interval of length π there is at least one discontinuity of Q. If not, the state would cross $\partial \mathscr{H}_{q_1,q_2}$ while spiralling around q_1 or q_2, and there would be nothing else to prove.

Suppose, by absurd, that $z_{z_0,Q}^F(t) \in \mathscr{H}_{q_1,q_2}$ for every $t \geq 0$. By Proposition 4.3.2, $z_{z_0,Q}^F(t) \in \mathscr{D}_{q_1,q_2}(z_0)$ for every $t \geq 0$. Let $H \triangleq \mathcal{M}_{q_2}^{q_1-q_2} \circ z_{z_0,Q}^F$, which is a continuous function, whose time derivative is

$$\dot{H}(t) = \nabla \mathcal{M}_{q_2}^{q_1-q_2}\left(z_{z_0,Q}^F(t)\right) \odot F\left(z_{z_0,Q}^F(t), Q(t)\right)$$

at every instant of time $t > 0$ at which Q is continuous. By (4.32), $\dot{H}(t) > 0$ during the time intervals in which $Q(t) = q_1$ and $\dot{H}(t) = 0$ during the time intervals in which $Q(t) = q_2$. Accordingly, H is monotonously increasing. There are two possible cases: $\{H(t) : t \geq 0\}$ is bounded above or not.

If $\{H(t) : t \geq 0\}$ is bounded above, there exists a finite limit

$$\lim_{t \to +\infty} H(t) = H(0) + \lim_{t \to +\infty} \int_0^t \dot{H}(t) \, dt < +\infty,$$

that asks for

$$\lim_{t \to +\infty} \dot{H}(t) = \lim_{t \to +\infty} \nabla \mathcal{M}_{q_2}^{q_1-q_2}\left(z_{z_0,Q}^F(t)\right) \odot F\left(z_{z_0,Q}^F(t), Q(t)\right) = 0. \tag{4.34}$$

Since Q is obliged to take the value q_1 at least once in every time interval of length π, and keep this value constant for at least $t_{dw} > 0$; the requirement (4.34) at the light of (4.32)–(4.33) allow to infer that

$$\mathcal{A}_{q_2}^{q_1-q_2}\left(z_{z_0,Q}^F(t)\right) \to 0$$

which means that $z_{z_0,Q}^F(t) \to \{q_2 + \rho(q_1 - q_2) : \rho > 0\} \cap \mathscr{D}_{q_1,q_2}(z_0) \subset \partial \mathscr{H}_{q_1,q_2}$. Once $z_{z_0,Q}^F(t)$ is sufficiently close to this line segment (whose distance to q_2 is positive), the obliged value q_2 that Q must take, for an interval of time of length greater than the given $t_{dw} > 0$, sweeps the state into $\left\{z \in \mathbb{C} : \mathcal{A}_{q_2}^{q_1-q_2}(z) \geq 0\right\} \subset \mathbb{C} \setminus \mathscr{H}_{q_1,q_2}$ by making it spiral counter-clock-wisely around q_2. This is absurd, because it was supposed that $z_{z_0,Q}^F(t) \in \mathscr{H}_{q_1,q_2}$ for every $t \geq 0$.

If $\{H(t) : t \geq 0\}$ is not bounded above, at some instant of time t_1, it must be $H(t_1) = \mathcal{M}_{q_2}^{q_1-q_2}\left(z_{z_0,Q}^F(t_1)\right) \gg \mathcal{M}_{q_2}^{q_1-q_2}(q_1)$. Actually, since H is monotonously increasing, $H(t) = \mathcal{M}_{q_2}^{q_1-q_2}\left(z_{z_0,Q}^F(t)\right) \gg \mathcal{M}_{q_2}^{q_1-q_2}(q_1)$ for every $t \geq t_1$. In addition, by Proposition 4.3.1, a $t_1' > t_1$ can be found such that $d\left(z_{z_0,Q}^F(t_1'), \partial \mathscr{H}_{q_1,q_2}\right) < \epsilon$ for an $\epsilon > 0$ as small as desired. In conclusion, there exists a t_1' such that $z_{z_0,Q}^F(t_1')$

is as far away from q_1 as desired and as close to the ray $\overrightarrow{q_2 q_1}$ as desired. From such point in state-space either q_1 or q_2 acting as the centre of a state-guiding α-equiangular spiral (maintained over a time interval greater than t_{dw}) sweeps the state away from $\mathscr{H}_{q_1,q_2}$ into $\mathbb{C} \backslash \mathscr{H}_{q_1,q_2}$. This is also absurd, because it was supposed that $z_{z_0,Q}^F(\mathsf{t}) \in \mathscr{H}_{q_1,q_2}$ for every $\mathsf{t} \geq 0$. $\qquad \square$

4.4. The underlying point-wise inf-sup problem

In contrast with the previous section, that was about *global* state temporal evolutions, this section is about *local* control action selection by each player.

It will become apparent soon the central role played by the family of point-wise inf-sup problems of the form

$$\inf_{u \in U} \sup_{\sigma \in \boldsymbol{\Sigma}} \{ p \odot f(z, u, \sigma) \}, \tag{4.35}$$

parametrized by $(z, p) \in \mathbb{C} \times \mathbb{C}$.

Once a $(z, p) \in \mathbb{C} \times \mathbb{C}$ has been fixed, the resulting problem (4.35) is said to be *solved* by a pair $(\hat{u}, \hat{\sigma}) \in U \times \boldsymbol{\Sigma}$, if

$$p \odot f(z, \hat{u}, \hat{\sigma}) = \inf_{u \in U} \sup_{\sigma \in \boldsymbol{\Sigma}} \{ p \odot f(z, u, \sigma) \}.$$

The following proposition summarizes essential facts, in connection with (4.35), that will be recurred to, in the following section and the following chapter.

Proposition 4.4.1.

1. *The* inf *and* sup *operations commute in* (4.35), *i.e.*,

$$\forall (z, p) \in \mathbb{C} \times \mathbb{C}, \quad \inf_{u \in U} \sup_{\sigma \in \boldsymbol{\Sigma}} \{ p \odot f(z, u, \sigma) \} = \sup_{\sigma \in \boldsymbol{\Sigma}} \inf_{u \in U} \{ p \odot f(z, u, \sigma) \}. \tag{4.36}$$

2. *Let* $u^* : \mathbb{C} \to U$ *and* $\sigma^* : \mathbb{C} \to \boldsymbol{\Sigma}$, *such that*

$$\begin{aligned} u^*(p) &\triangleq \quad \left(\frac{1 + i_o^{\triangledown}}{2} - \mathrm{sg}\left(-\bar{k}p, \mathrm{e}^{-\mathrm{j}2\beta} \right) \frac{1 - i_o^{\triangledown}}{2} \right) \\ &\quad + \mathrm{j} \left(\frac{1 + v_i^{\triangledown}}{2} - \mathrm{sg}\left(-\bar{k}p, \mathrm{e}^{\mathrm{j}\left(\frac{\pi}{2} - \beta \right)} \right) \frac{1 - v_i^{\triangledown}}{2} \right), \end{aligned} \tag{4.37}$$

$$\sigma^*(p) \triangleq \quad \left(\frac{1}{2} + \mathrm{sg}\left(-\bar{k}p, \mathrm{e}^{\mathrm{j}\left(\frac{\pi}{2} - \beta \right)} \right) \frac{1}{2} \right). \tag{4.38}$$

where $\mathrm{sg} : \mathbb{C} \times \mathbb{C} \to \{-1, 1\}$ *is defined by*

$$\mathrm{sg}(w_1, w_2) \triangleq \begin{cases} \mathrm{sgn}(w_1 \odot w_2) & \textit{if } w_1 \odot w_2 \neq 0, \\ \mathrm{sgn}(w_1 \otimes w_2) & \textit{if } w_1 \odot w_2 = 0, \end{cases}$$

and sgn $: \mathbb{R} \to \{-1, 0, 1\}$ *is defined by*

$$\operatorname{sgn}(\xi) \triangleq \begin{cases} 1 & \textit{if } \xi > 0, \\ 0 & \textit{if } \xi = 0, \\ -1 & \textit{if } \xi < 0. \end{cases}$$

For every $(z, p) \in \mathbb{C} \times \mathbb{C}$, *the pair* $(u^*(p), \sigma^*(p)) \in U \times \Sigma$ *solves* (4.35).

3. *Given* $(z, p) \in \mathbb{C} \times \mathbb{C}$, *such that* $\overline{k}p \odot \mathrm{e}^{-\mathrm{j}2\beta} \neq 0$ *and* $\overline{k}p \odot \mathrm{e}^{\mathrm{j}\left(\frac{\pi}{2} - \beta\right)} \neq 0$, *let* $(\hat{u}, \hat{\sigma}) \in U \times \Sigma$ *be any pair that solves* (4.35); *then,*

$$\mathsf{q}(\hat{u}, \hat{\sigma}) = \mathsf{q}(u^*(p), \sigma^*(p)).$$

Moreover,

$$\mathsf{q}(u^*(p), \sigma^*(p)) = \begin{cases} a & \textit{if } \left(-\overline{k}p\right) \odot \mathrm{e}^{-\mathrm{j}2\beta} > 0 \text{ and } \left(-\overline{k}p\right) \odot \mathrm{e}^{\mathrm{j}\left(\frac{\pi}{2} - \beta\right)} < 0, \\ b & \textit{if } \left(-\overline{k}p\right) \odot \mathrm{e}^{-\mathrm{j}2\beta} < 0 \text{ and } \left(-\overline{k}p\right) \odot \mathrm{e}^{\mathrm{j}\left(\frac{\pi}{2} - \beta\right)} < 0, \\ c & \textit{if } \left(-\overline{k}p\right) \odot \mathrm{e}^{-\mathrm{j}2\beta} < 0 \text{ and } \left(-\overline{k}p\right) \odot \mathrm{e}^{\mathrm{j}\left(\frac{\pi}{2} - \beta\right)} > 0, \\ d & \textit{if } \left(-\overline{k}p\right) \odot \mathrm{e}^{-\mathrm{j}2\beta} > 0 \text{ and } \left(-\overline{k}p\right) \odot \mathrm{e}^{\mathrm{j}\left(\frac{\pi}{2} - \beta\right)} > 0. \end{cases}$$

Proof. Let (z, p) be an arbitrary element of $\mathbb{C} \times \mathbb{C}$.

Recall that $f(z, u, \sigma) = k(z - \mathsf{q}(u, \sigma))$, so

$$p \odot f(z, u, \sigma) = p \odot (k(z - \mathsf{q}(u, \sigma))) = \left(p\overline{k}\right) \odot (z - \mathsf{q}(u, \sigma)) = \left(-\overline{k}p\right) \odot \mathsf{q}(u, \sigma) - \left(-\overline{k}p\right) \odot z,$$

for every $(u, \sigma) \in U \times \Sigma$. To simplify notation, let $r = -\overline{k}p$. Accordingly,

$$\inf_{u \in U} \sup_{\sigma \in \Sigma} \{p \odot f(z, u, \sigma)\} = \inf_{u \in U} \sup_{\sigma \in \Sigma} \{r \odot \mathsf{q}(u, \sigma) - r \odot z\}$$
$$= \inf_{u \in U} \sup_{\sigma \in \Sigma} \{r \odot \mathsf{q}(u, \sigma)\} - r \odot z.$$

Recall that $\mathsf{q}(u, \sigma) = -\mathrm{j}\delta_0 + \delta_1 \mathrm{e}^{-\mathrm{j}2\beta} \Re u + \delta_2 \mathrm{e}^{\mathrm{j}\left(\frac{\pi}{2} - \beta\right)} \sigma \Im u$, thus $r \odot \mathsf{q}(u, \sigma) = -\delta_0(r \odot \mathrm{j}) + \delta_1 \left(r \odot \mathrm{e}^{-\mathrm{j}2\beta}\right) \Re u + \delta_2 \left(r \odot \mathrm{e}^{\mathrm{j}\left(\frac{\pi}{2} - \beta\right)}\right) \sigma \Im u$. In addition, $\Sigma = [0, 1]$ and $U = \{i_o + \mathrm{j}v_i \ : \ i_o \in [i_o^\triangledown, 1], \ v_i \in [v_i^\triangledown, 1]\}$. Therefore,

$$\inf_{u \in U} \sup_{\sigma \in \Sigma} \{p \odot f(z, u, \sigma)\} = -\delta_0(r \odot \mathrm{j}) - r \odot z$$
$$+ \inf_{i_o \in [i_o^\triangledown, 1]} \left\{\delta_1 \left(r \odot \mathrm{e}^{-\mathrm{j}2\beta}\right) i_o\right\}$$
$$+ \inf_{v_i \in [v_i^\triangledown, 1]} \sup_{\sigma \in [0,1]} \left\{\delta_2 \left(r \odot \mathrm{e}^{\mathrm{j}\left(\frac{\pi}{2} - \beta\right)}\right) \sigma v_i\right\}. \quad (4.39)$$

It is clear that if the inf and sup operations commute in the last term of the RHS of the last equality, the above expansion can be reversed, with inf and sup interchanged, to conclude that

$$\inf_{u \in U} \sup_{\sigma \in \Sigma} \{p \odot f(z, u, \sigma)\} = \sup_{\sigma \in \Sigma} \inf_{u \in U} \{p \odot f(z, u, \sigma)\}.$$

Indeed,

$$\inf_{v_i \in \left[v_i^\triangledown, 1\right]} \sup_{\sigma \in [0,1]} \left\{ \delta_2 \left(r \odot \mathrm{e}^{\mathrm{j}\left(\frac{\pi}{2} - \beta\right)} \right) v_i \sigma \right\} = \sup_{\sigma \in [0,1]} \inf_{v_i \in \left[v_i^\triangledown, 1\right]} \left\{ \delta_2 \left(r \odot \mathrm{e}^{\mathrm{j}\left(\frac{\pi}{2} - \beta\right)} \right) v_i \sigma \right\},$$

because, recalling that δ_2 and $v_i^\triangledown$ are positive real numbers, direct execution of each alternative calculation leads to

$$\inf_{v_i \in \left[v_i^\triangledown, 1\right]} \sup_{\sigma \in [0,1]} \left\{ \delta_2 \left(r \odot \mathrm{e}^{\mathrm{j}\left(\frac{\pi}{2} - \beta\right)} \right) v_i \sigma \right\} = \begin{cases} \left(r \odot \mathrm{e}^{\mathrm{j}\left(\frac{\pi}{2} - \beta\right)} \right) v_i^\triangledown & \text{if } r \odot \mathrm{e}^{\mathrm{j}\left(\frac{\pi}{2} - \beta\right)} \geq 0, \\ 0 & \text{otherwise}; \end{cases}$$

$$\sup_{\sigma \in [0,1]} \inf_{v_i \in \left[v_i^\triangledown, 1\right]} \left\{ \delta_2 \left(r \odot \mathrm{e}^{\mathrm{j}\left(\frac{\pi}{2} - \beta\right)} \right) v_i \sigma \right\} = \begin{cases} \left(r \odot \mathrm{e}^{\mathrm{j}\left(\frac{\pi}{2} - \beta\right)} \right) v_i^\triangledown & \text{if } r \odot \mathrm{e}^{\mathrm{j}\left(\frac{\pi}{2} - \beta\right)} \geq 0, \\ 0 & \text{otherwise}. \end{cases}$$

This completes the proof of statement 1.

From (4.39) it is evident that problem (4.35) reduces to the following two problems:

$$\inf_{i_o \in \left[i_o^\triangledown, 1\right]} \left\{ \delta_1 \left(r \odot \mathrm{e}^{-\mathrm{j}2\beta} \right) i_o \right\}, \tag{4.40}$$

$$\inf_{v_i \in \left[v_i^\triangledown, 1\right]} \sup_{\sigma \in [0,1]} \left\{ \delta_2 \left(r \odot \mathrm{e}^{\mathrm{j}\left(\frac{\pi}{2} - \beta\right)} \right) v_i \sigma \right\}. \tag{4.41}$$

Using the expansion (4.39) and recalling that $\delta_1, \delta_2, v_i^\triangledown > 0$ and $i_o^\triangledown \geq 0$, it can be easily checked that the pair $(u^*(p), \sigma^*(p))$, as defined by (4.37)–(4.38), solves (4.35), as stated by statement 2.

Even though $(u^*(p), \sigma^*(p))$ may not be the unique solution of (4.35), note, however, that if $r \odot \mathrm{e}^{-\mathrm{j}2\beta} \neq 0$ and $r \odot \mathrm{e}^{\mathrm{j}\left(\frac{\pi}{2} - \beta\right)} \neq 0$, any solution $(\hat{u}, \hat{\sigma}) \in U \times \boldsymbol{\Sigma}$ of (4.35), must verify $\mathsf{q}(\hat{u}, \hat{\sigma}) = \mathsf{q}(u^*(p), \sigma^*(p))$. Indeed, if $(\hat{u}, \hat{\sigma})$ solves (4.35), according to the problem reduction (4.40)–(4.41) , $(\hat{u}, \hat{\sigma})$ must verify

$$\Re\hat{u} = \begin{cases} i_o^\triangledown & \text{if } r \odot \mathrm{e}^{-\mathrm{j}2\beta} > 0 \\ 1 & \text{if } r \odot \mathrm{e}^{-\mathrm{j}2\beta} < 0 \end{cases} = \Re(u^*(p)),$$

$$\hat{\sigma}\Im\hat{u} = \begin{cases} v_i^\triangledown & \text{if } r \odot \mathrm{e}^{\mathrm{j}\left(\frac{\pi}{2} - \beta\right)} > 0, \\ 0 & \text{if } r \odot \mathrm{e}^{\mathrm{j}\left(\frac{\pi}{2} - \beta\right)} < 0 \end{cases} = \sigma^*(p)\Im(u^*(p)).$$

Since $\mathsf{q}(u_1, \sigma_1) = \mathsf{q}(u_2, \sigma_2)$, for every $(u_1, u_2, \sigma_1, \sigma_2) \in U \times U \times \boldsymbol{\Sigma} \times \boldsymbol{\Sigma}$ such that $\Re u_1 = \Re u_2$ and $\sigma_1 \Im u_1 = \sigma_2 \Im u_2$; it follows that $\mathsf{q}(\hat{u}, \hat{\sigma}) = \mathsf{q}(u^*(p), \sigma^*(p))$, as stated by the first assertion of statement 3. The second one, follows from direct application of statement 2, under the hypothesis that $r \odot \mathrm{e}^{-\mathrm{j}2\beta} \neq 0$ and $r \odot \mathrm{e}^{\mathrm{j}\left(\frac{\pi}{2} - \beta\right)} \neq 0$. □

Remark 4. The pair $(u^*(p), \sigma^*(p))$, prescribed by (4.37)–(4.38) to solve (4.35), depends on p but not on z. In fact, it depends only on the argument of p, or equivalently, on the argument of $r = -\overline{k}p = (\sec\alpha)\,\mathrm{e}^{\mathrm{j}\left(\frac{\pi}{2} - \alpha\right)}p$ (see Figure 4.14). Only four values are possible for $\mathsf{q}(u^*(p), \sigma^*(p))$, namely, a, b, c and d (as defined in Table 3.6) which are the vertices of the parallelogram $\mathsf{q}\left([i_o^\triangledown, 1] + \mathrm{j}v_i^\triangledown, [0, 1]\right)$ (see Figures 3.7 and 3.8).

$$r_3 = -\overline{k}p_3$$
$$r_3 \odot e^{-j2\beta} < 0$$
$$r_3 \odot e^{j\left(\frac{\pi}{2}-\beta\right)} > 0$$
$$\mathsf{q}\left(u^*\left(p_3\right), \sigma^*\left(p_3\right)\right) = c$$

$$r_4 = -\overline{k}p_4$$
$$r_4 \odot e^{-j2\beta} > 0$$
$$r_4 \odot e^{j\left(\frac{\pi}{2}-\beta\right)} > 0$$
$$\mathsf{q}\left(u^*\left(p_4\right), \sigma^*\left(p_4\right)\right) = d$$

$$r_2 = -\overline{k}p_2$$
$$r_2 \odot e^{-j2\beta} < 0$$
$$r_2 \odot e^{j\left(\frac{\pi}{2}-\beta\right)} < 0$$
$$\mathsf{q}\left(u^*\left(p_2\right), \sigma^*\left(p_2\right)\right) = b$$

$$r_1 = -\overline{k}p_1$$
$$r_1 \odot e^{-j2\beta} > 0$$
$$r_1 \odot e^{j\left(\frac{\pi}{2}-\beta\right)} < 0$$
$$\mathsf{q}\left(u^*\left(p_1\right), \sigma^*\left(p_1\right)\right) = a$$
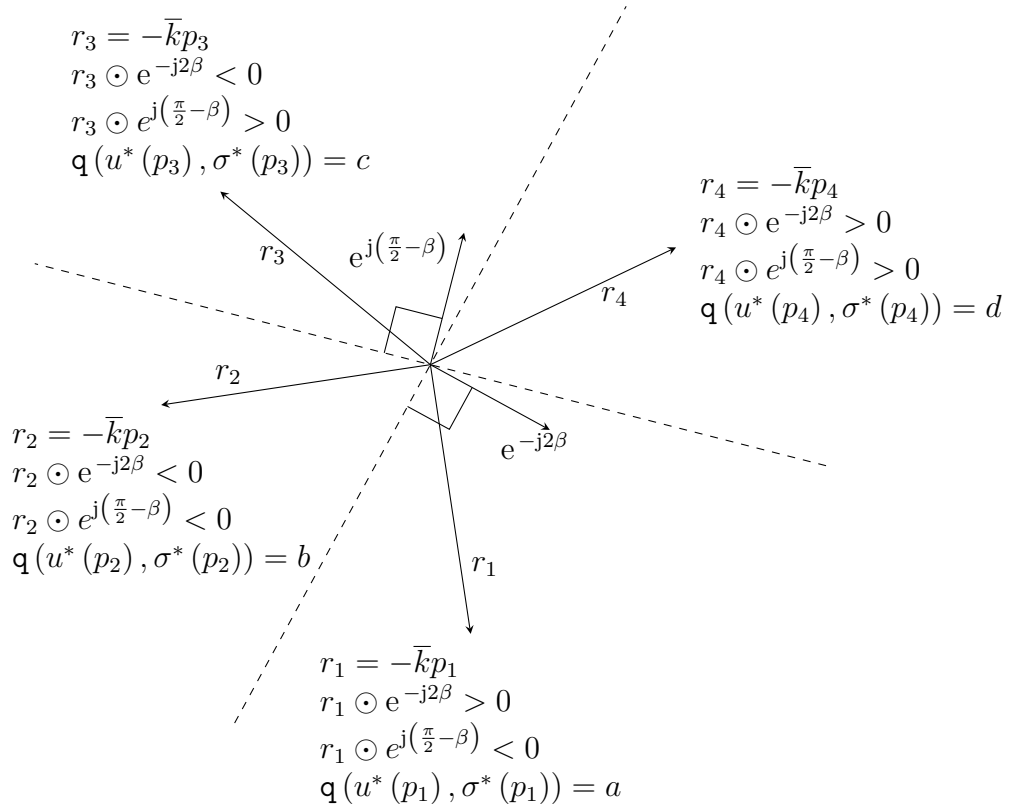
Figure 4.14: The pair $(u^*(p), \sigma^*(p))$ prescribed by the functions $u^* : \mathbb{C} \to U$ and $\sigma^* : \mathbb{C} \to \Sigma$ (defined in statement 2 of Proposition 4.4.1) to solve the inf-sup problem $\inf_{u\in U} \sup_{\sigma\in\Sigma}\{p \odot f(z,u,\sigma)\}$ depends only on the argument of $r \triangleq -\overline{k}p = (\sec\alpha)\,e^{j\left(\frac{\pi}{2}-\alpha\right)}p$; it does not depend on z.

Remark 5. Observe that $(u^*(p), \sigma^*(p))$ is not necessarily the only possible solution of (4.35), even if $\left(-\overline{k}p\right) \odot e^{-j2\beta} \neq 0$ and $\left(-\overline{k}p\right) \odot e^{j\left(\frac{\pi}{2}-\beta\right)} \neq 0$. For example, if $\left(-\overline{k}p\right) \odot e^{-j2\beta} > 0$ and $\left(-\overline{k}p\right) \odot e^{j\left(\frac{\pi}{2}-\beta\right)} < 0$, every pair $(i_o^{\triangledown} + jv_i, 0)$, with $v_i \in [v_i^{\triangledown}, 1]$, also solves (4.35) for every $z \in \mathbb{C}$. This is because every $(v_i, \sigma) \in [v_i^{\triangledown}, 1] \times \{0\}$ solves (4.41), if $\left(-\overline{k}p\right) \odot e^{j\left(\frac{\pi}{2}-\beta\right)} < 0$. However, non-unique solutions are not possible for the modified problem

$$\inf_{u\in U} \sup_{\sigma^{\triangledown}\leq\sigma\leq 1}\{p \odot f(z,u,\sigma)\}, \tag{4.42}$$

where $\sigma^{\triangledown} > 0$, if $\left(-\overline{k}p\right) \odot e^{-j2\beta} \neq 0$ and $\left(-\overline{k}p\right) \odot e^{j\left(\frac{\pi}{2}-\beta\right)} \neq 0$. The prescription $p \mapsto v_i^* = \Im(u^*(p))$, implicit in (4.37), is preferred over others that also solve (4.41) because it is somehow robust, i.e., it is the same that would result from solving (4.42) with arbitrarily small $\sigma^{\triangledown} > 0$, instead of (4.35).

Remark 6. As a by-product of the proof, the following expansion is obtained

$$
\begin{aligned}
\inf_{u \in U} \sup_{\sigma \in \mathbf{\Sigma}} \left\{ p \odot f\left(z, u, \sigma\right) \right\} = \sup_{\sigma \in \mathbf{\Sigma}} \inf_{u \in U} & \left\{ p \odot f\left(z, u, \sigma\right) \right\} \\
= & -\delta_0 \left(r \odot \mathrm{j} \right) - r \odot z \\
& + \inf_{i_o \in [i_o^\triangledown, 1]} \left\{ \delta_1 \left(r \odot \mathrm{e}^{-\mathrm{j}2\beta} \right) i_o \right\} \\
& + \inf_{v_i \in [v_i^\triangledown, 1]} \sup_{\sigma \in [0,1]} \left\{ \delta_2 \left(r \odot \mathrm{e}^{\mathrm{j}\left(\frac{\pi}{2} - \beta\right)} \right) v_i \sigma \right\}, \quad (4.43)
\end{aligned}
$$

where $r = -\overline{k} p$.

Remark 7. For the game in time, the running cost function (see section Subsection 2.1.2) is constant and equal to one, so the Hamiltonian function (see Subsection 2.6.1) adopts the form $(z, p, u, \sigma) \mapsto \mathcal{H}\left(z, p, u, \sigma\right) = p \odot f\left(z, u, \sigma\right) + 1$. For the game in distance, the running cost function is constant and equal to zero, so the Hamiltonian function adopts the form $(z, p, u, \sigma) \mapsto \mathcal{H}\left(z, p, u, \sigma\right) = p \odot f\left(z, u, \sigma\right)$. For both games, statement 1 of Proposition 4.4.1 implies that that the Isaacs' condition (see Subsection 2.6.2) holds, i.e.,

$$
\inf_{u \in U} \sup_{\sigma \in \mathbf{\Sigma}} \mathcal{H}\left(z, p, u, \sigma\right) = \sup_{\sigma \in \mathbf{\Sigma}} \inf_{u \in U} \mathcal{H}\left(z, p, u, \sigma\right).
$$

The functions $u^* : \mathbb{C} \to U$ and $\sigma^* : \mathbb{C} \to \mathbf{\Sigma}$, defined in statement 2 of the above proposition, will be used to build optimal strategies of the game in distance which is the matter of the following chapter. In particular, u^* and σ^* will be required to be evaluated at $p = \pm \mathrm{j}$. The following lemma paves the way for such evaluations.

Lemma 4.4.1. *If* $r^\pm = -\overline{k}\left(\pm \mathrm{j}\right)$*, then*

$$
r^\pm \odot \mathrm{e}^{-\mathrm{j}2\beta} \lesseqgtr 0, \tag{4.44}
$$
$$
r^\pm \odot \mathrm{e}^{\mathrm{j}\left(\frac{\pi}{2} - \beta\right)} \gtreqless 0. \tag{4.45}
$$

Proof. Evaluation of the dot products yields:

$$
r^\pm \odot \mathrm{e}^{-\mathrm{j}2\beta} = \mp \left(\mathrm{j}\overline{k} \right) \odot \mathrm{e}^{-\mathrm{j}2\beta} = \mp \overline{k} \otimes \mathrm{e}^{-\mathrm{j}2\beta} = \mp \Im \left(k \mathrm{e}^{-\mathrm{j}2\beta} \right),
$$
$$
r^\pm \odot \mathrm{e}^{\mathrm{j}\left(\frac{\pi}{2} - \beta\right)} = \mp \left(\mathrm{j}\overline{k} \right) \odot \mathrm{e}^{\mathrm{j}\left(\frac{\pi}{2} - \beta\right)} = \mp \overline{k} \otimes \mathrm{e}^{\mathrm{j}\left(\frac{\pi}{2} - \beta\right)} = \mp \Im \left(k \mathrm{e}^{\mathrm{j}\left(\frac{\pi}{2} - \beta\right)} \right).
$$

Since $k = -\kappa + \mathrm{j} = \sqrt{1 + \kappa^2} \mathrm{e}^{\mathrm{j}\left(\frac{\pi}{2} + \alpha\right)} = \dfrac{\mathrm{e}^{\mathrm{j}\left(\frac{\pi}{2} + \alpha\right)}}{\cos \alpha} = \left(\sec \alpha \right) \mathrm{e}^{\mathrm{j}\left(\frac{\pi}{2} + \alpha\right)}$, the above expressions become

$$
r^\pm \odot \mathrm{e}^{-\mathrm{j}2\beta} = \left(\mp \sec \alpha \right) \Im \left(\mathrm{e}^{\mathrm{j}\left(\frac{\pi}{2} + \alpha - 2\beta\right)} \right) = \left(\mp \sec \alpha \right) \sin \left(\frac{\pi}{2} + \alpha - 2\beta \right),
$$
$$
r^\pm \odot \mathrm{e}^{\mathrm{j}\left(\frac{\pi}{2} - \beta\right)} = \left(\mp \sec \alpha \right) \Im \left(\mathrm{e}^{\mathrm{j}\left(\pi + \alpha - \beta\right)} \right) = \left(\mp \sec \alpha \right) \sin \left(\pi + \alpha - \beta \right);
$$

or equivalently

$$
r^\pm \odot \mathrm{e}^{-\mathrm{j}2\beta} = \mp \sec \alpha \cos \left(\alpha - 2\beta \right),
$$
$$
r^\pm \odot \mathrm{e}^{\mathrm{j}\left(\frac{\pi}{2} - \beta\right)} = \pm \sec \alpha \sin \left(\alpha - \beta \right).
$$

To prove the lemma it is enough to prove the following inequalities:

$$\sec \alpha > 0,$$
$$\cos (\alpha - 2\beta) > 0,$$
$$\sin (\alpha - \beta) > 0.$$

Recall that the seven real parameters, which make up function f, must verify (4.2), (4.3) and (4.4). In particular, (4.2) is the logical conjunction of:

$$\alpha \in \left(0, \frac{\pi}{2}\right), \tag{4.46}$$
$$|\beta| < \alpha, \tag{4.47}$$
$$\tan \alpha - \tan \beta < \sec \alpha. \tag{4.48}$$

From (4.46)–(4.47), it is clear that $\sec \alpha > 0$ and $\sin (\alpha - \beta) > 0$. To prove that $\cos (\alpha - 2\beta) > 0$, the inequality (4.48) is needed as it is shown next.

Note that

$$\begin{aligned}
\cos (\alpha - 2\beta) &= \cos (2\beta - \alpha) = \cos (2\beta) \cos \alpha + \sin (2\beta) \sin \alpha \\
&= \frac{1 - \tan^2 \beta}{1 + \tan^2 \beta} \cos \alpha + \frac{2 \tan \beta}{1 + \tan^2 \beta} \sin \alpha \\
&= \frac{1}{1 + \tan^2 \beta} \left(\left(1 - \tan^2 \beta\right) \cos \alpha + 2 \tan \beta \sin \alpha\right) \\
&= \cos^2 \beta \left(\left(1 - \tan^2 \beta\right) \cos \alpha + 2 \tan \beta \sin \alpha\right) \\
&= \cos^2 \beta \left(\left(1 - \tan^2 \beta\right) \sqrt{1 - \sin^2 \alpha} + 2 \sin \alpha \tan \beta\right).
\end{aligned}$$

Let $\zeta \triangleq \sin \alpha$ and $\lambda \triangleq \cos \alpha (\tan \alpha - \tan \beta)$. From above,

$$\cos (\alpha - 2\beta) = \cos^2 \beta \left(\left(1 - \tan^2 \beta\right) \sqrt{1 - \zeta^2} + 2\zeta \tan \beta\right) \tag{4.49}$$

The difference between ζ and λ is

$$\begin{aligned}
\zeta - \lambda &= \sin \alpha - \cos \alpha (\tan \alpha - \tan \beta) = \cos \alpha \tan \beta \\
&= \sqrt{1 - \zeta^2} \tan \beta,
\end{aligned}$$

Solve for $\tan \beta$ in this last equation and substitute into (4.49) to obtain

$$\begin{aligned}
\cos (\alpha - 2\beta) &= \cos^2 \beta \left(\left(1 - \frac{(\zeta - \lambda)^2}{1 - \zeta^2}\right) \sqrt{1 - \zeta^2} + 2\zeta \frac{\zeta - \lambda}{\sqrt{1 - \zeta^2}}\right) \\
&= \frac{\cos^2 \beta}{\sqrt{1 - \zeta^2}} \left(1 - \zeta^2 - (\zeta - \lambda)^2 + 2\zeta (\zeta - \lambda)\right) \\
&= \frac{\cos^2 \beta}{\sqrt{1 - \zeta^2}} \left(1 - \lambda^2\right) \\
&= \frac{\cos^2 \beta}{\cos \alpha} (1 + \lambda) (1 - \lambda) \\
&= \frac{\cos^2 \beta}{\cos \alpha} (1 + \cos \alpha (\tan \alpha - \tan \beta)) (1 - \cos \alpha (\tan \alpha - \tan \beta)) \\
&= \cos^2 \beta (1 + \cos \alpha (\tan \alpha - \tan \beta)) (\sec \alpha - (\tan \alpha - \tan \beta))
\end{aligned}$$

Observe that, since $\alpha \in \left(0, \frac{\pi}{2}\right)$ and $|\beta| < \alpha$, the following inequalities hold: $\cos\alpha > 0$ and $\tan\alpha - \tan\beta > 0$. In addition, by (4.48), $\sec\alpha - (\tan\alpha - \tan\beta) > 0$. Consequently,

$$\cos(\alpha - 2\beta) > 0.$$

$\square$

Note 1. In the course of the proof of the previous lemma, ζ and λ were defined in terms of α and β in such a way that they happen to coincide with the *canonical parameters* ζ and λ of Subsection 3.4.4. Notice, however, that is was not necessary to recall their physical meaning to complete the proof, which follows exclusively from (4.2).

The following corollary, which follows logically from Proposition 4.4.1 and the previous lemma, characterizes the initial (in retrogressive sense) compound control actions for the retrogressive integration technique which is used, in the following chapter, to obtain candidate optimal trajectories of the game in distance.

Corollary 4.4.1. *For every $z \in \mathbb{C}$:*

$$\inf_{u\in U}\sup_{\sigma\in\Sigma}\left\{+\mathrm{j}\odot f\left(z,u,\sigma\right)\right\} = +\overline{k}\otimes(z-c), \tag{4.50}$$

$$\inf_{u\in U}\sup_{\sigma\in\Sigma}\left\{-\mathrm{j}\odot f\left(z,u,\sigma\right)\right\} = -\overline{k}\otimes(z-a). \tag{4.51}$$

Furthermore:

1. *if $(\hat{u},\hat{\sigma})$ solves the* inf*-sup* *problem in the* LHS *of* (4.50)*, then*

$$\mathsf{q}\left(\hat{u},\hat{\sigma}\right) = \mathsf{q}\left(u^{*}\left(+\mathrm{j}\right),\sigma^{*}\left(+\mathrm{j}\right)\right) = c;$$

2. *if $(\hat{u},\hat{\sigma})$ solves the* inf*-sup* *problem in the* LHS *of* (4.51)*, then*

$$\mathsf{q}\left(\hat{u},\hat{\sigma}\right) = \mathsf{q}\left(u^{*}\left(-\mathrm{j}\right),\sigma^{*}\left(-\mathrm{j}\right)\right) = a.$$

Proof. Consider the family (4.35) of point-wise inf-sup problems parametrized by $(z,p) \in \mathbb{C} \times \mathbb{C}$. Suppose p is either $+\mathrm{j}$ or $-\mathrm{j}$. To consider both alternatives simultaneously let $p^{\pm} = \pm\mathrm{j}$ and $r^{\pm} = -\overline{k}p^{\pm} = -\overline{k}\left(\pm\mathrm{j}\right)$. According to Lemma 4.4.1,

$$r^{\pm}\odot\mathrm{e}^{-\mathrm{j}2\beta} \lessgtr 0, \tag{4.52}$$

$$r^{\pm}\odot\mathrm{e}^{\mathrm{j}\left(\frac{\pi}{2}-\beta\right)} \gtrless 0. \tag{4.53}$$

Recalling statement 3 of Proposition 4.4.1, the inequalities (4.52) and (4.53) imply that

$$\inf_{u\in U}\sup_{\sigma\in\Sigma}\left\{p\odot f\left(z,u,\sigma\right)\right\} = \begin{cases} p\odot\left(k\left(z-c\right)\right) & \text{if } p=+\mathrm{j}, \\ p\odot\left(k\left(z-a\right)\right) & \text{if } p=-\mathrm{j}; \end{cases}$$

or equivalently

$$\inf_{u \in U} \sup_{\sigma \in \mathbf{\Sigma}} \{p \odot f(z, u, \sigma)\} = \begin{cases} \left(+\mathsf{j}\overline{k}\right) \odot (z - c) = +\overline{k} \otimes (z - c) & \text{if } p = +\mathsf{j}, \\ \left(-\mathsf{j}\overline{k}\right) \odot (z - a) = -\overline{k} \otimes (z - a) & \text{if } p = -\mathsf{j}. \end{cases}$$

It follows, from this last expression, that

$$\inf_{u \in U} \sup_{\sigma \in \mathbf{\Sigma}} \{+\mathsf{j} \odot f(z, u, \sigma)\} = +\overline{k} \otimes (z - c), \tag{4.54}$$

$$\inf_{u \in U} \sup_{\sigma \in \mathbf{\Sigma}} \{-\mathsf{j} \odot f(z, u, \sigma)\} = -\overline{k} \otimes (z - a). \tag{4.55}$$

In addition, by the same statement of Proposition 4.4.1, if $(\hat{u}, \hat{\sigma}) \in U \times \mathbf{\Sigma}$ solves the LHS of (4.54), the following equality must hold

$$\mathsf{q}(\hat{u}, \hat{\sigma}) = \mathsf{q}(u^*(+\mathsf{j}), \sigma^*(+\mathsf{j})) = c.$$

Similarly, if $(\hat{u}, \hat{\sigma}) \in U \times \mathbf{\Sigma}$ solves the LHS of (4.55), the following equality must hold

$$\mathsf{q}(\hat{u}, \hat{\sigma}) = \mathsf{q}(u^*(-\mathsf{j}), \sigma^*(-\mathsf{j})) = a.$$

$\square$

4.5. Semi-permeable curves

This section is devoted to the systematic search of semi-permeable surfaces (defined in Section 2.5) associated to the SE in (4.1). Since the state space, in this case, is the *two* dimensional real vector space $\mathbb{C}$, these subsets of the state space will be referred to as semi-permeable *curves.*

4.5.1. The unknowns

Consider a smooth curve $\mathscr{S} \subset \mathbb{C}$ given implicitly by $\mathscr{S} = \{w : \mathcal{U}(w) = 0\}$, where $\mathcal{U} : \mathscr{R} \to \mathbb{R}$ is a real valued function defined on a region $\mathscr{R}$ of $\mathbb{C}$. Without loss of generality, assume that, from both sides of the surface, E prefers the side $\{w : \mathcal{U}(w) > 0\}$ and P prefers the side $\{w : \mathcal{U}(w) < 0\}$.

Let $z \in \mathscr{S}$ and $p = \nabla \mathcal{U}(z)$. Since $\mathscr{S}$ is smooth, $p \neq 0$ is normal to $\mathscr{S}$ at z, and $\pm \mathsf{j}p$ are tangents to $\mathscr{S}$ at z. Let

$$r = -\overline{k}p = -\overline{(-\kappa + \mathsf{j})}p = (\kappa + \mathsf{j})p = \sqrt{1 + \kappa^2}\mathrm{e}^{\mathsf{j}\left(\frac{\pi}{2} - \alpha\right)}p = \frac{\mathrm{e}^{\mathsf{j}\left(\frac{\pi}{2} - \alpha\right)}}{\cos \alpha}p.$$

The objects just introduced will be referred to in the next three propositions. Keep in mind that p reflects the players' opposite preferences with respect to both sides of $\mathscr{S}$.

4.5.2. Characterization of semi-permeable curves

Proposition 4.5.1. *The curve $\mathscr{S}$ is semi-permeable at z, if and only if*

$$\inf_{u \in U} \sup_{\sigma \in \boldsymbol{\Sigma}} \{p \odot f(z, u, \sigma)\} = 0.$$

Proof. By definition of semi-permeability, the curve $\mathscr{S}$ is semi-permeable at z, if there exist controls $\hat{u} \in U$ and $\hat{\sigma} \in \boldsymbol{\Sigma}$ such that

$$\forall u \in U, \; \forall \sigma \in \boldsymbol{\Sigma}, \quad p \odot f(z, \hat{u}, \sigma) \leq p \odot f(z, \hat{u}, \hat{\sigma}) = 0 \leq p \odot f(z, u, \hat{\sigma}). \quad (4.56)$$

The interchangeability of the inf and sup operations in any problem of the form (4.35) (guaranteed by statement 1 of Proposition 4.4.1) allow for expressing the semi-permeability condition (4.56) simply as

$$\inf_{u \in U} \sup_{\sigma \in \boldsymbol{\Sigma}} \{p \odot f(z, u, \sigma)\} = 0,$$

as it was pointed out in Section 2.5 (within the $\mathbb{R}^n$ set-up of Chapter 2 instead of $\mathbb{C}$). $\qquad \square$

Proposition 4.5.2. *Assume that $r \odot \mathrm{e}^{-\mathrm{j}2\beta} \neq 0$ and $r \odot \mathrm{e}^{\mathrm{j}\left(\frac{\pi}{2} - \beta\right)} \neq 0$ and let $q = \mathsf{q}\left(u^*(p), \sigma^*(p)\right) \in \{a, b, c, d\}$ (see statements 2 and 3 of Proposition 4.4.1).*
Under these assumptions, the curve $\mathscr{S}$ is semi-permeable at z if and only if

$$p \odot (k(z - q)) = 0,$$

or, equivalently, if and only if

$$r \odot (z - q) = 0.$$

Proof. The statement 2 of Proposition 4.4.1, by means of functions u^* and σ^*, provides a pair $(u^*(p), \sigma^*(p)) \in U \times \boldsymbol{\Sigma}$, such that

$$p \odot f(z, u^*(p), \sigma^*(p)) = \inf_{u \in U} \sup_{\sigma \in \boldsymbol{\Sigma}} \{p \odot f(z, u, \sigma)\}.$$

Even though, there could be other pairs $(\hat{u}, \hat{\sigma}) \in U \times \boldsymbol{\Sigma}$, possibly different from $(u^*(p), \sigma^*(p))$, such that

$$p \odot f(z, \hat{u}, \hat{\sigma}) = \inf_{u \in U} \sup_{\sigma \in \boldsymbol{\Sigma}} \{p \odot f(z, u, \sigma)\};$$

statement 3 of Proposition 4.4.1 states that, if $r \odot \mathrm{e}^{-\mathrm{j}2\beta} \neq 0$ and $r \odot \mathrm{e}^{\mathrm{j}\left(\frac{\pi}{2} - \beta\right)} \neq 0$, the functional value $\mathsf{q}(\hat{u}, \hat{\sigma})$ must coincide with $\mathsf{q}(u^*(p), \sigma^*(p))$, which in turn must belong to the finite set $\{a, b, c, d\}$. This means that, if $r \odot \mathrm{e}^{-\mathrm{j}2\beta} \neq 0$ and $r \odot \mathrm{e}^{\mathrm{j}\left(\frac{\pi}{2} - \beta\right)} \neq 0$, the complex number $q \triangleq \mathsf{q}(u^*(p), \sigma^*(p)) \in \{a, b, c, d\}$ is the only one that satisfies

$$p \odot (k(z - q)) = \inf_{u \in U} \sup_{\sigma \in \boldsymbol{\Sigma}} \{p \odot f(z, u, \sigma)\}, \quad (4.57)$$

where it was used that, by definition, $f(z, u, \sigma) = k(z - \mathsf{q}(u, \sigma))$ for every $(z, u, \sigma) \in \mathbb{C} \times U \times \mathbf{\Sigma}$.

Consequently, assuming $r \odot \mathrm{e}^{-\mathrm{j}2\beta} \neq 0$ and $r \odot \mathrm{e}^{\mathrm{j}\left(\frac{\pi}{2} - \beta\right)} \neq 0$, it follows, from Proposition 4.5.1 and (4.57), that $\mathscr{S}$ is semi-permeable at z if and only if

$$p \odot (k(z - q)) = 0,$$

or, equivalently, if and only if

$$r \odot (z - q) = 0,$$

because $p \odot (k(z - q)) = \left(\overline{k}p\right) \odot (z - q) = -r \odot (z - q)$. $\square$

Proposition 4.5.3. *Define eight sectors of the complex plane as follows:*

$$\mathscr{A}_a^+ \triangleq \mathscr{A}_{a,\left(0, \frac{\pi}{2} + \beta\right)}^{a-b} = \left\{ w \ : \ (w - a) \otimes \mathrm{e}^{-\mathrm{j}2\beta} > 0 \ \wedge \ (w - a) \otimes \mathrm{e}^{\mathrm{j}\left(\frac{\pi}{2} - \beta\right)} < 0 \right\},$$

$$\mathscr{A}_a^- \triangleq \mathscr{A}_{a,\left(0, \frac{\pi}{2} + \beta\right)}^{b-a} = \left\{ w \ : \ (w - a) \otimes \mathrm{e}^{-\mathrm{j}2\beta} < 0 \ \wedge \ (w - a) \otimes \mathrm{e}^{\mathrm{j}\left(\frac{\pi}{2} - \beta\right)} > 0 \right\},$$

$$\mathscr{A}_b^+ \triangleq \mathscr{A}_{b,\left(0, \frac{\pi}{2} - \beta\right)}^{c-b} = \left\{ w \ : \ (w - b) \otimes \mathrm{e}^{-\mathrm{j}2\beta} < 0 \ \wedge \ (w - b) \otimes \mathrm{e}^{\mathrm{j}\left(\frac{\pi}{2} - \beta\right)} < 0 \right\},$$

$$\mathscr{A}_b^- \triangleq \mathscr{A}_{b,\left(0, \frac{\pi}{2} - \beta\right)}^{b-c} = \left\{ w \ : \ (w - b) \otimes \mathrm{e}^{-\mathrm{j}2\beta} > 0 \ \wedge \ (w - b) \otimes \mathrm{e}^{\mathrm{j}\left(\frac{\pi}{2} - \beta\right)} > 0 \right\},$$

$$\mathscr{A}_c^+ \triangleq \mathscr{A}_{c,\left(0, \frac{\pi}{2} + \beta\right)}^{c-d} = \left\{ w \ : \ (w - c) \otimes \mathrm{e}^{-\mathrm{j}2\beta} < 0 \ \wedge \ (w - c) \otimes \mathrm{e}^{\mathrm{j}\left(\frac{\pi}{2} - \beta\right)} > 0 \right\},$$

$$\mathscr{A}_c^- \triangleq \mathscr{A}_{c,\left(0, \frac{\pi}{2} + \beta\right)}^{d-c} = \left\{ w \ : \ (w - c) \otimes \mathrm{e}^{-\mathrm{j}2\beta} > 0 \ \wedge \ (w - c) \otimes \mathrm{e}^{\mathrm{j}\left(\frac{\pi}{2} - \beta\right)} < 0 \right\},$$

$$\mathscr{A}_d^+ \triangleq \mathscr{A}_{d,\left(0, \frac{\pi}{2} - \beta\right)}^{a-d} = \left\{ w \ : \ (w - d) \otimes \mathrm{e}^{-\mathrm{j}2\beta} > 0 \ \wedge \ (w - d) \otimes \mathrm{e}^{\mathrm{j}\left(\frac{\pi}{2} - \beta\right)} > 0 \right\},$$

$$\mathscr{A}_d^- \triangleq \mathscr{A}_{d,\left(0, \frac{\pi}{2} - \beta\right)}^{d-a} = \left\{ w \ : \ (w - d) \otimes \mathrm{e}^{-\mathrm{j}2\beta} < 0 \ \wedge \ (w - d) \otimes \mathrm{e}^{\mathrm{j}\left(\frac{\pi}{2} - \beta\right)} < 0 \right\}.$$

Assume that

$$r \notin \left\{ w \ : \ w \odot \mathrm{e}^{-\mathrm{j}2\beta} = 0 \ \vee \ w \odot \mathrm{e}^{\mathrm{j}\left(\frac{\pi}{2} - \beta\right)} = 0 \right\},$$

so that $q \triangleq \mathsf{q}\left(u^*(p), \sigma^*(p)\right)$ belongs $\{a, b, c, d\}$ (as detailed by statement 3 of Proposition 4.4.1), and suppose that

$$z \notin \{a, b, c, d\}.$$

If the curve $\mathscr{S}$ is semi-permeable at z, then either $z \in \mathscr{A}_q^+$ or $z \in \mathscr{A}_q^-$. Moreover,

$$p = \begin{cases} -\mathrm{j}\,|p|\,\dfrac{k(z-q)}{|k(z-q)|} & \text{if } z \in \mathscr{A}_q^+, \\ +\mathrm{j}\,|p|\,\dfrac{k(z-q)}{|k(z-q)|} & \text{if } z \in \mathscr{A}_q^-, \end{cases} \qquad r = \begin{cases} +\mathrm{j}\,\dfrac{(z-q)}{|z-q|}\,|kp| & \text{if } z \in \mathscr{A}_q^+, \\ -\mathrm{j}\,\dfrac{(z-q)}{|z-q|}\,|kp| & \text{if } z \in \mathscr{A}_q^-. \end{cases}$$
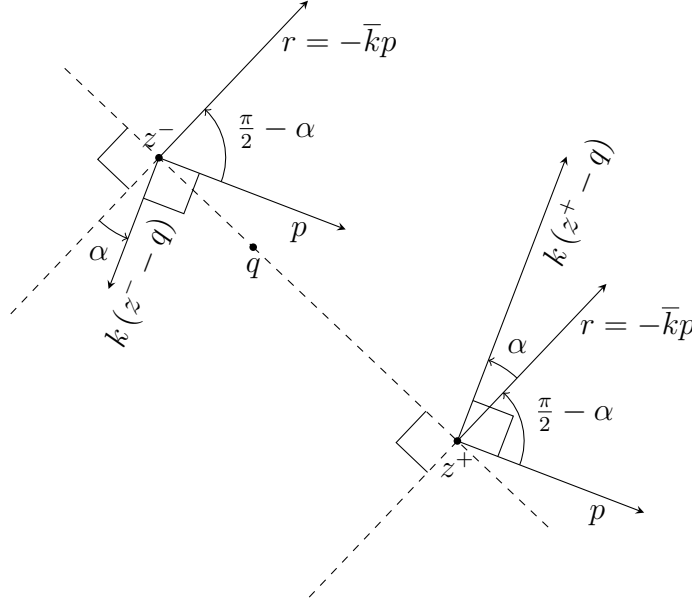
Figure 4.15: Let z be point of an unknown smooth curve $\mathscr{S}$ whose known normal at z is $p \neq 0$. If $z \notin \{a, b, c, d\}$ and $r \triangleq -\overline{k}p \notin \left\{ w \; : \; w \odot \mathrm{e}^{-\mathrm{j}2\beta} = 0 \;\vee\; w \odot \mathrm{e}^{\mathrm{j}\left(\frac{\pi}{2}-\beta\right)} = 0 \right\}$, $\mathscr{S}$ is semi-permeable at z if and only if $p \odot (k(z-q)) = 0$ where $q = \mathsf{q}\left(u^*(p), \sigma^*(p)\right) \in \{a, b, c, d\}$, being u^* and σ^* the functions defined in statement 2 of Proposition 4.4.1. These conditions restrict z to belong to either $\mathscr{A}_q^+$ (if $\frac{k(z-q)}{|z-q|} = +\mathrm{j}\frac{p}{|p|}$), or $\mathscr{A}_q^-$ (if $\frac{k(z-q)}{|z-q|} = -\mathrm{j}\frac{p}{|p|}$). These two alternatives are exemplified in the figure by the points $z^+ \in \mathscr{A}_q^+$ and $z^- \in \mathscr{A}_q^-$.

Proof. By hypothesis, $r \notin \left\{ w \; : \; w \odot \mathrm{e}^{-\mathrm{j}2\beta} = 0 \;\vee\; w \odot \mathrm{e}^{\mathrm{j}\left(\frac{\pi}{2}-\beta\right)} = 0 \right\}$ and the curve $\mathscr{S}$ is semi-permeable at z. Hence, by Proposition 4.5.2,

$$p \odot (k(z-q)) = 0 \tag{4.58}$$

and

$$r \odot (z - q) = 0,$$

where $q \triangleq \mathsf{q}\left(u^*(p), \sigma^*(p)\right) \in \{a, b, c, d\}$ (recall statement 3 of Proposition 4.4.1).

By hypothesis, $z \notin \{a, b, c, d\}$, so $z - q \neq 0$. Since $p \neq 0$, from (4.58) it follows that either $\frac{k(z-q)}{|k(z-q)|} = +\mathrm{j}\frac{p}{|p|}$ or $\frac{k(z-q)}{|k(z-q)|} = -\mathrm{j}\frac{p}{|p|}$ if , i.e., the direction of $k(z-q)$ must be one of the only two directions tangent to $\mathscr{S}$ at z (see Figure 4.15). Hence, p adopts different expressions, in terms of $(z-q)$, depending on the case:

$$p = \begin{cases} -\mathrm{j}\,|p|\,\frac{k(z-q)}{|k(z-q)|} & \text{if } \frac{k(z-q)}{|k(z-q)|} = +\mathrm{j}\frac{p}{|p|}, \\ +\mathrm{j}\,|p|\,\frac{k(z-q)}{|k(z-q)|} & \text{if } \frac{k(z-q)}{|k(z-q)|} = -\mathrm{j}\frac{p}{|p|}. \end{cases}$$

Accordingly, $r = -\overline{k}p$ also adopts different expressions, in terms of $(z-q)$, depending on the case:

$$r = \begin{cases} +\mathrm{j}\,\frac{(z-q)}{|z-q|}\,|kp| & \text{if } \frac{k(z-q)}{|k(z-q)|} = +\mathrm{j}\frac{p}{|p|}, \\ -\mathrm{j}\,\frac{(z-q)}{|z-q|}\,|kp| & \text{if } \frac{k(z-q)}{|k(z-q)|} = -\mathrm{j}\frac{p}{|p|}. \end{cases} \tag{4.59}$$

The point $q = \mathsf{q}\left(u^*\left(p\right), \sigma^*\left(p\right)\right)$ belongs to $\{a, b, c, d\}$. Specifically, as detailed by statement 3 of Proposition 4.4.1:

$$q = \begin{cases} a & \text{if } r \odot \mathrm{e}^{-\mathrm{j}2\beta} > 0 \text{ and } r \odot \mathrm{e}^{\mathrm{j}\left(\frac{\pi}{2}-\beta\right)} < 0, \\ b & \text{if } r \odot \mathrm{e}^{-\mathrm{j}2\beta} < 0 \text{ and } r \odot \mathrm{e}^{\mathrm{j}\left(\frac{\pi}{2}-\beta\right)} < 0, \\ c & \text{if } r \odot \mathrm{e}^{-\mathrm{j}2\beta} < 0 \text{ and } r \odot \mathrm{e}^{\mathrm{j}\left(\frac{\pi}{2}-\beta\right)} > 0, \\ d & \text{if } r \odot \mathrm{e}^{-\mathrm{j}2\beta} > 0 \text{ and } r \odot \mathrm{e}^{\mathrm{j}\left(\frac{\pi}{2}-\beta\right)} > 0. \end{cases} \qquad (4.60)$$

Suppose r is such that the first case of the RHS of (4.60) holds, then undoubtedly $q = a$. Moreover, in view of (4.59), z must satisfy either $(\mathrm{j}\left(z - a\right)) \odot \mathrm{e}^{-\mathrm{j}2\beta} > 0$ and $(\mathrm{j}\left(z - a\right)) \odot \mathrm{e}^{\mathrm{j}\left(\frac{\pi}{2}-\beta\right)} < 0$, or $(\mathrm{j}\left(z - a\right)) \odot \mathrm{e}^{-\mathrm{j}2\beta} < 0$ and $(\mathrm{j}\left(z - a\right)) \odot \mathrm{e}^{\mathrm{j}\left(\frac{\pi}{2}-\beta\right)} > 0$. Consequently, z must belong to either

$$\mathscr{A}_a^+ \triangleq \mathscr{A}_{a,\left(0,\frac{\pi}{2}+\beta\right)}^{a-b} = \left\{w \ : \ (w - a) \otimes \mathrm{e}^{-\mathrm{j}2\beta} > 0 \ \wedge \ (w - a) \otimes \mathrm{e}^{\mathrm{j}\left(\frac{\pi}{2}-\beta\right)} < 0\right\},$$

or

$$\mathscr{A}_a^- \triangleq \mathscr{A}_{a,\left(0,\frac{\pi}{2}+\beta\right)}^{b-a} = \left\{w \ : \ (w - a) \otimes \mathrm{e}^{-\mathrm{j}2\beta} < 0 \ \wedge \ (w - a) \otimes \mathrm{e}^{\mathrm{j}\left(\frac{\pi}{2}-\beta\right)} > 0\right\};$$

because $(\mathrm{j}w_1) \odot w_2 = w_1 \otimes w_2$, for every $w_1, w_2 \in \mathbb{C}$ (as already shown in (4.11)). Put differently, z must lie in a pair of opposite disjoint sectors with common vertex at a. Which of the two sectors does z actually belong to? If $\frac{k(z-q)}{|k(z-q)|} = +\mathrm{j}\frac{p}{|p|}$, then $z \in \mathscr{A}_a^+$; while if $\frac{k(z-q)}{|k(z-q)|} = -\mathrm{j}\frac{p}{|p|}$, then $z \in \mathscr{A}_a^-$ (see Figure 4.15).

Carrying on with the discussion for the remaining three cases in the RHS of (4.60), the thesis of the proposition follows. $\qquad \square$

4.5.3. Families of semi-permeable curves

Recall that $\mathscr{S}$ was introduced, at the beginning of this section, just as a smooth curve with normal p, at one of its points z, that points to the side of the curve preferred by E (being implicit that the opposite side is the one preferred by P). The above proposition states necessary conditions on z for $\mathscr{S}$ to be semi-permeable at z, under the assumption that $z \notin \{a, b, c, d\}$ and that $r = -\overline{k}p \notin \left\{w \ : \ w \odot \mathrm{e}^{-\mathrm{j}2\beta} = 0 \ \vee \ w \odot \mathrm{e}^{\mathrm{j}\left(\frac{\pi}{2}-\beta\right)} = 0\right\}$. These conditions, which can be interpreted geometrically with the aid of Figure 4.15, suggest that arcs of α-equiangular spirals, with common centre at $q = \mathsf{q}\left(u^*\left(p\right), \sigma^*\left(p\right)\right)$, are good candidates to be semi-permeable curves. Indeed, if z is now a moving point along one of these curves, the normal p_z at z varies continuously and so $r_z = -\overline{k}p_z$ also varies continuously while the centre of the spiral $q = \mathsf{q}\left(u^*\left(p_z\right), \sigma^*\left(p_z\right)\right)$ remains constant, at least as long as r_z does not reach the set

$$\left\{w \ : \ w \odot \mathrm{e}^{-\mathrm{j}2\beta} = 0 \ \vee \ w \odot \mathrm{e}^{\mathrm{j}\left(\frac{\pi}{2}-\beta\right)} = 0\right\}.$$

Note that r_z reaches this last set exactly when z reaches the following set

$$\left\{w \ : \ w \otimes \mathrm{e}^{-\mathrm{j}2\beta} = 0 \ \vee \ w \otimes \mathrm{e}^{\mathrm{j}\left(\frac{\pi}{2}-\beta\right)} = 0\right\},$$

because (from Proposition 4.5.3) during the approach

$$r_z = \begin{cases} +\mathrm{j}\frac{(z-q)}{|z-q|}\,|kp| & \text{if } \frac{k(z-q)}{|k(z-q)|} = +\mathrm{j}\frac{p}{|p|}, \\ -\mathrm{j}\frac{(z-q)}{|z-q|}\,|kp| & \text{if } \frac{k(z-q)}{|k(z-q)|} = -\mathrm{j}\frac{p}{|p|}, \end{cases} \tag{4.61}$$

must hold and $(\mathrm{j}w_1) \odot w_2 = w_1 \otimes w_2$, for every $w_1, w_2 \in \mathbb{C}$.

Following this insight, eight families of curves arise as indicated by the following bijection, which assigns a family to each sector defined within Proposition 4.5.3:

$$\mathscr{A}_a^+ \mapsto \mathscr{F}_a^+ \triangleq \mathscr{F}_{a,\left(0,\frac{\pi}{2}+\beta\right)}^{a-b} = \left\{ \mathscr{S}_{a,\left(0,\frac{\pi}{2}+\beta\right)}^{a-b}(\rho) \ : \ \rho > 0 \right\},$$

$$\mathscr{A}_a^- \mapsto \mathscr{F}_a^- \triangleq \mathscr{F}_{a,\left(0,\frac{\pi}{2}+\beta\right)}^{b-a} = \left\{ \mathscr{S}_{a,\left(0,\frac{\pi}{2}+\beta\right)}^{b-a}(\rho) \ : \ \rho > 0 \right\},$$

$$\mathscr{A}_b^+ \mapsto \mathscr{F}_b^+ \triangleq \mathscr{F}_{b,\left(0,\frac{\pi}{2}-\beta\right)}^{c-b} = \left\{ \mathscr{S}_{b,\left(0,\frac{\pi}{2}-\beta\right)}^{c-b}(\rho) \ : \ \rho > 0 \right\},$$

$$\mathscr{A}_b^- \mapsto \mathscr{F}_b^- \triangleq \mathscr{F}_{b,\left(0,\frac{\pi}{2}-\beta\right)}^{b-c} = \left\{ \mathscr{S}_{b,\left(0,\frac{\pi}{2}-\beta\right)}^{b-c}(\rho) \ : \ \rho > 0 \right\},$$

$$\mathscr{A}_c^+ \mapsto \mathscr{F}_c^+ \triangleq \mathscr{F}_{c,\left(0,\frac{\pi}{2}+\beta\right)}^{c-d} = \left\{ \mathscr{S}_{c,\left(0,\frac{\pi}{2}+\beta\right)}^{c-d}(\rho) \ : \ \rho > 0 \right\},$$

$$\mathscr{A}_c^- \mapsto \mathscr{F}_c^- \triangleq \mathscr{F}_{c,\left(0,\frac{\pi}{2}+\beta\right)}^{d-c} = \left\{ \mathscr{S}_{c,\left(0,\frac{\pi}{2}+\beta\right)}^{d-c}(\rho) \ : \ \rho > 0 \right\},$$

$$\mathscr{A}_d^+ \mapsto \mathscr{F}_d^+ \triangleq \mathscr{F}_{d,\left(0,\frac{\pi}{2}-\beta\right)}^{a-d} = \left\{ \mathscr{S}_{d,\left(0,\frac{\pi}{2}-\beta\right)}^{a-d}(\rho) \ : \ \rho > 0 \right\},$$

$$\mathscr{A}_d^- \mapsto \mathscr{F}_d^- \triangleq \mathscr{F}_{d,\left(0,\frac{\pi}{2}-\beta\right)}^{d-a} = \left\{ \mathscr{S}_{d,\left(0,\frac{\pi}{2}-\beta\right)}^{d-a}(\rho) \ : \ \rho > 0 \right\}.$$

Each family is a set of arcs of α-equiangular spirals with common centre and angular amplitude, which are, respectively: the vertex and the angular amplitude of the sector that corresponds to the family (see Figure 4.16). So, each sector coincides with the union of the arcs included within it, e.g.,

$$\mathscr{A}_a^+ = \bigcup \mathscr{F}_a^+ = \bigcup_\rho \left\{ \mathscr{S}_{a,\left(0,\frac{\pi}{2}+\beta\right)}^{a-b}(\rho) \ : \ \rho > 0 \right\}.$$

Note, however, that the eight sectors involved are not all pairwise disjoint, e.g., $\mathscr{A}_a^- \cap \mathscr{A}_c^+ \neq \emptyset$ and $\mathscr{A}_b^+ \cap \mathscr{A}_d^+ \neq \emptyset$, among other examples (see Figure 4.16).

The arcs of spirals that belong to these families are actually semi-permeable curves. For example, fix $\rho > 0$ and consider $\mathscr{S}_{a,\left(0,\frac{\pi}{2}+\beta\right)}^{a-b}(\rho)$ which is a member of $\mathscr{F}_a^+$. By definition,

$$\mathscr{S}_{a,\left(0,\frac{\pi}{2}+\beta\right)}^{a-b}(\rho) = \left\{ a + \rho\frac{a-b}{|a-b|}\mathrm{e}^{(-\tan\alpha+\mathrm{j})\theta} \ : \ \theta \in \left(0,\frac{\pi}{2}+\beta\right) \right\}$$

$$= \left\{ w \ : \ \mathcal{M}_a^{a-b}(w) = \rho \ \wedge \ \mathcal{A}_a^{a-b}(w) \in \left(0,\frac{\pi}{2}+\beta\right) \right\}.$$

Using (4.7), the two normal directions of $\mathscr{S}_{a,\left(0,\frac{\pi}{2}+\beta\right)}^{a-b}(\rho)$ at $z \in \mathscr{S}_{a,\left(0,\frac{\pi}{2}+\beta\right)}^{a-b}(\rho) \subset \mathscr{A}_a^+$ can be represented by the vectors

$$\pm\nabla\mathcal{M}_a^{a-b}(z) = \pm\mathrm{e}^{\kappa\mathcal{A}_a^{a-b}(z)}(1+\mathrm{j}\kappa)\frac{z-a}{|z-a|} = \pm\mathrm{e}^{\kappa\mathcal{A}_a^{a-b}(z)}(-\mathrm{j}k)\frac{z-a}{|z-a|},$$

which can both be checked to verify

$$\begin{cases} \left(-\overline{k}\,\nabla\mathcal{M}_a^{a-b}\left(z\right)\right)\odot\mathrm{e}^{-\mathrm{j}2\beta}\neq0 \quad\text{and}\quad \left(-\overline{k}\,\nabla\mathcal{M}_a^{a-b}\left(z\right)\right)\odot\mathrm{e}^{\mathrm{j}\left(\frac{\pi}{2}-\beta\right)}\neq0, \\ \nabla\mathcal{M}_a^{a-b}\left(z\right)\odot\left(k\left(z-a\right)\right)=0, \end{cases}$$

as required by Proposition 4.5.2 to prove that $\mathscr{S}_{a,\left(0,\frac{\pi}{2}+\beta\right)}^{a-b}\left(\rho\right)$ is semi-permeable at z. However, only $+\nabla\mathcal{M}_a^{a-b}\left(z\right)$ complies with Proposition 4.5.3, that is to say, that the selected normal (denoted p in the proposition) divided by $k\left(z-a\right)$ has to be a positive real multiple of $-\mathrm{j}$, as $z\in\mathscr{A}_a^+$. This normal direction, represented by $+\nabla\mathcal{M}_a^{a-b}\left(z\right)$, is the one preferred by E. For the remaining families similar conclusions can be arrived.

In Figure 4.16, normal directions preferred by E, represented by

$$p_{z_q^\pm}\triangleq\pm\nabla\mathcal{M}_q^{\pm\mathrm{v}(q)}\left(z_q^\pm\right)=\pm\mathrm{e}^{\kappa\mathcal{A}_q^{\pm\mathrm{v}(q)}\left(z_q^\pm\right)}\left(-\mathrm{j}k\right)\frac{z_q^\pm-q}{\left|z_q^\pm-q\right|},\qquad(4.62)$$

and velocity vectors

$$k\left(z_q^\pm-q\right),$$

are shown for $z_q^\pm\in\mathscr{A}_q^\pm$ and $q\in\{a,b,c,d\}$, being $\mathrm{v}:\{a,b,c,d\}\to\mathbb{C}$ such that

$$\mathrm{v}\left(q\right)\triangleq\begin{cases} +\left(a-b\right) & \text{if } q=a, \\ -\left(b-c\right) & \text{if } q=b, \\ +\left(c-d\right) & \text{if } q=c, \\ -\left(d-a\right) & \text{if } q=d. \end{cases}$$

For a certain $q\in\{a,b,c,d\}$, and a certain $z_0^\pm\in\mathscr{A}_q^\pm=\bigcup\mathscr{F}_q^\pm$ a semi-permeable curve contained in the family $\mathscr{F}_q^\pm$ is actually traversed by the system's state if the players adopt a pair of *semi-permeable strategies* $\left(\tilde{u}^*,\tilde{\sigma}^*\right)$ such that $\mathsf{q}\left(\tilde{u}^*\left(z\right),\tilde{\sigma}^*\left(z\right)\right)=q$. This can be checked by solving $\dot{z}=F\left(z,\mathsf{q}\left(\tilde{u}^*\left(z\right),\tilde{\sigma}^*\left(z\right)\right)\right)=k\left(z-q\right)$ with initial state z_0.

For each $q\in\{a,b,c,d\}$, the family $\mathscr{F}_q^+$ is classified as *positively oriented* while $\mathscr{F}_q^-$ is classified as *negatively oriented*, for the reason that follows. Observe that $\mathrm{sgn}\left(p_{z_q^\pm}\otimes\left(k\left(z_q^\pm-q\right)\right)\right)=\pm1$ for $z_q^\pm\in\mathscr{A}_q^\pm$, because

$$\begin{aligned} p_{z_q^\pm}\otimes\left(k\left(z_q^\pm-q\right)\right) &=\left(\mathrm{j}p_{z_q^\pm}\right)\odot\left(k\left(z_q^\pm-q\right)\right) \\ &=\left(\pm\mathrm{e}^{\kappa\mathcal{A}_q^{\pm\mathrm{v}(q)}\left(z_q^\pm\right)}k\frac{z_q^\pm-q}{\left|z_q^\pm-q\right|}\right)\odot\left(k\left(z_q^\pm-q\right)\right) \\ &=\pm\mathrm{e}^{\kappa\mathcal{A}_q^{\pm\mathrm{v}(q)}\left(z_q^\pm\right)}\left|k\right|^2\left|z_q^\pm-q\right|. \end{aligned}$$

This means that, along an arc of spiral that belongs to a *positively* oriented family, the direction of the velocity vector is obtained by an *anticlockwise* rotation of angle $\frac{\pi}{2}$ of the normal preferred by E; while along an arc of spiral that belongs to a *negatively* oriented family, the direction of the velocity vector is obtained by a *clockwise* rotation of angle $\frac{\pi}{2}$ of the normal preferred by E (see Figure 4.16).
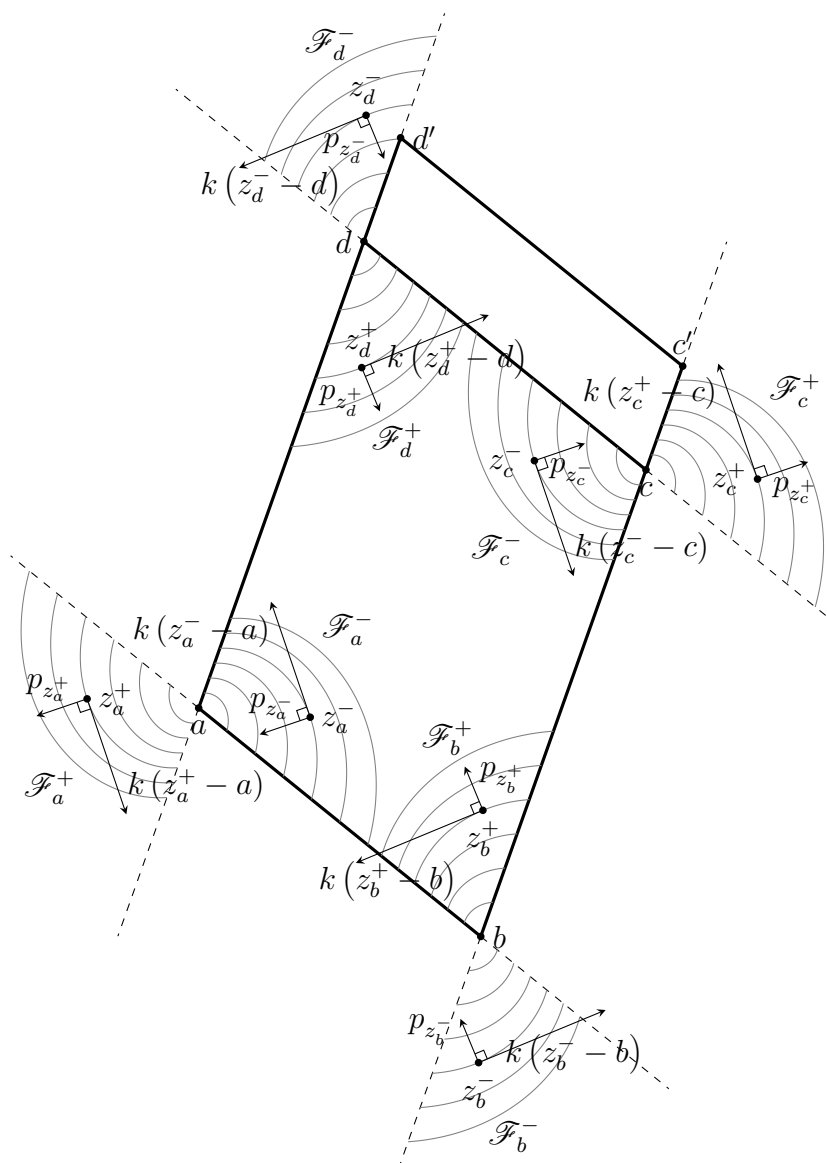
Figure 4.16: Families of semi-permeable curves: $\mathscr{F}_a^+$, $\mathscr{F}_a^-$, $\mathscr{F}_b^+$, $\mathscr{F}_b^-$, $\mathscr{F}_c^+$, $\mathscr{F}_c^-$, $\mathscr{F}_d^+$, $\mathscr{F}_d^-$. Each family is a collection of arcs α-equiangular spirals with common centre and angular amplitude.

4.5.4. Composite semi-permeable curves

Once all possible smooth semi-permeable curves have been characterized, it is natural to ask if two or more of such curves can be concatenated to from a new (possibly non-smooth) *composite* semi-permeable curve. Let the analysis be started by discarding false composite semi-permeable curves.

4.5.4.1. False composite semi-permeable curves

First, notice that a concatenation between a member of a *positively* oriented family and a member of a *negatively* oriented family does not make sense, because it would give rise to a composite curve that if it was to be traversed by the system's state along the direction dictated by the velocity vector, the preferred sides of the players would be reversed at the concatenation point. Imagine, for example, in Figure 4.16 an arc of $\mathscr{F}_b^+$ that intersects with an arc of $\mathscr{F}_a^-$ and examine E's preferred normal direction at a moving point that follows the velocity vector along both curves switching from the first one to the second one at the intersection point.

Second, observe that some pairs of families of semi-permeable curves do not even have a boundary in common, e.g., $\mathrm{d}\left(\bigcup \mathscr{F}_a^+, \bigcup \mathscr{F}_c^+\right) > 0$ and $\mathrm{d}\left(\bigcup \mathscr{F}_a^+, \bigcup \mathscr{F}_b^-\right) > 0$, so no candidate point of concatenation exists to try to concatenate a member of $\mathscr{F}_a^+$ with a member of $\mathscr{F}_c^+$, or a member of $\mathscr{F}_a^+$ with a member of $\mathscr{F}_b^-$ (see Figure 4.16).

Third, in some cases, the concatenation of two semi-permeable curves taken from equally oriented families "leaks" at the concatenation point.

As an example of this third kind of misleading concatenation of semi-permeable curves, consider the following arcs of spirals represented in Figure 4.17: $\mathscr{S}_a \in \mathscr{F}_a^-$, $\mathscr{S}_c \in \mathscr{F}_c^-$, $\mathscr{S}_b \in \mathscr{F}_b^+$, and $\mathscr{S}_d \in \mathscr{F}_d^+$. These arcs of spirals are taken in such a way that $\mathscr{S}_a$ and $\mathscr{S}_c$ intersect at two points inside $\mathrm{conv}\left(\{a, b, c, d\}\right)$ and likewise $\mathscr{S}_b$ and $\mathscr{S}_d$. Let $z_1, \ldots, z_4 \in \mathrm{conv}\left(\{a, b, c, d\}\right)$ be the intersection points as represented in Figure 4.17. Define the sets

$$\mathscr{U}_E \triangleq \left\{z \ : \ \mathcal{M}_a^{b-a}\left(z\right) \leq \mathcal{M}_a^{b-a}\left(z_1\right) \ \wedge \ \mathcal{M}_c^{d-c}\left(z\right) \leq \mathcal{M}_c^{d-c}\left(z_1\right)\right\},$$
$$\mathscr{U}_P \triangleq \left\{z \ : \ \mathcal{M}_b^{c-b}\left(z\right) \leq \mathcal{M}_b^{c-b}\left(z_3\right) \ \wedge \ \mathcal{M}_d^{a-d}\left(z\right) \leq \mathcal{M}_d^{a-d}\left(z_3\right)\right\},$$

represented as shaded areas in Figure 4.17.

Since both $\mathscr{S}_a$ and $\mathscr{S}_c$ belong to *negatively* oriented families, the non-empty set $\mathscr{U}_E$ delimited between them may be thought to be a set where E can keep the state in forever, since his preferred normal directions (represented generically by $p_{z_a^-}$ and $p_{z_c^-}$ in Figure 4.16) point *into* $\mathscr{U}_E$ at every point of $\partial \mathscr{U}_E$ where $\partial \mathscr{U}_E$ is *smooth*. However, this is false because if, for example, P decides to apply a constant control action $u = i_o^\triangledown + \mathrm{j} v_{i0}$ where $v_{i0} \in [v_i^\triangledown, 1]$, he forces the compound input q to belong to the segment $\left\{a + \delta_2 \mathrm{e}^{\mathrm{j}\left(\frac{\pi}{2} - \beta\right)} \sigma v_{i0} \ : \ \sigma \in [0, 1]\right\} \subset \mathrm{conv}\left(\{a, d'\}\right)$, and, by Proposition 4.3.1, the state must come, in finite time, arbitrarily close to the straight line through a and d', which lies in the exterior of $\mathscr{U}_E$.

Similarly, the set $\mathscr{U}_P$, delimited by $\mathscr{S}_b$ and $\mathscr{S}_d$ (both semi-permeable curves of *positively* oriented families), may be thought to be a set where P can keep
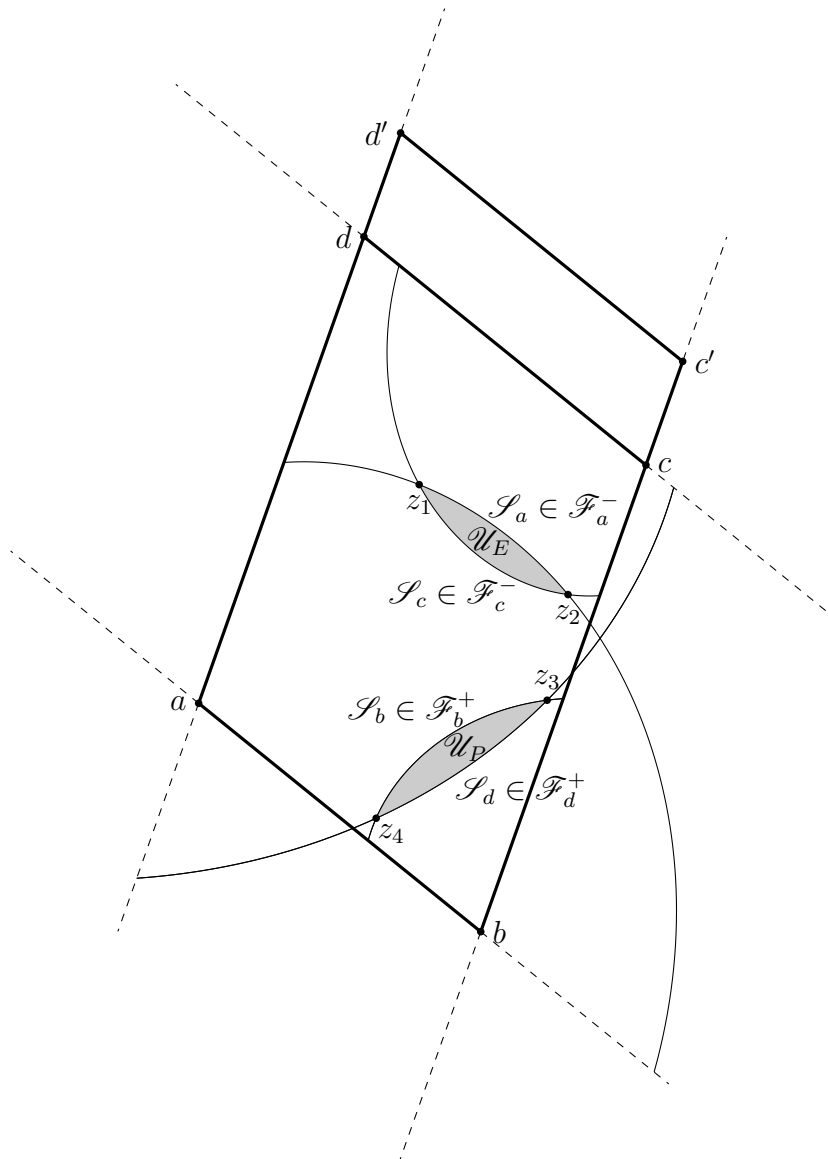
Figure 4.17: False semi-permeable composite closed curves $\partial \mathscr{U}_E$ and $\partial \mathscr{U}_P$, due to leaking corners at concatenation points: $z_1, \ldots, z_4$.

the state in forever, since his opponent's preferred normal directions (represented generically by $p_{z_b^+}$ and $p_{z_d^+}$ in Figure 4.16) point *out of* $\mathscr{U}_P$ at every point of $\partial \mathscr{U}_P$ where $\partial \mathscr{U}_P$ is *smooth*. However, this is also false because if, for example, E decides to apply a constant control action $\sigma = 0$, he forces the compound input q to belong to the segment $\mathrm{conv}\,(\{a, b\})$, and, by Proposition 4.3.1, the state must come, in finite time, arbitrarily close to the straight line through a and b, which lies in the exterior of $\mathscr{U}_P$.

The reason for this third kind of failure to concatenate two smooth semi-permeable surfaces is that the concatenation points $z_1, \ldots, z_4$ are *leaking corners* [60]. To examine this "leaking" issue, consider for example the point z_1. From (4.62), the normal direction to $\mathscr{S}_a \in \mathscr{F}_a^-$, at z_1, preferred by E is

$$p_a^- \triangleq -\nabla \mathcal{M}_a^{b-a}(z_1) = -\mathrm{e}^{\kappa \mathcal{A}_a^{b-a}(z_1)}\,(-\mathrm{j}k)\,\frac{z_1 - a}{|z_1 - a|},$$

and the normal direction to $\mathscr{S}_c \in \mathscr{F}_c^-$, at z_1, preferred by E is

$$p_c^- \triangleq -\nabla \mathcal{M}_c^{d-c}(z_1) = -\mathrm{e}^{\kappa \mathcal{A}_c^{d-c}(z_1)}\,(-\mathrm{j}k)\,\frac{z_1 - c}{|z_1 - c|}.$$

Let $\xi \in [0, 1]$ and consider the scalar product

$$\left((1 - \xi)\,p_a^- + \xi p_c^-\right) \odot k\,(z_1 - q),\tag{4.63}$$

where $q \in \mathrm{conv}\,(\{a, b, c', d'\})$ is unknown. It is just an algebraic exercise to prove that (4.63) is equal to

$$|k|^2 \left(\mathrm{e}^{\kappa \mathcal{A}_a^{b-a}(z_1)}\,(1 - \xi)\,\frac{a - z_1}{|a - z_1|} + \mathrm{e}^{\kappa \mathcal{A}_c^{d-c}(z_1)}\xi\,\frac{c - z_1}{|c - z_1|}\right) \otimes (q - z_1),$$

from where it follows that (4.63) is non-negative *for all* $\xi \in [0, 1]$, if and only if $(a - z_1) \otimes (q - z_1) \geq 0$ and $(c - z_1) \otimes (q - z_1) \geq 0$. Since $q \in \mathrm{conv}\,(\{a, b, c', d'\})$, the compound input q must belong to the set

$$\{w \;:\; (a - z_1) \otimes (w - z_1) \geq 0 \;\wedge\; (c - z_1) \otimes (w - z_1) \geq 0\} \cap \mathrm{conv}\,(\{a, b, c', d'\})\tag{4.64}$$

to make (4.63) positive. The set (4.64) is represented graphically in Figure 4.18. The problem for E is that for every q in (4.64) which makes the velocity vector $k\,(z - q)$ based at z_1 point into $\mathscr{U}_E$, there exists a $q' \in \mathrm{conv}\,(a, d')$ (eligible by P simply by choosing $i_o = i_o^\triangledown$) which makes the velocity vector based at z point into $\mathbb{C} \setminus \mathscr{U}_E$. Consequently, E lacks a *semi-permeable control* at $z = z_1$ for the composite curve $\partial \mathscr{U}_E$. If such semi-permeable control existed, it would make the velocity vector based at z_1 point into $\mathscr{U}_E$ regardless of what P does.

4.5.4.2. True composite semi-permeable curves

Having discarded most of the potential concatenations, observe however that there are some concatenations that give rise to true composite semi-permeable
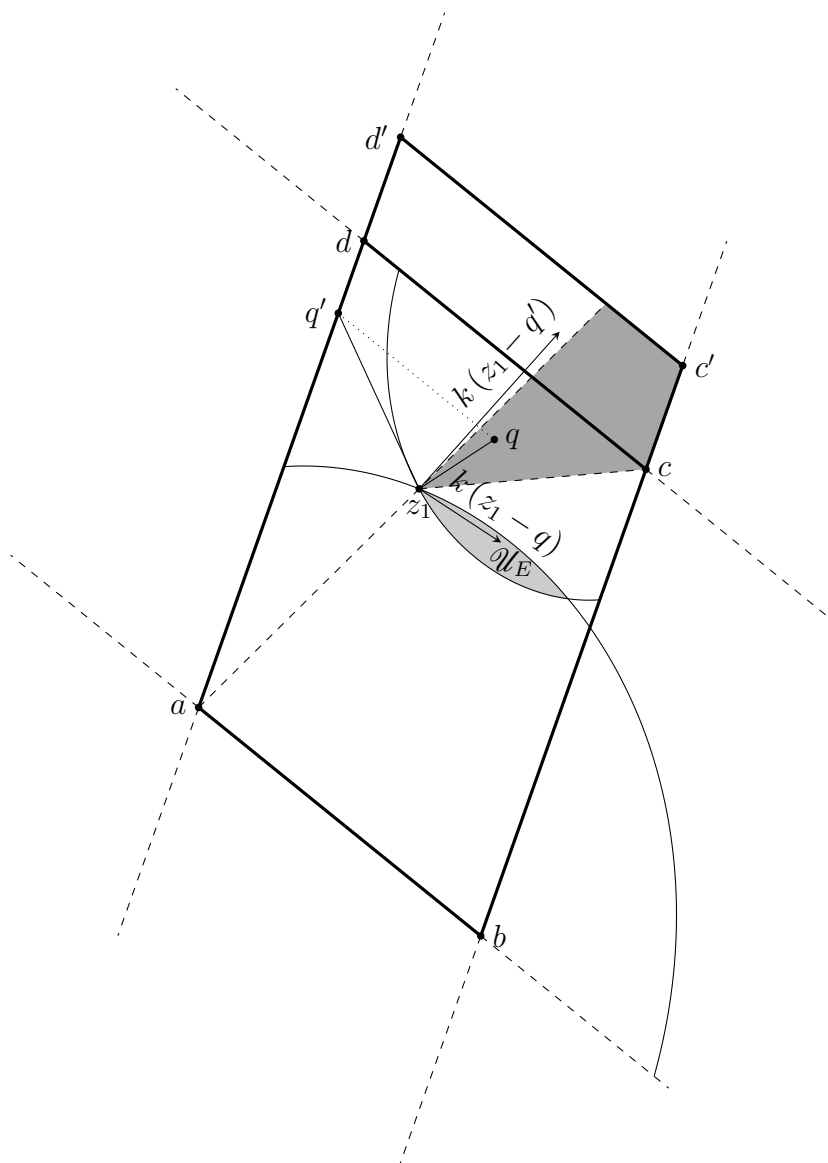
Figure 4.18: The point z_1 in the figure is an example of a leaking corner. If the state reaches the state z_1, E can not prevent the state from leaving $\mathscr{U}_E$ against certain control actions of P. For every q in the darkest shaded area that makes the velocity vector $k(z-q)$, based at z_1, point into $\mathscr{U}_E$, there exists a $q' \in \mathrm{conv}(a, d')$ that can be imposed by P simply by choosing $i_o = i_o^{\triangledown}$ that makes the velocity vector, based at z, point into $\mathbb{C} \setminus \mathscr{U}_E$. Consequently, E lacks a semi-permeable control at $z = z_1$ for the composite curve $\partial \mathscr{U}_E$.

curves. For example, curves of the family $\mathscr{F}_a^-$ can be successfully concatenated with curves of the family $\mathscr{F}_b^-$.

To justify this, consider the common boundary between $\bigcup \mathscr{F}_a^-$ and $\bigcup \mathscr{F}_b^-$ which is the ray $\left\{ z = b + \rho \frac{b-a}{|b-a|} \ : \ \rho > 0 \right\}$. Let $\rho_1 > 0$ and $z_1 = b + \rho_1 \frac{b-a}{|b-a|}$. The normal direction to $\mathscr{S}_a \in \mathscr{F}_a^-$, at z_1, preferred by E can be defined taking a natural limit in (4.62)

$$
\begin{aligned}
p_a^- &\triangleq \lim_{\mathscr{A}_a^- \ni z \to z_1} -\nabla \mathcal{M}_a^{b-a}(z) = -e^{\kappa \mathcal{A}_a^{b-a}(z_1)} (-\mathrm{j}k) \frac{z_1 - a}{|z_1 - a|} \\
&= e^{\kappa \mathcal{A}_a^{b-a}(z_1)} \left(1 + \frac{\rho_1}{|b-a|} \right) \mathrm{j}k\,(b-a).
\end{aligned}
$$

Analogously, the normal direction to $\mathscr{S}_b \in \mathscr{F}_b^-$, at z_1, preferred by E is can be defined as

$$
\begin{aligned}
p_b^- &\triangleq \lim_{\mathscr{A}_b^- \ni z \to z_1} -\nabla \mathcal{M}_b^{b-c}(z) = -e^{\kappa \mathcal{A}_b^{b-c}(z_1)} (-\mathrm{j}k) \frac{z_1 - b}{|z_1 - b|} \\
&= e^{\kappa \mathcal{A}_b^{b-c}(z_1)} \frac{1}{|b-a|} \mathrm{j}k\,(b-a).
\end{aligned}
$$

Consequently, p_a^- and p_b^- are oriented along the *same* direction $p \triangleq \mathrm{j}k\,(b-a)$. This direction should be the one preferred by E at the concatenation point. But, does the semi-permeability condition actually holds at z_1? If it does, it must be

$$
\inf_{u \in U} \sup_{\sigma \in \Sigma} \{ p \odot f(z, u, \sigma) \} = 0. \tag{4.65}
$$

as required by (4.5.1). The expansion of the LHS of (4.65) as suggested by Remark 6 yields

$$
\begin{aligned}
\inf_{u \in U} \sup_{\sigma \in \Sigma} \{ p \odot f(z, u, \sigma) \} &= \sup_{\sigma \in \Sigma} \inf_{u \in U} \{ p \odot f(z, u, \sigma) \} \\
&= -\delta_0\,(r \odot \mathrm{j}) - r \odot z \\
&\quad + \inf_{i_o \in [i_o^\triangledown, 1]} \left\{ \delta_1 \left(r \odot e^{-\mathrm{j}2\beta} \right) i_o \right\} \\
&\quad + \inf_{v_i \in [v_i^\triangledown, 1]} \sup_{\sigma \in [0,1]} \left\{ \delta_2 \left(r \odot e^{\mathrm{j}\left(\frac{\pi}{2} - \beta\right)} \right) v_i \sigma \right\}, \tag{4.66}
\end{aligned}
$$

where $i_o = \Re u$ and $v_i = \Im u$. Since $r \triangleq -\bar{k}p = -|k|^2\,\mathrm{j}\,(b-a) = -|k|^2\,\mathrm{j}\,|b-a|\,e^{-\mathrm{j}2\beta}$, the dot product $r \odot e^{-\mathrm{j}2\beta}$ vanishes causing an indeterminacy in the solution of the inf-sup problem (4.66), in particular in the selection of $i_o = \Re u$. But the dot product that rules the selection of v_i and σ, i.e.,

$$
\begin{aligned}
r \odot e^{\mathrm{j}\left(\frac{\pi}{2} - \beta\right)} &= -|k|^2\,|b-a| \left(\mathrm{j}e^{-\mathrm{j}2\beta} \right) \odot e^{\mathrm{j}\left(\frac{\pi}{2} - \beta\right)} \\
&= -|k|^2\,|b-a|\,e^{-\mathrm{j}2\beta} \otimes e^{\mathrm{j}\left(\frac{\pi}{2} - \beta\right)} \\
&= -|k|^2\,|b-a|\,\Im \left(e^{\mathrm{j}2\beta} e^{\mathrm{j}\left(\frac{\pi}{2} - \beta\right)} \right) \\
&= -|k|^2\,|b-a|\,\sin \left(\frac{\pi}{2} + \beta \right)
\end{aligned}
$$

is negative (because, from (4.2), $|\beta| < \frac{\pi}{2}$). Accordingly, $v_i = v_i^* = 1$ and $\sigma = \sigma^* = 0$ render the same inf-sup value in (4.66) for every $i_o \in [0,1]$. Otherwise stated,

$$\inf_{u \in U} \sup_{\sigma \in \Sigma} \{p \odot f(z, u, \sigma)\} = (jk(b-a)) \odot k(z_1 - q^*)$$

$$= |k|^2 (b-a) \otimes (z_1 - q^*), \qquad (4.67)$$

for every $q^* = \mathsf{q}(i_o + jv_i^*, \sigma^*) = \mathsf{q}(i_o + j, 0) \in \underline{ab} = \left\{ z \in \mathbb{C} \ : \ \frac{z-a}{b-a} \in [0,1] \right\}$. Since $z_1 = b + \rho_1 \frac{b-a}{|b-a|}$, the cross product in (4.67) is zero. This confirms that the proposed concatenation is semi-permeable at z_1.

Likewise, at every point of the ray $\left\{ b + \rho \frac{b-c}{|b-c|} \ : \ \rho > 0 \right\}$ a curve of the family $\mathscr{F}_b^-$ can be successfully concatenated with a curve of the family $\mathscr{F}_c^-$, at every point of the ray $\left\{ c + \rho \frac{d-c}{|d-c|} \ : \ \rho > 0 \right\}$ a curve of the family $\mathscr{F}_c^-$ can be successfully concatenated with a curve of the family $\mathscr{F}_d^-$, and at every point of the ray $\left\{ d + \rho \frac{d-a}{|d-a|} \ : \ \rho > 0 \right\}$ a curve of the family $\mathscr{F}_d^-$ can be successfully concatenated with a curve of the family $\mathscr{F}_a^-$ (see Figure 4.16). Analogous concatenations can be devised among members of the *positively* oriented families ($\mathscr{F}_a^+$, $\mathscr{F}_b^+$, $\mathscr{F}_d^+$, and $\mathscr{F}_d^+$).

In the following chapter, the *negatively* oriented families of semi-permeable curves and their successful concatenations will appear naturally giving form to the VF of the game in distance.

Chapter 5

The game in distance

5.1. Road map for the chapter

This chapter deals with the game in distance induced by the buck converter conflict introduced in Chapter 3. The final goal of this chapter is to find a meaningful solution for this pursuit-evasion game.

In Section 5.2 the precise formulation of the game in distance is reviewed and restricted to the particular case in which the input voltage to the buck converter remains constant. This restriction is postulated rather lately in this thesis because it is only aimed at simplifying the problem of solving the game, at the cost of sacrificing generality, though. The concept of solution to the game in distance is reviewed in this section to make clear what a meaningful solution of the game is.

The particular form of the target set that defines of the game in distance makes the game intrinsically bilateral. In Section 5.3, a decomposition into two unilateral games (an upward game and a downward game) is proposed to approach the problem of solving the bilateral game. In addition, the meaning of solving each of the two unilateral games is made clear and some preliminary properties in connection with the unilateral games are examined.

When the players engage in the play of one of the two unilateral games, somehow the outcome of the play finally turns out to be determined. The discussion of Section 5.4 is intended to figure out how such outcome takes place when both players play optimally, and to motivate the formulation of an ansatz to approach the problem of solving the upward unilateral game.

The ansatz, proposed in Section 5.5, has the form of a partial differential equation with a rather loosely defined boundary condition, which justifiably deserves to be called Isaacs' equation for the upward game. This equation is solved in Section 5.6 by the classical method of characteristics, which reduces the problem of solving a partial differential equation to the problem of solving a system of ordinary differential equations.

Inconveniently, the solution of Isaacs' equation, as obtained by the method of characteristics, does not provide a solution of the upward game in a clean manner. Instead, an artisanal construction, derived from the solution of Isaacs' equation,

has to be done in order to successfully validate it as the solution of the upward game. This is the subject of Sections 5.7 to 5.9. Each of these sections deals with a qualitatively different case that is determined by the game's concrete instance in its parameter space. In each case, a solution of the upward game is constructed and explained how to be validated. In particular, in Section 5.7 the validation process is carried out thoroughly in order to describe meticulously (at least for one of the three cases) the kind of arguments involved in the validation process.

Thanks to the sacrifice in generality paid by restricting the input voltage applied to the converter to be constant, the two unilateral games relate geometrically by a central inversion. This fact is exploited in Section 5.10 to argue that the solution of an unilateral game can be obtained from the solution of the other.

Finally, enriched with the knowledge obtained from having previously rigorously solved both unilateral games, in Section 5.11 the original bilateral game is attacked. The same three qualitatively different cases, that need to be distinguished when solving any of the two unilateral games, need to be distinguished when solving the bilateral game. For each case, a solution of the bilateral game is constructed and commented on how to validate it.

5.2. Formulation of the game in distance

5.2.1. The three main defining objects

Next, the formulation of the buck converter game in distance is briefly recalled.

The game is formulated by the following state equation (SE), target set (TS), and pay-off functional (PF).

$$
\mathcal{G}_{\text{dist}}
\begin{cases}
\text{SE}: & \frac{\mathrm{d}z}{\mathrm{d}t} = f(z, u, \sigma) \triangleq k(z - \mathsf{q}(u, \sigma)), \\
\text{TS}: & \mathscr{T} \triangleq \{z \in \mathbb{C} \ : \ |\Im z| \geq 1\}, \\
\text{PF}: & \mathcal{P}_{f, \mathscr{T}}^{\mathrm{d_o}}(z_0, u(\cdot), \sigma(\cdot)) \triangleq \inf\left\{ \mathrm{d_o}\left(z_{z_0, u(\cdot), \sigma(\cdot)}^{f}(\mathsf{t}), \mathscr{T} \right) \ : \ \mathsf{t} \geq 0 \right\};
\end{cases}
$$

where $f : \mathbb{C} \times U \times \mathbf{\Sigma} \to \mathbb{C}$ is defined by

$$
f(z, u, \sigma) \triangleq F(z, \mathsf{q}(u, \sigma)),
$$

being $F : \mathbb{C} \times \mathbb{C} \to \mathbb{C}$ such that $F(z, q) \triangleq k(z - q)$ and $\mathsf{q} : U \times \mathbf{\Sigma} \to \mathbb{C}$ such that $\mathsf{q}(u, \sigma) \triangleq -\mathrm{j}\delta_0 + \delta_1 \mathrm{e}^{-\mathrm{j}2\beta}\Re u + \delta_2 \mathrm{e}^{\mathrm{j}\left(\frac{\pi}{2} - \beta\right)}\sigma\Im u$, where

$$
\begin{aligned}
U &\triangleq \left\{ i_o + \mathrm{j}v_i \in \mathbb{C} \ : \ i_o^{\triangledown} \leq i_o \leq 1, \ v_i^{\triangledown} \leq v_i \leq 1 \right\}, \\
\mathbf{\Sigma} &\triangleq \left\{ \sigma \in \mathbb{R} \ : \ 0 \leq \sigma \leq 1 \right\}, \\
k &\triangleq -\kappa + \mathrm{j}, \quad \kappa \triangleq \tan\alpha.
\end{aligned}
$$

The function $\mathrm{d_o} : \mathbb{C} \times 2^{\mathbb{C}} \setminus \{\emptyset\} \to \mathbb{R}$ is defined by

$$
\mathrm{d_o}(z, \mathscr{W}) \triangleq
\begin{cases}
+\mathrm{d}(z, \mathscr{W}) & \text{if } z \in \mathscr{W}^{\complement}, \\
-\mathrm{d}\left(z, \mathscr{W}^{\complement}\right) & \text{if } z \in \mathscr{W};
\end{cases}
$$

where $\mathscr{W}^{\complement} = \mathbb{C} \setminus \mathscr{W}$ and $\mathrm{d}\,(z, \mathscr{W}) = \inf\{|z - w| : w \in \mathscr{W}\}$ for every $z \in \mathbb{C}$ and every non-empty subset $\mathscr{W}$ of $\mathbb{C}$. The unique state-space trajectory (solution of the SE) through an arbitrary initial state $z|_{\mathsf{t}=0} = z_0 \in \mathbb{C}$ due to arbitrary piecewise continuous control functions $u : [0, +\infty) \to U$ and $\sigma : [0, +\infty) \to \boldsymbol{\Sigma}$, is denoted $z^f_{z_0, u(\cdot), \sigma(\cdot)} : [0, +\infty) \to \mathbb{C}$ in the above formulation.

5.2.2. The game's original parameter-space

In Chapter 3, the physical assumptions (A1)–(A9) were introduced and argued to be reasonable for the buck converter control problem. Subsequently, the problem was stated as a pursuit-evasion conflict which can always be expressed in a canonical form in terms of seven real parameters introduced as *geometric parameters*: α, β, δ_0, δ_1, δ_2, $i_o^{\triangledown}$, and $v_i^{\triangledown}$. These parameters must satisfy

$$0 < \alpha < \frac{\pi}{2}, \quad -\alpha < \beta < \alpha, \qquad\qquad \tan\alpha - \tan\beta < \sec\alpha, \quad (5.1)$$

$$\delta_1, \delta_2 > 0, \qquad \delta_0 > 1 + (\tan\alpha - \tan\beta)\,\delta_1 \cos^2\beta, \qquad\qquad (5.2)$$

$$0 \le i_o^{\triangledown} < 1, \quad 0 < v_i^{\triangledown} \le 1, \qquad\qquad (5.3)$$

in order to comply with the original assumptions (A1)–(A9) as it was explained in Subsection 3.4.6. The conditions (5.1)–(5.3) were the conditions assumed to hold in Chapter 4, where basic facts about the canonized conflict's dynamics were evidenced, in particular all its families of semi-permeable curves.

5.2.3. A simplifying restriction on the game's parameter-space

The natural way to proceed from now on would be to maintain (5.1)–(5.3) as the valid set of assumptions to approach the game in distance formulated above in Subsection 5.2.1. However, a sacrifice of generality will be introduced next to simplify the game.

Concretely, the assumption

$$0 < V_{I\min} \le V_{I\max} \qquad\qquad (\text{A3})$$

introduced in Chapter 3, is transformed into

$$0 < V_{I\min} = V_{I\max}. \qquad\qquad (\text{A3!})$$

Accordingly, the condition

$$0 < v_i^{\triangledown} \le 1 \qquad\qquad (5.4)$$

in (5.3) becomes

$$0 < v_i^{\triangledown} = 1. \qquad\qquad (5.5)$$

The introduced modification on the set of assumptions leaves P with the load current drained from the converter (i_O, or i_o in its normalized form) as its single scalar control action, impeding him from acting on the converter's input voltage (v_I, or v_i in its normalized form). Otherwise stated, in the SE of the

conflict, P's control $u = i_o + \mathrm{j}v_i$ becomes $u = i_o + \mathrm{j}$ and its control set $U = \{i_o + \mathrm{j}v_i \in \mathbb{C} \ : \ i_o^\triangledown \leq i_o \leq 1, \ v_i^\triangledown \leq v_i \leq 1\}$ becomes $U = \{i_o + \mathrm{j} \in \mathbb{C} \ : \ i_o^\triangledown \leq i_o \leq 1\}$. In practice, this means that, within the control problem, the voltage supplied to the buck converter is assumed *constant*, i.e., $v_I = V_{I\max} = V_{I\min}$.

Clearly, (A3!) is not a minor deviation from the original assumption (A3) and it is introduced here solely because of the pragmatic reason that it introduces certain symmetry in the SE of $\mathcal{G}_{\mathrm{dist}}$ which facilitates the process of solving it.

From now on the parameter-space (5.1)–(5.3) restricted by (5.5) will be referred to as the *restricted parameter-space*.

5.2.4. Geometric reinterpretation of the canonical conflict

The *anchor points*, introduced in Subsection 3.5.2, are fixed points of the complex plane defined as follows in terms of the geometric parameters:

$$
\begin{aligned}
a &\triangleq -\mathrm{j}\delta_0 + i_o^\triangledown \delta_1 \mathrm{e}^{-\mathrm{j}2\beta} &, \\
b &\triangleq -\mathrm{j}\delta_0 + \quad \delta_1 \mathrm{e}^{-\mathrm{j}2\beta} &, \\
c &\triangleq -\mathrm{j}\delta_0 + \quad \delta_1 \mathrm{e}^{-\mathrm{j}2\beta} + v_i^\triangledown \delta_2 \mathrm{e}^{\mathrm{j}\left(\frac{\pi}{2}-\beta\right)}, \\
c' &\triangleq -\mathrm{j}\delta_0 + \quad \delta_1 \mathrm{e}^{-\mathrm{j}2\beta} + \quad \delta_2 \mathrm{e}^{\mathrm{j}\left(\frac{\pi}{2}-\beta\right)}, \\
d &\triangleq -\mathrm{j}\delta_0 + i_o^\triangledown \delta_1 \mathrm{e}^{-\mathrm{j}2\beta} + v_i^\triangledown \delta_2 \mathrm{e}^{\mathrm{j}\left(\frac{\pi}{2}-\beta\right)}, \\
d' &\triangleq -\mathrm{j}\delta_0 + i_o^\triangledown \delta_1 \mathrm{e}^{-\mathrm{j}2\beta} + \quad \delta_2 \mathrm{e}^{\mathrm{j}\left(\frac{\pi}{2}-\beta\right)}.
\end{aligned}
$$

Observe that the depart from (5.4) in favour of (5.5) causes that $c = c'$ and $d = d'$ in Figures 3.7 and 3.8, reducing the parallelogram where the compound control action

$$
q = \mathsf{q}(u,\sigma) = \mathsf{q}(i_o + \mathrm{j}v_i, \sigma) = -\mathrm{j}\delta_0 + i_o\delta_1 \mathrm{e}^{-\mathrm{j}2\beta} + \sigma v_i \delta_2 \mathrm{e}^{\mathrm{j}\left(\frac{\pi}{2}-\alpha\right)}
$$

takes values to the parallelogram $\mathrm{conv}\left(\{a,b,c,d\}\right)$, whose side lengths are:

$$
\begin{aligned}
\mu_1 &\triangleq |b-a| = |c-d| = \left(1 - i_o^\triangledown\right)\delta_1, \\
\mu_2 &\triangleq |c-b| = |d-a| = v_i^\triangledown \delta_2 = \delta_2.
\end{aligned}
$$

Recall that *instantaneously*, players P and E can be thought as disputing the position of the centre $q = \mathsf{q}(u,\sigma)$ of an α-equiangular spiral, that drives the state evolution. In Figure 5.1 the canonical conflict between P and E is geometrically reinterpreted for the restricted parameter-space. Notice that, because of the restriction on v_i, the compound input

$$
q = \mathsf{q}(u,\sigma) = \mathsf{q}(i_o + \mathrm{j}v_i, \sigma) = a + \left(i_o - i_o^\triangledown\right)\delta_1 \mathrm{e}^{-\mathrm{j}2\beta} + \sigma v_i \delta_2 \mathrm{e}^{\mathrm{j}\left(\frac{\pi}{2}-\alpha\right)}
$$

becomes

$$
q = \mathsf{q}(u,\sigma) = \mathsf{q}(i_o + \mathrm{j}, \sigma) = a + \left(i_o - i_o^\triangledown\right)\delta_1 \mathrm{e}^{-\mathrm{j}2\beta} + \sigma \delta_2 \mathrm{e}^{\mathrm{j}\left(\frac{\pi}{2}-\alpha\right)}, \qquad (5.6)
$$

i.e., P loses his influence along $\mathrm{e}^{\mathrm{j}\left(\frac{\pi}{2}-\alpha\right)}$.
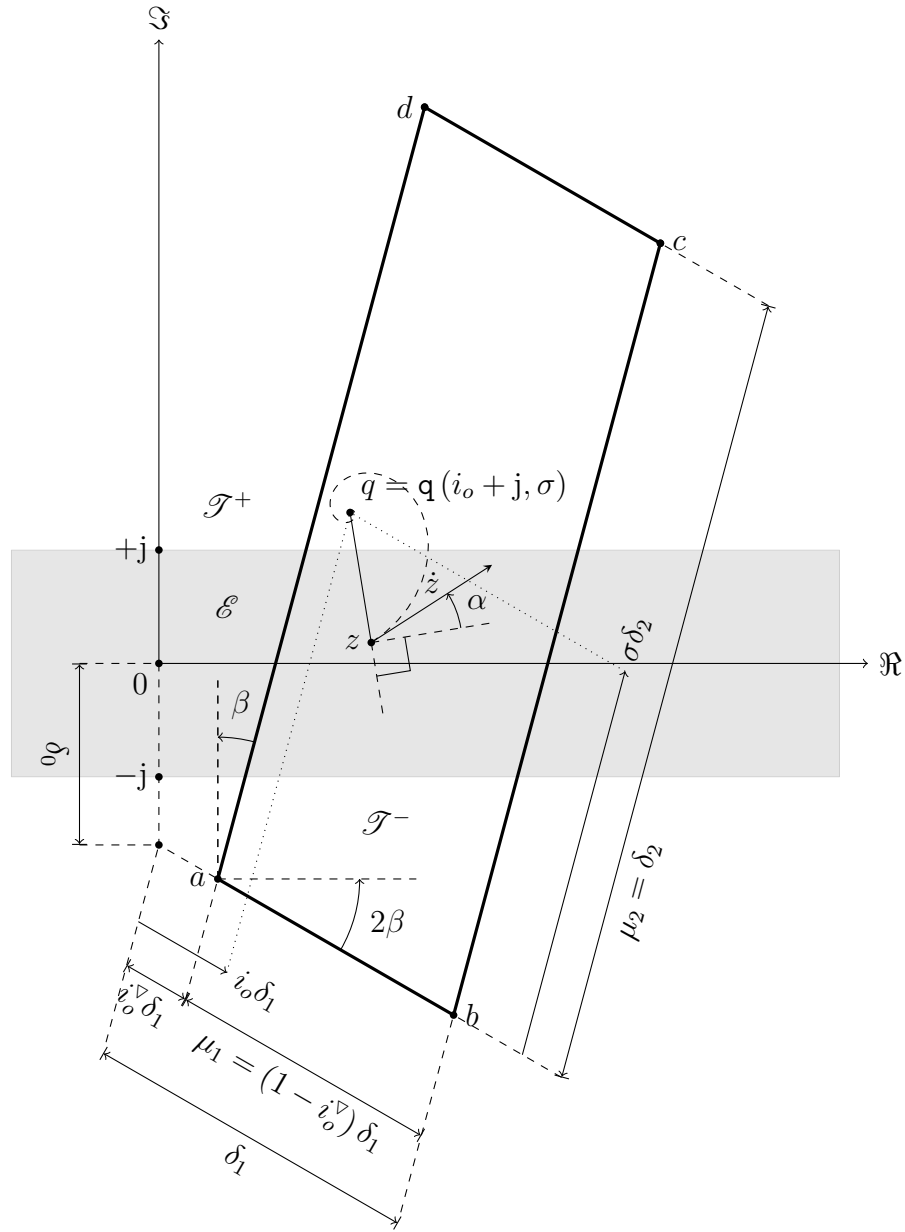
Figure 5.1: Geometric reinterpretation of the canonical conflict (for a case in which $\beta > 0$) after restricting its parameter-space to $0 < v_i^\triangledown = 1$ (compare with Figures 3.7 and 3.8). The TS is $\mathscr{T} = \mathscr{T}^+ \cup \mathscr{T}^-$, where $\mathscr{T}^+ = \{z \in \mathbb{C} \ : \ \Im z \geq +1\}$ and $\mathscr{T}^- = \{z \in \mathbb{C} \ : \ \Im z \leq -1\}$. The PS is $\mathscr{E} = \mathbb{C} \setminus \mathscr{T}$. The SE is $\dot{z} = k(z - q)$, where $q = \mathsf{q}(u, \sigma) = \mathsf{q}(i_o + \mathrm{j}, \sigma) = -\mathrm{j}\delta_0 + i_o\delta_1\mathrm{e}^{-\mathrm{j}2\beta} + \sigma\delta_2\mathrm{e}^{\mathrm{j}\left(\frac{\pi}{2}-\alpha\right)}$.

Disregard temporarily the fact that $u \in U$ and $\sigma \in \mathbf{\Sigma}$ were taken (because of their physical meaning) as P's and E's controls, respectively, in the formulation of $\mathcal{G}_{\text{dist}}$. Since (5.6) can be rewritten as

$$q = a + \left(i_o - i_o^{\triangledown}\right) \delta_1 \frac{b - a}{|b - a|} + \qquad \sigma \delta_2 \frac{d - a}{|d - a|} \qquad (5.7)$$

$$= c + \ (1 - i_o) \, \delta_1 \frac{d - c}{|d - c|} + (1 - \sigma) \, \delta_2 \frac{b - c}{|b - c|}, \qquad (5.8)$$

P's and E's controls may be alternatively taken as: either $i_o - i_o^{\triangledown} \in [0, 1 - i_o^{\triangledown}]$ and $\sigma \in [0, 1]$, respectively; or $1 - i_o \in [0, 1 - i_o^{\triangledown}]$ and $1 - \sigma \in [0, 1]$, respectively. Note how the vertices of the parallelogram conv $(\{a, b, c, d\})$ interchange their roles between (5.7) and (5.8).

The interplay $a \leftrightarrow c$, $b \leftrightarrow d$ between these two conceptions of how P's and E's controls could have alternatively been defined, is the aimed property behind the odd parameter-space restriction introduced in Subsection 5.2.3.

5.2.5. The solution concept

In this subsection the meaning of what is meant by a solution of the above formulated game is reviewed because the general solution concept given in Section 2.4 is not directly applicable due to the special form of the game's PF.

In an informal manner, the *game in distance* $\mathcal{G}_{\text{dist}}$ is just about how *close to* (resp. *deep into*) the TS does the system's state $z_{z_0, u(\cdot), \sigma(\cdot)}^{f}(t)$, ruled by the SE, *approaches* (resp. *penetrates*), along the course of an infinitely long *play* $(z_0, u(\cdot), \sigma(\cdot))$, initiated at a given arbitrary initial state $z(0) = z_0 \in \mathbb{C}$ and guided by control functions: $u : [0, +\infty) \to U$ and $\sigma : [0, +\infty) \to \mathbf{\Sigma}$. The pursuer (P), who controls u, wants the state to get deep into the TS while the evader (E), who controls σ, wants the state to remain as far away as possible from the TS. The closest proximity of the sate to the TS is quantified by the PF which assigns a value $\mathcal{P}_{f, \mathcal{T}}^{\text{do}}(z_0, u(\cdot), \sigma(\cdot)) = \inf \left\{ \text{d}_{\text{o}} \left(z_{z_0, u(\cdot), \sigma(\cdot)}^{f}(t), \mathcal{T} \right) \ : \ t \geq 0 \right\}$ to every possible play $(z_0, u(\cdot), \sigma(\cdot))$.

Recall, however, that a *feedback information structure* is implicitly assumed underlying the formulation of $\mathcal{G}_{\text{dist}}$, so, actually, the control functions u and σ must be considered the result of P's and E's decisions of applying *feedback strategies* $\tilde{u}$ and $\tilde{\sigma}$, respectively. Overloading the use of the word play, it can be said: for every *play* $(z_0, \tilde{u}, \tilde{\sigma})$ corresponds an *outcome* $\tilde{\mathcal{P}}_{f, \mathcal{T}}^{\text{do}}(z_0, \tilde{u}, \tilde{\sigma}) \triangleq \mathcal{P}_{f, \mathcal{T}}^{\text{do}}(z_0, u(\cdot), \sigma(\cdot))$ where the *realizations* $u(\cdot)$ and $\sigma(\cdot)$ of $\tilde{u}$ and $\tilde{\sigma}$, respectively, are obtained by solving the SE with controls functions u and σ substituted by strategies $\tilde{u}$ and $\tilde{\sigma}$, respectively.

In principle, the goal of this chapter is to find *saddle-point* strategies (also called *optimal* strategies) for $\mathcal{G}_{\text{dist}}$, i.e., strategies $\tilde{u}^*$ and $\tilde{\sigma}^*$ such that they verify the *saddle-inequalities*:

$$\tilde{\mathcal{P}}_{f, \mathcal{T}}^{\text{do}}(z, \tilde{u}^*, \tilde{\sigma}) \leq \underbrace{\tilde{\mathcal{P}}_{f, \mathcal{T}}^{\text{do}}(z, \tilde{u}^*, \tilde{\sigma}^*)}_{\mathcal{V}_{\text{do}}(z)} \leq \tilde{\mathcal{P}}_{f, \mathcal{T}}^{\text{do}}(z, \tilde{u}, \tilde{\sigma}^*) \quad \forall z, \tilde{u}, \tilde{\sigma}.$$

If a pair $(\tilde{u}^*, \tilde{\sigma}^*)$ of such strategies is found, the game $\mathcal{G}_{\mathrm{dist}}$ can be considered solved, being $\mathcal{V}_{\mathrm{d_o}}$ as defined above its value function (VF) (remember Proposition 2.2.2). In such case, the pair $(\tilde{u}^*, \tilde{\sigma}^*)$ is called an *saddle-point equilibrium* for $\mathcal{G}_{\mathrm{dist}}$.

Unfortunately, such pair of strategies could not be found, not even for a reduced version of the game in distance (to be presented in Section 5.3) which considers just one of the connected components of the target set. Although discouraging, this failure to find optimal feedback strategies, can be circumvent if a small error in the fulfilment of the saddle-inequalities is tolerated. For example, it may be considered that it is sufficient to find an ϵ-saddle-point (as introduced in Subsection 2.2.6), instead of a *pure* saddle-point equilibrium.

For a given $\epsilon \geq 0$, a pair $(\tilde{u}^{*\epsilon}, \tilde{\sigma}^{*\epsilon})$ is called an ϵ-*saddle-point* for the game $\mathcal{G}_{\mathrm{dist}}$ and its two components are called ϵ-*saddle-point strategies* if

$$\tilde{\mathcal{P}}^{\mathrm{d_o}}_{f,\mathscr{T}}(z, \tilde{u}^{*\epsilon}, \tilde{\sigma}) - \epsilon \leq \tilde{\mathcal{P}}^{\mathrm{d_o}}_{f,\mathscr{T}}(z, \tilde{u}^{*\epsilon}, \tilde{\sigma}^{*\epsilon}) \leq \tilde{\mathcal{P}}^{\mathrm{d_o}}_{f,\mathscr{T}}(z, \tilde{u}, \tilde{\sigma}^{*\epsilon}) + \epsilon \quad \forall z, \tilde{u}, \tilde{\sigma}. \qquad (5.9)$$

Observe that if a saddle-point equilibrium for $\mathcal{G}_{\mathrm{dist}}$ could be found, it would also be an ϵ-saddle point for the same game. In addition, as granted by Theorem 2.2.1, if for every $\epsilon > 0$ there exists an ϵ-saddle-point for $\mathcal{G}_{\mathrm{dist}}$, then $\mathcal{G}_{\mathrm{dist}}$ has a VF, and conversely.

Clearly, from a practical viewpoint, the distinction between an ϵ-saddle-point and a pure saddle-point is irrelevant for ϵ sufficiently small.

Hopefully, at the end of this chapter in Section 5.11, it will become intuitively clear how for every $\epsilon > 0$ an ϵ-saddle-point strategy can be conceived for each player of $\mathcal{G}_{\mathrm{dist}}$. To reach this level of understating of $\mathcal{G}_{\mathrm{dist}}$, a decomposition of it into two auxiliary games will be heavily relied on.

5.3. Decomposition of the game into two unilateral games

The TS, $\mathscr{T} = \{z \in \mathbb{C} : |\Im z| \geq 1\}$, is the union of a pair of disjoint half-planes: $\mathscr{T}^+ \triangleq \{z \in \mathbb{C} : \Im z \geq +1\}$ and $\mathscr{T}^- \triangleq \{z \in \mathbb{C} : \Im z \leq -1\}$. The simplicity of form of the target set manifests in the function value

$$\mathrm{d_o}(z, \mathscr{T}) = \min\left\{\mathrm{d_o}(z, \mathscr{T}^+), \mathrm{d_o}(z, \mathscr{T}^-)\right\} = \min\{1 - \Im z, 1 + \Im z\} \qquad (5.10)$$

assigned, by the *oriented distance* function $z \mapsto \mathrm{d_o}(z, \mathscr{T})$, to each $z \in \mathbb{C}$. Clearly, $\mathrm{d_o}(z, \mathscr{T}) > 0$ if $z \notin \mathscr{T}$, while $\mathrm{d_o}(z, \mathscr{T}) \leq 0$ if $z \in \mathscr{T}$.

The expression (5.10) suggests a way of decomposing the problem of solving the game $\mathcal{G}_{\mathrm{dist}}$. Consider the following two *unilateral* games: an *upward* game

$$\mathcal{G}^+_{\mathrm{dist}} \begin{cases} \text{SE}: & \frac{\mathrm{d}z}{\mathrm{d}t} = f(z, u, \sigma) = k(z - \mathsf{q}(u, \sigma)), \\ \text{TS}: & \mathscr{T}^+ \triangleq \{z \in \mathbb{C} : 1 - \Im z \leq 0\}, \\ \text{PF}: & \mathcal{P}^{\mathrm{d_o}}_{f,\mathscr{T}^+}(z_0, u(\cdot), \sigma(\cdot)) \triangleq \inf\left\{\mathrm{d_o}\left(z^f_{z_0, u(\cdot), \sigma(\cdot)}(\mathsf{t}), \mathscr{T}^+\right) : \mathsf{t} \geq 0\right\}, \end{cases}$$

associated with $\mathscr{T}^+$; and a *downward* game

$$\mathcal{G}^-_{\mathrm{dist}} \begin{cases} \text{SE}: & \frac{\mathrm{d}z}{\mathrm{d}t} = f(z, u, \sigma) = k(z - \mathsf{q}(u, \sigma)), \\ \text{TS}: & \mathscr{T}^- \triangleq \{z \in \mathbb{C} : 1 + \Im z \leq 0\}, \\ \text{PF}: & \mathcal{P}^{\mathrm{d_o}}_{f,\mathscr{T}^-}(z_0, u(\cdot), \sigma(\cdot)) \triangleq \inf\left\{\mathrm{d_o}\left(z^f_{z_0, u(\cdot), \sigma(\cdot)}(\mathsf{t}), \mathscr{T}^-\right) : \mathsf{t} \geq 0\right\}, \end{cases}$$

associated with $\mathscr{T}^-$. They both share the same SE as the original *bilateral* game $\mathcal{G}_{\text{dist}}$, but their TSs and PFs are each defined in relation to only one of the two connected components of the original target set $\mathscr{T}$.

The justification of why the decomposition just introduced will actually lead to the solution of the original (bilateral) game in distance is postponed to Section 5.11. For the moment, observe that (because of having replaced $0 < v_i^{\triangledown} \leq 1$ by $0 < v_i^{\triangledown} = 1$) there is no deep difference between $\mathcal{G}_{\text{dist}}^+$ and $\mathcal{G}_{\text{dist}}^-$ (see Figure 5.1). Actually, from a geometric standpoint, at the light of (5.7)–(5.8), it is visible that both unilateral games are different instances of the same essential game, the only difference due to the fact that in general $\mathrm{d_o}\left(a, \mathscr{T}^+\right) \neq \mathrm{d_o}\left(c, \mathscr{T}^-\right)$.

5.3.1. The solution concept for the unilateral games

For every *play* $(z_0, u\,(\cdot)\,, \sigma\,(\cdot))$, the pay-offs $\mathcal{P}_{f,\mathscr{T}^+}^{\mathrm{d_o}}\left(z_0, u\,(\cdot)\,, \sigma\,(\cdot)\right)$ (in the context of $\mathcal{G}_{\text{dist}}^+$) and $\mathcal{P}_{f,\mathscr{T}^-}^{\mathrm{d_o}}\left(z_0, u\,(\cdot)\,, \sigma\,(\cdot)\right)$ (in the context of $\mathcal{G}_{\text{dist}}^-$) are both *finite* because the state-space trajectory $\left\{ z_{z_0,u(\cdot),\sigma(\cdot)}^f\,(\mathsf{t}) \;:\; \mathsf{t} \geq 0 \right\}$ is *bounded*. Actually, an unbounded behaviour of $\mathsf{t} \mapsto z_{z_0,u(\cdot),\sigma(\cdot)}^f\,(\mathsf{t})$ for $\mathsf{t} \to +\infty$ does not match the distant vector field approximation of the SE (see Subsection 4.3.3) which generates shrinking solutions

$$[0, +\infty) \ni \mathsf{t} \to q_0 + \mathrm{e}^{k\mathsf{t}}\left(z_0 - q_0\right) \in \mathbb{C},$$

where $\Re k = -\kappa < 0$ and $q_0 \in \mathrm{conv}\left(\{a, b, c', d'\}\right)$, for every z_0 such that $|z_0 - q_0| \gg \mathrm{diam}\left(\mathrm{conv}\left(\{a, b, c', d'\}\right)\right)$.

Using in a natural way the notation already introduced for $\mathcal{G}_{\text{dist}}$, each game $\mathcal{G}_{\text{dist}}^{\pm}$ could be considered to be solved if *optimal* strategies, $\tilde{u}_{\pm}^*$ and $\tilde{\sigma}_{\pm}^*$, i.e., such that

$$\tilde{\mathcal{P}}_{f,\mathscr{T}^{\pm}}^{\mathrm{d_o}}\left(z, \tilde{u}_{\pm}^*, \tilde{\sigma}\right) \leq \underbrace{\tilde{\mathcal{P}}_{f,\mathscr{T}^{\pm}}^{\mathrm{d_o}}\left(z, \tilde{u}_{\pm}^*, \tilde{\sigma}_{\pm}^*\right)}_{\mathcal{V}_{\mathrm{d_o}}^{\pm}(z)} \leq \tilde{\mathcal{P}}_{f,\mathscr{T}^{\pm}}^{\mathrm{d_o}}\left(z, \tilde{u}, \tilde{\sigma}_{\pm}^*\right) \quad \forall z, \tilde{u}, \tilde{\sigma}, \qquad (5.11)$$

were found, being $\mathcal{V}_{\mathrm{d_o}}^{\pm}$ (as the defined above) the corresponding VF of the game. However, as anticipated before, for certain instances of $\mathcal{G}_{\text{dist}}^+$ or $\mathcal{G}_{\text{dist}}^-$ in the restricted parameter-space, such optimal strategies could not be found for *both* players.

Instead, the resulting conclusion from the following sections up to Section 5.9 inclusive will be that, regardless of the selected instance of $\mathcal{G}_{\text{dist}}^+$ in the restricted parameter-space, for every $\epsilon > 0$, there exists a pair $(\tilde{u}_+^{*\epsilon}, \tilde{\sigma}_+^{*\epsilon})$ such that

$$\tilde{\mathcal{P}}_{f,\mathscr{T}^+}^{\mathrm{d_o}}\left(z, \tilde{u}_+^{*\epsilon}, \tilde{\sigma}\right) - \epsilon \leq \tilde{\mathcal{P}}_{f,\mathscr{T}^+}^{\mathrm{d_o}}\left(z, \tilde{u}_+^{*\epsilon}, \tilde{\sigma}_+^{*\epsilon}\right) \leq \tilde{\mathcal{P}}_{f,\mathscr{T}^+}^{\mathrm{d_o}}\left(z, \tilde{u}, \tilde{\sigma}_+^{*\epsilon}\right) + \epsilon \quad \forall z, \tilde{u}, \tilde{\sigma}. \;(5.12)$$

This conclusion will be rigorously and constructively proved. The existence of analogous pairs $(\tilde{u}_-^{*\epsilon}, \tilde{\sigma}_-^{*\epsilon})$ of ϵ-saddle-point strategies for $\mathcal{G}_{\text{dist}}^-$ will follow from the existence of the former ones, as it will be argued in Section 5.10.

As a consequence of the existence of such ϵ-saddle-point strategy pairs, by Theorem 2.2.1, the existence of a VF for $\mathcal{G}_{\text{dist}}^+$ and a VF for $\mathcal{G}_{\text{dist}}^-$ can be inferred.

5.3.2. Semiplanes of dominance

The two unilateral games, $\mathcal{G}_{\mathrm{dist}}^{+}$ and $\mathcal{G}_{\mathrm{dist}}^{-}$, even though simpler than the original game $\mathcal{G}_{\mathrm{dist}}$, still have the problem that their PFs are not in the standard form (see Subsection 2.1.2), which is the prevalent form assumed in the literature on differential games. To overcome this difficulty, Isaacs' hint [49, Sec. 2.4] to treat the type of PF shared by $\mathcal{G}_{\mathrm{dist}}^{+}$ and $\mathcal{G}_{\mathrm{dist}}^{-}$ is followed in this section to guide the approach to solve $\mathcal{G}_{\mathrm{dist}}^{+}$ and $\mathcal{G}_{\mathrm{dist}}^{-}$. It consists in determining the regions of dominance of each player in connection with the sign of the time derivative of the oriented distance to the target set, as explained next.

As it is customary, name the directions $+1$, -1, $+j$, and $-j$ in the complex plane as "right", "left", "up", and "down", respectively. The unilateral games $\mathcal{G}_{\mathrm{dist}}^{+}$ and $\mathcal{G}_{\mathrm{dist}}^{-}$ are about how much *up* and how much *down*, respectively, can P force the state to go against E's resistance. Accordingly, it is pertinent to ask if there exists any subset of the state space where a player dominates the sign of the "vertical" component of the state's velocity.

Four combinations need to be considered. Define $P_{\uparrow}$, $P_{\downarrow}$, $E_{\uparrow}$, and $E_{\downarrow}$ by:

$$
P_{\uparrow} \triangleq \left\{ z \in \mathbb{C} \ : \ \inf_{u \in U} \sup_{\sigma \in \boldsymbol{\Sigma}} \left\{ -j \odot f\left(z, u, \sigma\right) \right\} < 0 \right\},
$$
$$
E_{\downarrow} \triangleq \left\{ z \in \mathbb{C} \ : \ \inf_{u \in U} \sup_{\sigma \in \boldsymbol{\Sigma}} \left\{ -j \odot f\left(z, u, \sigma\right) \right\} > 0 \right\},
$$
$$
P_{\downarrow} \triangleq \left\{ z \in \mathbb{C} \ : \ \inf_{u \in U} \sup_{\sigma \in \boldsymbol{\Sigma}} \left\{ +j \odot f\left(z, u, \sigma\right) \right\} < 0 \right\},
$$
$$
E_{\uparrow} \triangleq \left\{ z \in \mathbb{C} \ : \ \inf_{u \in U} \sup_{\sigma \in \boldsymbol{\Sigma}} \left\{ +j \odot f\left(z, u, \sigma\right) \right\} > 0 \right\}.
$$

Recall that, by virtue of statement 1 of Proposition 4.4.1, the order of the inf and sup operations in the above definitions does not matter. Note that the mnemotechnical names given to the sets reflect the following facts:

- P can force $\Im z$ to *increase* for every $z \in P_{\uparrow}$,

- E can force $\Im z$ to *decrease* for every $z \in E_{\downarrow}$,

- P can force $\Im z$ to *decrease* for every $z \in P_{\downarrow}$,

- E can force $\Im z$ to *increase* for every $z \in E_{\uparrow}$.

A direct consequence of Corollary 4.4.1 is that the sets $P_{\uparrow}$, $E_{\downarrow}$, $P_{\downarrow}$, and $E_{\uparrow}$ are
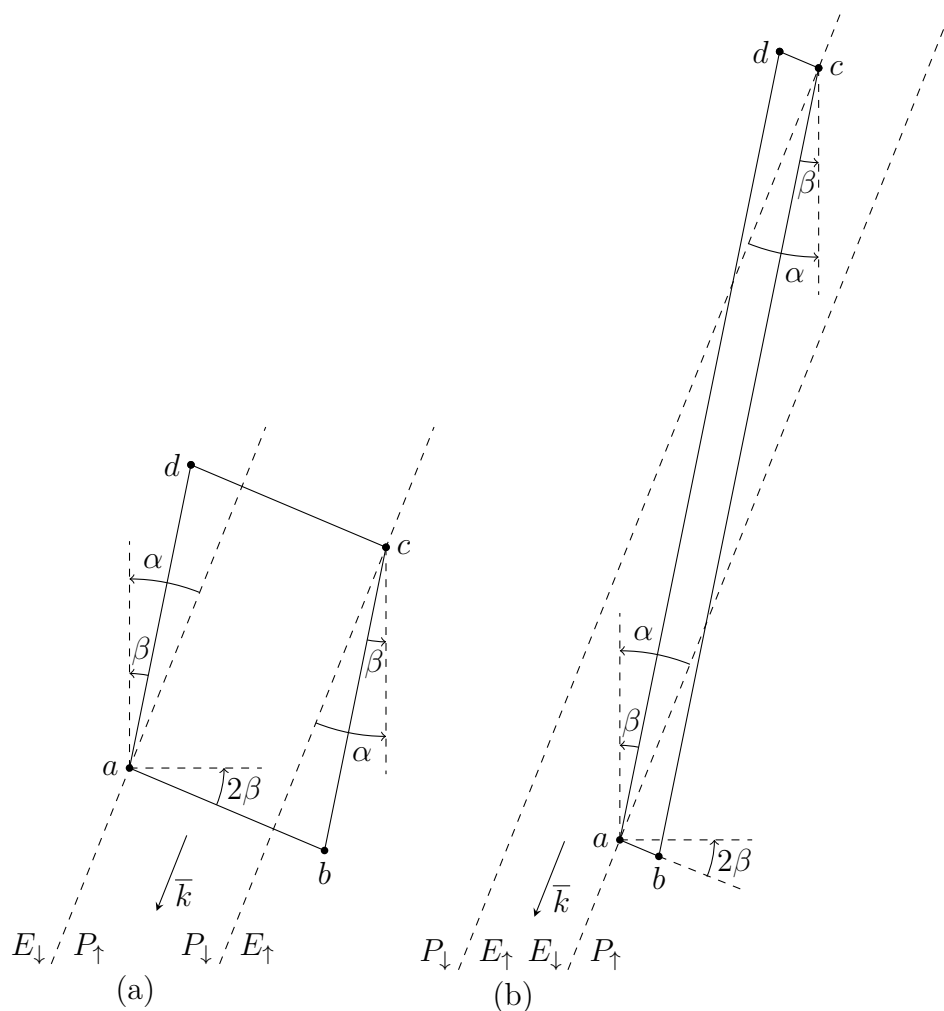
Figure 5.2: Semi-planes of vertical motion dominance of each player, for two qualitatively different cases: (a) $\overline{k} \otimes (c - a) > 0$ and (b) $\overline{k} \otimes (c - a) < 0$. For example, E can force $\Im z$ to *increase* for every z in the semi-plane $E_\uparrow = \left\{ z \in \mathbb{C} \ : \ \overline{k} \otimes (z - c) > 0 \right\}$, while P can force $\Im z$ to *decrease* for every z in the semi-plane $P_\downarrow = \left\{ z \in \mathbb{C} \ : \ \overline{k} \otimes (z - c) < 0 \right\}$. Likewise, E can force $\Im z$ to *decrease* for every z in the semi-plane $E_\downarrow = \left\{ z \in \mathbb{C} \ : \ -\overline{k} \otimes (z - a) > 0 \right\}$, while P can force $\Im z$ to *increase* for every z in the semi-plane $P_\uparrow = \left\{ z \in \mathbb{C} \ : \ -\overline{k} \otimes (z - a) < 0 \right\}$.

the following half-planes of the complex plane (see Figure 5.2):

$$P_\uparrow \triangleq \left\{ z \in \mathbb{C} \ : \ \inf_{u \in U} \sup_{\sigma \in \Sigma} \left\{ -\mathrm{j} \odot f\left(z,u,\sigma\right) \right\} < 0 \right\} = \left\{ z \in \mathbb{C} \ : \ -\overline{k} \otimes \left(z - a\right) < 0 \right\},$$

$$E_\downarrow \triangleq \left\{ z \in \mathbb{C} \ : \ \inf_{u \in U} \sup_{\sigma \in \Sigma} \left\{ -\mathrm{j} \odot f\left(z,u,\sigma\right) \right\} > 0 \right\} = \left\{ z \in \mathbb{C} \ : \ -\overline{k} \otimes \left(z - a\right) > 0 \right\},$$

$$P_\downarrow \triangleq \left\{ z \in \mathbb{C} \ : \ \inf_{u \in U} \sup_{\sigma \in \Sigma} \left\{ +\mathrm{j} \odot f\left(z,u,\sigma\right) \right\} < 0 \right\} = \left\{ z \in \mathbb{C} \ : \ +\overline{k} \otimes \left(z - c\right) < 0 \right\},$$

$$E_\uparrow \triangleq \left\{ z \in \mathbb{C} \ : \ \inf_{u \in U} \sup_{\sigma \in \Sigma} \left\{ +\mathrm{j} \odot f\left(z,u,\sigma\right) \right\} > 0 \right\} = \left\{ z \in \mathbb{C} \ : \ +\overline{k} \otimes \left(z - c\right) > 0 \right\}.$$

Note that the line $\partial P_\uparrow = \partial E_\downarrow$ is parallel to the line $\partial P_\downarrow = \partial E_\uparrow$, since they both share a common direction: $\overline{k}$. It may happen that $\overline{k} \otimes \left(c - a\right) = 0$, in which case both lines coincide; the two other possible cases are represented in Figure 5.2. The case $\overline{k} \otimes \left(c - a\right) > 0$, endows P with a subset $P_\uparrow \cap P_\downarrow \neq \emptyset$ where he has full control of the sign of the vertical component of the state's velocity, while $E_\uparrow \cap E_\downarrow = \emptyset$. Symmetrically, the case $\overline{k} \otimes \left(c - a\right) < 0$, endows E with a subset $E_\uparrow \cap E_\downarrow \neq \emptyset$ where he has full control of the sign of the vertical component of the state's velocity, while $P_\uparrow \cap P_\downarrow = \emptyset$.

5.4. The infimum oriented distance to the target set

5.4.1. Where can it be attained?

To fix ideas, from both games $\mathcal{G}_{\text{dist}}^+$ and $\mathcal{G}_{\text{dist}}^-$, consider just $\mathcal{G}_{\text{dist}}^+$ for the moment. Consider also a generic play: $\left(z_0, u\left(\cdot\right), \sigma\left(\cdot\right)\right)$ of $\mathcal{G}_{\text{dist}}^+$. Assume that $u\left(\cdot\right)$ and $\sigma\left(\cdot\right)$ are *piecewise continuous* realizations of feedback strategies. Therefore, the trajectory $\mathsf{t} \mapsto z_{z_0,u(\cdot),\sigma(\cdot)}^f\left(\mathsf{t}\right)$, described by the sate in $\mathbb{C}$, is *continuous* and *piecewise differentiable*. It was already argued that, since $\left\{ \mathrm{d_o}\left(z_{z_0,u(\cdot),\sigma(\cdot)}^f\left(\mathsf{t}\right), \mathscr{T}^+\right) \ : \ \mathsf{t} \geq 0 \right\}$ is bounded, $\mathcal{P}_{f,\mathscr{T}^+}^{\mathrm{d_o}}\left(z_0, u\left(\cdot\right), \sigma\left(\cdot\right)\right) = \inf \left\{ \mathrm{d_o}\left(z_{z_0,u(\cdot),\sigma(\cdot)}^f\left(\mathsf{t}\right), \mathscr{T}^+\right) \ : \ \mathsf{t} \geq 0 \right\}$ is *finite*.

Now suppose $u^*\left(\cdot\right)$ and $\sigma^*\left(\cdot\right)$ are piecewise continuous realizations that result from an *optimal* strategy pair $\left(\tilde{u}^*, \tilde{\sigma}^*\right)$ of $\mathcal{G}_{\text{dist}}^+$. Accordingly, the finite value $\mathcal{P}_{f,\mathscr{T}^+}^{\mathrm{d_o}}\left(z_0, u^*\left(\cdot\right), \sigma^*\left(\cdot\right)\right)$ equals the VF of $\mathcal{G}_{\text{dist}}^+$ at z_0, i.e., $\mathcal{P}_{f,\mathscr{T}^+}^{\mathrm{d_o}}\left(z_0, u^*\left(\cdot\right), \sigma^*\left(\cdot\right)\right) = \tilde{\mathcal{P}}_{f,\mathscr{T}^+}^{\mathrm{d_o}}\left(z, \tilde{u}^*, \tilde{\sigma}^*\right) = \mathcal{V}_{\mathrm{d_o}}^+\left(z_0\right)$. This finite value is a *global* infimum of the function $z \mapsto \mathrm{d_o}\left(z, \mathscr{T}^+\right)$ evaluated along the trajectory $\mathsf{t} \mapsto z_{z_0,u^*(\cdot),\sigma^*(\cdot)}^f\left(\mathsf{t}\right)$ which is either *attained* in finite time or *approximated* as $\mathsf{t} \to +\infty$. Suppose that it does not take place at the initial time $\mathsf{t} = 0$. If neither P nor E squander their dominant power (P in $P_\uparrow$ and E in $E_\downarrow$) the aforementioned infimum *occurs* (resp. *is approximated*) when the state *reaches* (resp. as the state *approaches*) the line

$$\partial P_\uparrow = \partial E_\downarrow = \left\{ z \in \mathbb{C} \ : \ -\overline{k} \otimes \left(z - a\right) = 0 \right\},$$

from the half-plane $P_\uparrow$. Recall that $\mathrm{d_o}\left(z, \mathscr{T}^+\right) = 1 - \Im z$, for every $z \in \mathbb{C}$. So, by definition of $P_\uparrow$, for every $z \in P_\uparrow$, P can cause $\mathrm{d_o}\left(z, \mathscr{T}^+\right)$ to *decrease*, whatever

E may do. Symmetrically, by definition of $E_\downarrow$, for every $z \in E_\downarrow$, E can cause $d_o(z, \mathscr{T}^+)$ to *increase*, whatever P may do.

Similarly, if $u^*(\cdot)$ and $\sigma^*(\cdot)$ are the realizations that result from an *optimal* strategy pair $(\tilde{u}^*, \tilde{\sigma}^*)$ of $\mathcal{G}_{\mathrm{dist}}^-$, observing that $d_o(z, \mathscr{T}^-) = 1 + \Im z$ for every $z \in \mathbb{C}$ and recalling the definitions of $P_\downarrow$ and $E_\uparrow$, it can be argued that the *global* infimum of $\mathsf{t} \mapsto d_o\left(z^f_{z_0,u^*(\cdot),\sigma^*(\cdot)}(\mathsf{t}), \mathscr{T}^-\right)$ *occurs* (resp. *is approximated*) when $z^f_{z_0,u^*(\cdot),\sigma^*(\cdot)}(\mathsf{t})$ *reaches* (resp. as the state *approaches*) the line

$$\partial P_\downarrow = \partial E_\uparrow = \left\{ z \in \mathbb{C} \ : \ +\overline{k} \otimes (z - c) = 0 \right\},$$

from $P_\downarrow$, if it supposed that it does not take place at the initial time $\mathsf{t} = 0$.

5.4.2. Characterization of the infimums that are not attained at the initial state

Let $\mathcal{G}_{\mathrm{dist}}^+$ be the main focus of attention again and let $z^* \in \partial P_\uparrow = \partial E_\downarrow$ be the point *reached* or *approached* from $P_\uparrow$ by $z^f_{z_0,u^*(\cdot),\sigma^*(\cdot)}(\mathsf{t})$ that corresponds to the global infimum of $\mathsf{t} \mapsto d_o\left(z^f_{z_0,u^*(\cdot),\sigma^*(\cdot)}(\mathsf{t}), \mathscr{T}^+\right)$, which is assumed *not* to take place at $\mathsf{t} = 0$. Consider a generic point z in an arbitrarily small neighbourhood of z^*. The second point of the final statement of Corollary 4.4.1 can be interpreted as follows: when P and E are doing their most to respectively *increase* $\Im z$ and *decrease* $\Im z$, their control actions, $\hat{u}$ and $\hat{\sigma}$ respectively, must be such that $\mathsf{q}(\hat{u}, \hat{\sigma}) = a$. So, the state velocity vector $\dot{z} = f(z, \hat{u}, \hat{\sigma}) = k(z - \mathsf{q}(\hat{u}, \hat{\sigma})) = k(z - a)$, based at z, must have the following orthogonal components

$$\Re \dot{z} = \Re(k(z-a)) = \overline{k} \odot (z-a), \tag{5.13}$$
$$\Im \dot{z} = \Im(k(z-a)) = \overline{k} \otimes (z-a). \tag{5.14}$$

This is the vector field, defined in an arbitrarily small neighbourhood of z^*, that must be followed by $z^f_{z_0,u^*(\cdot),\sigma^*(\cdot)}(\mathsf{t})$ along its way to z^*.

Nearby optimal trajectories *that attain* the infimum at points close to z^* in $\partial P_\uparrow = \partial E_\downarrow$ must follow the same local vector field. Observe that the flux, induced by this vector field, is made up of arcs of α-equiangular spirals centred at a, each of which is included in a member of either $\mathscr{F}_a^+$ or $\mathscr{F}_a^-$ (see Figures 4.16 and 5.2). If $z_0 \neq a$, the only stationary point ($z = a$) of the local vector field (5.13)–(5.14) cannot be the global infimum of $\mathsf{t} \mapsto d_o\left(z^f_{z_0,u^*(\cdot),\sigma^*(\cdot)}(\mathsf{t}), \mathscr{T}^-\right)$, because states close to a in $P_\uparrow$ are guided by the vector filed towards a point in $\partial P_\uparrow = \partial E_\downarrow$ with larger imaginary part than a. It could only be $z^* = a$, if $z_0 = a$ and $z^f_{z_0,u^*(\cdot),\sigma^*(\cdot)}(\mathsf{t}) = z^*$ for every $\mathsf{t} \geq 0$. But then, the global infimum of $z \mapsto d_o(z, \mathscr{T}^+)$ evaluated along the trajectory $\mathsf{t} \mapsto z^f_{z_0,u^*(\cdot),\sigma^*(\cdot)}(\mathsf{t})$ would take place at the initial time $\mathsf{t} = 0$, which is a case that has been deliberatively ruled out.

For $z = z^* \neq a$, the local vector field (5.13)–(5.14) asks for $\Im \dot{z} = 0$ and $\Re \dot{z} = \overline{k} \odot (z - a)$; since z^* must be *reached* or *approached* from $P_\uparrow$ (i.e., from the right), it must be $\overline{k} \odot (z^* - a) < 0$ (see Figure 5.2). Therefore, only the

family $\mathscr{F}_a^-$ provides a pertinent local description of how the global infimum of $\mathfrak{t} \mapsto \mathrm{d_o}\left(z_{z_0,u^*(\cdot),\sigma^*(\cdot)}^f(\mathfrak{t}), \mathscr{T}^+\right)$ is *attained* at $\partial P_\uparrow = \partial E_\downarrow$ (see Figure 4.16), if it is attained in finite time. It is clear that the local vector field (5.13)–(5.14), rules out the a priori possible situation in which $z^* \in \partial P_\uparrow = \partial E_\downarrow$ is approached but never reached by $z_{z_0,u^*(\cdot),\sigma^*(\cdot)}^f(\mathfrak{t})$, *except* in case z^* is approached by $z_{z_0,u^*(\cdot),\sigma^*(\cdot)}^f(\mathfrak{t})$ as the result of an infinite sequence of crossings of $\partial P_\uparrow = \partial E_\downarrow$. If this exceptional case is purposely disregarded for the moment, we conclude that the state is obliged to follow an arc of spiral in $P_\uparrow$ with unitary angular speed before *reaching z^** in

$$\left\{z \in \mathbb{C} \ : \ \overline{k} \otimes (z-a) = 0 \ \wedge \ \overline{k} \odot (z-a) < 0\right\} = \left\{a - \rho \frac{\overline{k}}{|k|} \ : \ \rho > 0\right\}. \quad (5.15)$$

Let $\mathscr{S}_a(z^*)$ be the unique semi-permeable curve of the family $\mathscr{F}_a^-$ that passes through z^*. The arc of spiral mentioned above is included in $\mathscr{S}_a(z^*)$. From (4.62), the normal direction to $\mathscr{S}_a(z^*)$ preferred by E, at z^*, is represented by

$$p_{z^*}^- = -\nabla \mathcal{M}_a^{b-a}(z^*) = -\mathrm{e}^{\kappa \mathcal{A}_a^{b-a}(z^*)} (-\mathrm{j}k) \frac{z^*-a}{|z^*-a|}.$$

In this last expression $\frac{z^*-a}{|z^*-a|} = -\frac{\overline{k}}{|k|}$ because $z^* \in \left\{a - \rho \frac{\overline{k}}{|k|} \ : \ \rho > 0\right\}$. Hence,

$$p_{z^*}^- = \mathrm{e}^{\kappa \mathcal{A}_a^{b-a}(z^*)} |k| (-\mathrm{j}),$$

i.e., the normal direction to $\mathscr{S}_a(z^*)$ preferred by E, at z^*, points "downwards". This is not surprise since z^* belongs to

$$\partial P_\uparrow = \partial E_\downarrow = \left\{z \in \mathbb{C} \ : \ \inf_{u \in U} \sup_{\sigma \in \Sigma} \{-\mathrm{j} \odot f(z,u,\sigma)\} = 0\right\}$$

and $\inf_{u \in U} \sup_{\sigma \in \Sigma} \{-\mathrm{j} \odot f(z,u,\sigma)\} = 0$ is, by Proposition 4.5.1, the condition for a curve (with normal $-\mathrm{j}$ preferred by E at z) to be semi-permeable at z.

In an analogous manner, similar conclusions can be derived for $\mathcal{G}_{\mathrm{dist}}^-$ which are stated next.

5.4.3. Conclusions

In the context of $\mathcal{G}_{\mathrm{dist}}^+$, the global infimum of $\mathfrak{t} \mapsto \mathrm{d_o}\left(z_{z_0,u^*(\cdot),\sigma^*(\cdot)}^f(\mathfrak{t}), \mathscr{T}^+\right)$, i.e., the value $\mathcal{V}_{\mathrm{d_o}}^+(z_0)$, is attained either: i) at $\mathfrak{t} = 0$, or ii) in infinite time as the limit of a sequence of crossings of $\partial P_\uparrow = \partial E_\downarrow$ by the trajectory $[0,\infty) \mathfrak{t} \mapsto z_{z_0,u^*(\cdot),\sigma^*(\cdot)}^f(\mathfrak{t})$, or iii) in finite time as the result of $z_{z_0,u^*(\cdot),\sigma^*(\cdot)}^f(\mathfrak{t})$ *reaching* a point z^* in the ray (5.15), from $P_\uparrow$, through an arc of spiral included in $\mathscr{S}_a(z^*)$, being $\mathscr{S}_a(z^*)$ the unique semi-permeable curve of the family $\mathscr{F}_a^-$ that passes through z^* (being $-\mathrm{j}$ the normal direction to $\mathscr{S}_a(z^*)$ preferred by E at z^*).

In the context of $\mathcal{G}_{\mathrm{dist}}^-$, the global infimum of $\mathfrak{t} \mapsto \mathrm{d_o}\left(z_{z_0,u^*(\cdot),\sigma^*(\cdot)}^f(\mathfrak{t}), \mathscr{T}^-\right)$, i.e., the value $\mathcal{V}_{\mathrm{d_o}}^-(z_0)$, is attained either: i) at $\mathfrak{t} = 0$, ii) in infinite time as the limit of
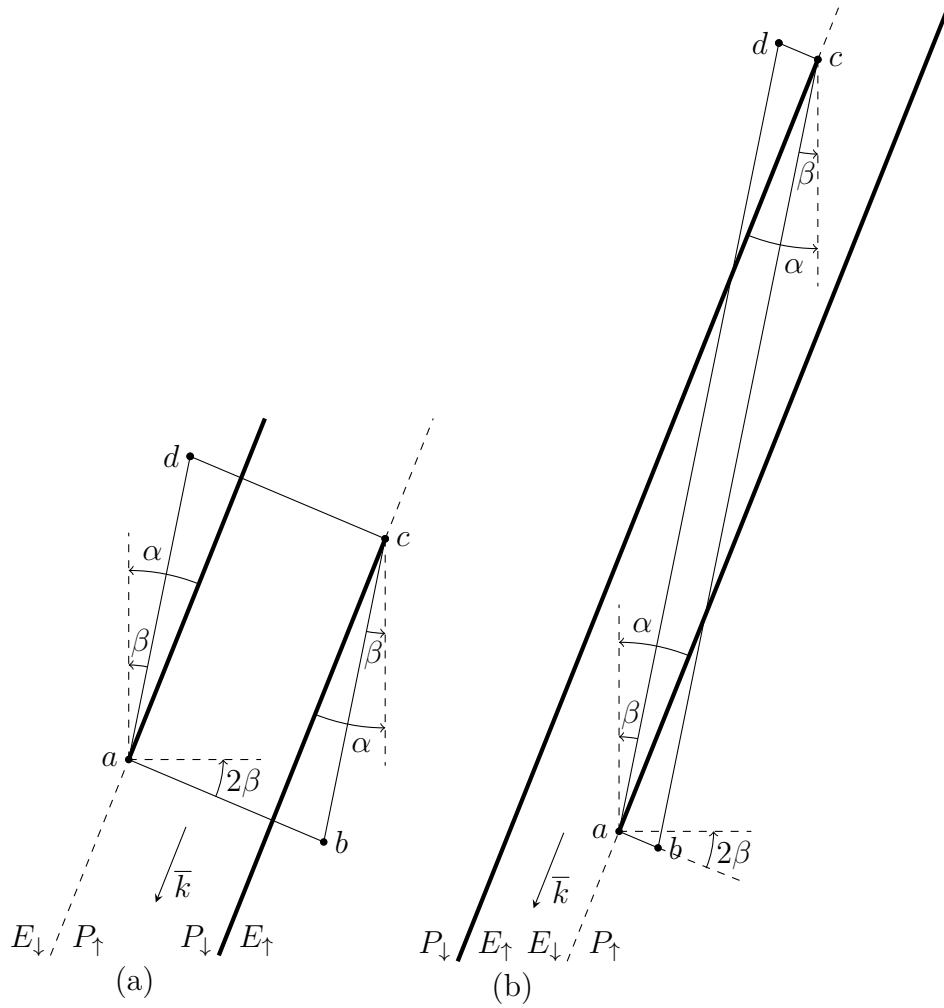
Figure 5.3: The sets $\left\{z = a - \rho\frac{\overline{k}}{|k|} \; : \; \rho \geq 0\right\} \subset \partial P_\uparrow = \partial E_\downarrow$ and $\left\{z = c + \rho\frac{\overline{k}}{|k|} \; : \; \rho \geq 0\right\} \subset$ $\partial P_\downarrow = \partial E_\uparrow$ are represented in the figure by thick rays with endpoints at a and c, respectively, for two qualitatively different cases: (a) $\overline{k} \otimes (c - a) > 0$ and (b) $\overline{k} \otimes (c - a) < 0$.

a sequence of crossings of $\partial P_\downarrow = \partial E_\uparrow$ by the trajectory $[0, \infty) \; t \mapsto z^f_{z_0, u^*(\cdot), \sigma^*(\cdot)}(t)$, or iii) in finite time as the result of $z^f_{z_0, u^*(\cdot), \sigma^*(\cdot)}(t)$ *reaching* a point z^* in the ray

$$\left\{z \in \mathbb{C} \; : \; \overline{k} \otimes (z - c) = 0 \; \wedge \; \overline{k} \odot (z - c) > 0\right\} = \left\{c + \rho\frac{\overline{k}}{|k|} \; : \; \rho > 0\right\}, \quad (5.16)$$

from $P_\downarrow$, through an arc of spiral included in $\mathscr{S}_c(z^*)$, being $\mathscr{S}_c(z^*)$ the unique semi-permeable curve of the family $\mathscr{F}_c^-$ that passes through z^* (being +j the normal direction to $\mathscr{S}_c(z^*)$ preferred by E at z^*).

The rays (5.15) and (5.16), the first included in $\bigcup \mathscr{F}_a^-$ and the second included in $\bigcup \mathscr{F}_c^-$, are represented in Figure 5.3 for the two qualitatively different cases commented at the end of Subsection 5.3.2. The families $\mathscr{F}_a^-$ and $\mathscr{F}_c^-$ are represented

in Figure 4.16.

5.5. An ansatz to approach the upward game problem

From now on the analysis will proceed exclusively focused on $\mathcal{G}_{\mathrm{dist}}^+$, since a parallel analysis for $\mathcal{G}_{\mathrm{dist}}^-$ can be developed analogously.

The conclusions of the previous section describe *locally* how an optimal trajectory $\mathfrak{t} \mapsto z_{z,u^*(\cdot),\sigma^*(\cdot)}^f(\mathfrak{t})$ of $\mathcal{G}_{\mathrm{dist}}^+$ that departs from $z \in \mathbb{C}$ (previously denoted z_0) *attains* or *approximates* $\mathcal{V}_{\mathrm{d_o}}^+(z)$, i.e., the global infimum of the function $\mathfrak{t} \mapsto \mathrm{d_o}\left(z_{z,u^*(\cdot),\sigma^*(\cdot)}^f(\mathfrak{t}), \mathscr{T}^+\right)$, if it is not attained right at $\mathfrak{t} = 0$, i.e., if $\mathcal{V}_{\mathrm{d_o}}^+(z) < \mathrm{d_o}(z, \mathscr{T}^+) = 1 - \Im z$. Suppose that $\mathfrak{t} \mapsto z_{z,u^*(\cdot),\sigma^*(\cdot)}^f(\mathfrak{t})$ *attains* $\mathcal{V}_{\mathrm{d_o}}^+(z)$ at some positive finite time.

Recalling: in $P_\uparrow$ and close to $\left\{a - \rho\frac{\overline{k}}{|k|} \ : \ \rho > 0\right\}$, the optimal trajectory coincides with an arc of spiral of the family $\mathscr{F}_a^-$ as it approaches and finally reaches the point in $\left\{a - \rho\frac{\overline{k}}{|k|} \ : \ \rho > 0\right\} \subset \partial P_\uparrow = \partial E_\downarrow$ where the infimum $\mathcal{V}_{\mathrm{d_o}}^+(z)$ is attained. Let $z_\rho = a - \rho\frac{\overline{k}}{|k|}$ be this point (which is different from the initial state z) and let $\mathscr{S}_a(z_\rho)$ be the unique member of $\mathscr{F}_a^-$ through z_ρ. It is clear that it must be $\mathcal{V}_{\mathrm{d_o}}^+(z) = 1 - \Im z_\rho < 1 - \Im z$. Moreover, as it was concluded before, the normal direction to $\mathscr{S}_a(z_\rho)$ preferred by E at z_ρ is represented by $-\mathrm{j}$. Notice that $\nabla(1 - \Im z) = -\mathrm{j}$ for every $z \in \mathbb{C}$.

The previous observations *suggest* that $\mathcal{V}_{\mathrm{d_o}}^+$ verifies the partial differential equation

$$\inf_{u \in U} \sup_{\sigma \in \Sigma} \nabla \mathcal{V}(z) \odot f(z, u, \sigma) = 0, \tag{5.17}$$

with the boundary conditions

$$\begin{cases} \mathcal{V}(z) = 1 - \Im z \\ \nabla \mathcal{V}(z) = -\mathrm{j} \end{cases} \quad z \in \left\{a - \rho\frac{\overline{k}}{|k|} \ : \ \rho > 0\right\}, \tag{5.18}$$

at least in a domain of the form

$$P_\uparrow \cap \left\{w \ : \ |w - z^*| < \epsilon\right\}, \tag{5.19}$$

for some $z^* \in \left\{a - \rho\frac{\overline{k}}{|k|} \ : \ \rho > 0\right\}$ and some $\epsilon > 0$, i.e., *locally* at the intersection of the half-plane $P_\uparrow$ with some neighbourhood of some unknown point z^* on the ray $\left\{a - \rho\frac{\overline{k}}{|k|} \ : \ \rho > 0\right\}$ included in the line $\partial P_\uparrow = \partial E_\downarrow$.

Note that from the conclusions arrived at the previous section it can not be inferred that necessarily *every* point of the ray $\left\{a - \rho\frac{\overline{k}}{|k|} \ : \ \rho > 0\right\}$ is actually a point of closest approach to $\mathscr{T}^+$ of some optimal state-space trajectory.

By Proposition 4.5.1, the equation (5.17) expresses a semi-permeability condition for the level sets of $\mathcal{V}$ which must coincide with the members of $\mathscr{F}_a^-$, at least in the unknown local domain (5.19) where the boundary conditions (5.18) are imposed.

5.5.1. Isaacs' equation

The partial differential equation (5.17) happens to coincide with *Isaacs' equation* for a pursuit-evasion differential game with the same SE as $\mathcal{G}^+_{\text{dist}}$, a TS included in $\left\{a - \rho\frac{\overline{k}}{|k|} \; : \; \rho > 0\right\}$, and a PF with identically null running cost $G \equiv 0$ that assigns a terminal cost $H(z) = 1 - \Im z$ to each play that terminates in the TS. Indeed, (5.17) may be written as Isaacs' main equation in its first form (ME$_1$) for such terminal game:

$$\inf_{u \in U} \sup_{\sigma \in \boldsymbol{\Sigma}} \mathcal{H}(z, \nabla \mathcal{V}(z), u, \sigma) = 0, \tag{5.20}$$

where $\mathcal{H} : \mathbb{C} \times \mathbb{C} \times U \times \boldsymbol{\Sigma} \to \mathbb{R}$ is a Hamiltonian function defined by

$$\mathcal{H}(z, p, u, \sigma) = p \odot f(z, u, \sigma) + \underbrace{G(z, u, \sigma)}_{=0} = \frac{\overline{p}k(z - \mathsf{q}(u, \sigma)) + p\overline{k}(\overline{z} - \overline{\mathsf{q}}(u, \sigma))}{2}.$$

Notice that *Isaacs' condition* holds in (5.17), i.e., the order of the inf and sup in (5.17) does not matter by virtue of the statement 1 of Proposition 4.4.1.

Although suggestive, the aforementioned coincidence will not be exploited further except for referring to (5.17) (or equivalently (5.20)) as *Isaacs' equation for* $\mathcal{G}^+_{\text{dist}}$, or just *Isaacs' equation*, since it expresses the same semi-permeability condition that would be required if $\mathcal{G}^-_{\text{dist}}$ was being treated instead of $\mathcal{G}^+_{\text{dist}}$.

It must be empathised that the problem (5.17)–(5.18) proposed above will be used *merely* to try to figure out how $\tilde{u}^*_+$ and $\tilde{\sigma}^*_+$ should be defined in order to verify (5.11) at least approximately for the case of the upward game $\mathcal{G}^+_{\text{dist}}$. Accordingly, (5.17)–(5.18) should be conceived at this stage simply as an ansatz to approach the problem of solving $\mathcal{G}^+_{\text{dist}}$.

5.6. Solving Isaacs' equation for the upward game

The condition (5.17), or equivalently (5.20), is a semi-permeability condition for the level curves of $\mathcal{V}$ through z, at the point z, for every z such that $\nabla \mathcal{V}(z)$ is well defined and $\nabla \mathcal{V}(z) \neq 0$. The E's preferred side of the level curve is the one pointed by the vector $\nabla \mathcal{V}(z)$ based at z. The opposite side is the one preferred by P.

Recall that, in Section 4.5, eight families of semi-permeable curves for the conflict's SE have been discovered and the possible concatenations among them have been discussed. If an arrangement of (possibly composite) semi-permeable curves can be envisaged, each one with an assigned real value and an endpoint in the ray $\left\{a - \rho\frac{\overline{k}}{|k|} \; : \; \rho > 0\right\}$, such that they jointly define a real valued function $\mathcal{V}$ (in some subset of the complex plane) that verifies the boundary condition (5.18); then $\mathcal{V}$ is a solution of (5.17)–(5.18). This arrangement of semi-permeable curves could be built ad hoc making use only of the results of Chapter 4, however, it will be obtained by the more classical method of characteristics as follows.

Recall the functions $u^* : \mathbb{C} \to U$ and $\sigma^* : \mathbb{C} \to \mathbf{\Sigma}$, introduced in statement 2 of Proposition 4.4.1. By the same proposition's statement, the pair

$$(u^* (\nabla \mathcal{V} (z)), \sigma^* (\nabla \mathcal{V} (z))) \tag{5.21}$$

is a solution of the point-wise inf-sup problem defined in the LHS of (5.20), for each $z \in \mathbb{C}$.

Substituting (5.21) into (5.20), Isaacs' main equation in its second form (ME$_2$) is obtained:

$$\mathcal{H} (z, \nabla \mathcal{V} (z), u^* (\nabla \mathcal{V} (z)), \sigma^* (\nabla \mathcal{V} (z))) = 0. \tag{5.22}$$

This is a partial differential equation whose unknown is the function $\mathcal{V}$. Next, the classical method of characteristics is applied to solve (5.22) with the boundary condition (5.18), in order to figure out an explicit expression for $\mathcal{V}_{\mathrm{do}}^+$ in closed form that matches its role of VF of $\mathcal{G}_{\mathrm{dist}}^+$.

5.6.1. The retrograde path equations

The retrograde path equations (RPE) or *characteristic equations* of (5.22) are

$$\mathring{z} = -2 \frac{\partial}{\partial \overline{p}} \mathcal{H} (z, p, u^* (p), \sigma^* (p)) = -f (z, u^* (p), \sigma^* (p))$$
$$= -k (z - \mathsf{q} (u^* (p), \sigma^* (p))), \tag{5.23}$$
$$\mathring{p} = +2 \frac{\partial}{\partial \overline{z}} \mathcal{H} (z, p, u^* (p), \sigma^* (p)) = \overline{k} p. \tag{5.24}$$

where $\mathring{\ }$ denotes differentiation with respect to *retrogressive time* τ. Note that Wirtinger calculus has been used to adapt the formulation of the RPE, as presented in Section 2.8, to its complex counterpart for the case in which the state-space $\mathbb{R}^2$ is identified with $\mathbb{C}$. The explicit dependence of z and p on τ has been omitted for clarity. Each solution of this system of ordinary differential equations supplies a *characteristic* state-space trajectory $\tau \mapsto z (\tau)$ and its corresponding *co-state* trajectory $\tau \mapsto p (\tau)$. The meaning of the co-state $p (\tau)$ is: $p (\tau) = \nabla \mathcal{V} (z (\tau))$. It must be noted however, that this presupposes that $\mathcal{V}$ is twice continuously real differentiable in the region covered by the characteristic trajectories.

5.6.2. Integration of the retrograde path equations

5.6.2.1. Generic initial conditions

It is remarkable that for $\mathcal{H}$, as defined before, the co-state retrograde path equation (5.24) can be solved independently of the state retrograde path equation (5.23). Indeed, the solution of (5.24) is readily found to be

$$\tau \mapsto p (\tau) = e^{\overline{k} \tau} p_0 = e^{-\kappa \tau} e^{-j \tau} p_0. \tag{5.25}$$

where $p_0 \triangleq p|_{\tau=0} \in \mathbb{C}$ is the initial (in retrogressive sense) co-state. Admit, for the moment, that $p_0 \neq 0$. Observe that $p (\tau)$ is a roto-homothety of p_0, for every $\tau \geq 0$.

Let $r\left(\tau\right) \triangleq -\overline{k}p\left(\tau\right) = \left(\sec\alpha\right)\mathrm{e}^{\mathrm{j}\left(\frac{\pi}{2}-\alpha\right)}p\left(\tau\right)$, for every $\tau \geq 0$. Not surprisingly, $r\left(\tau\right) = \mathrm{e}^{-\kappa\tau}\mathrm{e}^{-\mathrm{j}\tau}r_0$ is a roto-homothety of $r_0 \triangleq r|_{\tau=0}$, for every $\tau \geq 0$.

In the state retrograde path equation (5.23), $\mathsf{q}\left(u^*\left(p\left(\tau\right)\right),\sigma^*\left(p\left(\tau\right)\right)\right)$ remains constant and equal to $q_0 \triangleq \mathsf{q}\left(u^*\left(p_0\right),\sigma^*\left(p_0\right)\right)$ as long as $\mathrm{sg}\left(r\left(\tau\right),\mathrm{e}^{-\mathrm{j}2\beta}\right)$ and $\mathrm{sg}\left(r\left(\tau\right),\mathrm{e}^{\mathrm{j}\left(\frac{\pi}{2}-\beta\right)}\right)$ do not change (recall the definitions of u^* and σ^* in statement 2 of Proposition 4.4.1). As long as this happens (5.23) reads

$$\mathring{z} = -k\left(z - q_0\right),$$

whose solution

$$\tau \mapsto z\left(\tau\right) = q_0 + \mathrm{e}^{-k\tau}\left(z_0 - q_0\right) = q_0 + \mathrm{e}^{\kappa\tau}\mathrm{e}^{-\mathrm{j}\tau}\left(z_0 - q_0\right),$$

through $z_0 \triangleq z|_{\tau=0} \in \mathbb{C}$, is valid as long as $\mathrm{sg}\left(r\left(\tau\right),\mathrm{e}^{-\mathrm{j}2\beta}\right) = \mathrm{sg}\left(r_0,\mathrm{e}^{-\mathrm{j}2\beta}\right)$ and $\mathrm{sg}\left(r\left(\tau\right),\mathrm{e}^{\mathrm{j}\left(\frac{\pi}{2}-\beta\right)}\right) = \mathrm{sg}\left(r_0,\mathrm{e}^{\mathrm{j}\left(\frac{\pi}{2}-\beta\right)}\right)$. Clearly, $\tau \mapsto z\left(\tau\right)$ is the parametrization of an α-equiangular spiral, through z_0, centred at q_0 (parametrized by increasing values of τ along the un-shrinking direction of motion).

The retro-instants of time at which $\mathsf{q}\left(u^*\left(p\left(\tau\right)\right),\sigma^*\left(p\left(\tau\right)\right)\right)$ changes or *switches* are exactly the instants at which the vector $r\left(\tau\right) = \mathrm{e}^{-\kappa\tau}\mathrm{e}^{-\mathrm{j}\tau}r_0$, based at the origin of the complex plane, crosses one of the following straight lines which intersect at the origin: $\left\{w \in \mathbb{C} \ : \ w \odot \mathrm{e}^{-\mathrm{j}2\beta} = 0\right\}$ and $\left\{w \in \mathbb{C} \ : \ w \odot \mathrm{e}^{\mathrm{j}\left(\frac{\pi}{2}-\beta\right)} = 0\right\}$ (see Figure 4.14). Note that the argument of $r\left(\tau\right)$ is all that matters for this switching mechanism, not its magnitude. Note also that at each of such instants, switching is mandatory because $\frac{r(\tau)}{|r(\tau)|} = \mathrm{e}^{-\mathrm{j}\tau}\frac{r_0}{|r_0|}$ is a unit vector that rotates clock-wisely with unitary angular velocity. Therefore, $\mathsf{q}\left(u^*\left(p\left(\tau\right)\right),\sigma^*\left(p\left(\tau\right)\right)\right)$ periodically visits the points a, b, c, and d following a precisely timed switching sequence. Recall that these four points are the vertices of the parallelogram $\left\{\mathsf{q}\left(i_o + \mathrm{j},\sigma\right) \ : \ i_o \in [i_o^\triangledown, 1] \ \wedge \ \sigma \in [0,1]\right\}$ (see Figure 5.1), being $\mathsf{q}\left(u,\sigma\right) = -\mathrm{j}\delta_0 + i_o\delta_1\mathrm{e}^{-\mathrm{j}2\beta} + \sigma\delta_2\mathrm{e}^{\mathrm{j}\left(\frac{\pi}{2}-\beta\right)}$.

5.6.2.2. Particular initial conditions

The initial conditions z_0 and p_0 used above are generic. To solve (5.22) with (5.18) as boundary conditions, the particular initial conditions that ought to be used are

$$z_\rho|_{\tau=0} = z_{\rho,0} = a - \rho\frac{\overline{k}}{|k|}, \quad \rho > 0, \tag{5.26}$$

$$p|_{\tau=0} \ = \ p_0 \ = -\mathrm{j}, \tag{5.27}$$

where every $\rho > 0$ is considered a priori. In accordance with (5.27),

$$r|_{\tau=0} = r_0 = -\overline{k}p_0 = \mathrm{e}^{-\mathrm{j}\alpha}\sec\alpha,$$

as represented in Figure 5.4.

For each $\rho > 0$, using (5.26) and (5.27) as the initial conditions for the integration of the RPE, a characteristic trajectory $\tau \mapsto z_\rho\left(\tau\right)$ and its corresponding

$$r(\tau) = -\overline{k}p(\tau)$$
$$r(\tau) \odot \mathrm{e}^{-\mathrm{j}2\beta} < 0$$
$$r(\tau) \odot \mathrm{e}^{\mathrm{j}\left(\frac{\pi}{2}-\beta\right)} > 0$$
$$\mathsf{q}\left(u^*\left(p\left(\tau\right)\right), \sigma^*\left(p\left(\tau\right)\right)\right) = c$$

$$\mathrm{e}^{-\mathrm{j}2\beta}$$

$$r(\tau) = -\overline{k}p(\tau)$$
$$r(\tau) \odot \mathrm{e}^{-\mathrm{j}2\beta} > 0$$
$$r(\tau) \odot \mathrm{e}^{\mathrm{j}\left(\frac{\pi}{2}-\beta\right)} > 0$$
$$\mathsf{q}\left(u^*\left(p\left(\tau\right)\right), \sigma^*\left(p\left(\tau\right)\right)\right) = d$$

$$\tfrac{\pi}{2}+\beta$$

$$r(\tau)$$

$$\tfrac{\pi}{2}-\beta$$

$$\mathrm{e}^{\mathrm{j}\left(\frac{\pi}{2}-\beta\right)}$$

$$r_0$$

$$\alpha - \beta$$

$$r(\tau) = -\overline{k}p(\tau)$$
$$r(\tau) \odot \mathrm{e}^{-\mathrm{j}2\beta} < 0$$
$$r(\tau) \odot \mathrm{e}^{\mathrm{j}\left(\frac{\pi}{2}-\beta\right)} < 0$$
$$\mathsf{q}\left(u^*\left(p\left(\tau\right)\right), \sigma^*\left(p\left(\tau\right)\right)\right) = b$$

$$\tfrac{\pi}{2}-\beta$$

$$\tfrac{\pi}{2}+2\beta-\alpha$$

$$\mathrm{e}^{-\mathrm{j}\alpha}$$

$$r(\tau) = -\overline{k}p(\tau)$$
$$r(\tau) \odot \mathrm{e}^{-\mathrm{j}2\beta} > 0$$
$$r(\tau) \odot \mathrm{e}^{\mathrm{j}\left(\frac{\pi}{2}-\beta\right)} < 0$$
$$\mathsf{q}\left(u^*\left(p\left(\tau\right)\right), \sigma^*\left(p\left(\tau\right)\right)\right) = a$$
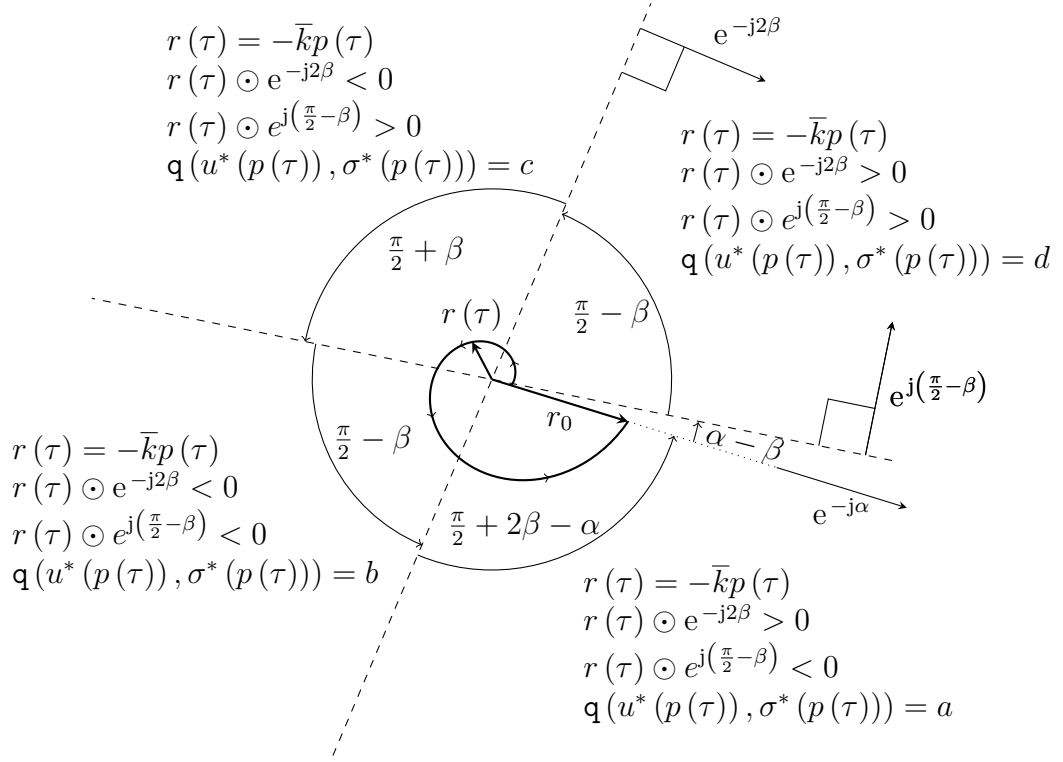
Figure 5.4: The r-trajectory $\tau \mapsto r(\tau)$, defined as the $-\overline{k}(\cdot) = (\sec\alpha)\,\mathrm{e}^{\mathrm{j}\left(\frac{\pi}{2}-\alpha\right)}(\cdot)$ roto-homothety of the co-state trajectory $[0, 2\pi) \ni \tau \mapsto p(\tau) = \mathrm{e}^{-\kappa\tau}\mathrm{e}^{-\mathrm{j}\tau}(-\mathrm{j})$, rules the switching instants of the piecewise constant function $\tau \mapsto \mathsf{q}\left(u^*\left(p\left(\tau\right)\right), \sigma^*\left(p\left(\tau\right)\right)\right)$. The arrows on the r-trajectory indicate the direction of motion along which retrogressive time τ *decreases*.

co-state trajectory $\tau \mapsto p(\tau)$ can be constructed as it was explained before with generic initial conditions.

The method of characteristics provides a way of determining the solution of (5.22)–(5.18), by setting

$$\mathcal{V}\left(z_\rho\left(\tau\right)\right) = \mathcal{V}\left(z_\rho|_{\tau=0}\right) = 1 - \Im\left(a - \rho\frac{\overline{k}}{|k|}\right) \tag{5.28}$$

at every point $z_\rho(\tau)$ reached by integration of the RPE, but it relies on the assumption that $\mathcal{V}$ is twice continuously real differentiable in the region covered by the characteristic trajectories.

5.6.2.3. The characteristic trajectories of Isaacs' equation

Since $p_0 = -\mathrm{j}$, the co-state trajectory (5.25) takes the form

$$\tau \mapsto p(\tau) = \mathrm{e}^{\overline{k}\tau}(-\mathrm{j}) = \mathrm{e}^{-\kappa\tau}\mathrm{e}^{-\mathrm{j}\tau}(-\mathrm{j}). \tag{5.29}$$

Accordingly,

$$\tau \mapsto r(\tau) = -\overline{k}p(\tau) = (\sec\alpha)\,\mathrm{e}^{\mathrm{j}\left(\frac{\pi}{2}-\alpha\right)}\mathrm{e}^{-\kappa\tau}\mathrm{e}^{-\mathrm{j}\tau}(-\mathrm{j}) = \mathrm{e}^{-\kappa\tau}\mathrm{e}^{-\mathrm{j}\tau}r_0. \tag{5.30}$$
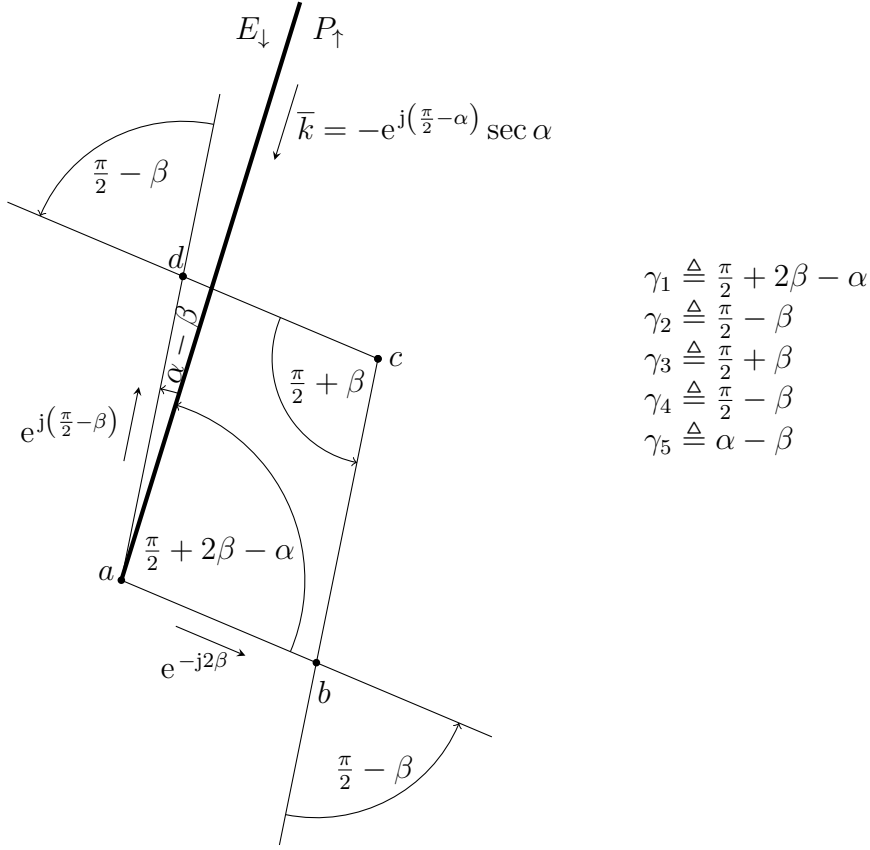
Figure 5.5: The geometric parameters α and β (recall Figures 3.7 and 3.8) reinterpreted at the light of the integration of the retrograde path equations.

Letting this *r-trajectory* blindly determine the retro-time instants at which $q\left(u^*\left(p\left(\tau\right)\right),\sigma^*\left(p\left(\tau\right)\right)\right)$ must switch (as represented in Figure 5.4), the following ρ-parametrized family of characteristic trajectories is obtained over a retro-time interval of length 2π:

$$\tau \mapsto z_\rho\left(\tau\right) = \begin{cases} a + \mathrm{e}^{(\kappa-\mathrm{j})(\tau-\tau_0)}\left(z_{\rho,0} - a\right) & \text{if } \tau \in [0,\tau_1], \\ b + \mathrm{e}^{(\kappa-\mathrm{j})(\tau-\tau_1)}\left(z_\rho\left(\tau_1\right) - b\right) & \text{if } \tau \in (\tau_1,\tau_2], \\ c + \mathrm{e}^{(\kappa-\mathrm{j})(\tau-\tau_2)}\left(z_\rho\left(\tau_2\right) - c\right) & \text{if } \tau \in (\tau_2,\tau_3], \\ d + \mathrm{e}^{(\kappa-\mathrm{j})(\tau-\tau_3)}\left(z_\rho\left(\tau_3\right) - d\right) & \text{if } \tau \in (\tau_3,\tau_4], \\ a + \mathrm{e}^{(\kappa-\mathrm{j})(\tau-\tau_4)}\left(z_\rho\left(\tau_4\right) - a\right) & \text{if } \tau \in (\tau_4,2\pi), \end{cases} \tag{5.31}$$

where $\tau_1 = \gamma_1 \triangleq \frac{\pi}{2} + 2\beta - \alpha$, $\tau_2 - \tau_1 = \gamma_2 \triangleq \frac{\pi}{2} - \beta$, $\tau_3 - \tau_2 = \gamma_3 \triangleq \frac{\pi}{2} + \beta$, $\tau_4 - \tau_3 = \gamma_4 \triangleq \frac{\pi}{2} - \beta$, $2\pi - \tau_4 = \gamma_5 \triangleq \alpha - \beta$. Of course, $\gamma_1 + \gamma_2 + \gamma_3 + \gamma_4 + \gamma_5 = 2\pi$.

The fact that the retro-time interval lengths $\gamma_1, \ldots, \gamma_5$ are all positive follows logically from the conditions (5.1). To prove that $\gamma_2, \ldots, \gamma_5 > 0$, it is enough to recall the condition $|\beta| < \alpha < \frac{\pi}{2}$. However, to prove that $\gamma_1 > 0$, this is not enough. Since $|\beta| < \alpha < \frac{\pi}{2}$, it must be $\gamma_1 = \frac{\pi}{2} + 2\beta - \alpha \in (-\pi, \pi)$. Hence, to prove

that $\gamma_1 > 0$, it suffices to prove that $\sin \gamma_1 = \sin\left(\frac{\pi}{2} + 2\beta - \alpha\right) = \cos(2\beta - \alpha)$ is positive, which was already incidentally proved in the proof of Lemma 4.4.1, using the condition $\tan\alpha - \tan\beta < \sec\alpha$ also required by (5.1).

In Figure 5.4 the r-trajectory $\{r(\tau) \ : \ \tau \in [0, 2\pi)\}$ is represented by a thickly traced arc of spiral, for a case in which $\beta > 0$. The r-trajectory is just the p-*trajectory* (co-state trajectory) transformed by the roto-homothety $(\sec\alpha)\,\mathrm{e}^{\mathrm{j}\left(\frac{\pi}{2}-\alpha\right)}(\cdot)$. The arrows on the r-trajectory indicate the direction of motion along which retrogressive time τ *decreases*, i.e., along which progressive time t *increases*. Note that $r_0 = -\bar{k}(-\mathrm{j})$ verifies the inequalities

$$r_0 \odot \mathrm{e}^{-\mathrm{j}2\beta} > 0,$$
$$r_0 \odot \mathrm{e}^{\mathrm{j}\left(\frac{\pi}{2}-\beta\right)} < 0,$$

which are guaranteed to hold by Lemma 4.4.1, even if $\beta \leq 0$. Consequently, $\mathsf{q}\left(u^*\left(p_0\right), \sigma^*\left(p_0\right)\right) = \mathsf{q}\left(u^*\left(-\mathrm{j}\right), \sigma^*\left(-\mathrm{j}\right)\right) = a$, as already established by the second point of the final statement of Corollary 4.4.1. Observe the perfect accordance between angular sweeps of $z_\rho(\tau)$ and $r(\tau)$ (see Figures 5.4 and 5.5), which also holds even if $\beta \leq 0$. As a consequence of this accordance, at the switching retrotime instants τ_1, τ_2, τ_3, and τ_4, the state $z_\rho(\tau)$ belongs to the straight line $\overleftrightarrow{ab}$, $\overleftrightarrow{cb}$, $\overleftrightarrow{cd}$, and $\overleftrightarrow{ad}$, respectively.

5.6.3. A return map for the flow of characteristic trajectories

Although parametrized by $\rho > 0$, the family of characteristic trajectories (5.31) may be considered from a slightly more general viewpoint by letting ρ be any real number in the initial condition (5.26), where $-\frac{\bar{k}}{|k|} = \mathrm{e}^{\mathrm{j}\left(\frac{\pi}{2}-\alpha\right)}$.

For example, let ρ' be a real number that takes the place of ρ in (5.31). For each retro-time $\tau \in [0, 2\pi)$, the point $z_{\rho'}(\tau)$ is reached from $z_{\rho',0} = z_{\rho'}(0)$ by moving *backwards* in time through the characteristic trajectory that passes through $z_{\rho',0}$. Consider, in particular, the limit as $\tau \to (2\pi)^-$. It can be verified that $\lim_{\tau\to(2\pi)^-} z_{\rho'}(\tau) \in \left\{a + \xi\mathrm{e}^{\mathrm{j}\left(\frac{\pi}{2}-\alpha\right)} \ : \ \xi \in \mathbb{R}\right\}$ for every $\rho' \in \mathbb{R}$, as it is done in Appendix B.1.

Hence, for every $\rho' \in \mathbb{R}$ there exists an unique $\rho \in \mathbb{R}$ such that

$$\lim_{\tau\to(2\pi)^-} z_{\rho'}(\tau) = z_\rho(0). \tag{5.32}$$

From this limit point a characteristic trajectory $[0, 2\pi) \ni \tau \mapsto z_\rho(\tau)$ (in general different from $[0, 2\pi) \ni \tau \mapsto z_{\rho'}(\tau)$) emanates retrogressively in time as represented in Figure 5.6. Therefore the well defined real-valued function

$$\left(z_{\rho'}(0) - a\right) \odot \mathrm{e}^{\mathrm{j}\left(\frac{\pi}{2}-\alpha\right)} = \rho' \mapsto \rho \triangleq \left(\underbrace{\lim_{\tau\to(2\pi)^-} z_{\rho'}(\tau)}_{z_\rho(0)} - a\right) \odot \mathrm{e}^{\mathrm{j}\left(\frac{\pi}{2}-\alpha\right)} \tag{5.33}$$
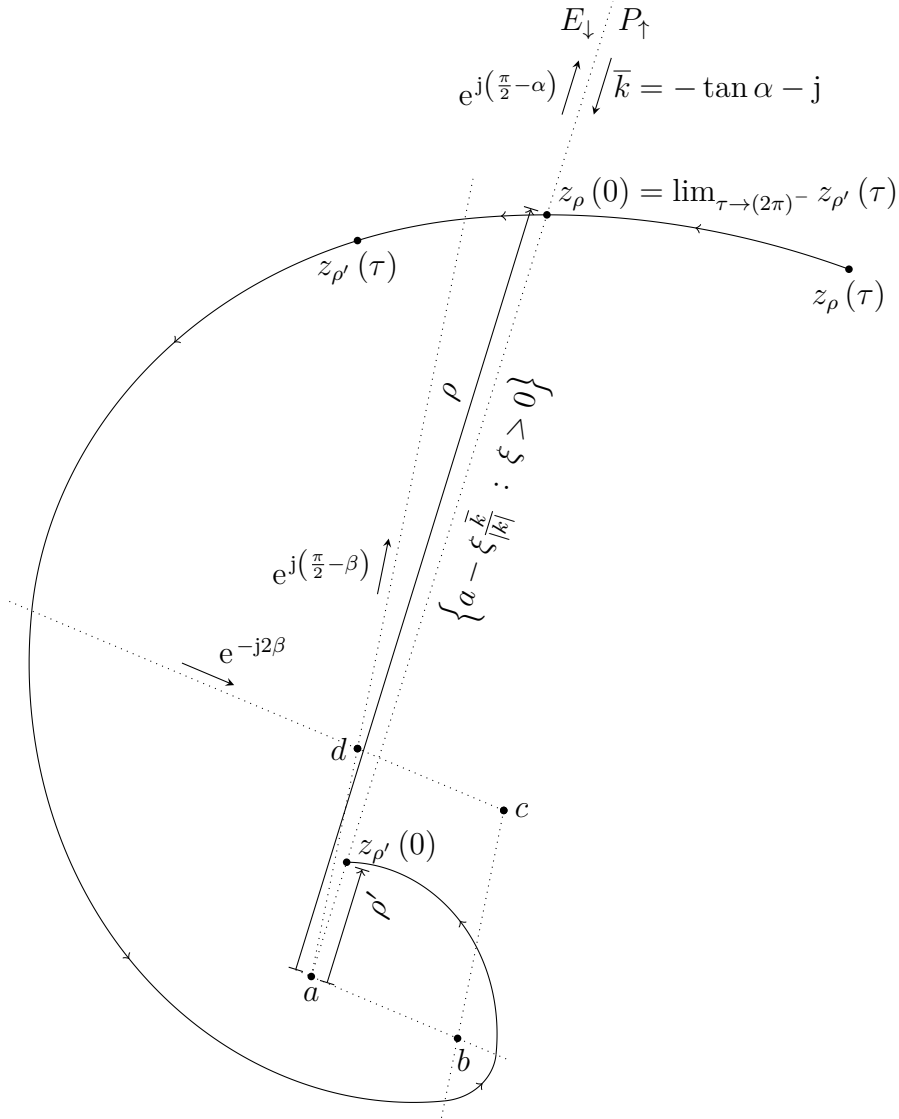
Figure 5.6: The function $z \mapsto a + P\left((z-a) \odot \mathrm{e}^{\mathrm{j}\left(\frac{\pi}{2}-\alpha\right)}\right)\mathrm{e}^{\mathrm{j}\left(\frac{\pi}{2}-\alpha\right)}$ assigns to every point $z_\rho(0) \in \left\{a + \xi\mathrm{e}^{\mathrm{j}\left(\frac{\pi}{2}-\alpha\right)} \; : \; \xi \in \mathbb{R}\right\}$ its *succeeding* point $z_{\rho'}(0) \in \left\{a + \xi\mathrm{e}^{\mathrm{j}\left(\frac{\pi}{2}-\alpha\right)} \; : \; \xi \in \mathbb{R}\right\}$, in the sense of (5.32). The underlying function $P : \mathbb{R} \to \mathbb{R}$ is just its coordinate expression.

may be used to assign to every point $z_{\rho'}(0) \in \left\{a + \xi\mathrm{e}^{\mathrm{j}\left(\frac{\pi}{2}-\alpha\right)} \; : \; \xi \in \mathbb{R}\right\}$ its *preceding* point $z_\rho(0) \in \left\{a + \xi\mathrm{e}^{\mathrm{j}\left(\frac{\pi}{2}-\alpha\right)} \; : \; \xi \in \mathbb{R}\right\}$, in the limit sense of (5.32).

The function (5.33) is invertible and its inverse $P : \mathbb{R} \to \mathbb{R}$ (calculated in Appendix B.1) is

$$\rho \mapsto \rho' = P(\rho) = \eta_1 \rho + \eta_0, \tag{5.34}$$

where:

$$\eta_1 \triangleq e^{-2\pi\kappa}, \quad \eta_0 \triangleq \left(2e^{-\kappa\pi}\cosh\frac{\kappa\pi}{2}\right)\left(\mu_1 e^{-\kappa(2\beta-\alpha)} - \mu_2 e^{-\kappa\left(\frac{\pi}{2}-(\alpha-\beta)\right)}\right).$$

The function $P : \mathbb{R} \to \mathbb{R}$ just introduced may be used to assign to every point $z_\rho(0)$ in $\left\{a + \xi e^{j\left(\frac{\pi}{2}-\alpha\right)} : \xi \in \mathbb{R}\right\}$ its *succeeding* point $z_{\rho'}(0) \in \left\{a + \xi e^{j\left(\frac{\pi}{2}-\alpha\right)} : \xi \in \mathbb{R}\right\}$, in the limit sense of (5.32), as follows:

$$z \mapsto a + P\left((z-a) \odot e^{j\left(\frac{\pi}{2}-\alpha\right)}\right) e^{j\left(\frac{\pi}{2}-\alpha\right)}. \tag{5.35}$$

Accordingly, (5.35) may be viewed as a *return map*, in the limit sense of (5.32), for the progressive time flow of characteristic state-space trajectories and $P : \mathbb{R} \to \mathbb{R}$ as its *coordinate expression* along the line $\left\{a + \xi e^{j\left(\frac{\pi}{2}-\alpha\right)} : \xi \in \mathbb{R}\right\}$, i.e., if a point z that belongs to $\left\{a + \xi e^{j\left(\frac{\pi}{2}-\alpha\right)} : \xi \in \mathbb{R}\right\}$ is such that $(z-a) \odot e^{j\left(\frac{\pi}{2}-\alpha\right)} = \rho$ and z' is the image of z by (5.35), then $(z'-a) \odot e^{j\left(\frac{\pi}{2}-\alpha\right)} = P(\rho)$.

It is easy to check that the function $P : \mathbb{R} \to \mathbb{R}$ verifies the following properties (see Appendix B.1):

$$\frac{dP}{d\rho}(\rho) = \eta_1 < 1, \tag{5.36}$$

$$P(\rho_{\text{lim}}) = \rho_{\text{lim}}, \tag{5.37}$$

$$P(\rho) < \rho \quad \Longleftrightarrow \quad \rho > \rho_{\text{lim}}, \tag{5.38}$$

$$P(\rho) > \rho \quad \Longleftrightarrow \quad \rho < \rho_{\text{lim}}, \tag{5.39}$$

$$P^{-1}(\rho) > \rho \quad \Longleftrightarrow \quad \rho > \rho_{\text{lim}}, \tag{5.40}$$

$$P^{-1}(\rho) < \rho \quad \Longleftrightarrow \quad \rho < \rho_{\text{lim}}, \tag{5.41}$$

$$\rho < \rho_{\text{lim}} \quad \Longleftrightarrow \quad P(\rho) < \rho_{\text{lim}}, \tag{5.42}$$

$$\rho > \rho_{\text{lim}} \quad \Longleftrightarrow \quad P(\rho) > \rho_{\text{lim}}, \tag{5.43}$$

$$\lim_{n \to +\infty}\left(\underbrace{P \circ \ldots \circ P}_{n}\right)(\rho) = \lim_{n \to +\infty} P^n(\rho) = \rho_{\text{lim}} \quad \forall \rho \in \mathbb{R}, \tag{5.44}$$

where:

$$\rho_{\text{lim}} \triangleq \frac{\eta_0}{1-\eta_1} = \frac{\mu_1 e^{-\kappa(2\beta-\alpha)} - \mu_2 e^{-\kappa\left(\frac{\pi}{2}-(\alpha-\beta)\right)}}{2\sinh\frac{\kappa\pi}{2}}. \tag{5.45}$$

The above properties tell us that in the family of characteristic trajectories (5.31), parametrized by $\rho \in \mathbb{R}$, there exists a special one, namely $[0, 2\pi) \ni \tau \mapsto z_{\rho_{\text{lim}}}(\tau)$, which verifies

$$\lim_{\tau \to (2\pi)^-} z_{\rho_{\text{lim}}}(\tau) = z_{\rho_{\text{lim}}}(0), \tag{5.46}$$

while each other characteristic trajectory $[0, 2\pi) \ni \tau \mapsto z_\rho(\tau)$ verifies either

$$\lim_{\tau \to (2\pi)^-} z_\rho(\tau) > z_\rho(0) \quad \text{if } \rho > \rho_{\text{lim}}, \tag{5.47}$$
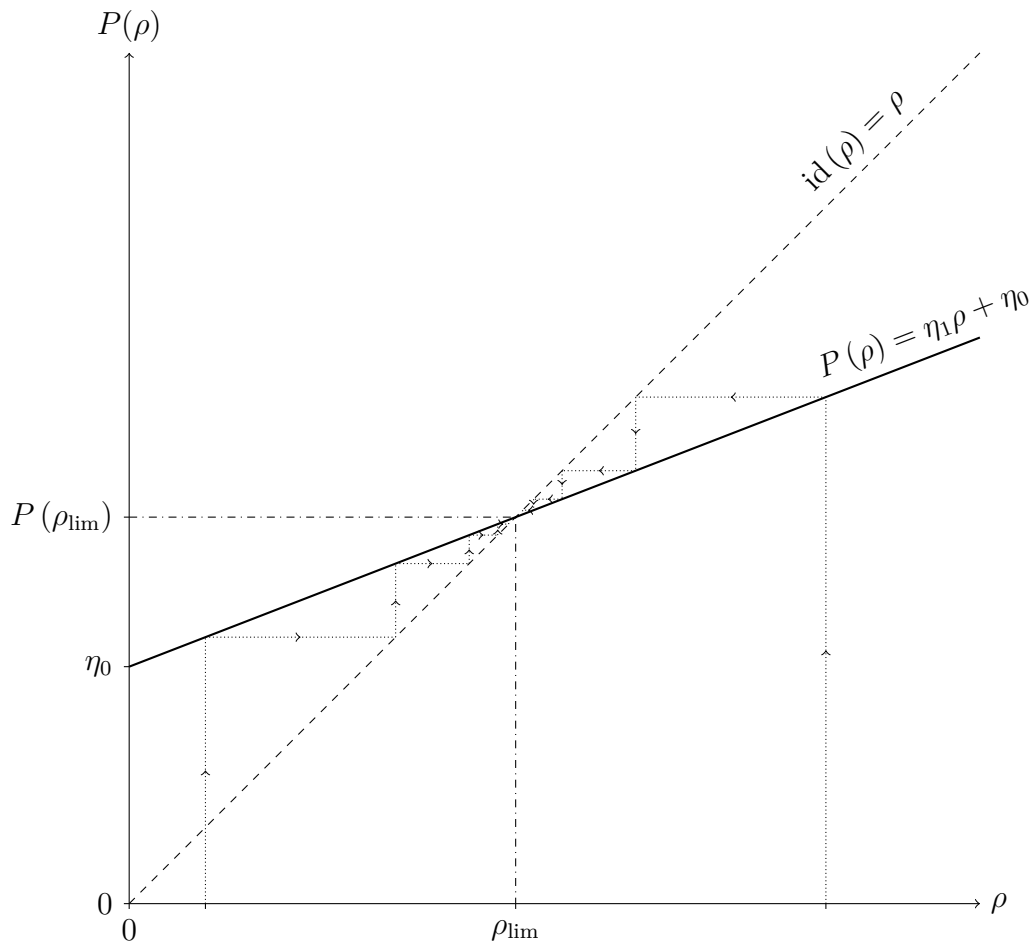
Figure 5.7: The properties (5.36)–(5.44) of the function $P : \mathbb{R} \to \mathbb{R}$ exposed graphically.

or

$$\lim_{\tau \to (2\pi)^-} z_\rho(\tau) < z_\rho(0) \quad \text{if } \rho < \rho_{\text{lim}}. \tag{5.48}$$

Now, for each $\rho \in \mathbb{R}$, instead of looking backwards to the *preceding* point of $z_\rho(0) = a + \rho e^{j\left(\frac{\pi}{2} + \alpha\right)}$, look forward to its succeeding point, and the succeeding point of its succeeding point, and so on (always in the limit sense of (5.32)), by looking at the coordinate expressions given by the successive iterates of ρ by P. Observe in Figure 5.7 that on the one hand if $\rho < \rho_{\text{lim}}$, the sequence $\{P^n(\rho)\}_{n \in \mathbb{N}}$ tends strictly monotonically *increasingly* to ρ_{lim} as $n \to \infty$, while on the other hand, if

$\rho > \rho_{\text{lim}}$, the sequence $\{P^n(\rho)\}_{n \in \mathbb{N}}$ tends strictly monotonically *decreasingly* to ρ_{lim} as $n \to \infty$. By contrast, the sequence $\{P^n(\rho_{\text{lim}})\}_{n \in \mathbb{N}}$ takes the constant value ρ_{lim}.

5.6.4. Three qualitatively different cases

Let

$$\mu \triangleq \frac{\mu_2}{\mu_1} e^{\kappa\left(\frac{\pi}{2}+\beta\right)} \tag{5.49}$$

Recall that $\mu_1 = |b - a| = |d - c|$ and $\mu_2 = |c - b| = |a - d|$ are the side lengths of the parallelogram conv $(\{a, b, c, d\})$ and $\kappa = \tan\alpha$.

In Sections 5.7 to 5.9, it will become clear that the restriction of (5.35) to $\left\{a - \xi\frac{\bar{k}}{|k|} \; : \; \xi > P^{-1}(\rho_{\text{min}})\right\}$, where the positive real number ρ_{min} is defined as

$$\rho_{\text{min}} \triangleq \begin{cases} \mu_1 e^{-\kappa\left(\frac{\pi}{2}+2\beta-\alpha\right)} & \text{if } \mu > 1, \\ \left((1-\mu)\exp^{-\kappa\pi} + 1\right)\mu_1 \exp^{-\kappa\left(\frac{\pi}{2}+2\beta-\alpha\right)} & \text{if } \mu \leq 1, \end{cases} \tag{5.50}$$

is actually a *first* return map (in the limit sense of (5.32)) for the progressive time flow of characteristic state-space trajectories, such that for each $\rho > \rho_{\text{min}}$ the curve $\{z_\rho(\tau) \; : \; \tau \in [0.2\pi)\}$ is semi-permeable and free of corners. Accept these facts for the moment and consider the following cases.

If $\rho_{\text{min}} < \rho_{\text{lim}}$, by (5.41), $P^{-1}(\rho_{\text{min}}) < \rho_{\text{min}}$. Hence, $P^{-1}(\rho_{\text{min}}) < \rho_{\text{lim}}$, which means that the point $z_{\rho_{\text{lim}}}(0) = a - \rho_{\text{lim}}\frac{\bar{k}}{|k|}$ belongs to the domain of the aforementioned first return map. In this case, (5.35) restricted to $\left\{a - \xi\frac{\bar{k}}{|k|} \; : \; \xi > P^{-1}(\rho_{\text{min}})\right\}$ acts like a *Poincaré map* for the trajectory through $z_{\rho_{\text{lim}}}(0)$ (which verifies (5.46)) on the *Poincaré section* $\left\{a - \xi\frac{\bar{k}}{|k|} \; : \; \xi > P^{-1}(\rho_{\text{min}})\right\}$.

If $\rho_{\text{min}} > \rho_{\text{lim}}$, by (5.40), $P^{-1}(\rho_{\text{min}}) > \rho_{\text{min}}$. Hence, $\rho_{\text{lim}} < P^{-1}(\rho_{\text{min}})$, which means that the point $z_{\rho_{\text{lim}}}(0) = a - \rho_{\text{lim}}\frac{\bar{k}}{|k|}$ does not belong to the domain of the aforementioned first return map. In this case, even though (5.46) still holds, the characteristic trajectory through $z_{\rho_{\text{lim}}}(0)$ loses its significance.

In connection with the above discussion, in Appendix B.1, the following double implications are proved:

$$\mu > 1 \iff \rho_{\text{min}} > \rho_{\text{lim}}, \tag{5.51}$$
$$\mu < 1 \iff \rho_{\text{min}} < \rho_{\text{lim}}. \tag{5.52}$$

Therefore, obviously

$$\mu = 1 \iff \rho_{\text{min}} = \rho_{\text{lim}}. \tag{5.53}$$

If $\rho_{\text{min}} = \rho_{\text{lim}}$, the curve $\{z_{\rho_{\text{min}}}(\tau) \; : \; \tau \in [0.2\pi)\}$ can be checked to be semi-permeable, though not free of corners.

Chapter 5. The game in distance

5.6.5. Geometric characterization of each case

A careful examination of the family of integral curves (5.31) (obtained by blind integration of the RPE), requires discriminating among the three cases (5.51)–(5.53). This is the matter of Sections 5.7 to 5.9. However, before delving into such examination, let us first characterize *geometrically* each of the three cases: $\mu > 1$, $\mu < 1$, and $\mu = 1$. The following sub-subsections, specially the last one, are devoted to this characterization.

In Figure 5.8 a geometric construction is built for each of the three cases. The points and curves indicated in the figure are introduced next.

5.6.5.1. Semi-permeable curves with a common endpoint at b

Let

$$b_a \triangleq a + e^{(-\kappa+j)\left(\frac{\pi}{2}+\beta\right)} (b-a), \tag{5.54}$$

$$b_c \triangleq c + e^{(+\kappa-j)\left(\frac{\pi}{2}+\beta\right)} (b-c). \tag{5.55}$$

as represented in Figure 5.8. Observe that

$$b_a - b = a - b + e^{(-\kappa+j)\left(\frac{\pi}{2}+\beta\right)} (b-a) = \left(e^{(-\kappa+j)\left(\frac{\pi}{2}+\beta\right)} - 1\right)(b-a),$$

$$b_c - b = c - b + e^{(+\kappa-j)\left(\frac{\pi}{2}+\beta\right)} (b-c) = \left(e^{(+\kappa-j)\left(\frac{\pi}{2}+\beta\right)} - 1\right)(b-c).$$

Hence, $\frac{b_c-b}{b_a-b} = \frac{e^{(+\kappa-j)\left(\frac{\pi}{2}+\beta\right)}-1}{e^{(-\kappa+j)\left(\frac{\pi}{2}+\beta\right)}-1}\frac{b-c}{b-a} = -e^{(\kappa-j)\left(\frac{\pi}{2}+\beta\right)}\frac{b-c}{b-a}$, but since

$$\frac{b-c}{b-a} = \frac{\mu_2 e^{j\left(\frac{3\pi}{2}-\beta\right)}}{\mu_1 e^{-j2\beta}} = -\frac{\mu_2}{\mu_1}e^{j\left(\frac{\pi}{2}+\beta\right)}, \tag{5.56}$$

after operating, the former quotient can be rewritten as

$$\frac{b_c-b}{b_a-b} = \frac{\mu_2}{\mu_1}e^{\kappa\left(\frac{\pi}{2}+\beta\right)} = \mu. \tag{5.57}$$

Therefore, the quotient $\frac{b_c-b}{b_a-b}$ is real and equal to the quantity μ which has to be compared against unity to determine which of the three cases applies. Notice that since $\frac{b_c-b}{b_a-b}$ is real, the points b, b_a and b_c are aligned. As it is apparent in Figure 5.8, the line through b, b_a and b_c separates the following arcs of α-equiangular spirals:

$$\widehat{b,b_a} \triangleq \left\{a + e^{(-\kappa+j)t}(b-a) \ : \ t \in \left(0, \frac{\pi}{2}+\beta\right)\right\}, \tag{5.58}$$

$$\widehat{b,b_c} \triangleq \left\{c + e^{(+\kappa-j)t}(b-c) \ : \ t \in \left(0, \frac{\pi}{2}+\beta\right)\right\}. \tag{5.59}$$

The curves $\widehat{b,b_a}$ and $\widehat{b,b_c}$ are semi-permeable curves which belong to the families $\mathscr{F}_a^-$ and $\mathscr{F}_c^-$, respectively. The endpoints of $\widehat{b,b_a}$ are b and b_a, while the endpoints of $\widehat{b,b_c}$ are b and b_c.

5.6.5.2. Semi-permeable curves with a common endpoint at d

If a is interchanged with c and b is interchanged with d in (5.58)–(5.59), the resulting curves

$$\widehat{d, d_c} \triangleq \left\{ c + \mathrm{e}^{(-\kappa+\mathrm{j})\mathfrak{t}} (d - c) \ : \ \mathfrak{t} \in \left(0, \frac{\pi}{2} + \beta \right) \right\}, \tag{5.60}$$

$$\widehat{d, d_a} \triangleq \left\{ a + \mathrm{e}^{(+\kappa-\mathrm{j})\mathfrak{t}} (d - a) \ : \ \mathfrak{t} \in \left(0, \frac{\pi}{2} + \beta \right) \right\}. \tag{5.61}$$

are also semi-permeable curves, the former belongs to the family $\mathscr{F}_c^-$ and the latter to the family $\mathscr{F}_a^-$. The endpoints of $\widehat{d, d_c}$ are d and d_c, while the endpoints of $\widehat{d, d_a}$ are d and d_a; being d_c and d_a the points that result from interchanging a with c and b with d in the definitions (5.54)–(5.55). Clearly, by construction, $\widehat{d, d_c}$ and $\widehat{b, b_a}$ are symmetric about the centre $\frac{a+c}{2} = \frac{b+d}{2}$ of the parallelogram conv $(\{a, b, c, d\})$. Similarly, $\widehat{d, d_a}$ and $\widehat{b, b_c}$ are symmetric about the same parallelogram's centre.

5.6.5.3. The three qualitative different cases of an homothetic transformation

The two arcs $\widehat{b, b_a}$ and $\widehat{d, d_a}$ belong to the same family $\mathscr{F}_a^-$ of arcs of α-equiangular spirals centred at a. Hence, $\widehat{d, d_a}$ and $\widehat{b, b_a}$ are related by an homothecy with centre at a and scaling factor

$$\frac{d - a}{b_a - a} = \frac{\mu_2 \mathrm{e}^{\mathrm{j}\left(\frac{\pi}{2}-\beta\right)}}{\mathrm{e}^{(-\kappa+\mathrm{j})\left(\frac{\pi}{2}+\beta\right)} (b - a)} = \frac{\mu_2 \mathrm{e}^{\mathrm{j}\left(\frac{\pi}{2}-\beta\right)}}{\mathrm{e}^{(-\kappa+\mathrm{j})\left(\frac{\pi}{2}+\beta\right)} \mu_1 \mathrm{e}^{-\mathrm{j}2\beta}} = \frac{\mu_2}{\mu_1} \mathrm{e}^{\kappa\left(\frac{\pi}{2}+\beta\right)} = \mu$$

equal to (5.57). Accordingly, the homothecy, with centre at a, that transforms $\widehat{b, b_a}$ into $\widehat{d, d_a}$ is a dilation if $\mu > 1$, is a contraction $\mu < 1$, and is an identity transformation if $\mu = 1$ (see Figure 5.8).

5.6.5.4. Six special horizontal tangents

Recall that $k = -\kappa + \mathrm{j}$ and let

$$b_a^* \triangleq \widehat{b, b_a} \cap \left\{ a - \rho \frac{\overline{k}}{|k|} \ : \ \rho > 0 \right\} = a + \mathrm{e}^{k\left(\frac{\pi}{2}+2\beta-\alpha\right)} (b - a),$$

$$d_a^* \triangleq \widehat{d, d_a} \cap \left\{ a - \rho \frac{\overline{k}}{|k|} \ : \ \rho > 0 \right\} = a + \mathrm{e}^{k\left(\frac{\pi}{2}+2\beta-\alpha\right)} (d_a - a),$$

$$d_c^* \triangleq \widehat{d, d_c} \cap \left\{ c + \rho \frac{\overline{k}}{|k|} \ : \ \rho > 0 \right\} = c + \mathrm{e}^{k\left(\frac{\pi}{2}+2\beta-\alpha\right)} (d - c),$$

$$b_c^* \triangleq \widehat{b, b_c} \cap \left\{ c + \rho \frac{\overline{k}}{|k|} \ : \ \rho > 0 \right\} = c + \mathrm{e}^{k\left(\frac{\pi}{2}+2\beta-\alpha\right)} (b_c - c),$$

$$b^* \triangleq \widehat{d_a, d_c} \cap \left\{ b - \rho \frac{\overline{k}}{|k|} \ : \ \rho > 0 \right\} = b + \mathrm{e}^{-k(\alpha-\beta)} (d_c - b),$$

$$d^* \triangleq \widehat{b_c, b_a} \cap \left\{ d + \rho \frac{\overline{k}}{|k|} \ : \ \rho > 0 \right\} = d + \mathrm{e}^{-k(\alpha-\beta)} (b_a - d).$$

Chapter 5. The game in distance

These points are special, because the tangents $k\,(b_a^* - a)$, $k\,(d_a^* - a)$, $k\,(d_c^* - c)$, $k\,(b_c^* - c)$, $k\,(b^* - b)$, and $k\,(d^* - d)$ to the arcs $\widehat{b, b_a}$, $\widehat{d, d_a}$, $\widehat{d, d_c}$, $\widehat{b, b_c}$, $\widehat{d_a, d_c}$, and $\widehat{b_c, b_a}$ at b_a^*, d_a^*, d_c^*, b_c^*, b^*, and d^*, respectively, have zero imaginary part, as it is manifest in Figure 5.8.

5.6.5.5. Each case represented by the shape of a single closed curve

From b_a and b_c definitions it follows that

$$b_a - d = a - d + \mathrm{e}^{(-\kappa+\mathrm{j})\left(\frac{\pi}{2}+\beta\right)}\,(b - a)\,,$$
$$b_c - d = c - d + \mathrm{e}^{(+\kappa-\mathrm{j})\left(\frac{\pi}{2}+\beta\right)}\,(b - c)\,;$$

where, by (5.56), $b - a = -\frac{\mu_1}{\mu_2}\mathrm{e}^{-\mathrm{j}\left(\frac{\pi}{2}+\beta\right)}\,(b - c)$ and $b - c = -\frac{\mu_2}{\mu_1}\mathrm{e}^{\mathrm{j}\left(\frac{\pi}{2}+\beta\right)}\,(b - a)$. Hence,

$$b_a - d = a - d - \mathrm{e}^{-\kappa\left(\frac{\pi}{2}+\beta\right)}\frac{\mu_1}{\mu_2}\,(b - c) = \left(1 - \frac{\mu_1}{\mu_2}\mathrm{e}^{-\kappa\left(\frac{\pi}{2}+\beta\right)}\right)(b - c)\,, \quad (5.62)$$

$$b_c - d = c - d - \mathrm{e}^{+\kappa\left(\frac{\pi}{2}+\beta\right)}\frac{\mu_2}{\mu_1}\,(b - a) = \left(1 - \frac{\mu_2}{\mu_1}\mathrm{e}^{+\kappa\left(\frac{\pi}{2}+\beta\right)}\right)(b - a)\,; \quad (5.63)$$

where it was used that $a - d = b - c$ and $c - d = b - a$. Accordingly,

$$\frac{b_a - d}{b_c - d} = -\frac{\mu_1}{\mu_2}\mathrm{e}^{-\kappa\left(\frac{\pi}{2}+\beta\right)}\frac{b - c}{b - a}\,,$$

where $\frac{b-c}{b-a} = -\frac{\mu_2}{\mu_1}\mathrm{e}^{\mathrm{j}\left(\frac{\pi}{2}+\beta\right)}$ by (5.56). So, $\frac{b_a - d}{b_c - d} = \mathrm{e}^{(-\kappa+\mathrm{j})\left(\frac{\pi}{2}+\beta\right)}$, or equivalently

$$b_a = d + \mathrm{e}^{(-\kappa+\mathrm{j})\left(\frac{\pi}{2}+\beta\right)}\,(b_c - d)\,,$$

i.e., the points b_c and b_a are the endpoints of the α-equiangular spiral

$$\widehat{b_c, b_a} \triangleq \left\{d + \mathrm{e}^{(-\kappa+\mathrm{j})\mathfrak{t}}\,(b_c - d)\ :\ \mathfrak{t} \in \left(0, \frac{\pi}{2}+\beta\right)\right\}.$$

Analogously, it can be shown that the points d_a and d_c are the endpoints of the α-equiangular spiral

$$\widehat{d_a, d_c} \triangleq \left\{b + \mathrm{e}^{(-\kappa+\mathrm{j})\mathfrak{t}}\,(d_a - b)\ :\ \mathfrak{t} \in \left(0, \frac{\pi}{2}+\beta\right)\right\}.$$

Both $\widehat{b_c, b_a}$ and $\widehat{d_a, d_c}$ are represented by dashed lines in Figure 5.8 to point out that they are *not* semi-permeable curves.

The union $\overset{\circ}{b} \triangleq \widehat{b, b_a} \cup \{b\} \cup \widehat{b, b_c} \cup \{b_c\} \cup \widehat{b_c, b_a} \cup \{b_a\}$ is a closed curve in the complex plane whose shape changes qualitatively according to the sign of $\frac{\mu_2}{\mu_1}\mathrm{e}^{\kappa\left(\frac{\pi}{2}+\beta\right)} - 1$. The same may be stated about the closed curve $\overset{\circ}{d} \triangleq \widehat{d, d_c} \cup \{d\} \cup \widehat{d, d_a} \cup \{d_a\} \cup \widehat{d_a, d_c} \cup \{d_c\}$ which, by construction, is symmetric to $\overset{\circ}{b}$ about the centre of the parallelogram $\mathrm{conv}\,(\{a, b, c, d\})$. Note that if $\frac{\mu_2}{\mu_1}\mathrm{e}^{\kappa\left(\frac{\pi}{2}+\beta\right)} = 1$, $\overset{\circ}{b} = \overset{\circ}{d}$.

144

(a) $\frac{\mu_2}{\mu_1}e^{\kappa\left(\frac{\pi}{2}+\beta\right)} > 1$:
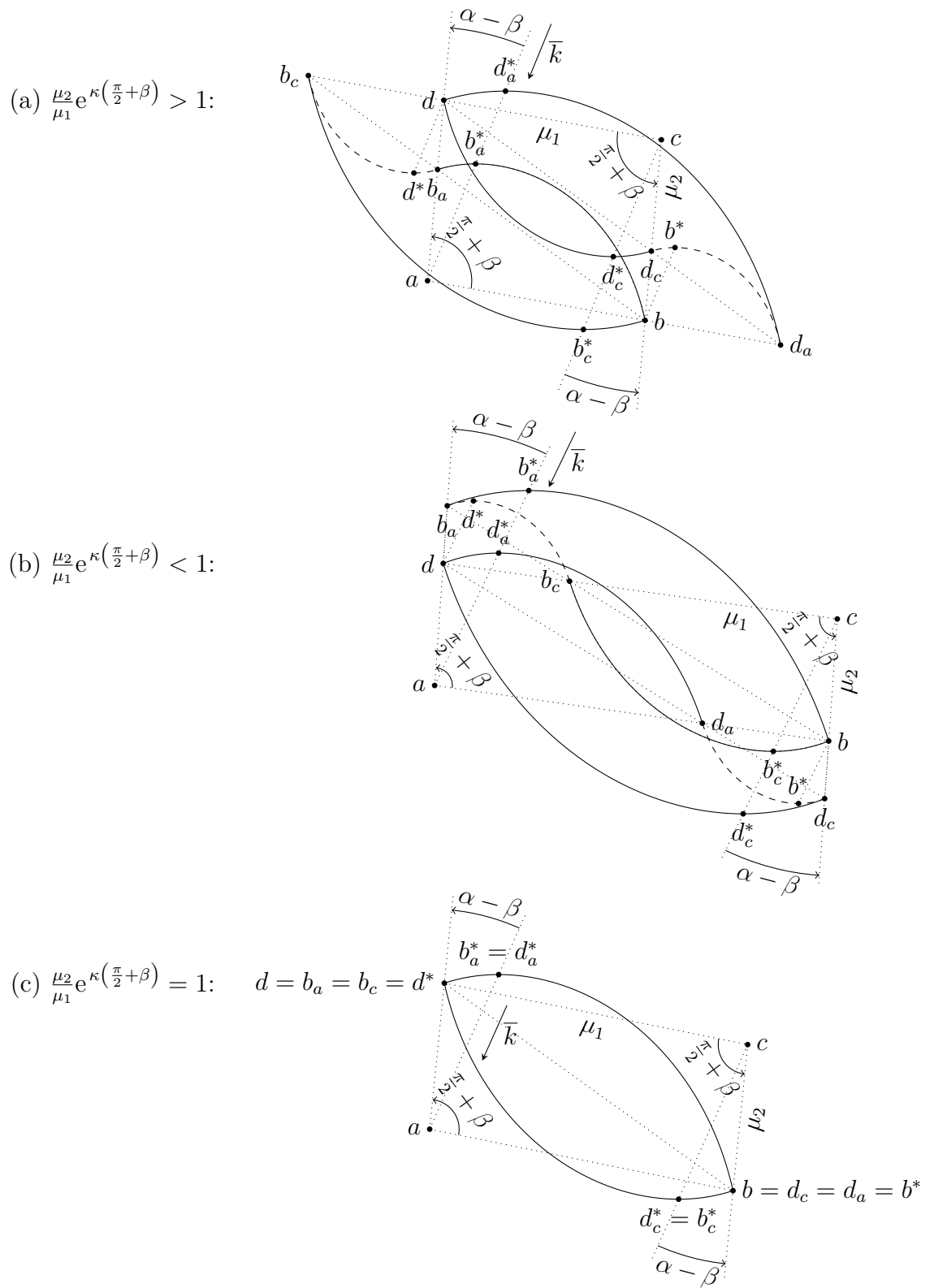
(b) $\frac{\mu_2}{\mu_1}e^{\kappa\left(\frac{\pi}{2}+\beta\right)} < 1$:

(c) $\frac{\mu_2}{\mu_1}e^{\kappa\left(\frac{\pi}{2}+\beta\right)} = 1$:

Figure 5.8: Three qualitatively different cases interpreted geometrically.

145

Accordingly, either $\overset{\circ}{b}$ or $\overset{\circ}{d}$ may be regarded as an *icon* which characterizes which of the three cases applies: either $\frac{\mu_2}{\mu_1}e^{\kappa\left(\frac{\pi}{2}+\beta\right)} > 1$, $\frac{\mu_2}{\mu_1}e^{\kappa\left(\frac{\pi}{2}+\beta\right)} < 1$, or $\frac{\mu_2}{\mu_1}e^{\kappa\left(\frac{\pi}{2}+\beta\right)} = 1$ (see Figure 5.8).

This geometric characterization of the sign of $\mu - 1$ is independent of the sign of β. In Figure 5.8, β is positive for the three illustrated cases, but the qualitative shape of $\overset{\circ}{b}$ and $\overset{\circ}{d}$ does not depend on the sign β but only on the sign of $\mu - 1$.

It will become patent in Sections 5.7 to 5.9 that either $\overset{\circ}{b}$ or $\overset{\circ}{d}$ lies at the geometrical core of the solution of the upward game $\mathcal{G}_{\text{dist}}^+$, depending on the sign of $\mu - 1$. The same may be stated if the game under consideration was the downward game $\mathcal{G}_{\text{dist}}^-$; however, with the roles of $\overset{\circ}{b}$ and $\overset{\circ}{d}$ interchanged. Actually, the rather artificial assumption (5.5) was introduced in this chapter to achieve this desirable reciprocity between $\mathcal{G}_{\text{dist}}^+$ and $\mathcal{G}_{\text{dist}}^-$.

5.7. Solution of the upward game for the case $\mu > 1$

Next, the solution of $\mathcal{G}_{\text{dist}}^+$ is worked out for the case $\mu > 1$. This case is elaborated further than the other two cases ($\mu < 1$, $\mu = 1$) with the intent of serving as an in detail example of the construction methods and arguments that will be recurred in a less detailed manner in Sections 5.8 and 5.9 when dealing with the remaining cases of $\mathcal{G}_{\text{dist}}^+$, and even in Section 5.11 when dealing with the bilateral game $\mathcal{G}_{\text{dist}}$.

5.7.1. The semi-permeable domain

Reconsider the family (5.31) of characteristic state-space trajectories, now parametrized by $\rho > 0$ as formulated by the initial condition (5.26) derived from the ansatz proposed in Section 5.5. In Figure 5.9, twelve characteristic trajectories of the family, which emanate retrogressively in time from the ray $\left\{a - \rho\frac{\overline{k}}{|k|} : \rho > 0\right\}$, are depicted for a case in which $\mu = \frac{\mu_2}{\mu_1}e^{\kappa\left(\frac{\pi}{2}+\beta\right)}$ is greater than one. Nine of them are represented by dashed lines and the other three are represented by continuous lines, for a reason that will be soon explained. The arrows indicate the direction of motion in which retrogressive time τ *decreases*, i.e., progressive time $\mathfrak{t}$ *increases*.

For every $\rho = |z_\rho(0) - a| > 0$, the curve $(0, 2\pi) \ni \tau \mapsto z_\rho(\tau)$ consists of the concatenation, in order as τ increases, of arcs of spirals with centres at a, b, c, d, and a. Each of these arcs belong to one of the eight families of possible semi-permeable curves: either $\mathscr{F}_a^+$, $\mathscr{F}_a^-$, $\mathscr{F}_b^+$, $\mathscr{F}_b^-$, $\mathscr{F}_c^+$, $\mathscr{F}_c^-$, $\mathscr{F}_d^+$, or $\mathscr{F}_d^-$ (see Figure 4.16). However, not every concatenation is valid for the goal of ending up with a semi-permeable curve.

To examine the failure of some of the integral curves to be semi-permeable, consider the first (in retrogressive sense) concatenation which occurs when $\tau = \gamma_1 = \frac{\pi}{2} + 2\beta - \alpha$. At this retro-instant, $z_\rho(\gamma_1) = a + e^{(\kappa - \mathrm{j})\gamma_1}(z_\rho(0) - a) = a + \rho e^{\kappa\gamma_1}\frac{b-a}{|b-a|} = a + \frac{\rho e^{\kappa\gamma_1}}{\mu_1}(b - a)$. If $\frac{\rho e^{\kappa\gamma_1}}{\mu_1} < 1$, blind integration of the RPE asks for concatenating
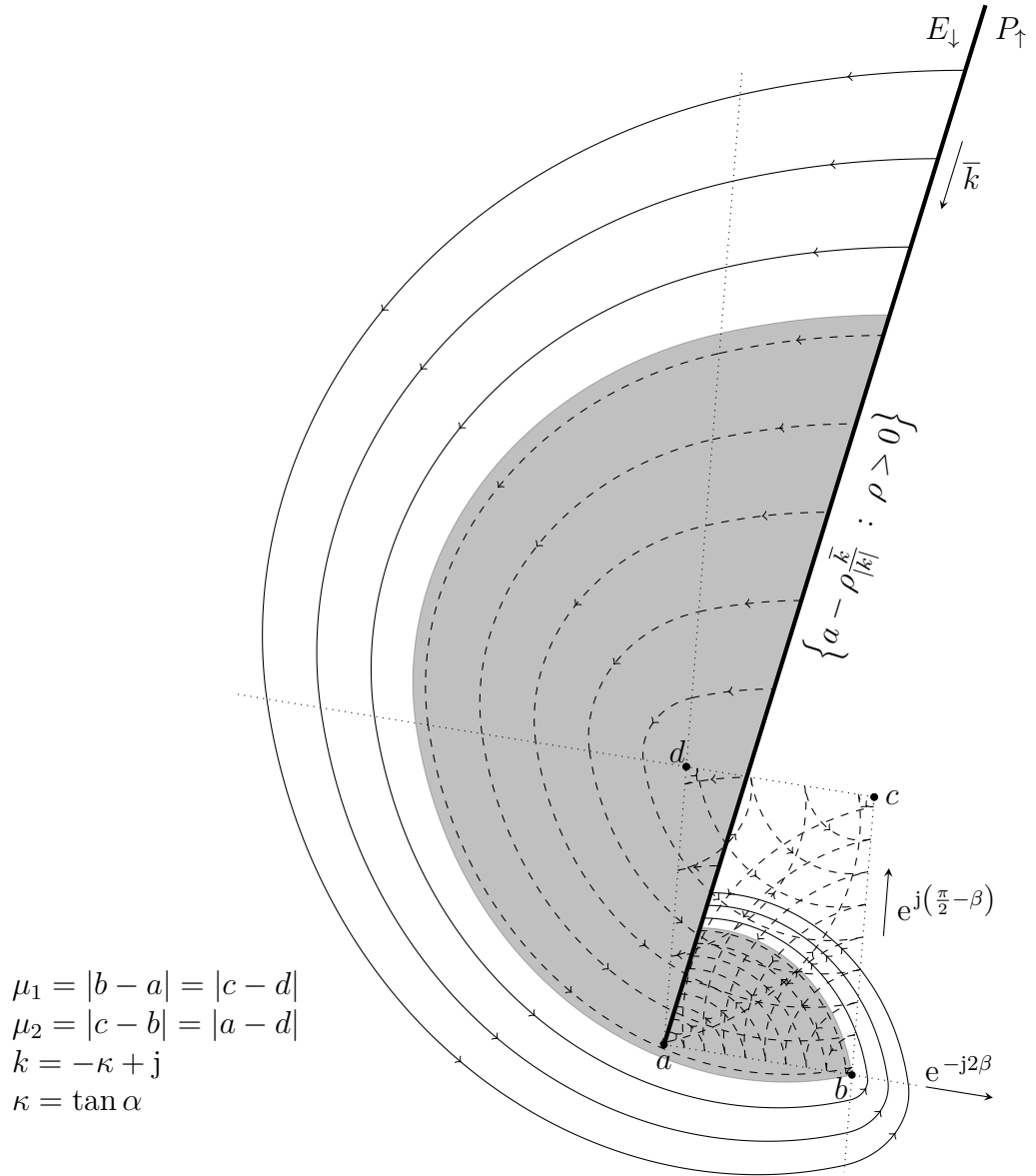
Figure 5.9: Characteristic trajectories of $\mathcal{G}_{\text{dist}}^{+}$, which emanate retrogressively in time from $\left\{ z = a - \rho \frac{\overline{k}}{|k|} \ : \ \rho > 0 \right\}$, as obtained by routine integration of the RPE for the case $\frac{\mu_2}{\mu_1} e^{\kappa \left(\frac{\pi}{2} + \beta \right)} > 1$. Every characteristic trajectory that lies in the interior of set represented by the shaded area fails to be semi-permeable at least at one of its points.

a member of $\mathscr{F}_a^-$ with a member of $\mathscr{F}_b^+$ (see Figure 4.16). As was commented in Subsection 4.5.4, the concatenation of a member of a *negatively* oriented family (named with a superscript $-$) with a member of a *positively* oriented family (named with a superscript $+$) fails to be semi-permeable at the concatenation point. This is the reason why every characteristic trajectory $\tau \mapsto z_\rho(\tau)$ such that $\rho < \mu_1 \mathrm{e}^{-\kappa\gamma_1}$ must be discarded.

The special curve $\{z_{\rho_{\min}}(\tau) \; : \; \tau \in [0, 2\pi)\}$, where $\rho_{\min} = \mu_1 \mathrm{e}^{-\kappa\gamma_1}$ (as defined by (5.50)), has no definite tangent direction at the point b. It includes the semi-permeable arcs $\widehat{b, b_a}$ and $\widehat{b, b_c}$ of the closed curve $\overset{\circ}{b} = \widehat{b, b_a} \cup \{b\} \cup \widehat{b, b_c} \cup \{b_c\} \cup \widehat{b_c, b_a} \cup \{b_a\}$ (introduced in Subsubsection 5.6.5.5 and represented by the dot-dashed line in Figure 5.10). The moving point $z_{\rho_{\min}}(\tau)$ belongs to $\widehat{b, b_a}$ (which is a member of $\mathscr{F}_a^-$) for $\tau \in (0, \gamma_1)$, while it belongs to $\widehat{b, b_c}$ (which is a member of $\mathscr{F}_c^-$) for $\tau \in (\gamma_3, \gamma_4)$. Curiously, however, $z_{\rho_{\min}}(\tau)$ remains stationary at the point b for $\tau \in (\gamma_1, \gamma_2)$. This is clearly suspicious for a time-invariant system, so $z_{\rho_{\min}}([0, 2\pi))$ will be left out of the analysis for the moment. Its role will become clear after studying what happens at both sides of it.

Consider the collection $\{z_\rho([0, 2\pi)) \; : \; \rho > \rho_{\min}\}$ of corner-free curves that covers the set

$$\mathscr{S}^+ \triangleq \bigcup_{\rho > \rho_{\min}} z_\rho([0, 2\pi)).$$

Each curve $(0, 2\pi) \ni \tau \mapsto z_\rho(\tau)$ is unquestionably semi-permeable at each of its points and it consists of concatenations among members of the negatively oriented families: $\mathscr{F}_a^-$, $\mathscr{F}_b^-$, $\mathscr{F}_c^-$, and $\mathscr{F}_d^-$. For this reason, $\mathscr{S}^+$ will be referred to as the *semi-permeable domain* of $\mathcal{G}_{\mathrm{dist}}^+$.

Notice in Figure 5.10 that each curve $\{z_\rho(\tau) \; : \; \tau \in ([0, 2\pi))\}$ such that $\rho > \rho_{\min}$ encloses the closed curve $\overset{\circ}{b}$. This fact prevents the members of the family $\{z_\rho([0, 2\pi)) \; : \; \rho > \rho_{\min}\}$ from intersecting themselves.

Observe that if the selected integration interval had been selected as $[0, \tau_{\max}]$ with $\tau_{\max} \geq 2\pi$, each member of the collection $\{z_\rho([0, \tau_{\max}]) \; : \; \rho > \rho_{\min}\}$ would have intersected another member of the same collection after a full rotation around the origin of its corresponding co-state because, by (5.40), $P^{-1}(\rho) > \rho \iff \rho > \rho_{\mathrm{lim}}$ and $\rho_{\min} > \rho_{\mathrm{lim}}$ for the case $\mu > 1$ as stated in (5.51).

5.7.2. The solution of Isaacs' equation in the semi-permeable domain

The collection $\{z_\rho([0, 2\pi)) \; : \; \rho > \rho_{\min}\}$ provides a solution $\mathcal{V}$ of (5.17)–(5.18) defined on $\mathscr{S}^+$ which will be next given in close form after a verbal explanation of how to compute $\mathcal{V}(z)$ for each $z \in \mathscr{S}^+$.

Consider, for example, the point z represented in Figure 5.10. Imagine a moving point that follows the characteristic trajectory through z, along *decreasing* retro-time τ. The moving point spirals around a, then around d, c, b, and finally around a again, to end at a point z' in $\left\{a - \rho\frac{\overline{k}}{|k|} \; : \; \rho > 0\right\}$. Actually, z

is first transformed by $a + \mathrm{e}^{k\left(\frac{\pi}{2} + \beta - \mathrm{Arg}\,\frac{\cdot - a}{b - a}\right)}\,(\cdot - a)$ to reach the ray $\underrightarrow{ad}$, then by $d + \mathrm{e}^{k\left(\frac{\pi}{2} - \beta\right)}\,(\cdot - d)$ to reach $\underrightarrow{cd}$, then by $c + \mathrm{e}^{k\left(\frac{\pi}{2} + \beta\right)}\,(\cdot - c)$ to reach $\underrightarrow{cb}$, then by $b + \mathrm{e}^{k\left(\frac{\pi}{2} - \beta\right)}\,(\cdot - b)$ to reach $\underrightarrow{ab}$, and finally by $a + \mathrm{e}^{k\left(\frac{\pi}{2} + 2\beta - \alpha\right)}\,(\cdot - a)$ to reach $\left\{a - \rho\frac{\overline{k}}{|k|} \ : \ \rho > 0\right\}$ at z'. The assigned value to $\mathcal{V}(z)$ is $1 - \Im(z')$. Notice that for other points, different from the starting point z of the example, the chain of roto-homotheties may be shorter. It is apparent that the level sets of $\mathcal{V}$ are semi-permeable curves, each of them with an endpoint in $\left\{a - \rho\frac{\overline{k}}{|k|} \ : \ \rho > \rho_{\min}\right\}$.

Each of the roto-homotheties mentioned in the previous example is associated with one the following sets:

$$\mathscr{A}_1 \triangleq \left\{w \in \mathbb{C} \ : \ \mathcal{M}_a^{b-a}(w) > \mu_1 \ \wedge \ \mathcal{A}_a^{b-a}(w) \in [0, \gamma_1]\right\},$$
$$\mathscr{A}_2 \triangleq \left\{w \in \mathbb{C} \ : \ \mathcal{M}_b^{b-c}(w) > 0 \ \wedge \ \mathcal{A}_b^{b-c}(w) \in [0, \gamma_2]\right\},$$
$$\mathscr{A}_3 \triangleq \left\{w \in \mathbb{C} \ : \ \mathcal{M}_c^{d-c}(w) > \mu_2 \mathrm{e}^{\kappa\gamma_3} \ \wedge \ \mathcal{A}_c^{d-c}(w) \in [0, \gamma_3)\right\},$$
$$\mathscr{A}_4 \triangleq \left\{w \in \mathbb{C} \ : \ \mathcal{M}_d^{d-a}(w) > (\mu_2 \mathrm{e}^{\kappa\gamma_3} - \mu_1)\mathrm{e}^{\kappa\gamma_4} \ \wedge \ \mathcal{A}_d^{d-a}(w) \in [0, \gamma_4)\right\},$$
$$\mathscr{A}_5 \triangleq \left\{w \in \mathbb{C} \ : \ \mathcal{M}_a^{b-a}(w) > ((\mu_2 \mathrm{e}^{\kappa\gamma_3} - \mu_1)\mathrm{e}^{\kappa\gamma_4} + \mu_2)\mathrm{e}^{\kappa\gamma_3} \ \wedge \ \mathcal{A}_a^{b-a}(w) \in (\gamma_1, \gamma_3)\right\};$$

where the angles $\gamma_1, \ldots, \gamma_4$ are defined, in terms of α and β, as indicated in Figure 5.5, and the functions $\mathcal{A}_o^v : \mathbb{C}\backslash\{o\} \to (-\pi, \pi]$ and $\mathcal{M}_o^v : \mathbb{C} \to [0, \infty)$, parametric on $o, v \in \mathbb{C}$ such that $v \neq 0$, are the ones introduced in Subsubsections 4.2.2.2 and 4.2.2.3. The collection $\{\mathscr{A}_1, \ldots, \mathscr{A}_5\}$ is a partition of $\mathscr{S}^+$, because:

$$\mathscr{S}^+ = \bigcup_{i \in \{1, \ldots, 5\}} \mathscr{A}_i \quad \text{and} \quad \mathscr{A}_i \cap \mathscr{A}_j = \emptyset \text{ for } i \neq j.$$

For every $z \in \mathscr{S}^+$, the functional value of $\mathcal{V}$ at z is given by

$$\mathcal{V}(z) \triangleq \begin{cases} 1 - \Im\left(\mathcal{R}_a^{\gamma_1 - \mathcal{A}_a^{b-a}(z)}(z)\right) & \text{if } z \in \mathscr{A}_1, \\[2mm] 1 - \Im\left(\mathcal{R}_a^{\gamma_1} \circ \mathcal{R}_b^{\gamma_2 - \mathcal{A}_b^{b-c}(z)}(z)\right) & \text{if } z \in \mathscr{A}_2, \\[2mm] 1 - \Im\left(\mathcal{R}_a^{\gamma_1} \circ \mathcal{R}_b^{\gamma_2} \circ \mathcal{R}_c^{\gamma_3 - \mathcal{A}_c^{d-c}(z)}(z)\right) & \text{if } z \in \mathscr{A}_3, \\[2mm] 1 - \Im\left(\mathcal{R}_a^{\gamma_1} \circ \mathcal{R}_b^{\gamma_2} \circ \mathcal{R}_c^{\gamma_3} \circ \mathcal{R}_d^{\gamma_4 - \mathcal{A}_d^{d-a}(z)}(z)\right) & \text{if } z \in \mathscr{A}_4, \\[2mm] 1 - \Im\left(\mathcal{R}_a^{\gamma_1} \circ \mathcal{R}_b^{\gamma_2} \circ \mathcal{R}_c^{\gamma_3} \circ \mathcal{R}_d^{\gamma_4} \circ \mathcal{R}_a^{\gamma_3 - \mathcal{A}_a^{b-a}(z)}(z)\right) & \text{if } z \in \mathscr{A}_5, \end{cases}$$

where $\mathcal{R}_q^\theta : \mathbb{C} \to \mathbb{C}$ is a roto-homothety, of centre $q \in \mathbb{C}$ and angle $\theta \in \mathbb{R}$, given by

$$\mathcal{R}_q^\theta(z) \triangleq q + \mathrm{e}^{k\theta}(z - q),$$

where $k = -\kappa + \mathrm{j}$, being $\kappa = \tan \alpha$.

The function $\mathcal{V} : \mathscr{S}^+ \to \mathbb{R}$ just described is real differentiable in $\mathscr{S}^+$, so it conveys recommended strategies defined in $\mathscr{S}^+$ for both players, namely:

$$z \mapsto \tilde{u}_\mathcal{V}^*(z) \triangleq u^*(\nabla\mathcal{V}(z)), \tag{5.64}$$
$$z \mapsto \tilde{\sigma}_\mathcal{V}^*(z) \triangleq \sigma^*(\nabla\mathcal{V}(z)), \tag{5.65}$$
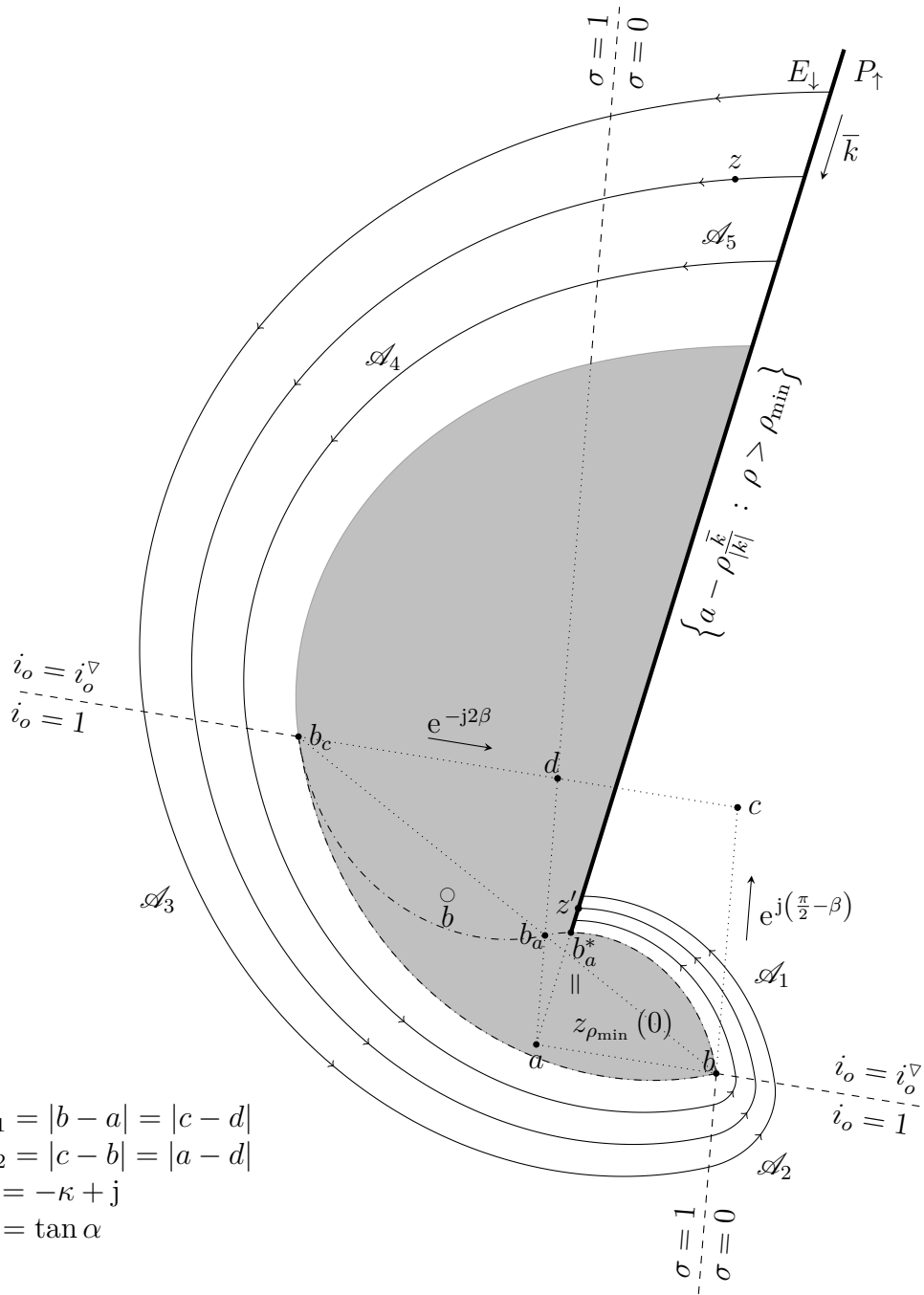
Figure 5.10: Semi-permeable characteristic trajectories of $\mathcal{G}^+_{\mathrm{dist}}$ for the case $\frac{\mu_2}{\mu_1}\mathrm{e}^{\kappa\left(\frac{\pi}{2}+\beta\right)} > 1$. The shape of the closed curve indicated by the dot-dashed line characterizes this case. The dashed rays are switching curves.

provided that it is understood that $\nabla \mathcal{V}(z_\rho(0)) \triangleq \lim_{\tau \to 0^+} \nabla \mathcal{V}(z_\rho(\tau))$, for every $\rho > \rho_{\min}$ (notice that $\mathcal{V}$ is discontinuous at $z_\rho(0)$ for every $\rho > \rho_{\min}$). Recall that the functions $u^* : \mathbb{C} \to U$ and $\sigma^* : \mathbb{C} \to \Sigma$ evaluated in (5.64)–(5.65) are the functions introduced in statement 2 of Proposition 4.4.1.

Note that, by the essence of the method of characteristics, the recommended strategies $\tilde{u}_\mathcal{V}^*$ and $\tilde{\sigma}_\mathcal{V}^*$ could have been defined in an equivalent way to (5.64)–(5.65) as follows: for each $z \in \mathscr{S}^+$, find ρ and τ such that $z = z_\rho(\tau)$ and let

$$z \mapsto \tilde{u}_\mathcal{V}^*(z) \triangleq u^*(p(\tau)),$$
$$z \mapsto \tilde{\sigma}_\mathcal{V}^*(z) \triangleq \sigma^*(p(\tau)).$$

The dashed rays in Figure 5.10 indicate the *switching* rays that result from (5.64)–(5.65). Each of these switching rays lies in one of the following common boundaries: either $(\partial \mathscr{A}_1) \cap (\partial \mathscr{A}_2)$, $(\partial \mathscr{A}_2) \cap (\partial \mathscr{A}_3)$, $(\partial \mathscr{A}_3) \cap (\partial \mathscr{A}_4)$, or $(\partial \mathscr{A}_4) \cap (\partial \mathscr{A}_5)$.

5.7.3. The pursuer's counter-clockwise circulation power in the semi-permeable domain

It will be argued next that for every initial state in $\mathscr{S}^+$ the strategy $\tilde{u}_\mathcal{V}^*$ recommended for P as specified before, generates state-space motions such that the state remains in $\mathscr{S}^+$ until (sooner or later) it reaches $\left\{a - \rho \frac{\bar{k}}{|k|} : \rho > \rho_{\min}\right\}$ from half-plane $P_\uparrow$, regardless of the strategy adopted by E. The argument relies on the repeated application of Corollary 4.3.1, followed by the application of Propositions 4.3.1 and 4.3.2.

Take an arbitrary initial state z_5 in $\mathscr{A}_5$ (see Figure 5.11). As long as the state remains in $\mathscr{A}_5$, P's strategy (5.64) mandates $u(\mathsf{t}) = i_o^\triangledown + \mathsf{j}$. Hence, the compound control $Q(\mathsf{t}) = \mathsf{q}(u(\mathsf{t}), \sigma(\mathsf{t})) = \mathsf{q}(i_o^\triangledown + \mathsf{j}, \sigma(\mathsf{t}))$ belongs to the segment $\underline{da}$. Applying Corollary 4.3.1, with $z_0 = z_5$, $q_1 = d$, $q_2 = a$, and $\theta = 0$, it can be inferred that the state must reach the line $\overleftrightarrow{da}$ in finite time and E can do nothing to prevent this from happening. Moreover, as the state approaches the line $\overleftrightarrow{da}$, it remains in the set $\mathscr{K}_{d,a}^0(z_5)$ (as defined in Corollary 4.3.1) represented by the thin shaded area that emanates from z_5 in Figure 5.11. This assures that the state does not abandon $\mathscr{S}^+$ during its approach to $\overleftrightarrow{da}$, whatever E does. Furthermore, since Corollary 4.3.1 also states that $\mathscr{K}_{d,a}^0(z_5) \backslash \{z_5\} \subset \{z \in \mathbb{C} : (z_5 - a) \otimes (z - a) > 0\}$, the state must remain in the half-plane $\{z \in \mathbb{C} : (z_5 - a) \otimes (z - a) > 0\}$ during its approach to $\overleftrightarrow{da}$; thus, E cannot direct the state towards $\left\{a - \rho \frac{\bar{k}}{|k|} : \rho > \rho_{\min}\right\}$ as it moves in $\mathscr{A}_5$. The condition $\mathscr{K}_{d,a}^0(z_5) \cap \mathscr{C}_{d,a} = \emptyset$, required by Corollary 4.3.1, can be checked to be fulfilled. In fact, it follows from Remark 3, after verifying that $\mathcal{M}_a^{d-a}(z_5) > |d - a|$ for every $z_5 \in \mathscr{A}_5$.

While the state moves in $\mathscr{K}_{d,a}^0(z_5)$ towards $\overleftrightarrow{da}$, E is recommended to apply $\sigma(\mathsf{t}) = 0$ in order to prevent the state from crossing the semi-permeable characteristic trajectories in the *outward* direction. Once the state reaches a point $z_5{}'$ in $\overleftrightarrow{da} \cap \mathscr{K}_{d,a}^0(z_5)$, E is recommended to switch from $\sigma = 0$ to $\sigma = 1$. Regardless of whether he follows this recommendation or not, at $z_5{}'$, he must select a velocity vector from the set $\{k(z_5{}' - q) : q \in \underline{ad}\}$. *All* of these vectors, based at $z_5{}'$ point into
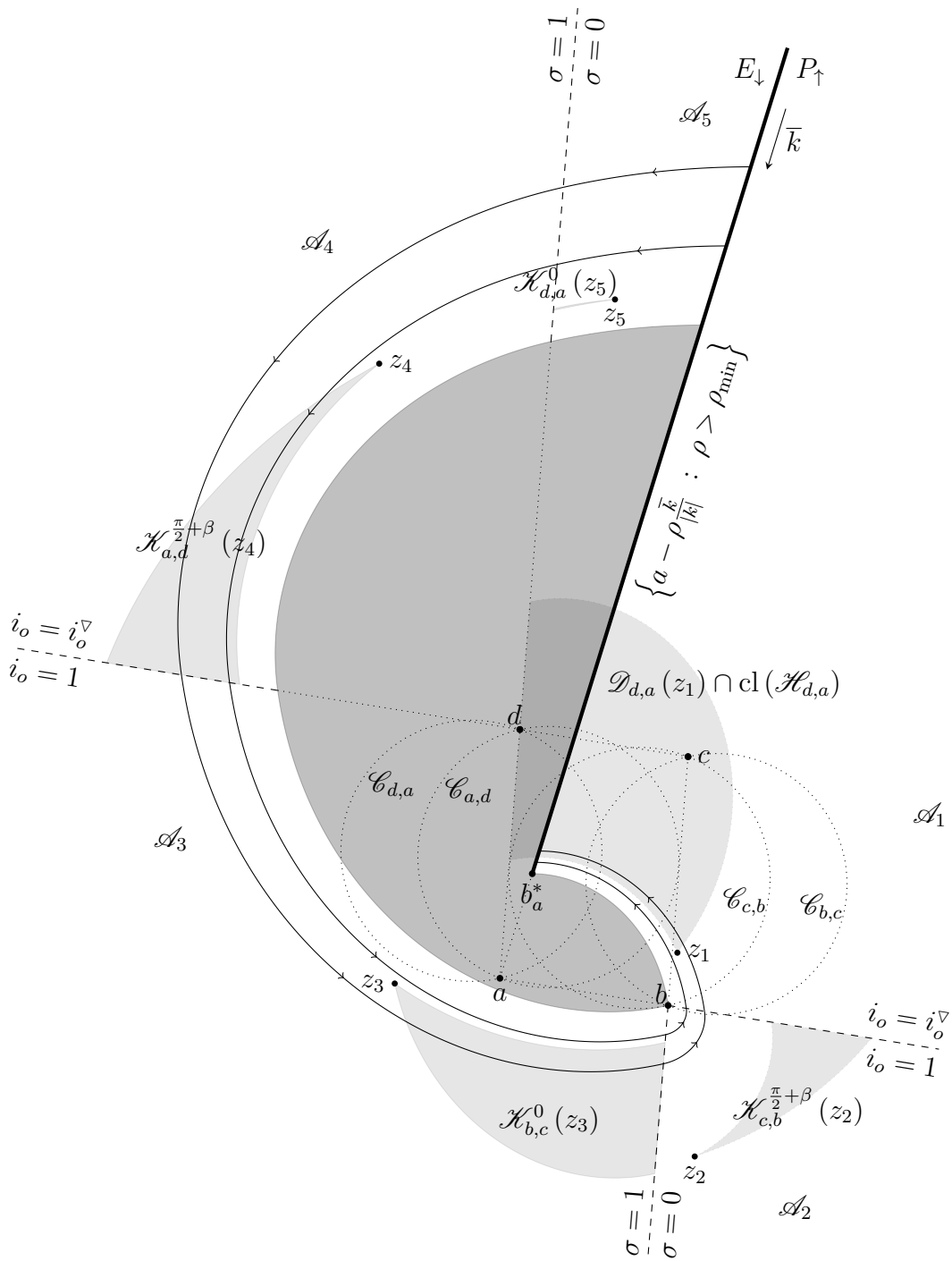
Figure 5.11: The pursuer's counter-clockwise circulation power in the semi-permeable domain $\mathscr{S}^+ = \bigcup_{\rho > \rho_{\min}} z_\rho\left([0, 2\pi)\right) = \bigcup_{i \in \{1, ..., 5\}} \mathscr{A}_i$.

$\mathscr{A}_4$, so E cannot prevent the state from continuing into $\mathscr{A}_4$. This last statement relies on the fact that $z_5' \in \left\{ \mathcal{R}_d^{-\left(\frac{\pi}{2}-\beta\right)}(b_c) + \xi e^{j\left(\frac{\pi}{2}-\beta\right)} \ : \ \xi > 0 \right\}$ and $\mathcal{R}_d^{-\left(\frac{\pi}{2}-\beta\right)}(b_c) = d + e^{-k\left(\frac{\pi}{2}-\beta\right)}(b_c - d)$ necessarily belongs to the ray $\left\{ d + \xi e^{j\left(\frac{\pi}{2}-\beta\right)} \ : \ \xi > 0 \right\}$, because b_c lies in $\left\{ d - \xi e^{j2\beta} \ : \ \xi > 0 \right\}$ (as can be verified looking at (5.63) and recalling that $b - a = -(d - c)$ and $\frac{\mu_2}{\mu_1} e^{\kappa\left(\frac{\pi}{2}+\beta\right)} > 1$).

For an initial state z_4 in $\mathscr{A}_4$, which could be a visited state of a play initiated in $\mathscr{A}_5 \cup ((\partial\mathscr{A}_5) \cap (\partial\mathscr{A}_4))$ or the starting point of another play, P's strategy still mandates the same control $u(\mathrm{t}) = i_o^\triangledown + \mathrm{j}$, as in $\mathscr{A}_5$. Hence, the compound control $Q(\mathrm{t}) = \mathsf{q}(u(\mathrm{t}), \sigma(\mathrm{t})) = \mathsf{q}(i_o^\triangledown + \mathrm{j}, \sigma(\mathrm{t}))$ still belongs to the segment $\underline{ad}$. Applying Corollary 4.3.1 again, but now with $z_0 = z_4$, $q_1 = a$, $q_2 = d$, and $\theta = \frac{\pi}{2} + \beta$, it can be inferred that the state must reach the line $\overleftrightarrow{cd}$ in finite time and E can do nothing to prevent this from happening. Moreover, as the state approaches the line $\overleftrightarrow{cd}$, it remains in the set $\mathscr{K}_{a,d}^{\frac{\pi}{2}+\beta}(z_4)$ (as defined in Corollary 4.3.1) represented by the shaded area that emanates from z_4 in Figure 5.11. This assures that that the state does not abandon $\mathscr{S}^+$ during its approach to $\overleftrightarrow{cd}$. Furthermore, since Corollary 4.3.1 also states that $\mathscr{K}_{a,d}^{\frac{\pi}{2}+\beta}(z_4) \setminus \{z_4\} \subset \{z \in \mathbb{C} \ : \ (z_4 - d) \otimes (z - d) > 0\}$, the state must remain in the half-plane $\{z \in \mathbb{C} \ : \ (z_4 - d) \otimes (z - d) > 0\}$ during its approach to $\overleftrightarrow{cd}$; thus, E cannot direct the state to $(\partial\mathscr{A}_4) \cap (\partial\mathscr{A}_5)$ as it moves in $\mathscr{A}_4$. The condition $\mathscr{K}_{a,d}^{\frac{\pi}{2}+\beta}(z_4) \cap \mathscr{C}_{a,d} = \emptyset$, required by Corollary 4.3.1, can be checked to be fulfilled recalling Remark 3 and verifying that $\mathcal{M}_d^{a-d}(z_4) > |a - d|$ for every $z_4 \in \mathscr{A}_4$.

Take an initial state z_3 that belongs to $((\partial\mathscr{A}_4) \cap (\partial\mathscr{A}_3)) \cup \mathscr{A}_3$. As before, this state may be the starting point of a play, or a visited state of a play initiated somewhere in $\mathscr{A}_5 \cup ((\partial\mathscr{A}_5) \cap (\partial\mathscr{A}_4)) \cup \mathscr{A}_4 \cup ((\partial\mathscr{A}_4) \cap (\partial\mathscr{A}_3))$. Applying Corollary 4.3.1, with $z_0 = z_3$, $q_1 = b$, $q_2 = c$, and $\theta = 0$, it can be inferred that the state must reach the line $\overleftrightarrow{bc}$ in finite time and E can do nothing to prevent this from happening. Moreover, as the state approaches the line $\overleftrightarrow{bc}$, it remains in the set $\mathscr{K}_{b,c}^0(z_3)$ (as defined in Corollary 4.3.1) represented by the shaded area that emanates from z_3 in Figure 5.11. This assures that the state does not abandon $\mathscr{S}^+$ during its approach to $\overleftrightarrow{bc}$, whatever E does. Furthermore, since Corollary 4.3.1 also states that $\mathscr{K}_{b,c}^0(z_3) \setminus \{z_3\} \subset \{z \in \mathbb{C} \ : \ (z_3 - c) \otimes (z - c) > 0\}$, the state must remain in the half-plane $\{z \in \mathbb{C} \ : \ (z_3 - c) \otimes (z - c) > 0\}$ during its approach to $\overleftrightarrow{bc}$; thus, E cannot direct the state back into $\mathscr{A}_4$ as it moves in $\mathscr{A}_3$. Once again, the condition $\mathscr{K}_{b,c}^0(z_3) \cap \mathscr{C}_{b,c} = \emptyset$, required by Corollary 4.3.1, can be checked to be fulfilled recalling Remark 3 and verifying that $\mathcal{M}_c^{b-c}(z_3) > |b - c|$ for every $z_3 \in ((\partial\mathscr{A}_4) \cap (\partial\mathscr{A}_3)) \cup \mathscr{A}_3$.

While the state moves in $\mathscr{K}_{b,c}^0(z_3)$ towards $\overleftrightarrow{bc}$, E is recommended to apply $\sigma(\mathrm{t}) = 1$ in order to prevent the state from crossing the semi-permeable characteristic trajectories in the *outward* direction. Once the state reaches a point z_3' in $\overleftrightarrow{bc} \cap \mathscr{K}_{b,c}^0(z_3)$, E is recommended to switch from $\sigma = 1$ to $\sigma = 0$. Regardless of whether he follows this recommendation or not, at z_3', he must select a velocity vector from the set $\{k(z_3' - q) \ : \ q \in \underline{bc}\}$. Clearly, *all* of these vectors, based at

$z_3{}'$ point into $\mathscr{A}_2$, so E cannot prevent the state from continuing into $\mathscr{A}_2$.

An argumentation along similar lines as the ones applied to the initial state in $\mathscr{A}_4$ may be applied to an initial state $z_2 \in \mathscr{A}_2$, to infer that the state must move in $\mathscr{K}_{c,b}^{\frac{\pi}{2}+\beta}(z_2)$ while it approaches and finally reaches the line $\overleftrightarrow{ab}$.

At last, take an initial state $z_1 \in ((\partial\mathscr{A}_2) \cap (\partial\mathscr{A}_1)) \cup \mathscr{A}_1$. If $z_1 \in (\partial\mathscr{A}_2) \cap (\partial\mathscr{A}_1)$, Corollary 4.3.1 can be applied, as it was applied for the initial state z_3, but now *only* to show that the state cannot move back into $\mathscr{A}_2$, and to do so θ must be taken as $\theta = \frac{\pi}{2} + \beta - \epsilon$, with $\epsilon > 0$ sufficiently small, in order to comply with the condition $\mathscr{K}_{d,a}^{\theta}(z_1) \cap \mathscr{C}_{d,a} = \emptyset$. For $z_1 \in ((\partial\mathscr{A}_2) \cap (\partial\mathscr{A}_1)) \cup \mathscr{A}_1$, Corollary 4.3.1 *cannot* be applied as it was applied for the initial condition z_5, because with $\theta = 0$ the condition $\mathscr{K}_{d,a}^{\theta}(z_1) \cap \mathscr{C}_{d,a} = \emptyset$ does not hold for every $z_1 \in ((\partial\mathscr{A}_2) \cap (\partial\mathscr{A}_1)) \cup \mathscr{A}_1$. However, Propositions 4.3.1 and 4.3.2 *can* be applied. Applying Proposition 4.3.1 with $z_0 = z_1$, $q_1 = d$, and $q_2 = a$, it can be proved that the state must come arbitrarily close to the line $\overleftrightarrow{ad}$ in finite time (not necessarily reaching it). In addition, by Proposition 4.3.2, as long as the state remains in $\mathrm{cl}\,(\mathscr{H}_{d,a})$, it must remain in the set $\mathscr{D}_{d,a}(z_1)$ (as defined in Proposition 4.3.2). The set $\mathscr{D}_{d,a}(z_1) \cap \mathrm{cl}\,(\mathscr{H}_{d,a})$ is represented by the shaded area that emanates from z_1 in Figure 5.11. Thus, the state, along its way to $\overleftrightarrow{ad}$, must necessarily *reach* the ray $\left\{a - \rho\frac{\overline{k}}{|k|} \ : \ \rho > \rho_{\min}\right\}$ in finite time.

Observe that, along the motions previously described the state can only cross the semi-permeable curves of the collection $\{z_\rho([0,2\pi)) \ : \ \rho > \rho_{\min}\}$ in the direction preferred by P, i.e., in the *outward* direction that results in higher imaginary part of the state when it inevitably reaches the ray $\left\{a - \rho\frac{\overline{k}}{|k|} \ : \ \rho > \rho_{\min}\right\}$ from $P_\uparrow$. This is because P sticks to the strategy (5.64) recommended for him, derived from the semi-permeable characteristic trajectories. The best that E can do in order to minimize the imaginary part of the state when it reaches $\left\{a - \rho\frac{\overline{k}}{|k|} \ : \ \rho > \rho_{\min}\right\}$ is to stick to the strategy (5.65) recommended for him, also derived from the semi-permeable characteristic trajectories. Only if P temporary abandons the strategy (5.64), can E force the state to cross the semi-permeable characteristic trajectories in the *inward* direction preferred by him.

In conclusion, for every initial state z_0 in $\mathscr{S}^+$, P can force the state to circulate counter-clock-wisely in $\mathscr{S}^+$ while preventing it from crossing the semi-permeable curves in the inward direction, so as to make it reach the ray $\left\{a - \rho\frac{\overline{k}}{|k|} \ : \ \rho > \rho_{\min}\right\}$, from half-plane $P_\uparrow$, at an oriented distance to $\mathscr{T}^+$ that is equal or less than $\mathcal{V}(z_0)$. If $\mathrm{d}_{\mathrm{o}}(z_0, \mathscr{T}^+) > \mathcal{V}(z_0)$ the use of such circulation power will clearly benefit him, while if $\mathrm{d}_{\mathrm{o}}(z_0, \mathscr{T}^+) \leq \mathcal{V}(z_0)$ he will not reduce the initial oriented distance to $\mathscr{T}^+$ by making use of such power.

5.7.4. The island not covered by semi-permeable corner-free characteristic state-space trajectories

The set $\mathscr{S}^+ = \bigcup_{\rho > \rho_{\min}} z_\rho \left([0, 2\pi) \right)$ covered by semi-permeable characteristic trajectories has a non-empty complement

$$\mathscr{I}^+ \triangleq \mathbb{C} \setminus \mathscr{S}^+$$

which will be referred to as the *island* of $\mathcal{G}_{\mathrm{dist}}^+$. In Figure 5.10, the set $\mathscr{I}^+$ corresponds to the union of the interior of the shaded area and the curve $z_{\rho_{\min}} \left([0, 2\pi) \right)$ which is included in the boundary of $\mathscr{S}^+$. In fact, $\mathscr{I}^+$ can be partitioned as:

$$\mathscr{I}^+ = \mathrm{int} \left(\mathscr{I}^+ \right) \cup z_{\rho_{\min}} \left([0, 2\pi) \right) \quad \text{being} \quad \mathrm{int} \left(\mathscr{I}^+ \right) \cap z_{\rho_{\min}} \left([0, 2\pi) \right) = \emptyset.$$

Observe that the special point b is the unique corner of $\{ z_{\rho_{\min}} (\tau) \; : \; \tau \in (0, 2\pi) \}$. Moreover, by construction of $\mathscr{S}^+$, the point b does not belong to $\mathscr{S}^+$. However, every other point of the line $\overleftrightarrow{bc}$, that belongs to a sufficiently small neighbourhood of b, *is* a member of $\mathscr{S}^+$. This may be checked comparing the directions of the lateral tangents $k \left(b - a \right) = -\lim_{\tau \to \tau_1^-} z_{\rho_{\min}} (\tau)$ and $-k \left(b - c \right) = \lim_{\tau \to \tau_2^+} z_{\rho_{\min}} (\tau)$ with respect to the direction $\mathrm{e}^{\mathrm{j} \left(\frac{\pi}{2} - \beta \right)}$ of the line $\overleftrightarrow{bc}$ as follows:

$$\mathrm{e}^{\mathrm{j} \left(\frac{\pi}{2} - \beta \right)} \otimes \left(k \left(b - a \right) \right) = \mu_1 \sec \alpha \sin \left(\alpha - \beta \right) > 0,$$
$$\mathrm{e}^{\mathrm{j} \left(\frac{\pi}{2} - \beta \right)} \otimes \left(-k \left(b - c \right) \right) = \mu_2 \sec \alpha \cos \alpha \qquad > 0,$$

where the inequalities result from $0 < \alpha < \frac{\pi}{2}$ and $|\beta| < \alpha$, as assured by (5.1).

5.7.5. The pursuer's pull-back manoeuvre

Recall that at $b_a^* = z_{\rho_{\min}} (0)$, the direction of the lateral tangent $k \left(b_a^* - a \right) = -\lim_{\tau \to 0^+} z_{\rho_{\min}} (\tau)$ is horizontal because $k \left(b_a^* - a \right) = 0$.

Consider an arbitrary initial state $z \in \mathrm{int} \left(\mathscr{I}^+ \right)$ such that $\Im z \leq \Im b_a^*$ (as represented in Figure 5.12) and suppose that P maintains $u \left(\mathsf{t} \right) = i_o + \mathsf{j}$ constant, where $i_o = 1$. This insistence by P, forces the compound input $Q \left(\mathsf{t} \right) = \mathsf{q} \left(u \left(\mathsf{t} \right), \sigma \left(\mathsf{t} \right) \right)$ to belong to the segment $\underline{bc}$. Otherwise stated, E is forced to select the instantaneous centre of the α-equiangular state-guiding spiral through the current state from the set of points that lie in the segment $\underline{bc}$. It follows logically from Proposition 4.3.1 (taking $q_1 = b$, $q_2 = c$, and $z_0 = z$) that the state must come arbitrarily close to the line $\overleftrightarrow{bc}$ in finite time. Therefore, if E manages to prevent the state from entering into $\{ w \; : \; \Im w > \Im b_a^* \} \cup \mathrm{cl} \left(\mathscr{S}^+ \right)$, the state must necessarily come arbitrarily close to b in finite time. This is true without any kind of limitation imposed on E. If E happens to be limited by a positive dwell time between consecutive switchings, as explained in Subsubsection 4.3.6.7 where E's control set $\Sigma = [0, 1]$ was temporarily supposed to be replaced by $\{0, 1\}$, he cannot prevent the state from reaching the line $\overleftrightarrow{bc}$ in finite time (as it follows from the application of Proposition 4.3.4 taking $q_1 = b$, $q_2 = c$, and $z_0 = z$) and therefore reaching either $\mathrm{cl} \left(\mathscr{S}^+ \right)$ or $\{ w \; : \; \Im w > \Im b_a^* \}$.
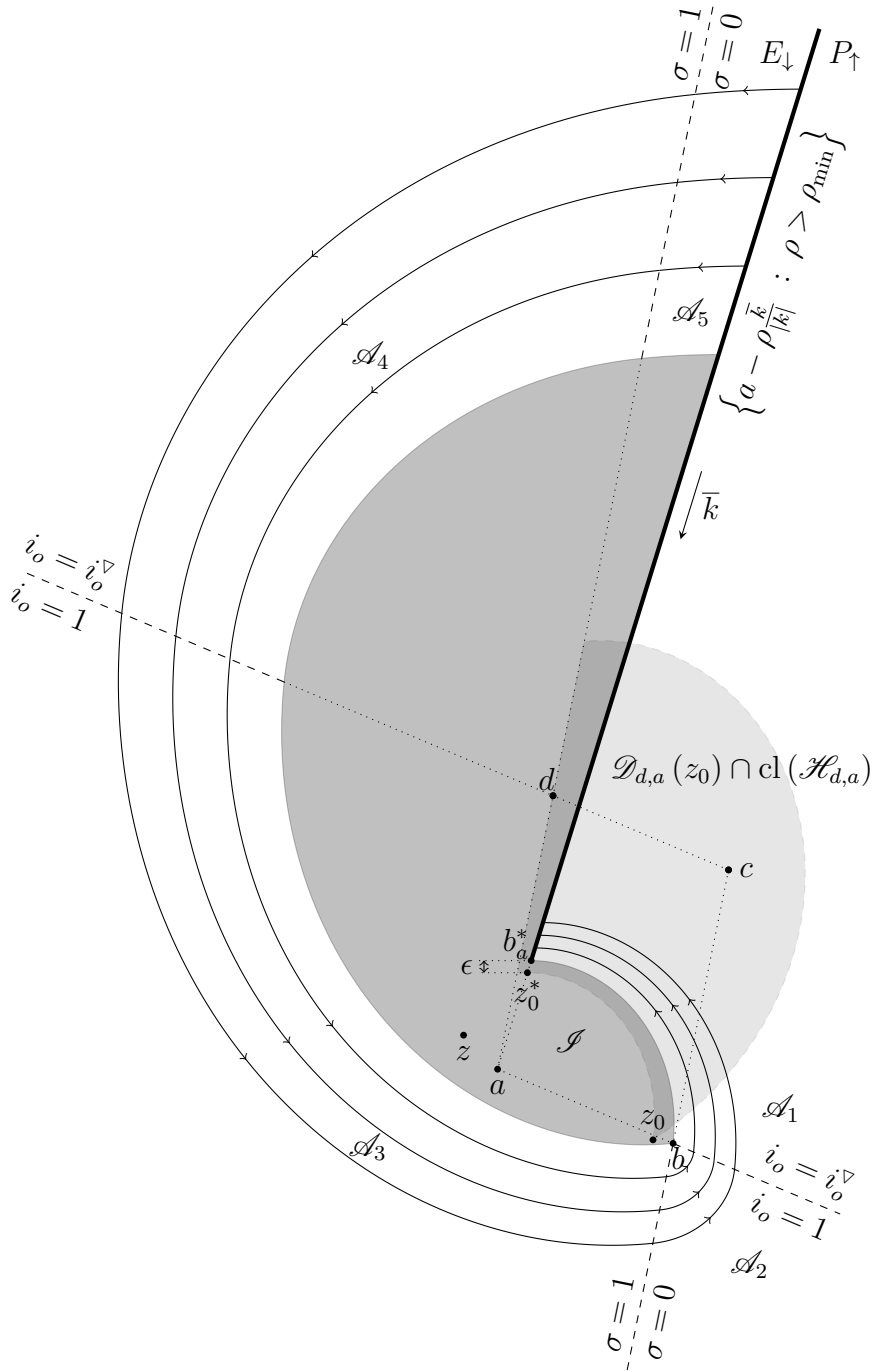
Figure 5.12: The set called island is defined as $\mathscr{I}^+ = \mathscr{S}^{+\complement}$, i.e., as the complement of the semi-permeable domain $\mathscr{S}^+ = \bigcup_{\rho > \rho_{\min}} z_\rho([0, 2\pi)) = \bigcup_{i \in \{1,\dots,5\}} \mathscr{A}_i$. The point $b_a^* = z_{\rho_{\min}}(0)$ has an oriented distance to $\mathscr{T}^+$ equal to $1 - \Im b_a^*$. For plays that initiate in $\mathrm{int}(\mathscr{I}^+) \cap \{w : \Im w \le \Im z_b^*\}$, if E manages to prevent the state from reaching $\{w : \Im w > \Im z_b^*\} \cup \mathrm{cl}(\mathscr{S}^+)$, given any $\epsilon > 0$, P can force the state to come as close as it is necessary to $b \in \partial \mathscr{S}^+$ in order to guarantee himself a future attainable oriented distance to $\mathscr{T}^+$ that is at most $1 - \Im(b_a^*) + \epsilon$.

The above observation sheds light on the reason why the integration of the RPE failed to cover the island $\mathscr{I}^+$ with semi-permeable trajectories. For plays that initiate in int $(\mathscr{I}^+) \cap \{w \; : \; \Im w \leq \Im z_b^*\}$, if E manages to prevent the state from entering $\{w \; : \; \Im w > \Im z_b^*\} \cup \mathrm{cl}\,(\mathscr{S}^+)$, P can take the state as close as he wants to b, in finite time. This ability possessed by P will be referred to as *P's pull-back manoeuvre* against E's resistance to let the state into $\{w \; : \; \Im w > \Im b_a^*\} \cup \mathrm{cl}\,(\mathscr{S}^+)$.

Once P is satisfied with the proximity achieved to b, loosely speaking lets say for example when the state is at the point z_0 indicated in Figure 5.12, P can switch to $u\,(\mathfrak{t}) = i_o^\triangledown + \mathfrak{j}$ (the same control action recommended in $\mathscr{A}_1$ by (5.64)) and keep it constant. Under this new condition, application of Proposition 4.3.1 once again (but now with $q_1 = d$, $q_2 = a$ and z_0 as represented in Figure 5.12) allows to infer that the state must come arbitrarily close to the line $\overleftrightarrow{da}$, in finite time. Moreover, Proposition 4.3.2, states that as long as the state remains in $\mathrm{cl}\,(\mathscr{H}_{d,a})$ the state must move in set $\mathscr{D}_{d,a}\,(z_0)$ along its way to $\overleftrightarrow{da}$. The set $\mathscr{D}_{d,a}\,(z_0) \cap \mathrm{cl}\,(\mathscr{H}_{d,a})$ is represented in Figure 5.12 by the shaded area that emanates from z_0 (both $\mathscr{D}_{d,a}\,(\cdot)$ and $\mathscr{H}_{d,a}$ are defined as in Proposition 4.3.2 with $q_1 = d$ and $q_2 = a$). Consequently, the state must *reach* the ray $\left\{a - \rho \frac{\overline{k}}{|k|} \; : \; \rho > 0\right\}$ from half-plane $P_\uparrow$ in finite time, at a point whose oriented distance to $\mathscr{T}^+$ is *at most* equal to $1 - \Im\,(b_a^*) + \epsilon$, where $\epsilon = \Im\,(b_a^* - z_0^*)$ is the imaginary part of the difference between $b_a^* = z_{\rho_{\min}}\,(0)$ and the point z_0^* of minimal imaginary part in the segment $\mathscr{D}_{d,a} \cap \mathrm{cl}\,(\mathscr{H}_{d,a}) \cap \left\{a - \rho \frac{\overline{k}}{|k|} \; : \; \rho > 0\right\}$, as represented in Figure 5.12. It is clear that P could have made the positive difference ϵ as small as he wanted, provided he had led the state approximate b as much as it was necessary in the previous pull-back stage. Note, however, that during this previous stage, P must also take care that that the approximation to b becomes sufficient so that the arguments just given invoking Propositions 4.3.1 and 4.3.2 for the next stage are actually valid. In Subsection 5.7.8 this issue will be treated more precisely.

For plays that initiate at states which belong to the curve $z_{\rho_{\min}}\,([0, 2\pi)) = \mathscr{I}^+ \cap \partial\mathscr{I}^+$, P can force the state to reach $\left\{a - \rho \frac{\overline{k}}{|k|} \; : \; \rho > 0\right\}$ at a point where the oriented distance to $\mathscr{T}^+$ is *at most* equal to $1 - \Im b_a^*$ by extending continuously the strategy (5.64), defined in $\mathscr{S}^+$, to the curve $z_{\rho_{\min}}\,([0, 2\pi))$ (similar arguments to the ones used in Subsection 5.7.3 may be invoked). However, some care must be taken to define P's strategy at the point b where the continuous extension is not well defined. At this point, the extension must be taken from $\mathscr{A}_1$, so that the arguments given in Subsection 5.7.3 for the case of an initial state $z_1 \in ((\partial\mathscr{A}_2) \cap (\partial\mathscr{A}_1)) \cup \mathscr{A}_1$ remain valid for the particular case $z_1 = b$ (see Figure 5.11).

The above facts, suggest that a reasonable extension for $\mathcal{V}$ in $\mathscr{I}^+$ is to define it constant and equal to $1 - \Im b_a^* = 1 - \Im\left(a - \rho_{\min} \frac{\overline{k}}{|k|}\right) = 1 - \Im a - \rho_{\min} \cos\alpha$, at least for those states in $\mathscr{I}^+$ such that their oriented distance to $\mathscr{T}^+$ is greater or equal than $1 - \Im b_a^*$, as it will be done in Subsection 5.7.6.

5.7.6. A candidate solution

At first glance, the function $\mathcal{V}$ introduced in Subsection 5.7.2 looks promising for verifying the saddle inequalities (5.11) that correspond to $\mathcal{V}_{d_o}^+$, at least for initial states $z \in \mathscr{S}^+$ such that $1 - \Im z \geq \mathcal{V}(z)$, i.e., such that their oriented distance $d_o(z, \mathscr{T}^+) = 1 - \Im z$ to $\mathscr{T}^+$ is greater or equal than the oriented distance $\mathcal{V}(z)$ to $\mathscr{T}^+$ that P can guarantee for himself as an upper bound of the final outcome. On the one hand, as was shown in Subsection 5.7.3, from every $z \in \mathscr{S}^+$, P can force a counter-clockwise state motion in $\mathscr{S}^+$ towards $\left\{ a - \rho \frac{\overline{k}}{|k|} \; : \; \rho > \rho_{\min} \right\}$ (reached from $P_\uparrow$) that attains a minimum oriented distance to $\mathscr{T}^+$ that is *at most* equal to $\mathcal{V}(z)$. On the other hand, E can guarantee for himself that this oriented distance to $\mathscr{T}^+$ will be at *at least* equal to $\mathcal{V}(z)$, by not allowing the state to cross the semi-permeable characteristic trajectories in the outward direction, as the state motion progress counter-clock-wisely towards $\left\{ a - \rho \frac{\overline{k}}{|k|} \; : \; \rho > \rho_{\min} \right\}$.

However, to put under test the saddle inequalities (5.11) that correspond $\mathcal{G}_{\text{dist}}^+$, the following objects, *globally* defined in the complex plane, are needed first: i) a candidate value function $\mathcal{V}_{d_o}^+$; and ii) candidate strategies $\tilde{u}_+^*$ and $\tilde{\sigma}_+^*$ for P and E, respectively. These objects are synthesized next from $\mathcal{V}$, by a two-step constructive method devised taking into account the facts discussed not only in Subsection 5.7.3 but also in Subsections 5.7.4 and 5.7.5. The resulting synthesised objects will be proved to be meaningful in Subsection 5.7.8, where a relaxed version of (5.11) will be proved.

1. <u>Extension</u> – Define $\mathcal{V}_{\text{aux}} : \mathbb{C} \to \mathbb{R}$ and $\tilde{p}_{\text{aux}}^* : \mathbb{C} \to \mathbb{C}$ as the following extensions of $\mathcal{V}$ and $\nabla \mathcal{V}$, respectively, to the whole complex plane:

$$\mathcal{V}_{\text{aux}}(z) \triangleq \begin{cases} \mathcal{V}(z) & \text{if } z \in \mathscr{S}^+, \\ 1 - \Im(z_{\rho_{\min}}(0)) & \text{if } z = z_{\rho_{\min}}(0), \\ \lim_{\mathscr{S}^+ \ni w \to z} \mathcal{V}(w) = 1 - \Im(z_{\rho_{\min}}(0)) & \text{if } z \in z_{\rho_{\min}}((0, 2\pi)), \\ \lim_{\mathscr{S}^+ \ni w \to b} \mathcal{V}(w) = 1 - \Im(z_{\rho_{\min}}(0)) & \text{otherwise, i.e., } z \in \text{int}(\mathscr{I}^+); \end{cases}$$

$$\tilde{p}_{\text{aux}}^*(z) \triangleq \begin{cases} \nabla \mathcal{V}(z) & \text{if } z \in \mathscr{S}^+, \\ -j & \text{if } z = z_{\rho_{\min}}(0), \\ \lim_{\mathscr{S}^+ \ni w \to z} \nabla \mathcal{V}(w) & \text{if } z \in z_{\rho_{\min}}((0, 2\pi)) \setminus \{b\}, \\ \lim_{\mathscr{A}_1 \ni w \to b} \nabla \mathcal{V}(w) & \text{if } z = b, \\ e^{\frac{1}{2}\left(\frac{\pi}{2} - \beta\right)\overline{k}} \lim_{\mathscr{A}_1 \ni w \to b} \nabla \mathcal{V}(w) & \text{otherwise, i.e., } z \in \text{int}(\mathscr{I}^+). \end{cases}$$

2. <u>Comparison</u> – Use $\mathcal{V}_{\text{aux}}$ and $\tilde{p}_{\text{aux}}^*$ as defined above, to define $\mathcal{V}_{d_o}^+ : \mathbb{C} \to \mathbb{R}$ and $\tilde{p}_+^* : \mathbb{C} \to \mathbb{C}$ as follows:

$$\mathcal{V}_{d_o}^+(z) \triangleq \min\{\mathcal{V}_{\text{aux}}(z), 1 - \Im z\}; \tag{5.66}$$

$$\tilde{p}_+^*(z) \triangleq \begin{cases} \tilde{p}_{\text{aux}}^*(z) & \text{if } \mathcal{V}_{\text{aux}}(z) \leq 1 - \Im z, \\ -j & \text{otherwise.} \end{cases} \tag{5.67}$$

Finally, use $\tilde{p}_+^*$ to define $\tilde{u}_+^* : \mathbb{C} \to U$ and $\tilde{\sigma}_+^* : \mathbb{C} \to \boldsymbol{\Sigma}$ as follows:

$$\tilde{u}_+^* (z) \triangleq u^* \left(\tilde{p}_+^* (z) \right), \tag{5.68}$$

$$\tilde{\sigma}_+^* (z) \triangleq \sigma^* \left(\tilde{p}_+^* (z) \right); \tag{5.69}$$

where $u^* : \mathbb{C} \to U$ and $\sigma^* : \mathbb{C} \to \boldsymbol{\Sigma}$ are the functions defined in statement 2 of Proposition 4.4.1.

Observe that the candidate value function $\mathcal{V}_{\mathrm{d_o}}^+$ is defined in terms of $\mathcal{V}_{\mathrm{aux}}$ which in turn is defined in terms of $\mathcal{V}$. The function $\mathcal{V}_{\mathrm{aux}}$ is continuous in $\mathbb{C} \setminus \left\{ a - \rho \frac{\bar{k}}{|k|} \ : \ \rho > \rho_{\min} \right\}$. In $\mathscr{S}^+$ the function $\mathcal{V}_{\mathrm{aux}}$ coincides with $\mathcal{V}$, but in $\mathscr{I}^+$ (where $\mathcal{V}$ is not defined) it takes the constant value

$$\mathrm{d_o} \left(b_a^*, \mathscr{T}^+ \right) = 1 - \Im b_a^* = 1 - \Im z_{\rho_{\min}} (0) = 1 - \Im a - \rho_{\min} \cos \alpha,$$

which equals $\sup_{z \in \mathscr{S}^+} \mathcal{V} (z) = \lim_{\mathscr{S}^+ \ni z \to b} \mathcal{V} (z) = \max_{z \in \mathbb{C}} \mathcal{V}_{\mathrm{aux}} (z)$.

Notice also that the newly defined strategies $\tilde{u}_+^*$ and $\tilde{\sigma}_+^*$ provide control action recommendations to both players not only in $\mathscr{S}^+$, but also in $\mathscr{I}^+ = \mathbb{C} \setminus \mathscr{S}^+$. In fact, for every $z \in \mathbb{C}$, the *upward game's pseudo-gradient* $\tilde{p}_+^* (z)$ provides well defined control actions for both players if it used as the argument of $\tilde{u}_+^*$ and $\tilde{\sigma}_+^*$, even if $\nabla \mathcal{V}_{\mathrm{d_o}}^+ (z) = 0$ or $\mathcal{V}_{\mathrm{d_o}}^+$ is not real-differentiable at z. If $\mathcal{V}_{\mathrm{d_o}}^+$ is real differentiable at z and $\mathcal{V}_{\mathrm{d_o}}^+ (z) \neq 0$, the pseudo-gradient $\tilde{p}_+^* (z)$ equals $\nabla \mathcal{V}_{\mathrm{d_o}}^+ (z)$.

For points $z \in \mathrm{int} \left(\mathscr{I}^+ \right)$ such that $\mathcal{V}_{\mathrm{aux}} (z) \leq 1 - \Im z$, the strategies $\tilde{u}_+^*$ and $\tilde{\sigma}_+^*$ are defined in such a way that they provide the same control actions recommended by the original strategies (5.64) and (5.65) in $\mathscr{A}_2$. This is done by defining $\tilde{p}_{\mathrm{aux}}^* (z)$ as an intermediate value between $\lim_{\mathscr{A}_1 \ni w \to b} \nabla \mathcal{V} (w)$ and $\lim_{\mathscr{A}_3 \ni w \to b} \nabla \mathcal{V} (w)$ (recall that $p (\tau)$ evolves according to (5.29) as τ varies in $[0, 2\pi)$; see also Figure 4.14). The purpose of doing this is just to endow P with a strategy that forces the state to approach $b \in \mathrm{cl} \left(\mathscr{S}^+ \right)$ in case E offers resistance against the state entering $\{ w \ : \ \Im w > \Im b_a^* \} \cup \mathrm{cl} \left(\mathscr{S}^+ \right)$ as explained in Subsection 5.7.5. In other words, P's pull-back manoeuvre is encoded in the definition of $\tilde{u}_+^*$. However, E's resistance against this pull-back is not encoded in $\tilde{\sigma}_+^*$, because it is futile (except for an $\epsilon > 0$ in the final outcome in favour of E which P can make arbitrarily small).

For points $z \in z_{\rho_{\min}} ([0, 2\pi))$ such that $\mathcal{V}_{\mathrm{aux}} (z) \leq 1 - \Im z$, the strategies $\tilde{u}_+^*$ and $\tilde{\sigma}_+^*$ are defined by extension of (5.64) and (5.65), taking care at $z = b$ where the extension fails to be well defined. This way, the control actions recommended by $\tilde{u}_+^*$ and $\tilde{\sigma}_+^*$ for each z in the curve $z_{\rho_{\min}} ([0, 2\pi)) \cap \{ w \ : \ \mathcal{V} (w) \leq 1 - \Im w \}$ are in fact semi-permeable controls for the same curve.

5.7.6.1. Pruning of the semi-permeable trajectories

The candidate value function (VF), $\mathcal{V}_{\mathrm{d_o}}^+$, is defined from $\mathcal{V}_{\mathrm{aux}}$ in (5.104) by taking the minimum between $1 - \Im z$ and $\mathcal{V}_{\mathrm{aux}} (z)$, for each $z \in \mathscr{S}^+$. This is nothing else than a comparison between the *current* oriented distance to $\mathscr{T}^+$ (i.e., $1 - \Im z = \mathrm{d_o} \left(z, \mathscr{T}^+ \right)$) and the best *future* potentially attainable oriented distance to $\mathscr{T}^+$ that P can assure for himself against optimal opposition from E (i.e.,

$\mathcal{V}_{\text{aux}}(z) = \mathcal{V}(z)$, except possibly for an arbitrarily small difference in favour of E, which is under P's control, in case $z \in \text{int}\,(\mathscr{I}^+) \cap \{w \;:\; \Im w < \Im b_a^*\}$).

Next, the effect that the comparison just described has on each curve $[0, 2\pi) \ni \tau \mapsto z_\rho(\tau)$ included in $\mathscr{S}^+ \cup z_{\rho_{\min}}([0, 2\pi)) = \bigcup_{\rho \geq \rho_{\min}} z_\rho([0, 2\pi))$ is examined.

Fix ρ such that $\rho \geq \rho_{\min}$ and imagine a moving point $z_\rho(\tau)$ as retrogressive time τ increases (see Figure 5.13). Recall that $\tau_1 = \gamma_1 = \frac{\pi}{2} + 2\beta - \alpha$, $\tau_2 - \tau_1 = \gamma_2 = \frac{\pi}{2} - \beta$, $\tau_3 - \tau_2 = \gamma_3 = \frac{\pi}{2} + \beta$, $\tau_4 - \tau_3 = \gamma_4 = \frac{\pi}{2} - \beta$, $2\pi - \tau_4 = \gamma_5 = \alpha - \beta$ and accordingly $\gamma_1 + \gamma_2 + \gamma_3 + \gamma_4 + \gamma_5 = 2\pi$ (see Figure 5.5).

On the one hand, the *future* potentiality attainable oriented distance to $\mathscr{T}^+$ that P can assure for himself, departing from $z_\rho(\tau)$, against optimal opposition from E is

$$\mathcal{V}_{\text{aux}}(z_\rho(\tau)) = \mathcal{V}(z_\rho(\tau)) = \mathcal{V}(z_\rho(0)) = 1 - \Im z_\rho(0) = 1 - \Im a - \rho \cos\alpha, \quad (5.70)$$

which remains constant as τ increases.

On the other hand, the *current* oriented distance to $\mathscr{T}^+$, at $z_\rho(\tau)$, is

$$d_o\left(z_\rho(\tau), \mathscr{T}^+\right) = 1 - \Im z_\rho(\tau), \quad (5.71)$$

which varies continuously as τ increases. Actually, $\tau \mapsto 1 - \Im z_\rho(\tau)$ is strictly monotonously *increasing* in the interval $(0, \gamma_1 + \gamma_2 + \gamma_5)$ and strictly monotonously *decreasing* in the interval $(\gamma_1 + \gamma_2 + \gamma_5, 2\pi)$. At $\tau = 0$, (5.71) equals (5.70). At $\tau = \gamma_1 + \gamma_2 + \gamma_5$, (5.71) attains its maximum value in the interval $[0, 2\pi)$. The point $z_\rho(\gamma_1 + \gamma_2 + \gamma_5)$ where the maximum is attained belongs to the ray $\left\{c + \xi \frac{\bar{k}}{|k|} \;:\; \xi > 0\right\}$ as it is patent in Figure 5.13. As $\tau \to (2\pi)^-$, the oriented distance (5.71) tends to

$$\lim_{\tau \to (2\pi)^-} d_o\left(z_\rho(\tau), \mathscr{T}^+\right) = \lim_{\tau \to (2\pi)^-} (1 - \Im z_\rho(\tau)) = 1 - \Im\left(a - P^{-1}(\rho)\frac{\bar{k}}{|k|}\right)$$
$$= 1 - \Im a - P^{-1}(\rho)\cos\alpha \quad (5.72)$$

where $P : \mathbb{R} \to \mathbb{R}$ is given by (5.34).

Hence, (5.71) increases from a value given by (5.70) to a maximum value given by $1 - \Im z_\rho(\gamma_1 + \gamma_2 + \gamma_5)$ and then decreases and tends to a value given by (5.72) as $\tau \to (2\pi)^-$. Compare (5.72) with (5.70). From (5.40), $P^{-1}(\rho) > \rho$ for $\rho > \rho_{\text{lim}}$, and in fact $\rho > \rho_{\text{lim}}$ (because $\rho \geq \rho_{\min}$ and $\rho_{\min} > \rho_{\text{lim}}$ for the case $\mu > 1$ as stated by (5.51)). Since (5.71) varies continuously in $[0, 2\pi)$, there exists a $\tau_{\max} = \tau_{\max}(\rho) \in (0, 2\pi)$ such that $1 - \Im z_\rho(\tau_{\max}) = 1 - \Im z_\rho(0)$, i.e., $\Im z_\rho(\tau_{\max}) = \Im z_\rho(0)$ (see Figure 5.13). Otherwise stated, as retrogressive time τ increases in the interval $[0, 2\pi)$, the imaginary part of $z_\rho(\tau)$ varies from $\Im z_\rho(0)$ to the minimum value $\Im z_\rho(\gamma_1 + \gamma_2 + \gamma_5)$ and then increases again until it necessarily attains the value $\Im z_\rho(0)$ for a second time at $\tau = \tau_{\max}(\rho) \in (0, 2\pi)$.

This means that for every $\rho \geq \rho_{\min}$, there exists a retro-time instant $\tau_{\max} = \tau_{\max}(\rho)$ such that $\Im z_\rho(\tau_{\max}(\rho)) = \Im z_\rho(0)$. Accordingly, for each $\rho \geq \rho_{\min}$ the characteristic trajectory $z_\rho([0, 2\pi))$ is pruned by the comparison (5.104) which defines $\mathcal{V}_{d_o}^+$. The resulting *pruning curve of* $\mathcal{G}_{\text{dist}}^+$

$$\text{PC}^+ = \{z_\rho(\tau_{\max}(\rho)) \;:\; \rho \geq \rho_{\min}\} \quad (5.73)$$
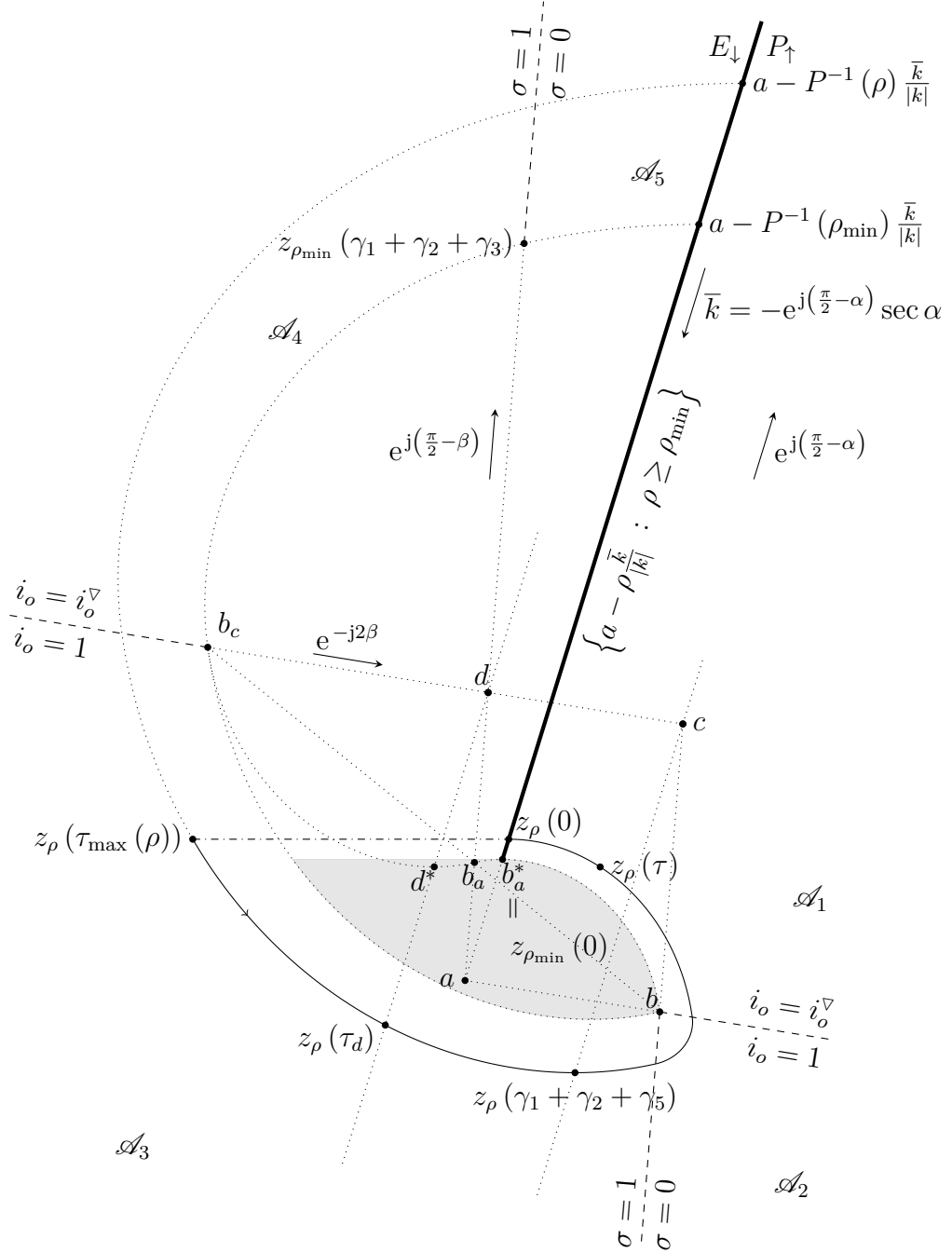
Figure 5.13: Construction of the pruning curve $\mathrm{PC}^+ = \{z_\rho\left(\tau_{\max}\left(\rho\right)\right) \ : \ \rho \geq \rho_{\min}\}$. For every $\rho \geq \rho_{\min}$, there exists a retro-time instant $\tau_{\max} = \tau_{\max}\left(\rho\right)$ such that $\Im z_\rho\left(\tau_{\max}\left(\rho\right)\right) = \Im z_\rho\left(0\right)$.

certainly impacts on the topography of the candidate value function $\mathcal{V}_{d_o}^+$ defined from $\mathcal{V}_{\mathrm{aux}}$. In Figure 5.14 some semi-permeable characteristic trajectories are pruned as just explained to manifest graphically the origin of the pruning curve. From the figure it may be thought that the pruning curve must lie in $\mathscr{A}_3$, however this is false in general. An example of a pruning curve that crosses from $\mathscr{A}_3$ to $\mathscr{A}_4$ is shown in Figure 5.15.

What is clear is that each of the *pruning points* which conform the pruning curve (5.73) must be of the form $z_\rho\left(\tau_{\max}\right)$ with $\tau_{\max} \in \left(\tau_2, 2\pi\right)$, because $\tau \mapsto \Im z_\rho\left(\tau\right)$ is monotonously decreasing in $[0, \tau_2]$, In fact, at $\tau = \tau_2$, the imaginary part of $z_\rho\left(\tau\right)$ has not attained its minimum yet (as τ increases) which is attained at $\tau = \tau_2 + \gamma_5 = \gamma_1 + \gamma_2 + \gamma_5 > \tau_2$. Hence, the pruning points belong to

$$\left(\mathscr{A}_5 \cup z_{\rho_{\min}}\left(\left(\tau_4, 2\pi\right)\right)\right) \cup \left(\mathscr{A}_4 \cup z_{\rho_{\min}}\left(\left(\tau_3, \tau_4\right]\right)\right) \cup \left(\mathscr{A}_3 \cup z_{\rho_{\min}}\left(\left(\tau_2, \tau_3\right]\right)\right).$$

However, more than this can be stated. The points in $\left(\mathscr{A}_3 \cup z_{\rho_{\min}}\left(\left(\tau_2, \tau_3\right]\right)\right)$ that lie in the half-plane $\{z \in \mathbb{C} \ : \ (z - d) \otimes (d^* - d) \leq 0\}$ cannot be pruning points as it is justified next.

Fix $\rho \geq \rho_{\min}$ and let τ_d be the first retrogressive time instant at which $\tau \mapsto z_\rho\left(\tau\right)$ crosses the straight line $\overleftrightarrow{dd^*} = \{z \in \mathbb{C} \ : \ (z - d) \otimes (d^* - d) = 0\}$ as τ increases in the interval $[0, 2\pi)$ (see Figure 5.13). At the retro-time instant $\tau = \tau_d$, still

$$\Im z_\rho\left(\tau_d\right) < \Im d^* < \Im b_a^* < \Im z_\rho\left(0\right), \tag{5.74}$$

so $\Im z_\rho\left(\tau\right)$ has to keep on increasing to attain the value $\Im z_\rho\left(0\right)$ at some $\tau_{\max} > \tau_d$ and thus $z_\rho\left(\tau\right)$ has to get into the half-plane $\{z \in \mathbb{C} \ : \ (z - d) \otimes (d^* - d) > 0\}$. This argument is sustained by the fact that $\Im b_a^* - \Im d^* = \Im\left(b_a^* - d^*\right) > 0$ and that for every $\rho \geq \rho_{\min}$ the point $z_\rho\left(\tau\right)$ rotates clockwisely around the closed curve $\overset{\circ}{b} \triangleq \widehat{b, b_a} \cup \{b\} \cup \widehat{b, b_c} \cup \{b_c\} \cup \widehat{b_c, b_a} \cup \{b_a\}$ as τ increases in the interval $[0, 2\pi)$. In Appendix B.2 it is proved that $\Im\left(b_a^* - d^*\right) > 0$ and $\Re\left(b_a^* - d^*\right) > 0$, as it is visualized in Figures 5.13 to 5.15.

In conclusion, the pruning curve (5.73) is included in the set

$$\left(\mathscr{A}_5 \cup z_{\rho_{\min}}\left(\left(\tau_4, 2\pi\right)\right)\right) \qquad\qquad\qquad \cup$$
$$\left(\mathscr{A}_4 \cup z_{\rho_{\min}}\left(\left(\tau_3, \tau_4\right]\right)\right) \qquad\qquad\qquad \cup$$
$$\left(\left(\mathscr{A}_3 \cup z_{\rho_{\min}}\left(\left(\tau_2, \tau_3\right]\right)\right) \cap \{z \in \mathbb{C} \ : \ (z - d) \otimes (d^* - d) > 0\}\right).$$

This fact will be invoked in Subsection 5.7.8 along the validation of the proposed candidate solution.

5.7.7. The topography of the candidate value function

The comparison that transforms $\mathcal{V}_{\mathrm{aux}}$ into $\mathcal{V}_{d_o}^+$ takes effect in the set

$$\mathscr{R}^+ \triangleq \{z \in \mathbb{C} \ : \ 1 - \Im z < \mathcal{V}_{\mathrm{aux}}\left(z\right)\}.$$

This set, included in $E_\downarrow$, will be referred to as the *ramp* of $\mathcal{G}_{\mathrm{dist}}^+$ because of the form of the graph of $\mathcal{V}_{d_o}^+$ therein. In Figure 5.14 part of the set $\mathscr{R}^+$ is represented

Figure 5.14: The pruning curve of the upward game (PC^+) arises by comparison between the *current* oriented distance to the target set $\mathscr{T}^+$ and P's *potentially attainable* oriented distance to $\mathscr{T}^+$ against optimal opposition from E.
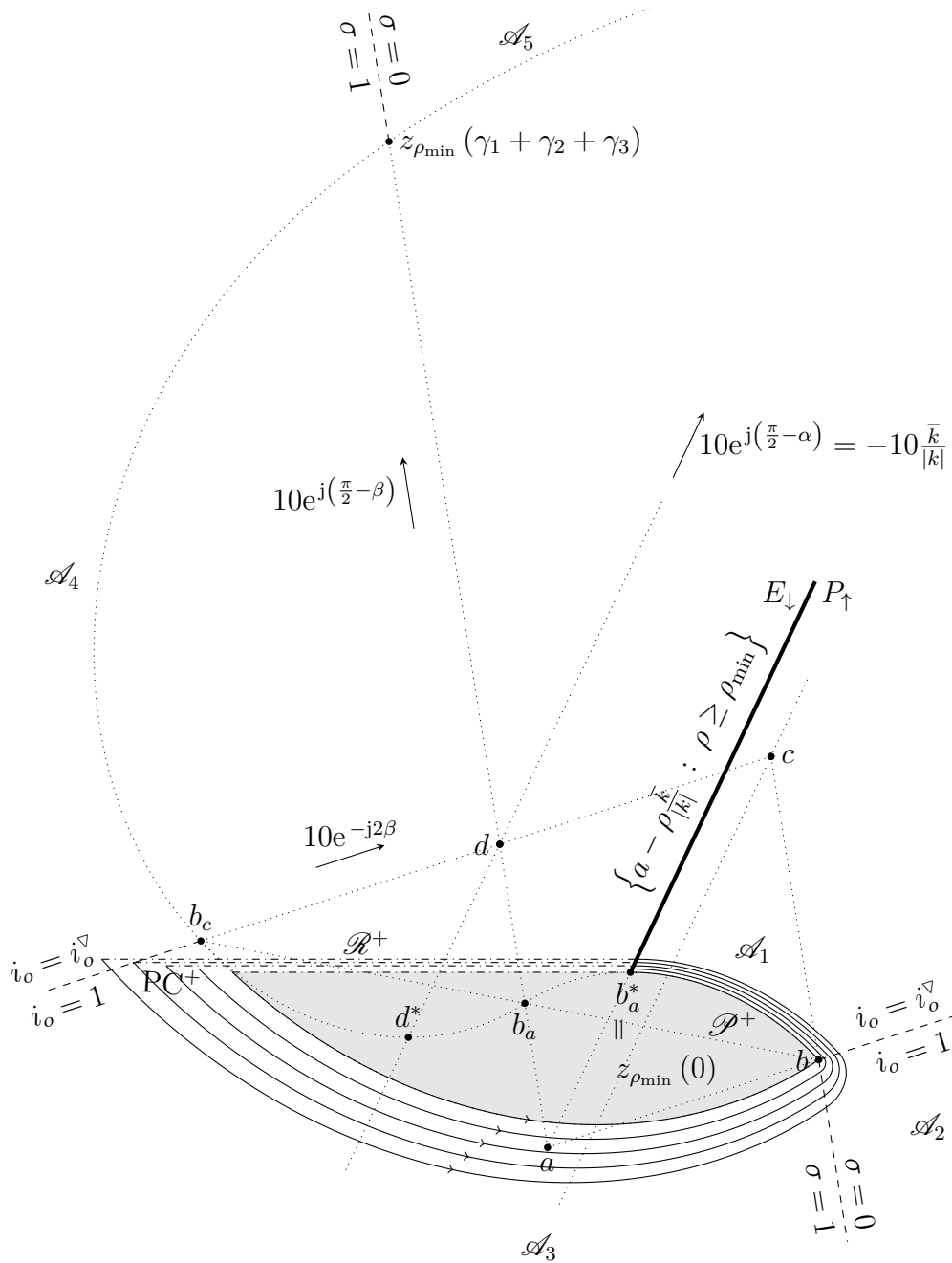
Figure 5.15: In this example, the pruning curve of the upward game (PC^+) crosses one of the two switching rays for i_o (the one that lies on the boundary between $\mathscr{A}_3$ and $\mathscr{A}_4$).

by the area filled by the dot-dashed segments that equalize the imaginary part of the endpoints of each depicted pruned semi-permeable characteristic trajectory.

Since $\mathscr{R}^+ \subset E_\downarrow$, E can instantaneously force $\Im z$ to decrease for every $z \in \mathscr{R}^+$. Moreover, in $\mathscr{R}^+$, P cannot foresee a future oriented distance to $\mathscr{T}^+$ lower than the "current" one $1 - \Im z$. Accordingly, for $z \in \mathscr{R}^+$, is sensible for both players to select control actions $\hat{u} \in U$ and $\hat{\sigma} \in \boldsymbol{\Sigma}$ such that

$$-\mathrm{j} \odot f(z, \hat{u}, \hat{\sigma}) = \inf_{u \in U} \sup_{\sigma \in \boldsymbol{\Sigma}} \left\{ -\mathrm{j} \odot f(z, u, \sigma) \right\},$$

i.e., with the focus on the *current rate of change* of the oriented distance to $\mathscr{T}^+$, rather than the minimum oriented distance to the $\mathscr{T}^+$ on an infinite time horizon. For this reason, $\tilde{u}_+^*(z)$ and $\tilde{\sigma}_+^*(z)$ are defined as $u^*(-\mathrm{j})$ and $\sigma^*(-\mathrm{j})$, respectively, for each $z \in \mathscr{R}^+$ (recall definitions (5.105)–(5.107)).

Coming back to Figure 5.14, notice that the union of each of the dot-dashed segments with its corresponding pruned semi-permeable characteristic trajectory constitutes a level curve of $\mathcal{V}_{d_o}^+$ included in $\mathscr{S}^+ \cup \mathscr{R}^+$. Actually, the set $\mathscr{S}^+ \cup \mathscr{R}^+$ may be expressed in terms of level sets of $\mathcal{V}_{d_o}^+$ as

$$\mathscr{S}^+ \cup \mathscr{R}^+ = \bigcup_{\lambda < 1 - \Im z_{\rho_{\min}}(0)} \left\{ z \ : \ \mathcal{V}_{d_o}^+(z) = \lambda \right\}.$$

It is important to notice that, by the way in which $\mathcal{V}_{d_o}^+$ was constructed, it follows immediately that for each $\lambda \in \mathbb{R}$ its λ-*sup-level set* $\mathcal{V}_{d_o}^+$, defined as

$$\mathscr{L}_{\mathcal{V}_{d_o}^+}(\lambda) \triangleq \left\{ z \ : \ \mathcal{V}_{d_o}^+(z) \geq \lambda \right\},$$

is a convex set. This fact, makes of $\mathcal{V}_{d_o}^+$ a *quasi-concave* function. This property of $\mathcal{V}_{d_o}^+$ will be exploited in Section 5.11 to deal with the (bilateral) game $\mathcal{G}_{\text{dist}}$.

The set

$$\mathscr{P}^+ \triangleq \arg\max_{w \in \mathbb{C}} \mathcal{V}_{d_o}^+(w)$$

will be referred to as the *plateau* of $\mathcal{G}_{\text{dist}}^+$ because the function $\mathcal{V}_{d_o}^+$ takes the constant value $\max_{z \in \mathbb{C}} \mathcal{V}_{d_o}^+(z) = 1 - \Im z_{\rho_{\min}}(0)$ in this closed subset of $\mathbb{C}$. It can be checked that, by the way in which function $\mathcal{V}_{d_o}^+$ was constructed,

$$\mathscr{P}^+ = \mathscr{I}^+ \setminus \mathscr{R}^+.$$

For points $z \in \mathscr{P}^+ \setminus z_{\rho_{\min}}([0, 2\pi))$, the strategies $\tilde{u}_+^*$ and $\tilde{\sigma}_+^*$ are defined in such a way that they recommend the same control actions prescribed by the original strategies (5.64) and (5.65) in $\mathscr{A}_2$. This is just to endow P with a strategy that forces the state to approach $z_{\rho_{\min}}([0, \tau_{\max}(\rho_{\min})]) \subset \mathrm{cl}(\mathscr{S}^+)$, in case E manages to keep the state in $\mathscr{P}^+ \setminus z_{\rho_{\min}}([0, 2\pi))$ (recall P's pull-back manoeuvre).

For points $z \in \mathscr{P}^+ \cap z_{\rho_{\min}}([0, 2\pi)) = z_{\rho_{\min}}([0, \tau_{\max}(\rho_{\min})])$, the strategies $\tilde{u}_+^*$ and $\tilde{\sigma}_+^*$ are defined by extension of (5.64) and (5.65), taking care at $z = b$, as it was already explained. This way, P's counter-clockwise circulation power is extended from $\mathscr{S}^+$ to the curve $z_{\rho_{\min}}([0, \tau_{\max}(\rho_{\min})]) \subset \partial \mathscr{S}^+$

Finally, observe in (5.105) that $\tilde{p}_+^*(z)$ is defined as $\tilde{p}_{\mathrm{aux}}^*(z)$ in the limit case $\mathcal{V}_{\mathrm{aux}}(z) = 1 - \Im z$ (instead of being defined as $-\mathrm{j}$ as it done in case $\mathcal{V}_{\mathrm{aux}}(z) > 1 - \Im z$). This implies that at every point $z \in \mathrm{PC}^+$, which verifies $\mathcal{V}_{\mathrm{aux}}(z) = 1 - \Im z$, P activates its counter-clockwise circulation power, even if he cannot foresee a future oriented distance to the target set lower than the current one $1 - \Im z$. P loses nothing with this unnecessary exercise, while it completes a consistent definition of P's counter-clockwise circulation power in whole closed set $\mathrm{cl}\left(\mathscr{S}^+ \setminus \mathscr{R}^+\right)$.

The whole complex plane may be expressed as

$$
\begin{aligned}
\mathbb{C} = \mathscr{S}^+ \cup \mathscr{S}^{+\complement} &= \mathscr{S}^+ \cup \mathscr{I}^+ \\
&= \left[\left(\mathscr{S}^+ \setminus \mathscr{R}^+\right) \cup \left(\mathscr{S}^+ \cap \mathscr{R}^+\right)\right] \cup \left[\left(\mathscr{I}^+ \setminus \mathscr{R}^+\right) \cup \left(\mathscr{I}^+ \cap \mathscr{R}^+\right)\right] \\
&= \left(\mathscr{S}^+ \setminus \mathscr{R}^+\right) \cup \underbrace{\left(\mathscr{I}^+ \setminus \mathscr{R}^+\right)}_{\mathscr{P}^+} \cup \underbrace{\left(\mathscr{S}^+ \cap \mathscr{R}^+\right) \cup \left(\mathscr{I}^+ \cap \mathscr{R}^+\right)}_{(\mathscr{S}^+ \cup \mathscr{I}^+) \cap \mathscr{R}^+ = \mathbb{C} \cap \mathscr{R}^+ = \mathscr{R}^+} \\
&= \left(\mathscr{S}^+ \setminus \mathscr{R}^+\right) \cup \mathscr{P}^+ \cup \mathscr{R}^+,
\end{aligned}
$$

where $\left(\mathscr{S}^+ \setminus \mathscr{R}^+\right) \cap \mathscr{P}^+ = \emptyset$, $\mathscr{P}^+ \cap \mathscr{R}^+ = \emptyset$, and obviously $\left(\mathscr{S}^+ \setminus \mathscr{R}^+\right) \cap \mathscr{R}^+ = \emptyset$. Hence, $\left\{\mathscr{S}^+ \setminus \mathscr{R}^+, \mathscr{P}^+, \mathscr{R}^+\right\}$ is a partition of $\mathbb{C}$.

5.7.8. Validation of the candidate solution

To assert that the proposal $\left(\mathcal{V}_{\mathrm{d_o}}^+, \tilde{u}_+^*, \tilde{\sigma}_+^*\right)$ constructed before actually solves the upward game $\mathcal{G}_{\mathrm{dist}}^+$ for the case $\mu > 1$, the following saddle inequalities should be proved:

$$
\tilde{\mathcal{P}}_{f,\mathscr{T}^+}^{\mathrm{d_o}}\left(z, \tilde{u}_+^*, \tilde{\sigma}\right) \leq \mathcal{V}_{\mathrm{d_o}}^+(z) \leq \tilde{\mathcal{P}}_{f,\mathscr{T}^+}^{\mathrm{d_o}}\left(z, \tilde{u}, \tilde{\sigma}_+^*\right) \qquad \forall z, \tilde{u}, \tilde{\sigma}. \tag{5.75}
$$

However, strictly speaking, the leftmost inequality of (5.75) is false. The problem arises because in the interior of $\mathscr{P}^+$ (represented by the light-shaded area in Figures 5.14 and 5.15), the strategy $\tilde{u}_+^*$ mandates $i_o = 1$ forcing E to choose instantaneous centres q, for the state-guiding α-equiangular spiral, from the set of points that belong to the segment $\underline{bc}$. The porpouse of P behind this mandate is to pull the state towards the line $\overleftrightarrow{bc}$ and thereby force it to either: i) reach the boundary $\partial \mathscr{P}^+ \setminus \mathrm{cl}\left(\mathscr{S}^+\right) \subset \left\{w : \Im w = \Im z_{\rho_{\min}}(0)\right\}$, or ii) approach $z_{\rho_{\min}}\left([0, \tau_{\max}(\rho_{\min})]\right) = \partial \mathscr{P}^+ \cap \mathrm{cl}\left(\mathscr{S}^+\right)$, as explained in Subsection 5.7.4 relaying on Proposition 4.3.1. If the state reaches $z_{\rho_{\min}}\left([0, \tau_{\max}(\rho_{\min})]\right)$ in finite time, P can make use of its counter-clockwise circulation power and assure for himself an outcome which is *at most* $\mathrm{d_o}\left(z_{\rho_{\min}}(0), \mathscr{T}^+\right) = 1 - \Im z_{\rho_{\min}}(0)$. This is why, $\mathcal{V}_{\mathrm{d_o}}^+$ was constructed such that it takes the constant value $1 - \Im z_{\rho_{\min}}(0)$ in $\mathscr{P}^+$. Nevertheless, E may manage to avoid the state from reaching $z_{\rho_{\min}}\left([0, \tau_{\max}(\rho_{\min})]\right)$ in finite time, for example if he is able to select instantaneous centres $q \in \underline{bc}$ such that the velocity vector $F(z, q) = k(z - q)$, based at the current state $z \in \mathrm{int}\left(\mathscr{P}^+\right)$, points directly to b. The resulting dynamics of the situation just described is exactly the one analysed in Subsubsection 4.3.6.2 and depicted graphically in Figure 4.6, if q_1 is taken as b and q_2 is taken as c. Recall however that, as analysed in Subsubsection 4.3.6.7, this defensive manoeuvre can be performed by E only at the

cost of infinitely fast switching in case E's control set $\boldsymbol{\Sigma} = [0, 1]$ is replaced by the more realistic control set $\{0, 1\}$, making E's control action function non-piecewise continuous. At this point of the discussion, if we adopt P's perspective, we cannot disregard the possibility that E might exhibit such defensive resistance precluding the leftmost inequality of (5.75).

For the reason just explained, sometimes it is preferable for P to resign a small departure from the optimal value promised by $\mathcal{V}_{\mathrm{d_o}}^+$ and bring the play to an end in finite time, than continuing struggling in a never ending play. This issue calls for a slight modification of the strategy $\tilde{u}_+^*$, which has to be made attending the tolerance $\epsilon > 0$ admitted by P with respect to the aimed value $1 - \Im z_{\rho_{\min}}(0)$.

More precisely, define an ϵ-*modification of* $\tilde{u}_+^* : \mathbb{C} \to U$ *for the case* $\mu > 1$ as a function $\tilde{u}_+^{*\epsilon} : \mathbb{C} \to U$ such that

$$\tilde{u}_+^{*\epsilon}(z) \triangleq \begin{cases} i_o^\triangledown + \mathrm{j} & \text{if } z \in \mathscr{B}_{\epsilon'}, \\ \tilde{u}_+^*(z) & \text{otherwise,} \end{cases} \tag{5.76}$$

where

$$\mathscr{B}_{\epsilon'} \triangleq \mathscr{P}^+ \cap$$

$$\left\{ w \in \mathbb{C} \ : \ \mathcal{M}_a^{d-a}(w) \geq \left(\rho_{\min} - \frac{\epsilon'}{\cos\alpha}\right) \mathrm{e}^{-\kappa(\alpha-\beta)} \ \wedge \ \mathcal{A}_a^{d-a}(w) \leq -(\alpha - \beta) \right\}, \tag{5.77}$$

and $\epsilon' \in (0, \epsilon)$ is sufficiently small to guarantee the existence of a unique transverse intersection point in half-plane $\left\{ w \ : \ \overline{k} \otimes (w - a) > 0 \right\}$ between the a-centred arc of α-equiangular spiral

$$\left\{ w \in \mathbb{C} \ : \ \mathcal{M}_a^{d-a}(w) = \left(\rho_{\min} - \frac{\epsilon'}{\cos\alpha}\right) \mathrm{e}^{-\kappa(\alpha-\beta)} \ \wedge \ \mathcal{A}_a^{d-a}(w) \leq 0 \right\} \tag{5.78}$$

and the c-centred arc α-equiangular spiral $\widehat{b, b_c}$ (see Figure 5.16 where the former arc of spiral is indicated by the dash-dot-dotted curve and the intersection point is labelled i).

The conditions involved in the above definition are *sufficient* to guarantee a geometric configuration (as the one depicted in Figure 5.16) such that Propositions 4.3.1 and 4.3.2 can be applied successfully to each initial state in $\mathscr{B}_{\epsilon'}$ in order to prove that the state must cross the ray $\left\{ a - \rho\frac{\overline{k}}{|k|} \ : \ \rho > 0 \right\}$ in finite time (along its way to the line $\overleftrightarrow{dq}$) at a point whose imaginary part is not less than $\Im z_{\rho_{\min}}(0) - \epsilon$.

Now, the following result can be stated as an approximate alternative to (5.75).

Proposition 5.7.1. *In case the parameters of $\mathcal{G}_{\mathrm{dist}}^+$ are such that $\mu > 1$, for every $\epsilon > 0$, there exists an ϵ-modification of $\tilde{u}_+^* : \mathbb{C} \to U$ for the case $\mu > 1$, denoted $\tilde{u}_+^{*\epsilon} : \mathbb{C} \to U$, such that*

$$\tilde{\mathcal{P}}_{f,\mathscr{T}^+}^{\mathrm{d_o}}\left(z, \tilde{u}_+^{*\epsilon}, \tilde{\sigma}\right) - \epsilon \leq \mathcal{V}_{\mathrm{d_o}}^+(z) \leq \tilde{\mathcal{P}}_{f,\mathscr{T}^+}^{\mathrm{d_o}}\left(z, \tilde{u}, \tilde{\sigma}_+^*\right) \quad \forall z, \tilde{u}, \tilde{\sigma}, \tag{5.79}$$

where $\mathcal{V}_{\mathrm{d_o}}^+ : \mathbb{C} \to \mathbb{R}$, $\tilde{u}_+^* : \mathbb{C} \to U$ and $\tilde{\sigma}_+^* : \mathbb{C} \to \boldsymbol{\Sigma}$ are the functions defined in Subsection 5.7.6.

Figure 5.16: If $\mu > 1$, the band $\mathscr{B}_{\epsilon'}$ (represented by the darkest shaded area) is defined so as to extend P's circulation power from $\mathscr{A}_1$ slightly into $\mathscr{P}^+$. Accordingly, in the darkest-shaded area P's modified strategy is defined as $i_o^\nabla + \mathrm{j}$.

Figure 5.17: Illustration of how P can achieve an outcome which is *at most* equal to $1 - \Im z_{\rho_{\min}}(0) + \epsilon' = \mathcal{V}_{d_o}(z) + \epsilon'$ from each initial state $z \in \mathscr{B}_{\epsilon'}$.

Proof. Let $z \in \mathbb{C}$ be an arbitrary initial state for P and E to play $\mathcal{G}_{\text{dist}}^+$.

The proof will be divided into two parts to be enumerated next. From the first one, the leftmost inequality of (5.100) will be derived, while from the second one, the rightmost.

1. P's candidate optimal strategy
   Given $\epsilon > 0$, choose $\epsilon' \in (0, \epsilon)$ to use in (5.76)–(5.77) such that

$$\left\{ w \in \mathbb{C} \ : \ \mathcal{M}_a^{d-a}(w) = \left(\rho_{\min} - \frac{\epsilon'}{\cos \alpha} \right) \mathrm{e}^{-\kappa(\alpha-\beta)} \ \wedge \ \mathcal{A}_a^{d-a}(w) \leq 0 \right\} \cap \widehat{b, b_c},$$

is a transverse intersection with an unique member point i that lies on $\left\{ w \ : \ \overline{k} \otimes (w - a) > 0 \right\}$, as represented in Figure 5.16. To recognize that such ϵ' exists, note that i can be chosen arbitrarily close to b, by taking ϵ' sufficiently small.

Having chosen ϵ', assume that P sticks to the strategy $\tilde{u}_+^{*\epsilon} : \mathbb{C} \to U$, constructed from $\tilde{u}_+^* : \mathbb{C} \to U$ as specified by (5.76)–(5.77).

It was already noted that $\{ \mathscr{S}^+ \setminus \mathscr{R}^+, \mathscr{P}^+, \mathscr{R}^+ \}$ is a partition of $\mathbb{C}$. In addition, $\mathscr{P}^+$ may be partitioned as $\mathscr{P}^+ = \mathscr{B}_{\epsilon'} \cup (\mathscr{P}^+ \setminus \mathscr{B}_{\epsilon'})$. Consequently, the initial state z belongs to only one of the following four sets: either $\mathscr{S}^+ \setminus \mathscr{R}^+$, $\mathscr{B}_{\epsilon'}$, $\mathscr{P}^+ \setminus \mathscr{B}_{\epsilon'}$, or $\mathscr{R}^+$. Next, each case is considered separately.

   a) $z \in \mathscr{S}^+ \setminus \mathscr{R}^+$ – The union set of pruned semi-permeable characteristics. By applying $\tilde{u}_+^{*\epsilon}$, which coincides with $\tilde{u}_+^*$ in $\mathscr{S}^+ \setminus \mathscr{R}^+$, P can force the state to reach $\left\{ a - \rho \frac{\overline{k}}{|k|} \ : \ \rho > \rho_{\min} \right\}$, from the half-plane $P_\uparrow$, at a point where the minimum oriented distance to $\mathscr{T}^+$ is equal or less than $\mathcal{V}_{\mathrm{d_o}}^+(z) = \mathcal{V}(z)$, whatever E does (recall Subsection 5.7.3). This proves that $\tilde{\mathcal{P}}_{f,\mathscr{T}}^{\mathrm{d_o}}(z, \tilde{u}_+^{*\epsilon}, \tilde{\sigma}) \leq \mathcal{V}_{\mathrm{d_o}}(z)$ for every strategy $\tilde{\sigma}$ of E. Thus, trivially, $\tilde{\mathcal{P}}_{f,\mathscr{T}}^{\mathrm{d_o}}(z, \tilde{u}_+^{*\epsilon}, \tilde{\sigma}) \leq \mathcal{V}_{\mathrm{d_o}}(z) + \epsilon$ for every $\tilde{\sigma}$.

   b) $z \in \mathscr{B}_{\epsilon'}$ – P's ϵ'-tolerance band.
      While the state remains in $\mathscr{B}_{\epsilon'}$, the strategy $\tilde{u}_+^{*\epsilon}$ prescribes $i_o^\triangledown + \mathrm{j}$ (as $\tilde{u}_+^*$ does in $\mathscr{A}_1$), forcing E to pick up centres q, for the state-guiding α-equiangular spiral, in the segment $\underline{da}$. Reasoning along the same lines already exposed in Subsection 5.7.5, Proposition 4.3.1 can be applied (with $q_1 = d$, $q_2 = a$) to acknowledge that the state is pulled towards the line $\overleftrightarrow{dq}$, whatever E may do. Moreover, Proposition 4.3.2 states that as long as the state remains in closed half-plane $\mathrm{cl}(\mathscr{H}_{d,a})$, the state must move in $\mathscr{D}_{d,a}(z)$ along its way to $\overleftrightarrow{dq}$ (being $\mathscr{H}_{d,a}$ and $\mathscr{D}_{d,a}(\cdot)$ as defined in Proposition 4.3.2 with $q_1 = d$ and $q_2 = a$). In Figure 5.17 the situation is represented graphically with the set $\mathscr{D}_{d,a}(\cdot) \cap \mathrm{cl}(\mathscr{H}_{d,a})$ represented by the curved shaded area with a vertex at z. While the state moves in $\mathscr{D}_{d,a} \cap P_\uparrow$ it may enter $\mathscr{S}^+ \setminus \mathscr{R}^+$, but it cannot cross

$$\left\{ w \in \mathbb{C} \ : \ \mathcal{M}_a^{d-a}(w) = \left(\rho_{\min} - \frac{\epsilon'}{\cos \alpha} \right) \mathrm{e}^{-\kappa(\alpha-\beta)} \ \wedge \ \mathcal{A}_a^{d-a}(w) \leq 0 \right\}$$

because that would mean that it escapes from $\mathscr{D}_{d,a}$. Consequently, the state must *reach* the ray $\left\{ a - \rho \frac{\bar{k}}{|k|} \ : \ \rho \geq \rho_{\min} - \frac{\epsilon'}{\cos \alpha} \right\}$ from half-plane $P_{\uparrow}$ in finite time, at a point whose oriented distance to $\mathscr{T}^+$ is *at most* equal to $1 - \Im z_{\rho_{\min}}(0) + \epsilon'$, i.e., $\tilde{\mathcal{P}}^{\mathrm{d_o}}_{f,\mathscr{T}}(z, \tilde{u}^{*\epsilon}_+, \tilde{\sigma}) \leq \mathcal{V}_{\mathrm{d_o}}(z) + \epsilon'$ regardless of E's strategy $\tilde{\sigma}$. Consequently, $\tilde{\mathcal{P}}^{\mathrm{d_o}}_{f,\mathscr{T}}(z, \tilde{u}^{*\epsilon}_+, \tilde{\sigma}) \leq \mathcal{V}_{\mathrm{d_o}}(z) + \epsilon$ for every $\tilde{\sigma}$, because $\epsilon' < \epsilon$.

c) $z \in \mathscr{P}^+ \setminus \mathscr{B}_{\epsilon'}$ – The set where P pulls the state towards the line $\overleftrightarrow{bc}$.

While the state remains in $\mathscr{P}^+ \setminus \mathscr{B}_{\epsilon'}$, the strategy $\tilde{u}^{*\epsilon}_+$ (which coincides with $\tilde{u}^*_+$ in $\mathscr{P}^+ \setminus \mathscr{B}_{\epsilon'}$) dictates $1 + \mathrm{j}$, forcing E to pick up centres q, for the state-guiding α-equiangular spiral, in the segment $\underline{bc}$. Proposition 4.3.1, with $q_1 = b$, $q_2 = c$, assures that the state must come arbitrarily close to the line $\overleftrightarrow{bc}$ in finite time (see Figure 5.16). Therefore, the state must either enter: i) the union set of pruned semipermeable characteristics $\mathscr{S}^+ \setminus \mathscr{R}^+$, or ii) P's ϵ'-tolerance band $\mathscr{B}_{\epsilon'}$, or iii) the ramp $\mathscr{R}^+$. For cases i) and ii), P can guarantee for himself a final outcome such that $\tilde{\mathcal{P}}^{\mathrm{d_o}}_{f,\mathscr{T}}(z, \tilde{u}^{*\epsilon}_+, \tilde{\sigma}) \leq \mathcal{V}_{\mathrm{d_o}}(z) + \epsilon$ for every $\tilde{\sigma}$, as it was already explained in Items 1*a* and 1*b*, respectively. In fact, for case i), $\tilde{\mathcal{P}}^{\mathrm{d_o}}_{f,\mathscr{T}}(z, \tilde{u}^{*\epsilon}_+, \tilde{\sigma}) < \mathcal{V}_{\mathrm{d_o}}(z) = 1 - \Im z_{\rho_{\min}}(0)$, because the state enters the semi-permeable domain. For case iii), since the state enters $\mathscr{R}^+$, it reaches a set where the oriented distance to $\mathscr{T}^+$ is lower than $\mathcal{V}_{\mathrm{d_o}}(z) = 1 - \Im z_{\rho_{\min}}(0)$. Thus, necessarily $\tilde{\mathcal{P}}^{\mathrm{d_o}}_{f,\mathscr{T}}(z, \tilde{u}^{*\epsilon}_+, \tilde{\sigma}) < \mathcal{V}_{\mathrm{d_o}}(z)$. Trivially, $\tilde{\mathcal{P}}^{\mathrm{d_o}}_{f,\mathscr{T}}(z, \tilde{u}^{*\epsilon}_+, \tilde{\sigma}) \leq \mathcal{V}_{\mathrm{d_o}}(z) + \epsilon$ for every $\tilde{\sigma}$.

d) $z \in \mathscr{R}^+$ – The set of indifference for P.

While the state is in $\mathscr{R}^+$, P has no way of guaranteeing himself a future oriented distance to $\mathscr{T}^+$ lower than the current one. Consequently, any control action is valid for him in this set. The selected one by $\tilde{u}^{*\epsilon}_+$, which coincides with the one given by $\tilde{u}^*_+$ in $\mathscr{R}^+$, is the one that results from solving inf-sup problem $\inf_{u \in U} \sup_{\sigma \in \mathbf{\Sigma}} \{ -\mathrm{j} \odot f(w, u, \sigma) \}$, in order to slow down, as much as possible, the current rate of increase of the oriented distance to $\mathscr{T}^+$ (a rate of increase that can be imposed to be positive by E because $\mathscr{R}^+ \subset E_{\downarrow}$). Whatever happens in the future, it will be true that $\tilde{\mathcal{P}}^{\mathrm{d_o}}_{f,\mathscr{T}^+}(z, \tilde{u}^{*\epsilon}_+, \tilde{\sigma}) \leq 1 - \Im z = \mathcal{V}^+_{\mathrm{d_o}}(z)$, regardless of E's strategy $\tilde{\sigma}$. Hence, $\tilde{\mathcal{P}}^{\mathrm{d_o}}_{f,\mathscr{T}^+}(z, \tilde{u}^{*\epsilon}_+, \tilde{\sigma}) \leq \mathcal{V}^+_{\mathrm{d_o}}(z) + \epsilon$ for each $\tilde{\sigma}$.

2. E's candidate optimal strategy

Assume that E sticks to the strategy σ^*_+. Recall that z is a generic but already fixed initial state.

Consider the sup-level set

$$\mathscr{N}(z) \triangleq \mathscr{L}_{\mathcal{V}^+_{\mathrm{d_o}}}\left(\mathcal{V}^+_{\mathrm{d_o}}(z) \right) = \left\{ w \in \mathbb{C} \ : \ \mathcal{V}^+_{\mathrm{d_o}}(w) \geq \mathcal{V}^+_{\mathrm{d_o}}(z) \right\}.$$

Its boundary $\partial \mathscr{N}(z) = \left\{ w \in \mathbb{C} \ : \ \mathcal{V}^+_{\mathrm{d_o}}(w) = \mathcal{V}^+_{\mathrm{d_o}}(z) \right\}$, which is a level curve of $\mathcal{V}^+_{\mathrm{d_o}}$, is a closed curve in the complex plane, comprised by the disjoint

union of an open curve $\mathscr{C}_{\mathrm{curve}}(\rho)$ and a straight line segment $\mathscr{C}_{\mathrm{straight}}(\rho)$ that joins its endpoints:

$$\partial \mathscr{N}(z) = \underbrace{z_\rho\left([0, \tau_{\max}(\rho)]\right)}_{\mathscr{C}_{\mathrm{curve}}(\rho)} \cup \underbrace{\left\{ w \in \mathbb{C} \;:\; \frac{w - z_\rho(0)}{z_\rho(\tau_{\max}(\rho)) - z_\rho(0)} \in (0,1) \right\}}_{\mathscr{C}_{\mathrm{straight}}},$$

for some $\rho \geq \rho_{\min}$ which *depends* on z. If $\mathcal{V}_{\mathrm{d_o}}^+(z) < 1 - \Im z_{\rho_{\min}}(0)$, the curve $\partial \mathscr{N}(z)$ encloses $\mathscr{P}^+$ and $\rho > \rho_{\min}$, while if $\mathcal{V}_{\mathrm{d_o}}^+(z) = 1 - \Im z_{\rho_{\min}}(0)$ the curve $\partial \mathscr{N}(z)$ coincides with $\partial \mathscr{P}^+$ and $\rho = \rho_{\min}$. In Figure 5.13, the dot-dashed segment with endpoints at $z_\rho(\tau_{\max}(\rho))$ and $z_\rho(0)$ represents $\mathscr{C}_{\mathrm{straight}}(\rho)$, and the solid curve that joins the same two endpoints represents $\mathscr{C}_{\mathrm{curve}}(\rho)$.

Every point in $\mathscr{N}(z)$ has an oriented distance to $\mathscr{T}^+$ equal or greater than $\mathcal{V}_{\mathrm{d_o}}^+(z)$ (see Figure 5.13). So, to prove that $\mathcal{V}_{\mathrm{d_o}}^+(z) \leq \tilde{\mathcal{P}}_{f,\mathscr{T}^+}^{\mathrm{d_o}}(z, \tilde{u}, \tilde{\sigma}_+^*)$ for every strategy $\tilde{u}$ eligible by P, it is enough to prove that the state remains in the sup-level set $\mathscr{N}(z)$.

For each state $w \in \mathscr{C}_{\mathrm{curve}}(\rho)$, E applies a control action $\sigma_+^*(w)$, derived from the semi-permeability of $\mathscr{C}_{\mathrm{curve}}(\rho) \subset \mathrm{cl}\left(\mathscr{S}^+\right)$, which prevents the state velocity vector, based at w, from pointing into $\bigcup_{\lambda > \rho} z_\lambda[0, 2\pi) \subset \mathbb{C} \setminus \mathscr{N}(z)$.

For each point $w \in \mathscr{C}_{\mathrm{straight}}(\rho) \subset E_\downarrow$, E applies a control action $\sigma_+^*(w) = 0$, which prevents the imaginary part of the state from *increasing*.

A hasty conclusion of the previous two paragraphs may be the following: at every point $w \in \partial \mathscr{N}(z)$, the state velocity vector, based at w, *does not point into* $\mathbb{C} \setminus \mathscr{N}(z)$, whatever P does. Thus,

$$\mathcal{V}_{\mathrm{d_o}}^+(z) \leq \tilde{\mathcal{P}}_{f,\mathscr{T}^+}^{\mathrm{d_o}}(z, \tilde{u}, \tilde{\sigma}_+^*) \quad \forall \tilde{u} \tag{5.80}$$

as required to prove the rightmost inequality of (5.100). However, to definitely prove this claim, the corner points of $\partial \mathscr{N}(z)$ must be examined closer.

If $\mathcal{V}_{\mathrm{d_o}}^+(z) \geq 1 - \Im z_{\rho_{\min}}(0)$ the level curve $\partial \mathscr{N}(z)$ coincides with $\partial \mathscr{P}^+$ which has two corner points: b and $z_\rho(\tau_{\max}(\rho))$ where $\rho = \rho_{\min}$. If $\mathcal{V}_{\mathrm{d_o}}^+(z) < 1 - \Im z_{\rho_{\min}}(0)$, the level curve $\partial \mathscr{N}(z)$ has a single corner point: $z_\rho(\tau_{\max}(\rho))$ where $\rho > \rho_{\min}$. It can be easily checked that the strategy $\tilde{\sigma}_+^*$ (which was carefully defined to take the value 0 at the point b) prevents the velocity vector $f(b, u, \tilde{\sigma}_+^*(b))$, based at b, from pointing into $\mathbb{C} \setminus \mathscr{N}(z)$ for every $u \in U$; so let the focus be on the corner point $z_\rho(\tau_{\max}(\rho))$ where ρ may be greater than or equal to $\rho_{\min}$ (see Figure 5.13).

At $z_\rho(\tau_{\max}(\rho))$, E applies a control action $\tilde{\sigma}_+^*(z_\rho(\tau_{\max}(\rho)))$ that guarantees him that the state does not cross $\partial \mathscr{N}(z)$ into $\bigcup_{\lambda > \rho} z_\lambda[0, 2\pi)$. But, can E be sure that the same control action prevents the state from crossing $\partial \mathscr{N}(z)$ into the set $\{w \;:\; \Im w > \Im z_\rho(0)\}$? This could only happen if the imaginary part of the velocity vector $f(z_\rho(\tau_{\max}(\rho)), u, \tilde{\sigma}_+^*(z_\rho(\tau_{\max}(\rho))))$ results to be positive for some control action $u \in U$ eligible by P. However, making use of the results of Subsection 4.3.5, it will be argued next that this hypothetical possibility can be ruled out.

As it was shown in Subsubsection 5.7.6.1, $z_\rho \left(\tau_{\max}(\rho)\right) \in \mathrm{PC}^+$ must belong to

$$\left(\mathscr{A}_5 \cup z_{\rho_{\min}}\left(\left(\tau_4, 2\pi\right)\right)\right) \qquad\qquad\qquad \cup$$
$$\left(\mathscr{A}_4 \cup z_{\rho_{\min}}\left(\left(\tau_3, \tau_4\right]\right)\right) \qquad\qquad\qquad \cup$$
$$\left(\left(\mathscr{A}_3 \cup z_{\rho_{\min}}\left(\left(\tau_2, \tau_3\right]\right)\right) \cap \left\{w \in \mathbb{C} \ : \ (w-d) \otimes (d^* - d) > 0\right\}\right).$$

Firstly, if $z_\rho \left(\tau_{\max}(\rho)\right) \in \left(\mathscr{A}_5 \cup z_{\rho_{\min}}\left(\left(\tau_4, 2\pi\right)\right)\right)$, the control action prescribed to E is $\tilde{\sigma}_+^* \left(z_\rho \left(\tau_{\max}(\rho)\right)\right) = 0$. Therefore, the state velocity vector, based at $z_\rho \left(\tau_{\max}(\rho)\right)$, is

$$f\left(z_\rho \left(\tau_{\max}(\rho)\right), u, \tilde{\sigma}_+^* \left(z_\rho \left(\tau_{\max}(\rho)\right)\right)\right) = F\left(z_\rho \left(\tau_{\max}(\rho)\right), q\right)$$

with $q \in \underline{ab} = \left\{w \in \mathbb{C} \ : \ \frac{w-a}{b-a} \in [0,1]\right\}$. Assimilate, $\underline{ab}$ as the set $\mathscr{Q}$ of Subsection 4.3.5; the corresponding set $I^- \triangleq \left\{w \in \mathbb{C} \ : \ \Im F(w, q) < 0 \quad \forall q \in \mathscr{Q}\right\}$ was proved to coincide with $\left\{w \in \mathbb{C} \ : \ \overline{k} \otimes (w-q) < 0 \quad \forall q \in \mathscr{Q}\right\}$ in Subsection 4.3.5, i.e., I^- is the following supporting half-plane of the set $\mathscr{Q}$:

$$I^- = \left\{w \in \mathbb{C} \ : \ \overline{k} \otimes (w-q) < 0 \quad \forall q \in \mathscr{Q}\right\}. \qquad (5.81)$$

In the current context, this supporting half-plane takes the form of

$$\left\{w \in \mathbb{C} \ : \ (w - b_a^*) \otimes (a - b_a^*) > 0\right\}$$

which includes the set $\left(\mathscr{A}_5 \cup z_{\rho_{\min}}\left(\left(\tau_4, 2\pi\right)\right)\right)$ where the point $z_\rho \left(\tau_{\max}(\rho)\right)$ lies. Consequently, $\Im f\left(z_\rho \left(\tau_{\max}(\rho)\right), u, \tilde{\sigma}_+^* \left(z_\rho \left(\tau_{\max}(\rho)\right)\right)\right) < 0$ for every $u \in U$.

Secondly, if $z_\rho \left(\tau_{\max}(\rho)\right)$ belongs to

$$\left(\mathscr{A}_4 \cup z_{\rho_{\min}}\left(\left(\tau_3, \tau_4\right]\right)\right) \qquad\qquad\qquad\qquad \cup$$
$$\left(\left(\mathscr{A}_3 \cup z_{\rho_{\min}}\left(\left(\tau_2, \tau_3\right]\right)\right) \cap \left\{w \in \mathbb{C} \ : \ (w-d) \otimes (d^* - d) > 0\right\}\right), \quad (5.82)$$

an analogous argument based on the assimilation of the segment $\underline{dc} = \left\{w \in \mathbb{C} \ : \ \frac{w-d}{c-d} \in [0,1]\right\}$ as the set $\mathscr{Q}$ of Subsection 4.3.5, allows to conclude that $\Im f\left(z_\rho \left(\tau_{\max}(\rho)\right), u, \tilde{\sigma}_+^* \left(z_\rho \left(\tau_{\max}(\rho)\right)\right)\right) < 0$ for every $u \in U$. In this case, the supporting half-plane (5.81) of $\mathscr{Q} = \underline{dc}$ takes the form of

$$\left\{w \in \mathbb{C} \ : \ (w - d) \otimes (d^* - d) > 0\right\}$$

which includes the set (5.82) where $z_\rho \left(\tau_{\max}(\rho)\right)$ lies.

Therefore, at every point (corner or not) of $\partial \mathscr{N}(z)$, the strategy $\tilde{\sigma}_+^*$ adopted by E prevents the state velocity vector, based at the same point, from pointing into $\mathbb{C} \setminus \mathscr{N}(z)$. In conclusion, (5.80) holds.

$$\square$$

The previous proposition paves the way for the two following important results.

Corollary 5.7.1. *In case the parameters of $\mathcal{G}_{\mathrm{dist}}^+$ are such that $\mu > 1$, for every $\epsilon > 0$, there exists an $\frac{\epsilon}{2}$-modification of $\tilde{u}_+^*$, denoted $\tilde{u}_+^{*\frac{\epsilon}{2}}$, such that the pair $\left(\tilde{u}_+^{*\frac{\epsilon}{2}}, \tilde{\sigma}_+^* \right)$ is an ϵ-saddle point for $\mathcal{G}_{\mathrm{dist}}^+$.*

Proof. The following proof follows very closely the proof of the sufficiency part of Theorem 4.1 found in [59, Ch. 4], whose statement was transcribed literally as the statement of Theorem 2.2.1 in Subsection 2.2.6.

Given an $\epsilon > 0$, use $\frac{\epsilon}{2}$ to invoke Proposition 5.7.1 which asserts that there exists $\tilde{u}_+^{*\frac{\epsilon}{2}}$ such that

$$\tilde{\mathcal{P}}_{f,\mathscr{T}+}^{\mathrm{d_o}} \left(z, \tilde{u}_+^{*\frac{\epsilon}{2}}, \tilde{\sigma} \right) - \frac{\epsilon}{2} \leq \mathcal{V}_{\mathrm{d_o}}^+ (z) \leq \tilde{\mathcal{P}}_{f,\mathscr{T}+}^{\mathrm{d_o}} (z, \tilde{u}, \tilde{\sigma}_+^*) \quad \forall z, \tilde{u}, \tilde{\sigma}. \qquad (5.83)$$

Rewrite (5.83) as

$$\tilde{\mathcal{P}}_{f,\mathscr{T}+}^{\mathrm{d_o}} \left(z, \tilde{u}_+^{*\frac{\epsilon}{2}}, \tilde{\sigma} \right) \leq \mathcal{V}_{\mathrm{d_o}}^+ (z) + \frac{\epsilon}{2} \quad \forall z, \tilde{\sigma}, \qquad (5.84)$$

$$\tilde{\mathcal{P}}_{f,\mathscr{T}+}^{\mathrm{d_o}} (z, \tilde{u}, \tilde{\sigma}_+^*) \geq \mathcal{V}_{\mathrm{d_o}}^+ (z) \qquad \forall z, \tilde{u}. \qquad (5.85)$$

Since $\epsilon > 0$, from (5.85) trivially follows that

$$\tilde{\mathcal{P}}_{f,\mathscr{T}+}^{\mathrm{d_o}} (z, \tilde{u}, \tilde{\sigma}_+^*) \geq \mathcal{V}_{\mathrm{d_o}}^+ (z) - \frac{\epsilon}{2} \quad \forall z, \tilde{u}. \qquad (5.86)$$

Adding ϵ to both sides of (5.86) yields

$$\tilde{\mathcal{P}}_{f,\mathscr{T}+}^{\mathrm{d_o}} (z, \tilde{u}, \tilde{\sigma}_+^*) + \epsilon \geq \mathcal{V}_{\mathrm{d_o}}^+ (z) + \frac{\epsilon}{2} \geq \tilde{\mathcal{P}}_{f,\mathscr{T}+}^{\mathrm{d_o}} \left(z, \tilde{u}_+^{*\frac{\epsilon}{2}}, \tilde{\sigma}_+^* \right) \quad \forall z, \tilde{u}, \qquad (5.87)$$

where the rightmost inequality follows from (5.84) by letting $\tilde{\sigma} = \tilde{\sigma}_+^*$. Analogously, adding $-\epsilon$ to (5.84)

$$\tilde{\mathcal{P}}_{f,\mathscr{T}+}^{\mathrm{d_o}} \left(z, \tilde{u}_+^{*\frac{\epsilon}{2}}, \tilde{\sigma} \right) - \epsilon \leq \mathcal{V}_{\mathrm{d_o}}^+ (z) - \frac{\epsilon}{2} \leq \tilde{\mathcal{P}}_{f,\mathscr{T}+}^{\mathrm{d_o}} \left(z, \tilde{u}_+^{*\frac{\epsilon}{2}}, \tilde{\sigma}_+^* \right) \quad \forall z, \tilde{\sigma}, \qquad (5.88)$$

where the rightmost inequality follows from (5.86) by letting $\tilde{u} = \tilde{u}_+^{*\frac{\epsilon}{2}}$.

From (5.87) and (5.88):

$$\tilde{\mathcal{P}}_{f,\mathscr{T}+}^{\mathrm{d_o}} \left(z, \tilde{u}_+^{*\frac{\epsilon}{2}}, \tilde{\sigma} \right) - \epsilon \leq \tilde{\mathcal{P}}_{f,\mathscr{T}+}^{\mathrm{d_o}} \left(z, \tilde{u}_+^{*\frac{\epsilon}{2}}, \tilde{\sigma}_+^* \right) \leq \tilde{\mathcal{P}}_{f,\mathscr{T}+}^{\mathrm{d_o}} (z, \tilde{u}, \tilde{\sigma}_+^*) + \epsilon \quad \forall z, \tilde{u}, \tilde{\sigma}.$$

Consequently, the pair $\left(\tilde{u}_+^{*\frac{\epsilon}{2}}, \tilde{\sigma}_+^* \right)$ is an ϵ-saddle point for $\mathcal{G}_{\mathrm{dist}}^+$. $\qquad \square$

By means of Theorem 2.2.1, the previous corollary implies that $\mathcal{G}_{\mathrm{dist}}^+$ has a value function. Its explicit form is given by the next corollary.

Corollary 5.7.2. *In case the parameters of $\mathcal{G}_{\mathrm{dist}}^+$ are such that $\mu > 1$, the function $\mathcal{V}_{\mathrm{d_o}}^+ : \mathbb{C} \to \mathbb{R}$, as defined in Subsection 5.7.6, is the value function of $\mathcal{G}_{\mathrm{dist}}^+$.*

Proof. From Proposition 5.7.1 we have that for every $\epsilon > 0$, there exists $\tilde{u}_+^{*\epsilon}$ such that

$$\tilde{\mathcal{P}}_{f,\mathscr{T}+}^{\mathrm{d_o}}\left(z,\tilde{u}_+^{*\epsilon},\tilde{\sigma}\right) - \epsilon \leq \mathcal{V}_{\mathrm{d_o}}^+\left(z\right) \leq \tilde{\mathcal{P}}_{f,\mathscr{T}+}^{\mathrm{d_o}}\left(z,\tilde{u},\tilde{\sigma}_+^*\right) \quad \forall z,\tilde{u},\tilde{\sigma}. \qquad (5.89)$$

Firstly, supremizing the leftmost expression in (5.89) we obtain

$$\sup_{\tilde{\sigma}} \tilde{\mathcal{P}}_{f,\mathscr{T}+}^{\mathrm{d_o}}\left(z,\tilde{u}_+^{*\epsilon},\tilde{\sigma}\right) - \epsilon \leq \mathcal{V}_{\mathrm{d_o}}^+\left(z\right) \leq \tilde{\mathcal{P}}_{f,\mathscr{T}+}^{\mathrm{d_o}}\left(z,\tilde{u},\tilde{\sigma}_+^*\right) \leq \sup_{\tilde{\sigma}} \tilde{\mathcal{P}}_{f,\mathscr{T}+}^{\mathrm{d_o}}\left(z,\tilde{u},\tilde{\sigma}\right) \quad \forall z,\tilde{u},$$

where the introduced right inequality is trivial. Now, infimizing the rightmost expression we obtain

$$\inf_{\tilde{u}} \sup_{\tilde{\sigma}} \tilde{\mathcal{P}}_{f,\mathscr{T}+}^{\mathrm{d_o}}\left(z,\tilde{u},\tilde{\sigma}\right) - \epsilon \leq \sup_{\tilde{\sigma}} \tilde{\mathcal{P}}_{f,\mathscr{T}+}^{\mathrm{d_o}}\left(z,\tilde{u}_+^{*\epsilon},\tilde{\sigma}\right) - \epsilon \leq \mathcal{V}_{\mathrm{d_o}}^+\left(z\right) \leq \inf_{\tilde{u}} \sup_{\tilde{\sigma}} \tilde{\mathcal{P}}_{f,\mathscr{T}+}^{\mathrm{d_o}}\left(z,\tilde{u},\tilde{\sigma}\right)$$

for every $z \in \mathbb{C}$, where the introduced leftmost inequality is trivial. By definition of upper value function, $\overline{\mathcal{V}_{\mathrm{d_o}}^+}\left(z\right) = \inf_{\tilde{u}} \sup_{\tilde{\sigma}} \tilde{\mathcal{P}}_{f,\mathscr{T}+}^{\mathrm{d_o}}\left(z,\tilde{u},\tilde{\sigma}\right)$. Hence, for every $\epsilon > 0$,

$$\overline{\mathcal{V}_{\mathrm{d_o}}^+}\left(z\right) - \epsilon \leq \mathcal{V}_{\mathrm{d_o}}^+\left(z\right) \leq \overline{\mathcal{V}_{\mathrm{d_o}}^+}\left(z\right) \quad \forall z \in \mathbb{C}.$$

Consequently, $\mathcal{V}_{\mathrm{d_o}}^+ \equiv \overline{\mathcal{V}_{\mathrm{d_o}}^+}$.

Secondly, infimizing the rightmost expression in (5.89), we obtain

$$\inf_{\tilde{u}} \tilde{\mathcal{P}}_{f,\mathscr{T}+}^{\mathrm{d_o}}\left(z,\tilde{u},\tilde{\sigma}\right) - \epsilon \leq \tilde{\mathcal{P}}_{f,\mathscr{T}+}^{\mathrm{d_o}}\left(z,\tilde{u}_+^{*\epsilon},\tilde{\sigma}\right) - \epsilon \leq \mathcal{V}_{\mathrm{d_o}}^+\left(z\right) \leq \inf_{\tilde{u}} \tilde{\mathcal{P}}_{f,\mathscr{T}+}^{\mathrm{d_o}}\left(z,\tilde{u},\tilde{\sigma}_+^*\right) \quad \forall z,\tilde{\sigma},$$

where the introduced leftmost inequality is trivial. Now, supremizing the leftmost expression we obtain

$$\sup_{\tilde{\sigma}} \inf_{\tilde{u}} \tilde{\mathcal{P}}_{f,\mathscr{T}+}^{\mathrm{d_o}}\left(z,\tilde{u},\tilde{\sigma}\right) - \epsilon \leq \mathcal{V}_{\mathrm{d_o}}^+\left(z\right) \leq \inf_{\tilde{u}} \tilde{\mathcal{P}}_{f,\mathscr{T}+}^{\mathrm{d_o}}\left(z,\tilde{u},\tilde{\sigma}_+^*\right) \leq \sup_{\tilde{\sigma}} \inf_{\tilde{u}} \tilde{\mathcal{P}}_{f,\mathscr{T}+}^{\mathrm{d_o}}\left(z,\tilde{u},\tilde{\sigma}_+^*\right)$$

for every $z \in \mathbb{C}$, where the introduced rightmost inequality is trivial. By definition of lower value function, $\underline{\mathcal{V}_{\mathrm{d_o}}^+}\left(z\right) = \sup_{\tilde{\sigma}} \inf_{\tilde{u}} \tilde{\mathcal{P}}_{f,\mathscr{T}+}^{\mathrm{d_o}}\left(z,\tilde{u},\tilde{\sigma}\right)$. Hence, for every $\epsilon > 0$,

$$\underline{\mathcal{V}_{\mathrm{d_o}}^+}\left(z\right) - \epsilon \leq \mathcal{V}_{\mathrm{d_o}}^+\left(z\right) \leq \underline{\mathcal{V}_{\mathrm{d_o}}^+}\left(z\right) \quad \forall z \in \mathbb{C}.$$

Consequently, $\mathcal{V}_{\mathrm{d_o}}^+ \equiv \underline{\mathcal{V}_{\mathrm{d_o}}^+}$.

Since, $\underline{\mathcal{V}_{\mathrm{d_o}}^+} \equiv \mathcal{V}_{\mathrm{d_o}}^+ \equiv \overline{\mathcal{V}_{\mathrm{d_o}}^+}$, the function $\mathcal{V}_{\mathrm{d_o}}^+$ is the VF of $\mathcal{G}_{\mathrm{dist}}^+$. $\qquad \square$

5.8. Solution of the upward game for the case $\mu < 1$

In this section, the solution of $\mathcal{G}_{\mathrm{dist}}^+$ is worked out for the case $\mu < 1$, relaying on similar methods and arguments as the ones already used for the case $\mu > 1$.

Interestingly, the solution for the case $\mu < 1$ differs qualitatively from the solution obtained for the case $\mu > 1$. Therefore, the focus of this section is on emphasizing the differences, not only between the solutions themselves, but also between the argumentations that validate them.

5.8.0.1. The semi-permeable domain

As in the previous section, reconsider the family (5.31) of characteristic state-space trajectories, parametrized by $\rho > 0$ as formulated by the initial condition (5.26) derived from the ansatz proposed in Section 5.5. In Figure 5.18, nine characteristic trajectories of the sub-family $\{[0, 2\pi) \ni \tau \mapsto z_\rho(\tau) \; : \; \rho > \rho_{\min}\}$ are depicted for a case in which $\mu < 1$, being $\rho_{\min}$ the μ-dependent positive real defined by (5.50). They emanate retrogressively in time from the ray $\left\{a - \rho\frac{\overline{k}}{|k|} \; : \; \rho > \rho_{\min}\right\}$. The arrows indicate the direction of motion in which retrogressive time τ *decreases*, i.e., progressive time $\mathfrak{t}$ *increases*.

For each $\rho > \rho_{\min}$, the curve $\{z_\rho(\tau) \; : \; \tau \in (0, 2\pi)\}$ can be checked to be free of corners and semi-permeable at each of its points. In fact, each of these curves consists of concatenations among members of the negatively oriented families: $\mathscr{F}_a^-$, $\mathscr{F}_b^-$, $\mathscr{F}_c^-$, and $\mathscr{F}_d^-$ (see Figure 4.16). In accordance with the nomenclature of the previous section, the set

$$\mathscr{S}^+ \triangleq \bigcup_{\rho > \rho_{\min}} z_\rho\left([0, 2\pi)\right), \tag{5.90}$$

covered by such curves, will be referred to as the *semi-permeable domain* of $\mathcal{G}_{\mathrm{dist}}^+$. Note that the definition (5.90) adapts to each case automatically, because $\rho_{\min}$ depends on μ.

This definition does not include the special curve $\{z_{\rho_{\min}}(\tau) \; : \; \tau \in [0, 2\pi)\} \subset \partial\mathscr{S}^+$, which passes through $z_{\rho_{\min}}(0)$, d, and tends to $d_a^* = a - P^{-1}(\rho_{\min})\frac{\overline{k}}{|k|}$ as $\tau \to (2\pi)^-$, because even though $z_{\rho_{\min}}((0, 2\pi))$ can be checked to be semi-permeable at each of its points, it is not free of corners: at d it has no definite tangent direction (see Figure 5.18). The special characteristic trajectory $\{z_{\rho_{\min}}(\tau) \; : \; \tau \in [0, 2\pi)\}$ is included in the closed curve $\overset{\circ}{d} = \widehat{d, d_c} \cup \{d\} \cup \widehat{d, d_a} \cup \{d_a\} \cup \widehat{d_a, d_c} \cup \{d_c\}$, introduced in Subsubsection 5.6.5.5 and represented by the dot-dashed line in Figure 5.18. Notice the difference with respect to the case $\mu > 1$ in which $z_{\rho_{\min}}([0, 2\pi))$ is included in the characteristic closed curve $\overset{\circ}{b}$ (compare Figures 5.10 and 5.18 and recall the geometric characterization exhibited in Figure 5.8).

The curves of the collection $\{z_\rho((0, 2\pi)) \; : \; \rho < \rho_{\min}\}$ are also left out the definition of $\mathscr{S}^+$, because they fail to be semi-permeable. For example, in Figure 5.19 seven of such curves are indicated by the dashed curves that lie in the shaded areas. They all require of the concatenation of a member of $\mathscr{F}_c^-$ with a member of $\mathscr{F}_d^+$ (recall Figure 4.16). As every concatenation between members of opposite oriented families, such concatenations fail to be semi-permeable at the concatenation point.

Recall the properties of the function P consolidated into Figure 5.7 and (5.46)–(5.47)–(5.48) rewritten here for ease of use:

$$\lim_{\tau \to (2\pi)^-} z_{\rho_{\lim}}(\tau) = z_{\rho_{\lim}}(0), \tag{5.91}$$

$$\lim_{\tau \to (2\pi)^-} z_\rho(\tau) > z_\rho(0) \qquad \text{if } \rho > \rho_{\lim}, \tag{5.92}$$

$$\lim_{\tau \to (2\pi)^-} z_\rho(\tau) < z_\rho(0) \qquad \text{if } \rho < \rho_{\lim}. \tag{5.93}$$
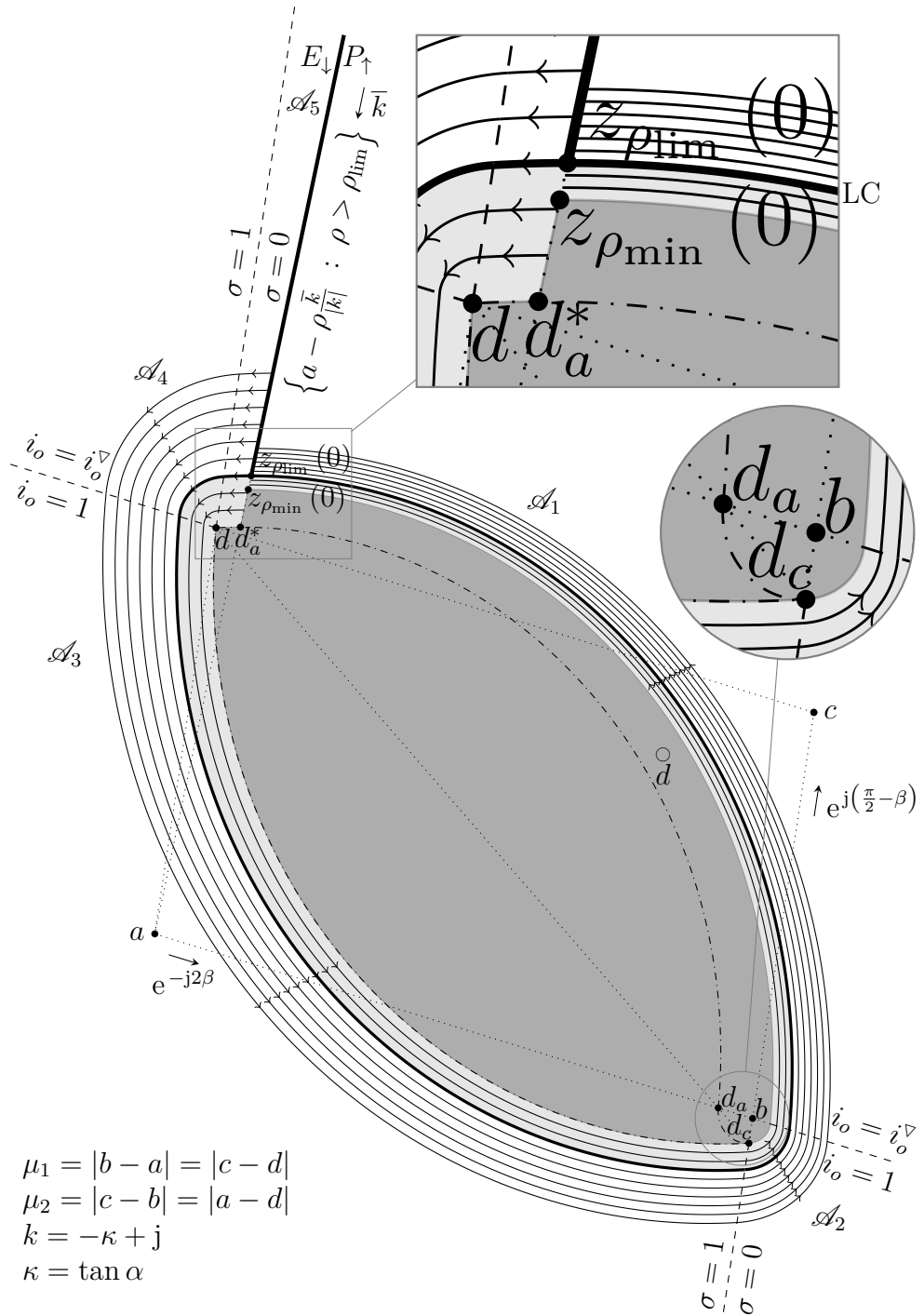
Figure 5.18: Nine representative semi-permeable corner-free characteristic curves of $\mathcal{G}_{\text{dist}}^{+}$ that belong to the collection $\{z_\rho\left([0,2\pi)\right)\ :\ \rho > \rho_{\min}\}$, for the case $\frac{\mu_2}{\mu_1}e^{\kappa\left(\frac{\pi}{2}+\beta\right)} < 1$. The shape of the closed curve indicated by the dot-dashed line characterizes this case. The dashed rays are switching curves.
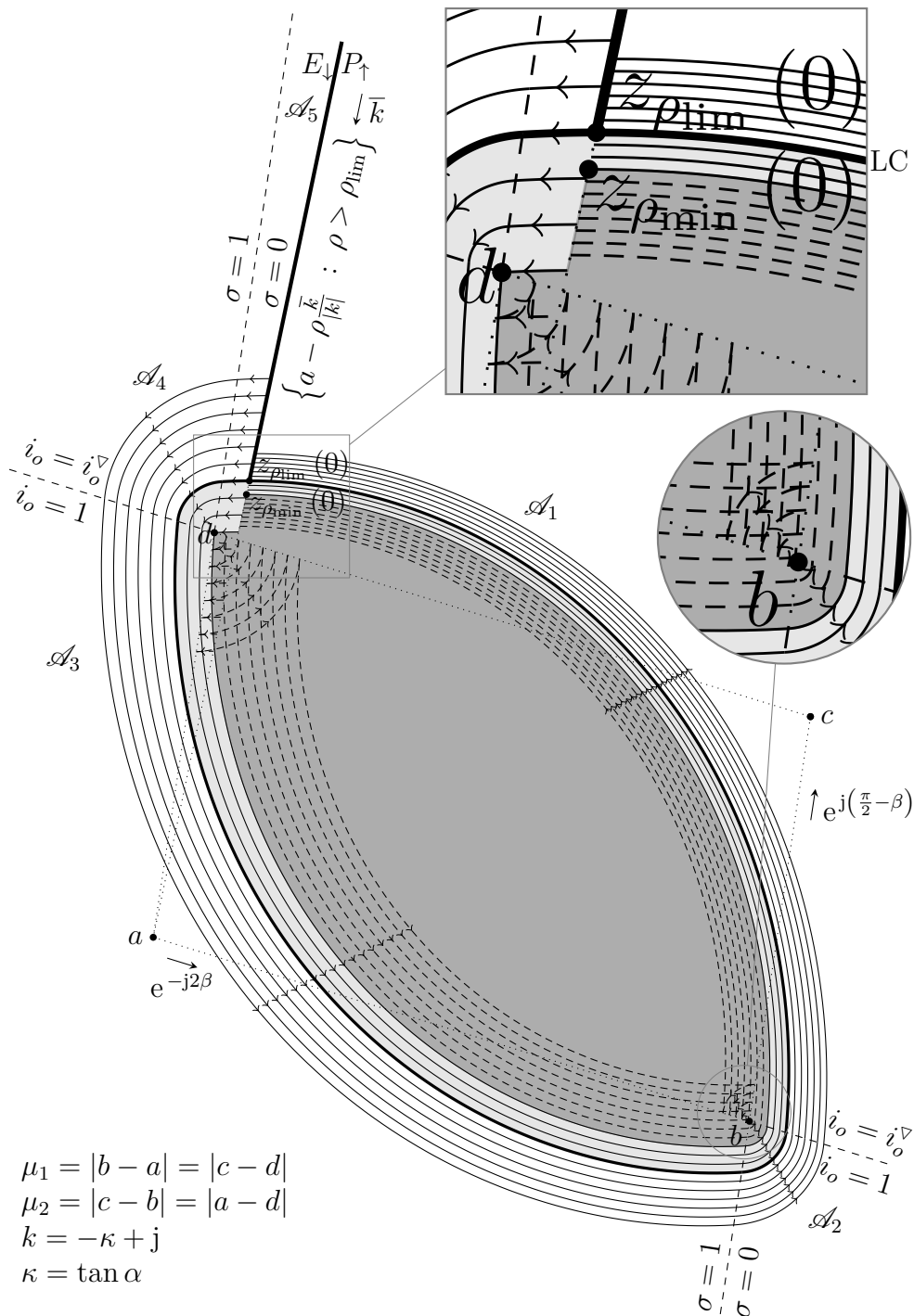
Figure 5.19: The integral curves $(0, 2\pi) \ni \tau \mapsto z_\rho(\tau)$ such that $\rho < \rho_{\min}$, fail to be semi-permeable over the whole integration interval $(0, 2\pi)$ selected for integration of the RPE. The seven dashed *curves* are examples of such curves. The four dashed *rays* are switching curves.

Since $\mu < 1$, from (5.52), $\rho_{\min} < \rho_{\lim}$. Hence, $z_{\rho_{\lim}}\left([0, 2\pi)\right) \subset \mathscr{S}^+$ as opposed to the case $\mu > 1$ in which $z_{\rho_{\lim}}\left([0, 2\pi)\right) \subset \mathbb{C} \setminus \mathscr{S}^+$ because $\rho_{\lim} < \rho_{\min}$. To clearly differentiate among the behaviours (5.91)–(5.92)–(5.93) of the trajectories included in $\mathscr{S}^+$, it is convenient to introduce the following partition of $\mathscr{S}^+$:

$$\mathscr{S}^+ = \mathscr{S}_E^+ \cup z_{\rho_{\lim}}\left([0, 2\pi)\right) \cup \mathscr{S}_C^+,$$

where

$$\mathscr{S}_E^+ \triangleq \bigcup_{\rho_{\min} < \rho < \rho_{\lim}} z_\rho\left([0, 2\pi)\right) \quad \text{and} \quad \mathscr{S}_C^+ \triangleq \bigcup_{\rho_{\lim} < \rho} z_\rho\left([0, 2\pi)\right).$$

Interpreting (5.91)–(5.92)–(5.93) as progressive time t increases (i.e., as retrogressive time τ decreases), the set $\mathscr{S}_C^+$ may be associated with a *contractive* behaviour in the sense of (5.92), while the set $\mathscr{S}_E^+$ may be associated with an *expansive* behaviour in the sense of (5.93). The set $z_{\rho_{\lim}}\left([0, 2\pi)\right)$ lies at the common boundary between $\mathscr{S}_C^+$ and $\mathscr{S}_E^+$. In Figures 5.18 and 5.19, $\mathscr{S}_E^+$ is indicated by the light-shaded area, while the (non-bounded) non-shaded area corresponds to $\mathscr{S}_C^+$.

Note that for $\rho \geq \rho_{\lim}$ the length 2π selected for the integration interval of the RPE, was correct. If it had been selected as $[0, \tau_{\max}]$ with $\tau_{\max} \geq 2\pi$, each member of the collection $\{z_\rho\left([0, \tau_{\max}]\right) : \rho > \rho_{\lim}\}$ would have intersected another member of the same collection after a full rotation around the origin of its corresponding co-state. But for $\rho < \rho_{\lim}$, the integration of the RPE could have been carried out over a retro-time interval of length larger than 2π. Since all that matters about the co-state (for the integration of the state retrograde path equation) is its direction, but not its magnitude, the integration could have been continued seamlessly concatenating (backwards in time): $z_\rho\left([0, 2\pi)\right)$, $z_{P^{-1}(\rho)}\left([0, 2\pi)\right)$, ..., $z_{P^{-n}(\rho)}\left([0, 2\pi)\right)$ into a single trajectory for every $n \in \mathbb{N}$. However, since $\lim_{n\to\infty} P^{-n}\left(\rho\right) = -\infty$ for $\rho < \rho_{\lim}$, there exists a $N = N\left(\rho\right) \in \mathbb{N}$ such that $P^{-N}\left(\rho\right) < \rho_{\min}$. Consequently, the concatenated trajectory $\bigcup_{n=0}^{N} z_{P^{-n}(\rho)}\left([0, 2\pi)\right)$ fails to be semi-permeable at some point of $z_{P^{-N}(\rho)}\left([0, 2\pi)\right)$. However, for $\rho > P^{-1}\left(\rho_{\min}\right)$, the concatenation (now, forward in time) of the trajectories $z_\rho\left([0, 2\pi)\right)$, $z_{P(\rho)}\left([0, 2\pi)\right)$, ..., $z_{P^n(\rho)}\left([0, 2\pi)\right)$, ..., is not limited by loss of semi-permeability. The resulting concatenated trajectory $\bigcup_{n=0}^{\infty} z_{P^n(\rho)}\left([0, 2\pi)\right)$ has $z_{\rho_{\lim}}\left([0, 2\pi)\right)$ as its limit cycle, represented by the thick curve labelled LC in Figures 5.18 and 5.19.

The existence of this one-sided limit cycle (from the inside) in the semi-permeable domain $\mathscr{S}^+$ is the most salient difference of the case $\mu > 1$ with respect to the case $\mu < 1$.

5.8.1. The solution of the Isaacs' equation in the semi-permeable domain

From the collection $\{z_\rho\left([0, 2\pi)\right) : \rho > \rho_{\min}\}$ a solution $\mathcal{V}$ of (5.17)–(5.18), defined on $\mathscr{S}^+$, can be constructed for the case $\mu < 1$ analogously to case $\mu > 1$ redefining, however, the sets $\mathscr{A}_1, \ldots, \mathscr{A}_5$ introduced in Subsection 5.7.2 as follows:

$$\mathscr{A}_1 \triangleq \left\{ w \in \mathbb{C} \; : \; \mathcal{M}_a^{b-a}\left(w\right) > \left(\mu_1 \mathrm{e}^{-\kappa\left(\frac{\pi}{2}+\beta\right)} - \mu_2\right) \mathrm{e}^{-\kappa\left(\frac{\pi}{2}-\beta\right)} + \mu_1 \; \wedge \; \mathcal{A}_a^{b-a}\left(w\right) \in [0,\gamma_1] \right\},$$

$$\mathscr{A}_2 \triangleq \left\{ w \in \mathbb{C} \; : \; \mathcal{M}_b^{b-c}\left(w\right) > \mu_1 \mathrm{e}^{-\kappa\left(\frac{\pi}{2}+\beta\right)} - \mu_2 \; \wedge \; \mathcal{A}_b^{b-c}\left(w\right) \in [0,\gamma_2] \right\},$$

$$\mathscr{A}_3 \triangleq \left\{ w \in \mathbb{C} \; : \; \mathcal{M}_c^{d-c}\left(w\right) > \mu_1 \; \wedge \; \mathcal{A}_c^{d-c}\left(w\right) \in [0,\gamma_3] \right\},$$

$$\mathscr{A}_4 \triangleq \left\{ w \in \mathbb{C} \; : \; \mathcal{M}_d^{d-a}\left(w\right) > 0 \; \wedge \; \mathcal{A}_d^{d-a}\left(w\right) \in [0,\gamma_4] \right\},$$

$$\mathscr{A}_5 \triangleq \left\{ w \in \mathbb{C} \; : \; \mathcal{M}_a^{b-a}\left(w\right) > \mu_2 \mathrm{e}^{\kappa\gamma_3} \; \wedge \; \mathcal{A}_a^{b-a}\left(w\right) \in (\gamma_1,\gamma_3) \right\};$$

where the angles $\gamma_1, \ldots, \gamma_4$ are defined, in terms of α and β, as indicated in Figure 5.5, and the functions $\mathcal{A}_o^v : \mathbb{C}\setminus\{o\} \to (-\pi,\pi]$ and $\mathcal{M}_o^v : \mathbb{C} \to [0,\infty)$, parametric on $o,v \in \mathbb{C}$ such that $v \neq 0$, are the ones introduced in Subsubsections 4.2.2.2 and 4.2.2.3. The collection $\{\mathscr{A}_1, \ldots, \mathscr{A}_5\}$, as just specified, is a partition of $\mathscr{S}^+$ for the case $\mu < 1$.

Having redefined, for $\mu < 1$, the sets $\mathscr{A}_1, \ldots, \mathscr{A}_5$, the construction of the functions $\mathcal{V} : \mathscr{S}^+ \to \mathbb{R}$, $\tilde{u}_\mathcal{V}^* : \mathscr{S}^+ \to U$, and $\tilde{\sigma}_\mathcal{V}^* : \mathscr{S}^+ \to \Sigma$ follows the same formulation detailed in Subsection 5.7.2.

Observe in Figure 5.18 the *switching* rays that result from the recommended strategies $\tilde{u}_\mathcal{V}^*$ and $\tilde{\sigma}_\mathcal{V}^*$ derived from $\mathcal{V}$. Each of these switching rays lies in one of the following common boundaries: either $(\partial\mathscr{A}_1)\cap(\partial\mathscr{A}_2)$, $(\partial\mathscr{A}_2)\cap(\partial\mathscr{A}_3)$, $(\partial\mathscr{A}_3)\cap(\partial\mathscr{A}_4)$, or $(\partial\mathscr{A}_4)\cap(\partial\mathscr{A}_5)$.

5.8.2. A candidate solution

In accordance with the nomenclature of the previous section, the *island*

$$\mathscr{I}^+ \triangleq \mathbb{C} \setminus \mathscr{S}^+$$

(represented in Figure 5.18 by the dark-shaded area) seems, a priori, somehow mysterious. However, considering analogous arguments to the ones used in Subsections 5.7.3 and 5.7.4, its nature is readily revealed also for the case $\mu < 1$.

Recall P's counter-clockwise circulation power in the semi-permeable domain discussed in Subsection 5.7.3. This power can be checked to be at P's disposal for every state in $\mathscr{S}^+ = \mathscr{S}_E^+ \cup z_{\rho_\mathrm{lim}}\left([0,2\pi)\right) \cup \mathscr{S}_C^+$. In addition, it can be extended naturally form $\mathscr{S}^+$ to $z_{\rho_\mathrm{min}}\left([0,2\pi)\right) \subset \mathrm{cl}\left(\mathscr{S}^+\right)$, taking care to extend P's strategy at the corner point $d \in z_{\rho_\mathrm{min}}\left([0,2\pi)\right)$ from $\mathscr{A}_3$ (not from $\mathscr{A}_4$ or $\mathscr{A}_5$). Note that for the case $\mu < 1$, the point $d \notin \mathscr{S}^+$ plays the roll point b plays for the case $\mu > 1$, i.e., d is the unique corner of $\{z_{\rho_\mathrm{min}}\left(\tau\right) \; : \; \tau \in (0,2\pi)\}$.

Consider a play that starts at a point $z \in \mathrm{int}\left(\mathscr{I}^+\right)$. The following are observations in connection with the possible progressive time evolutions of the play.

First, if E manages to prevent the state from entering into $\mathrm{cl}\left(\mathscr{S}^+\right)$, P can pull the state to come arbitrarily close to d in finite time by applying the constant control action $i_o^\triangledown + \mathrm{j}$. Proposition 4.3.1 provides the logical support for this claim (if it is invoked taking $q_1 = d$, $q_2 = a$, and $z_0 = z$).[1] This manoeuvre will be

---

[1]If E happens to be limited by a discrete control set of the form $\{0,1\}$ and a positive
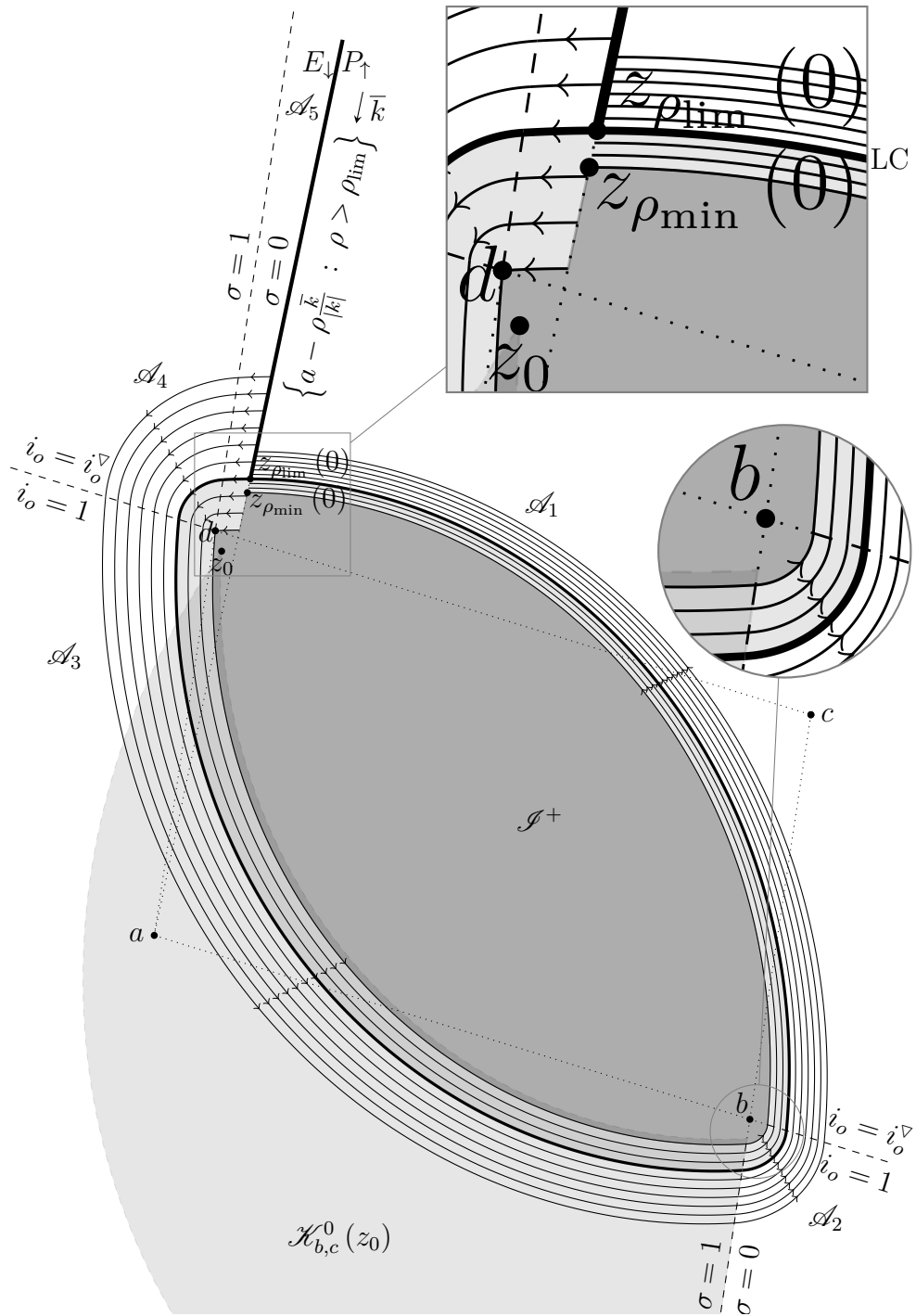
Figure 5.20: Illustration of how P's counter-clockwise circulation power can be extended from $\mathscr{A}_3$ slightly into $\mathscr{I}^+$.

referred as *P's pull-back manoeuvre* as in Subsection 5.7.5, although now, for the case $\mu < 1$, P pulls the state towards the line $\overleftrightarrow{da}$ (instead of the line $\overleftrightarrow{bc}$). Assume that E effectively manages to prevent the state from entering $\mathrm{cl}\left(\mathscr{S}^{+}\right)$.

Second, once the state is sufficiently close to d, such that P's circulation power can be extended, from $\mathscr{A}_3$, $\mathscr{A}_2$, and $\mathscr{A}_1$, slightly into $\mathscr{I}^+$ (loosely speaking for example when the state is at the point z_0 in Figure 5.20); P can force the state to circulate counter-clock-wisely (as it would do in $\mathscr{S}^+$). In Figure 5.20, the first of the three stages of the aforementioned state circulation takes place in the set $\mathscr{K}_{b,d}^0\left(z_0\right)$ (as defined in Corollary 4.3.1) represented by the curved shaded area with a vertex at z_0 which does not fit entirely into the figure. After the state circulates close to $\mathscr{A}_3$, $\mathscr{A}_2$, and $\mathscr{A}_1$ (perhaps entering one of these sets if E plays unwisely), P achieves an oriented distance to $\mathscr{T}^+$ which is *at most* an approximation from above of $\mathrm{d}_{\mathrm{o}}\left(z_{\rho_{\min}}\left(0\right),\mathscr{T}^+\right) = 1 - \Im z_{\rho_{\min}}\left(0\right)$. If E prevents the state from entering $\mathscr{S}^+$, P can still obtain *arbitrarily* good approximations (from above) of $1 - \Im z_{\rho_{\min}}\left(0\right)$ by first letting the state approach the point d *sufficiently*. If this is the case, by contrast with the case $\mu > 1$, when P attains such approximation he does not content himself. Instead, he *continues* the play forcing the state into $\mathscr{S}_E^+$ (the light-shaded area in Figure 5.18).

Third, once the state is in $\mathscr{S}_E^+$, by unlimited use of its circulation power over an infinite time horizon, P can guarantee for himself an outcome which is *at most* $\mathrm{d}_{\mathrm{o}}\left(z_{\rho_{\lim}}\left(0\right),\mathscr{T}^+\right) = 1 - \Im z_{\rho_{\lim}}\left(0\right)$. If E continues playing optimally this outcome is only approximated (not attained) as $\mathfrak{t} \to \infty$, because the state follows and expanding trajectory in $\mathscr{S}_E^+$ towards the limit cycle $z_{\rho_{\lim}}\left(\left[0, 2\pi\right)\right)$.

Summing up, for each initial state in $\mathscr{I}^+$, P can take the state into $\mathscr{S}_E^+$ in finite time and from there guarantee for himself an outcome which is at most $1 - \Im z_{\rho_{\lim}}\left(0\right)$ by unlimited use of its counter-clockwise circulation power. This asks for defining $1 - \Im z_{\rho_{\lim}}\left(0\right)$ as the value of the game in the set $\mathbb{C}\backslash\mathscr{S}_C^+ = \mathscr{I}^+ \cup \mathscr{S}_E^+ \cup z_{\rho_{\lim}}\left(\left[0, 2\pi\right)\right)$ which has the limit cycle $z_{\rho_{\lim}}\left(\left[0, 2\pi\right)\right)$ as its boundary.

For an initial state $z \in \mathscr{S}_C^+$, the value $\mathcal{V}\left(z\right)$ promised by $\mathcal{V}$ to P, provided he makes use of its circulation power, looks reasonable if $\mathcal{V}\left(z\right) \leq 1 - \Im z$. However, if $1 - \Im z < \mathcal{V}\left(z\right)$ the value $\mathcal{V}\left(z\right)$ is misleading because the state is "already" at an oriented distance to $\mathscr{T}^+$ which is less than the value promised by $\mathcal{V}$. This asks for the pruning of the semi-permeable characteristic trajectories of $\mathscr{S}_C^+$, in analogous manner as the trajectories of (the whole of) $\mathscr{S}^+$ must be pruned for the case $\mu > 1$, as explained in Subsubsection 5.7.6.1.

Taking into account the above considerations, next the formulation of the a *candidate solution* for the case $\mu < 1$ is provided. As for the case $\mu > 1$, the construction involves the two steps: extension and comparison.

1. <u>Extension</u> – Define $\mathcal{V}_{\mathrm{aux}} : \mathbb{C} \to \mathbb{R}$ and $\tilde{p}_{\mathrm{aux}}^* : \mathbb{C} \to \mathbb{C}$ as the following

---

dwell time between consecutive switchings, he cannot prevent the state from reaching the line $\overleftrightarrow{ad}$ in finite time (as granted by Proposition 4.3.4, taking $q_1 = d$, $q_2 = a$, and $z_0 = z$) and therefore reaching $\mathrm{cl}\left(\mathscr{S}^+\right)$.

extensions of $\mathcal{V}$ and $\nabla\mathcal{V}$, respectively, to the whole complex plane:

$$\mathcal{V}_{\mathrm{aux}}(z) \triangleq \begin{cases} \mathcal{V}(z) & \text{if } z \in \mathscr{S}_C^+, \\ 1 - \Im\left(z_{\rho_{\lim}}(0)\right) & \text{otherwise, i.e., } z \in \mathscr{I}^+ \cup \mathscr{S}_E^+ \cup z_{\rho_{\lim}}([0, 2\pi)); \end{cases}$$

$$\tilde{p}_{\mathrm{aux}}^*(z) \triangleq \begin{cases} \nabla\mathcal{V}(z) & \text{if } z \in \mathscr{S}^+, \\ -\mathrm{j} & \text{if } z = z_{\rho_{\min}}(0), \\ \displaystyle\lim_{\mathscr{S}^+ \ni w \to z} \nabla\mathcal{V}(w) & \text{if } z \in z_{\rho_{\min}}((0, 2\pi)) \setminus \{d\}, \\ \displaystyle\lim_{\mathscr{A}_3 \ni w \to d} \nabla\mathcal{V}(w) & \text{if } z = d, \\ \mathrm{e}^{\frac{1}{2}\left(\frac{\pi}{2} - \beta\right)\overline{k}} \displaystyle\lim_{\mathscr{A}_3 \ni w \to d} \nabla\mathcal{V}(w) & \text{otherwise, i.e., } z \in \mathrm{cl}\left(\mathscr{I}^+\right) \setminus z_{\rho_{\min}}([0, 2\pi)). \end{cases}$$

2. $\underline{\text{Comparison}}$ – Use $\mathcal{V}_{\mathrm{aux}}$ and $\tilde{p}_{\mathrm{aux}}^*$ as defined above, to define $\mathcal{V}_{\mathrm{d_o}}^+ : \mathbb{C} \to \mathbb{R}$ and $\tilde{p}_+^* : \mathbb{C} \to \mathbb{C}$ as follows:

$$\mathcal{V}_{\mathrm{d_o}}^+(z) \triangleq \min\left\{\mathcal{V}_{\mathrm{aux}}(z), 1 - \Im z\right\}; \tag{5.94}$$

$$\tilde{p}_+^*(z) \triangleq \begin{cases} \tilde{p}_{\mathrm{aux}}^*(z) & \text{if } \mathcal{V}_{\mathrm{aux}}(z) \leq 1 - \Im z, \\ -\mathrm{j} & \text{otherwise.} \end{cases} \tag{5.95}$$

Finally, use $\tilde{p}_+^*$ to define $\tilde{u}_+^* : \mathbb{C} \to U$ and $\tilde{\sigma}_+^* : \mathbb{C} \to \Sigma$ as follows:

$$\tilde{u}_+^*(z) \triangleq u^*\left(\tilde{p}_+^*(z)\right), \tag{5.96}$$

$$\tilde{\sigma}_+^*(z) \triangleq \sigma^*\left(\tilde{p}_+^*(z)\right); \tag{5.97}$$

where $u^* : \mathbb{C} \to U$ and $\sigma^* : \mathbb{C} \to \Sigma$ are the functions defined in statement 2 of Proposition 4.4.1.

From the comparison step the set

$$\mathscr{R}^+ \triangleq \left\{z \in \mathbb{C} \ : \ 1 - \Im z < \mathcal{V}_{\mathrm{aux}}(z)\right\},$$

called the *ramp* arises, in accordance with the nomenclature of the previous section. In Figure 5.21 part of the set $\mathscr{R}^+$ is represented by the area filled by the dot-dashed segments that equalize the imaginary part of the endpoints of each depicted pruned semi-permeable characteristic trajectory.

As explained in Subsection 5.7.7, when the state is in $\mathscr{R}^+$, the focus of both players turns to the *current rate of change* of the oriented distance to $\mathscr{T}^+$, rather than the minimum oriented distance to the $\mathscr{T}^+$ on an infinite time horizon. For this reason, $\tilde{u}_+^*(z)$ and $\tilde{\sigma}_+^*(z)$ are defined (also for the case $\mu < 1$) as $u^*(-\mathrm{j})$ and $\sigma^*(-\mathrm{j})$, respectively.

In accordance with the nomenclature of the previous section, the set

$$\mathscr{P}^+ \triangleq \underset{w \in \mathbb{C}}{\arg\max} \ \mathcal{V}_{\mathrm{d_o}}^+(w)$$

will be referred to as the *plateau* of $\mathcal{G}_{\mathrm{dist}}^+$ because the function $\mathcal{V}_{\mathrm{d_o}}^+$ (as defined in above) takes the constant value $\max_{z \in \mathbb{C}} \mathcal{V}_{\mathrm{d_o}}^+(z) = 1 - \Im z_{\rho_{\lim}}(0)$ in this closed
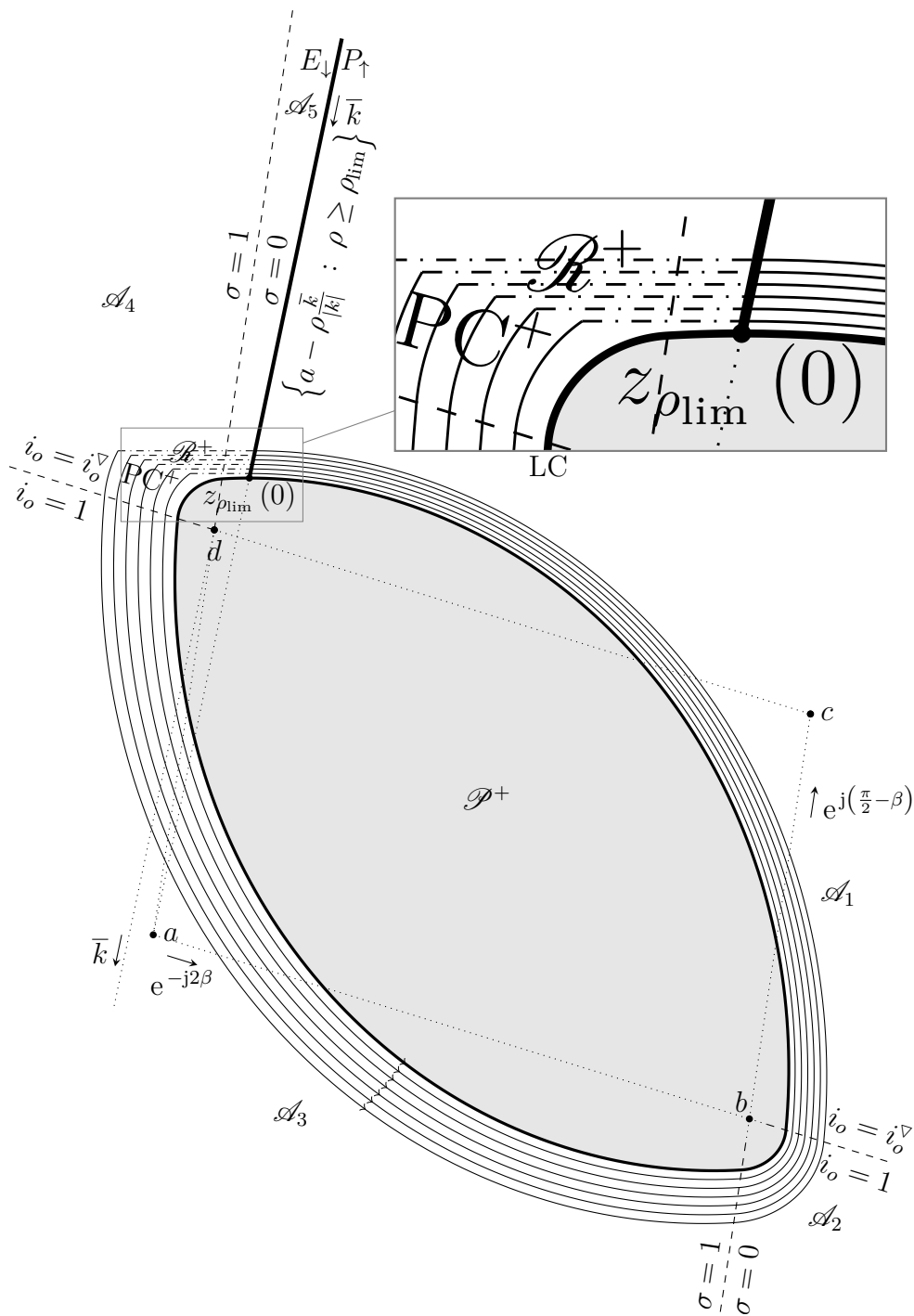
Figure 5.21: The pruning curve (PC^+) arises by comparison of the *current* oriented distance to the target set and P's *potentially attainable* oriented distance to the target set against optimal opposition from E, regardless of the sign of $\mu - 1$. However, if $\mu < 1$, as for the case illustrated, it has an endpoint at the point $z_{\rho_{\lim}}(0)$ which belongs to the limit cycle (LC).

subset of $\mathbb{C}$. For the case $\mu > 1$ it was mentioned that $\mathscr{P}^+ = \mathscr{I}^+ \setminus \mathscr{R}^+$. By contrast for the case $\mu < 1$ it can be verified that

$$\mathscr{P}^+ = \mathbb{C} \setminus \mathscr{S}_C^+ = \mathscr{I}^+ \cup z_{\rho_{\min}}\left([0, 2\pi)\right) \cup \mathscr{S}_E^+. \tag{5.98}$$

Observe that the topography of $\mathcal{V}_{\mathrm{d_o}}^+$ for the case $\mu > 1$ is clearly differentiable from the case $\mu < 1$ by the shape of $\mathscr{P}^+$ (compare Figures 5.14 and 5.21). For the former case, $\partial \mathscr{P}^+$ is a curve with two corner points, while for the later is corner-free curve (in fact it is the curve $z_{\rho_{\lim}}\left([0, 2\pi)\right)$). In both cases, $\mathcal{V}_{\mathrm{d_o}}^+$ results to be a quasi-concave function, since all its sup-level sets are convex.

5.8.3. Validation of the candidate solution

The candidate solution proposed in Subsection 5.8.2 for the case $\mu < 1$ can be validated following an analogous approach to the one described in Subsection 5.7.8 for the case $\mu > 1$.

The first step of such approach is to define a slight modification of P's strategy in order to endow P with a way of forcing the state into $\mathscr{S}_E^+$ from initial states in $\mathscr{I}^+$. More precisely, define an ϵ-modification of $\tilde{u}_+^* : \mathbb{C} \to U$ for the case $\mu < 1$ as a function $\tilde{u}_+^{*\epsilon} : \mathbb{C} \to U$ such that

$$\tilde{u}_+^{*\epsilon}(z) \triangleq \begin{cases} i_o^{\triangledown} + \mathsf{j} & \text{if } z \in \mathscr{B}_{\epsilon'}, \\ \tilde{u}_+^*(z) & \text{otherwise,} \end{cases} \tag{5.99}$$

where

$$\mathscr{B}_{\epsilon'} \triangleq \mathscr{I}^+ \cap \left(\left\{ w \in \mathbb{C} : \mathcal{M}_a^{b-a}(w) \geq \left(\rho_{\min} - \frac{\epsilon'}{\cos \alpha} \right) \mathrm{e}^{\kappa \gamma_1} \wedge \mathcal{A}_a^{b-a}(w) \in [0, \gamma_1] \right\} \right.$$

$$\cup \left\{ w \in \mathbb{C} : \mathcal{M}_b^{b-c}(w) \geq \left(\left(\rho_{\min} - \frac{\epsilon'}{\cos \alpha} \right) \mathrm{e}^{\kappa \gamma_1} - \mu_1 \right) \mathrm{e}^{\kappa \gamma_2} \wedge \mathcal{A}_b^{b-c}(w) \in [0, \gamma_2] \right\}$$

$$\left. \cup \left\{ w \in \mathbb{C} : \mathcal{M}_c^{b-c}(w) \geq \left(\left(\rho_{\min} - \frac{\epsilon'}{\cos \alpha} \right) \mathrm{e}^{\kappa \gamma_1} - \mu_1 \right) \mathrm{e}^{\kappa \gamma_2} + \mu_2 \wedge \mathcal{A}_c^{b-c} < 0 \right\} \right)$$

and $\epsilon' \in (0, \epsilon)$ is such that:

- $\left(\rho_{\min} - \frac{\epsilon'}{\cos \alpha} \right) \mathrm{e}^{\kappa \gamma_1} > \mu_1$, i.e., such that the auxiliary point

$$e \triangleq b + \mathrm{e}^{-k\gamma_2} \left(a + \mathrm{e}^{-k\gamma_1} \left(z_{\rho_{\min}}(0) + \frac{\epsilon'}{\cos \alpha} \frac{\overline{k}}{|k|} - a \right) - b \right)$$

  lies between b and d_c in segment $\underline{bd_c}$ (see Figure 5.16);

- there exists an unique transverse intersection point between the c-centred arc of α-equiangular spiral

$$\left\{ w \in \mathbb{C} : \mathcal{M}_c^{b-c}(w) = \left(\left(\rho_{\min} - \frac{\epsilon'}{\cos \alpha} \right) \mathrm{e}^{\kappa \gamma_1} - \mu_1 \right) \mathrm{e}^{\kappa \gamma_2} + \mu_2 \wedge \mathcal{A}_c^{b-c}(w) < 0 \right\}$$
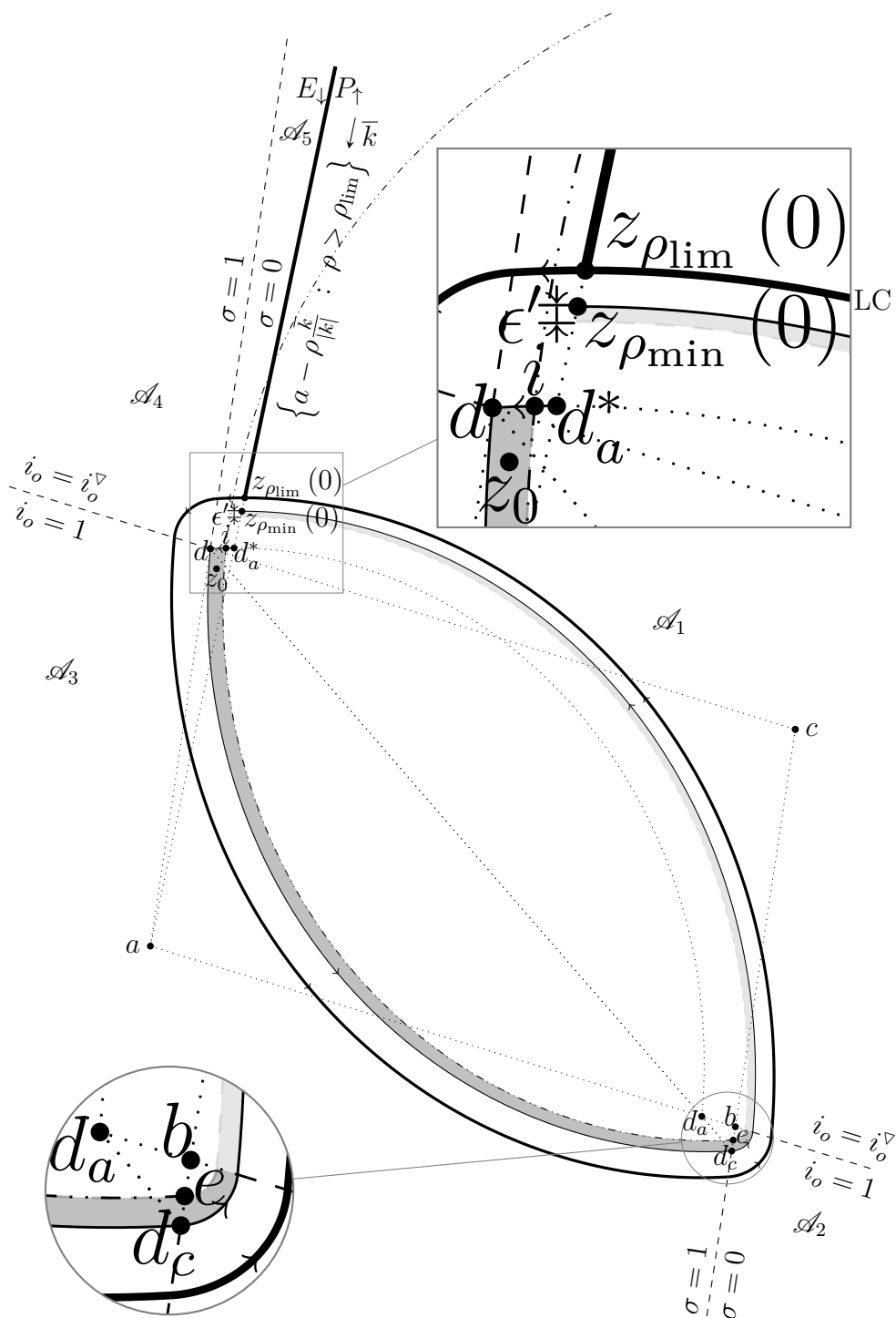
Figure 5.22: If $\mu < 1$, the band $\mathscr{B}_{\epsilon'}$ (represented by the union of the two shaded areas) is defined so as to extend P's circulation power from $\mathscr{A}_1$, $\mathscr{A}_2$, and $\mathscr{A}_3$, slightly into $\mathscr{I}^+$. Accordingly, in the light-shaded area P's modified strategy is defined as $i_o^\triangledown + \mathsf{j}$, while in the dark-shaded area it is defined as $1 + \mathsf{j}$.

and the a-centred arc α-equiangular spiral $\widehat{d, d_a^*}$ (see Figure 5.16 where the former arc of spiral is indicated by the dash-dot-dotted curve and the intersection point is labelled i).

The conditions involved in the above definition of $\tilde{u}_+^{*\epsilon}$ are *sufficient* to guarantee a geometric configuration (as the one depicted in Figure 5.22) such that P can exploit his circulation power in $\mathscr{B}_{\epsilon'}$ in order to force the state to cross the ray $\left\{ a - \rho \frac{\overline{k}}{|k|} \ : \ \rho > 0 \right\}$ (from $P_\uparrow$ to $E_\downarrow$) in finite time (along its way to the line $\overleftrightarrow{da}$) at a point whose imaginary part is not less than $\Im z_{\rho_{\min}}(0) - \epsilon'$. Corollary 4.3.1 and Propositions 4.3.1 and 4.3.2 used analogously as in Subsection 5.7.3 justify this loose statement more rigorously. Hereby, P can force the state out of $\mathscr{B}_{\epsilon'}$ into $\mathscr{S}_E^+$, from where he can obtain an outcome which is at most equal to $\mathrm{d_o}\left(z_{\rho_{\lim}}(0), \mathscr{T}^+ \right) = 1 - z_{\rho_{\lim}}(0)$, by unlimited use of its circulation power.

If the state is originally in $\mathscr{I}^+$, P can force it into either into $\mathscr{B}_{\epsilon'}$ or $\mathscr{S}_E^+$ in finite time just by applying $u = i_o^\triangledown + \mathrm{j}$ while the state remains in $\mathscr{I}^+ \setminus \mathscr{B}_{\epsilon'}$, as prescribed by $\tilde{u}_+^*$.

Now, the following proposition can be stated to validate the proposed candidate solution.

Proposition 5.8.1. *In case the parameters of $\mathcal{G}_{\mathrm{dist}}^+$ are such that $\mu < 1$, there exists an ϵ-modification of $\tilde{u}_+^* : \mathbb{C} \to U$ for the case $\mu < 1$, denoted $\tilde{u}_+^{*\epsilon} : \mathbb{C} \to U$, such that*

$$\tilde{\mathcal{P}}_{f,\mathscr{T}^+}^{\mathrm{d_o}}\left(z, \tilde{u}_+^{*\epsilon}, \tilde{\sigma} \right) \leq \mathcal{V}_{\mathrm{d_o}}^+(z) \leq \tilde{\mathcal{P}}_{f,\mathscr{T}^+}^{\mathrm{d_o}}\left(z, \tilde{u}, \tilde{\sigma}_+^* \right) \quad \forall z, \tilde{u}, \tilde{\sigma}, \qquad (5.100)$$

where $\mathcal{V}_{\mathrm{d_o}}^+ : \mathbb{C} \to \mathbb{R}$, $\tilde{u}_+^* : \mathbb{C} \to U$ and $\tilde{\sigma}_+^* : \mathbb{C} \to \mathbf{\Sigma}$ are the functions defined in Subsection 5.8.2 .

Proof. The proof goes along the same line of the proof of Proposition 5.7.1. However, certain particularities should be mentioned.

First, the construction of an ϵ-modification of $\tilde{u}_+^* : \mathbb{C} \to U$ for the case $\mu < 1$ (clearly defined differently from the case $\mu > 1$) is needed to guarantee that P can take the state away from $\mathscr{I}^+$ into $\mathscr{S}_E^+$. For such construction any $\epsilon > 0$ is useful, because the relevant existence conditions are imposed on $\epsilon' \in (0, \epsilon)$ within the definition of $\tilde{u}_+^{*\epsilon}$. However, once the state is in $\mathscr{S}_E^+$, P can force the state to circulate closer and closer to the limit cycle $z_{\rho_{\lim}}([0, 2\pi))$ in case E manages to keep the state in $\mathscr{S}_E^+$. For this reason $\tilde{\mathcal{P}}_{f,\mathscr{T}^+}^{\mathrm{d_o}}\left(z, \tilde{u}_+^{*\epsilon}, \tilde{\sigma} \right) \leq \mathcal{V}_{\mathrm{d_o}}^+(z) = 1 - \Im z_{\rho_{\lim}}(0)$ for every $z \in \mathscr{I}^+ \cup \mathscr{S}_E^+ \cup z_{\rho_{\lim}}([0, 2\pi))$ without the presence of an ϵ quantity disfavouring P in the leftmost inequality (as it is the case if $\mu > 1$ according to Proposition 5.7.1).

Second, as in the proof of Proposition 5.7.1, special attention must be given to the corner points of the boundary of each sup-level set of $\mathcal{V}_{\mathrm{d_o}}^+$. The possibility that E might be unable to prevent the leakage of the state through one of such corner points from one level set into a lower sup-level set must be proved to be impossible. To this end, consider the following argument which, although similar, is simpler than for the case $\mu > 1$.

Now, for the case $\mu < 1$, every corner point of a sup-level set of $\mathcal{V}_{d_o}^+$ is necessarily a point that belongs to the pruning curve (see Figure 5.21) which by construction lies in $\mathscr{S}_C^+ \cap \{w \; : \; \Im w > \Im z_{\rho_{\lim}}(0)\}$. In addition, as for the case $\mu > 1$, the pruning curve must necessarily have each of its points in

$$\left(\mathscr{A}_5 \cup z_{\rho_{\min}}((\tau_4, 2\pi))\right) \cup \left(\mathscr{A}_4 \cup z_{\rho_{\min}}((\tau_3, \tau_4])\right) \cup \left(\mathscr{A}_3 \cup z_{\rho_{\min}}((\tau_2, \tau_3])\right). \quad (5.101)$$

Fix $z \in \mathscr{S}_C^+$ and let

$$\mathscr{N}(z) \triangleq \mathscr{L}_{\mathcal{V}_{d_o}^+}\left(\mathcal{V}_{d_o}^+(z)\right) = \left\{w \in \mathbb{C} \; : \; \mathcal{V}_{d_o}^+(w) \geq \mathcal{V}_{d_o}^+(z)\right\}$$

be its corresponding sup-level set. Let $\rho > \rho_{\lim}$ be the real number in terms of which the boundary of $\mathscr{N}(z)$ may be expressed as

$$\partial\mathscr{N}(z) = \underbrace{z_\rho\left([0, \tau_{\max}(\rho)]\right)}_{\mathscr{C}_{\mathrm{curve}}(\rho)} \cup \underbrace{\left\{w \in \mathbb{C} \; : \; \frac{w - z_\rho(0)}{z_\rho(\tau_{\max}(\rho)) - z_\rho(0)} \in (0, 1)\right\}}_{\mathscr{C}_{\mathrm{straight}}},$$

where the pruning point $z_\rho(\tau_{\max}(\rho))$, which belongs to (5.101), is the a-priori possibly leaking corner for E.

At $z_\rho(\tau_{\max}(\rho))$, E applies a control action $\tilde{\sigma}_+^*(z_\rho(\tau_{\max}(\rho)))$ that guarantees him that the state does not cross $\partial\mathscr{N}(z)$ into $\bigcup_{\lambda > \rho} z_\lambda[0, 2\pi)$. But, can E be sure that the same control action prevents the state from crossing $\partial\mathscr{N}(z)$ into the set $\{w \; : \; \Im w > \Im z_\rho(0)\}$? This could only happen if the imaginary part of the velocity vector $f\left(z_\rho(\tau_{\max}(\rho)), u, \tilde{\sigma}_+^*(z_\rho(\tau_{\max}(\rho)))\right)$ results to be positive for some control action $u \in U$ eligible by P. However, making use of the results of Subsection 4.3.5, it will be argued next that this hypothetical possibility can be ruled out. Consider the following cases:

- $z_\rho(\tau_{\max}(\rho)) \in \left(\mathscr{A}_5 \cup z_{\rho_{\min}}((\tau_4, 2\pi))\right)$.
  E's strategy $\tilde{\sigma}_+^*$ prescribes $\tilde{\sigma}_+^*(z_\rho(\tau_{\max}(\rho))) = 0$. Therefore, the state velocity vector, based at $z_\rho(\tau_{\max}(\rho))$, is

$$f\left(z_\rho(\tau_{\max}(\rho)), u, \tilde{\sigma}_+^*(z_\rho(\tau_{\max}(\rho)))\right) = F\left(z_\rho(\tau_{\max}(\rho)), q\right)$$

  with $q \in \underline{ab} = \left\{w \in \mathbb{C} \; : \; \frac{w-a}{b-a} \in [0,1]\right\}$. Assimilate, $\underline{ab}$ as the set $\mathscr{Q}$ of Subsection 4.3.5; the corresponding set $I^- \triangleq \left\{w \in \mathbb{C} \; : \; \Im F(w, q) < 0 \quad \forall q \in \mathscr{Q}\right\}$ was proved to coincide with $\left\{w \in \mathbb{C} \; : \; \overline{k} \otimes (w - q) < 0 \quad \forall q \in \mathscr{Q}\right\}$ in Subsection 4.3.5. In the current context, this supporting half-plane takes the form

$$\left\{w \in \mathbb{C} \; : \; (w - a) \otimes \overline{k} > 0\right\}$$

  which includes the set $\left(\mathscr{A}_5 \cup z_{\rho_{\min}}((\tau_4, 2\pi))\right)$ where the point $z_\rho(\tau_{\max}(\rho))$ lies. Thus, $\Im f\left(z_\rho(\tau_{\max}(\rho)), u, \tilde{\sigma}_+^*(z_\rho(\tau_{\max}(\rho)))\right) < 0$ for every $u \in U$.

- $z_\rho(\tau_{\max}(\rho)) \in \left(\mathscr{A}_4 \cup z_{\rho_{\min}}((\tau_3, \tau_4])\right) \cup \left(\mathscr{A}_3 \cup z_{\rho_{\min}}((\tau_2, \tau_3])\right)$.
  E's strategy $\tilde{\sigma}_+^*$ prescribes $\tilde{\sigma}_+^*(z_\rho(\tau_{\max}(\rho))) = 1$. Therefore, the state velocity vector, based at $z_\rho(\tau_{\max}(\rho))$, is

$$f\left(z_\rho(\tau_{\max}(\rho)), u, \tilde{\sigma}_+^*(z_\rho(\tau_{\max}(\rho)))\right) = F\left(z_\rho(\tau_{\max}(\rho)), q\right)$$

with $q \in \underline{dc} = \left\{ w \in \mathbb{C} \ : \ \frac{w-d}{c-d} \in [0,1] \right\}$. Assimilate, $\underline{dc}$ as the set $\mathscr{Q}$ of Subsection 4.3.5; the corresponding set $I^- \triangleq \left\{ w \in \mathbb{C} \ : \ \Im F(w,q) < 0 \quad \forall q \in \mathscr{Q} \right\}$ takes the form

$$\left\{ w \in \mathbb{C} \ : \ (w-d) \otimes \overline{k} > 0 \right\}. \tag{5.102}$$

The pruning point $z_\rho(\tau_{\max}(\rho)) \in (\mathscr{A}_4 \cup z_{\rho_{\min}}((\tau_3, \tau_4])) \cup (\mathscr{A}_3 \cup z_{\rho_{\min}}((\tau_2, \tau_3]))$ belongs to (5.102) because: i) by construction of the pruning curve for the case $\mu < 1$, each of its points has an imaginary part greater than $z_{\rho_{\lim}}(0)$, and ii) $\Im z_{\rho_{\lim}}(0) > \Im z_{\rho_{\min}}(0) > \Im a - P^{-1}(\rho_{\min}) \frac{\overline{k}}{|k|} = d_a^* > \Im d$ (see Figure 5.18). Thus, $\Im f\left(z_\rho(\tau_{\max}(\rho)), u, \tilde{\sigma}_+^*(z_\rho(\tau_{\max}(\rho))) \right) < 0$ for every $u \in U$.

$\square$

Proposition 5.8.1 tell us that, for the case $\mu < 1$, at least a pair of saddle-point strategies, denoted $(\tilde{u}_+^{*\epsilon}, \tilde{\sigma}_+^*)$, exists for $\mathcal{G}_{\text{dist}}^+$, i.e., a pair of strategies such that

$$\tilde{\mathcal{P}}_{f,\mathscr{T}+}^{\text{do}}(z, \tilde{u}_+^{*\epsilon}, \tilde{\sigma}) \leq \tilde{\mathcal{P}}_{f,\mathscr{T}+}^{\text{do}}(z, \tilde{u}_+^{*\epsilon}, \tilde{\sigma}_+^*) \leq \tilde{\mathcal{P}}_{f,\mathscr{T}+}^{\text{do}}(z, \tilde{u}, \tilde{\sigma}_+^*) \quad \forall z, \tilde{u}, \tilde{\sigma}.$$

From this fact, by application of Proposition 2.2.2, it can be concluded that $\mathcal{V}_{\text{do}}^+(\cdot) = \tilde{\mathcal{P}}_{f,\mathscr{T}+}^{\text{do}}(\cdot, \tilde{u}_+^{*\epsilon}, \tilde{\sigma}_+^*)$ is the VF of $\mathcal{G}_{\text{dist}}^+$ for the case $\mu < 1$.

5.9. Solution of the upward game for the case $\mu = 1$

This short section deals with the border case $\mu = 1$.

As before, the *semi-permeable domain* of $\mathcal{G}_{\text{dist}}^+$ is defined as

$$\mathscr{S}^+ \triangleq \bigcup_{\rho > \rho_{\min}} z_\rho([0, 2\pi)), \tag{5.103}$$

because for each $\rho < \rho_{\min}$, the characteristic trajectory $\{ z_\rho(\tau) \ : \ \tau \in (0, 2\pi) \}$ fails to be semi-permeable. The special curve $z_{\rho_{\min}}([0, 2\pi))$ clearly differentiates the case $\mu = 1$ from the other two because it presents *two* corner points, namely b and d. Recall that $z_{\rho_{\min}}([0, 2\pi))$ has b as its single corner point if $\mu > 1$, while it has d as its single corner point if $\mu < 1$. Even though semi-permeable, $z_{\rho_{\min}}([0, 2\pi))$ is not free of corners, as the semi-permeable characteristic curves included in $\mathscr{S}^+$.

Since $\mu = 1$, by (5.53), $\rho_{\min} = \rho_{\lim}$. On one hand, by contrast with the case $\mu < 1$, in this case $\mathscr{S}^+$, *lacks* an expansive subset in the sense of (5.93). On the other hand, by contrast with the case $\mu > 1$, the special trajectory $z_{\rho_{\lim}}([0, 2\pi))$, that verifies (5.91), *is* included in $\partial \mathscr{S}^+$. In fact, $z_{\rho_{\lim}}([0, 2\pi)) = z_{\rho_{\min}}([0, 2\pi)) = \partial \mathscr{S}^+$ if $\mu = 1$.

Although $z_{\rho_{\lim}}([0, 2\pi))$ verifies (5.91), it is *not* a limit cycle as in the case $\mu < 1$. Now, the maximal interval over which the RPE can be integrated without self-overlapping of the family of semi permeable state-space characteristics is $[0, 2\pi)$, for *every* member of the family.

The case $\mu = 1$ is the only case in which the closed curves $\overset{\circ}{b} = \widehat{b, b_a} \cup \{b\} \cup \widehat{b, b_c} \cup \{b_c\} \cup \widehat{b_c, b_a} \cup \{b_a\}$ and $\overset{\circ}{d} = \widehat{d, d_c} \cup \{d\} \cup \widehat{d, d_a} \cup \{d_a\} \cup \widehat{d_a, d_c} \cup \{d_c\}$ coincide (see Figure 5.8). Actually, $z_{\rho_{\lim}}([0, 2\pi)) = z_{\rho_{\min}}([0, 2\pi)) = \overset{\circ}{b} = \overset{\circ}{d}$ if $\mu = 1$.

The *island*

$$\mathscr{I}^+ \triangleq \mathbb{C} \setminus \mathscr{S}^+$$

not covered by semi-permeable corner-free characteristic state-space trajectories is comprised by the curve $z_{\rho_{\lim}}\left([0, 2\pi)\right)$ and the area enclosed by it.

As for the case $\mu > 1$, for initial states in $\mathscr{I}^+$, P must choose between either an outcome that is at most an arbitrarily good approximation (from above) of $\mathrm{d_o}\left(z_{\rho_{\min}}(0), \mathscr{T}^+\right)$, or the possibility of engaging himself in a never ending play while struggling to achieve an outcome that is at most equal to $\mathrm{d_o}\left(z_{\rho_{\min}}(0), \mathscr{T}^+\right)$. For this reason, the construction of a candidate solution of $\mathcal{G}_{\mathrm{dist}}^+$ and its validation for the case $\mu = 1$, has more in common with the case $\mu > 1$ than with the case $\mu < 1$. For completeness, this natural construction is formulated next.

For the case $\mu = 1$, define $\mathscr{A}_1$, …, $\mathscr{A}_5$, $\mathcal{V} : \mathscr{S}^+ \to \mathbb{R}$, $\tilde{u}_{\mathcal{V}}^* : \mathscr{S}^+ \to U$, and $\tilde{\sigma}_{\mathcal{V}}^* : \mathscr{S}^+ \to \boldsymbol{\Sigma}$ as in Subsection 5.7.2, and follow the next two steps.

1. <u>Extension</u> – Define $\mathcal{V}_{\mathrm{aux}} : \mathbb{C} \to \mathbb{R}$ and $\tilde{p}_{\mathrm{aux}}^* : \mathbb{C} \to \mathbb{C}$ as the following extensions of $\mathcal{V}$ and $\nabla \mathcal{V}$, respectively, to the whole complex plane:

$$\mathcal{V}_{\mathrm{aux}}(z) \triangleq \begin{cases} \mathcal{V}(z) & \text{if } z \in \mathscr{S}^+, \\ 1 - \Im\left(z_{\rho_{\min}}(0)\right) & \text{if } z = z_{\rho_{\min}}(0), \\ \lim\limits_{\mathscr{S}^+ \ni w \to z} \mathcal{V}(w) = 1 - \Im\left(z_{\rho_{\min}}(0)\right) & \text{if } z \in z_{\rho_{\min}}\left((0, 2\pi)\right), \\ \lim\limits_{\mathscr{S}^+ \ni w \to b} \mathcal{V}(w) = 1 - \Im\left(z_{\rho_{\min}}(0)\right) & \text{otherwise, i.e., } z \in \mathrm{int}\left(\mathscr{I}^+\right); \end{cases}$$

$$\tilde{p}_{\mathrm{aux}}^*(z) \triangleq \begin{cases} \nabla \mathcal{V}(z) & \text{if } z \in \mathscr{S}^+, \\ -\mathrm{j} & \text{if } z = z_{\rho_{\min}}(0), \\ \lim\limits_{\mathscr{S}^+ \ni w \to z} \nabla \mathcal{V}(w) & \text{if } z \in z_{\rho_{\min}}\left((0, 2\pi)\right) \setminus \{b, d\}, \\ \lim\limits_{\mathscr{A}_1 \ni w \to b} \nabla \mathcal{V}(w) & \text{if } z = b, \\ \lim\limits_{\mathscr{A}_3 \ni w \to d} \nabla \mathcal{V}(w) & \text{if } z = d, \\ \mathrm{e}^{\frac{1}{2}\left(\frac{\pi}{2} - \beta\right)\overline{k}} \lim\limits_{\mathscr{A}_1 \ni w \to b} \nabla \mathcal{V}(w) & \text{otherwise, i.e., } z \in \mathrm{int}\left(\mathscr{I}^+\right). \end{cases}$$

2. <u>Comparison</u> – Use $\mathcal{V}_{\mathrm{aux}}$ and $\tilde{p}_{\mathrm{aux}}^*$ as defined above, to define $\mathcal{V}_{\mathrm{d_o}}^+ : \mathbb{C} \to \mathbb{R}$ and $\tilde{p}_+^* : \mathbb{C} \to \mathbb{C}$ as follows:

$$\mathcal{V}_{\mathrm{d_o}}^+(z) \triangleq \min\left\{\mathcal{V}_{\mathrm{aux}}(z), 1 - \Im z\right\}; \tag{5.104}$$

$$\tilde{p}_+^*(z) \triangleq \begin{cases} \tilde{p}_{\mathrm{aux}}^*(z) & \text{if } \mathcal{V}_{\mathrm{aux}}(z) \le 1 - \Im z, \\ -\mathrm{j} & \text{otherwise.} \end{cases} \tag{5.105}$$

Finally, use $\tilde{p}_+^*$ to define $\tilde{u}_+^* : \mathbb{C} \to U$ and $\tilde{\sigma}_+^* : \mathbb{C} \to \boldsymbol{\Sigma}$ as follows:

$$\tilde{u}_+^*(z) \triangleq u^*\left(\tilde{p}_+^*(z)\right), \tag{5.106}$$

$$\tilde{\sigma}_+^*(z) \triangleq \sigma^*\left(\tilde{p}_+^*(z)\right); \tag{5.107}$$

where $u^* : \mathbb{C} \to U$ and $\sigma^* : \mathbb{C} \to \boldsymbol{\Sigma}$ are the functions defined in statement 2 of Proposition 4.4.1.
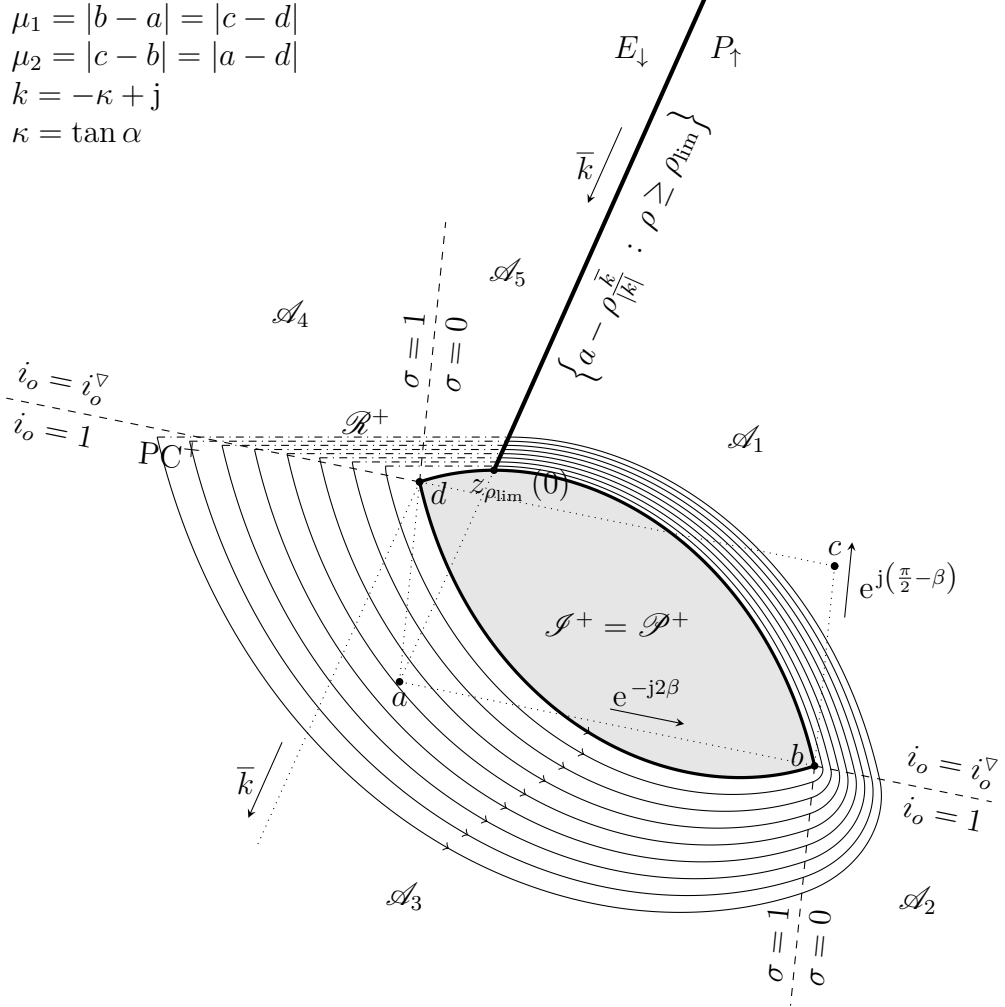
Figure 5.23: The topography of the VF of $\mathcal{G}_{\text{dist}}^{+}$ for a case such that $\frac{\mu_2}{\mu_1} e^{\kappa\left(\frac{\pi}{2}+\beta\right)} = 1$.

In Figure 5.23, the topography of the above constructed function $\mathcal{V}_{\text{d}_\text{o}}^{+} : \mathbb{C} \to \mathbb{R}$ is shown. Notice, that for $\mu = 1$, the *plateau*, defined as

$$\mathscr{P}^{+} \triangleq \arg\max_{w \in \mathbb{C}} \mathcal{V}_{\text{d}_\text{o}}^{+}(w)$$

coincides with $\mathscr{I}^{+} = \mathbb{C} \setminus \mathscr{S}^{+}$. In addition, as for the case $\mu < 1$, the pruning curve lies in $\{w : \Im w > \Im z_{\rho_{\text{lim}}}(0)\}$, having $z_{\rho_{\text{lim}}}(0)$ as its limiting endpoint.

The validation of the above construction is analogous to the case $\mu > 1$. Defining an ϵ-modification of $\tilde{u}_{+}^{*} : \mathbb{C} \to U$ for the case $\mu = 1$ exactly as for the case $\mu > 1$, natural analogous versions of Proposition 5.7.1 and Corollaries 5.7.1 and 5.7.2 for the case $\mu = 1$ can be stated and similarly proved. However, in the proof of the counterpart Proposition 5.7.1, to show that $\tilde{\sigma}_{+}^{*}$ prevents the leakage of the state from each sup-level to set of $\mathcal{V}_{\text{d}_\text{o}}^{+}$, even at the corner points of its

boundary, the argument goes simpler as in the proof of Proposition 5.8.1 (which deals with the case $\mu < 1$), relaying on the fact that every point of the pruning curve has an imaginary part greater than $\Im z_{\rho_{\lim}}(0)$ if $\mu \leq 1$.

5.10. The downward game

As it was mentioned before, the downward game $\mathcal{G}_{\mathrm{dist}}^-$ can be treated analogously to the upward game $\mathcal{G}_{\mathrm{dist}}^+$. The whole process by which a solution for $\mathcal{G}_{\mathrm{dist}}^+$ was first devised and finally validated, can be recreated step by step for $\mathcal{G}_{\mathrm{dist}}^-$.

However, making use of the geometric considerations exposed at the end of Subsection 5.2.4, this process may be spiked recognizing that both unilateral games are different instances of the same (coordinate-free) underlying game, being the only difference due to the fact that in general $d_o(a, \mathcal{T}^+) \neq d_o(c, \mathcal{T}^-)$, that is to say: $\Im a + \Im c \neq 0$ in general. In the particular case that $d_o(a, \mathcal{T}^+) = d_o(c, \mathcal{T}^-)$, i.e., in case the centre $\frac{a+c}{2} = \frac{b+d}{2}$ of the parallelogram $\mathrm{conv}(\{a, b, c, d\})$ lies on the real axis, each unilateral game is a central inversion version of the other, being $\frac{a+c}{2} = \frac{b+d}{2}$ the inversion point.

Whatever may be the path selected to approach the downward game, the counterparts $\mathcal{V}_{\mathrm{d}_o}^-$, $\tilde{u}_-^*$, and $\tilde{\sigma}_-^*$ (within $\mathcal{G}_{\mathrm{dist}}^-$) of $\mathcal{V}_{\mathrm{d}_o}^+$, $\tilde{u}_+^*$, and $\tilde{\sigma}_+^*$ (within $\mathcal{G}_{\mathrm{dist}}^+$), respectively, can be checked to verify

$$\mathcal{V}_{\mathrm{d}_o}^-(z) = \mathcal{V}_{\mathrm{d}_o}^+(a + c - z) - (1 - \Im a) + (1 + \Im c), \qquad (5.108)$$

$$\tilde{u}_-^*(z) = u^*\left(\tilde{p}_+^*(a + c - z)\right), \qquad (5.109)$$

$$\tilde{\sigma}_-^*(z) = \sigma^*\left(\tilde{p}_+^*(a + c - z)\right), \qquad (5.110)$$

for every $z \in \mathbb{C}$, where $\mathcal{V}_{\mathrm{d}_o}^+ : \mathbb{C} \to \mathbb{R}$ and $\tilde{p}_+^* : \mathbb{C} \to \mathbb{C}$ are constructed as explained in Sections 5.7 to 5.9 (the specific section depending on the sign of $\mu - 1$). In agreement with the notation used throughout these three sections, the functions $u^* : \mathbb{C} \to U$ and $\sigma^* : \mathbb{C} \to \Sigma$ involved in (5.109) and (5.110) are the functions defined in statement 2 of Proposition 4.4.1.

The central inversion $z \mapsto a + c - z = a + \mathrm{e}^{\mathrm{j}\pi}(z - c) = \frac{a+c}{2} - \left(z - \frac{a+c}{2}\right)$ in (5.109)–(5.110) express algebraically how $\mathcal{G}_{\mathrm{dist}}^-$ must be though "up-side down" in order to conceive it as an instance of $\mathcal{G}_{\mathrm{dist}}^+$. With the mismatch $1 - \Im a = d_o(a, \mathcal{T}^+) \neq d_o(c, \mathcal{T}^-) = 1 + \Im c$ corrected in (5.108), though.

Thus, presented this way, the problem of solving $\mathcal{G}_{\mathrm{dist}}^-$ reduces to solving $\mathcal{G}_{\mathrm{dist}}^+$.

Relying on the previous arguments, define the *downward game's pseudo-gradient function* $\tilde{p}_-^* : \mathbb{C} \to \mathbb{C}$ as

$$\tilde{p}_-^*(z) \triangleq \tilde{p}_+^*(a + c - z)$$

for every $z \in \mathbb{C}$, in order to conveniently express the strategies (5.109)–(5.110) as

$$\tilde{u}_-^*(z) = u^*\left(\tilde{p}_-^*(z)\right),$$

$$\tilde{\sigma}_-^*(z) = \sigma^*\left(\tilde{p}_-^*(z)\right).$$

Finally, observe that $\mathcal{V}_{\mathrm{d}_o}^-$ (given by (5.108) in terms of $\mathcal{V}_{\mathrm{d}_o}^+$) shares with $\mathcal{V}_{\mathrm{d}_o}^+$ the following important properties that may be checked reviewing the construction of

$\mathcal{V}_{d_o}^+$. First, $\mathcal{V}_{d_o}^+$ is continuous, upper bounded, lower unbounded, quasi-concave and globally defined on $\mathbb{C}$. Second, the family of sup-level sets of $\mathcal{V}_{d_o}^+$ is a family of nested compact subsets of $\mathbb{C}$ that cover the whole complex plane. The arguments of the next section make use of these properties.

5.11. The bilateral game

In this section the original game in distance $\mathcal{G}_{\text{dist}}$ is finally approached. After all, its solution is the main goal of this chapter.

The bilateral nature of $\mathcal{G}_{\text{dist}}$, due to the fact that its target set $\mathscr{T}^+$ is split up into to connected components, was used to focus first on its two related unilateral games, namely $\mathcal{G}_{\text{dist}}^+$ and $\mathcal{G}_{\text{dist}}^-$. Having solved these two games, the way is paved for proposing a solution of $\mathcal{G}_{\text{dist}}$.

As for the unilateral games, the distinction of whether $\mu > 1$ or $\mu \leq 1$ is required to formulate a candidate solution.

5.11.1. Solution of the game in distance for the case $\mu > 1$

This case is treated first because it presents certain peculiarities that require a more careful analysis than the case $\mu \leq 1$.

5.11.1.1. A first attempt in proposing a solution

From the knowledge acquired while solving $\mathcal{G}_{\text{dist}}^+$ recall the following facts. Consider a play that starts at an arbitrary initial state $z \in \mathbb{C}$. On the one hand, for $z \in \mathscr{R}^{+\complement} = (\mathscr{S}^+ \setminus \mathscr{R}^+) \cup \mathscr{P}^+$, is P the player who actively forces matters so that the outcome of the play turns out to be (in the future) less or equal than $\mathcal{V}_{d_o}^+(z) + \epsilon$, being $\epsilon > 0$ an arbitrarily small number selected by P. In particular, if $z \in \text{cl}(\mathscr{S}^+ \setminus \mathscr{R}^+)$, P can force the final outcome to be at most $\mathcal{V}_{d_o}^+(z)$ by making use of its counter-clockwise circulation power. For $z \in \mathscr{P}^+ \setminus \text{cl}(\mathscr{S}^+ \setminus \mathscr{R}^+)$, P needs to perform a sufficiently long pull-back manoeuvre before applying its counter-clockwise circulation power to finally achieve an outcome bounded from above by $\mathcal{V}_{d_o}^+(z) + \epsilon$, being $\epsilon > 0$ as small as he wants. Against this, E may battle for a vanishing quantity ϵ, or simply defend himself so that the final outcome does not fall below $\mathcal{V}_{d_o}^+(z)$ materializing this defence by simply preventing the state from crossing the closed level curve of $\mathcal{V}_{d_o}^+$ that corresponds to the value $\mathcal{V}_{d_o}^+(z)$ in the outward direction. On the other hand, for $z \in \mathscr{R}^+$, P cannot enforce a future oriented distance to $\mathscr{T}^+$ lower than the current one $d_o(z, \mathscr{T}^+)$ (which obviously has already been attained). While the state remains in $\mathscr{R}^+$, E can impose a positive rate of change of the oriented distance to $\mathscr{T}^+$, but this does not alter the infimum oriented distance to $\mathscr{T}^+$ already attained by P (in the past).

Thinking about the four possibly non-empty intersections $\mathscr{R}^{+\complement} \cap \mathscr{R}^{-\complement}$, $\mathscr{R}^+ \cap \mathscr{R}^{-\complement}$, $\mathscr{R}^{+\complement} \cap \mathscr{R}^-$, and $\mathscr{R}^+ \cap \mathscr{R}^-$ that might occur between the sets $\mathscr{R}^{+\complement}$ and $\mathscr{R}^+$ of $\mathcal{G}_{\text{dist}}^+$, and the counterpart sets $\mathscr{R}^{-\complement}$ and $\mathscr{R}^-$ of $\mathcal{G}_{\text{dist}}^-$, it seems reasonable that if

faced with problem of having to choose between $\mathcal{G}_{\text{dist}}^+$ and $\mathcal{G}_{\text{dist}}^-$ at z, P will choose to play the game whose value function evaluated at z renders him the lower value (either already attained or to be attained in the future).

Note however that this argument implicitly assumes that if the outcome of the game has not already been attained at z, once P decides to play either $\mathcal{G}_{\text{dist}}^+$ or $\mathcal{G}_{\text{dist}}^-$, he will not doubt again an he will continue to play the selected game until its corresponding outcome is finally attained. Moreover, the possibility that P might continuously threaten E against *both* unilateral games is disregarded in the previous argument.

Even so, carrying along with the initiated line of reasoning let $\mathcal{V}_{\min} : \mathbb{C} \to \mathbb{R}$, defined as

$$\mathcal{V}_{\min}(z) \triangleq \min \left\{ \mathcal{V}_{\text{d}_{\text{o}}}^+(z), \mathcal{V}_{\text{d}_{\text{o}}}^-(z) \right\}, \tag{5.111}$$

be proposed as a first attempt in the synthesis of a VF for $\mathcal{G}_{\text{dist}}$. In accordance, the player's candidate optimal strategies should be defined as

$$\tilde{u}_{\min}^*(z) \triangleq u^*(\tilde{p}_{\min}^*(z)), \tag{5.112}$$

$$\tilde{\sigma}_{\min}^*(z) \triangleq \sigma^*(\tilde{p}_{\min}^*(z)), \tag{5.113}$$

where $u^* : \mathbb{C} \to U$ and $\sigma^* : \mathbb{C} \to \boldsymbol{\Sigma}$ are the functions defined in statement 2 of Proposition 4.4.1, and $\tilde{p}_{\min}^* : \mathbb{C} \to \mathbb{C}$ is defined as

$$\tilde{p}_{\min}^*(z) \triangleq \begin{cases} \tilde{p}_+^*(z) & \text{if } \mathcal{V}_{\text{d}_{\text{o}}}^+(z) < \mathcal{V}_{\text{d}_{\text{o}}}^-(z), \\ \tilde{p}_-^*(z) & \text{if } \mathcal{V}_{\text{d}_{\text{o}}}^-(z) < \mathcal{V}_{\text{d}_{\text{o}}}^+(z), \\ \tilde{p}_-^*(z) & \text{if } \mathcal{V}_{\text{d}_{\text{o}}}^+(z) = \mathcal{V}_{\text{d}_{\text{o}}}^-(z) \ \wedge \ \tilde{p}_+^*(z) \otimes \tilde{p}_-^*(z) > 0, \\ \tilde{p}_+^*(z) & \text{if } \mathcal{V}_{\text{d}_{\text{o}}}^+(z) = \mathcal{V}_{\text{d}_{\text{o}}}^-(z) \ \wedge \ \tilde{p}_+^*(z) \otimes \tilde{p}_-^*(z) < 0, \\ \tilde{p}_+^*(z) & \text{if } \mathcal{V}_{\text{d}_{\text{o}}}^+(z) = \mathcal{V}_{\text{d}_{\text{o}}}^-(z) \ \wedge \ \tilde{p}_+^*(z) \otimes \tilde{p}_-^*(z) = 0. \end{cases} \tag{5.114}$$

The thorough definition of $\tilde{p}_{\min}^*$ is done so as to preserve P's counter-clockwise circulation power even at the points where the functional values of $\mathcal{V}_{\text{d}_{\text{o}}}^+$ and $\mathcal{V}_{\text{d}_{\text{o}}}^-$ coincide, as it will be explained soon.

Observe that $\mathcal{V}_{\min}$ is continuous because it is defined as the minimum of two continuous functions. In Figure 5.24, a game $\mathcal{G}_{\text{dist}}$ such that $\mu < 1$ is taken as an example to illustrate how iso-valued level curves taken from $\mathcal{V}_{\text{d}_{\text{o}}}^+$ and $\mathcal{V}_{\text{d}_{\text{o}}}^-$ engender the level curves of $\mathcal{V}_{\min}$ (indicated by the thick closed curves). Each of these level curves obviously encloses a sup-level set of $\mathcal{V}_{\min}$. Recalling the notation

$$\mathscr{L}_g(\lambda) \triangleq \{ z \in \mathbb{C} \ : \ g(z) \geq \lambda \}$$

for the λ-sup level set of a function $g : \mathbb{C} \to \mathbb{R}$, note that

$$\mathscr{L}_{\mathcal{V}_{\min}}(\lambda) = \mathscr{L}_{\mathcal{V}_{\text{d}_{\text{o}}}^+}(\lambda) \cap \mathscr{L}_{\mathcal{V}_{\text{d}_{\text{o}}}^-}(\lambda),$$

as it can be easily proved.

In the particular example of Figure 5.24, the highest-valued sup-level set of $\mathcal{V}_{\min}$ inherits its value 0.704 from the plateau of $\mathcal{G}_{\text{dist}}^-$, i.e., $\mathscr{P}^- = \arg\max_{z \in \mathbb{C}} \mathcal{V}_{\text{d}_{\text{o}}}^-(z)$,
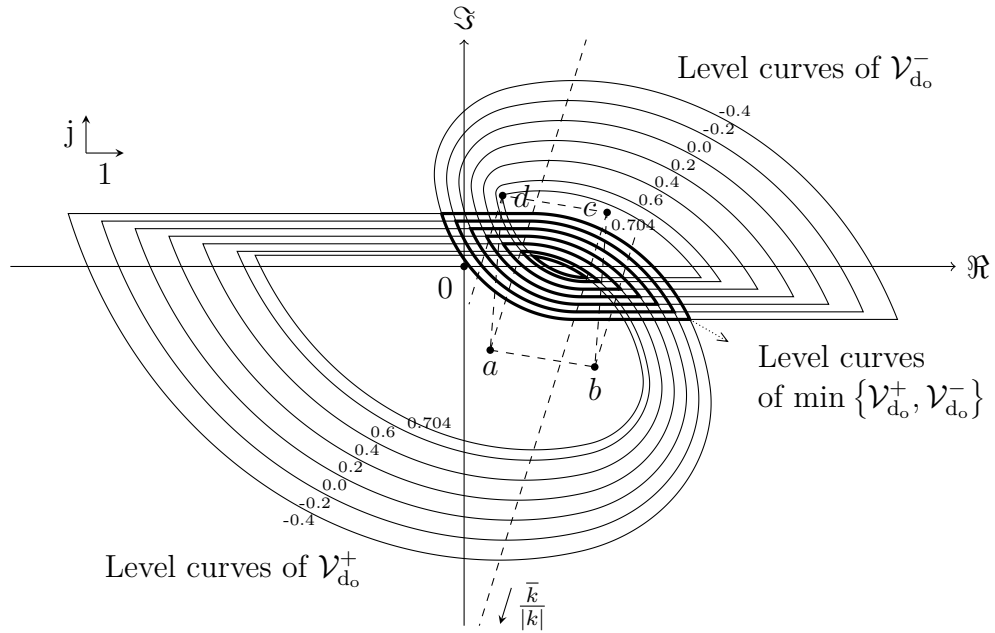
Figure 5.24: The level curves of $\mathcal{V}_{\min} = \min\left\{\mathcal{V}_{d_o}^+, \mathcal{V}_{d_o}^-\right\}$ (indicated by the thick closed curves) are engendered by iso-valued level curves of $\mathcal{V}_{d_o}^+$ and $\mathcal{V}_{d_o}^-$. The quasi-concavity of $\mathcal{V}_{\min}$ inherited from the quasi-concavity of $\mathcal{V}_{d_o}^+$ and $\mathcal{V}_{d_o}^-$, guarantees the convexity of each sup-level set of $\mathcal{V}_{\min}$.

which has d as a corner point of its boundary. However, in general, the highest-valued sup-level set of $\mathcal{V}_{\min}$ can be inherited form either $\mathscr{P}^+$, $\mathscr{P}^-$, or neither of them.

Since both $\mathcal{V}_{d_o}^+$ and $\mathcal{V}_{d_o}^-$ are quasi-concave functions, $\mathcal{V}_{\min} = \min\left\{\mathcal{V}_{d_o}^+, \mathcal{V}_{d_o}^-\right\}$ must also be quasi-concave function. Accordingly, the sup-level sets of $\mathcal{V}_{\min}$ are convex sets, i.e., $\mathscr{L}_{\mathcal{V}_{\min}}(\lambda)$ is a convex set for each $\lambda \in \mathbb{R}$.

As the family of sup-level sets of $\mathcal{V}_{d_o}^+$ and the family of sup-level sets of $\mathcal{V}_{d_o}^-$, the family $\left\{\mathscr{L}_{\mathcal{V}_{\min}}(\lambda) : \lambda \in \mathbb{R}\right\}$ of sup-level sets of $\mathcal{V}_{\min}$ is a nested family of compact subsets of $\mathbb{C}$ that covers the whole complex plane.

As $\mathcal{V}_{d_o}^+$ and $\mathcal{V}_{d_o}^-$, $\mathcal{V}_{\min}$ is bounded above and, by the Bolzano–Weierstrass extreme value theorem, attains its supremum at some point of $\mathbb{C}$. However, the point where the maximum is attained is not necessarily unique. Quite obviously, in the example of Figure 5.24 the maximum of $\mathcal{V}_{\min}$ is attained at every point of the set $\mathscr{L}_{\mathcal{V}_{\min}}(0.704)$, represented in the figure by the area enclosed by the innermost thick closed curve.

In Figure 5.25 the particular 0.65-level curve of $\mathcal{V}_{\min}$ (represented by the thick closed curve) is taken as an example to illustrate why $\tilde{p}_{\min}^*$ was defined so carefully at the points where both unilateral VFs take the same functional value. The points z_1 and z_2 represented in the figure are the only two points that solve $\mathcal{V}_{d_o}^+(z) = \mathcal{V}_{d_o}^-(z) = 0.65$. If P wants to extend consistently his counter-clockwise circulation power (described in Subsection 5.7.3) from the curved parts of the level curve

195
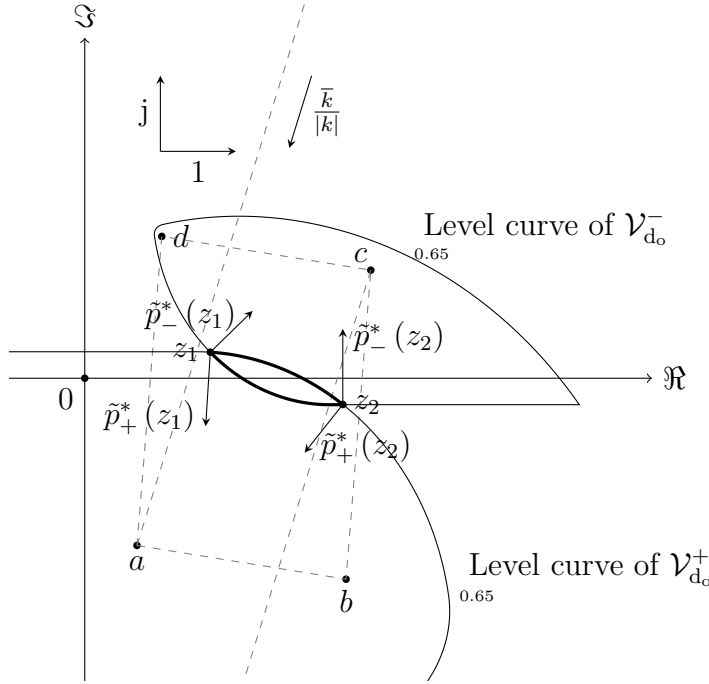
Figure 5.25: The thick closed curve is the 0.65-level curve of the function $\mathcal{V}_{\min} = \min\{\mathcal{V}_{d_o}^+, \mathcal{V}_{d_o}^-\}$. It has two corner points: z_1 and z_2 where the functional values of $\mathcal{V}_{d_o}^+$ and $\mathcal{V}_{d_o}^-$ coincide at 0.65. At z_1, P must choose to play $\mathcal{G}_{\text{dist}}^-$ to make use of its counter-clockwise circulation power consistently along (or around) the lower arc between z_1 and z_2. At z_2 he must choose to play $\mathcal{G}_{\text{dist}}^+$ to make use of its counter-clockwise circulation power consistently along (or around) the upper arc between z_2 and z_1. For each $i \in \{1, 2\}$, at the corner point z_i, P must choose $\mathcal{G}_{\text{dist}}^-$ if $\tilde{p}_+^*(z_i) \otimes \tilde{p}_-^*(z_i) > 0$ while he must choose $\mathcal{G}_{\text{dist}}^+$ if $\tilde{p}_+^*(z_i) \otimes \tilde{p}_-^*(z_i) < 0$.

$\{z : \mathcal{V}_{\min}(z) = 0.65\}$ to its corner points z_1 and z_2, the vector $\tilde{p}_{\min}^*(z_1)$ must be taken as $\tilde{p}_-^*(z_1)$ and the vector $\tilde{p}_{\min}^*(z_2)$ must be taken as $\tilde{p}_+^*(z_2)$, as ruled by the sign of the the cross product involved in the definition (5.114). If $\mathcal{V}_{d_o}^+(z) = \mathcal{V}_{d_o}^-(z)$ and $\tilde{p}_+^*(z) \otimes \tilde{p}_-^*(z) = 0$ for some $z \in \mathbb{C}$, either $\tilde{p}_+^*(z)$ or $\tilde{p}_-^*(z)$ can be selected as $\tilde{p}_{\min}^*(z)$; in definition (5.114), for definiteness, $\tilde{p}_+^*(z)$ is selected.

5.11.1.2. Criticism of the proposed solution

The example of Figure 5.24 evidences a serious flaw in the attempted solution of $\mathcal{G}_{\text{dist}}$. If the level curves of $\mathcal{V}_{\min}$ (indicated by the thick closed curves in the figure) were the true level curves of the VF of $\mathcal{G}_{\text{dist}}$, then E would be always able to prevent the sate from crossing each of them in the outward direction. However, this turns out to be false.

Consider for example the sup-level set $\mathscr{L}_{\mathcal{V}_{\min}}(0.6) = \mathscr{L}_{\mathcal{V}_{d_o}^+}(0.6) \cap \mathscr{L}_{\mathcal{V}_{d_o}^-}(0.6)$. For each $z \in \partial \mathscr{L}_{\mathcal{V}_{d_o}^+}(0.6)$, E can force the state velocity vector $\dot{z}$, based at z, to point into $\mathscr{L}_{\mathcal{V}_{d_o}^+}(0.6)$. Similarly, for each $z \in \partial \mathscr{L}_{\mathcal{V}_{d_o}^-}(0.6)$, E can force $\dot{z}$, based at

z, to point into $\mathscr{L}_{\mathcal{V}_{\mathrm{do}}^-}(0.6)$. However, he might be unable to force $\dot{z}$, based at z, to point into $\mathscr{L}_{\mathcal{V}_{\min}}(0.6) = \mathscr{L}_{\mathcal{V}_{\mathrm{do}}^+}(0.6) \cap \mathscr{L}_{\mathcal{V}_{\mathrm{do}}^-}(0.6)$. Therefore, the corner points of the level curves of $\mathcal{V}_{\min}$ constitute a serious challenge for E, since they may be *leaking corners.*

In fact, the leftmost corner point of $\mathscr{L}_{\mathcal{V}_{\min}}(0.6)$ *is* a leaking corner. An enlightening way of proving it is to invoke Proposition 4.3.1 with z_0 taken as the this corner point, q_1 taken as d, and q_2 taken as a. The result of the invocation is that the state must abandon $\mathscr{L}_{\mathcal{V}_{\mathrm{do}}^-}(0.6)$ because it must come arbitrarily close to the line $\overleftrightarrow{da}$ in finite time (see Figure 5.24). All that P has to do to develop this arbitrarily proximity to the line $\overleftrightarrow{da}$ is to keep $i_o = i_o^\triangledown$ constant during a sufficiently large (but finite) interval of time. By means of this *bilateral pull-back manoeuvre* (which clearly resembles P's pull-back manoeuvre in the context of any of the unilateral games), P is able to bring the state to a level curve of $\mathcal{V}_{\min}$ (lower than $\partial\mathscr{L}_{\mathcal{V}_{\min}}(0.6)$) that is as close as he wishes to the line $\overleftrightarrow{da}$; let say for example $\partial\mathscr{L}_{\mathcal{V}_{\min}}(0.4)$. From this new level curve he can make full use of its counter-clockwise circulation power (in the context of $\mathcal{G}_{\mathrm{dist}}^-$). Thereby, preventing the state from crossing $\partial\mathscr{L}_{\mathcal{V}_{\min}}(0.4)$ in the inward direction, while simultaneously reducing the current oriented distance to $\mathscr{T}^-$ along its way to the ray $\left\{w \ : \ c + \rho\frac{\overline{k}}{|k|}\right\}$ where P finally attains an outcome (in the context of $\mathcal{G}_{\mathrm{dist}}^-$ *and* $\mathcal{G}_{\mathrm{dist}}$) that is *at most* 0.4.

5.11.1.3. A candidate solution

The discussion of the previous example, suggests a way of fixing the detected flaw in the proposal (5.111)–(5.114). Let

$$\hat{\lambda} = \max\left\{\mathcal{V}_{\min}(z) \ : \ z \in \mathbb{C}\right\} = \max\left\{\lambda \ : \ \mathscr{L}_{\mathcal{V}_{\min}}(\lambda) \neq \emptyset\right\}, \qquad (5.115)$$

Hence, $\mathscr{L}_{\mathcal{V}_{\min}}(\hat{\lambda})$ is the highest sup-level set of $\mathcal{V}_{\min}$. Suppose that (as in the previous example) $\mathscr{L}_{\mathcal{V}_{\min}}(\hat{\lambda})$ does not intersect *both* lines $\overleftrightarrow{da}$ and $\overleftrightarrow{bc}$. Being $\left\{\mathscr{L}_{\mathcal{V}_{\min}}(\lambda) \ : \ \lambda \leq \hat{\lambda}\right\}$ a family of nested compact subsets of $\mathbb{C}$ that covers the whole complex plane, we can search in this family for the largest λ^* such that $\mathscr{L}_{\mathcal{V}_{\min}}(\lambda)$ intersects *both* $\overleftrightarrow{da}$ and $\overleftrightarrow{bc}$. The nature of the nested family $\left\{\mathscr{L}_{\mathcal{V}_{\min}}(\lambda) \ : \ \lambda \leq \hat{\lambda}\right\}$ not only guarantees that the searched number

$$\lambda^* \triangleq \max\left\{\lambda \ : \ \lambda \leq \hat{\lambda} \ \wedge \ \mathscr{L}_{\mathcal{V}_{\min}}(\lambda) \cap \overleftrightarrow{da} \neq \emptyset \ \wedge \ \mathscr{L}_{\mathcal{V}_{\min}}(\lambda) \cap \overleftrightarrow{bc} \neq \emptyset\right\} \quad (5.116)$$

exists, but also, that at least one of the two intersections involved above is a singleton. The singleton one, indicates P which of the two lines he must select to carry out his bilateral pull back manoeuvre. If both are singletons, any of the two selections serves for P's purpose.

Recognizing these facts, let $\mathcal{V}_{\mathrm{do}} : \mathbb{C} \to \mathbb{R}$, defined as

$$\mathcal{V}_{\mathrm{do}}(z) \triangleq \min\left\{\mathcal{V}_{\min}(z), \lambda^*\right\}, \qquad (5.117)$$

be a candidate VF of $\mathcal{G}_{\mathrm{dist}}$ for the case $\mu > 1$, and let the set

$$\mathscr{M} \triangleq \arg\max_{z \in \mathbb{C}} \mathcal{V}_{\mathrm{do}}(z) = \mathscr{L}_{\mathcal{V}_{\min}}(\lambda^*) \qquad (5.118)$$
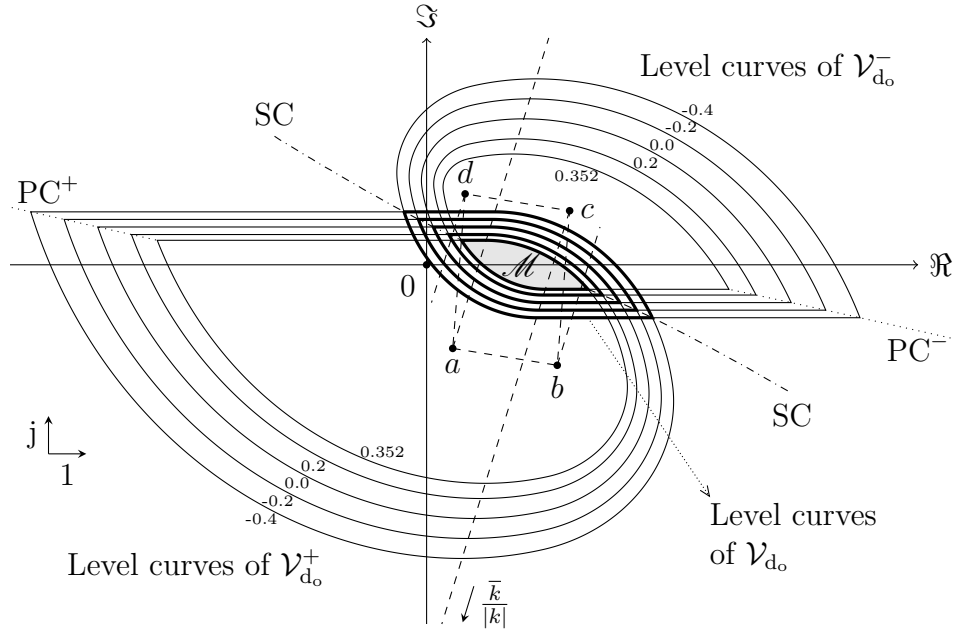
Figure 5.26: The function $\mathcal{V}_{d_o} : \mathbb{C} \to \mathbb{R}$ is defined in terms of $\mathcal{V}_{\min} = \min\left\{\mathcal{V}_{d_o}^+, \mathcal{V}_{d_o}^-\right\}$ as $\mathcal{V}_{d_o} = \min\left\{\mathcal{V}_{\min}, \lambda^*\right\}$, where λ^* is the largest real number λ such that the λ-sup-level set $\mathscr{L}_{\mathcal{V}_{\min}}(\lambda)$ intersects *both* of the following two straight lines: the one through points b and c, and the one through points d and a. Consequently, the function $\mathcal{V}_{d_o}$ is a truncated version of $\mathcal{V}_{\min}$ and attains its maximum in the set $\mathscr{M} = \mathscr{L}_{\mathcal{V}_{\min}}(\lambda^*)$, called the *summit* of $\mathcal{G}_{\text{dist}}^+$ (represented in the figure by the light-shaded area and its border). In this example, the maximum of $\mathcal{V}_{d_o}$ is 0.352.

be referred to a as the *summit* of $\mathcal{G}_{\text{dist}}$ in order to remember that $\mathcal{V}_{d_o}$ takes its maximum therein. The corresponding candidate strategies $\tilde{u}^* : \mathbb{C} \to U$ and $\tilde{\sigma}^* : \mathbb{C} \to \boldsymbol{\Sigma}$ are defined by

$$\tilde{u}^*(z) \triangleq u^*(\tilde{p}^*(z)), \tag{5.119}$$

$$\tilde{\sigma}^*(z) \triangleq \sigma^*(\tilde{p}^*(z)), \tag{5.120}$$

where $u^* : \mathbb{C} \to U$ and $\sigma^* : \mathbb{C} \to \boldsymbol{\Sigma}$ are the already known functions defined in statement 2 of Proposition 4.4.1, and $\tilde{p}^* : \mathbb{C} \to \mathbb{C}$ is defined, in terms of the function $\tilde{p}_{\min}^* : \mathbb{C} \to \mathbb{C}$, as

$$\tilde{p}^*(z) \triangleq \begin{cases} \tilde{p}_{\min}^*(z) & \text{if } z \notin \text{int}(\mathscr{M}), \\ \tilde{p}_+^*(b) & \text{if } z \in \text{int}(\mathscr{M}) \text{ and } \mathscr{L}_{\mathcal{V}_{\min}}(\lambda^*) \cap \overleftrightarrow{bc} \text{ is a singleton,} \\ \tilde{p}_-^*(d) & \text{if } z \in \text{int}(\mathscr{M}) \text{ and } \mathscr{L}_{\mathcal{V}_{\min}}(\lambda^*) \cap \overleftrightarrow{bc} \text{ is not a singleton,} \end{cases} \tag{5.121}$$

The strategies defined above materialize P's bilateral pull back manoeuvre in $\text{int}(\mathscr{M})$ as explained before. For E, the definition of his strategy in $\text{int}(\mathscr{M})$ is not important because he cannot prevent the state from being pulled towards $\overleftrightarrow{da}$ or $\overleftrightarrow{bc}$ once P has taken a decision in this respect. However, both player's strategies
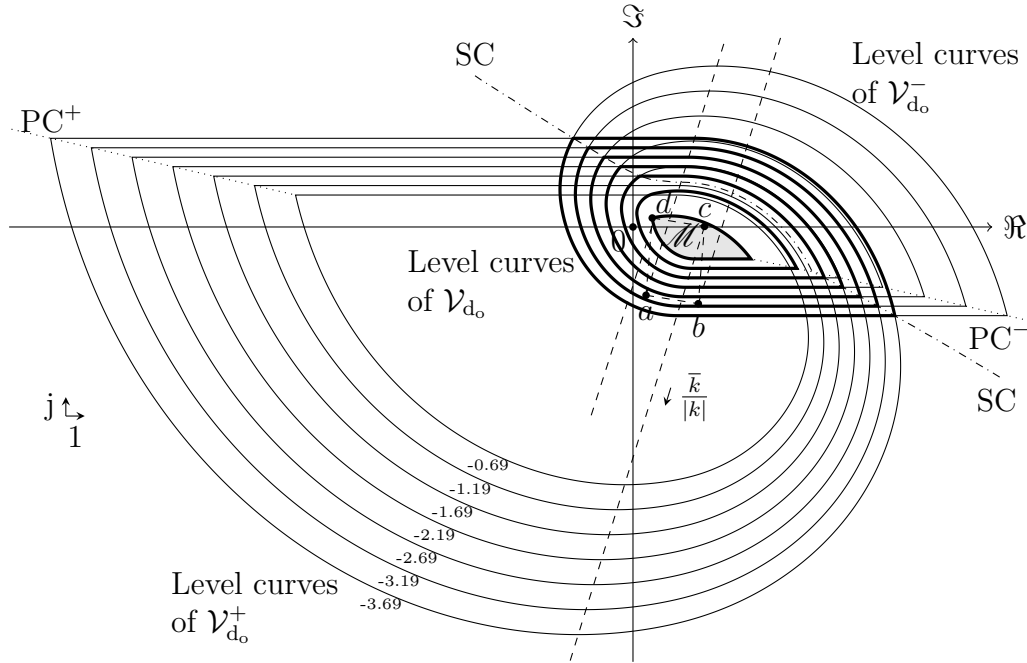
Figure 5.27: For $\mu > 1$, an instance of $\mathcal{G}_{\text{dist}}^+$ such that some level curves of $\mathcal{V}_{\text{d}_{\text{o}}}$ coincide with the level curves of $\mathcal{V}_{\text{d}_{\text{o}}}^-$. In this case, $\mathcal{M} = \mathscr{P}^-$, i.e., the highest sup-level set of $\mathcal{V}_{\text{d}_{\text{o}}}$ coincides with the highest sup-level set of $\mathcal{V}_{\text{d}_{\text{o}}}^-$.

are defined in $\mathrm{int}\,(\mathcal{M})$ in such a way that P and E behave in $\mathrm{int}\,(\mathcal{M})$ either as they would do in $\mathscr{P}^+ \setminus \mathrm{cl}\,(\mathscr{S}^+ \setminus \mathscr{R}^+)$ in case $\mathcal{M} \cap \overleftrightarrow{bc}$ is a singleton, or as they would do in $\mathscr{P}^- \setminus \mathrm{cl}\,(\mathscr{S}^- \setminus \mathscr{R}^-)$ in case $\mathcal{M} \cap \overleftrightarrow{bc}$ is not singleton (i.e., in case $\mathscr{L}_{\mathcal{V}_{\min}}\,(\lambda^*) \cap \overleftrightarrow{da}$ is a singleton).

In Figure 5.26 the same example of Figure 5.24 is reconsidered to show the topography of the function $\mathcal{V}_{\text{d}_{\text{o}}}$, defined in terms of $\mathcal{V}_{\min}$ as explained before. Consider the sets:

$$\mathrm{EQ} \triangleq \left\{ z \in \mathbb{C} \;:\; \mathcal{V}_{\text{d}_{\text{o}}}^+\,(z) = \mathcal{V}_{\text{d}_{\text{o}}}^-\,(z) \right\} \quad \text{and} \quad \mathrm{SC} \triangleq \mathrm{EQ} \setminus \mathcal{M}.$$

For the example being considered, the set SC is the union of two curves that emanate from $\mathcal{M}$ as represented in Figure 5.26 by the dot-dashed curves. Each of these curves is a *separation curve* in the sense that it separates the upward game from the downward game in the context of the bilateral game.

In Figure 5.27 another example of $\mathcal{G}_{\text{dist}}^+$ for the case $\mu > 1$ is considered to illustrate that not necessarily SC splits into two curves as in Figure 5.26. In Figure 5.27, the set SC is a single separation curve that bypasses $\mathcal{M}$. In this case, in fact, $\mathcal{M} = \mathscr{P}^-$, i.e., the highest sup-level set of $\mathcal{V}_{\text{d}_{\text{o}}}$ coincides with the highest sup-level set of $\mathcal{V}_{\text{d}_{\text{o}}}^-$. Note also that in the example of Figure 5.27, the corner points of the level curves of $\mathcal{V}_{\text{d}_{\text{o}}}$ may be either points of SC or points of PC$^-$ (the pruning curve of $\mathcal{G}_{\text{dist}}^-$). By contrast, in Figure 5.26 every corner point of a level curve of $\mathcal{V}_{\text{d}_{\text{o}}}$ is a point of SC.

5.11.1.4. Validation of the candidate solution

The validation of the candidate solution of $\mathcal{G}_{\mathrm{dist}}$ proposed above for the case $\mu > 1$ can be carried out using the same approach used for the unilateral game $\mathcal{G}_{\mathrm{dist}}^{+}$, particularly explained in detail for the case $\mu > 1$ in Subsection 5.7.8. Similar issues [2] as the ones discussed therein arise in connection with P having to appeal for ϵ-saddle strategies, if faced with E's stubbornness for fighting for a vanishing quantity under P's control. The detailed validation is not carried out here for brevity, since the arguments are similar.

Nevertheless, there *is* a significant difference in connection with E's ability to prevent the state from crossing the level sets of $\mathcal{V}_{\mathrm{d_o}}$ in the outward (i.e., decreasing) direction. This difference deserves the following comments.

When the unilateral game $\mathcal{G}_{\mathrm{dist}}^{+}$ was dealt with, special attention was given to the corner points of the level sets of $\mathcal{V}_{\mathrm{d_o}}^{+}$, which except for b (in case $\mu \geq 1$) are the points of the pruning curve PC^{+}. Whether $\mu > 1$ or $\mu \leq 1$ a different argument was given in each case to show that the points of PC^{+} are not leaking corners for E. This, of course, also holds for the points of PC^{-} by the reduction of $\mathcal{G}_{\mathrm{dist}}^{+}$ to $\mathcal{G}_{\mathrm{dist}}^{-}$.

By contrast, in $\mathcal{G}_{\mathrm{dist}}$ the arising of SC poses a *new* source of corner points for the level curves of $\mathcal{V}_{\mathrm{d_o}}$. Observe in Figures 5.26 and 5.27 how SC may interact, or not, with the pruning curves of the unilateral games to conform the corner points of the level sets of $\mathcal{V}_{\mathrm{d_o}}$. In particular, observe in Figure 5.26 that every point of the left branch of SC is a corner point of a level set of $\mathcal{V}_{\mathrm{d_o}}$ and that some of them belong to the angular sector $\left\{ z \in \mathbb{C} \; : \; (z - d) \otimes (a - d) \geq 0 \; \wedge \; (z - d) \otimes \overline{k} \leq 0 \right\}$, whose vertex is at d. The corner points of $\mathcal{V}_{\mathrm{d_o}}$ which belong to this sector need special attention in order to successfully validate E's strategy (5.120), because the arguments used at the corner points originated by the pruning curves do not hold for the corner points in this sector. Similarly, by symmetry between the upper and the lower game, special attention deserve the corner points of $\mathcal{V}_{\mathrm{d_o}}$ that belong to the angular sector $\left\{ z \in \mathbb{C} \; : \; (z - b) \otimes (c - b) \geq 0 \; \wedge \; (z - b) \otimes \left(-\overline{k} \right) \leq 0 \right\}$ whose vertex is at b. Next, by means of analysing a representative example, it is argued that even at the presence of this new kind of corner points in the level curves of the proposed candidate VF, E is still able to prevent the state from crossing them in the outward (i.e., decreasing) direction.

Reconsider the game instance used to generate Figures 5.24 and 5.26. This example was used before to show that $\mathcal{V}_{\min} = \min \left\{ \mathcal{V}_{\mathrm{d_o}}^{+}, \mathcal{V}_{\mathrm{d_o}}^{-} \right\}$ is *not* a good candidate VF for $\mathcal{G}_{\mathrm{dist}}$. As an alternative, the function $\mathcal{V}_{\mathrm{d_o}}$, defined as the truncation of $\mathcal{V}_{\min}$ above its λ^{*}-sup-level set, was proposed as a candidate VF for $\mathcal{G}_{\mathrm{dist}}$. In Figure 5.28 some level curves of $\mathcal{V}_{\min}$ are magnified. Clearly, for each $\lambda \leq \lambda^{*} = 0.352$, the λ-level-curve of $\mathcal{V}_{\min}$ coincides with the λ-level-curve of $\mathcal{V}_{\mathrm{d_o}}$. The λ^{*}-level-curve of $\mathcal{V}_{\min}$ (not shown in the figure) is the only level curve of $\mathcal{V}_{\min}$ that intersects the

---

[2]For plays that initiate in $\mathrm{int}\,(\mathcal{M})$, P needs to perform a bilateral pull-back manoeuvre, whose bilateral aspect is related to the fact that he continuously threatens E against both unilateral games while he pulls the state towards: either $\overleftrightarrow{bc}$ or $\overleftrightarrow{da}$.

line $\underleftrightarrow{dq}$ at exactly one single point, namely the intersection of

$$\mathrm{EQ} \triangleq \left\{ z \in \mathbb{C} \ : \ \mathcal{V}_{\mathrm{d_o}}^+ (z) = \mathcal{V}_{\mathrm{d_o}}^- (z) \right\} \tag{5.122}$$

and $\underleftrightarrow{dq}$. The set $\mathcal{M}$, defined by (5.118), is precisely the set enclosed by the λ^*-level-curve of $\mathcal{V}_{\min}$.

The porpouse of the remaining paragraphs of this subsection is to validate E's strategy (5.120) in $\mathbb{C} \setminus \mathrm{int}\,(\mathcal{M})$. In $\mathrm{int}\,(\mathcal{M})$, as it was explained before, E cannot prevent P from making use of its bilateral pull-back manoeuvre. Since the emended strategy (5.120) coincides with the first attempted strategy (5.113) in $\mathbb{C} \setminus \mathrm{int}\,(\mathcal{M})$, it can be assumed without inconvenience that E sticks to (5.113) instead of (5.120). This substitution of strategies will not affect the validation of (5.120) in $\mathbb{C} \setminus \mathrm{int}\,(\mathcal{M})$ and, as a by-product, will make evident why the first attempt (5.113) fails in $\mathrm{int}\,(\mathcal{M})$. Notice that $\mathcal{V}_{\mathrm{d_o}}$ coincides with $\mathcal{V}_{\min}$ in $\mathbb{C} \setminus \mathrm{int}\,(\mathcal{M})$.

Let

$$\mathrm{EQ}^+ \triangleq \left\{ z \in \mathbb{C} \ : \ \mathcal{V}_{\mathrm{d_o}}^+ (z) < \mathcal{V}_{\mathrm{d_o}}^- (z) \right\}, \tag{5.123}$$

$$\mathrm{EQ}^- \triangleq \left\{ z \in \mathbb{C} \ : \ \mathcal{V}_{\mathrm{d_o}}^- (z) < \mathcal{V}_{\mathrm{d_o}}^+ (z) \right\}. \tag{5.124}$$

Consider the points of EQ represented in Figure 5.28 by the dot-dashed curve. According to (5.113), on the dot-dashed line and below it (i.e., in EQ^-) E is mandated to play $\sigma = 1$, whereas above the dot-dashed line (i.e., in EQ^+) E is mandated to play $\sigma = 0$. As it was assumed, E sticks to this mandate.

The point z_1 is a corner point of the level curve $\partial \mathscr{L}_{\mathcal{V}_{\min}} (0.05)$ that lies in half-plane $\left\{ z \in \mathbb{C} \ : \ (z - d) \otimes \overline{k} > 0 \right\}$. At z_1, E plays $\sigma = 1$. Therefore P is forced to select a centre q (of the instantaneous α-equiangular state-guiding spiral through z_1) from the segment $\underline{dc}$. If P selects $q = c$, as mandated by (5.112), the state departs from z_1 tangentially to the level curve $\partial \mathscr{L}_{\mathcal{V}_{\min}} (0.05)$ along the counter-clock-wise direction. If P selects any other point q of the segment $\underline{dc}$, the state velocity vector $F(z_1, q)$, based at z_1, points towards *higher* sup-level sets of $\mathcal{V}_{\min}$. Even in the extreme case $q = d$, the velocity vector $F(z_1, d)$ still has a *negative* imaginary part, because z_1 lies in the half-plane $\left\{ z \in \mathbb{C} \ : \ (z - d) \otimes \overline{k} > 0 \right\}$ which coincides with the supporting half-plane $I^- = \left\{ z \in \mathbb{C} \ : \ \Im F(z, q) < 0 \quad \forall q \in \mathcal{Q} \right\}$ for the case $\mathcal{Q} = \underline{cd}$ (recall Subsection 4.3.5). Therefore, z_1 is similar in nature to the corner points of the level curves $\mathcal{V}_{\mathrm{d_o}}^+$ engendered by the pruning curve PC^+ in the following sense: E has at z_1 a control action that prevents the velocity vector, based at z_1, from pointing into a higher sup-level set of the candidate VF, *whatever* P's control may be (see Figure 5.28).

Different is the case for z_2 which is a corner point of the level curve $\partial \mathscr{L}_{\mathcal{V}_{\min}} (0.30)$ that lies in half-plane $\left\{ z \in \mathbb{C} \ : \ (z - d) \otimes \overline{k} < 0 \right\}$. As before, E plays $\sigma = 1$ at z_2 and P is forced to select a centre q from the segment $\underline{dc}$. However, since z_2 lies in $\left\{ z \in \mathbb{C} \ : \ (z - d) \otimes \overline{k} < 0 \right\}$, now P can select a control action that enforces the velocity vector to have a *positive* imaginary part. For example, if P plays $q = d$, the velocity vector $F(z_2, d)$, based at z_2, points to a *lower* sup-level set of $\mathcal{V}_{\min}$ (see Figure 5.28). This means that a new kind of argumentation (radically different from the one used in the context of the uppward unilateral game) is needed to
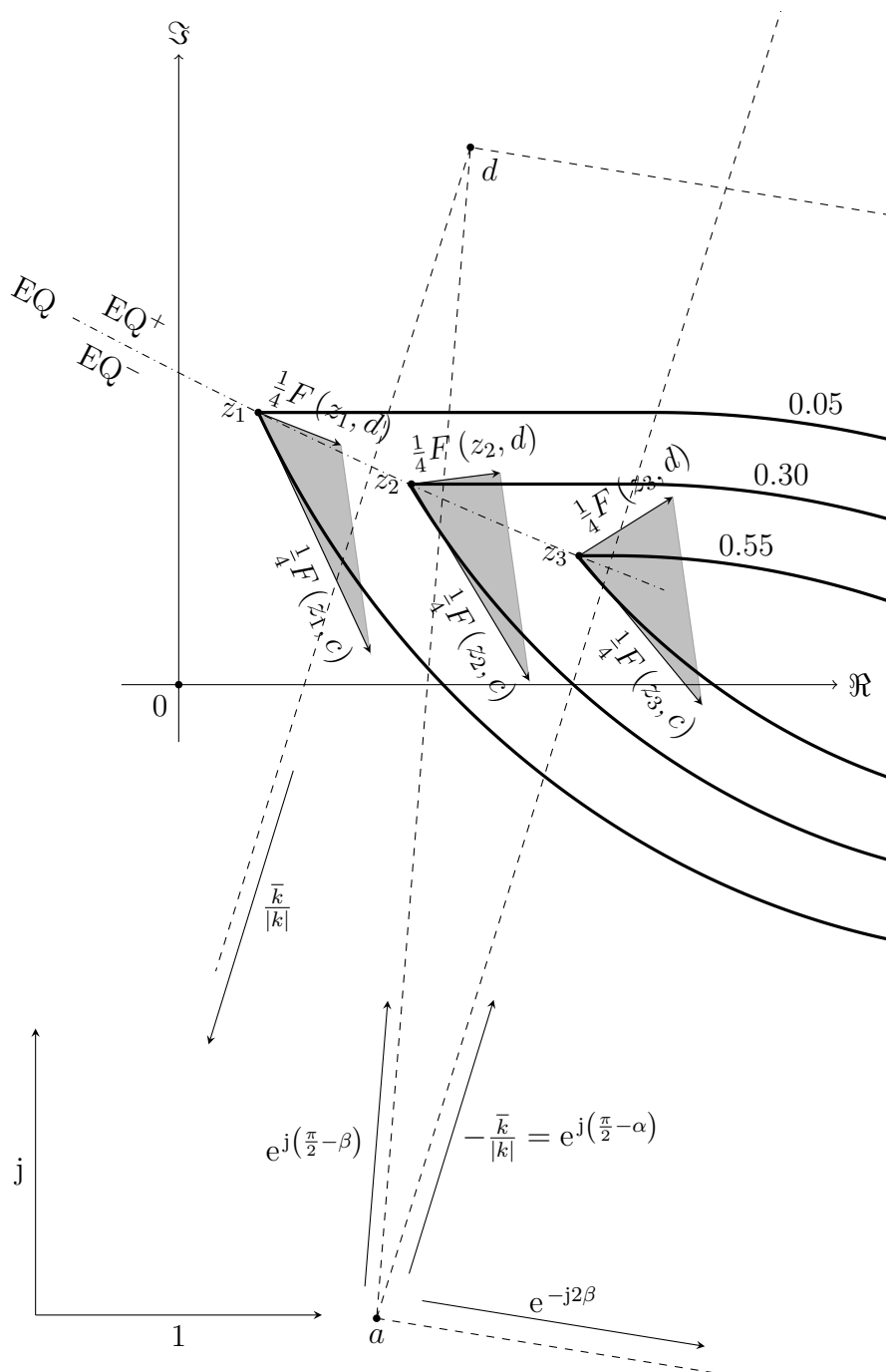
Figure 5.28: The points z_1, z_2, and z_3 are corner points of the level curves of $\mathcal{V}_{\min}$ with associated values 0.05, 0.30 and 0.55, respectively. For each $i \in \{1, 2, 3\}$, the vectogram $\{F(z_i, q) = k(z_i - q) \ : \ q \in \mathrm{conv}(\{c, d\})\}$ available for P at z_i is represented by the shaded area with a vertex at z_i, under the assumption that E sticks to strategy (5.113) which forces q to belong to the segment $\mathrm{conv}(\{c, d\})$ for states on $\mathrm{EQ} = \{z \in \mathbb{C} \ : \ \mathcal{V}_{\mathrm{d_o}}^+(z) = \mathcal{V}_{\mathrm{d_o}}^-(z)\}$.

validate E's proposed strategy if there is any chance to validate it at all. Furthermore, why would (5.113) be fruitful for E at a corner point like $z_2 \in \mathbb{C} \setminus \text{int}(\mathscr{M})$ but not at a corner point like $z_3 \in \mathscr{M}$, as represented in Figure 5.28? The answer is derived from the following observations.

Notice in Figure 5.28 that at each corner point z_i, where $i \in \{1, 2, 3\}$, P is able to make the velocity vector $F(z_i, q)$, based at z_i, point into the set EQ^+. At z_1 he obtains no benefit from this ability because he cannot direct $F(z_1, q)$, based at z_1, into $\mathbb{C} \setminus \mathscr{L}_{\mathcal{V}_{\min}}(0.05)$. However, at z_2 he *can* direct $F(z_2, q)$, based at z_2, into $\mathbb{C} \setminus \mathscr{L}_{\mathcal{V}_{\min}}(0.30)$. Similarly, at z_3 he can direct $F(z_3, q)$, based at z_3, into $\mathbb{C} \setminus \mathscr{L}_{\mathcal{V}_{\min}}(0.55)$. Therefore, P might be tempted to play $q = d$ at z_2 and z_3 (instead of playing $q = c$ which only leads the state to a tangential counter-clockwise circulation along a level curve).

If P plays $q = d$ at z_2 or z_3, as soon as the state enters EQ^+, E reacts switching from $\sigma = 1$ to $\sigma = 0$, forcing P to select a new centre q from the segment $\underline{ab}$. Recognizing that z_2, z_3 lie in $\left\{ z \in \mathbb{C} \ : \ (z - a) \otimes \overline{k} > 0 \right\}$ which coincides with $\{ z \in \mathbb{C} \ : \ \Im F(z, q) < 0 \quad \forall q \in \underline{ab} \}$, it follows (recalling Subsection 4.3.5) that E's reaction leads the state downwards towards EQ again.

Once the state is back on EQ, P might repeat his opportunistic behaviour, so E might be forced to be continuously switching between $\sigma = 1$ (on EQ) and $\sigma = 0$ (in EQ^+, above and close to EQ). If this happens, a *sliding* trajectory along EQ arises. The key point here is determining in which direction along EQ does the state z slides as time increases: either the direction in which the $\mathcal{V}_{\min}$ decreases (which is desirable for P), or the direction in which the $\mathcal{V}_{\min}$ increases (which is desirable for E). As it will be seen, the direction depends on the sign of the cross product $(a - z) \otimes (d - z)$ which is positive for $z = z_2$ while it is negative for $z = z_3$.

Recall that

- if the state z is on EQ, or in EQ^- close to EQ, P must select a velocity vector $F(z, q) = k(z - q)$ with $q \in \underline{cd}$, while

- if the state z is in EQ^+ close to EQ, P must select a velocity vector $F(z, q) = k(z - q)$ with $q \in \underline{ab}$;

because E sticks to (5.113).

First, consider the representative corner point $z_2 \in \mathbb{C} \setminus \text{int}(\mathscr{M})$. When the state z is in a sufficiently small neighbourhood of z_2, the velocity vector $\dot{z}$ must arbitrarily approximate a vector of the vectogram $V_2 \triangleq \{ F(z_2, q) \ : \ q \in \text{conv}(\{a, b, c, d\}) \}$. The most extreme directions of $\{ z_2 - q \ : \ q \in \text{conv}(\{a, b, c, d\}) \}$ are $z_2 - a$ and $z_2 - d$. Accordingly, the most extreme directions of V_2 are $F(z_2, a) = k(z_2 - a)$ and $F(z_2, d) = k(z_2 - d)$. All the possible *directions* represented by the vectors of V_2 are equally well represented by the set of vectors $\{ F(z_2, q) \in \mathbb{C} \ : \ q \in \underline{ad} \}$ indicated by the shaded area with a vertex at z_2 in Figure 5.29. By definition of EQ and the level curves of $\mathcal{V}_{\min}$, there exists an unique vector $v_s \in \{ F(z_2, q) \in \mathbb{C} \ : \ q \in \underline{ad} \}$ tangent to EQ at z_2. The direction represented by v_s is the direction that should reasonably be associated with the sliding trajectory possibly induced by P. Since $F(z_2, a) \otimes F(z_2, d) = |k|^2 (a - z_2) \otimes (d - z_2) > 0$, v_s must point towards *increasing* values of $\mathcal{V}_{\min}$ (see Figure 5.29). Hence, inducing E into a sliding trajectory from
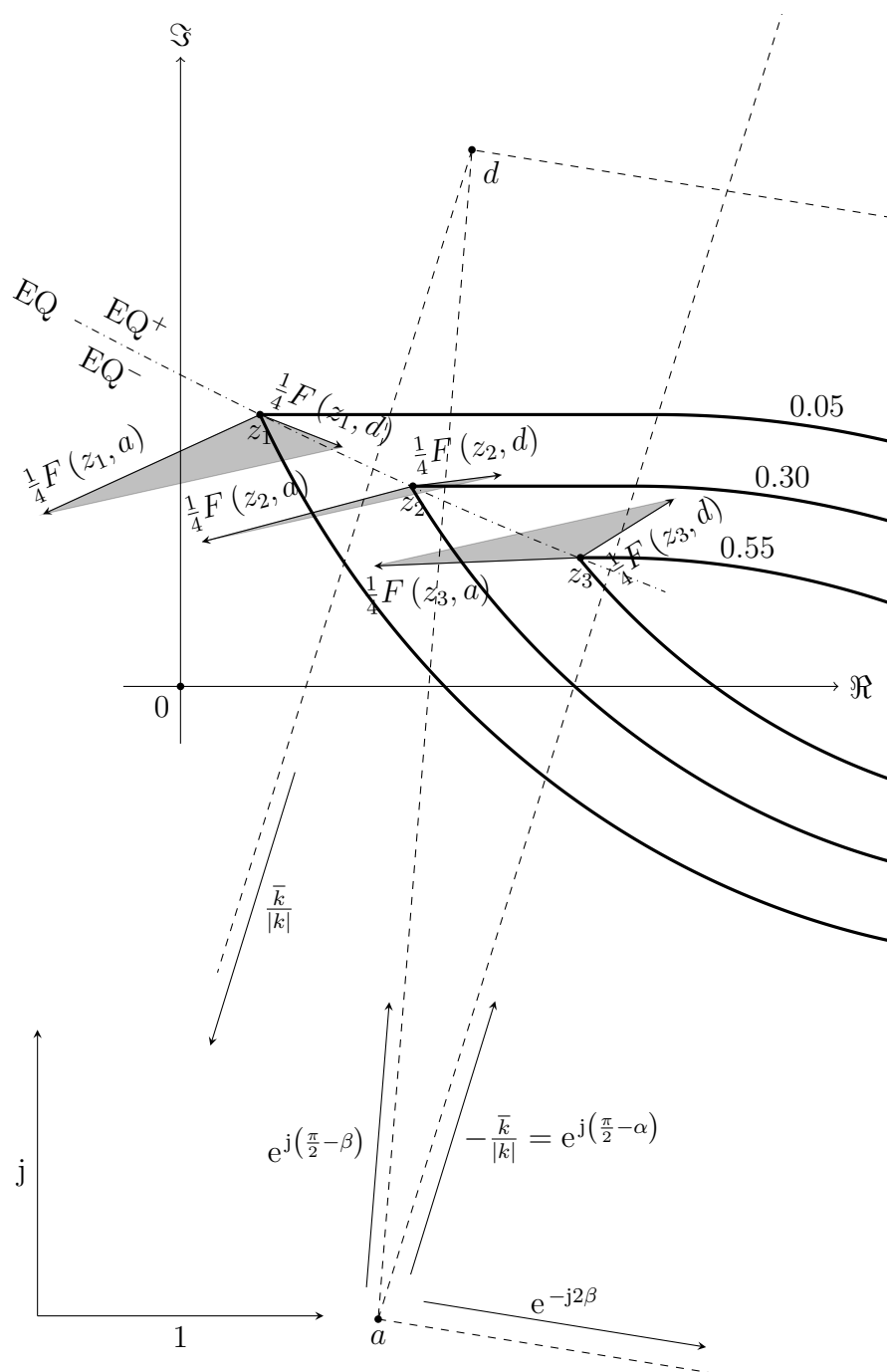
Figure 5.29: The same level curves and corner points of Figure 5.28 are represented in the figure. Also, as in Figure 5.28, E is assumed to stick to strategy (5.113), whatever P may do. From points on EQ such as z_1, z_2, P can (unwisely) induce E into a sliding trajectory such that $\mathcal{V}_{\min}$ *increases* as the state *slides* through EQ. From points on EQ such as z_3 P can put into practice his bilateral pull-back manoeuvre just by keeping $i_o = i_o^\triangledown$ constant, thereby pulling the state towards the line through points a and d. Against this pull-back, E's strategy (5.113) is futile because the state slides through EQ in the direction that $\mathcal{V}_{\min}$ *decreases*.

z_2 is not a wise option for P. Nevertheless, the point that is worthy of notice here is that the argument just given validates E's strategy even against such unwise opposition from P. Generalizing the conclusion just arrived at this example, it can be stated that the strategy (5.120) (which coincides with (5.113) in $\mathbb{C} \setminus \mathrm{int}\,(\mathcal{M})$), prevents $\mathcal{V}_{\mathrm{d_o}}$ (which coincides with $\mathcal{V}_{\mathrm{min}}$ in $\mathbb{C} \setminus \mathrm{int}\,(\mathcal{M})$) from *decreasing* as long as the state remains in $\mathbb{C} \setminus \mathrm{int}\,(\mathcal{M})$. Since every corner point of a level curve of $\mathcal{V}_{\mathrm{d_o}}$ is either $b \in \mathcal{M}$, $d \in \mathcal{M}$, a point of PC^+, a point of PC^-, or a point of $\mathrm{SC} \subset \mathrm{EQ}$, and argument is known for each corner point case, the conclusion generalized from the concrete example is valid.

Second, consider the representative corner point $z_3 \in \mathrm{int}\,(\mathcal{M})$. As before E is supposed to stick to (5.113), but now suppose that P applies his bilateral pull-back manoeuvre as dictated by (5.119) for states in $\mathrm{int}\,(\mathcal{M})$, which (for the example being considered) consists in keeping $u = i_o^{\triangledown} + \mathrm{j}$ constant so as to pull the state towards the line $\overleftrightarrow{ad}$. E is consequently forced to pick up centres q from the segment $\underline{ad}$. When the state z is in a sufficiently small neighbourhood of z_3, the velocity vector $\dot{z}$ must arbitrarily approximate a vector of the vectogram $V_3 \triangleq \{F\,(z_3, q) \ : \ q \in \underline{ad}\}$. The most extreme directions of $\{z_3 - q \ : \ q \in \underline{ad}\}$ are $z_3 - a$ and $z_3 - d$. Accordingly, the most extreme directions of V_3 are $F\,(z_3, a) = k\,(z_3 - a)$ and $F\,(z_3, d) = k\,(z_3 - d)$. All the possible *directions* represented by the vectors of V_3 are equally well represented by the set of vectors $\{F\,(z_3, q) \in \mathbb{C} \ : \ q \in \underline{ad}\}$ indicated by the shaded area with a vertex at z_3 in Figure 5.29. By definition of EQ and the level curves of $\mathcal{V}_{\mathrm{min}}$, there exists an unique vector $v_s \in \{F\,(z_3, q) \in \mathbb{C} \ : \ q \in \underline{ad}\}$ tangent to EQ at z_3. The direction represented by v_s is the direction that should reasonably be associated with the sliding behaviour that results from E trying to defend himself from P's bilateral pull-back manoeuvre. Since $F\,(z_3, a) \otimes F\,(z_3, d) = |k|^2\,(a - z_3) \otimes (d - z_3) < 0$, v_s must point towards *decreasing* values of $\mathcal{V}_{\mathrm{min}}$. This shows vividly the *leakage* of the state through the corner point $z_3 \in \mathrm{int}\,(\mathcal{M})$ of the sup-level set $\mathscr{L}_{\mathcal{V}_{\mathrm{min}}}\,(0.55)$, and confirms the already known fact that (5.113) is futile for E in $\mathrm{int}\,(\mathcal{M})$.

5.11.2. Solution of the game in distance for the case $\mu \leq 1$

In the context of the bilateral game $\mathcal{G}_{\mathrm{dist}}$, there is as important difference between the case $\mu > 1$ and the case $\mu \leq 1$ that has to do with how the sets $\mathscr{P}^+$ and $\mathscr{P}^-$ relate to each other.

Regardless the case (whether $\mu > 1$ or $\mu \leq 1$), $\mathscr{P}^-$ is the image of $\mathscr{P}^+$ through the central inversion $z \mapsto \frac{a+c}{2} - (z - \frac{a+c}{2})$ (recall Section 5.10). As it is almost evident from Figure 5.24, the sets $\mathscr{P}^- = \arg\max_{z \in \mathbb{C}} \mathcal{V}_{\mathrm{d_o}}^-\,(z)$ (with a corner point at d) and $\mathscr{P}^+ = \arg\max_{z \in \mathbb{C}} \mathcal{V}_{\mathrm{d_o}}^+\,(z)$ (with a corner point at b) do *not* coincide for the case $\mu > 1$. However, if $\mu \leq 1$, $\mathscr{P}^+$ has point symmetry with respect to the point $\frac{a+c}{2}$ (see Figure 5.21 for the case $\mu < 1$ and Figure 5.23 for the case $\mu = 1$). Therefore, for the case $\mu \leq 1$, the set $\mathscr{P}^-$ coincides with $\mathscr{P}^+$. This fact simplifies the topography of the candidate VF to be proposed next for the case $\mu \leq 1$.

5.11.2.1. A candidate solution

Reasoning along the same lines as in Subsubsection 5.11.1.1 for the case $\mu > 1$, the first natural candidate VF for $\mathcal{G}_{\text{dist}}$ that can be thought of for the case $\mu \leq 1$ is $\min \left\{ \mathcal{V}_{\text{d}_\text{o}}^+, \mathcal{V}_{\text{d}_\text{o}}^- \right\}$. Fortunately, by contrast with the case $\mu > 1$, taking the minimum between $\mathcal{V}_{\text{d}_\text{o}}^+$ and $\mathcal{V}_{\text{d}_\text{o}}^-$ turns out to be fruitful for the case $\mu \leq 1$.

For the sake of explicitness, consider the following formulation. Let $\mathcal{V}_{\text{d}_\text{o}} : \mathbb{C} \to \mathbb{R}$, defined as

$$\mathcal{V}_{\text{d}_\text{o}} (z) \triangleq \min \left\{ \mathcal{V}_{\text{d}_\text{o}}^+ (z), \mathcal{V}_{\text{d}_\text{o}}^- (z) \right\}, \tag{5.125}$$

be proposed as a candidate VF for $\mathcal{G}_{\text{dist}}$ for the case $\mu \leq 1$. In accordance, the player's candidate optimal strategies should be defined as

$$\tilde{u}^* (z) \triangleq u^* (\tilde{p}^* (z)), \tag{5.126}$$

$$\tilde{\sigma}^* (z) \triangleq \sigma^* (\tilde{p}^* (z)), \tag{5.127}$$

where $u^* : \mathbb{C} \to U$ and $\sigma^* : \mathbb{C} \to \mathbf{\Sigma}$ are the functions defined in statement 2 of Proposition 4.4.1, and $\tilde{p}^* : \mathbb{C} \to \mathbb{C}$ is defined as

$$\tilde{p}^* (z) \triangleq \begin{cases} \tilde{p}_+^* (z) & \text{if } \mathcal{V}_{\text{d}_\text{o}}^+ (z) < \mathcal{V}_{\text{d}_\text{o}}^- (z), \\ \tilde{p}_-^* (z) & \text{if } \mathcal{V}_{\text{d}_\text{o}}^- (z) < \mathcal{V}_{\text{d}_\text{o}}^+ (z), \\ \tilde{p}_-^* (z) & \text{if } \mathcal{V}_{\text{d}_\text{o}}^+ (z) = \mathcal{V}_{\text{d}_\text{o}}^- (z) \ \wedge \ \tilde{p}_+^* (z) \otimes \tilde{p}_-^* (z) > 0, \\ \tilde{p}_+^* (z) & \text{if } \mathcal{V}_{\text{d}_\text{o}}^+ (z) = \mathcal{V}_{\text{d}_\text{o}}^- (z) \ \wedge \ \tilde{p}_+^* (z) \otimes \tilde{p}_-^* (z) < 0, \\ \tilde{p}_+^* (z) & \text{if } \mathcal{V}_{\text{d}_\text{o}}^+ (z) = \mathcal{V}_{\text{d}_\text{o}}^- (z) \ \wedge \ \tilde{p}_+^* (z) \otimes \tilde{p}_-^* (z) = 0. \end{cases} \tag{5.128}$$

Notice, that this formulation of a candidate solution for $\mathcal{G}_{\text{dist}}$ for the case $\mu \leq 1$ coincides exactly with the first attempted candidate solution for the case $\mu > 1$ (formulated in Subsubsection 5.11.1.1), which was proved to be defective (as demonstrated in Subsubsection 5.11.1.2). For the case $\mu \leq 1$, however, the above formulation *does* constitute a valid solution of $\mathcal{G}_{\text{dist}}$ for the case $\mu \leq 1$ as it argued next.

5.11.2.2. Validation of the candidate solution

Before focusing on the validation of the candidate VF, recall first the acquired knowledge about the solution of $\mathcal{G}_{\text{dist}}^+$ for the case $\mu < 1$. Remember that, the interior of $\mathscr{P}^+$ (represented by the interior of the shaded area in Figure 5.21) is the union of the island $\mathscr{I}^+$ (represented by the dark-shaded area and its border in Figure 5.18) and the expansive semi-permeable domain $\mathscr{S}_E^+$ (represented by interior of the light-shaded area in Figure 5.18). In $\text{int} \left(\mathscr{I}^+ \right)$, P activates his pull-back manoeuvre which pulls the state towards the line $\overleftrightarrow{dq}$ thereby taking the state to the proximities of $\mathscr{S}_E^+$, from where P can make use of its counter-clockwise *expansive* circulation power to make the state spiral outwards towards the limit cycle LC $= \partial \mathscr{P}^+$ assuming E exhibits optimal opposition. In the border case $\mu = 1$, the expansive semi-permeable domain $\mathscr{S}_E^+$ reduces to the empty set and P's pull-back manoeuvre takes over the whole interior of $\mathscr{P}^+$. An analogous

description of the action in $\mathrm{int}\,(\mathscr{P})^-$ holds for $\mathcal{G}^-_{\mathrm{dist}}$, with the difference that P's pull-back manoeuvre pulls the state towards the line $\overleftrightarrow{bc}$ (instead of the line $\overleftrightarrow{da}$)

Now, consider the context of the bilateral game $\mathcal{G}_{\mathrm{dist}}$ for initial states in $\mathrm{int}\,(\mathscr{P}^+)$. As was commented before, $\mathscr{P}^+ = \mathscr{P}^-$ for the case $\mu \leq 1$. Hence, being by definition $\mathscr{P}^+ = \arg\max_{w \in \mathbb{C}} \mathcal{V}^+_{\mathrm{d_o}}(w)$ and $\mathscr{P}^- = \arg\max_{w \in \mathbb{C}} \mathcal{V}^-_{\mathrm{d_o}}(w)$, it must be necessarily the case that both $\mathcal{V}^+_{\mathrm{d_o}}$ and $\mathcal{V}^-_{\mathrm{d_o}}$ are constant in $\mathscr{P}^+ = \mathscr{P}^-$. If $\mathcal{V}^+_{\mathrm{d_o}}$ is less than $\mathcal{V}^-_{\mathrm{d_o}}$ in $\mathscr{P}^+$, the action in $\mathrm{int}\,(\mathscr{P})$ is as recalled above for the unilateral game $\mathcal{G}^+_{\mathrm{dist}}$, because P chooses it as the most convenient unilateral game to play, while if $\mathcal{V}^-_{\mathrm{d_o}}$ is less than $\mathcal{V}^+_{\mathrm{d_o}}$ in $\mathscr{P}^+$, the action in $\mathrm{int}\,(\mathscr{P})$ is as for the unilateral game $\mathcal{G}^-_{\mathrm{dist}}$ because of an analogous reason. If $\mathcal{V}^+_{\mathrm{d_o}}$ equals $\mathcal{V}^-_{\mathrm{d_o}}$, P may choose any of the two unilateral games in $\mathrm{int}\,(\mathscr{P})$, for definiteness assume P chooses $\mathcal{G}^+_{\mathrm{dist}}$ in this particular case.

As for the case $\mu > 1$, define

$$\mathscr{M} \triangleq \arg\max_{z \in \mathbb{C}} \mathcal{V}_{\mathrm{d_o}}(z)$$

The description just recalled of what happens in the interior of $\mathscr{P}^+$ which coincides with $\mathscr{P}^-$ and $\mathscr{M}$, corresponds to what is mathematically encoded in (5.126)–(5.128), and shows the validity of $\mathcal{V}_{\mathrm{d_o}} = \min\left\{\mathcal{V}^+_{\mathrm{d_o}}, \mathcal{V}^-_{\mathrm{d_o}}\right\}$ as the value function of $\mathcal{G}^+_{\mathrm{dist}}$ in $\mathrm{int}\,(\mathscr{M})$. In fact, in $\mathrm{int}\,(\mathscr{M})$ both players are playing either $\mathcal{G}^+_{\mathrm{dist}}$ or $\mathcal{G}^-_{\mathrm{dist}}$, without switching from one unilateral game to the other. So, the validation of the candidate value function (5.125) and the strategies (5.126)–(5.127) in $\mathrm{int}\,(\mathscr{M})$ reduces to the validation in the context of one of the two unilateral games.

In $\mathbb{C} \setminus \mathscr{M}$, however, switching between both unilateral games may occur. In Figure 5.30 the arising of the level curves of $\mathcal{V}_{\mathrm{d_o}} = \min\left\{\mathcal{V}^+_{\mathrm{d_o}}, \mathcal{V}^-_{\mathrm{d_o}}\right\}$ from the corresponding iso-level curves of $\mathcal{V}^+_{\mathrm{d_o}}$ and $\mathcal{V}^-_{\mathrm{d_o}}$ is illustrated for an instance of $\mathcal{G}_{\mathrm{dist}}$ such that $\mu < 1$. As for the case $\mu > 1$, let

$$\mathrm{EQ} \triangleq \left\{z \in \mathbb{C} \,:\, \mathcal{V}^+_{\mathrm{d_o}}(z) = \mathcal{V}^-_{\mathrm{d_o}}(z)\right\} \quad \text{and} \quad \mathrm{SC} \triangleq \mathrm{EQ} \setminus \mathscr{M}.$$

For $\mu < 1$, in general, the set EQ coincides with SC and is a curve that separates the domains of both unilateral games in the context of the bilateral game. In Figure 5.30, the players play $\mathcal{G}^+_{\mathrm{dist}}$ above SC and play $\mathcal{G}^-_{\mathrm{dist}}$ below SC. The only case in which $\mathrm{EQ} \neq \mathrm{SC}$ is the case such that $\max\left\{\mathcal{V}^+_{\mathrm{d_o}}(z) \,:\, z \in \mathbb{C}\right\} = \max\left\{\mathcal{V}^-_{\mathrm{d_o}}(z) \,:\, z \in \mathbb{C}\right\}$, because in this case EQ degenerates from a curve into a set that includes $\mathscr{M} = \mathscr{P}^+ = \mathscr{P}^-$. This singular case occurs when $\frac{a+c}{2}$ is a real number, i.e., when the parallelogram $\mathrm{conv}\,(\{a, b, c, d\})$ half of its area at either side of the real axis. If $\Im\frac{a+c}{2} > 0$, the separation curve SC avoids $\mathscr{M}$ by passing *below* it (as it is the case in Figure 5.30). If $\Im\frac{a+c}{2} < 0$, the separation curve SC avoids $\mathscr{M}$ by passing *above* it.

The validation of the candidate value function (5.125) and strategies (5.126)–(5.127) in $\mathbb{C} \setminus \mathrm{int}\,(\mathscr{M})$ presents no new challenges. Analogous arguments to the ones used for the unilateral game $\mathcal{G}^+_{\mathrm{dist}}$ for the case $\mu \leq 1$ can be successfully applied because, by contrast with the case $\mu > 1$, the corner points of $\mathcal{V}_{\mathrm{d_o}}$ that belong to SC cannot take place in neither of the following two problematic angular sectors:
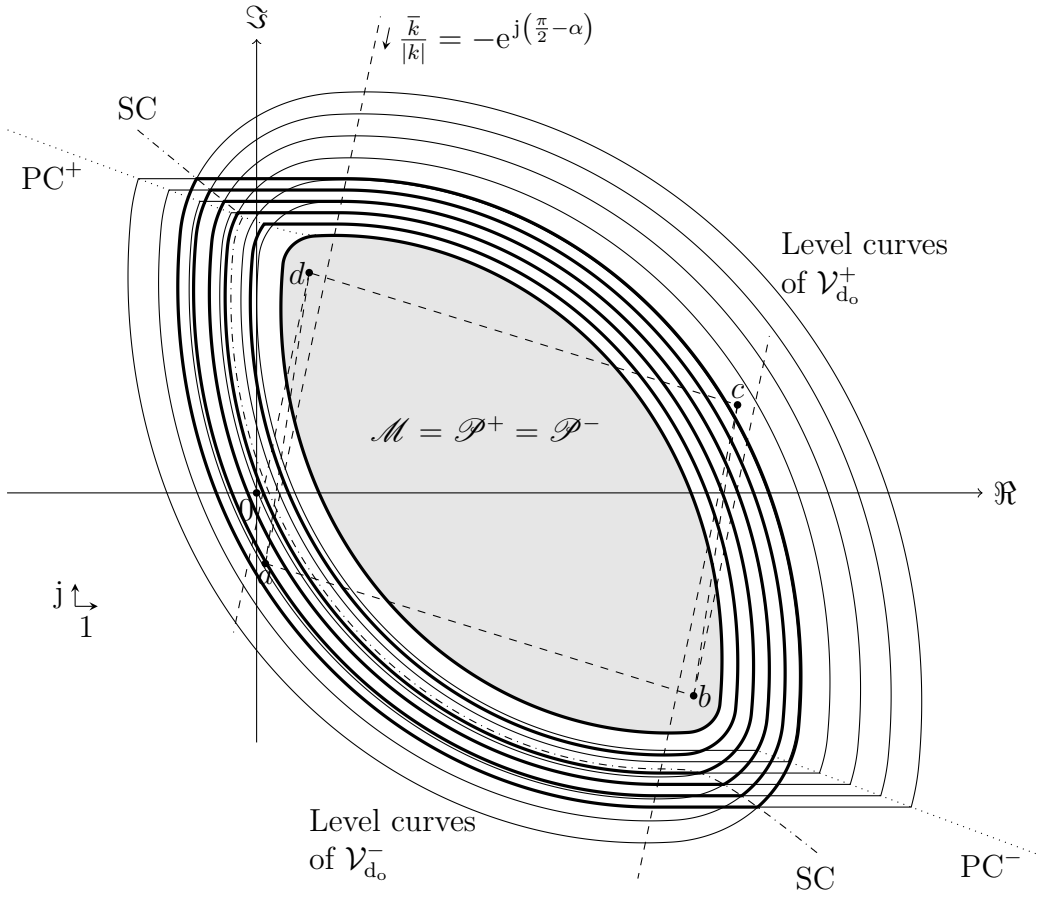
Figure 5.30: The thick closed lines represent the level curves of $\min\left\{\mathcal{V}_{d_o}^+, \mathcal{V}_{d_o}^-\right\}$ that result from the corresponding iso-valued level curves of $\mathcal{V}_{d_o}^+$ and $\mathcal{V}_{d_o}^-$ (represented by the thin closed curves). By contrast with the case $\mu > 1$, for the case $\mu \leq 1$ (exemplified in the figure) taking $\mathcal{V}_{d_o} = \min\left\{\mathcal{V}_{d_o}^+, \mathcal{V}_{d_o}^-\right\}$ as a candidate VF for $\mathcal{G}_{\text{dist}}$, actually renders the true VF of $\mathcal{G}_{\text{dist}}$.

$$\left\{z \in \mathbb{C} \ : \ (z-d) \otimes (a-d) \geq 0 \ \wedge \ (z-d) \otimes \overline{k} \leq 0\right\} \text{ and}$$
$$\left\{z \in \mathbb{C} \ : \ (z-b) \otimes (c-b) \geq 0 \ \wedge \ (z-b) \otimes \left(-\overline{k}\right) \leq 0\right\} \text{ (see Figure 5.30).}$$

5.11.3. The maximum of the value function

It is worth noting that regardless of the case (whether $\mu > 1$ or $\mu \geq 1$), the summit $\mathscr{M} = \arg\max_{z \in \mathbb{C}} \mathcal{V}_{d_o}(z)$, where the value function of $\mathcal{G}_{\text{dist}}$ attains it maximum value, has a shape such that its oriented distance to $\mathscr{T}$ is necessarily less than one, i.e.,

$$\min\left\{d_o(z, \mathscr{T}) \ : \ z \in \mathscr{M}\right\} < 1, \tag{5.129}$$

as it can be verified observing that $\mathscr{M}$ is not included in the line $\{z \in \mathbb{C} \ : \ \Im z = 0\}$, regardless of the case. In addition, the functional value of $\mathcal{V}_{d_o} : \mathbb{C} \to \mathbb{R}$ in $\mathscr{M}$

coincides with left-hand value of the inequality (5.129) regardless of the case, as it can be checked recalling the construction of $\mathcal{V}_{d_o}$. Therefore,

$$\max \left\{ \mathcal{V}_{d_o}(z) \ : \ z \in \mathbb{C} \right\} < 1. \tag{5.130}$$

This last equality, has a remarkable consequence: even if a play starts on the line $\{z \in \mathbb{C} \ : \ \Im z = 0\}$, i.e., at maximum oriented distance from $\mathscr{T}$, E cannot prevent P from taking the state away from this line into a place where the oriented distance to $\mathscr{T}$ is less than one.

5.12. Concluding remarks

In Chapter 3, a buck converter control problem of practical interest was shown to be properly modelled by a pursuit-evasion conflict, in which the controller takes the role of the evader (E) and the disturbances on the input voltage and the load current take the role of the pursuer (P). From such conflict, two natural pursuit-evasion games may be considered: a game in distance and a game in time.

This chapter was initially intended to solve a canonized version of the former one, which is the most relevant from the controller designer's perspective. The pursuit-evasion game in distance models the struggle between the controller and the disturbances for the control of the converter-system's state. In particular, in connection with its distance to an unsafe (from E's viewpoint) subset of the state-space where the control requirements can not be assured to be fulfilled, i.e., P's target set. The concept of oriented distance used in the formulation of the game in distance allows to study in an unified way, to which *degree* the controller either succeeds or fails in preventing the state from entering the unsafe subset.

Regrettably, to be able to solve the game in distance, it was necessary to assume that P's does not command the converter's input voltage, thereby reducing considerably the aimed scope of this work. Nevertheless, interesting results were found considering that P acts only on the load current, which is usually the most significant disturbance in most buck converter applications.

Working with two unilateral auxiliary games derived from the original bilateral game in distance, the parameter-space of the game (restricted to the case in which the input voltage of the converter is constant) was found to be partitioned into three sub-spaces that give rise to qualitatively different families of optimal trajectories.

This knowledge was exploited to construct a candidate solution and validate it as a true solution of the original bilateral game. Since the construction was performed with an eye on implementation, it can be easily translated into program code in order to: i) generate optimal strategies for both players, and ii) evaluate the value function of the game at a given arbitrary initial state.

Accordingly, knowing the values of the parameters of the game, for a given initial state, the relevant problem *of kind* of determining if there exists a controller able to guarantee the fulfilment of the control problem requirements, reduces to an algorithmic evaluation of the sign of the value function of the game at the

initial state. If it is positive, such a controller exists; for example, the controller that results from programming the strategy given by the solution of the game for E. In fact, this special controller, is the best one from the family of succeeding controllers, in the sense that it is the one which keeps the state as much far away as possible from the unsafe set (i.e., to the largest degree). If the sign of value function evaluation is not positive, no such controller exists, and every defiant controller claimed to be able to prevent the state from entering the unsafe set, can be proved to disappoint its designers by letting it play against the strategy given by the solution of the game for P.

Chapter 6

Simulations

This chapter is organized around different application aspects of the solution of the buck converter game in distance. In connection with each of these aspects, numerical simulations, performed in Matlab-Simulink, are reported.

Before delving into the discussion of each aspect, in the following section, the physically meaningful concepts that will be required are recalled, highlighted, and linked to the solution (obtained in Chapter 5) for the canonical form of the game.

6.1.   The absolute worst-case error function and the absolute worst-case error value function

In Section 3.2 the (instantaneous) worst-case error $\mathrm{e}^{\mathrm{wc}}\left(\boldsymbol{y}\right)$ at state $\boldsymbol{y} \in \mathbb{R}^2$ was introduced, by (3.12), as the error (between the reference voltage $v_R = V_{LL0} - R_{LL}i_O$ and the converter's output voltage v_O) whose absolute value is maximized by the selection of an (instantaneous) worst-case load current (3.13) when the buck's converter state is $\boldsymbol{y} = \begin{bmatrix} i_L & v_C \end{bmatrix}^\top$. Recall that in these expressions $\boldsymbol{l} = \begin{bmatrix} R_C & 1 \end{bmatrix}^\top$ and the resistance mismatch $R_M = R_C - R_{LL}$ is the difference between the capacitor's parasitic ESR and the characteristic load line resistance. Therefore, for each $\boldsymbol{y} \in \mathbb{R}^2$, the real number $\mathrm{e}^{\mathrm{wc}}\left(\boldsymbol{y}\right)$ condenses a worst-case *instantaneous* concept.

The significance of the (original) game in distance

$$\boldsymbol{\mathcal{G}_{\mathbf{dist}}}' \begin{cases} \mathrm{SE}: & \frac{\mathrm{d}\boldsymbol{y}}{\mathrm{d}t} = \boldsymbol{f}'\left(\boldsymbol{y}, \boldsymbol{v}, \sigma\right) = \boldsymbol{A}'\boldsymbol{y} + \boldsymbol{B}'\boldsymbol{S}\left(\sigma\right)\boldsymbol{v}, \\ \mathrm{TS}: & \boldsymbol{\mathscr{T}}' = \left\{ \boldsymbol{y} \in \mathbb{R}^2 \ : \ |\boldsymbol{l}^\top\boldsymbol{y} - V| \geq D \right\}, \\ \mathrm{PF}: & \left(\boldsymbol{y_0}, \boldsymbol{v}, \sigma\right) \mapsto \mathcal{P}_{\boldsymbol{f}', \boldsymbol{\mathscr{T}}'}^{\mathrm{dist_o}}\left(\boldsymbol{y_0}, \boldsymbol{v}, \sigma\right) = \inf\left\{ \mathrm{dist_o}\left(\boldsymbol{y}_{\boldsymbol{y_0}, \boldsymbol{v}, \sigma}^{\boldsymbol{f}'}\left(t\right), \boldsymbol{\mathscr{T}}'\right) \ : \ t \geq 0 \right\}, \end{cases}$$

(formulated in Subsection 3.2.3) was established by the relation

$$\sqrt{R_C^2 + 1} \, \mathrm{dist_o}\left(\boldsymbol{y}, \boldsymbol{\mathscr{T}}'\right) = E - \left|\mathrm{e}^{\mathrm{wc}}\left(\boldsymbol{y}\right)\right|$$

that exists between the absolute worst-case error $\left|\mathrm{e}^{\mathrm{wc}}\left(\boldsymbol{y}\right)\right|$ and the oriented distance $\mathrm{dist_o}\left(\boldsymbol{y}, \boldsymbol{\mathscr{T}}'\right)$ to $\boldsymbol{\mathscr{T}}'$, for every $\boldsymbol{y} \in \mathbb{R}^2$, where E is the error tolerance specification.

Actually, as argued in Subsection 3.2.4, to solve $\boldsymbol{\mathcal{G}_{dist}}'$ is equivalent to solve

$$\boldsymbol{\mathcal{G}_{|e^{wc}|}}' \begin{cases} \text{SE}: & \frac{\mathrm{d}\boldsymbol{y}}{\mathrm{d}t} = \boldsymbol{f}'(\boldsymbol{y}, \boldsymbol{v}, \sigma) = \boldsymbol{A}'\boldsymbol{y} + \boldsymbol{B}'\boldsymbol{S}(\sigma)\boldsymbol{v}, \\ \text{TS}: & \boldsymbol{\mathcal{T}}' = \left\{ \boldsymbol{y} \in \mathbb{R}^2 \ : \ |\boldsymbol{l}^\top \boldsymbol{y} - V| \geq D \right\}, \\ \text{PF}: & (\boldsymbol{y_0}, \boldsymbol{v}, \sigma) \mapsto \mathcal{P}_{\boldsymbol{f}', \boldsymbol{\mathcal{T}}'}^{|e^{wc}|}(\boldsymbol{y_0}, \boldsymbol{v}, \sigma) = \inf\left\{ \left| e^{wc}\left(\boldsymbol{y}_{\boldsymbol{y_0}, \boldsymbol{v}, \sigma}^{\boldsymbol{f}'}(t) \right) \right| \ : \ t \geq 0 \right\}. \end{cases}$$

if the roles of P and E are interchanged letting P become the supremizer and letting E become the infimizer. The *absolute worst-case error value function* $\mathcal{V}_{|e^{wc}|} : \mathbb{R}^2 \to \mathbb{R}$, i.e., the value function of the game $\boldsymbol{\mathcal{G}_{|e^{wc}|}}'$, gives, for every initial state $\boldsymbol{y} \in \mathbb{R}^2$, the worst-case error $\mathcal{V}_{|e^{wc}|}(\boldsymbol{y})$ along an infinite time horizon assuming P and E play optimally. Therefore, for every $\boldsymbol{y} \in \mathbb{R}^2$, the real number $\mathcal{V}_{|e^{wc}|}(\boldsymbol{y})$ condenses a worst-case *looking ahead* concept.

Consequently, it is worth noting that: the *(instantaneous) absolute worst-case error function* $\boldsymbol{y} \mapsto |e^{wc}(\boldsymbol{y})|$ and the *absolute worst-case error value function* $\boldsymbol{y} \mapsto \mathcal{V}_{|e^{wc}|}(\boldsymbol{y})$ provide an *instantaneous* and *looking ahead* worst-case description of the buck converter's state-space, respectively.

As it was noted in Subsection 3.2.2, in general, the worst-case error cannot be nullified even at states that lie at maximum oriented distance from $\boldsymbol{\mathcal{T}}'$, because in

$$|e^{wc}(\boldsymbol{y})| = \left| \underbrace{V_{LL0} + R_M \frac{I_{O\min} + I_{O\max}}{2}}_{V} - \boldsymbol{l}^\top \boldsymbol{y} \right| + |R_M| \frac{I_{O\max} - I_{O\min}}{2}. \tag{6.1}$$

the last term is zero only if $R_M = 0$ (because assumption (A2) states that $I_{O\max}$ is strictly greater than $I_{O\min}$). *Only if* the mismatch $R_M = R_C - R_{LL}$ is zero, the instantaneous worst-case error is equal to zero for states lying on the line $\left\{ \boldsymbol{y} \in \mathbb{R}^2 \ : \ \boldsymbol{l}^\top \boldsymbol{y} = V \right\}$, at maximum oriented distance $\frac{D}{\sqrt{R_C^2+1}}$ from $\boldsymbol{\mathcal{T}}'$. The voltage difference

$$D = E - |R_C - R_{LL}| \frac{I_{O\max} - I_{O\min}}{2} \tag{6.2}$$

is assumed positive by assumption (A7) in order to prevent the case of an empty playing set (PS):

$$\boldsymbol{\mathcal{E}}' = \left\{ \boldsymbol{y} \in \mathbb{R}^2 \ : \ |e^{wc}(\boldsymbol{y})| < E \right\}.$$

The case $\boldsymbol{\mathcal{E}}' = \emptyset$ is ruled out, because it leaves E without any chance of fulfilling the control requirement: $|e(t)| < E$ for every $t \geq 0$, being $e = v_R - v_O$ the error signal.

In Chapter 5, the canonical game in distance

$$\mathcal{G}_{dist} \begin{cases} \text{SE}: & \frac{\mathrm{d}z}{\mathrm{d}t} = f(z, u, \sigma) = k(z - q(u, \sigma)), \\ \text{TS}: & \mathcal{T} = \{ z \in \mathbb{C} \ : \ |\Im z| \geq 1 \}, \\ \text{PF}: & (z_0, u, \sigma) \mapsto \mathcal{P}_{f, \mathcal{T}}^{dist_o}(z_0, u, \sigma) \triangleq \inf\left\{ d_o\left(z_{z_0, u, \sigma}^f(t), \mathcal{T} \right) \ : \ t \geq 0 \right\}, \end{cases}$$

was solved, which is just a canonical for $\boldsymbol{\mathcal{G}_{dist}}'$ formulated in the complex plane. As explained at the end of Subsubsection 3.5.2.3, the value function of $\mathcal{G}_{dist}$, denoted $\mathcal{V}_{d_o} : \mathbb{C} \to \mathbb{R}$, relates to $\mathcal{V}_{|e^{wc}|} : \mathbb{R}^2 \to \mathbb{R}$ (the value function of $\boldsymbol{\mathcal{G}_{|e^{wc}|}}'$) by

$$D\,\mathcal{V}_{d_o}(z) = E - \mathcal{V}_{|e^{wc}|}(\boldsymbol{y}), \tag{6.3}$$

where $z = \begin{bmatrix} 1 & \mathrm{j} \end{bmatrix} \boldsymbol{x} = \langle \boldsymbol{x}, \hat{\boldsymbol{e}}_1 \rangle + \mathrm{j} \langle \boldsymbol{x}, \hat{\boldsymbol{e}}_2 \rangle$ and $\boldsymbol{x} = \boldsymbol{h}^{-1}(\boldsymbol{y}) = \frac{1}{D}\left(\boldsymbol{P}^{-1}\boldsymbol{y} - V\hat{\boldsymbol{e}}_2\right)$, for every $\boldsymbol{y} \in \mathbb{R}^2$, being $\boldsymbol{h} : \mathbb{R}^2 \to \mathbb{R}^2$ the state-space transformation introduced in Subsection 3.4.1 that transforms the realistic state-space into the canonical state space. In particular, from (6.3),

$$D \max_{z \in \mathbb{C}} \mathcal{V}_{\mathrm{d_o}}(z) = E - \min_{\boldsymbol{y} \in \mathbb{R}^2} \mathcal{V}_{|\mathrm{e^{wc}}|}(\boldsymbol{y}). \tag{6.4}$$

Similarly, the oriented distance function $z \mapsto \mathrm{d_o}(z, \mathscr{T})$ to the target set $\mathscr{T}$ in the canonical state-space relates to the worst-case error in the realistic state-space $\boldsymbol{y} \mapsto \mathrm{e^{wc}}(\boldsymbol{y})$ by

$$D\,\mathrm{d_o}(z) = E - |\mathrm{e^{wc}}(\boldsymbol{y})|. \tag{6.5}$$

Unfortunately (from E's perspective), even in the case of exact resistance matching, i.e., $R_C = R_{LL}$, a zero worst-case error, $\mathrm{e^{wc}}(\boldsymbol{y_0}) = 0$, associated with an initial state $\boldsymbol{y_0}$ lying on the line $\left\{ \boldsymbol{y} \in \mathbb{R}^2 \ : \ \boldsymbol{l}^\top \boldsymbol{y} = V \right\}$ at $t = 0$, cannot be granted for every $t \geq 0$. This is because

$$\min_{\boldsymbol{y} \in \mathbb{R}^2} \mathcal{V}_{|\mathrm{e^{wc}}|}(\boldsymbol{y}) > |R_M| \frac{I_{O\max} - I_{O\min}}{2} \tag{6.6}$$

as it results from (5.130), (6.4), and (6.2). However, if $\min_{\boldsymbol{y} \in \mathbb{R}^2} \mathcal{V}_{|\mathrm{e^{wc}}|}(\boldsymbol{y}) < E$, E can still fulfil the control requirement by using the feedback strategy

$$\boldsymbol{y} \mapsto \tilde{\sigma}^*\left(\left\langle \boldsymbol{h}^{-1}(\boldsymbol{y}), \hat{\boldsymbol{e}}_1 \right\rangle + \mathrm{j}\left\langle \boldsymbol{h}^{-1}(\boldsymbol{y}), \hat{\boldsymbol{e}}_2 \right\rangle\right) \tag{6.7}$$

where $\tilde{\sigma}^* : \mathbb{C} \to \boldsymbol{\Sigma}$ is E's optimal strategy for $\mathcal{G}_{\mathrm{dist}}$ as constructed in Chapter 5. If $\min_{\boldsymbol{y} \in \mathbb{R}^2} \mathcal{V}_{|\mathrm{e^{wc}}|}(\boldsymbol{y}) \geq E$, P can break completely E's expectancy for fulfilling the control requirement by using the feedback strategy

$$\boldsymbol{y} \mapsto \begin{bmatrix} I_{O\max}\,\Re\tilde{u}^*\left(\left\langle \boldsymbol{h}^{-1}(\boldsymbol{y}), \hat{\boldsymbol{e}}_1 \right\rangle + \mathrm{j}\left\langle \boldsymbol{h}^{-1}(\boldsymbol{y}), \hat{\boldsymbol{e}}_2 \right\rangle\right) \\ V_{I\max}\,\Im\tilde{u}^*\left(\left\langle \boldsymbol{h}^{-1}(\boldsymbol{y}), \hat{\boldsymbol{e}}_1 \right\rangle + \mathrm{j}\left\langle \boldsymbol{h}^{-1}(\boldsymbol{y}), \hat{\boldsymbol{e}}_2 \right\rangle\right) \end{bmatrix} \tag{6.8}$$

where $\tilde{u}^* : \mathbb{C} \to U$ is P's optimal strategy for $\mathcal{G}_{\mathrm{dist}}$ as constructed in Chapter 5, or some ϵ-modification of it (as explained in Chapter 5) in case E is not limited by a positive switching dwell time. In this more practically oriented chapter, it is assumed that E *is* actually limited by a positive switching dwell time and that its control set is the discrete set $\{0, 1\}$, so no modification of the strategy $\tilde{u}^* : \mathbb{C} \to U$ will be needed by P. Instead, a relaxation of E's optimal strategy (6.7) will be introduced in Subsection 6.3.3 in order to prevent P from inducing E into excessive chattering, even under the realistic limitation of a switching dwell time $t_{\mathrm{dw}} > 0$ of the order of nanoseconds. Recall that in Chapter 5 the contrived assumption of constant input voltage was introduced in order to solve the game, so in (6.8) only the first (load current) component is actually relevant, because the other component is equal to the constant $V_I \triangleq V_{I\min} = V_{I\max}$.

As the state variable $\boldsymbol{y} = \begin{bmatrix} i_L & v_C \end{bmatrix}^\top$ will be preferred, along this chapter, over the dimensionless complex state variable z because of its physical meaning, so will be the case of the real time t over the normalized time $\mathsf{t} = \omega_d t$ (introduced in Subsection 3.4.3 while developing the canonical form of the conflict).

6.2. A first guiding example

Parameter	Description	Value	Unit
L	Inductor's inductance	310	nH
R_L	Inductor's parasitic ESR	10	mΩ
C	Capacitor's capacitance	1.1	mF
R_C	Capacitor's parasitic ESR	1.6	mΩ
$I_{O\min}$	Minimum load current	1	A
$I_{O\max}$	Maximum load current	50	A
$V_I = V_{I\min} = V_{I\max}$	Input voltage	5	V
V_{LL0}	Open-circ. load ref. voltage	1.5	V
R_{LL}	Load line resistance	1.25	mΩ
E	Error tolerance	80	mV

Table 6.1: Parameter values of a buck converter control problem example.

As an example, take the case of the control problem specified by the parameter values detailed in Table 6.1. The absolute worst-case error value function $\boldsymbol{y} \mapsto \mathcal{V}_{|\mathrm{e}^{\mathrm{wc}}|}(\boldsymbol{y})$ and the instantaneous absolute worst-case error function $\boldsymbol{y} \mapsto |\mathrm{e}^{\mathrm{wc}}(\boldsymbol{y})|$ for this example are represented graphically by their contour plots at the bottom of Figure 6.1. At the upper part of the same figure the corresponding functions $z \mapsto \mathcal{V}_{\mathrm{d_o}}(z)$ and $z \mapsto \mathrm{d_o}(z)$, related to the former ones by (6.3) and (6.5), respectively, are represented by their contour plots.

Observe in the contour plot of $\boldsymbol{y} \mapsto |\mathrm{e}^{\mathrm{wc}}(\boldsymbol{y})|$ that the minimum instantaneous absolute worst-case error is approximately 8.6 mV, which corresponds to the evaluation of the second term in the RHS of (6.1).

The error tolerance for this example is $E = 80$ mV. The control requirement, i.e., $|\mathrm{e}(t)| < E$ for every $t \geq 0$, can be expected to be fulfilled by E, if he plays optimally, for every initial state lying in the escape set (ES)

$$\mathscr{E}_{\mathbf{E}} = \left\{ \boldsymbol{y} \in \mathbb{R}^2 \ : \ \mathcal{V}_{|\mathrm{e}^{\mathrm{wc}}|}(\boldsymbol{y}) < E \right\}. \tag{6.9}$$

As it is visualized in Figure 6.1, obviously $\mathscr{E}_{\mathbf{E}} \subset \mathscr{E}' = \{\boldsymbol{y} \in \mathbb{R}^2 \ : \ |\mathrm{e}^{\mathrm{wc}}(\boldsymbol{y})| < E\}$, i.e., the ES (which is non-empty for this example) must be necessarily included in the PS. The name escape set given to $\mathscr{E}_{\mathbf{E}}$ follows from the metaphorical reference to the event of the control requirement being violated as the event of P "capturing" E.

Figure 6.1: Four related contour maps for the example of Table 6.1. *Above:* for $z \in \mathbb{C}$, contours of $z \mapsto \mathcal{V}_{\mathrm{d_o}}(z)$ (coloured closed curves) and contours of $z \mapsto \mathrm{d_o}(z, \mathscr{T}) = 1 - |\Im z|$ (dashed lines). *Below:* for $\boldsymbol{y} = i_L \hat{\boldsymbol{e}}_{\boldsymbol{1}} + v_C \hat{\boldsymbol{e}}_{\boldsymbol{2}} \in \mathbb{R}^2$, contours of $\boldsymbol{y} \mapsto \mathcal{V}_{|\mathrm{e^{wc}}|}(\boldsymbol{y})$ (coloured closed curves) and contours of $\boldsymbol{y} \mapsto |\mathrm{e^{wc}}(\boldsymbol{y})|$ (dashed lines). The lines $v_C = V_{LL0} - R_{LL}i_L$ (dot-dashed), and $i_L = I_{O\min}$, $i_L = I_{O\max}$ (densely dotted) in the i_L–v_C plane (at the bottom), and their counterparts in the canonical state-space (at the top) are just helping lines.

6.3.   The solution as a control method

This is probably the most straightforward application of the solution of the game in distance. Any optimal strategy for E is a natural feedback law to be considered, at least theoretically, as a possible control law for a real buck converter control problem.

6.3.1.   The evader's optimal strategy as it was proposed

To actually escape form P for every play starting in $\mathscr{E}_{\mathbf{E}}$, E has to apply, for example, the optimal strategy (6.7) (in the context of $\boldsymbol{\mathcal{G}_{\mathbf{dist}}}'$ or equivalently $\boldsymbol{\mathcal{G}_{|e^{\mathbf{wc}}|}}'$) that results from the solution proposed in Chapter 5 for the canonical game $\mathcal{G}_{\mathrm{dist}}$.

E's optimal strategy (6.7) for the current example is described graphically in the upper part of Figure 6.2 by the coloured areas that cover the converter's realistic state-space taken as the plane i_L–v_C. For each point of this plane a well defined control action is prescribed for E: either $\sigma = 1$ (switch ON), or $\sigma = 0$ (switch OFF).

To test this strategy, consider a play, starting at $\boldsymbol{y}\,(0) = [i_L\,(0)\,, v_C\,(0)]^\top = [40\,\mathrm{A}, 1.4\,\mathrm{V}]^\top$, such that P keeps the load current $i_O\,(t)$ constant at its maximum possible value $I_{O\max} = 50\,\mathrm{A}$ for every $t \geq 0$, and E puts into practice the strategy (6.7), as described by the coloured areas in Figure 6.2, except for the fact that his switching action is limited by a dwell time constant $t_{\mathrm{dw}} = 50\,\mathrm{ns}$ which prevents successive switchings separated by an interval of time of length equal or less than t_{dw}.

The state-space trajectory of the numerically simulated play is represented in Figure 6.2 by the black curve with an endpoint at the initial condition $[40\,\mathrm{A}, 1.4\,\mathrm{V}]^\top$. Observe that when the state reaches the boundary of the (convex) *valley of* $\boldsymbol{\mathcal{G}_{|e^{\mathbf{wc}}|}}'$, defined as the set

$$\mathscr{V} = \left\{ \boldsymbol{y} \in \mathbb{R}^2 \ : \ \mathcal{V}_{|\mathrm{e^{wc}}|}\,(\boldsymbol{y}) = \min_{\boldsymbol{y}' \in \mathbb{R}^2} \mathcal{V}_{|\mathrm{e^{wc}}|}\,(\boldsymbol{y}') \right\} \tag{6.10}$$

where the function $\boldsymbol{y} \mapsto \mathcal{V}_{|\mathrm{e^{wc}}|}\,(\boldsymbol{y})$ attains its minimum

$$\min_{\boldsymbol{y} \in \mathbb{R}^2} \mathcal{V}_{|\mathrm{e^{wc}}|}\,(\boldsymbol{y}) \approx 64.7\,\mathrm{mV}, \tag{6.11}$$

E's strategy (6.7) leads him into undesirable high frequency chattering (of the order of megahertz), as it is appreciated in the plot of $|\mathrm{e^{wc}}\,(t)|$ versus t at the bottom of Figure 6.2. In fact, if E had not been limited by a positive dwell time t_{dw}, the situation would have been even worst because the converter's state would have incurred into a *sliding motion* along the boundary of $\mathscr{V}$ towards the line $i_L = I_{O\max}$.
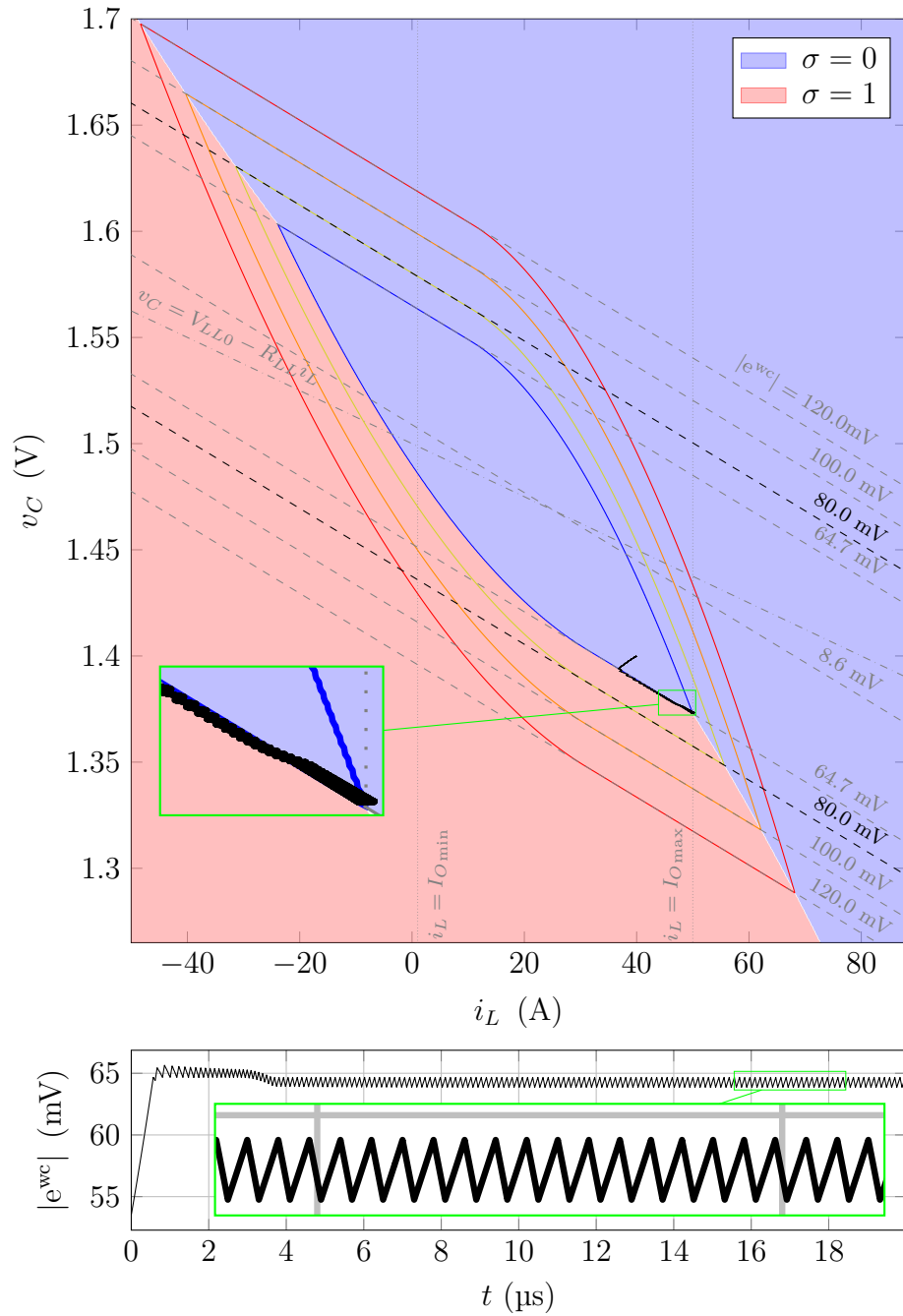
Figure 6.2: For the example of Table 6.1, simulation of a play that starts at $\boldsymbol{y}(0) = [i_L(0), v_C(0)]^\top = [40\,\mathrm{A}, 1.4\,\mathrm{V}]^\top$. For each $t \geq 0$, P applies a constant load current $i_O(t) = I_{O\max} = 50\,\mathrm{A}$, and E selects the switching action $\sigma(t)$ dictated by the strategy derived for him from the proposed solution of the game in distance (indicated by the coloured areas in the i_L–v_C state-space). Even though this strategy is optimal for E, it is not free from sliding trajectories. To limit the converter's switching frequency, the switch is purposely limited by a $50\,\mathrm{ns}$ dwell time which gives rise to the observed chattering at $7.5\,\mathrm{MHz}$.

6.3.2. An equivalent optimal strategy for the evader

The observed chattering is unnecessary and is due to the arbitrary way in which E's strategy was defined in the valley $\mathscr{V}$ of $\mathcal{G}_{|e^{wc}|}{}'$ (or more properly in the summit $\mathscr{M}$ of $\mathcal{G}_{\mathrm{dist}}$ in Chapter 5). In fact, all that is required from an optimal strategy for E to be such, is that it can prevent the state from crossing the level curves of $\mathcal{V}_{|e^{wc}|}$ in the *increasing* direction. Since $\mathcal{V}_{|e^{wc}|}$ is constant in the valley $\mathscr{V}$, E's optimal strategy is not uniquely defined in $\mathscr{V}$.

Recognizing these facts, an emendation of (6.7) is proposed as described graphically by the coloured and non-coloured area of the i_L–v_C plane represented in Figure 6.3. The proposal relies on the simple idea of not requiring E to act unless the state $\boldsymbol{y}$ reaches the boundary of the valley (6.10) where $\mathcal{V}_{|e^{wc}|}(\boldsymbol{y})$ is at risk of increasing. The introduced hysteresis in E's optimal strategy transforms it into a control method that cannot be properly referred to as a *feedback* strategy. However, it is still an optimal strategy for $\mathcal{G}_{|e^{wc}|}{}'$.

The proposed alternative for E's original optimal strategy, as described graphically in Figure 6.3, is tested in a simulated play with the same conditions that were used before, that is to say: initial state at $\boldsymbol{y}(0) = [i_L(0), v_C(0)]^\top = [40\,\mathrm{A}, 1.4\,\mathrm{V}]^\top$, constant maximum load current $i_O(t) = I_{O\max} = 50\,\mathrm{A}$ applied by P for every $t \geq 0$, and a switching action limitation imposed on E by a dwell time constant $t_{\mathrm{dw}} = 50\,\mathrm{ns}$. The resulting state-space trajectory is illustrated in the i_L–v_C plane represented in Figure 6.3 by the black curve with an endpoint at the initial state. The state clearly "bounces" between the two smooth pieces of the boundary of $\mathscr{V}$ as the state approaches the line $i_L = I_{O\max}$. Even though this state-space trajectory is free from sliding motions, it presents an undesirable *Zeno behaviour* which is only limited by the purposely imposed 50 ns dwell time on the switching action. The resulting steady-state switching frequency, of the order of megahertz, still precludes the proposed control method from being convenient from a practical standpoint.

Note in Figure 6.3 that E cannot prevent the state from slightly abandoning $\mathscr{V}$ in an small neighbourhood of the intersection point of $\mathscr{V}$ and the line $i_L = I_{O\max}$, because of the positive dwell time limitation imposed on its switching action. This fact (which confirms the practical implications of Proposition 4.3.4), allows P to do without ϵ-saddle-point strategies in case he pretends to play optimally against a dwell-time-limited evader.
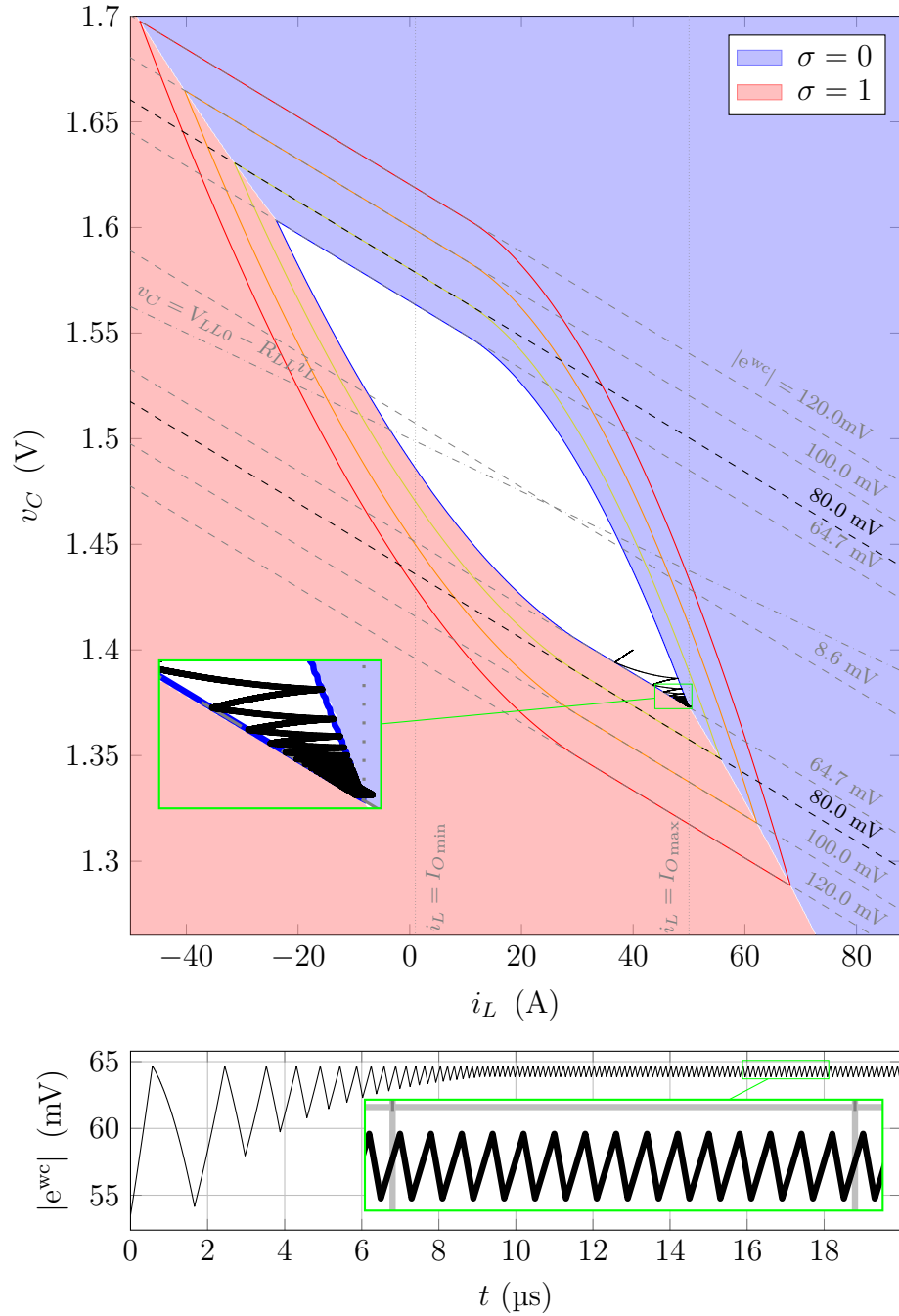
Figure 6.3: For the example of Table 6.1, simulation of a play starting at $\boldsymbol{y}(0) = [i_L(0), v_C(0)]^\top = [40\,\mathrm{A}, 1.4\,\mathrm{V}]^\top$. For each $t \geq 0$, P applies a constant load current $i_O(t) = I_{O\max} = 50\,\mathrm{A}$, and E selects the switching action $\sigma(t)$ dictated by the strategy derived for him from the proposed solution of the game in distance *if* $\mathcal{V}_{|\mathrm{e^{wc}}|}(\boldsymbol{y}(t)) > \min\{\mathcal{V}_{|\mathrm{e^{wc}}|}(\boldsymbol{y}) : \boldsymbol{y} \in \mathbb{R}^2\} \approx 64.7\,\mathrm{mV}$ (see the coloured areas in the i_L–v_C state-space), *otherwise* E leaves $\sigma(t) = \lim_{s \to t^-} \sigma(s)$ unchanged (see the non-coloured area in the i_L–v_C state-space). It is assumed that $\lim_{s \to 0^-} \sigma(s) = 0$. This strategy is not properly a feedback strategy, but still is optimal for E. However, it may produce Zeno behaviour as in this example; limited, though, by the switch's $50\,\mathrm{ns}$ dwell time which causes chattering at $7.5\,\mathrm{MHz}$.

6.3.3. A relaxation of the evader's strategy

From the observation of the two previous simulation results, the remedy to undesired sliding motions and Zeno behaviours appears to be clear. It comes at the cost of sacrificing performance, in an administrable manner, though.

Suppose that for plays that start at $\boldsymbol{y}\left(0\right)$ in $\mathscr{V}$, E resigns his ambition of keeping the state $\boldsymbol{y}\left(t\right)$ in $\mathscr{V}$ for every $t \geq 0$. For example, let $\lambda > 0$ quantify E's permissibility in this respect assuming that he does not act on the converter's switch unless the state escapes from $\left\{\boldsymbol{y} \in \mathbb{R}^2 \ : \ \mathcal{V}_{|\mathrm{e^{wc}}|}\left(\boldsymbol{y}\right) \leq \lambda\right\}$, in which case he applies the switching action dictated by his optimal strategy (6.7). As long as λ can be chosen such that

$$\min_{\boldsymbol{y}\in\mathbb{R}^2} \mathcal{V}_{|\mathrm{e^{wc}}|}\left(\boldsymbol{y}\right) < \lambda < E,$$

the just proposed *relaxed evader's strategy (RES) of permissibility* λ does not put at risk the control requirement for plays that initiate in (6.9) while it extends the remedial hysteresis outside from $\mathscr{V}$.

In Figure 6.4 a RES of permissibility $\lambda = 0.95E = 76\,\mathrm{mV}$ is described graphically (by the coloured areas and the non-coloured area of the represented i_L–v_C plane) for the example of Table 6.1 being considered. This is the maximum relaxation that can be introduced while still letting a 5 % guard band of E's active control against control requirement violations.

As before, a play starting at $\boldsymbol{y}\left(0\right) = \left[i_L\left(0\right), v_C\left(0\right)\right]^\top = \left[40\,\mathrm{A}, 1.4\,\mathrm{V}\right]^\top$, such that P applies $i_O\left(t\right) = I_{O\max} = 50\,\mathrm{A}$ for every $t \geq 0$, is simulated to test the proposed relaxation of E's optimal strategy, as described in Figure 6.4, except for the realistic imposed limitation of a 50 ns dwell time constant on the switching action.

By contrast with the previous simulation results, the resulting trajectory is free from the (7.5 MHz)-frequency chattering that resulted from potential sliding motions and Zeno behaviours that pushed the switching action to the limit of the dwell time constant. Observe at the bottom of Figure 6.4 how $|\mathrm{e^{wc}}\left(\boldsymbol{y}\left(t\right)\right)|$ remains below $E = 80\,\mathrm{mV}$ for every $t \geq 0$, exhibiting an almost steady-state frequency approximately equal to 700 kHz.

Having already addressed the problems related to sliding motions and Zeno behaviours, consider the block diagram depicted in Figure 6.5. It describes how a *RES controller* is proposed to control a buck converter. The access to the converter's state $\boldsymbol{y}\left(t\right) = \left[i_L\left(t\right), v_C\left(t\right)\right]^\top$ allows the RES controller to act on the converter's switch so as to prevent $\mathcal{V}_{|\mathrm{e^{wc}}|}\left(\boldsymbol{y}\left(t\right)\right)$ from increasing. However this presupposes, from the RES controller, an *exact* knowledge of the parameters present in Table 6.1, in particular of the parameters L, R_L, C, and R_C which characterize the plant (i.e., the converter) under control. Such is the confidence on the converter's model encoded in the RES controller that error feedback information is done away with, as graphically emphasised in the block diagram of Figure 6.5.
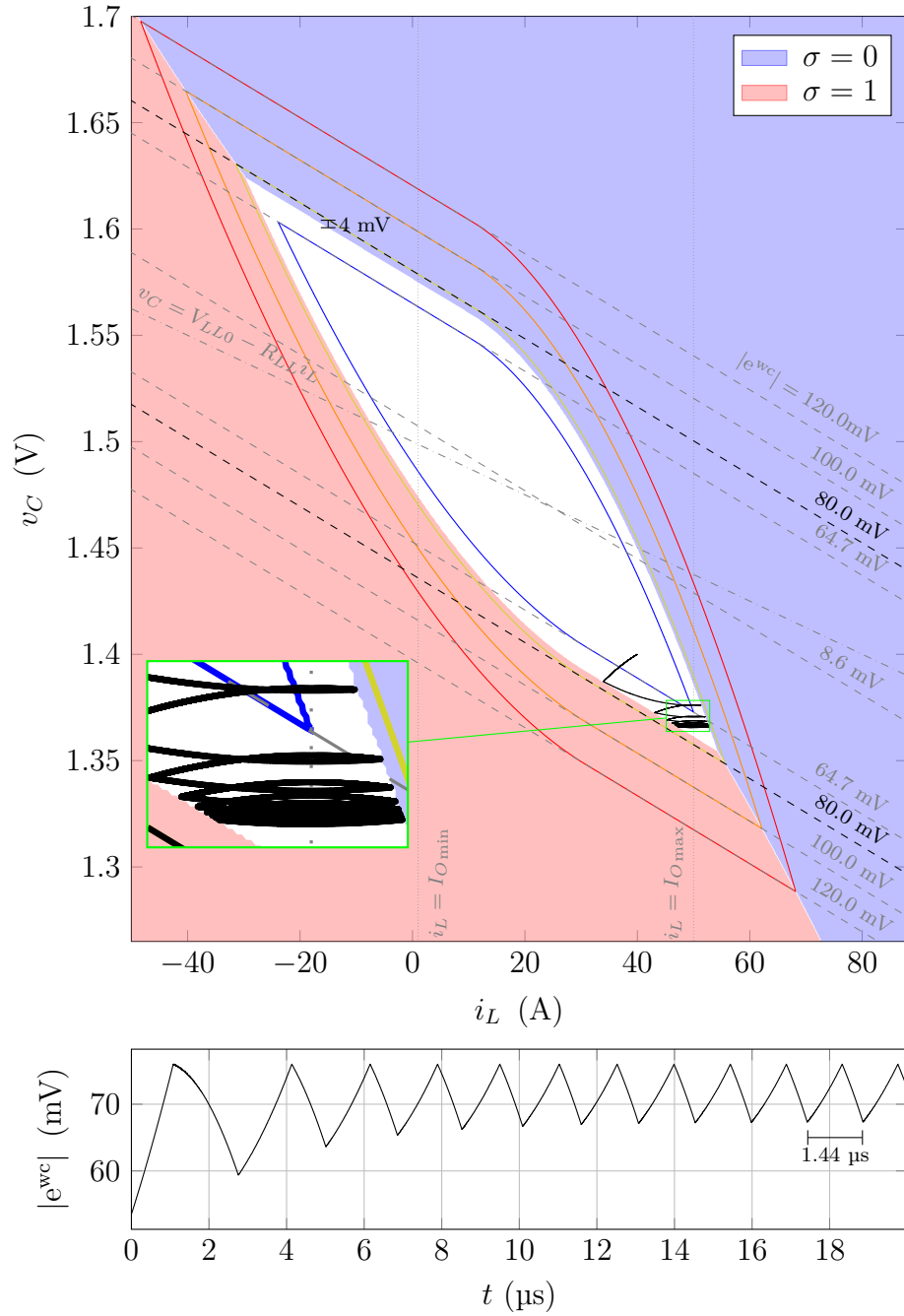
Figure 6.4: For the example of Table 6.1, simulation of a play that starts at $\boldsymbol{y}(0) = [i_L(0), v_C(0)]^\top = [40\,\text{A}, 1.4\,\text{V}]^\top$. For each $t \geq 0$, P applies a constant load current $i_O(t) = I_{O\max} = 50\,\text{A}$, and E selects the switching action $\sigma(t)$ dictated by the strategy derived for him from the proposed solution of the game in distance *if* $\mathcal{V}_{|e^{\text{wc}}|}(\boldsymbol{y}(t)) > 0.95E = 76\,\text{mV}$ (see the coloured areas), *otherwise* E leaves $\sigma(t) = \lim_{s \to t^-} \sigma(s)$ unchanged (see the non-coloured area in the i_L–v_C state-space). It is assumed that $\lim_{s \to 0^-} \sigma(s) = 0$. This *relaxed* version of E's optimal strategy is free from the $7.5\,\text{MHz}$ chattering observed in Figures 6.2 and 6.3 (related to the $50\,\text{ns}$ dwell time of the converter's switch), at least for $\boldsymbol{y}(0)$ such that $\mathcal{V}_{|e^{\text{wc}}|}(\boldsymbol{y}(0)) \leq 76\,\text{mV}$. The almost steady-state $694.4\,\text{kHz}$ frequency observed in the figure is much lower than $7.5\,\text{MHz}$.
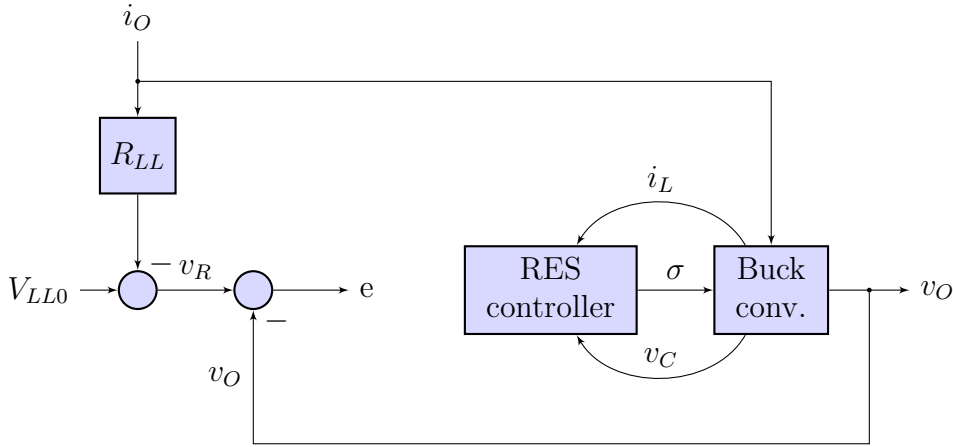
Figure 6.5: Block diagram of the RES-controlled buck converter, under the assumption of constant input voltage.

6.3.4. Some common methods of buck converter control

To explore the RES (proposed in Subsection 6.3.3) as a control method for the example of Table 6.1, its disturbance rejection performance was evaluated and compared to other few common control methods, as will be reported in Subsection 6.3.5, by simulating the controlled converter response to an extreme load current pulse driving signal.

The selected controllers against which the RES controller was compared are the following: a) PID controller, b) hysteresis (H) controller, and c) SM controller. This subsection is devoted to briefly explain how each controller was virtually implemented and tuned.

The ideal of a fair comparison among the considered controllers influences each tuning method, particularly in connection with the maximum demanded switching frequency. Nonetheless, since the information required by each controller varies from case to case, the comparison among them is just illustrative and not claimed to be completely fair.

6.3.4.1. The PID controller

The PID controller is by far the most common control algorithm used in industry and buck converter control is not an exception in this respect.

Recall the simplified buck converter model described by the circuit diagram of Figure 3.2. The equations (3.4)–(3.6) that rule the dynamics of this model are rewritten next for ease of use:

$$L\frac{\mathrm{d}i_L}{\mathrm{d}t} = \sigma V_I - R_L i_L - v_C - R_C\left(i_L - i_O\right), \tag{6.12}$$

$$C\frac{\mathrm{d}v_C}{\mathrm{d}t} = i_L - i_O, \tag{6.13}$$

$$v_O = R_C\left(i_L - i_O\right) + v_C, \tag{6.14}$$

where v_I was substituted by V_I to remind that the input voltage is assumed constant. Actually, for the example of Table 6.1 being considered, and for all the examples of this chapter the symbol V_I is used to denote the constant $V_{I\min} = V_{I\max}$.

Under *synchronous operation* of the buck converter, the switching action $t \mapsto \sigma(t)$, which appears in (6.12), results from a PWM technique that encodes a control signal $t \mapsto d(t)$ as the *duty cycle* of $t \mapsto \sigma(t)$. The technique is modelled as follows. A periodic sawtooth signal of period $T_{\mathrm{s}} > 0$ and unitary amplitude defined as

$$t \mapsto w(t) = \frac{t - iT_{\mathrm{s}}}{T_{\mathrm{s}}} \quad \text{if} \quad t \in [iT_{\mathrm{s}}, (i+1)\,T_{\mathrm{s}}),$$

for every $i \in \mathbb{Z}$, is compared to a control signal $t \mapsto d(t) \in [0,1]$ to generate

$$t \mapsto \sigma(t) = \begin{cases} 1 & \text{if } t \in [iT_{\mathrm{s}}, (i+1)\,T_{\mathrm{s}}) \text{ and } d(t') \geq w(t') \text{ for every } t' \in [iT_{\mathrm{s}}, t], \\ 0 & \text{otherwise,} \end{cases}$$

for every $i \in \mathbb{Z}$. Notice that for each $i \in \mathbb{Z}$, the idealised converter's switch is compulsorily turned on at the beginning of the period interval $[iT_{\mathrm{s}}, (i+1)\,T_{\mathrm{s}})$, and the comparison between both signals (that eventually turns off the switch during the same period interval) remains active *only* if the switch has not already been turned off during the same period interval. Once the switch has been turned off during the period interval $[iT_{\mathrm{s}}, (i+1)\,T_{\mathrm{s}})$, it cannot be turned on again until the beginning of the next period interval $[(i+1)\,T_{\mathrm{s}}, (i+2)\,T_{\mathrm{s}})$. This *latched* PWM prevents multiple switchings during the same period interval in case the control signal $t \mapsto d(t)$ varies too quickly with respect to $t \mapsto w(t)$.

Averaging the equations (6.12)–(6.14) over a moving-average-window of length T_{s}, the following *averaged model* is obtained for the buck converter under synchronous operation:

$$L\frac{\mathrm{d}\langle i_L \rangle}{\mathrm{d}t} = V_I d - R_L \langle i_L \rangle - \langle v_C \rangle - R_C\left(\langle i_L \rangle - \langle i_O \rangle\right), \tag{6.15}$$

$$C\frac{\mathrm{d}\langle v_C \rangle}{\mathrm{d}t} = \langle i_L \rangle - \langle i_O \rangle, \tag{6.16}$$

$$\langle v_O \rangle = R_C\left(\langle i_L \rangle - \langle i_O \rangle\right) + \langle v_C \rangle, \tag{6.17}$$

where $\langle x \rangle$ stands for the *averaged signal*

$$t \mapsto \langle x \rangle(t) \triangleq \frac{1}{T_{\mathrm{s}}} \int_{t-T_{\mathrm{s}}}^{t} x(t)\,\mathrm{d}t$$

of the generic signal $t \mapsto x(t)$. Observe that $d = \langle \sigma \rangle$ in (6.15).

Taking Laplace transforms (assuming zero initial conditions) in the above equations and isolating $\langle vO \rangle(s)$ in terms of $\langle d \rangle(s)$ and $\langle i_O \rangle(s)$, we get

$$\langle v_O \rangle(s) = V_I \underbrace{\frac{R_C C s + 1}{LC s^2 + (R_L + R_C)\,Cs + 1}}_{H_{\mathrm{BUCK}}^d(s)} d(s) - \underbrace{\frac{(Ls + R_L)\,(R_C C s + 1)}{LC s^2 + (R_L + R_C)\,Cs + 1}}_{H_{\mathrm{BUCK}}^{iO}(s)} \langle i_O \rangle(s)$$

$$\tag{6.18}$$

where, abusing notation, $s \mapsto \langle v_O \rangle (s)$, $s \mapsto d(s)$, and $s \mapsto i_O(s)$ stand for the Laplace transforms of $t \mapsto \langle v_O \rangle (t)$, $t \mapsto d(t)$, and $t \mapsto \langle i_O \rangle (t)$, respectively. The transfer functions, H_{BUCK}^d and $H_{\mathrm{BUCK}}^{i_O}$, introduced above provide an input-output description of the synchronous buck converter averaged model, under the assumption of constant input voltage. Recalling definitions (3.35) this *second order model* may be expressed as

$$\langle v_O \rangle (s) = V_I \underbrace{\frac{\omega_n^2 \left(R_C C s + 1 \right)}{s^2 + 2\zeta\omega_n s + \omega_n^2}}_{H_{\mathrm{BUCK}}^d(s)} d(s) - \underbrace{\frac{\omega_n^2 \left(L s + R_L \right) \left(R_C C s + 1 \right)}{s^2 + 2\zeta\omega_n s + \omega_n^2}}_{H_{\mathrm{BUCK}}^{i_O}(s)} \langle i_O \rangle (s) \quad (6.19)$$

where $\omega_n = \frac{1}{\sqrt{LC}}$ and $\zeta = \frac{R_L + R_C}{2\omega_n L}$ are its natural frequency and its damping ratio, respectively. Observe that $\zeta < 1$ and $\omega_n < \frac{1}{R_C C}$ because of assumptions (A8) and (A9), respectively

The PID controller is compelled to act on d so as to keep the error e $= V_{LL0} - R_{LL} i_O - v_O$ as close to zero as possible. Therefore, it has to compensate, to the best of its ability, the disturbing effect that i_O has on the error e (see the block diagram of Figure 6.6). A signal $t \mapsto d_{\mathrm{PID}}(t)$ is computed by the PID controller such that its Laplace transform $s \mapsto d_{\mathrm{PID}}(s)$ is given (assuming zero initial conditions) by

$$d_{\mathrm{PID}}(s) = \underbrace{K_P \left(1 + \frac{1}{T_I s} + \frac{T_D s}{\frac{T_D}{N_D}s + 1} \right)}_{H_{\mathrm{PID}}(s)} \mathrm{e}(s), \quad (6.20)$$

where $s \mapsto \mathrm{e}(s)$ is the Laplace transform of the error signal $t \mapsto \mathrm{e}(t)$, and H_{PID} is the transfer function of the PID controller. The factor $\frac{T_D}{N_D}s + 1$ is deliberatively introduced into the otherwise pure PID transfer function, i.e., $K_P \left(1 + \frac{1}{T_I s} + T_D s \right)$, so that high-frequency measurement noise is amplified *at most* by a factor $K_P N_D$. However, the signal that is actually used as input for the latched PWM is necessarily of the saturated form

$$d(t) = \begin{cases} 1 & \text{if } d_{\mathrm{PID}}(t) > 1, \\ 0 & \text{if } d_{\mathrm{PID}}(t) < 0, \\ d_{\mathrm{PID}}(t) & \text{otherwise.} \end{cases} \quad (6.21)$$

To prevent integral windup, i.e., to prevent the integral action from becoming too large when saturation of $d(t)$ takes place (either towards 1 or 0), an anti-windup mechanism is incorporated in the simulated PID controller. The selected mechanism, which consists in stopping integration if $d_{\mathrm{PID}}(t) \neq d(t)$ *and* e $(t) d_{\mathrm{PID}}(t) > 0$, is reported in [78] to be the best scheme among other variants of the *conditional integration* approach to avoid integral windup.

Let $a \triangleq T_I T_D \left(1 + \frac{1}{N_D} \right)$, $b \triangleq T_I + \frac{T_D}{N_D}$, and $c \triangleq \frac{T_D}{N_D}$, so that the *open-loop* transfer function can be expressed as

$$H_{\mathrm{OL}}(s) \triangleq H_{\mathrm{BUCK}}^d(s) H_{\mathrm{PID}}(s) = \frac{K_P V_I}{T_I s} \omega_n^2 a \left(\frac{s^2 + \frac{b}{a}s + \frac{1}{a}}{s^2 + 2\zeta\omega_n s + \omega_n^2} \right) \frac{R_C C s + 1}{cs + 1}.$$
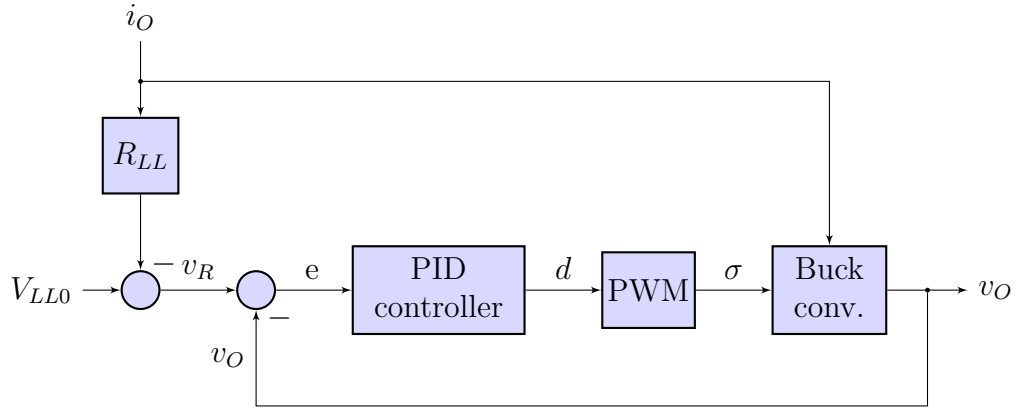
Figure 6.6: Block diagram of the PID-controlled synchronous buck converter, under the assumption of constant input voltage.

To tune the PID controller parameters a classical *loop-shaping* methodology is followed, based on the following criteria which seeks an uniform $-20 \frac{\text{dB}}{\text{dec}}$ slope of the straight-line magnitude Bode approximation of H_{OL} without recourse to *non-real* zero-pole cancellations, and an open-loop unit gain bandwidth as high as possible but not so high as to risk the validity of the averaged model thereby incurring excessive ripple on the output voltage.

- PID controller tuning criteria:

  1. *Medium frequency real zeros at the converter's natural frequency.*
     The zeros of H_{PID} are demanded to be real and to have an angular frequency equal to ω_n.

  2. *High-frequency pole placed so as to achieve zero-pole cancellation.*
     The high-frequency pole of H_{PID} must cancel the zero of H_{BUCK}^d.

  3. *Compromise selection of the open-loop unit gain bandwidth.*
     The gain crossover frequency of H_{OL} must be equal to one sixth of the PWM frequency.

- PID controller tuning methodology:
  Firstly, from criterion 1: $a = \frac{1}{\omega_n^2}$ and $b = \frac{2}{\omega_n}$, so that $s^2 + \frac{b}{a}s + \frac{1}{a} = s^2 + 2\omega_n s + \omega_n^2 = (s + \omega_n)^2$. Secondly, from criterion 2: $c = R_C C$. Thirdly, having determined the values of a, b, and c, the values of T_I, T_D and N_D are obtained as follows:

$$T_I = b - c,$$
$$T_D = \frac{a}{b-c} - c,$$
$$N_D = \frac{a}{c(b-c)} - 1.$$

225
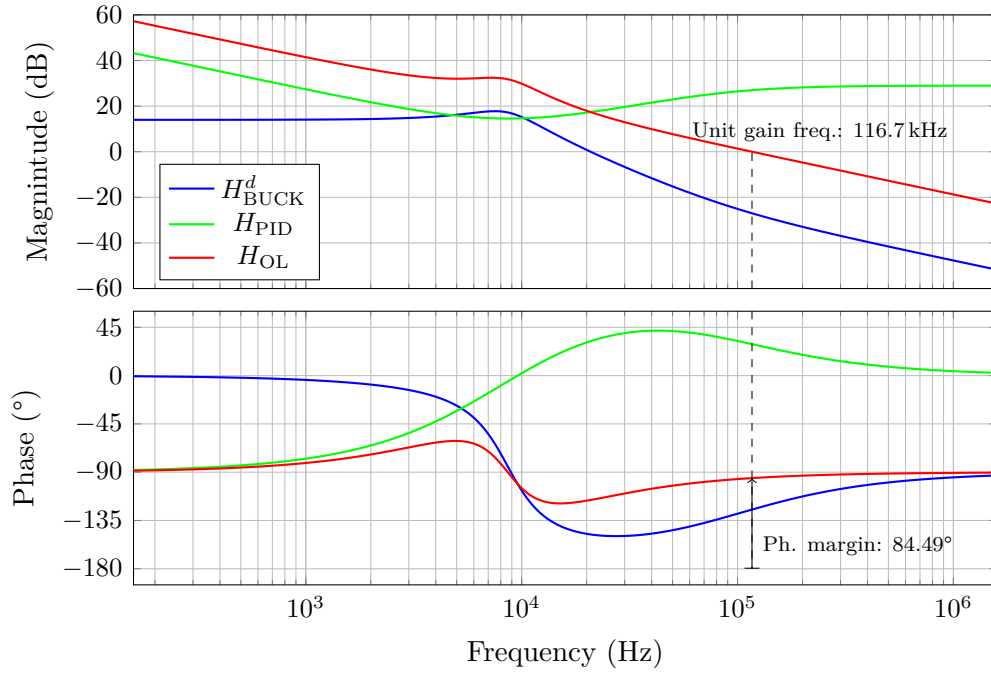
Figure 6.7: For the control problem example of Table 6.1, Bode plots of the frequency response of: the buck converter subsystem H^d_{BUCK}, the tuned PID-controller H_{PID}, and the resulting open-loop $H_{\mathrm{OL}} = H^d_{\mathrm{BUCK}} H_{\mathrm{PID}}$.

Finally, from 3:

$$
K_P = \left. \frac{1}{\left| 1 + \frac{1}{T_I s} + \frac{T_D s}{\frac{T_D}{N_D} s + 1} \right| \left| H^d_{\mathrm{BUCK}}(s) \right|} \right|_{s = j\frac{2\pi}{6T_s}}.
$$

Choosing a *PWM switching frequency* $f_s \triangleq T_s^{-1}$ of 700 kHz and following the just described tuning methodology for the example of Table 6.1, the following parameter values were obtained for the PID controller: $K_P = 5.107\,\mathrm{V}^{-1}$, $T_I = 35.17\,\mu\mathrm{s}$, $T_D = 7.935\,\mu\mathrm{s}$, $N_D = 4.509$. The corresponding Bode plots of H^d_{BUCK}, H_{PID}, and H_{OL} are illustrated in Figure 6.7.

Aiming fairness between the PID controller and the RES controller, the PWM switching frequency was chosen close to the steady-state switching frequency exhibited by the RES of permissibility $\lambda = 76\,\mathrm{mV}$ under maximum constant load current (as observed in Figure 6.4). This is the constant load condition found to demand the highest switching frequency from the RES-controller for the current example. A fact that can be intuitively attributable to the proximity of the the the line $\{(i_L, v_C) \; : \; i_L = I_{O\max}\}$ to "rightmost" corner point of $\{\boldsymbol{y} \; : \; \mathcal{V}_{|\mathrm{e^{wc}}|}(\boldsymbol{y}) \leq \lambda\}$ (see Figure 6.4).

6.3.4.2. Tuning of the hysteresis controller

The hysteresis (H) controller acts on the converter's idealised switch according the following simple error-dependent law:

$$
\sigma(t) = \begin{cases} 1 & \text{if } e(t) \geq E_H, \\ 0 & \text{if } e(t) \leq -E_H, \\ \lim_{t' \to t^-} \sigma(t') & \text{otherwise}, \end{cases} \tag{6.22}
$$

where $e(t) = v_R(t) - v_O(t) = V_{LL0} - R_{LL}i_O(t) - v_O(t)$ is the voltage error (see Figure 6.8). The amplitude $E_H > 0$ of the hysteresis band is the only parameter that needs to be set a value in order to tune the H controller.

With the aim of achieving comparable maximum switching frequencies, among the different controllers being tested on the example of Table 6.1, the parameter E_H was selected by iterative trial-and-error simulations until the observed steady-state switching frequency of the H-controlled converter was close to $700\,\text{kHz}$, while being driven by maximum constant load current. The resulting value was $E_H = 0.05E = 4\,\text{mV}$.
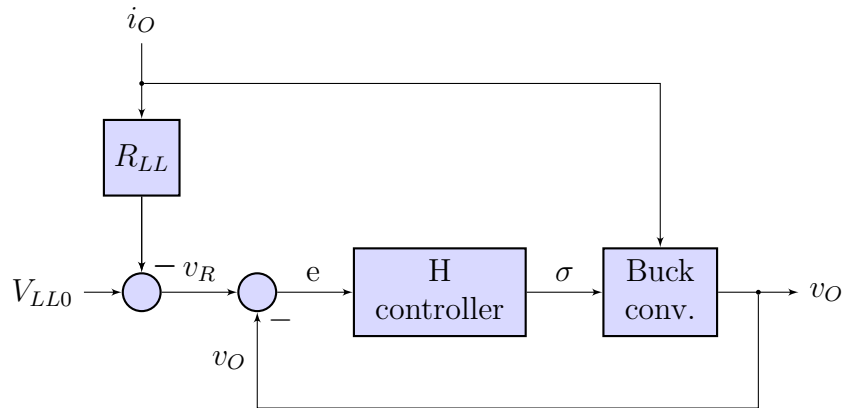
Figure 6.8: Block diagram of the H-controlled buck converter, under the assumption of constant input voltage.

6.3.4.3. Tuning of the sliding mode controller

As a third and last alternative to the RES controller (described in Subsection 6.3.3), a sliding mode (SM) controller proposed in [25] was simulated in charge of the control problem of Table 6.1.

In [25] the load of the converter is modelled by a resistance. However, in our set-up the load of the converter is modelled a by an independent current source (see Figure 3.2). To adapt the SM controller proposal described in [25] to our set-up, the following converter's nominal parameters are defined: *nominal load current* $I_{O\text{nom}} \triangleq \frac{1}{2}(I_{O\text{min}} + I_{O\text{max}})$, *nominal output voltage* $V_{O\text{nom}} \triangleq V_{LL0} - R_{LL}I_{O\text{nom}}$, and *nominal output resistance* $R_{\text{nom}}^{\text{load}} \triangleq \frac{V_{O\text{nom}}}{I_{O\text{nom}}}$.
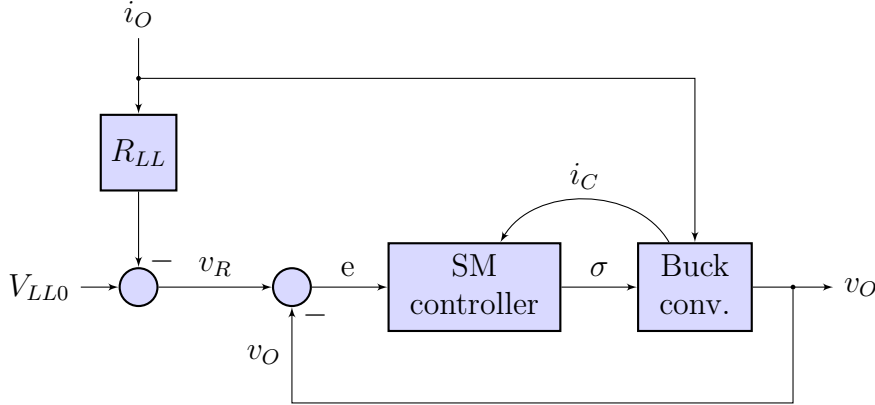
Figure 6.9: Block diagram of the SM-controlled buck converter, under the assumption of constant input voltage.

The SM controller (as proposed in [25]) acts on the converter's switch according to

$$\sigma(t) = \begin{cases} 1 & \text{if } S\left(\mathrm{e}\left(t\right), i_C\left(t\right)\right) \geq \kappa, \\ 0 & \text{if } S\left(\mathrm{e}\left(t\right), i_C\left(t\right)\right) \leq -\kappa, \\ \lim_{t' \to t^-} \sigma\left(t'\right) & \text{otherwise.} \end{cases} \tag{6.23}$$

where

$$\kappa = \frac{V_{O\mathrm{nom}}\left(1 - \frac{V_{O\mathrm{nom}}}{V_I}\right)}{2 f_{\mathrm{Sd}} L} \tag{6.24}$$

is the amplitude of an hysteresis band deliberately introduced to avoid *sliding-mode chattering*. The desired nominal switching frequency f_{Sd} determines the amplitude of the hysteresis band. The *switching function*

$$\left(\mathrm{e}, i_C\right) \mapsto S\left(\mathrm{e}, i_C\right) = \frac{1}{R_{\mathrm{nom}}^{\mathrm{load}}} \mathrm{e} - i_C, \tag{6.25}$$

where $\mathrm{e} = v_R - v_O = V_{LL0} - R_{LL} i_O - v_O$ is the voltage error (see Figure 6.9) and $i_C = C \frac{\mathrm{d} v_C}{\mathrm{d} t}$ is the current through the converter's capacitor (see Figure 3.2), defines a *switching line* $\{(\mathrm{e}, i_C) \ : \ S(\mathrm{e}, i_C) = 0\}$ towards which the moving point $(\mathrm{e}(t), i_C(t))$ is directed to by the SM controller's action. Once $(\mathrm{e}(t), i_C(t))$ reaches the switching line, *if* $(\mathrm{e}(t), i_C(t))$ starts tracking the sliding line towards $(0, 0)$, the controlled system is said to enter into *sliding mode*. In [25], the precise sliding mode *existence regions* in the e–i_C plane are studied. The controller formulated above is proposed by the authors as a practical and systematic way of approaching buck converter control with a SM control methodology.

Having introduced $I_{O\mathrm{nom}}$, $V_{O\mathrm{nom}}$, and $R_{\mathrm{nom}}^{\mathrm{load}}$ in terms of the parameters of Table 6.1 as just detailed, the only parameter value that needs to be set in order to tune the simulated SM controller is the desired switching frequency f_{Sd}. Aiming a fair as possible comparison among the tested controllers, this parameter value was set to $f_{\mathrm{Sd}} = 700\,\mathrm{kHz}$.

6.3.5. Disturbance rejection performance

The four controllers (RES, PID, H, and SM), tuned as explained before, were virtually put in charge of the buck converter control problem of Table 6.1. In particular, the performance of each of them was evaluated in response to a disturbing driving pulse of maximum amplitude ($I_{O\max} - I_{O\min} = 49\,\text{A}$) in the load current, departing from the controlled steady-state regime that corresponds to constant minimum load current ($I_{O\min} = 1\,\text{A}$). The pulse's 120 μs length was selected so as to let each response reach an almost steady-state regime.

In Figure 6.10 the simulated disturbance and resulting output voltage signal for each case are plotted. Alongside each output voltage (continuous line), the reference voltage (dot-dashed line) and the $\pm E$-tolerance band (dashed lines) are also plotted to ease the checking of the control requirement.

Notice that, as it was intended, the maximum switching frequencies are comparable among the different cases. However, the switching frequency range exhibited by the RES-controlled buck is much more wider than for the rest of the cases. Depending on the application, this may be an issue or not. The RES controller, as it was defined, requires a minimal switching effort in the sense that it acts only when the control requirement fulfilment is put at risk. This property is desirable if a variable-frequency output voltage ripple is of no concern. However, if the frequency range of the output voltage ripple is required to be narrow, the RES does not seem to be an attractive control method.

On the other hand, the RES controller is clearly the only one which actually fulfils the control requirement. This is achieved, however, at the cost of a much more complicated control algorithm, specifically designed to verify the control requirement (if it is possible at all), based on: i) exact knowledge of each of the control problem parameters, and ii) perfect full-state feedback.

Observe that, interestingly, while the controllers PID, H, and SM actively seek to reduce the steady-state error, the RES controller maintains it at a quite high level (close to the tolerance E) in order to "cover himself" against future load current transients. This salient difference is explained by the fact that the RES focuses in keeping low the future potentially attainable absolute worst-case error $\mathcal{V}_{|e^{wc}|}(\boldsymbol{y}(t))$, while all the other tested controllers focus on keeping low the current absolute error $|e(t)|$.

In Figure 6.11 the time interval $[110\,\mu\text{s}, 190\,\mu\text{s}]$, during which the load current steps down at the instant 120 μs, is examined closely for each tested controller. At the left side of the figure the absolute error $|e(t)|$ and the absolute worst-case error $|e^{wc}(t)|$ are plotted versus time t. At the right side of the figure the state-space trajectory $[110\,\mu\text{s}, 190\,\mu\text{s}] \ni t \mapsto \boldsymbol{y}(t) = \begin{bmatrix} i_L(t) & v_C(t) \end{bmatrix}^\top$ is plotted on the i_L–v_C plane enhanced with the contour maps of $\boldsymbol{y} \mapsto \mathcal{V}_{|e^{wc}|}(\boldsymbol{y})$ (coloured closed lines) and $\boldsymbol{y} \mapsto |e^{wc}(\boldsymbol{y})|$ (dashed straight lines). The dot-dashed line in the i_L–v_C plane represents the line $\{(i_L, v_C) : v_C = V_{LL0} - R_{LL}i_L\}$ where the average steady-state error is zero (because, from (6.16), it must be $\langle i_L \rangle = \langle iO \rangle$ in steady-state, and consequently, from (6.17), $\langle v_O \rangle = \langle v_C \rangle$)[1].

---

[1]Averaging is understood here over a moving-average window whose length is equal to
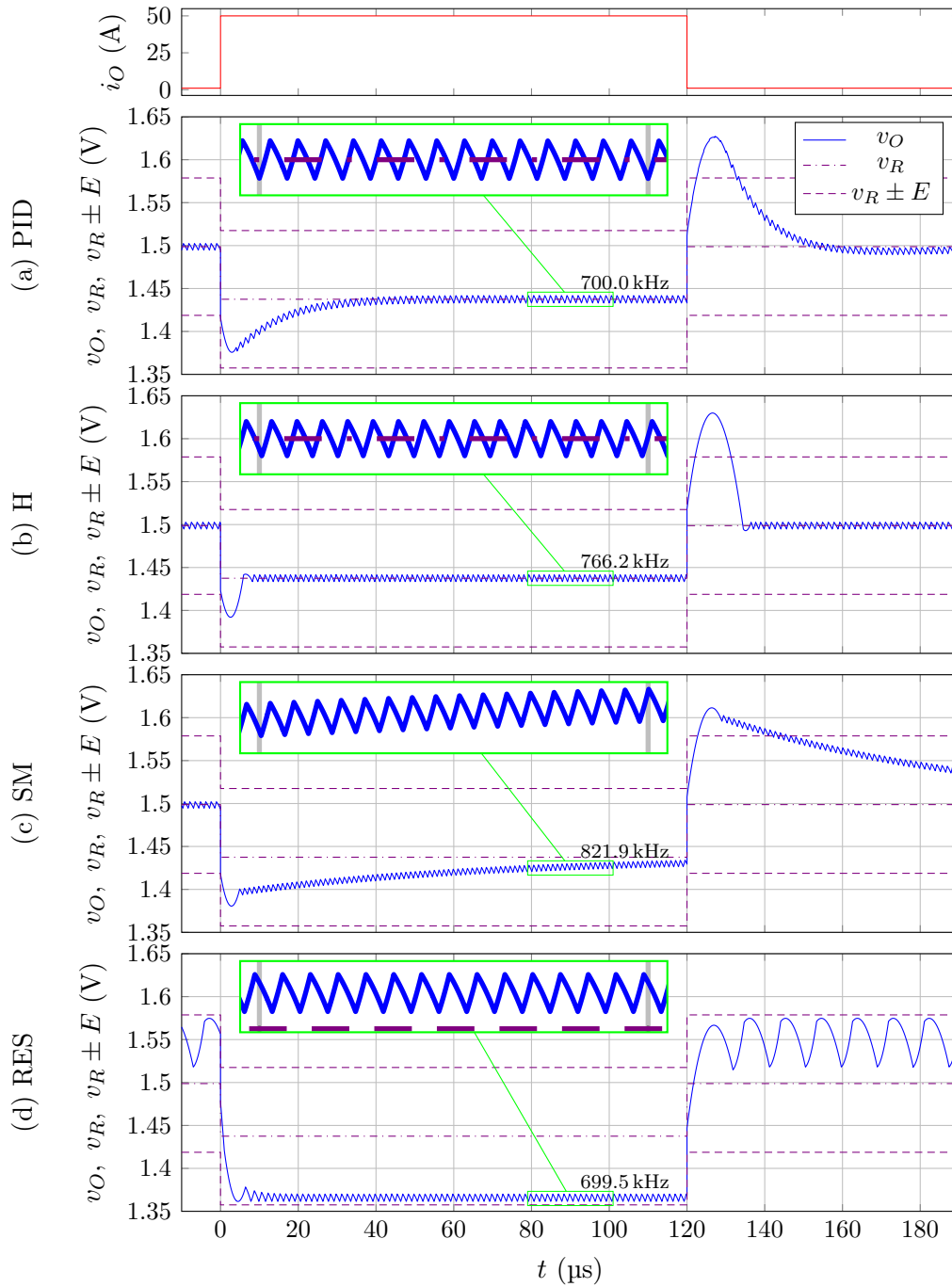
Figure 6.10: For the example of Table 6.1, a pulse in the load current (i_O), of amplitude $I_{O\max} - I_{O\min} = 49\,\text{A}$ and duration $120\,\mu\text{s}$, is used as the driving disturbance to simulate the response of the converter controlled by different controllers: (a) Proportional-Integral-Derivative (PID) controller, (b) Hysteresis (H) controller, (c) Sliding Mode (SM) controller, (d) Relaxed Evader's Strategy (RES) controller. In each case, the input voltage (v_I) is kept constant at $V_I = 5\,\text{V}$ and the converter's switch is limited by a $50\,\text{ns}$ dwell time. The synchronous PID-controlled buck is operated at $700\,\text{kHz}$ which is approximately the same steady-state frequency exhibited by the RES-controlled buck at maximum load current. The H controller and the SM controller are tuned so as to exhibit comparable switching frequencies.
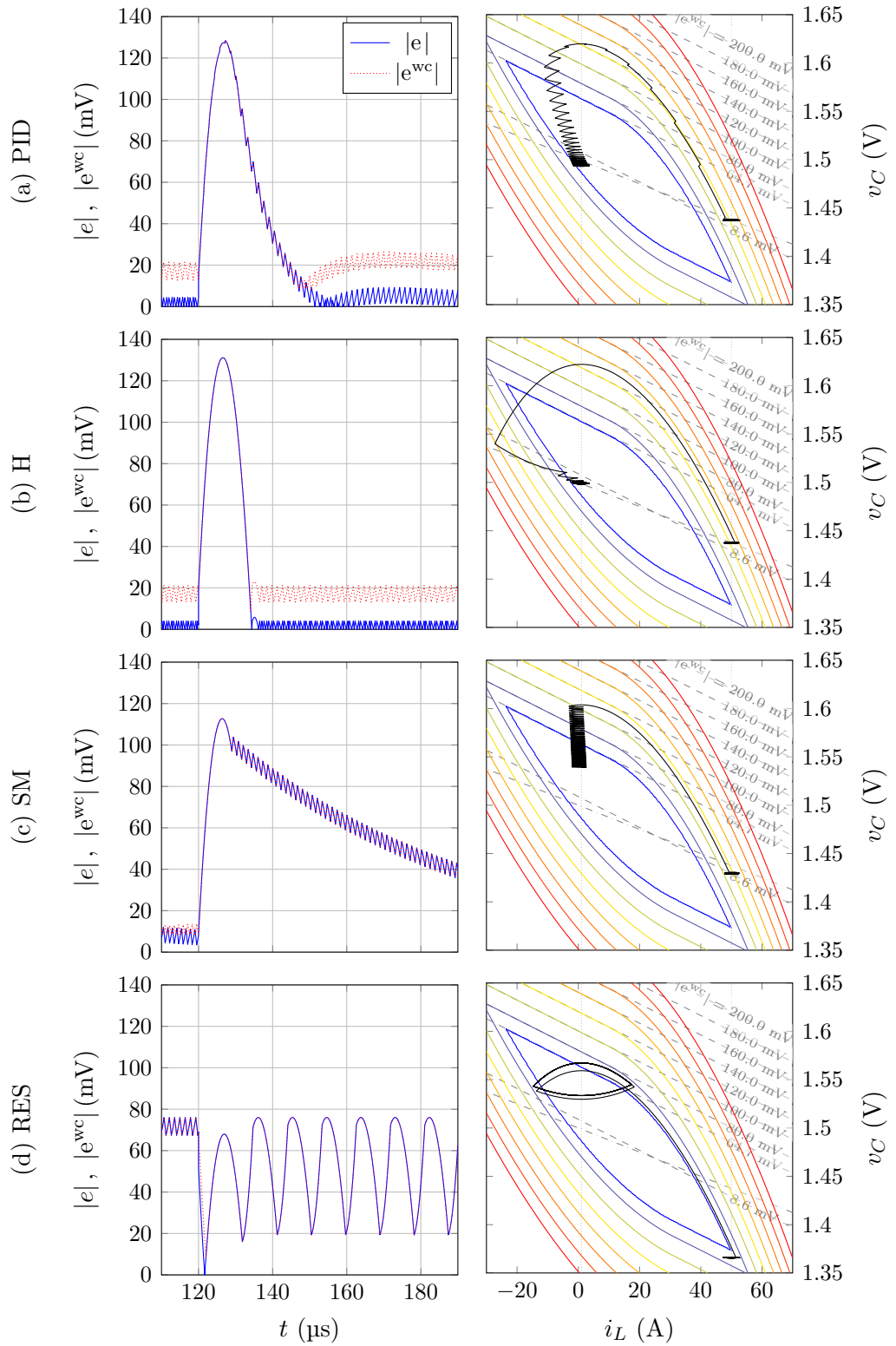
Figure 6.11: For each controller case and for $t \in [110\,\mu s, 190\,\mu s]$, the absolute error $t \mapsto |e(t)|$ and the absolute worst-case error $t \mapsto |e^{wc}(y(t))|$ (at the *left*), and the state-space trajectory $t \mapsto y(t) = [i_L(t), v_C(t)]^\top$ (at the *right*), that corresponds to same case in Figure 6.10.

Observe that every tested controller, except the RES controller, seeks the zero steady-state error condition. If the buck converter is not controlled by the RES controller, before the load current falling edge the state fluctuates around the *right* endpoint of the segment $\{(i_L, v_C) \ : \ v_C = V_{LL0} - R_{LL}i_L \ \wedge \ i_L \in [I_{O\min}, I_{O\max}]\}$, while after the load current falling edge the state tends to fluctuate around the *left* endpoint of the same segment. Quite differently, the RES controller disregards the relative position of the state to the line $\{(i_L, v_C) \ : \ v_C = V_{LL0} - R_{LL}i_L\}$. Instead, the RES controller continuously monitors the current-state evaluation of the absolute worst-case error value function, i.e., $\mathcal{V}_{|e^{wc}|}(\boldsymbol{y}(t))$, and takes a corrective action only when it reaches a risky level, namely the permissibility level $\lambda = 76\,\mathrm{mV}$. This causes the RES-controlled buck's state to fluctuate around a point on the line $\{(i_L, v_C) \ : \ i_L = I_{O\max}\}$, before the load current falling edge, that is distant from the zero average steady-state error line $\{(i_L, v_C) \ : \ v_C = V_{LL0} - R_{LL}i_L\}$. Similarly, after the load current falling edge, the state tends to steady-state fluctuation around a point on the line $\{(i_L, v_C) \ : \ i_L = I_{O\min}\}$ that is distant from $\{(i_L, v_C) \ : \ v_C = V_{LL0} - R_{LL}i_L\}$. As it is appreciated at the left side of Figure 6.11, this particular behaviour of the RES controller exchanges steady-state performance for worst-case transient disturbance rejection performance.

6.3.6. Robustness of performance to model parametric uncertainty

The superior disturbance rejection performance exhibited by the RES controller over the other tested controllers, is worthy of attention only if it is at least minimally robust against uncertainty in the converter's model. This is an issue of practical importance that, although deserves deep analysis, has been left out of the scope of this thesis. However, just in order to get a better overall look of the simulation results reported before, a simple sensitivity analysis with respect to variations in the converter's model parameters is exposed next.

Consider the values detailed in Table 6.1 for the parameters L, R_L, C, and R_C as *nominal* values. There are sixteen ways of simultaneously varying $\pm 10\,\%$ each of these nominal values. Each way is identified by a value setting identification number between 1 and 16 in Table 6.2, where "+" denotes a 10 % increment of the nominal value, "−" denotes a 10 % decrement of the nominal value, and "·" denotes no deviation from the nominal value. The identification number 0 in Table 6.2 corresponds to parameters L, R_L, C, and R_C set to nominal values.

For each value-setting of the converter's parameters L, R_L, C, and R_C, the quantity

$$\min_{\boldsymbol{y}\in\mathbb{R}^2} \mathcal{V}_{|e^{wc}|}(\boldsymbol{y}), \qquad (6.26)$$

is given in Table 6.2 at the left of the double vertical line. The absolute worst-case error value function $\mathcal{V}_{|e^{wc}|}$ attains its minimum (6.26) in the convex set (6.10) introduced before as the valley of $\mathcal{G}_{|e^{wc}|}'$. For nominal values, this set is represented

---

the steady-state period, which varies from case to case. For the PID case the steady-state period is known beforehand because it must equal the PWM period T_s; for each other case, it can be determined from the simulation results.

by the area delimited by the innermost level curve at the bottom of Figure 6.1. The minimum (6.26) and the valley where it is attained by $\mathcal{V}_{|\mathrm{e^{wc}}|}$ depend on *all* the parameter values present in Table 6.1 (which define an instance of $\mathcal{G}_{|e^{\mathbf{wc}}|}'$), but since the only values that vary along the rows of Table 6.2 are the values of L, R_L, C, and R_C, the quantity (6.26) may be regarded (as used in the current context) as a *theoretical minimum error figure of merit* of the converter's parameters selection with regard to the control requirement, regardless of the applied control method. The higher this figure, the more difficult it is for a controller (any) to fulfil the control requirement; because the higher (6.26), the smaller the escape set (6.9).

The remaining values reported in Table 6.2 were obtained as follows. For each value-setting of the converter's parameters L, R_L, C, and R_C, the four controllers under test (PID, H, SM, and RES) were put in charge of the converter's control, without modifying their originally tuned parameter values (intended for nominal values of L, R_L, C, and R_C). The performance exhibited by each controller against the same disturbing load current driving pulse used in Subsection 6.3.5, was quantified by evaluating the performance index

$$\max_{t \in [-10\,\mathrm{\mu s}, 190\,\mathrm{\mu s}]} |\mathrm{e}\,(t)|\,, \tag{6.27}$$

reported in Table 6.2, at the right of the double vertical line, for each value-setting of the converter's parameters. Accordingly, the last four columns of Table 6.2 express how the performance of each controller improves or deteriorates as the converter's parameter values deviate from the nominal ones.

In the bar chart of Figure 6.12 the controller's performances are compared graphically among each other and to the minimum of $\mathcal{V}_{|\mathrm{e^{wc}}|}$, for each value-setting identification number. Notice that the (6.27) fluctuations roughly follow the (6.26) fluctuations regardless the control method, corroborating the role of (6.26) as a theoretical minimum error figure of merit for the converter's parameters with respect to the control requirement. Moreover, observe that the RES controller outperforms each of the other three controllers, for every value setting. Even for the RES controller's worst performance, which takes place for the value setting identified by number 10, the RES controller achieves the best performance (118.7 mV), followed by the SM controller (143.1 mV). The simulated signals for this particular value setting are plotted in Figure 6.13.

Assuming the control problem given by Table 6.1 is a truly representative example, it may concluded from the previous simulation results that the RES controller performs quite satisfactorily, and that it has an acceptable robustness against moderate parametric uncertainty in the converter's model. That being said, it is clear that further (simulated and real) experiments need to be carried out in order to evaluate the performance and robustness of the proposed control method with broader generality. Besides, even if the previous simulations were conceded general value, it may well be considered that a 112.7 mV − 76.0 mV = 36.7 mV performance increase for the nominal converter (which deteriorates to 143.1 mV − 118.7 mV = 24.4 mV in case of 10 % simultaneous deviations from the nominal one) is not worth the cost of implementing a much more complicated control method than the SM control.

Id.	L	R_L	C	R_C	$\min\limits_{\boldsymbol{y}\in\mathbb{R}^2}\mathcal{V}_{\lvert\mathrm{e}^{\mathrm{wc}}\rvert}(\boldsymbol{y})$ (mV)	$\max\limits_{t\in[-10\,\mu\mathrm{s},190\,\mu\mathrm{s}]}\lvert\mathrm{e}(t)\rvert$ (mV)			
						PID	H	SM	RES
0	·	·	·	·	64.7	128.4	131.1	112.7	76.0
1	-	-	-	-	65.8	139.1	115.6	131.8	75.6
2	-	-	-	+	66.9	129.2	142.2	109.2	78.7
3	-	-	+	-	49.5	108.0	107.1	94.7	75.6
4	-	-	+	+	51.0	99.1	102.3	90.3	78.4
5	-	+	-	-	62.6	133.1	136.1	128.0	75.6
6	-	+	-	+	63.7	122.4	129.6	107.0	79.2
7	-	+	+	-	46.9	103.4	92.8	94.0	75.6
8	-	+	+	+	48.5	93.8	102.4	80.9	78.4
9	+	-	-	-	85.9	178.3	152.9	166.2	118.3
10	+	-	-	+	86.6	168.6	154.4	143.1	118.7
11	+	-	+	-	65.8	140.5	139.2	120.5	78.5
12	+	-	+	+	66.9	131.8	138.2	120.7	80.5
13	+	+	-	-	82.0	171.0	143.2	153.7	92.7
14	+	+	-	+	82.8	161.6	168.5	153.7	102.3
15	+	+	+	-	62.6	134.2	135.8	125.8	75.6
16	+	+	+	+	63.7	126.0	111.6	112.2	79.4

Table 6.2: For the control problem example of Table 6.1, results of a comparative disturbance rejection performance sensitivity analysis with respect to $10\,\%$ simultaneous deviations from nominal values (as indicated in Table 6.1) of the converter's parameters: L, R_L, C, and R_C.
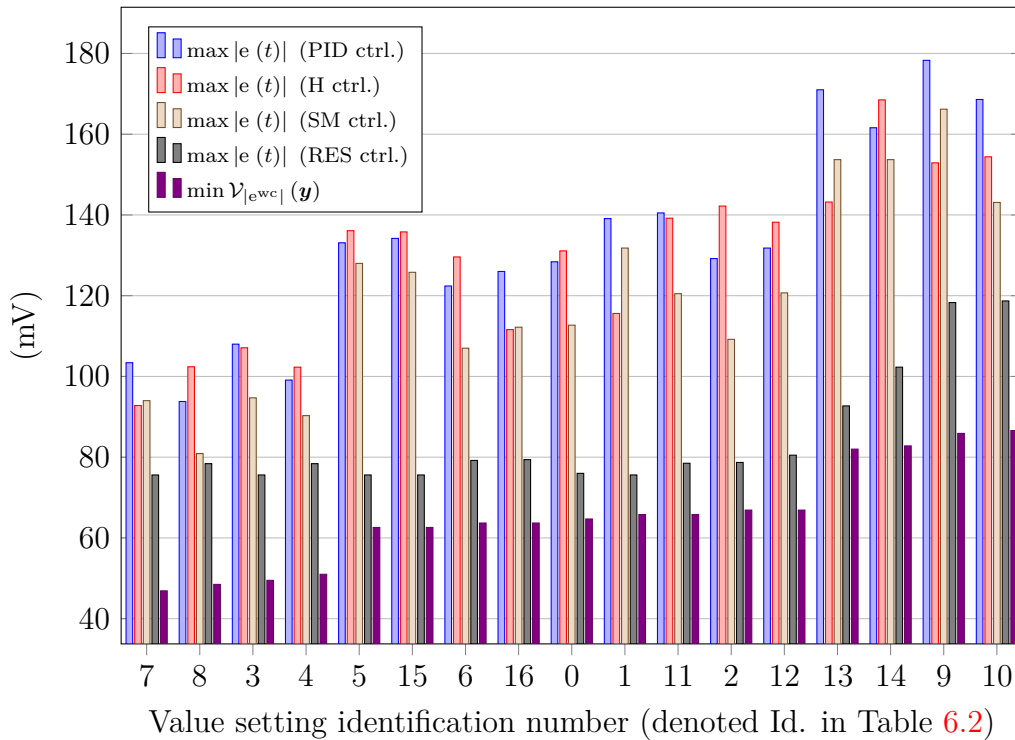
Figure 6.12: Graphical representation of the values of Table 6.2. The value setting identification numbers are ordered from left to right according to increasing values of $\min_{\boldsymbol{y}\in\mathbb{R}^2}\mathcal{V}_{\lvert\mathrm{e}^{\mathrm{wc}}\rvert}(\boldsymbol{y})$.
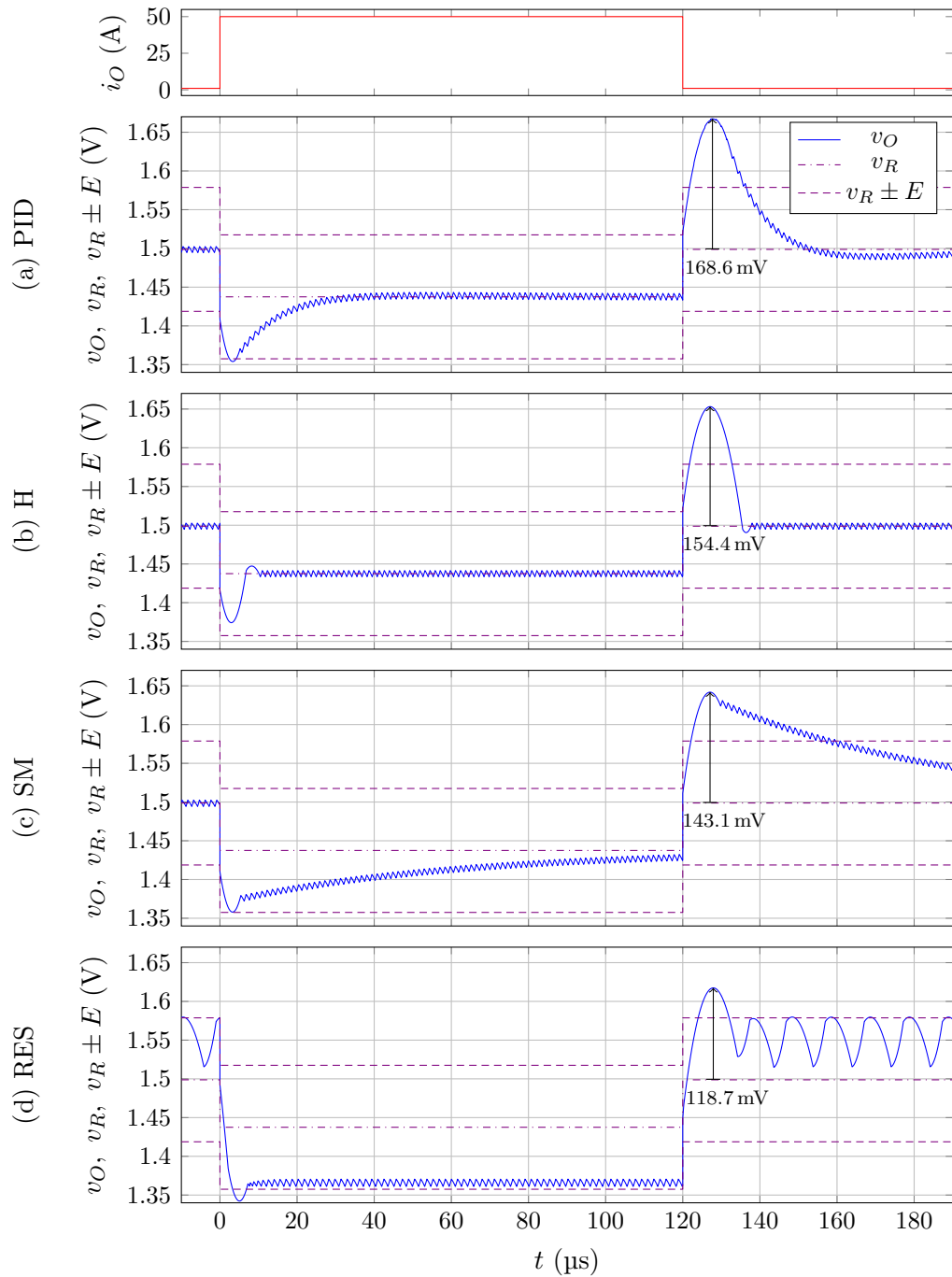
Figure 6.13: Pulse response simulations analogous to the ones of Figure 6.10 except for the fact that the parameters L and R_C are set 10 % higher than their nominal values, and the parameters R_L and C are set 10 % lower than their nominal values, while the controllers are left tuned for nominal values of L, R_L, C, and R_C.

6.4. The solution as a benchmark for control methods

Within the differential game theory framework, in which the buck converter control problem was formulated, both players (P and E) compete on equal terms. They both have access to perfect full state feedback and they both have exact knowledge of the converter's dynamics. Therefore, P's optimal strategy, obtained as part of the solution of the game in distance, can be considered as a benchmark test for *any* buck converter controller candidate. This *benchmarking* aspect of the game's solution is explored in this section by numerical simulations in which the previously introduced controllers are embodied in E to play against P's optimal strategy.

Reconsider the control problem specified by the parameters of Table 6.1 as a concrete instance of the game in distance $\mathcal{G}_{\mathbf{dist}}'$ with P as the infimizer and E as the supremizer (or equivalently the game $\mathcal{G}_{|e^{wc}|}'$ with P as the supremizer and E as the infimizer) in which $V_I = V_{I\min} = V_{I\max}$. In this context, P's load current optimal strategy (given by the first component of (6.8)) is represented graphically in Figure 6.14. P can play optimally against E without recurring to ϵ-modifications of this strategy because (as throughout this chapter) it is assumed that E is limited by a 50 ns dwell time between consecutive switchings.

In the same context, consider E adopting different strategies to play against P. In particular, consider E playing like: a) a proportional-integral-derivative (PID) controller, b) an hysteresis (H) controller, c) a sliding mode (SM) controller, and d) a relaxed evader's strategy (RES) controller of permissibility $\lambda = 0.95E = 76\,\mathrm{mV}$. In each case, with the controller tuned as explained in the previous section. Suppose that for $t < 0$, P plays a constant nominal load current $I_{O\,\mathrm{nom}} = \frac{I_{O\min} + I_{O\max}}{2} = 25.5\,\mathrm{A}$, but at $t = 0$ he starts playing according to his optimal strategy (as described by Figure 6.14). Let the time origin be defined such that at $t = 0$, the controlled buck has already reached a steady-state regime, regardless of the particular controller role adopted by E.

The load current $t \mapsto i_O(t)$ and output voltage $t \mapsto v_O(t)$ that results from each of the just conceived simulated plays are plotted in Figure 6.15. Along with each output voltage signal, the reference voltage $t \mapsto v_R(t)$ and its $\pm E$ tolerance band are also plotted. The corresponding absolute errors $t \mapsto |\mathrm{e}(t)|$, absolute worst-case errors $t \mapsto |\mathrm{e}^{wc}(\boldsymbol{y}(t))|$, and the state-space trajectories $t \mapsto \boldsymbol{y}(t) = [i_L(t), v_C(t)]^\top$, restricted to $t \in [-20\,\mu\mathrm{s}, 200\,\mu\mathrm{s}]$ are plotted in Figure 6.16.

Notice that the performance of each controller incarnated in E is quite good, except for the H controller which is mislead by P into a limit cycle with points that lie significantly beyond the boundary of $\{\boldsymbol{y} \in \mathbb{R}^2 \ : \ |\mathrm{e}^{wc}(\boldsymbol{y})| < E = 80\,\mathrm{mV}\}$.

These simulation results look deceptive at first glance. As a benchmark for the control problem, P's optimal strategy does not seem sufficiently harmful to the PID, SM, and RES controllers. However, nothing is wrong behind these results. For each initial state $\boldsymbol{y} \in \mathbb{R}^2$ at $t = 0$, P's optimal strategy (6.8) must secure P an absolute worst-case error, to be attained at some $t > 0$, greater or equal than $\mathcal{V}_{|e^{wc}|}(\boldsymbol{y})$. At the right side of Figure 6.16 it can be confirmed that this is indeed the case, regardless the particular type of opposition faced from E. Of course, P
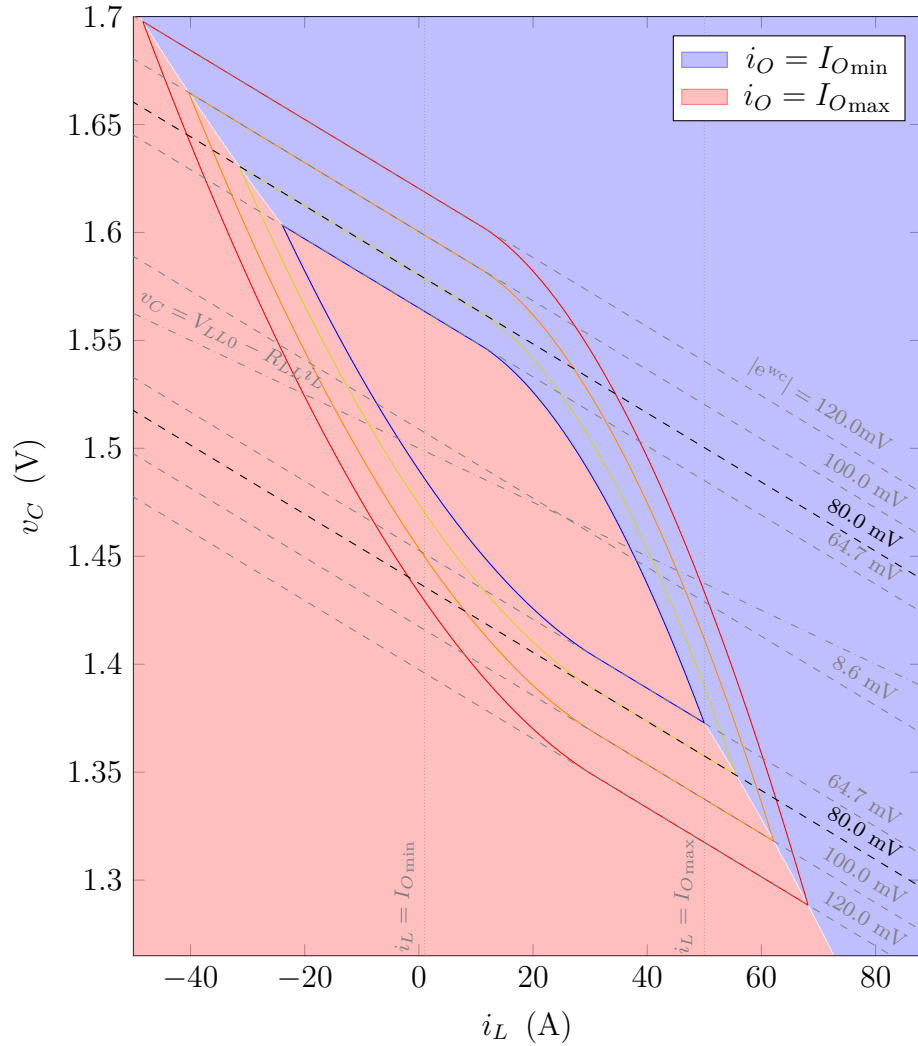
Figure 6.14: For the example of Table 6.1, P's optimal strategy (indicated by the coloured areas in the figure) for the game in distance $\mathcal{G}_{\mathbf{dist}}{}'$ or, equivalently, $\mathcal{G}_{|e^{wc}|}{}'$.

could do more to increase the outcome of the play played, for example, against E in its role of PID controller. However, doing so would not be optimal for P, because he would be risking to end up with an outcome lower than $\mathcal{V}_{|e^{wc}|}(\boldsymbol{y})$ in case E decides not to play as a PID controller, but as an optimal opponent instead.

Notice in Figure 6.16 that, for the previous simulations, the initial condition lies in the valley (6.10), regardless the control method adopted by E. This is due to the benevolent choice (from E's viewpoint) of having set the load current to its constant *nominal* value, before transferring the control of the load current to P's optimal strategy at $t = 0$. If analogous plays to ones previously simulated are started from the steady-state regime that corresponds to constant *maximum* load current (instead of nominal load current), the harmfulness of P's optimal strategy becomes more evident as it can be appreciated in Figures 6.17 and 6.18.
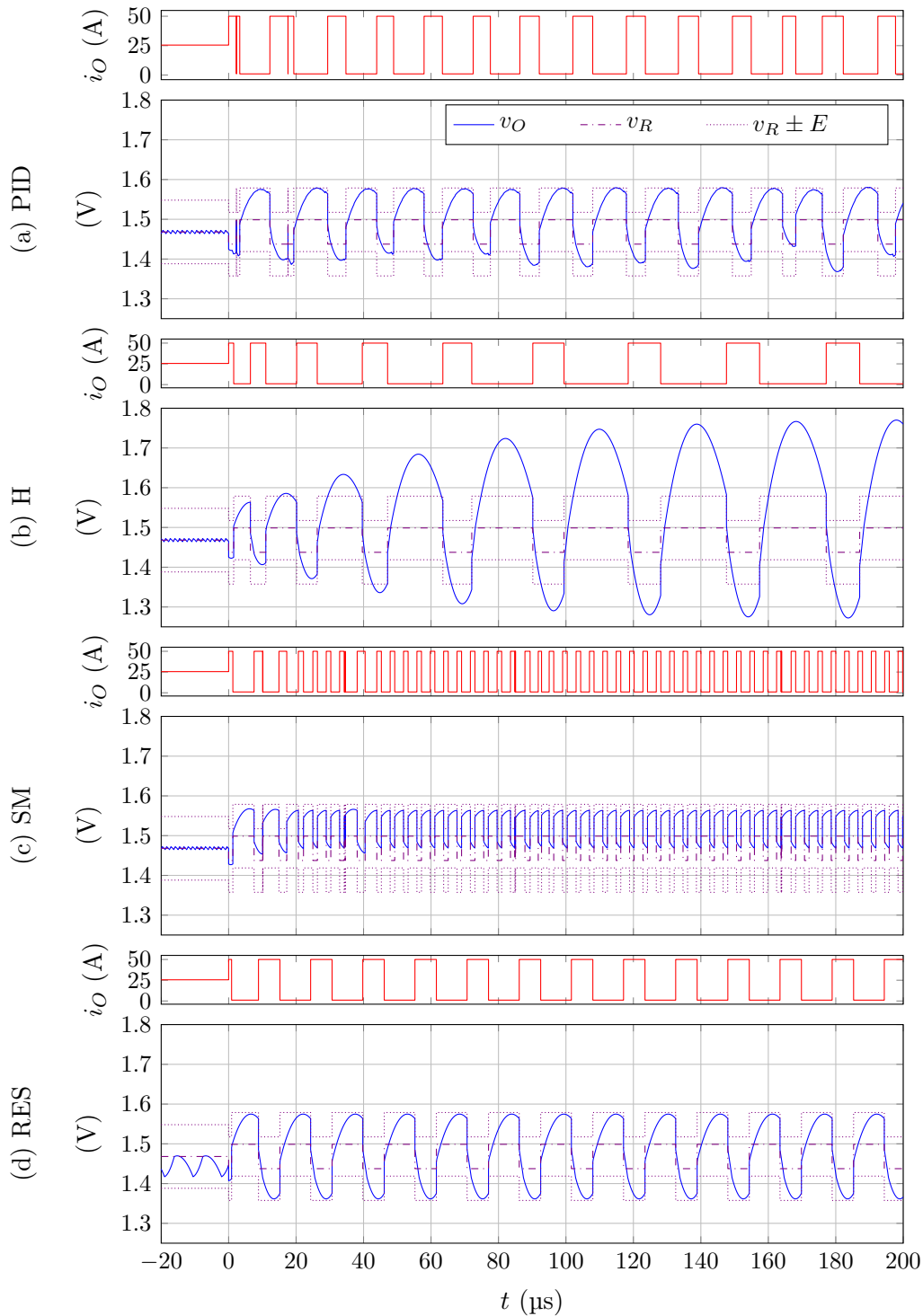
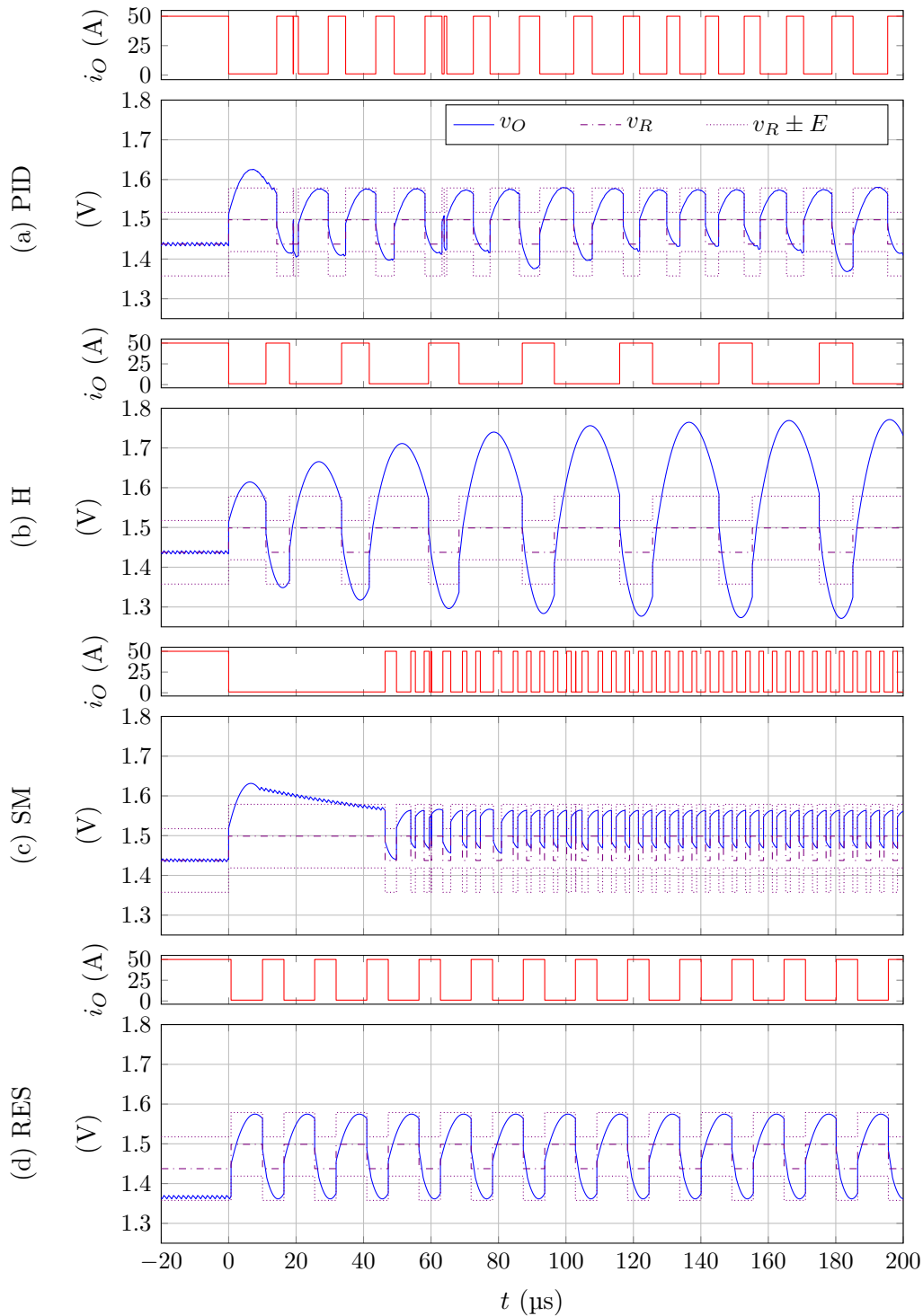Figure 6.15: For the example of Table 6.1, E plays against P's optimal strategy as different controllers. The controllers are: (a) Proportional-Integral-Derivative (PID) controller, (b) Hysteresis (H) controller, (c) Sliding Mode (SM) controller, (d) Relaxed Evader's Strategy (RES) controller. For $t \geq 0$, P applies his optimal strategy, but for $t < 0$, the load current is held constant at its nominal value $I_{O\,\mathrm{nom}} = 25.5\,\mathrm{A}$. At $t = 0$, the controlled buck has already reached a steady-state regime, regardless the particular controller role adopted by E.
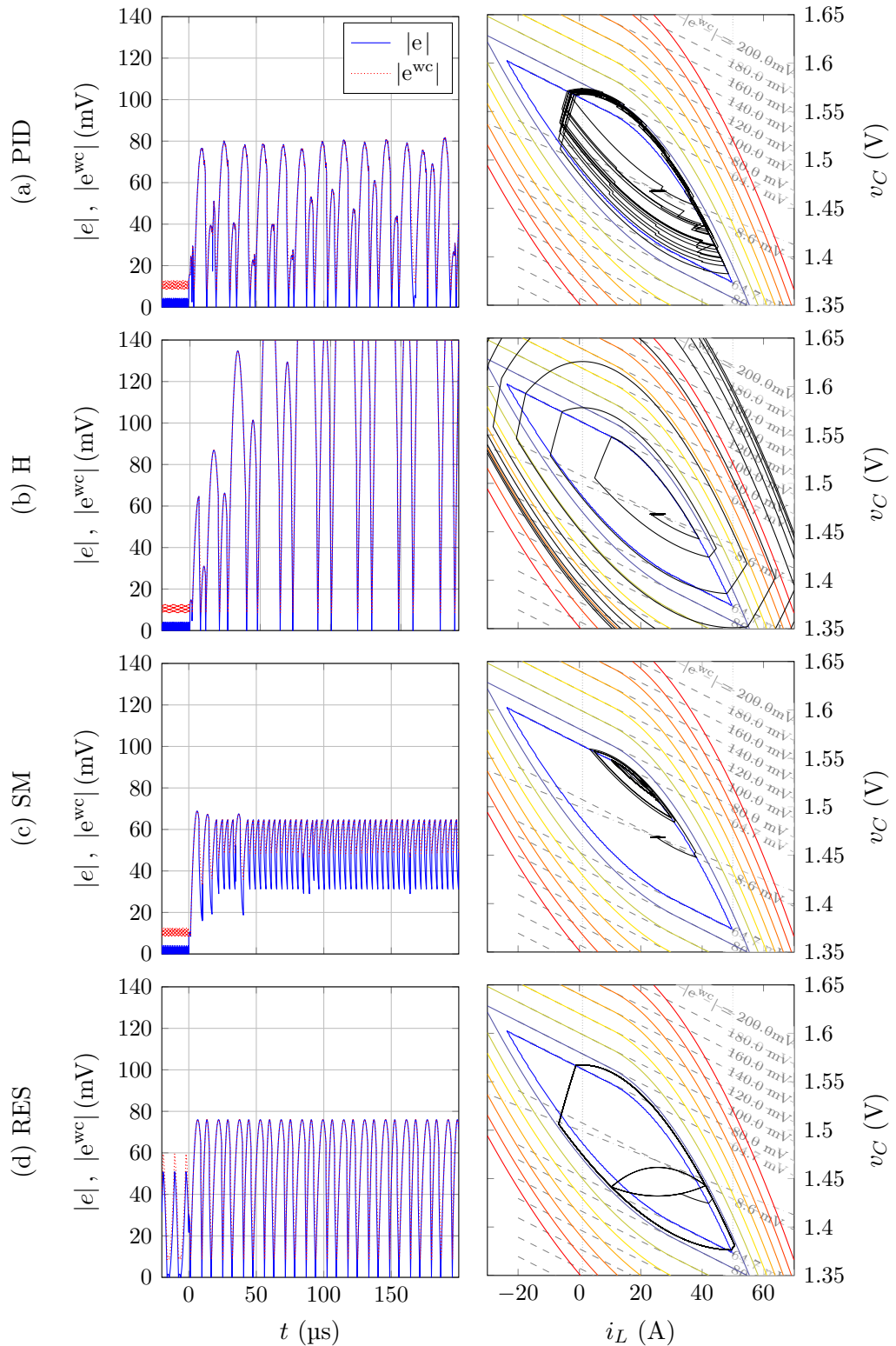
Figure 6.16: For each controller case and for $t \in [-20\,\mu s, 200\,\mu s]$, the absolute error $t \mapsto |e(t)|$ and the absolute worst-case error $t \mapsto |e^{wc}(y(t))|$ (at the *left*), and the state-space trajectory $t \mapsto y(t) = [i_L(t), v_C(t)]^\top$ (at the *right*), that corresponds to same case in Figure 6.15.

Figure 6.17: For the example of Table 6.1, E plays against P's optimal strategy as different controllers. The controllers are: (a) Proportional-Integral-Derivative (PID) controller, (b) Hysteresis (H) controller, (c) Sliding Mode (SM) controller, (d) Relaxed Evader's Strategy (RES) controller. For $t \geq 0$, P applies his optimal strategy, but for $t < 0$, the load current is held constant at its maximum value $I_{O\max} = 50\,\mathrm{A}$. At $t = 0$, the controlled buck has already reached a steady-state regime, regardless the particular controller role adopted by E.

Figure 6.18: For each controller case and for $t \in [-20\,\mu\text{s}, 200\,\mu\text{s}]$, the absolute error $t \mapsto |\text{e}\,(t)|$ and the absolute worst-case error $t \mapsto |\text{e}^{\text{wc}}\,(\boldsymbol{y}\,(t))|$ (at the *left*), and the state-space trajectory $t \mapsto \boldsymbol{y}\,(t) = [i_L\,(t)\,, v_C\,(t)]^{\top}$ (at the *right*), that corresponds to same case in Figure 6.17.

Before P starts applying its optimal strategy, i.e., for $t < 0$, every tested controller, except RES, achieves a steady-state regime with the state of the converter fluctuating closely around the point $(i_L, v_C) = (I_{O\max}, V_{LL0} - R_{LL}I_{O\max})$ where the function $\mathcal{V}_{|e^{wc}|}$ takes a value close to $120\,\text{mV}$. The RES controller instead, achieves a steady-state regime such that the state fluctuates around a point on the line $\{(i_L, v_C) \,:\, i_L = I_{O\max}\}$ without crossing the $76\,\text{mV}$-level curve of the function $\mathcal{V}_{|e^{wc}|}$ in the increasing direction. Therefore, when the control of the load current is transferred to P's optimal strategy, the RES controller is in a much better initial condition to start facing his optimal opponent than the rest of the tested controllers. However, this is at the cost of tolerating higher error peaks at the steady-state regime attained before $t = 0$ than the other controllers.

The atypical treatment given by the RES controller to the steady-state initial regime driven by maximum load current, makes the difference after the control of the load current is taken by P's optimal strategy. While the RES controller can fulfil the requirement of keeping the error below $80\,\text{mV}$ for every $t \geq 0$, the other controllers cannot prevent the error voltage from climbing up to more than $120\,\text{mV}$, as it can be observed in Figure 6.18.

6.5. The solution as a design tool

The aspect to be discussed in this section, was already introduced in Subsection 6.3.6 where the minimum of the absolute worst-case error value function was proposed to quantify how the difficulty of the buck converter control problem changes, as the values set for the converter's parameters L, R_L, C, and R_C deviate from the nominal ones.

The family $\left\{\left\{\boldsymbol{y} \in \mathbb{R}^2 \,:\, \mathcal{V}_{|e^{wc}|}(\boldsymbol{y}) \leq \lambda\right\} \,:\, \lambda \geq 0\right\}$ of inf-level sets of the function $\mathcal{V}_{|e^{wc}|}$ is a family of nested convex compact subsets of $\mathbb{R}^2$ that covers the whole state-space. Therefore, the value taken by $\mathcal{V}_{|e^{wc}|}$ at its lowest inf-level set, i.e., the valley $\mathscr{V} = \left\{\boldsymbol{y} \in \mathbb{R}^2 \,:\, \mathcal{V}_{|e^{wc}|}(\boldsymbol{y}) = \min_{\boldsymbol{y}' \in \mathbb{R}^2} \mathcal{V}_{|e^{wc}|}(\boldsymbol{y}')\right\}$, appears to be an appropriate *theoretical minimum error figure of merit* to quantify (globally) the suitability of the converter's parameters with regard to the control problem; the higher this figure, the more difficult the control problem. The brief numerical analysis reported in this section supports this idea.

Suppose that within the buck converter control problem detailed in Table 6.1 the values $L_n = 310\,\text{nH}$ and $C_n = 1.1\,\text{mF}$ given for parameters L and C, respectively, are just preliminary nominal values chosen during a first design phase of the buck converter, which can still be varied $\pm 50\,\%$ before selecting the final values. Leaving aside every design issue other than the control requirement, the designer could ask himself how to select these two values so as to achieve the best performance from the control system. For example, the designer might temporarily disregard cost, current ripple, output voltage ripple, heat dissipation, and physical dimensions, among other specific design issues, to focus solely on how the selection of the converter's inductor and capacitor affects the control problem's difficulty. Of course, the selection of these two components impacts on the values
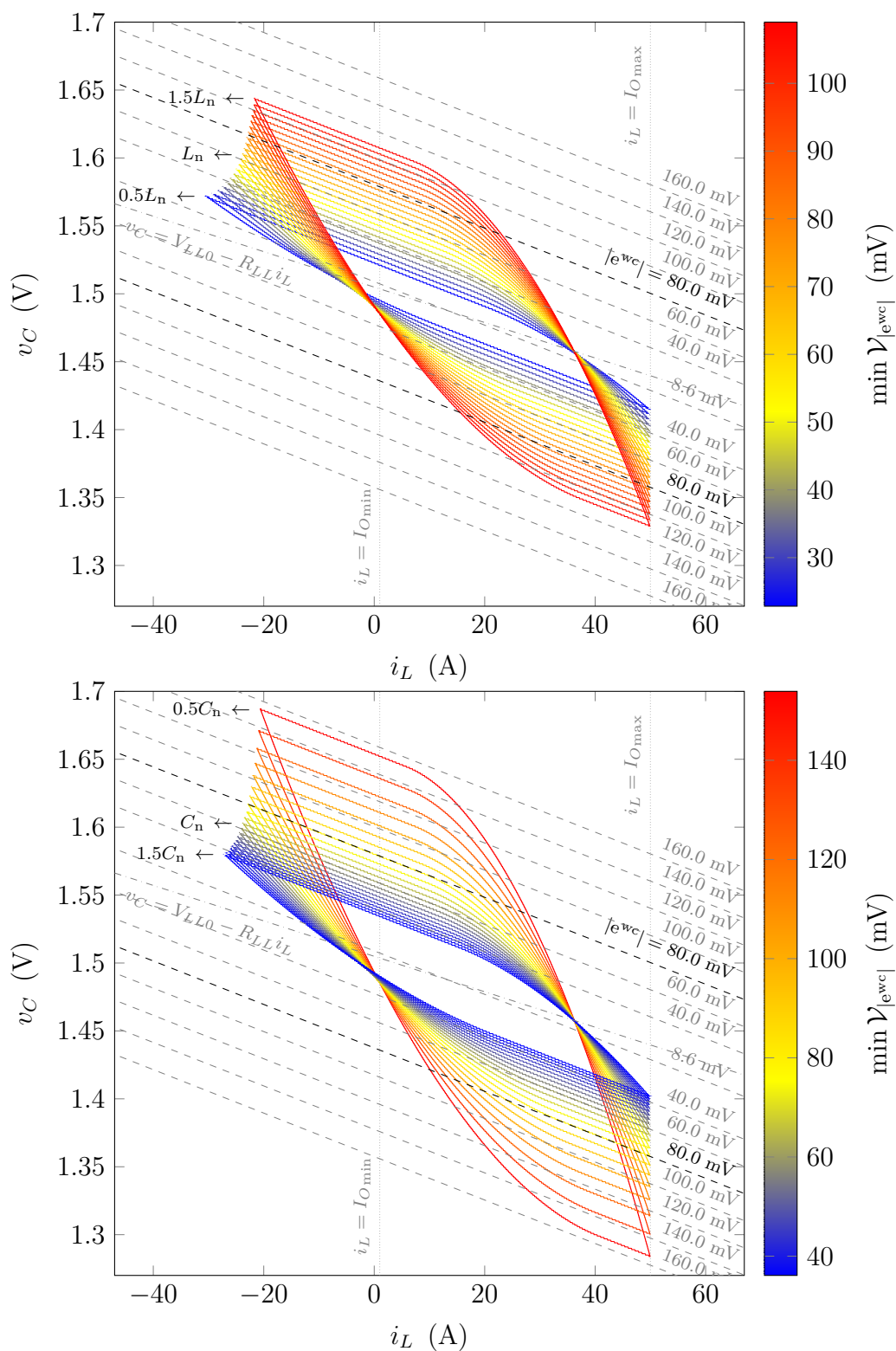
Figure 6.19: For the example of Table 6.1, deformation of the set $\mathcal{V}$ (i.e., the valley of $\mathcal{G}_{|e^{wc}|}{}'$) as L and C deviate independently from the nominal preliminary values $L_n = 310\,\text{nH}$ and $C_n = 1.1\,\text{mF}$. *Above:* L varies from $0.5L$ to $1.5L$ while $C = C_n$ is held constant. *Below:* C varies from $0.5C$ to $1.5C$ while $L = L_n$ is held constant.

243

of the *four* converter's parameters L, R_L, C, and R_C. However, for simplicity, it is assumed here that the values indicated in Table 6.1 for the ESRs R_L and R_C, remain unchanged even if the values of L and C vary. If, for example, R_L and R_C where known functions of L and C, respectively, such dependencies could be easily included in the numerical analysis presented next.

In Figure 6.19 different instances of the valley $\mathcal{V}$ are represented by its boundary as the values set to L and C vary independently. At the upper part of the figure, L varies from $0.5L_n$ to $1.5L_n$ while $C = C_n$ remains constant. A the lower part of the figure, C varies from $0.5C_n$ to $1.5C_n$ while $L = L_n$ remains constant. The colour-map indicates the value $\min_{\boldsymbol{y} \in \mathbb{R}^2} \mathcal{V}_{|\mathrm{e^{wc}}|}(\boldsymbol{y})$ attained by $\mathcal{V}_{|\mathrm{e^{wc}}|}$ at each of the represented particular instances of $\mathcal{V}$. Observe how the shape of $\mathcal{V}$ adapts better to the level curves of $\boldsymbol{y} \mapsto |\mathrm{e^{wc}}(\boldsymbol{y})|$ (which are pairs of straight lines) as L *decreases* or as C *increases*. In particular, it adapts better to the pair of straight lines (represented by dashed black lines) which delimit the safe band in state-space where P cannot violate the $80\,\mathrm{mV}$ control requirement by an instantaneous selection of an appropriate extreme load current value.

The observed trends suggest that, making use of the stipulated restricted freedom of choice for the values of L and C, the buck converter's designer should set
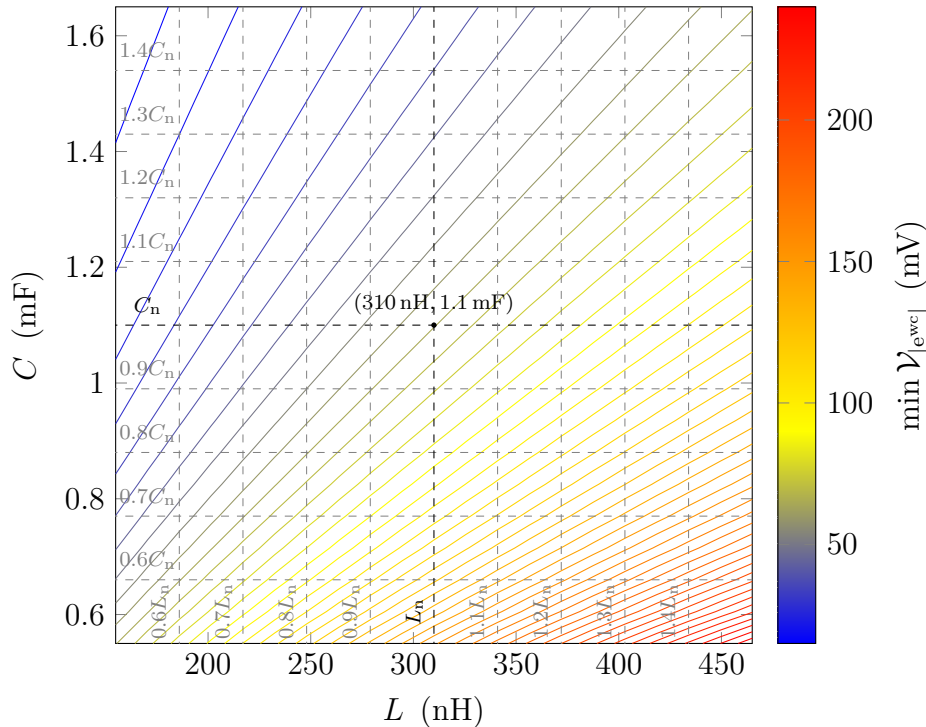

Figure 6.20: For preliminary nominal values for L and C selected as $L_n = 310\,\mathrm{nH}$ and $L_n = 1.1\,\mathrm{mF}$, respectively, the contour map of $(L, C) \mapsto \min_{\boldsymbol{y} \in \mathbb{R}^2} \mathcal{V}_{|\mathrm{e^{wc}}|}(\boldsymbol{y})$ defined with every parameter other than L and C set as indicated in Table 6.1. The figure of merit $\min_{\boldsymbol{y} \in \mathbb{R}^2} \mathcal{V}_{|\mathrm{e^{wc}}|}(\boldsymbol{y})$ is minimized, in the restricted domain $[0.5L_n, 1.5L_n] \times [0.5C_n, 1.5C_n]$, by selecting $L = 0.5L_n = 155\,\mathrm{nH}$ and $C = 1.5C_n = 1.65\,\mathrm{mF}$.
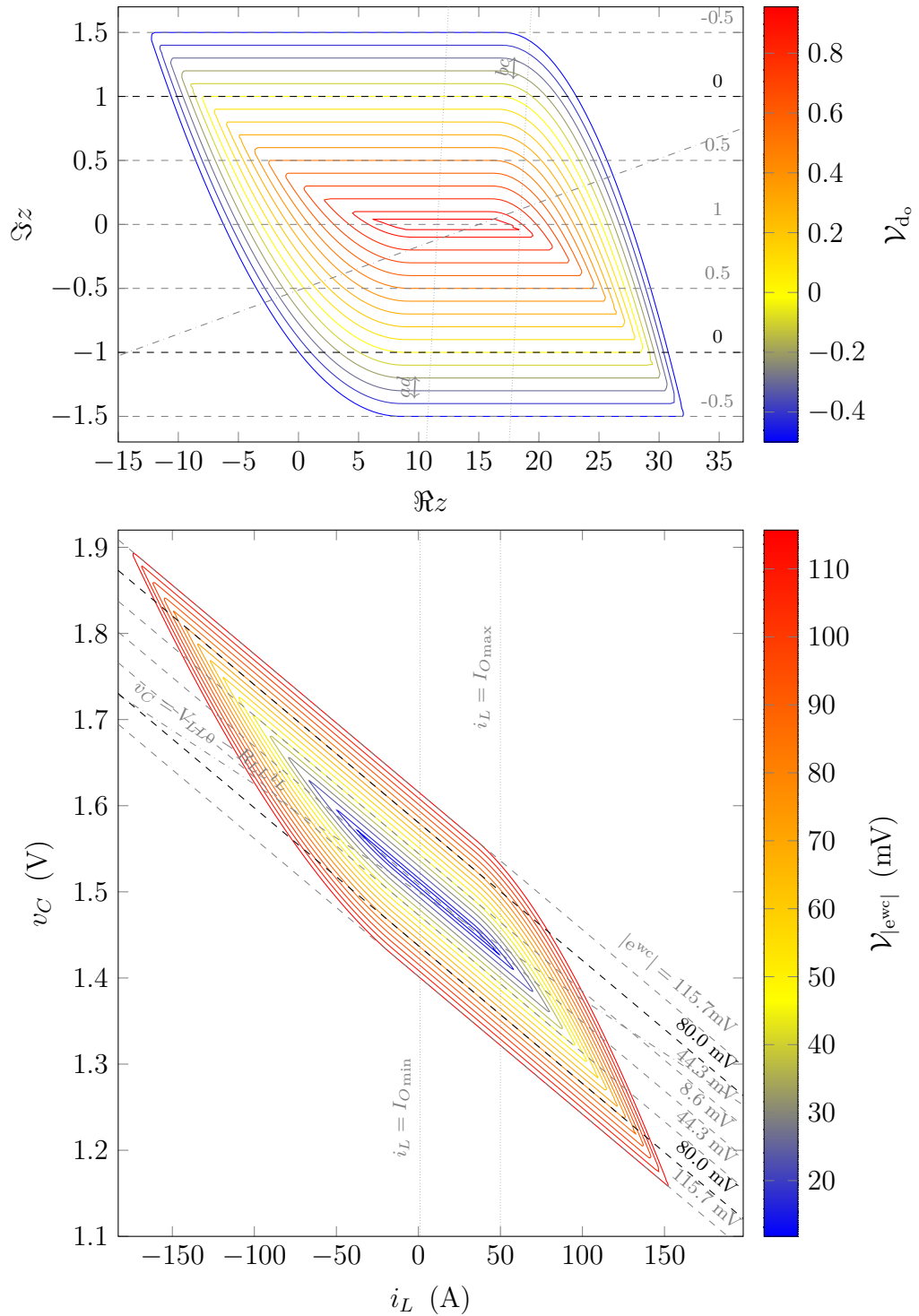
Figure 6.21: Four related contour maps for the example of Table 6.1 after decreasing $50\,\%$ the value specified for L and after increasing $50\,\%$ the value specified for C. *Above:* for $z \in \mathbb{C}$, contours of $z \mapsto \mathcal{V}_{\mathrm{d_o}}(z)$ (coloured closed curves) and contours of $z \mapsto \mathrm{d_o}(z, \mathscr{T}) = 1 - |\Im z|$ (dashed lines). *Below:* for $\boldsymbol{y} = i_L \hat{\boldsymbol{e}}_{\mathbf{1}} + v_C \hat{\boldsymbol{e}}_{\mathbf{2}} \in \mathbb{R}^2$, contours of $\boldsymbol{y} \mapsto \mathcal{V}_{|\mathrm{e^{wc}}|}(\boldsymbol{y})$ (coloured closed curves) and contours of $\boldsymbol{y} \mapsto |\mathrm{e^{wc}}(\boldsymbol{y})|$ (dashed lines). The lines $v_C = V_{LL0} - R_{LL} i_L$ (dot-dashed), and $i_L = I_{O\min}$, $i_L = I_{O\max}$ (densely dotted) in the i_L–v_C plane (at the bottom), and their counterparts in the canonical state-space (at the top) are just helping lines.

$L = 0.5L_n = 155\,\mathrm{nH}$ and $C = 1.5C_n = 1.65\,\mathrm{mF}$, in order to prioritize the prospect of the converter to fulfil the control requirement above every other design issue. These suggestion is confirmed by the contour map illustrated in Figure 6.20 which corresponds to the function $(L, C) \mapsto \min_{\boldsymbol{y} \in \mathbb{R}^2} \mathcal{V}_{|\mathrm{e^{wc}}|}(\boldsymbol{y})$ defined such that every parameter other than L and C is set as indicated in Table 6.1. The contour map shows that the figure of merit $\min\left\{\mathcal{V}_{|\mathrm{e^{wc}}|}(\boldsymbol{y}) \; : \; \boldsymbol{y} \in \mathbb{R}^2\right\}$ is minimized, in the restricted domain $[0.5L_n, 1.5L_n] \times [0.5C_n, 1.5C_n]$, by selecting $L = 0.5L_n$ and $C = 1.5C_n$.

At the bottom of Figure 6.21 the absolute worst-case error value function $\boldsymbol{y} \mapsto \mathcal{V}_{|\mathrm{e^{wc}}|}(\boldsymbol{y})$ and the instantaneous absolute worst-case error function $\boldsymbol{y} \mapsto |\mathrm{e^{wc}}(\boldsymbol{y})|$ for the finally selected values ($L = 155\,\mathrm{nH}$ and $C = 1.65\,\mathrm{mF}$) are represented graphically by their contour plots. At the upper part of the same figure the corresponding functions $z \mapsto \mathcal{V}_{\mathrm{d_o}}(z)$ and $z \mapsto \mathrm{d_o}(z)$, related to the former ones by (6.3) and (6.5), respectively, are represented by their contour plots. Compare the contour plots of Figure 6.21, which correspond to the optimized converter's design, with the contour plots of Figure 6.1, which correspond to the non-optimized preliminary converter's design. Qualitatively, the level curves of $\mathcal{V}_{|\mathrm{e^{wc}}|}$ adapt much better to the level curves of $|\mathrm{e^{wc}}|$ for the optimized design than for the non-optimized one. Quantitatively, $\min_{\boldsymbol{y} \in \mathbb{R}^2} \mathcal{V}_{|\mathrm{e^{wc}}|}(\boldsymbol{y})$ is reduced from $64.7\,\mathrm{mV}$ to $11.8\,\mathrm{mV}$ by the optimized selection of values for L and C. Each of these two values is the expression of an error that the converter's controller cannot avoid in a worst-case scenario, regardless its virtues, even if the converter's initial state conveniently lies in $\mathscr{V}$. For this reason, $\min_{\boldsymbol{y} \in \mathbb{R}^2} \mathcal{V}_{|\mathrm{e^{wc}}|}(\boldsymbol{y})$ was introduced in Subsection 6.3.6 as a theoretical minimum *error* figure of merit. Notice that an approximate 82 % reduction (i.e., improvement) of this figure was achieved by two simultaneous ± 50 % deviations from preliminary nominal values.

To test the optimized design, simulations analogous to the ones disused in Section 6.4 were carried out and are reported next. The controllers previously embodied in E to play against P's optimal strategy for the nominal parameters of Table 6.1, were retuned for the optimized converter's design (i.e., taking into account the new values $155\,\mathrm{nH}$ and $1.65\,\mathrm{mF}$ set to L and C, respectively) following the same tuning criteria described in Subsection 6.3.4. In particular, the RES controller was retuned to a permissibility of $23\,\mathrm{mV}$ which yields a switching frequency of $671.7\,\mathrm{kHz}$ at maximum load current, and the amplitude of the hysteresis band of the H controller was set to $9\,\mathrm{mV}$ which yields a switching frequency of $681.3\,\mathrm{kHz}$ at maximum load current. The PID controller was retuned acknowledging the new values for L and C, but its switching frequency was maintained at $700\,\mathrm{kHz}$. Accordingly, the SM controller needed not be re-tuned, because its desired switching frequency was consistently set to equal the switching frequency of the PID-controlled converter.

For each simulated play, the control of the load current is transferred to P's optimal strategy at $t = 0$, after a controlled steady-state regime has already been reached. The simulation results are graphically shown in Figures 6.22 and 6.23. Compare these figures with Figures 6.17 and 6.18, which correspond to analogous simulations for the non-optimized converter. It is evident that the optimization
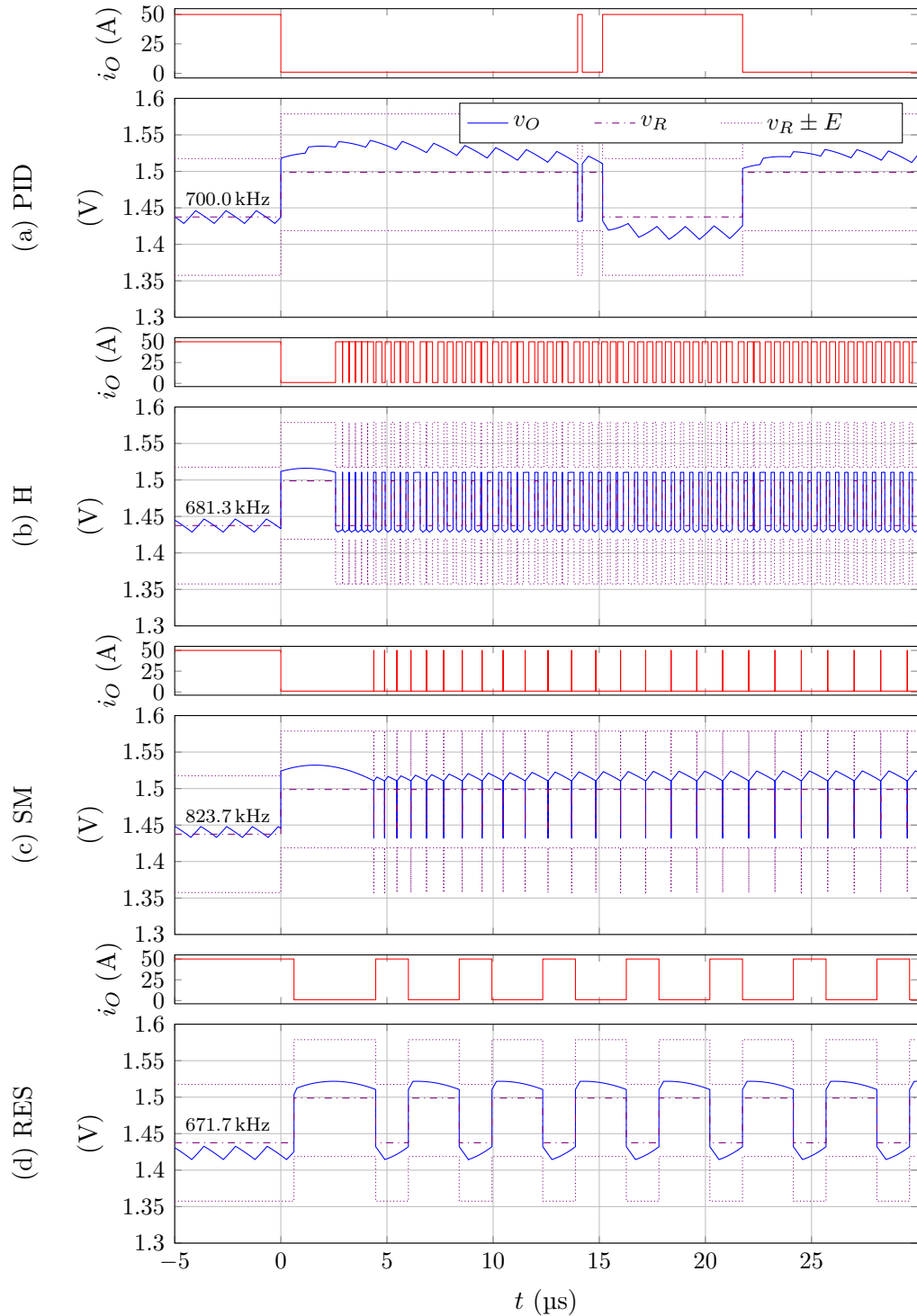
Figure 6.22: For the example of Table 6.1, with the values of L and C changed so as to minimize $\min_{\boldsymbol{y} \in \mathbb{R}^2} \mathcal{V}_{|e^{wc}|}(\boldsymbol{y})$, E plays against P's optimal strategy as different controllers: (a) Proportional-Integral-Derivative (PID) controller, (b) Hysteresis (H) controller, (c) Sliding Mode (SM) controller, (d) Relaxed Evader's Strategy (RES) controller. For $t \geq 0$, P applies his optimal strategy, but for $t < 0$, the load current is held constant at its maximum value $I_{O\max} = 50\,\mathrm{A}$. At $t = 0$, the controlled buck has already reached a steady-state regime.
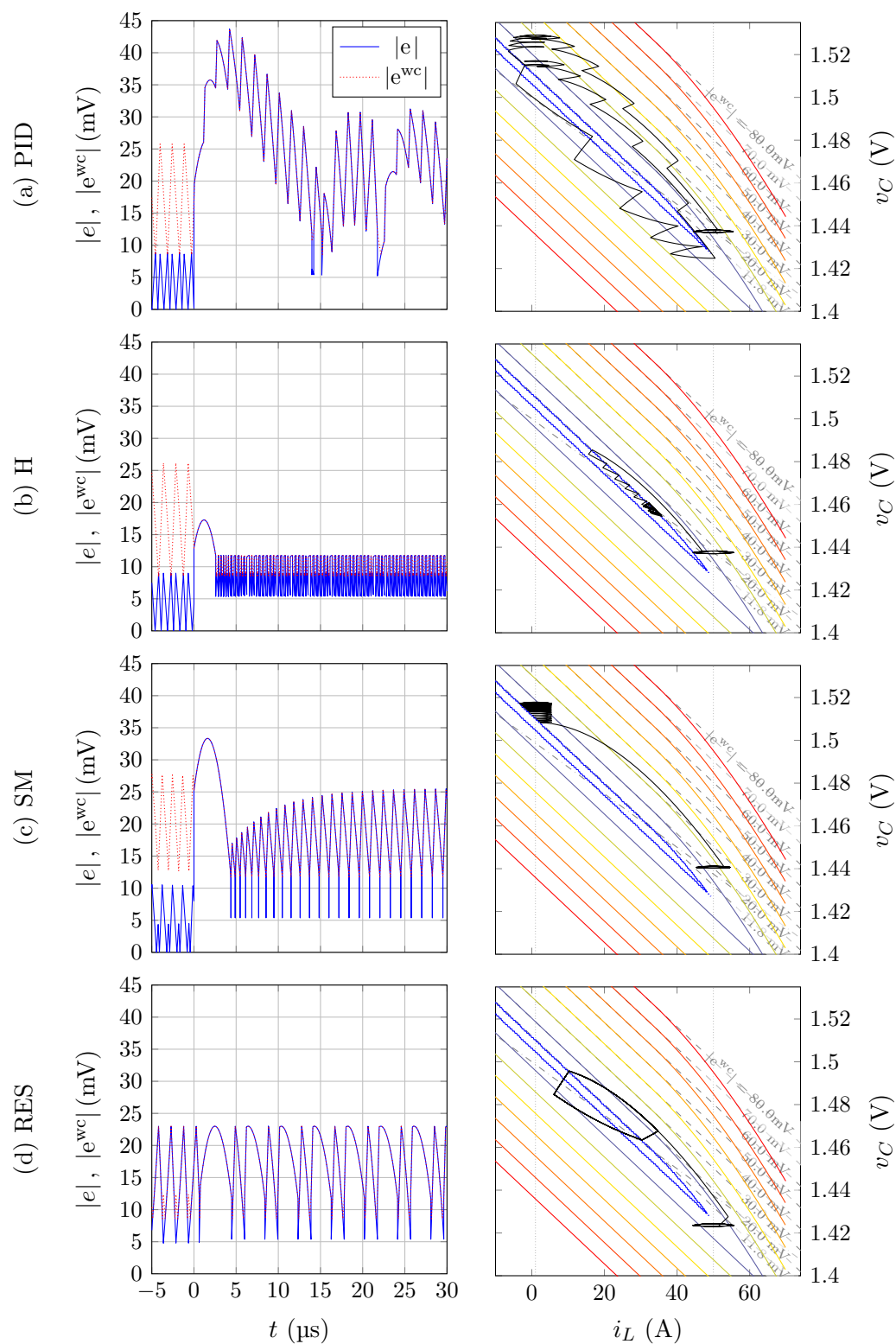
Figure 6.23: For each controller case the absolute error $t \mapsto |\mathrm{e}\,(t)|$ and the absolute worst-case error $t \mapsto |\mathrm{e}^{\mathrm{wc}}\,(\boldsymbol{y}\,(t))|$ (at the *left*), and the state-space trajectory $t \mapsto \boldsymbol{y}\,(t) = [i_L\,(t)\,, v_C\,(t)]^{\top}$ (at the *right*), that corresponds to same case in Figure 6.22.

of the figure of merit $\min_{\boldsymbol{y} \in \mathbb{R}^2} \mathcal{V}_{|\mathrm{e}^{\mathrm{wc}}|}(\boldsymbol{y})$, with respect to L and C in the stipulated restricted domain of optimization, has eased the job of each tested controller.

Even though, the RES controller is still the one that exhibits the best performance (evaluated by the performance index $\max_{t \in [-5\,\mu\mathrm{s}, 30\,\mu\mathrm{s}]} |\mathrm{e}\,(t)|$) in rejecting the disturbance synthesised by P, the other controllers also perform quite satisfactorily. Indeed, none of them fails to fulfil the control requirement which requires $|\mathrm{e}\,(t)| < E = 80\,\mathrm{mV}$ for every $t \geq 0$. In case of the PID and SM controllers, without incurring into high frequency chattering as is the case for the H controller.

These results show that the RES controller may not be as desirable as it may seem at first glance, at least if there is some room for optimization of some of the parameters that pose the control problem (i.e., some of the parameters present in Table 6.1). Any reasonable designer would not abandon the well established PID-control method, if there was no good reason for doing it.

In real-world buck converter designs, several factor are considered. One of them is the performance of the control system. The solution of the buck converter game in distance contributes qualitatively and quantitatively to address the design of the converter with an eye on the control problem.

6.6. The solution as a design verification tool

This last aspect of the solution of the game in distance arises from the observation that it embeds the solution of the game of kind associated to the underlying pursuit-evasion (buck converter) conflict, which is common to both games. Although a seemingly trivial observation, it is worth noting because of the theoretical and practical relevance of functional verification in electronic design. By contrast with the game in distance, the game of kind is concerned only with the determination of whether the control requirement can be fulfilled or not, but not to which extent. Accordingly, the solution of the game of kind answers some of the "yes" or "no" type of questions that a buck converter design verification tool should raise.

6.6.1. Negative verification of the control requirement

Take as an example the buck converter control problem given by the parameter values listed in Table 6.3. Suppose that an hypothetical novel control method is claimed to fulfil the requirement $|\mathrm{e}\,(t)| < E$ for every $t \geq 0$, for every initial state in the non-empty set $\mathscr{X} \subset \mathbb{R}^2$, regardless the load current disturbance signal. This claim can be true only if

$$\begin{cases} \mathscr{E}_{\mathbf{E}} \neq \emptyset, \\ \mathscr{X} \subset \mathscr{E}_{\mathbf{E}}, \end{cases} \tag{6.28}$$

where $\mathscr{E}_{\mathbf{E}} = \left\{ \boldsymbol{y} \in \mathbb{R}^2 \ : \ \mathcal{V}_{|\mathrm{e}^{\mathrm{wc}}|}(\boldsymbol{y}) < E \right\}$ is the escape set (for E).

The claim about the hypothetical controller's competence can be promptly proved to be false by noticing that the evaluation of the converter's *theoretical*

Parameter	Description	Value	Unit
L	Inductor's inductance	800	nH
R_L	Inductor's parasitic ESR	10	mΩ
C	Capacitor's capacitance	1	mF
R_C	Capacitor's parasitic ESR	1.65	mΩ
$I_{O\min}$	Minimum load current	5	A
$I_{O\max}$	Maximum load current	100	A
$V_I = V_{I\min} = V_{I\max}$	Input voltage	12	V
V_{LL0}	Open-circ. load ref. voltage	1	V
R_{LL}	Load line resistance	1.25	mΩ
E	Error tolerance	80	mV

Table 6.3: Parameter values of an unsolvable buck converter control problem example.

minimum error figure of merit

$$\min_{\boldsymbol{y}\in\mathbb{R}^2} \mathcal{V}_{|e^{wc}|}(\boldsymbol{y}) \tag{6.29}$$

exceeds the error tolerance, i.e., $\min_{\boldsymbol{y}\in\mathbb{R}^2} \mathcal{V}_{|e^{wc}|}(\boldsymbol{y}) \approx 965\,\text{mV} > E = 80\,\text{mV}$. Hence, $\mathscr{E}_\mathbf{E} = \left\{ \boldsymbol{y} \in \mathbb{R}^2 \; : \; \mathcal{V}_{|e^{wc}|}(\boldsymbol{y}) < E \right\} = \emptyset$ violating the first condition in (6.28).

In the context of the *canonical* buck converter game of kind, the escape set is $\mathscr{E}_\mathrm{E} = \{ z \in \mathbb{C} \; : \; \mathcal{V}_{\mathrm{d_o}}(z) > 0 \}$. Besides, since (6.29) is related to the *normalized maximum oriented distance figure of merit*

$$\max_{z\in\mathbb{C}} \mathcal{V}_{\mathrm{d_o}}(z) \tag{6.30}$$

by (6.4), determining whether $\mathscr{E}_\mathbf{E}$ (or $\mathscr{E}_\mathrm{E}$) is empty or not is equivalent to determining whether (6.30) is positive or not. For the example, $\max_{z\in\mathbb{C}} \mathcal{V}_{\mathrm{d_o}}(z) \approx -14.5 < 0$, which confirms that the hypothetical control method is actually a fiasco.

Examining Figure 6.24, where the contour maps of $\mathcal{V}_{\mathrm{d_o}}$ and $\mathcal{V}_{|e^{wc}|}$ are illustrated, the same conclusion may be arrived recognizing that the *highest sup-level set* of $\mathcal{V}_{\mathrm{d_o}}$ is not included in $\mathscr{E} = \{ z \in \mathbb{C} \; : \; |\Im z| < 1 \}$ (the canonical PS), or equivalently recognizing that the *lowest inf-level set* of $\mathcal{V}_{|e^{wc}|}$ is not included in $\mathscr{E}' = \{ \boldsymbol{y} \in \mathbb{R}^2 \; : \; |e^{wc}(\boldsymbol{y})| < E \}$ (the realistic PS). However, it is worth noticing that for proving the infeasibility of the hypothetical controller, all that is actually needed is to evaluate the sign of (6.30).

In conclusion, the evaluation of the sign of (6.30) may be used as a *negative verification* of a converter's design (meaning values selected for L, R_L, C, R_C, $I_{O\min}$, $I_{O\max}$, and V_I) with respect to a control requirement (meaning values selected for V_{LL0}, R_{LL}, and E). If (6.30) is negative, there exists no controller capable of fulfilling the control requirement in a worst-case scenario. If (6.30) is positive, (6.30) quantifies, in the normalized range $(0,1)$, the available room for designing
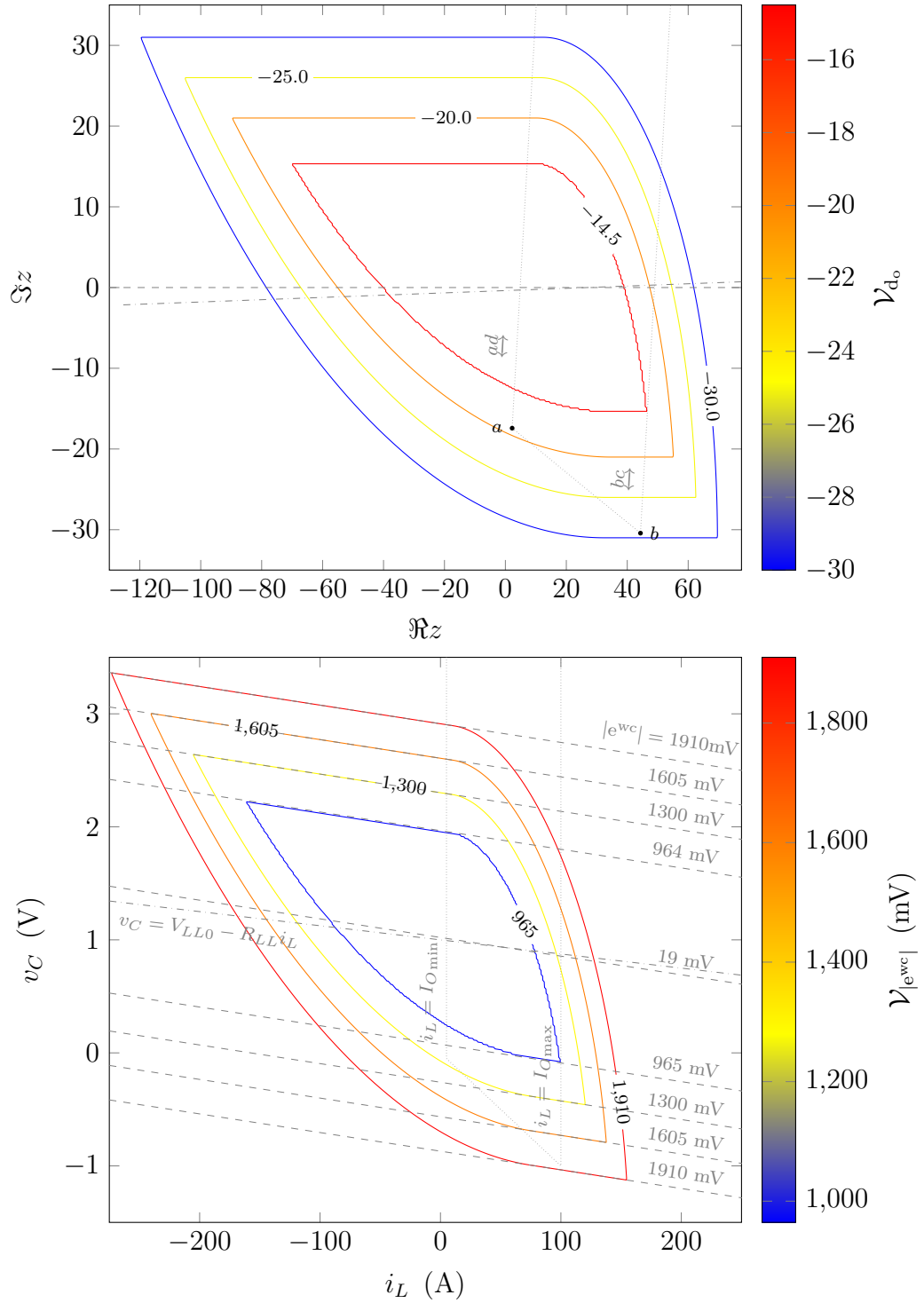
Figure 6.24: Four related contour maps for the example of Table 6.3. *Above:* for $z \in \mathbb{C}$, contours of $z \mapsto \mathcal{V}_{d_o}(z)$ (coloured closed curves) and contours of $z \mapsto d_o(z, \mathscr{T}) = 1 - |\Im z|$ (dashed lines). *Below:* for $\boldsymbol{y} = i_L \hat{\boldsymbol{e}}_1 + v_C \hat{\boldsymbol{e}}_2 \in \mathbb{R}^2$, contours of $\boldsymbol{y} \mapsto \mathcal{V}_{|e^{wc}|}(\boldsymbol{y})$ (coloured closed curves labelled with values implicitly expressed in mV) and contours of $\boldsymbol{y} \mapsto |e^{wc}(\boldsymbol{y})|$ (dashed lines labelled with values explicitly expressed in mV). The lines $v_C = V_{LL0} - R_{LL}i_L$, $i_L = I_{O\min}$, $i_L = I_{O\max}$ in the $\mathbb{R}^2$, and their counterparts in $\mathbb{C}$ are just helping lines.

a controller with better performance than the strictly necessary. In voltage units, the available room can be expressed as (recall (6.4)):

$$D \max_{z \in \mathbb{C}} \mathcal{V}_{d_o}(z) = E - \min_{\boldsymbol{y} \in \mathbb{R}^2} \mathcal{V}_{|e^{wc}|}(\boldsymbol{y}). \qquad (6.31)$$

Observe that the evaluation of (6.30) involves solving an unrestricted maximization problem, which is amenable to numerical treatment because its objective function is quasi-concave and defined solely in terms of normalized dimensionless parameter values.

If a vivid proof of the infeasibility of the hypothetical controller is demanded, a simulation of a play of E, playing as the controller, against P, applying his optimal strategy, can be performed as it is exemplified next. For the control problem being considered, the four controllers (PID, H, SM, and RES), already introduced, were taken as examples of the hypothetical overestimated controller imagined before. Each of them was tuned following the same tuning methodology already used, though tailored to the parameters of Table 6.3. The PWM switching frequency f_s, of the PID-controlled buck, was selected as 250 kHz. The SM-controller's desired frequency f_{Sd} was set equal to f_s. The parameters E_H and λ (of the H and RES controllers, respectively) were set (by trial and error) to 6.5 mV and 1 V, respectively, so as to achieve closed-loop switching frequencies, at maximum load current, comparable to f_s. Each simulated play, during which E plays as one of the four controllers, starts at $t = 0$ from a steady-state regime, driven by constant maximum load current ($I_{O\max} = 100$ A). For $t \geq 0$, the control of the load current is assigned to P's optimal strategy.

The results of these simulations are represented graphically in Figures 6.25 and 6.26. Plainly evident, every tested controller fails to keep e $(t) < E$ for every $t \geq 0$.

In each of the four simulations carried out, the initial steady-state regime was selected to be driven by the maximum load current ($I_{O\max} = 100$ A), so that the initial condition for every controlled buck, other than the RES-controlled one, lies as far away as possible from the valley

$$\mathscr{V} = \left\{ \boldsymbol{y} \in \mathbb{R}^2 \ : \ \mathcal{V}_{|e^{wc}|}(\boldsymbol{y}) = \min_{\boldsymbol{y}' \in \mathbb{R}^2} \mathcal{V}_{|e^{wc}|}(\boldsymbol{y}') \right\},$$

where $\min_{\boldsymbol{y}' \in \mathbb{R}^2} \mathcal{V}_{|e^{wc}|}(\boldsymbol{y}') \approx 965$ mV. In this way, the superior performance of the RES controller, over the other three ones, is clearly appreciated, even for this unsolvable control problem. Nevertheless, a more benevolent initial steady-state regime driven by, for example nominal current ($I_{O\text{nom}} = \frac{I_{O\min} + I_{O\max}}{2} = 52.5$ A), could have been equally chosen to prove the controllers infeasibility. Even though $\mathcal{V}_{|e^{wc}|}$ is constant in $\mathscr{V}$, P's optimal strategy, as it was defined, is able to pull the state towards the boundary of $\mathscr{V}$ and subsequently force matters so that a worst case error greater or equal than $\min_{\boldsymbol{y} \in \mathbb{R}^2} \mathcal{V}_{|e^{wc}|}(\boldsymbol{y}) \approx 965$ mV is attained at last.

6.6.2. Negative verification of the claimed performance

The buck converter design example of Table 6.3 did not pass the negative verification, proposed above, with respect to the fulfilment of the control requirement.

If it had passed it, the ultimate fulfilment or not of the control requirement would have obviously depended on the selection of the controller.

In general, once a controller has been selected, it can be verified against false performance claims as follows. Let $\eta \in (0,1)$, and suppose the selected controller is claimed to be able to keep $|e(t)| < \eta E$ for every $t \geq 0$, for every initial state in the non-empty set $\mathscr{X} \subset \mathbb{R}^2$. In this hypothetical context, in addition to (6.28), the following condition must also hold

$$\eta E \geq \min_{\boldsymbol{y}\in\mathbb{R}^2} \mathcal{V}_{|e^{wc}|}(\boldsymbol{y}).\tag{6.32}$$

Otherwise, the claim is false. Hence, the inequality (6.32) may be used as *negative verification* of the selected controller's claimed performance (quantified by η) with respect to the control problem (posed by the values given to L, R_L, C, R_C, $I_{O\min}$, $I_{O\max}$, V_I, V_{LL0}, R_{LL}, and E). Notice that, by virtue of (6.31), the verification (6.32) does not require to solve a new optimization problem if (6.30) has already been solved.

Again, if a vivid proof of the claim's falsehood is demanded, a simulation can be carried out. As an example, reconsider the problem posed by Table 6.1 and the simulations of Figures 6.15 and 6.16. These simulations are the vivid proof that neither PID, H, SM, nor RES can fulfil $|e(t)| < \eta E$, for every $t \geq 0$, if $\eta < \frac{\min_{\boldsymbol{y}\in\mathbb{R}^2} \mathcal{V}_{|e^{wc}|}(\boldsymbol{y})}{E} \approx \frac{64.7\,\mathrm{mV}}{80\,\mathrm{mV}} \approx 0.809$.
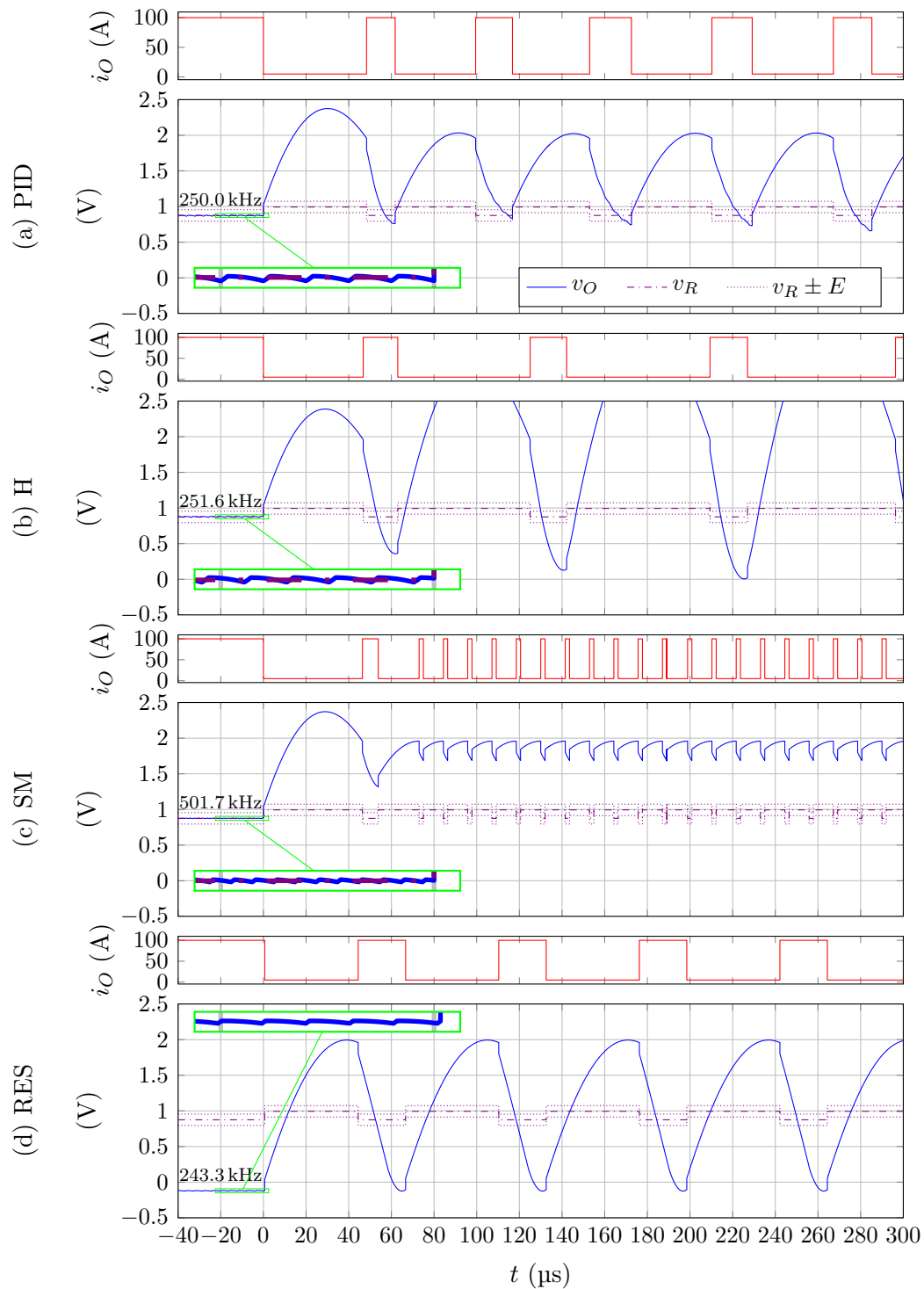
Figure 6.25: For the example of Table 6.3, E plays against P's optimal strategy as different controllers. The controllers are: (a) Proportional-Integral-Derivative (PID) controller, (b) Hysteresis (H) controller, (c) Sliding Mode (SM) controller, (d) Relaxed Evader's Strategy (RES) controller. For $t \geq 0$, P applies his optimal strategy, but for $t < 0$, the load current is held constant at its maximum value $I_{O\max} = 100\,\text{A}$. At $t = 0$, the controlled buck has already reached a steady-state regime, regardless the particular controller role adopted by E.
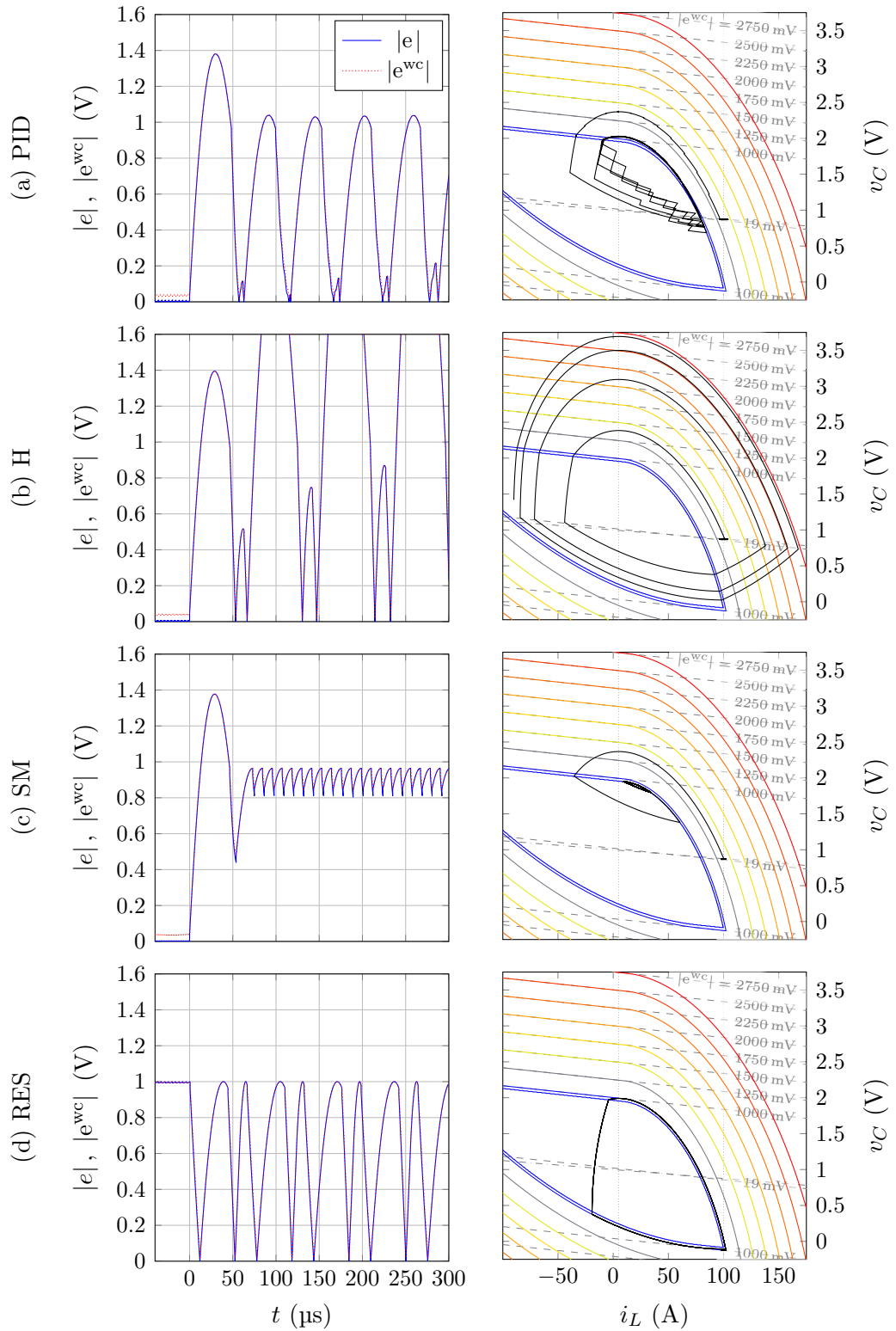
Figure 6.26: For each controller case, the absolute error $t \mapsto |e(t)|$ and the absolute worst-case error $t \mapsto |e^{wc}(\boldsymbol{y}(t))|$ (at the *left*), and the state-space trajectory $t \mapsto \boldsymbol{y}(t) = [i_L(t), v_C(t)]^\top$ (at the *right*), that corresponds to same case in Figure 6.25.

6.7. Concluding remarks

Different application aspects of the solution of the buck converter game in distance were explored in this chapter.

A relaxed version of the evader's optimal strategy was proposed as a buck converter's control method and was tested in numerical simulations. Not surprisingly, being a computationally expensive control method that requires full-state feedback, it exhibited quite good disturbance rejection performance, without incurring into high frequency chattering as the non-relaxed (pure) optimal strategy does. However, it was observed that steady-state performance is exchanged for transient performance, and that the switching frequency varies significantly from a steady-state regime to another. More significant is the finding that, by contrast to what was expected, the proposed control method showed an acceptable degree of robustness against moderate model parameter uncertainty, at least for the case studied. Nevertheless, this desirable property, needs further confirmation.

The counterpart of the evader's optimal strategy is the pursuer's optimal strategy, which was shown to be an appropriate disturbance synthesiser in simulated benchmark tests, set up for buck converter controller candidates. As the evader's optimal strategy, its implementation requires full-state feedback and exact knowledge of the converter's parameters, to continuously evaluate the current value of the game's value function. Such level of complexity, which may be impractical for a converter's controller, may be justifiable for an automated benchmarking platform. Yet, the selection of the initial state, from where each benchmark test is initiated, must be selected with some care in order to actually reproduce the intended worst case scenario. This selection is easily guided by the examination of the contour plot of the game's value function.

Actually, it is the exploitation of the game's value function, rather than its optimal strategies, what appears to be more fruitful from a practical standpoint. In particular, it was argued and supported by simulations that the global finite extremum of the game's value function quantifies the suitability of the converter with respect to the control requirement. Accordingly, this quantity was proposed as *figure of merit* of each possible converter–requirement *pair* instance that may result from a particular assignment of vales to the game's parameters. The proposed figure of merit can be evaluated to perform negative verifications on finished buck converter designs, or partially optimized (with respect to one or more parameters under given restrictions) during the design process itself to ease as much as possible the controller's job.

Chapter 7

Conclusions and future work

7.1. Conclusions

- The buck converter control problem, was precisely formulated in the realm of differential game theory as a pursuit-evasion conflict where the controller acts as the evader (E) and the disturbances on the load current and the input voltage act as the pursuer (P). The conflict gives rise to at least two natural pursuit-evasion games *of degree*: a *game in distance* (actually *oriented distance*) and a *game in time.* Roughly stated, for each possible converter's initial condition, the value function of the former game quantifies to which extent the control requirement can be fulfilled or not, while the value function of the second game, quantifies how long the violation of the control requirement can be delayed, always considering a *worst-case scenario* from E's viewpoint. The related *game of kind*, which is concerned only with the determination of whether the control requirement can be fulfilled or not (but not to which extent), is plainly embedded in both games of degree. However, for the buck controller's designer, the solution of the game in distance is, from both games of degree, the one that renders more valuable information. In addition, the game in distance, as it turned out to be the case, has the numerically desirable virtue of having a *continuous* value function, which is not the case for the game in time if the *escape set* is not empty, i.e., if there exists at least one initial condition from where the control requirement can be fulfilled. As pointed out in [50], the boundary of the escape set, i.e., the *barrier* of the game may be conveniently computed in an intrinsically numerically robust manner as the zero level set of the value function of the game in distance (because its gradient does not vanishes and is finite there). For these reasons, the game in distance derived from the buck converter conflict was taken as the central object of study of this thesis.

- The real Jordan form underlying the autonomous converter's dynamics was used along a non-dimensionalisation process of the original conflict formulation to propose a *canonical form* for the buck converter conflict, and its related games, under quite general assumptions. Accordingly, every buck

converter conflict originally posed in a 11-dimensional parameter-space can be reduced to its *canonical form* in a 7-dimensional parameter-space of dimensionless parameters. This reduction allows to systematically and consistently analyse the general buck converter control problem in the realm of differential game theory. Moreover, the proposed canonical form can be easily interpreted geometrically as a kinematic conflict in the plane, enhancing thereby intuition about the converter's switched model dynamics.

- The Isaacs' condition was proved to hold for both the game in distance and the game in time, even though the related Hamiltonians are not separable due to the multiplicative interaction between the input voltage and the switching action.

- Every semi-permeable curve associated to the dynamics of canonical buck converter conflict was found to belong to one of the eight possible families of such curves characterized in Section 4.5. The four negatively oriented families were shown to be the elementary building blocks underlying the solution of the game in distance.

- The game in distance was solved under quite general natural assumptions, except for one: the assumption that the converter's input voltage is constant. The sacrifice in generality introduced by this contrived assumption is compensated by the presence of central symmetry in the game, making it reducible to two unilateral (simpler) games.

- Three qualitative different cases, associated with how a positive dimensionless derived parameter compares to unity, were identified in the parameter-space of the game in distance. From the two non-limiting cases, one is distinguished by the existence of a limit cycle in the field of optimal trajectories.

- Different application aspects of the solution of the game in distance were suggested and supported by numerical simulations. Among these, the one that appears to contribute more to the real problem of buck converter control, is the aspect related with the possibility of quantifying the suitableness of the converter to the control problem by a *figure of merit*, computable by finding the finite extremum of the game's value function. The awareness of this figure allows for its optimization whenever it is possible, and expounds the inevitable theoretical limits to what can be expected from any control method.

7.2. Future work

- Determine whether the value function of the canonical game in distance (under the assumptions it was solved) is concave in general, or not. It is quasi-concave, and no evidence of non-concavity was found in the examples considered. However, a proof of generic concavity is still pending. Such proof

would endow the figure of merit mentioned before with an additional virtue, since concave maximization is particularly suited for numerical treatment.

- Solve the game in distance as it was formulated in Chapter 3, i.e., without assuming that the converter's input voltage is constant. Removing this assumption would make the solution of the game in distance much more relevant, since it would allow the model to take account of the fact that in real applications buck converters are usually fed by poorly regulated voltage sources.

- Develop the generic solution of the game in distance in a mathematically rigorous state-of-the-art theoretical framework. In this thesis Isaacs-Breakwell classical approach was followed to address the buck converter game in distance. This problem-solution oriented approach was proved adequate to yield immediate practical results. Nevertheless, a modern approach to the same problem would serve to corroborate the results reported here, and maybe, hopefully, would also shed light about the two previously enumerated items. The most reasonable theoretical framework to carry out this plan seems to be the widespread theory of viscosity solutions [65]. A rare example in which this theory is applied to a game in distance, instead of a game of time, is found in [50], where the "second order servomechanism problem" (a problem that has a lot in common with the buck converter conflict) is addressed. Another possible approach could be the theory of minimax solutions [64]. Attending the exactness of a purely numerical approach, even viability theory [66], which relies on set-valued analysis, should be invoked, as suggested in [50]. Closer investigation of these theories constitutes another further work in itself.

- Explore further the application aspects of the solution of the game in distance briefly discussed in Chapter 6. In particular, the benchmarking aspect of the solution of the game in distance, could be exploited to perform a broad comparison of an up-to-date set of the numerous control methods proposed in the literature for buck converter control. Another aspect that deserves a more realistic discussion than the one presented here, is the one related to the benefit of optimizing (at least to a certain degree) the proposed figure of merit.

Esta página ha sido intencionalmente dejada en blanco.

Appendix A

Geometric interpretation of the state-space transformation

A.1.   Some basic planar affine transformations

A function $\mathbf{T} : \mathbb{R}^n \to \mathbb{R}^n$ is called a an *affine transformation* if $\mathbf{T}\left((1-s)\,\boldsymbol{x} + s\boldsymbol{y}\right) = (1-s)\,\mathbf{T}\left(\boldsymbol{x}\right) + s\mathbf{T}\left(\boldsymbol{y}\right)$ for any $\boldsymbol{x}, \boldsymbol{y} \in \mathbb{R}^n$ and $s \in \mathbb{R}$. So, by definition, affine transformations preserve collinearity and proportions on lines.

Given an affine transformation $\mathbf{T} : \mathbb{R}^2 \to \mathbb{R}^2$, there exists a unique linear transformation $\mathbf{L}$ (called the *linear part* of $\mathbf{T}$) and a unique vector $\boldsymbol{y} \in \mathbb{R}^2$, such that $\mathbf{T}\left(\cdot\right) = \mathbf{L}\left(\cdot\right) + \boldsymbol{y}$. If $\det\left(\mathbf{L}\right) > 0$, $\mathbf{T}$ is *orientation-preserving*; if $\det\left(\mathbf{L}\right) < 0$, $\mathbf{T}$ it is *orientation-reversing*.

The following functions are examples of affine planar transformations. In each definition, $\theta, k \in \mathbb{R}$ and $\boldsymbol{y} \in \mathbb{R}^2$.

1. *Rotation of angle θ:* $\boldsymbol{x} \mapsto \mathbf{R}_\theta\left(\boldsymbol{x}\right) \triangleq \begin{bmatrix} \cos\theta & -\sin\theta \\ \sin\theta & \cos\theta \end{bmatrix} \boldsymbol{x}.$

2. *Positive right-angle rotation:* $\boldsymbol{x} \mapsto \boldsymbol{x}^\perp \triangleq \mathbf{R}_{\frac{\pi}{2}}\left(\boldsymbol{x}\right).$

3. *Shear of factor k along $\hat{\boldsymbol{e}}_{\mathbf{1}}$:* $\boldsymbol{x} \mapsto \mathbf{Sh}_{\hat{\boldsymbol{e}}_{\mathbf{1}},k}\left(\boldsymbol{x}\right) \triangleq \begin{bmatrix} 1 & k \\ 0 & 1 \end{bmatrix} \boldsymbol{x}.$

4. *Shear of factor k along $\hat{\boldsymbol{e}}_{\mathbf{2}}$:* $\boldsymbol{x} \mapsto \mathbf{Sh}_{\hat{\boldsymbol{e}}_{\mathbf{2}},k}\left(\boldsymbol{x}\right) \triangleq \begin{bmatrix} 1 & 0 \\ k & 1 \end{bmatrix} \boldsymbol{x}.$

5. *Scaling of factor k along $\hat{\boldsymbol{e}}_{\mathbf{1}}$:* $\boldsymbol{x} \mapsto \mathbf{Sc}_{\hat{\boldsymbol{e}}_{\mathbf{1}},k}\left(\boldsymbol{x}\right) \triangleq \begin{bmatrix} k & 0 \\ 0 & 1 \end{bmatrix} \boldsymbol{x}.$

6. *Scaling of factor k along $\hat{\boldsymbol{e}}_{\mathbf{2}}$:* $\boldsymbol{x} \mapsto \mathbf{Sc}_{\hat{\boldsymbol{e}}_{\mathbf{2}},k}\left(\boldsymbol{x}\right) \triangleq \begin{bmatrix} 1 & 0 \\ 0 & k \end{bmatrix} \boldsymbol{x}.$

7. *Translation by $\boldsymbol{y}$:* $\boldsymbol{x} \mapsto \mathbf{Tr}_{\boldsymbol{y}}\left(\boldsymbol{x}\right) \triangleq \boldsymbol{x} + \boldsymbol{y}.$

Except for the translation, all these transformations are linear transformations. Note that $\boldsymbol{x}^{\perp^\perp} = -\boldsymbol{x}$ and $\mathbf{R}_\theta\left(\boldsymbol{x}\right) = \boldsymbol{x}\cos\theta + \boldsymbol{x}^\perp \sin\theta.$

A.2.   Decomposition of the state space transformation

In Subsection 3.4.1 a function $\boldsymbol{h} : \mathbb{R}^2 \to \mathbb{R}^2$ is defined as

$$\boldsymbol{h}\left(\boldsymbol{x}\right) \triangleq \boldsymbol{P}\left(D\boldsymbol{x} + V\hat{\boldsymbol{e}}_{\boldsymbol{2}}\right),$$

where $\boldsymbol{P} \triangleq \frac{\sqrt{1-\zeta^2}}{(\zeta-\lambda)^2 + 1 - \zeta^2}\frac{1}{R}\begin{bmatrix} 1 & -\frac{\zeta-\lambda}{\sqrt{1-\zeta^2}} \\ -\lambda R & \frac{(1-\zeta\lambda)}{\sqrt{1-\zeta^2}}R \end{bmatrix}$, $V \triangleq V_{LL0} + R_M\frac{I_{O\min}+I_{O\max}}{2}, D \triangleq E - |R_M|\frac{I_{O\max}-I_{O\min}}{2}$, $R_M \triangleq R_C - R_{LL}$, $\omega_n \triangleq \frac{1}{\sqrt{LC}}$, $\zeta \triangleq \frac{1}{2\omega_n}\left(\frac{R_L+R_C}{L}\right)$, $R \triangleq \sqrt{\frac{L}{C}}$, and $\lambda \triangleq \frac{R_C}{R}$. What is more, its inverse $\boldsymbol{h}^{-1} : \mathbb{R}^2 \to \mathbb{R}^2$ defines a state-space transformation

$$\boldsymbol{y} = [i_L, v_C]^\top \mapsto [x_1, x_2]^\top = \boldsymbol{x} = \boldsymbol{h}^{-1}\left(\boldsymbol{y}\right) = \frac{1}{D}\left(\boldsymbol{P}^{-1}\boldsymbol{y} - V\hat{\boldsymbol{e}}_{\boldsymbol{2}}\right). \tag{A.1}$$

which allows for canonization of the buck converter conflict presented.

The state-space transformation (A.1) admits a simple geometric interpretation in terms of affine transformations that follows from the following matrix decomposition:

$$\boldsymbol{P}^{-1} = \begin{bmatrix} \frac{1-\zeta\lambda}{\sqrt{1-\zeta^2}}R & \frac{\zeta-\lambda}{\sqrt{1-\zeta^2}} \\ \lambda R & 1 \end{bmatrix} = \begin{bmatrix} s_1 & 0 \\ 0 & 1 \end{bmatrix}\begin{bmatrix} 1 & k_1 \\ 0 & 1 \end{bmatrix}\begin{bmatrix} 1 & 0 \\ k_2 & 1 \end{bmatrix}, \tag{A.2}$$

where $s_1 = \frac{(\zeta-\lambda)^2+1-\zeta^2}{\sqrt{1-\zeta^2}}R > 0$, $k_1 = \frac{\zeta-\lambda}{(\zeta-\lambda)^2+1-\zeta^2}R^{-1}$ and $k_2 = \lambda R > 0$. Substitution of (A.2) in (A.1) makes explicit the fact that $\boldsymbol{h}^{-1}$ is a shear along $\hat{\boldsymbol{e}}_{\boldsymbol{2}}$, followed by a shear along $\hat{\boldsymbol{e}}_{\boldsymbol{1}}$, followed by scalings (along $\hat{\boldsymbol{e}}_{\boldsymbol{1}}$ and $\hat{\boldsymbol{e}}_{\boldsymbol{2}}$), followed by a translation along $\hat{\boldsymbol{e}}_{\boldsymbol{2}}$:

$$
\begin{aligned}
\boldsymbol{x} = \boldsymbol{h}^{-1}\left(\boldsymbol{y}\right) &= \frac{1}{D}\boldsymbol{P}^{-1}\boldsymbol{y} - \frac{V}{D}\hat{\boldsymbol{e}}_{\boldsymbol{2}} \\
&= \frac{1}{D}\begin{bmatrix} s_1 & 0 \\ 0 & 1 \end{bmatrix}\begin{bmatrix} 1 & k_1 \\ 0 & 1 \end{bmatrix}\begin{bmatrix} 1 & 0 \\ k_2 & 1 \end{bmatrix}\boldsymbol{y} - \frac{V}{D}\hat{\boldsymbol{e}}_{\boldsymbol{2}} \\
&= \begin{bmatrix} \frac{s_1}{D} & 0 \\ 0 & 1 \end{bmatrix}\begin{bmatrix} 1 & 0 \\ 0 & \frac{1}{D} \end{bmatrix}\begin{bmatrix} 1 & k_1 \\ 0 & 1 \end{bmatrix}\begin{bmatrix} 1 & 0 \\ k_2 & 1 \end{bmatrix}\boldsymbol{y} - \frac{V}{D}\hat{\boldsymbol{e}}_{\boldsymbol{2}} \\
&= \left(\mathbf{Tr}_{-\frac{V}{D}\hat{\boldsymbol{e}}_{\boldsymbol{2}}} \circ \mathbf{Sc}_{\hat{\boldsymbol{e}}_{\boldsymbol{1}},\frac{s_1}{D}} \circ \mathbf{Sc}_{\hat{\boldsymbol{e}}_{\boldsymbol{2}},\frac{1}{D}} \circ \mathbf{Sh}_{\hat{\boldsymbol{e}}_{\boldsymbol{1}},k_1} \circ \mathbf{Sh}_{\hat{\boldsymbol{e}}_{\boldsymbol{2}},k_2}\right)\left(\boldsymbol{y}\right).
\end{aligned}
$$

Similarly,

$$\boldsymbol{P} = \frac{\sqrt{1-\zeta^2}}{(\zeta-\lambda)^2+1-\zeta^2}\frac{1}{R}\begin{bmatrix} 1 & -\frac{\zeta-\lambda}{\sqrt{1-\zeta^2}} \\ -\lambda R & \frac{1-\zeta\lambda}{\sqrt{1-\zeta^2}}R \end{bmatrix} = \begin{bmatrix} 1 & 0 \\ -k_2 & 1 \end{bmatrix}\begin{bmatrix} 1 & -k_1 \\ 0 & 1 \end{bmatrix}\begin{bmatrix} \frac{1}{s_1} & 0 \\ 0 & 1 \end{bmatrix},$$

$$\tag{A.3}$$

$$\frac{1}{D}\boldsymbol{P}^{-1}\cdot = \mathbf{Sc}_{\hat{\boldsymbol{e}}_1,\frac{s_1}{D}} \circ \mathbf{Sc}_{\hat{\boldsymbol{e}}_2,\frac{1}{D}} \circ \mathbf{Sh}_{\hat{\boldsymbol{e}}_1,k_1} \circ \mathbf{Sh}_{\hat{\boldsymbol{e}}_2,k_2}$$

$$\boldsymbol{y} \xrightarrow{\hspace{6cm}} \boldsymbol{x}-\boldsymbol{y}$$

$$\boldsymbol{h}^{-1}$$

$$\mathbf{Tr}_{\boldsymbol{y_0}} \uparrow \qquad\qquad \downarrow \mathbf{Tr}_{\boldsymbol{x_0}}$$

$$\boldsymbol{y}-\boldsymbol{y_0} \xleftarrow{\hspace{6cm}} \boldsymbol{x}$$

$$D\boldsymbol{P}\cdot = \mathbf{Sh}_{\hat{\boldsymbol{e}}_2,-k_2} \circ \mathbf{Sh}_{\hat{\boldsymbol{e}}_1,-k_1} \circ \mathbf{Sc}_{\hat{\boldsymbol{e}}_2,D} \circ \mathbf{Sc}_{\hat{\boldsymbol{e}}_1,\frac{D}{s_1}}$$
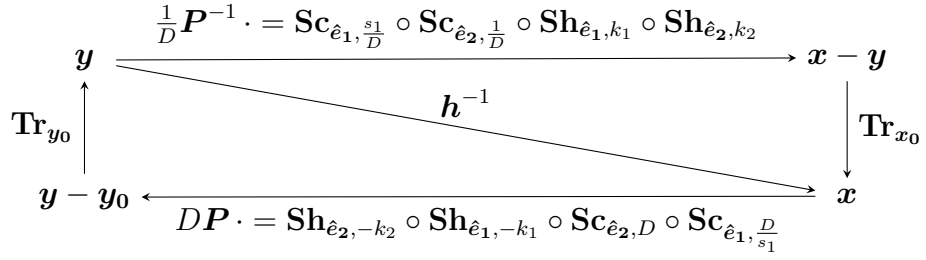
Figure A.1: Decomposition of the state space transformation $\boldsymbol{h}^{-1} : \mathbb{R}^2 \to \mathbb{R}^2$ and its inverse.

and therefore

$$\begin{aligned}
\boldsymbol{y} = \boldsymbol{h}\left(\boldsymbol{x}\right) &= D\boldsymbol{P}\boldsymbol{x} + V\boldsymbol{P}\hat{\boldsymbol{e}}_2 \\
&= D \begin{bmatrix} 1 & 0 \\ -k_2 & 1 \end{bmatrix} \begin{bmatrix} 1 & -k_1 \\ 0 & 1 \end{bmatrix} \begin{bmatrix} \frac{1}{s_1} & 0 \\ 0 & 1 \end{bmatrix} \boldsymbol{x} + V\boldsymbol{P}\hat{\boldsymbol{e}}_2 \\
&= \begin{bmatrix} 1 & 0 \\ -k_2 & 1 \end{bmatrix} \begin{bmatrix} 1 & -k_1 \\ 0 & 1 \end{bmatrix} \begin{bmatrix} 1 & 0 \\ 0 & D \end{bmatrix} \begin{bmatrix} \frac{D}{s_1} & 0 \\ 0 & 1 \end{bmatrix} \boldsymbol{x} + V\boldsymbol{P}\hat{\boldsymbol{e}}_2 \\
&= \left(\mathbf{Tr}_{+V\boldsymbol{P}\hat{\boldsymbol{e}}_2} \circ \mathbf{Sh}_{\hat{\boldsymbol{e}}_2,-k_2} \circ \mathbf{Sh}_{\hat{\boldsymbol{e}}_1,-k_1} \circ \mathbf{Sc}_{\hat{\boldsymbol{e}}_2,D} \circ \mathbf{Sc}_{\hat{\boldsymbol{e}}_1,\frac{D}{s_1}} \right)\left(\boldsymbol{x}\right).
\end{aligned}$$

Naming

$$\boldsymbol{y_0} \triangleq \boldsymbol{h}\left(\mathbf{0}\right) = V\boldsymbol{P}\hat{\boldsymbol{e}}_2 = \frac{\sqrt{1-\zeta^2}}{(\zeta-\lambda)^2 + 1 - \zeta^2} \frac{V}{R} \begin{bmatrix} -\frac{\zeta-\lambda}{\sqrt{1-\zeta^2}} \\ \frac{1-\zeta\lambda}{\sqrt{1-\zeta^2}}R \end{bmatrix},$$

$$\boldsymbol{x_0} \triangleq \boldsymbol{h}^{-1}\left(\mathbf{0}\right) = -\frac{V}{D}\hat{\boldsymbol{e}}_2 = -\frac{V}{D}\begin{bmatrix} 0 \\ 1 \end{bmatrix},$$

the commutative diagram of Figure A.1 summarizes this *active* plane-deformation interpretation of $\boldsymbol{h}^{-1}$ and its inverse.

Observe that $\boldsymbol{h}^{-1}$ is a composition of orientation preserving transformations, so it must preserve orientation. This can be verified by noting that its Jacobian $\det\left(\frac{\partial \boldsymbol{h}^{-1}}{\partial \boldsymbol{y}}\left(\boldsymbol{y}\right)\right) = \frac{1}{D^2}(\det \boldsymbol{P})^{-1}$ is positive.

Another way of looking at $\boldsymbol{h}^{-1}$, results from introducing

$$\boldsymbol{y_1} \triangleq \boldsymbol{h}\left(\hat{\boldsymbol{e}}_1\right) - \boldsymbol{y_0} = D\boldsymbol{P}\hat{\boldsymbol{e}}_1 = \frac{\sqrt{1-\zeta^2}}{(\zeta-\lambda)^2 + 1 - \zeta^2} \frac{D}{R} \begin{bmatrix} 1 \\ -\lambda R \end{bmatrix},$$

$$\boldsymbol{y_2} \triangleq \boldsymbol{h}\left(\hat{\boldsymbol{e}}_2\right) - \boldsymbol{y_0} = D\boldsymbol{P}\hat{\boldsymbol{e}}_2 = \frac{\sqrt{1-\zeta^2}}{(\zeta-\lambda)^2 + 1 - \zeta^2} \frac{D}{R} \begin{bmatrix} -\frac{\zeta-\lambda}{\sqrt{1-\zeta^2}} \\ \frac{1-\zeta\lambda}{\sqrt{1-\zeta^2}}R \end{bmatrix}.$$

Vectors $\boldsymbol{y_1}$ and $\boldsymbol{y_2}$ are, respectively, the first and second columns of matrix $D\boldsymbol{P}$. They are linearly independent because $\det\left(D\boldsymbol{P}\right) = D^2 \det \boldsymbol{P} > 0$, so $\{\boldsymbol{y_1}, \boldsymbol{y_2}\}$ is an ordered base of $\mathbb{R}^2$. The normalized state was introduced as $\boldsymbol{x} \triangleq h^{-1}\left(\boldsymbol{y}\right) =$

$\frac{1}{D}\left(\boldsymbol{P}^{-1}\boldsymbol{y} - V\hat{\boldsymbol{e}}_{\mathbf{2}}\right)$, but this is equivalent to define $\boldsymbol{x}$ as the coordinate vector of $\boldsymbol{y} - \boldsymbol{y_0}$ relative to $\{\boldsymbol{y_1}, \boldsymbol{y_2}\}$, i.e.,

$$\boldsymbol{x} = \begin{bmatrix} x_1 \\ x_2 \end{bmatrix} \triangleq [\boldsymbol{y} - \boldsymbol{y_0}]_{\{\boldsymbol{y_1}, \boldsymbol{y_2}\}}, \tag{A.4}$$

because $\boldsymbol{x} = \frac{1}{D}\left(\boldsymbol{P}^{-1}\boldsymbol{y} - V\hat{\boldsymbol{e}}_{\mathbf{2}}\right)$ if and only if $\boldsymbol{y} - \boldsymbol{y_0} = D\boldsymbol{P}\boldsymbol{x} = x_1\boldsymbol{y_1} + x_2\boldsymbol{y_2}$.

Likewise, introducing

$$\boldsymbol{x_1} \triangleq \boldsymbol{h}^{-1}\left(\hat{\boldsymbol{e}}_{\mathbf{1}}\right) - \boldsymbol{x_0} = \frac{1}{D}\boldsymbol{P}^{-1}\hat{\boldsymbol{e}}_{\mathbf{1}} = \frac{1}{D}\begin{bmatrix} \frac{1-\zeta\lambda}{\sqrt{1-\zeta^2}}R \\ \lambda R \end{bmatrix},$$

$$\boldsymbol{x_2} \triangleq \boldsymbol{h}^{-1}\left(\hat{\boldsymbol{e}}_{\mathbf{2}}\right) - \boldsymbol{x_0} = \frac{1}{D}\boldsymbol{P}^{-1}\hat{\boldsymbol{e}}_{\mathbf{2}} = \frac{1}{D}\begin{bmatrix} \frac{\zeta-\lambda}{\sqrt{1-\zeta^2}} \\ 1 \end{bmatrix},$$

$\boldsymbol{y}$ can be recovered back from x as

$$\boldsymbol{y} = \begin{bmatrix} z_1 \\ z_2 \end{bmatrix} = [\boldsymbol{x} - \boldsymbol{x_0}]_{\{\boldsymbol{x_1}, \boldsymbol{x_2}\}}, \tag{A.5}$$

because $\boldsymbol{y} = D\boldsymbol{P}\boldsymbol{x} + V\boldsymbol{P}\hat{\boldsymbol{e}}_{\mathbf{2}}$ if and only if $\boldsymbol{x} - \boldsymbol{x_0} = \frac{1}{D}\boldsymbol{P}^{-1}\boldsymbol{y} = z_1\boldsymbol{x_1} + z_2\boldsymbol{x_2}$.

In this *passive* interpretation of $\boldsymbol{h}^{-1}$, the components of $\boldsymbol{x} = \boldsymbol{h}^{-1}\left(\boldsymbol{y}\right)$ are the coordinates of vector $\boldsymbol{y}$ with respect to the *referential* $\{\boldsymbol{y_0}, \{\boldsymbol{y_1}, \boldsymbol{y_2}\}\}$. Note that this is a very special referential; the line through $\boldsymbol{y_0}$ oriented along $\boldsymbol{y_1}$ is the middle axis of the band $\mathcal{E}' = \{\boldsymbol{y} \in \mathbb{R}^2 \ : \ |\langle \boldsymbol{l}, \boldsymbol{y} \rangle - V| < D\}$, because $|\langle \boldsymbol{l}, \boldsymbol{y_0} \rangle - V| = 0$ and $\langle \boldsymbol{l}, \boldsymbol{y_1} \rangle = 0$. Also, the point $\boldsymbol{y_0} + \boldsymbol{y_2}$ lays on the boundary of $\mathcal{E}'$ that corresponds to the ROVC, because $\langle \boldsymbol{l}, \boldsymbol{y_2} \rangle - V = D$.

Regarded with the usual inner product of $\mathbb{R}^2$, the basis $\{\boldsymbol{y_1}, \boldsymbol{y_2}\}$ is not orthogonal, but if each of its elements is mapped by the linear part of $\boldsymbol{h}^{-1}$, the standard basis of $\mathbb{R}^2$ is obtained, i.e., $\left\{\frac{1}{D}\boldsymbol{P}^{-1}\boldsymbol{y_1}, \frac{1}{D}\boldsymbol{P}^{-1}\boldsymbol{y_2}\right\} = \{\hat{\boldsymbol{e}}_{\mathbf{1}}, \hat{\boldsymbol{e}}_{\mathbf{2}}\}$. In addition, $\frac{1}{D}\boldsymbol{P}^{-1}\cdot$, the unique linear transformation that relate both ordered bases, has positive determinant $\det\left(\frac{1}{D}\boldsymbol{P}^{-1}\right) = \frac{1}{D^2}(\det\boldsymbol{P})^{-1}$, so (by definition of the orientation of a basis in a vector space) the basis $\{\boldsymbol{y_1}, \boldsymbol{y_2}\}$ has the *same orientation* as $\{\hat{\boldsymbol{e}}_{\mathbf{1}}, \hat{\boldsymbol{e}}_{\mathbf{2}}\}$. This last one is usually conventionally declared as *positively oriented*.

Since $\{\boldsymbol{y_1}, \boldsymbol{y_2}\}$ is a basis of $\mathbb{R}^2$, the original state space can be parametrized as the plane $\{\boldsymbol{y_0} + x_1\boldsymbol{y_1} + x_2\boldsymbol{y_2} \ : \ x_1, x_2 \in \mathbb{R}\}$. The function $\boldsymbol{h}^{-1}$ takes any point $\boldsymbol{y} = \boldsymbol{y_0} + x_1\boldsymbol{y_1} + x_2\boldsymbol{y_2}$ of this plane to

$$\begin{aligned} \boldsymbol{h}^{-1}\left(\boldsymbol{y}\right) &= \frac{1}{D}\boldsymbol{P}^{-1}\left(\boldsymbol{y_0} + x_1\boldsymbol{y_1} + x_2\boldsymbol{y_2}\right) - \frac{V}{D}\hat{\boldsymbol{e}}_{\mathbf{2}} \\ &= \frac{1}{D}\boldsymbol{P}^{-1}\left(V\boldsymbol{P}\hat{\boldsymbol{e}}_{\mathbf{2}}\right) + x_1\frac{1}{D}\boldsymbol{P}^{-1}\boldsymbol{y_1} + x_2\frac{1}{D}\boldsymbol{P}^{-1}\boldsymbol{y_2} - \frac{V}{D}\hat{\boldsymbol{e}}_{\mathbf{2}} \\ &= x_1\hat{\boldsymbol{e}}_{\mathbf{1}} + x_2\hat{\boldsymbol{e}}_{\mathbf{2}}. \end{aligned}$$

These equalities, show explicitly that $\boldsymbol{y_0}$ is mapped to the origin, lines oriented along $\boldsymbol{y_1}$ are mapped to lines oriented along $\hat{\boldsymbol{e}}_{\mathbf{1}}$, and lines oriented along $\boldsymbol{y_2}$ are mapped to lines oriented along $\hat{\boldsymbol{e}}_{\mathbf{2}}$.

Appendix B

Miscellaneous calculations

B.1. The derivation of the return map

In Section 5.6, the ρ-parametrized family of state-space characteristic traject-
ories that results form integrating the RPE given by (5.23)–(5.24) with initial
conditions

$$z_\rho|_{\tau=0} = z_{\rho,0} = a - \rho\frac{\overline{k}}{|k|}, \tag{B.1}$$

$$p|_{\tau=0} \;=\; p_0 \;=\; -\mathrm{j}, \tag{B.2}$$

over a retro-time interval of length 2π was found to be

$$\tau \mapsto z_\rho(\tau) = \begin{cases} a + \mathrm{e}^{(\kappa-\mathrm{j})(\tau-\tau_0)}(z_{\rho,0} - a) & \text{if } \tau \in [0, \tau_1], \\ b + \mathrm{e}^{(\kappa-\mathrm{j})(\tau-\tau_1)}(z_\rho(\tau_1) - b) & \text{if } \tau \in (\tau_1, \tau_2], \\ c + \mathrm{e}^{(\kappa-\mathrm{j})(\tau-\tau_2)}(z_\rho(\tau_2) - c) & \text{if } \tau \in (\tau_2, \tau_3], \\ d + \mathrm{e}^{(\kappa-\mathrm{j})(\tau-\tau_3)}(z_\rho(\tau_3) - d) & \text{if } \tau \in (\tau_3, \tau_4], \\ a + \mathrm{e}^{(\kappa-\mathrm{j})(\tau-\tau_4)}(z_\rho(\tau_4) - a) & \text{if } \tau \in (\tau_4, 2\pi), \end{cases} \tag{B.3}$$

where $\tau_1 = \gamma_1 \triangleq \frac{\pi}{2} + 2\beta - \alpha$, $\tau_2 - \tau_1 = \gamma_2 \triangleq \frac{\pi}{2} - \beta$, $\tau_3 - \tau_2 = \gamma_3 \triangleq \frac{\pi}{2} + \beta$, $\tau_4 - \tau_3 = \gamma_4 \triangleq \frac{\pi}{2} - \beta$, and $2\pi - \tau_4 = \gamma_5 \triangleq \alpha - \beta$ are positive; and $\gamma_1 + \gamma_2 + \gamma_3 + \gamma_4 + \gamma_5 = 2\pi$.

The parameter ρ was assumed to be positive in (B.1) (because of the analysis
carried out in Section 5.4), but it may well be allowed to be any real number.
In that case, the ρ-parametrized family (B.3) is still the family of state-space
characteristic trajectories that results from integrating blindly the RPE. Here,
this broader conception of the initial condition (B.1) is assumed.

For notational convenience, let $\rho' \in \mathbb{R}$ take the place of ρ in (B.1) and (B.3)
so that the symbol ρ is free to be used next, i.e.,

$$z_{\rho'}|_{\tau=0} = z_{\rho',0} = a + \rho'\mathrm{e}^{\mathrm{j}\left(\frac{\pi}{2}-\alpha\right)}, \quad \rho' \in \mathbb{R}, \tag{B.4}$$

Appendix B. Miscellaneous calculations

$$
\tau \mapsto z_{\rho'}(\tau) = \begin{cases}
a + e^{-k(\tau-\tau_0)} \left(z_{\rho',0} - a \right) & \text{if } \tau \in [0, \tau_1], \\
b + e^{-k(\tau-\tau_1)} \left(z_{\rho'}(\tau_1) - b \right) & \text{if } \tau \in (\tau_1, \tau_2], \\
c + e^{-k(\tau-\tau_2)} \left(z_{\rho'}(\tau_2) - c \right) & \text{if } \tau \in (\tau_2, \tau_3], \\
d + e^{-k(\tau-\tau_3)} \left(z_{\rho'}(\tau_3) - d \right) & \text{if } \tau \in (\tau_3, \tau_4], \\
a + e^{-k(\tau-\tau_4)} \left(z_{\rho'}(\tau_4) - a \right) & \text{if } \tau \in (\tau_4, 2\pi),
\end{cases} \tag{B.5}
$$

where $-\frac{\overline{k}}{|k|}$ was replaced by $e^{\mathrm{j}\left(\frac{\pi}{2}-\alpha\right)}$ in (B.4) and $\kappa - \mathrm{j}$ was replaced by $-k$ in (B.5).

Also for notational convenience, let

$$
z_{\rho'}\left((2\pi)^-\right) \triangleq \lim_{\tau \to (2\pi)^-} z_{\rho'}(\tau). \tag{B.6}
$$

Proposition B.1.1. *For every $\rho' \in \mathbb{R}$, the point $z_{\rho'}\left((2\pi)^-\right)$ lies on the line $\left\{ a + \xi e^{\mathrm{j}\left(\frac{\pi}{2}-\alpha\right)} \ : \ \xi \in \mathbb{R} \right\}$. Moreover,*

$$
z_{\rho'}\left((2\pi)^-\right) = a + \rho e^{\mathrm{j}\left(\frac{\pi}{2}-\alpha\right)}
$$

where

$$
\rho = e^{2\pi\kappa} \left(\rho' - \mu_1 \left(e^{-\kappa\left(\frac{\pi}{2}+2\beta-\alpha\right)} + e^{-\kappa\left(\frac{3\pi}{2}+2\beta-\alpha\right)} \right) + \mu_2 \left(e^{-\kappa(\pi+\beta-\alpha)} + e^{-\kappa(2\pi+\beta-\alpha)} \right) \right).
$$

Proof. Taking the limit (B.6) in (B.5) to isolate $z_{\rho'}(\tau_4)$ in terms of $z_{\rho'}\left((2\pi)^-\right)$, yields

$$
z_{\rho'}(\tau_4) = a + e^{k\gamma_5} \left(z_{\rho'}\left((2\pi)^-\right) - a \right). \tag{B.7}
$$

Similarly, in (B.5), we may isolate $z_{\rho'}(\tau_3)$ in terms of $z_{\rho'}(\tau_4)$ as

$$
z_{\rho'}(\tau_3) = d + e^{k\gamma_4} \left(z_{\rho'}(\tau_4) - d \right), \tag{B.8}
$$

Analogously,

$$
z_{\rho'}(\tau_2) = c + e^{k\gamma_3} \left(z_{\rho'}(\tau_3) - c \right), \tag{B.9}
$$

$$
z_{\rho'}(\tau_1) = b + e^{k\gamma_2} \left(z_{\rho'}(\tau_2) - b \right), \tag{B.10}
$$

$$
z_{\rho'}(0) = z_{\rho',0} = a + e^{k\gamma_1} \left(z_{\rho'}(\tau_1) - a \right). \tag{B.11}
$$

Now, from (B.7)–(B.11):

$$
\begin{aligned}
z_{\rho'}(0) &= a + e^{k\gamma_1} \left(b + e^{k\gamma_2} \left(z_{\rho'}(\tau_2) - b \right) - a \right) \\
&= a + e^{k\gamma_1} (b-a) + e^{k(\gamma_1+\gamma_2)} \left(z_{\rho'}(\tau_2) - b \right) \\
&= a + e^{k\gamma_1} (b-a) + e^{k(\gamma_1+\gamma_2)} \left(c + e^{k\gamma_3} \left(z_{\rho'}(\tau_3) - c \right) - b \right) \\
&= a + e^{k\gamma_1} (b-a) + e^{k(\gamma_1+\gamma_2)} (c-b) + e^{k(\gamma_1+\gamma_2+\gamma_3)} \left(z_{\rho'}(\tau_3) - c \right) \\
&= a + e^{k\gamma_1} (b-a) + e^{k(\gamma_1+\gamma_2)} (c-b) + e^{k(\gamma_1+\gamma_2+\gamma_3)} \left(d + e^{k\gamma_4} \left(z_{\rho'}(\tau_4) - d \right) - c \right) \\
&= a + \left(e^{k\gamma_1} - e^{k(\gamma_1+\gamma_2+\gamma_3)} \right) (b-a) + e^{k(\gamma_1+\gamma_2)} (c-b) + e^{k(\gamma_1+\gamma_2+\gamma_3+\gamma_4)} \left(z_{\rho'}(\tau_4) - d \right) \\
&= a + \left(e^{k\gamma_1} - e^{k(\gamma_1+\gamma_2+\gamma_3)} \right) (b-a) + e^{k(\gamma_1+\gamma_2)} (c-b) \\
&\quad + e^{k(\gamma_1+\gamma_2+\gamma_3+\gamma_4)} \left(a + e^{k\gamma_5} \left(z_{\rho'}\left((2\pi)^-\right) - a \right) - d \right) \\
&= a + \left(e^{k\gamma_1} - e^{k(\gamma_1+\gamma_2+\gamma_3)} \right) (b-a) + \left(e^{k(\gamma_1+\gamma_2)} - e^{k(\gamma_1+\gamma_2+\gamma_3+\gamma_4)} \right) (c-b) \\
&\quad + e^{k(\gamma_1+\gamma_2+\gamma_3+\gamma_4+\gamma_5)} \left(z_{\rho'}\left((2\pi)^-\right) - a \right)
\end{aligned}
$$

where it was used that $d - c = -(b - a)$ and $a - d = -(c - b)$. Accordingly,

$$
\begin{aligned}
z_{\rho'}(0) - a &= \left(\mathrm{e}^{(-\kappa+\mathrm{j})\gamma_1} - \mathrm{e}^{(-\kappa+\mathrm{j})(\gamma_1+\gamma_2+\gamma_3)} \right)(b - a) \\
&\quad + \left(\mathrm{e}^{(-\kappa+\mathrm{j})(\gamma_1+\gamma_2)} - \mathrm{e}^{(-\kappa+\mathrm{j})(\gamma_1+\gamma_2+\gamma_3+\gamma_4)} \right)(c - b) \\
&\quad + \mathrm{e}^{(-\kappa+\mathrm{j})(\gamma_1+\gamma_2+\gamma_3+\gamma_4+\gamma_5)} \left(z_{\rho'}\left((2\pi)^-\right) - a \right) \\
&= \left(\mathrm{e}^{(-\kappa+\mathrm{j})\left(\frac{\pi}{2}+2\beta-\alpha\right)} - \mathrm{e}^{(-\kappa+\mathrm{j})\left(\frac{3\pi}{2}+2\beta-\alpha\right)} \right) \mu_1 \mathrm{e}^{-\mathrm{j}2\beta} \\
&\quad + \left(\mathrm{e}^{(-\kappa+\mathrm{j})(\pi+\beta-\alpha)} - \mathrm{e}^{(-\kappa+\mathrm{j})(2\pi+\beta-\alpha)} \right) \mu_2 \mathrm{e}^{\mathrm{j}\left(\frac{\pi}{2}-\beta\right)} \\
&\quad + \mathrm{e}^{(-\kappa+\mathrm{j})(2\pi)} \left(z_{\rho'}\left((2\pi)^-\right) - a \right) \\
&= \left(\mathrm{e}^{-\kappa\left(\frac{\pi}{2}+2\beta-\alpha\right)} + \mathrm{e}^{-\kappa\left(\frac{3\pi}{2}+2\beta-\alpha\right)} \right) \mu_1 \mathrm{e}^{\mathrm{j}\left(\frac{\pi}{2}-\alpha\right)} \\
&\quad + \left(-\mathrm{e}^{-\kappa(\pi+\beta-\alpha)} - \mathrm{e}^{-\kappa(2\pi+\beta-\alpha)} \right) \mu_2 \mathrm{e}^{\mathrm{j}\left(\frac{\pi}{2}-\alpha\right)} \\
&\quad + \mathrm{e}^{-\kappa(2\pi)} \left(z_{\rho'}\left((2\pi)^-\right) - a \right)
\end{aligned}
$$

where it was used that $k = -\kappa + \mathrm{j}$, $b - a = \mu_1 \mathrm{e}^{-\mathrm{j}2\beta}$, $c - b = \mu_2 \mathrm{e}^{\mathrm{j}\left(\frac{\pi}{2}-\beta\right)}$, $\gamma_1 = \frac{\pi}{2} + 2\beta - \alpha$, $\gamma_2 = \frac{\pi}{2} - \beta$, $\gamma_3 = \frac{\pi}{2} + \beta$, $\gamma_4 = \frac{\pi}{2} - \beta$, and $\gamma_5 = \alpha - \beta$.

Consequently, $z_{\rho'}\left((2\pi)^-\right) - a$ relates to $z_{\rho'}(0) - a$ as follows:

$$
\begin{aligned}
\mathrm{e}^{-2\pi\kappa} \left(z_{\rho'}\left((2\pi)^-\right) - a \right) &= z_{\rho'}(0) - a \\
&\quad - \left(\mathrm{e}^{-\kappa\left(\frac{\pi}{2}+2\beta-\alpha\right)} + \mathrm{e}^{-\kappa\left(\frac{3\pi}{2}+2\beta-\alpha\right)} \right) \mu_1 \mathrm{e}^{\mathrm{j}\left(\frac{\pi}{2}-\alpha\right)} \\
&\quad + \left(\mathrm{e}^{-\kappa(\pi+\beta-\alpha)} + \mathrm{e}^{-\kappa(2\pi+\beta-\alpha)} \right) \mu_2 \mathrm{e}^{\mathrm{j}\left(\frac{\pi}{2}-\alpha\right)}
\end{aligned}
$$

where $z_{\rho'}(0) - a = \rho' \mathrm{e}^{\mathrm{j}\left(\frac{\pi}{2}-\alpha\right)}$ because of the initial condition (B.4). Hence,

$$
\begin{aligned}
\mathrm{e}^{-2\pi\kappa} \left(z_{\rho'}\left((2\pi)^-\right) - a \right) &= \rho' \mathrm{e}^{\mathrm{j}\left(\frac{\pi}{2}-\alpha\right)} \\
&\quad - \left(\mathrm{e}^{-\kappa\left(\frac{\pi}{2}+2\beta-\alpha\right)} + \mathrm{e}^{-\kappa\left(\frac{3\pi}{2}+2\beta-\alpha\right)} \right) \mu_1 \mathrm{e}^{\mathrm{j}\left(\frac{\pi}{2}-\alpha\right)} \\
&\quad + \left(\mathrm{e}^{-\kappa(\pi+\beta-\alpha)} + \mathrm{e}^{-\kappa(2\pi+\beta-\alpha)} \right) \mu_2 \mathrm{e}^{\mathrm{j}\left(\frac{\pi}{2}-\alpha\right)}
\end{aligned}
$$

which evidences that $z_{\rho'}\left((2\pi)^-\right)$ lies on the straight line $\left\{ a + \xi \mathrm{e}^{\mathrm{j}\left(\frac{\pi}{2}-\alpha\right)} \ : \ \xi \in \mathbb{R} \right\}$. More explicitly,

$$
z_{\rho'}\left((2\pi)^-\right) = a + \rho \mathrm{e}^{\mathrm{j}\left(\frac{\pi}{2}-\alpha\right)}
$$

where

$$
\rho = \mathrm{e}^{2\pi\kappa} \left(\rho' - \mu_1 \left(\mathrm{e}^{-\kappa\left(\frac{\pi}{2}+2\beta-\alpha\right)} + \mathrm{e}^{-\kappa\left(\frac{3\pi}{2}+2\beta-\alpha\right)} \right) + \mu_2 \left(\mathrm{e}^{-\kappa(\pi+\beta-\alpha)} + \mathrm{e}^{-\kappa(2\pi+\beta-\alpha)} \right) \right).
$$

$\square$

The previous proposition, asserts that for every $\rho' \in \mathbb{R}$, the characteristic trajectory $[0, 2\pi) \ni \tau \mapsto z_{\rho'}(\tau)$ through the point $z_{\rho'}(0) = a + \rho' \mathrm{e}^{\mathrm{j}\left(\frac{\pi}{2}-\alpha\right)}$ which lies on the line $\left\{ a + \xi \mathrm{e}^{\mathrm{j}\left(\frac{\pi}{2}-\alpha\right)} \ : \ \xi \in \mathbb{R} \right\}$, is such that the limit $z_{\rho'}\left((2\pi)^-\right) = \lim_{\tau \to (2\pi)^-} z_{\rho'}(\tau)$ *also* lies on the line $\left\{ a + \xi \mathrm{e}^{\mathrm{j}\left(\frac{\pi}{2}-\alpha\right)} \ : \ \xi \in \mathbb{R} \right\}$. In addition, it

establishes how to compute $\rho = \left(z_{\rho'}\left((2\pi)^- \right) - a \right) \odot \mathrm{e}^{\mathrm{j}\left(\frac{\pi}{2} - \alpha \right)}$ in terms of $\rho' = \left(z_{\rho'}(0) - a \right) \odot \mathrm{e}^{\mathrm{j}\left(\frac{\pi}{2} - \alpha \right)}$. Inverting the map $\rho' \mapsto \rho$, we obtain the map

$$\rho \mapsto \rho' = P(\rho) = \eta_1 \rho + \eta_0$$

where

$$
\begin{aligned}
\eta_0 &\triangleq \left(\mathrm{e}^{-\kappa\left(\frac{\pi}{2} + 2\beta - \alpha \right)} + \mathrm{e}^{-\kappa\left(\frac{3\pi}{2} + 2\beta - \alpha \right)} \right) \mu_1 - \left(\mathrm{e}^{-\kappa(\pi + \beta - \alpha)} + \mathrm{e}^{-\kappa(2\pi + \beta - \alpha)} \right) \mu_2 \\
&= \left(1 + \mathrm{e}^{-\kappa\pi} \right) \left(\mathrm{e}^{-\kappa\left(\frac{\pi}{2} + 2\beta - \alpha \right)} \mu_1 - \mathrm{e}^{-\kappa(\pi + \beta - \alpha)} \mu_2 \right) \\
&= \left(\mathrm{e}^{\kappa\frac{\pi}{2}} + \mathrm{e}^{-\kappa\frac{\pi}{2}} \right) \mathrm{e}^{-\kappa\frac{\pi}{2}} \left(\mathrm{e}^{-\kappa\left(\frac{\pi}{2} + 2\beta - \alpha \right)} \mu_1 - \mathrm{e}^{-\kappa(\pi + \beta - \alpha)} \mu_2 \right) \\
&= \left(2\mathrm{e}^{-\kappa\frac{\pi}{2}} \cosh \frac{\kappa\pi}{2} \right) \left(\mathrm{e}^{-\kappa\left(\frac{\pi}{2} + 2\beta - \alpha \right)} \mu_1 - \mathrm{e}^{-\kappa(\pi + \beta - \alpha)} \mu_2 \right) \\
&= \left(2\mathrm{e}^{-\kappa\pi} \cosh \frac{\kappa\pi}{2} \right) \left(\mu_1 \mathrm{e}^{-\kappa(2\beta - \alpha)} - \mu_2 \mathrm{e}^{-\kappa\left(\frac{\pi}{2} - (\alpha - \beta) \right)} \right), \\
\eta_1 &\triangleq \mathrm{e}^{-2\pi\kappa}.
\end{aligned}
$$

In Subsection 5.6.3, some properties of $P : \mathbb{R} \to \mathbb{R}$ were stated in (5.36)–(5.44) and exposed graphically in Figure 5.7. In particular (5.44), which states that for every $\rho \in \mathbb{R}$ the sequence of iterates $\{ P^n(\rho) \}_{n \in \mathbb{N}}$ converges to

$$
\begin{aligned}
\rho_{\lim} &\triangleq \lim_{n \to \infty} P^n(\rho) = \lim_{n \to \infty} \left(\rho \eta_1^n + \eta_0 \sum_{i=0}^n \eta_1^i \right) = \rho \lim_{n \to \infty} \eta_1^n + \eta_0 \sum_{i=0}^{\infty} \eta_1^i = 0 + \eta_0 \frac{1}{1 - \eta_1} \\
&= \frac{\eta_0}{1 - \eta_1} = \eta_0 \frac{1}{1 - \mathrm{e}^{-2\pi\kappa}} = \eta_0 \frac{\mathrm{e}^{\kappa\pi}}{\mathrm{e}^{\kappa\pi} - \mathrm{e}^{-\kappa\pi}} \\
&= \frac{\eta_0 \mathrm{e}^{\kappa\pi}}{2 \sinh(\kappa\pi)} = \frac{\cosh \frac{\kappa\pi}{2}}{\sinh(\kappa\pi)} \left(\mu_1 \mathrm{e}^{-\kappa(2\beta - \alpha)} - \mu_2 \mathrm{e}^{-\kappa\left(\frac{\pi}{2} - (\alpha - \beta) \right)} \right) \\
&= \frac{\cosh \frac{\kappa\pi}{2}}{2 \sinh \frac{\kappa\pi}{2} \cosh \frac{\kappa\pi}{2}} \left(\mu_1 \mathrm{e}^{-\kappa(2\beta - \alpha)} - \mu_2 \mathrm{e}^{-\kappa\left(\frac{\pi}{2} - (\alpha - \beta) \right)} \right) \\
&= \frac{\mu_1 \mathrm{e}^{-\kappa(2\beta - \alpha)} - \mu_2 \mathrm{e}^{-\kappa\left(\frac{\pi}{2} - (\alpha - \beta) \right)}}{2 \sinh \frac{\kappa\pi}{2}}.
\end{aligned}
$$

The remaining properties (5.36)–(5.43) are trivial. For example, consider (5.38):

$$P(\rho) < \rho \iff \eta_1 \rho + \eta_0 < \rho \iff \rho > \frac{\eta_0}{1 - \eta_1} = \rho_{\lim}.$$

The next proposition states that the sign of $\frac{\mu_2}{\mu_1} \mathrm{e}^{\kappa\left(\frac{\pi}{2} + \beta \right)} - 1$ coincides with the sign of $\rho_{\min} - \rho_{\lim}$, being $\rho_{\min}$ the positive real number defined in (5.50).

Proposition B.1.2.

$$
\begin{aligned}
\frac{\mu_2}{\mu_1} \mathrm{e}^{\kappa\left(\frac{\pi}{2} + \beta \right)} > 1 &\iff \rho_{\min} > \rho_{\lim}, \\
\frac{\mu_2}{\mu_1} \mathrm{e}^{\kappa\left(\frac{\pi}{2} + \beta \right)} < 1 &\iff \rho_{\min} < \rho_{\lim},
\end{aligned}
$$

Proof. To prove the proposition, it is enough to prove that

$$\frac{\mu_2}{\mu_1}\mathrm{e}^{\kappa\left(\frac{\pi}{2}+\beta\right)} > 1 \Rightarrow \rho_{\min} > \rho_{\lim}, \tag{B.12}$$

$$\frac{\mu_2}{\mu_1}\mathrm{e}^{\kappa\left(\frac{\pi}{2}+\beta\right)} < 1 \Rightarrow \rho_{\min} < \rho_{\lim}, \tag{B.13}$$

$$\frac{\mu_2}{\mu_1}\mathrm{e}^{\kappa\left(\frac{\pi}{2}+\beta\right)} = 1 \Rightarrow \rho_{\min} = \rho_{\lim}, \tag{B.14}$$

The positive real number $\rho_{\min}$ is defined by

$$\rho_{\min} \triangleq \begin{cases} \mu_1 \mathrm{e}^{-\kappa\left(\frac{\pi}{2}+2\beta-\alpha\right)} & \text{if } \frac{\mu_2}{\mu_1}\mathrm{e}^{\kappa\left(\frac{\pi}{2}+\beta\right)} > 1, \\ \left(\left(1 - \frac{\mu_2}{\mu_1}\exp^{\kappa\left(\frac{\pi}{2}+\beta\right)}\right)\exp^{-\kappa\pi} + 1\right)\mu_1 \exp^{-\kappa\left(\frac{\pi}{2}+2\beta-\alpha\right)} & \text{if } \frac{\mu_2}{\mu_1}\mathrm{e}^{\kappa\left(\frac{\pi}{2}+\beta\right)} \leq 1, \end{cases}$$

and the real number $\rho_{\lim}$ is given by

$$\rho_{\lim} = \frac{1 + \mathrm{e}^{-\kappa\pi}}{1 - \mathrm{e}^{-2\kappa\pi}}\left(\mu_1 \mathrm{e}^{-\kappa\left(\frac{\pi}{2}+2\beta-\alpha\right)} - \mu_2 \mathrm{e}^{-\kappa(\pi+\beta-\alpha)}\right).$$

Defining $\mu \triangleq \frac{\mu_2}{\mu_1}\mathrm{e}^{\kappa\left(\frac{\pi}{2}+\beta\right)}$, $\hat{\mu} \triangleq (1-\mu)\exp^{-\kappa\pi} + 1$, and $\bar{\rho} \triangleq \mu_1 \mathrm{e}^{-\kappa\left(\frac{\pi}{2}+2\beta-\alpha\right)}$, both $\rho_{\min}$ and $\rho_{\lim}$ may be expressed more succinctly as follows:

$$\rho_{\min} = \begin{cases} \bar{\rho} & \text{if } \mu > 1, \\ \hat{\mu}\bar{\rho} & \text{if } \mu \leq 1; \end{cases} \qquad \rho_{\lim} = \frac{1 + \mathrm{e}^{-\kappa\pi}}{1 - \mathrm{e}^{-2\kappa\pi}}\left(\bar{\rho} - \mu_2 \mathrm{e}^{-\kappa(\pi+\beta-\alpha)}\right).$$

First, suppose that $\mu > 1$. To prove that $\rho_{\min} > \rho_{\lim}$ we must show that

$$\bar{\rho} > \frac{1 + \mathrm{e}^{-\kappa\pi}}{1 - \mathrm{e}^{-2\kappa\pi}}\left(\bar{\rho} - \mu_2 \mathrm{e}^{-\kappa(\pi+\beta-\alpha)}\right),$$

which is logically equivalent to $\left(1 - \mathrm{e}^{-2\kappa\pi}\right)\bar{\rho} > \left(1 + \mathrm{e}^{-\kappa\pi}\right)\left(\bar{\rho} - \mu_2 \mathrm{e}^{-\kappa(\pi+\beta-\alpha)}\right)$. Expanding terms at both sides of the inequality we get

$$\bar{\rho} - \bar{\rho}\mathrm{e}^{-2\kappa\pi} > \bar{\rho} - \mu_2 \mathrm{e}^{-\kappa(\pi+\beta-\alpha)} + \bar{\rho}\mathrm{e}^{-\kappa\pi} - \mu_2 \mathrm{e}^{-\kappa(2\pi+\beta-\alpha)}.$$

Cancelling and rearranging terms we obtain

$$\left(1 + \mathrm{e}^{-\kappa\pi}\right)\mu_2 \mathrm{e}^{-\kappa(\pi+\beta-\alpha)} > \left(1 + \mathrm{e}^{-\kappa\pi}\right)\bar{\rho}\mathrm{e}^{-\kappa\pi},$$

or equivalently $\left(1 + \mathrm{e}^{-\kappa\pi}\right)\mathrm{e}^{-\kappa\pi}\mu_2 \mathrm{e}^{\kappa(\alpha-\beta)} > \left(1 + \mathrm{e}^{-\kappa\pi}\right)\mathrm{e}^{-\kappa\pi}\bar{\rho}$. Simplifying,

$$\mu_2 \mathrm{e}^{\kappa(\alpha-\beta)} > \bar{\rho}.$$

Substitution of $\bar{\rho}$ renders $\mu_2 \mathrm{e}^{\kappa(\alpha-\beta)} > \mu_1 \mathrm{e}^{-\kappa\left(\frac{\pi}{2}+2\beta-\alpha\right)}$. This last inequality is logically equivalent to

$$\frac{\mu_2}{\mu_1}\mathrm{e}^{\kappa\left(\frac{\pi}{2}+\beta\right)} > 1,$$

which certainly holds because μ was supposed to be greater than unity. This proves (B.12).

Now, suppose that $\mu \leq 1$. To prove that $\rho_{\min} \leq \rho_{\lim}$ we must show that

$$\hat{\mu}\bar{\rho} \leq \frac{1 + e^{-\kappa\pi}}{1 - e^{-2\kappa\pi}} \left(\bar{\rho} - \mu_2 e^{-\kappa(\pi + \beta - \alpha)}\right)$$

which is logically equivalent to $\left(\frac{1 + e^{-\kappa\pi}}{1 - e^{-2\kappa\pi}} - \hat{\mu}\right)\bar{\rho} \geq \frac{1 + e^{-\kappa\pi}}{1 - e^{-2\kappa\pi}} e^{-\kappa(\pi + \beta - \alpha)}\mu_2$. Simplifying,

$$\left(1 + e^{-\kappa\pi} - \left(1 - e^{-2\kappa\pi}\right)\hat{\mu}\right)\bar{\rho} \geq \left(1 + e^{-\kappa\pi}\right)e^{-\kappa(\pi + \beta - \alpha)}\mu_2.$$

Substitution of $\bar{\rho}$ yields

$$\left(1 + e^{-\kappa\pi} - \left(1 - e^{-2\kappa\pi}\right)\hat{\mu}\right)\mu_1 e^{-\kappa\left(\frac{\pi}{2} + 2\beta - \alpha\right)} \geq \left(1 + e^{-\kappa\pi}\right)e^{-\kappa(\pi + \beta - \alpha)}\mu_2,$$

or equivalently

$$1 + e^{-\kappa\pi} - \left(1 - e^{-2\kappa\pi}\right)\hat{\mu} \geq \left(1 + e^{-\kappa\pi}\right)\frac{\mu_2}{\mu_1}e^{\kappa\left(\beta - \frac{\pi}{2}\right)}.$$

In the last inequality, expressing $\frac{\mu_2}{\mu_1}e^{\kappa\left(\beta - \frac{\pi}{2}\right)}$ as $\mu e^{-\kappa\pi}$ and substituting $\hat{\mu}$ by $(1 - \mu)\exp^{-\kappa\pi} + 1$ renders

$$1 + e^{-\kappa\pi} - \left(1 - e^{-2\kappa\pi}\right)\left((1 - \mu)\exp^{-\kappa\pi} + 1\right) \geq \left(1 + e^{-\kappa\pi}\right)\mu e^{-\kappa\pi}.$$

Expanding terms at both sides of the last inequality we get

$$1 + e^{-\kappa\pi} - e^{-\kappa\pi} + \mu e^{-\kappa\pi} - 1 + e^{-3\kappa\pi} - \mu e^{-3\kappa\pi} + e^{-2\kappa\pi} \geq \mu e^{-\kappa\pi} + \mu e^{-2\kappa\pi}.$$

After cancelling terms and re-factorizing, the following inequality shows up

$$(1 - \mu)\left(1 + e^{-\kappa\pi}\right)e^{-2\kappa\pi} \geq 0,$$

which certainly holds because it was supposed that $\mu \leq 1$. Moreover, the inequality is strict unless $\mu = 1$. This proves (B.13)–(B.14). $\qquad\square$

B.2. Both rectangular components of $b_a^* - d^*$ are positive

The purpose of this section is to prove that both the real part and the imaginary part of the difference $b_a^* - d^*$ are positive.

Proposition B.2.1.

$$\Re\left(b_a^* - d^*\right) > 0,$$
$$\Im\left(b_a^* - d^*\right) > 0.$$

Proof. The points b_a^* and d^* are defined as

$$b_a^* \triangleq a + e^{k\left(\frac{\pi}{2} + 2\beta - \alpha\right)}(b - a),$$
$$d^* \triangleq d + e^{-k(\alpha - \beta)}(b_a - d).$$

B.2. Both rectangular components of $b_a^* - d^*$ are positive

Hence, $b_a^* - d^* = a + \mathrm{e}^{k\left(\frac{\pi}{2}+2\beta-\alpha\right)}(b-a) - \left(d + \mathrm{e}^{-k(\alpha-\beta)}(b_a - d)\right)$. The definition of b_a is

$$b_a \triangleq a + \mathrm{e}^{k\left(\frac{\pi}{2}+\beta\right)}(b-a).$$

Substitution of b_a in the former expression for the difference $b_a^* - d^*$ yields

$$b_a^* - d^* = a + \mathrm{e}^{k\left(\frac{\pi}{2}+2\beta-\alpha\right)}(b-a) - \left(d + \mathrm{e}^{-k(\alpha-\beta)}\left(a + \mathrm{e}^{k\left(\frac{\pi}{2}+\beta\right)}(b-a) - d\right)\right),$$

$$= (d-a)\left(\mathrm{e}^{-k(\alpha-\beta)} - 1\right) + (b-a)\left(\mathrm{e}^{k\left(\frac{\pi}{2}+2\beta-\alpha\right)} - \mathrm{e}^{-k(\alpha-\beta)}\mathrm{e}^{k\left(\frac{\pi}{2}+\beta\right)}\right)$$

$$= (d-a)\left(\mathrm{e}^{-k(\alpha-\beta)} - 1\right) = \mu_2 \mathrm{e}^{\mathrm{j}\left(\frac{\pi}{2}-\beta\right)}\left(\mathrm{e}^{-k(\alpha-\beta)} - 1\right), \tag{B.15}$$

where $d - a = \mu_2 \mathrm{e}^{\mathrm{j}\left(\frac{\pi}{2}-\beta\right)}$ because the anchor points a and d are defined by

$$\begin{aligned} a &\triangleq -\mathrm{j}\delta_0 + i_o^{\triangledown}\delta_1 \mathrm{e}^{-\mathrm{j}2\beta} \\ d &\triangleq -\mathrm{j}\delta_0 + i_o^{\triangledown}\delta_1 \mathrm{e}^{-\mathrm{j}2\beta} + v_i^{\triangledown}\delta_2 \mathrm{e}^{\mathrm{j}\left(\frac{\pi}{2}-\beta\right)}, \end{aligned}$$

and $\mu_2 \triangleq |d-a|$.

Recalling that $k \triangleq -\kappa + \mathrm{j}$ and taking real and imaginary part in (B.15):

$$\Re\left(b_a^* - d^*\right) = \mu_2\left(\mathrm{e}^{\kappa(\alpha-\beta)}\sin\alpha - \sin\beta\right),$$

$$\Im\left(b_a^* - d^*\right) = \mu_2\left(\mathrm{e}^{\kappa(\alpha-\beta)}\cos\alpha - \cos\beta\right).$$

By (5.2)–(5.3), $\mu_2 = v_i^{\triangledown}\delta_2 > 0$. Moreover, by (5.1), $|\beta| < \alpha < \frac{\pi}{2}$.

It is clear that $\sin\alpha > 0$, $\sin\alpha > \sin\beta$, and $0 < \cos\alpha < \cos\beta$. In addition, $\mathrm{e}^{\kappa(\alpha-\beta)} > 1$ because $\alpha - \beta > 0$ and $\kappa \triangleq \tan\alpha > 0$.

Consequently, $\Re\left(b_a^* - d^*\right) = \mu_2\left(\mathrm{e}^{\kappa(\alpha-\beta)}\sin\alpha - \sin\beta\right) > \mu_2\left(\sin\alpha - \sin\beta\right) > 0$, which completes part of the proof.

It is clear now that the proof of $\Im\left(b_a^* - d^*\right) > 0$ reduces to the proof of

$$\mathrm{e}^{(\alpha-\beta)\tan\alpha}\cos\alpha > \cos\beta.$$

Since $\cos\theta = \frac{1}{\sqrt{1+\tan^2\theta}}$ for every $\theta \in \left(-\frac{\pi}{2}, \frac{\pi}{2}\right)$, the last inequality can be rewritten as $\frac{\mathrm{e}^{(\alpha-\beta)\tan\alpha}}{\sqrt{1+\tan^2\alpha}} > \frac{1}{\sqrt{1+\tan^2\beta}}$, or equivalently as

$$\frac{\mathrm{e}^{\alpha\tan\alpha}}{\sqrt{1+\tan^2\alpha}} > \frac{\mathrm{e}^{\beta\tan\alpha}}{\sqrt{1+\tan^2\beta}}. \tag{B.16}$$

Since $-\frac{\pi}{2} < -\alpha < \beta < \alpha < \frac{\pi}{2}$, to show that (B.16) holds, it suffices to prove that the function $\theta \mapsto \frac{\mathrm{e}^{\theta\tan\alpha}}{\sqrt{1+\tan^2\theta}}$ is strictly monotonously increasing in $(-\alpha, \alpha)$.

Let $g : \left(-\frac{\pi}{2}, \frac{\pi}{2}\right) \to \mathbb{R}$ be defined by $g(\theta) = \frac{\mathrm{e}^{\theta\tan\alpha}}{\sqrt{1+\tan^2\theta}}$. The derivative function of g is given by

$$g'(\theta) = \frac{\mathrm{e}^{\theta\tan\alpha}}{\sqrt{1+\tan^2\theta}}\left(\tan\alpha - \tan\theta\right).$$

Since, $g'(\theta) > 0$ for every $\theta \in (-\alpha, \alpha)$, the function g is strictly monotonously increasing in $(-\alpha, \alpha)$, and consequently (B.16) holds, proving that $\Im\left(b_a^* - d^*\right)$ is positive. $\qquad\square$

Esta página ha sido intencionalmente dejada en blanco.

Bibliography

[1] R. Erickson and D. Maksimovic, *Fundamentals of Power Electronics.* Power electronics, Springer, 2001.

[2] N. Mohan, T. Undeland, and W. Robbins, *Power Electronics: Converters, Applications, and Design.* No. v. 1 in Power Electronics: Converters, Applications, and Design, John Wiley & Sons, 2003.

[3] B. Bose, "Energy, environment, and advances in power electronics," *Power Electronics, IEEE Transactions on*, vol. 15, pp. 688–701, Jul 2000.

[4] B. Bose, "The past, present, and future of power electronics [guest introduction]," *Industrial Electronics Magazine, IEEE*, vol. 3, pp. 7–11, 14, June 2009.

[5] A. Bindra, "Growth in merchant power supplies: A look at the market trends propelled by emerging applications," *Power Electronics Magazine, IEEE*, vol. 1, pp. 32–34, March 2014.

[6] G. Eirea, *Estimation and Control Techniques in Power Converters.* PhD thesis, University of California, Berkeley, 2006.

[7] H. Sira-Ramirez and R. Silva-Ortigoza, *Control Design Techniques in Power Electronics Devices.* Power Systems, Springer, 2006.

[8] F. Vasca and L. Iannelli, *Dynamics and Control of Switched Electronic Systems: Advanced Perspectives for Modeling, Simulation and Control of Power Converters.* Advances in Industrial Control, Springer London, 2012.

[9] S. Bacha, I. Munteanu, and A. Bratcu, *Power Electronic Converters Modeling and Control: with Case Studies.* Advanced Textbooks in Control and Signal Processing, Imprint: Springer, 2013.

[10] R. Middlebrook and S. Cuk, "A general unified approach to modelling switching-converter power stages," in *Power Electronics Specialists Conference, 1976 IEEE*, pp. 18–34, June 1976.

[11] A. Forsyth and S. Mollov, "Modelling and control of DC-DC converters," *Power Engineering Journal*, vol. 12, pp. 229–236, Oct 1998.

Bibliography

[12] R. Mammano, "Switching power supply topology voltage mode vs. current mode." Design Note. Online; Accessed: 2015-05-23; http://www.ti.com/lit/an/slua119/slua119.pdf.

[13] R. Ridley, "Current mode or voltage mode?," *Switching Power Magazine*, pp. 4–5,9, October 2000.

[14] A. Pressman, K. Billings, and T. Morey, *Switching Power Supply Design, 3rd Ed.* McGraw-Hill Education, 2009.

[15] Y.-F. Liu and P. Sen, "A general unified large signal model for current programmed DC-to-DC converters," *Power Electronics, IEEE Transactions on*, vol. 9, pp. 414–424, Jul 1994.

[16] R. Erickson, S. Cuk, and R. Middlebrook, "Large-signal modelling and analysis of switching regulators," in *Power Electronics Specialists conference, 1982 IEEE*, pp. 240–250, June 1982.

[17] D. Hamill, J. Deane, and D. Jefferies, "Modeling of chaotic DC-DC converters by iterated nonlinear mappings," *Power Electronics, IEEE Transactions on*, vol. 7, pp. 25–36, Jan 1992.

[18] B. P. Schweitzer and A. B. Rosenstein, "Free running-switching mode power regulator: Analysis and design," *Aerospace, IEEE Transactions on*, vol. 2, pp. 1171–1180, Oct 1964.

[19] I. Babaa, T. Wilson, and Y. Yu, "Analytic solutions of limit cycles in a feedback-regulated converter system with hysteresis," *Automatic Control, IEEE Transactions on*, vol. 13, pp. 524–531, Oct 1968.

[20] G. Wester, "Describing-function analysis of a ripple regulator with slew-rate limits and time delays," in *Power Electronics Specialists Conference, 1990. PESC '90 Record., 21st Annual IEEE*, pp. 341–346, 1990.

[21] R. Redl and J. Sun, "Ripple-based control of switching regulators - an overview," *Power Electronics, IEEE Transactions on*, vol. 24, pp. 2669–2680, Dec 2009.

[22] V. Utkin, J. Guldner, and M. Shijun, *Sliding Mode Control in Electromechanical Systems.* Automation and Control Engineering, Taylor & Francis, 1999.

[23] H. Sira-Ramirez, "Sliding motions in bilinear switched networks," *Circuits and Systems, IEEE Transactions on*, vol. 34, pp. 919–933, Aug 1987.

[24] S. Tan, Y. Lai, and C. Tse, *Sliding Mode Control of Switching Power Converters: Techniques and Implementation.* CRC Press, 2011.

[25] S.-C. Tan, Y. Lai, M. Cheung, and C. Tse, "On the practical design of a sliding mode voltage controlled buck converter," *Power Electronics, IEEE Transactions on*, vol. 20, pp. 425–437, March 2005.

[26] S.-C. Tan, Y. Lai, and C. Tse, "An evaluation of the practicality of sliding mode controllers in DC-DC converters and their general design issues," in *Power Electronics Specialists Conference, 2006. PESC '06. 37th IEEE*, pp. 1–7, June 2006.

[27] S.-C. Tan, Y. Lai, and C. Tse, "General design issues of sliding-mode controllers in DC-DC converters," *Industrial Electronics, IEEE Transactions on*, vol. 55, pp. 1160–1174, March 2008.

[28] R. Munzert and P. Krein, "Issues in boundary control [of power convertors]," in *Power Electronics Specialists Conference, 1996. PESC '96 Record., 27th Annual IEEE*, vol. 1, pp. 810–816 vol.1, Jun 1996.

[29] M. Greuel, R. Muyshondt, and P. Krein, "Design approaches to boundary controllers," in *Power Electronics Specialists Conference, 1997. PESC '97 Record., 28th Annual IEEE*, vol. 1, pp. 672–678 vol.1, Jun 1997.

[30] K. Leung and H. Chung, "A comparative study of the boundary control of buck converters using first- and second-order switching surfaces -part i: Continuous conduction mode," in *Power Electronics Specialists Conference, 2005. PESC '05. IEEE 36th*, pp. 2133–2139, June 2005.

[31] G. Pitel and P. Krein, "Minimum-time transient recovery for DC-DC converters using raster control surfaces," *Power Electronics, IEEE Transactions on*, vol. 24, pp. 2692–2703, Dec 2009.

[32] G. Pitel and P. Krein, "Trajectory paths for Dc - Dc converters and limits to performance," in *Computers in Power Electronics, 2006. COMPEL '06. IEEE Workshops on*, pp. 40–47, July 2006.

[33] M. Ordonez, J. Quaicoe, and M. Iqbal, "Critical parameters in the transient response of synchronous buck converters," in *Power Electronics Specialists Conference, 2007. PESC 2007. IEEE*, pp. 2189–2195, June 2007.

[34] I. Galiano Zurbriggen, M. Ordonez, and M. Anun, "Dynamic physical limits of buck converters: The t0/4 transient benchmark rule," in *Applied Power Electronics Conference and Exposition (APEC), 2013 Twenty-Eighth Annual IEEE*, pp. 421–428, March 2013.

[35] J. Galvez, M. Ordonez, and M. Anun, "Normalized geometrical analysis: unified theory and derivation of natural trajectories for basic dc-dc topologies," in *Control and Modeling for Power Electronics (COMPEL), 2013 IEEE 14th Workshop on*, pp. 1–5, June 2013.

[36] M. Ordonez, M. Iqbal, and J. Quaicoe, "Selection of a curved switching surface for buck converters," *Power Electronics, IEEE Transactions on*, vol. 21, pp. 1148–1153, July 2006.

[37] J. Galvez, M. Ordonez, F. Luchino, and J. Quaicoe, "Improvements in boundary control of boost converters using the natural switching surface," in *Energy Conversion Congress and Exposition (ECCE), 2011 IEEE*, pp. 3362–3369, Sept 2011.

[38] J. Galvez, M. Ordonez, T. Nguyen, and F. Luchino, "Boundary control of buck-boost converters: normalized trajectories and the natural switching surface," in *Energy Conversion Congress and Exposition (ECCE), 2012 IEEE*, pp. 358–363, Sept 2012.

[39] I. Galiano Zurbriggen, M. Ordonez, and M. Anun, "PWM-geometric modeling and centric control of basic DC-DC topologies for sleek and reliable large-signal response," *Industrial Electronics, IEEE Transactions on*, vol. 62, pp. 2297–2308, April 2015.

[40] I. Galiano Zurbriggen, M. Anun, and M. Ordonez, "Dual-loop geometric-based control of buck converters," in *Applied Power Electronics Conference and Exposition (APEC), 2015 IEEE*, pp. 392–396, March 2015.

[41] D. Maksimovic, R. Zane, and R. Erickson, "Impact of digital control in power electronics," in *Power Semiconductor Devices and ICs, 2004. Proceedings. ISPSD '04. The 16th International Symposium on*, pp. 13–22, May 2004.

[42] M. Shirazi, R. Zane, D. Maksimovic, L. Corradini, and P. Mattavelli, "Auto-tuning techniques for digitally-controlled point-of-load converters with wide range of capacitive loads," in *Applied Power Electronics Conference, APEC 2007 - Twenty Second Annual IEEE*, pp. 14–20, Feb 2007.

[43] L. Corradini, A. Bjeletić, R. Zane, and D. Maksimović, "Fully digital hysteretic modulator for DC-DC switching converters," *Power Electronics, IEEE Transactions on*, vol. 26, pp. 2969–2979, Oct 2011.

[44] J. Xiao, A. Peterchev, and S. Sanders, "Architecture and IC implementation of a digital VRM controller," in *Power Electronics Specialists Conference, 2001. PESC. 2001 IEEE 32nd Annual*, vol. 1, pp. 38–47 vol. 1, 2001.

[45] A. Babazadeh and D. Maksimovic, "Hybrid digital adaptive control for fast transient response in synchronous buck DC-DC converters," *Power Electronics, IEEE Transactions on*, vol. 24, pp. 2625–2638, Nov 2009.

[46] A. Barrado, R. Vazquez, E. Olias, A. Roldan, and J. Pleite, "Fast transient response in hybrid sources with combined linear-non-linear control," in *Power Electronics Specialists Conference, 2002. pesc 02. 2002 IEEE 33rd Annual*, vol. 4, pp. 1599–1604, 2002.

[47] A. Radić, Z. Lukic, A. Prodić, and R. de Nie, "Minimum deviation digital controller ic for single and two phase dc-dc switch-mode power supplies," in *Applied Power Electronics Conference and Exposition (APEC), 2010 Twenty-Fifth Annual IEEE*, pp. 1–6, Feb 2010.

[48] A. Barrado, A. Roldan, J. Pleite, R. Vazquez, J. Vazquez, and E. Olias, "Linear-non-linear control (LnLc) for DC-DC buck converters: stability and transient response analysis," in *Applied Power Electronics Conference and Exposition, 2004. APEC '04. Nineteenth Annual IEEE*, vol. 2, pp. 1329–1335 vol.2, 2004.

[49] R. Isaacs, *Differential games: a mathematical theory with applications to warfare and pursuit, control and optimization.* Dover books on mathematics, Dover Publications, 1999.

[50] P. Bernhard and S. Crepey, "Comparison of two numerical approaches for the barrier and value of a simple pursuit—evasion game," in *Advances in Dynamic Games and Applications* (T. Başar, E. Altman, and O. Pourtallier, eds.), vol. 6 of *Annals of the International Society of Dynamic Games*, pp. 253–273, Birkhäuser Boston, 2001.

[51] A. W. Merz, *The homicidal chauffeur – a differential game.* PhD thesis, Stanford University, 1971.

[52] V. Patsko and V. Turova, "Homicidal chauffeur game: History and modern studies," in *Advances in Dynamic Games* (M. Breton and K. Szajowski, eds.), vol. 11 of *Annals of the International Society of Dynamic Games*, pp. 227–251, Birkhäuser Boston, 2011.

[53] V. Patsko and V. Turova, "Numerical solution of two-dimensional differential games." Preprint, Institute of Mathematics and Mechanics, Ekaterinburg, 1995.

[54] P. Cardaliaguet, M. Quincampoix, and P. Saint-Pierre, "Set-valued numerical analysis for optimal control and differential games," in *Stochastic and Differential Games* (M. Bardi, T. Raghavan, and T. Parthasarathy, eds.), vol. 4 of *Annals of the International Society of Dynamic Games*, pp. 177–247, Birkhäuser Boston, 1999.

[55] M. Bardi, M. Falcone, and P. Soravia, "Numerical methods for pursuit-evasion games via viscosity solutions," in *Stochastic and Differential Games* (M. Bardi, T. Raghavan, and T. Parthasarathy, eds.), vol. 4 of *Annals of the International Society of Dynamic Games*, pp. 105–175, Birkhäuser Boston, 1999.

[56] P. Hagedorn and J. V. Breakwell, "A differential game with two pursuers and one evader," in *Multicriteria Decision Making and Differential Games* (G. Leitmann, ed.), Mathematical Concepts and Methods in Science and Engineering, pp. 443–457, Springer US, 1976.

[57] J. Breakwell, "Lecture notes," in *Differential Games and Applications* (P. Hagedorn, H. Knobloch, and G. Olsder, eds.), vol. 3 of *Lecture Notes in Control and Information Sciences*, pp. 70–95, Springer Berlin Heidelberg, 1977.

Bibliography

[58] P. Cardaliaguet, "Introduction to differential games." University Lecture, 2010. Online; Accessed: 2013-06-06; https://www.ceremade.dauphine.fr/~cardalia/CoursJeuxDiff.pdf.

[59] T. Başar and G. Olsder, *Dynamic noncooperative game theory.* Classics in applied mathematics, SIAM, 1999.

[60] J. Lewin, *Differential games: theory and methods for solving game problems with singular surfaces.* Springer-Verlag, 1994.

[61] P. Bernhard, "Singular surfaces in differential games an introduction," in *Differential Games and Applications* (P. Hagedorn, H. Knobloch, and G. Olsder, eds.), vol. 3 of *Lecture Notes in Control and Information Sciences*, pp. 1–33, Springer Berlin / Heidelberg, 1977.

[62] M. H. Breitner, "Rufus Philip Isaacs and the early years of differential games," IWI Discussion Paper Series 1, Institut für Wirtschaftsinformatik, Universität Hannover, 2003.

[63] A. Friedman, *Differential Games.* Dover Books on Mathematics Series, Dover Publications, 2006.

[64] A. Subbotin, *Generalized solutions of first-order PDEs: the dynamical optimization perspective.* Systems & control, Birkhäuser, 1995.

[65] M. Bardi and I. Capuzzo-Dolcetta, *Optimal control and viscosity solutions of Hamilton-Jacobi-Bellman equations.* Systems & control, Birkhäuser, 2008.

[66] J. Aubin, *Viability theory.* Systems & control, Birkhäuser, 1991.

[67] A. E. Rapaport, "Characterization of barriers of differential games," *Journal of Optimization Theory and Applications*, vol. 97, pp. 151–179, 1998.

[68] A. Melikyan, *Generalized characteristics of first order PDEs: applications in optimal control and differential games.* Birkhäuser, 1998.

[69] E. A. Coddington and N. Levinson, *Theory of ordinary differential equations.* McGraw-Hill Book Company, Inc., New York-Toronto-London, 1955.

[70] M. Hirsch, R. Devaney, and S. Smale, *Differential Equations, Dynamical Systems, and Linear Algebra.* Pure and Applied Mathematics, Elsevier Science, 1974.

[71] L. Ahlfors, *Complex Analysis.* McGraw-Hill, 1966.

[72] C. Zwikker, *The advanced geometry of plane curves and their applications: (formerly titled: Advanced plane geometry).* Dover Publications, 1963.

[73] I. Shafarevich and A. Remizov, *Linear Algebra and Geometry.* SpringerLink : Bücher, Springer Berlin Heidelberg, 2012.

[74] L. Hahn, *Complex Numbers and Geometry.* MAA spectrum, "The" Mathematical Association of America, 1994.

[75] I. Yaglom, *Complex numbers in geometry.* Academic paperbacks, Academic Press, 1968.

[76] R. Remmert, *Theory of Complex Functions: Readings in Mathematics.* Graduate Texts in Mathematics, Springer-Verlag, 1991.

[77] K. Kreutz-Delgado, "The complex gradient operator and the CR-calculus." University Lecture, 2009.

[78] A. Visioli, "Modified anti-windup scheme for pid controllers," *Control Theory and Applications, IEE Proceedings*, vol. 150, pp. 49–54, Jan 2003.

Esta página ha sido intencionalmente dejada en blanco.

Acronyms

LnLC   linear-non-linear control 8

ME_1 main equation in its first form 29, 30, 132
ME_2 main equation in its second form 29, 32, 33, 133
MTC   minimum-time control 7

NSS   natural switching surface 7

OVC   over-voltage constraint 40

P   pursuer 14–23, 25, 26, 30, 32, 34, 40, 41, 46, 47, 49, 52, 61–64, 68, 73, 74, 78, 94, 103, 107, 111, 113, 114, 119, 120, 122, 125–128, 132, 151, 153–160, 163, 165–172, 180–182, 184–188, 190, 193–207, 209, 210, 212–214, 216–221, 236–238, 240, 242, 244, 246, 247, 249, 252, 254, 257
PF   pay-off functional 14–17, 24, 25, 27, 29, 30, 46, 47, 52, 62, 63, 118, 122–125, 132, 211, 212
PID   proportional-integral-derivative 3, 7, 222, 224–226, 229, 232, 233, 236, 237, 246, 249, 252, 253
POL   point of load 2
PS   playing set 15, 16, 25, 34, 41, 42, 44–46, 48, 50, 59, 64, 121, 212, 214, 250
PWM   pulse-width modulation 3, 4, 6–8, 223–226, 232, 252

RES   relaxed evader's strategy 220, 222, 226, 227, 229, 232, 233, 236, 242, 246, 249, 252, 253
RHS   right-hand side 15, 33, 91, 97, 107, 214
ROVC   robust over-voltage constraint 41, 43, 44, 264
RPE   retrograde path equations 33, 34, 133–135, 142, 146, 147, 157, 178, 179, 189, 265
RUVC   robust under-voltage constraint 41, 43, 44

SE   state equation 14–19, 24, 26, 27, 29, 30, 33, 46, 48, 50, 52, 59, 60, 62, 67, 68, 73–75, 80, 103, 118–124, 132, 211, 212
SM   sliding mode 5, 6, 222, 227–229, 233, 236, 246, 249, 252, 253
SMPS   switched-mode power supply 2
SS   switching surface 6–8

TS   target set 14–17, 27, 29, 30, 34, 41, 44–46, 52, 59, 62, 64, 67, 68, 118, 121–124, 132, 211, 212

UP	usable part 34
USA	United States of America 14
UVC	under-voltage constraint 40
VF	value function 20, 21, 23, 25–30, 34, 47, 63, 79, 116, 123, 124, 127, 133, 158, 159, 174, 175, 189, 191, 194–197, 200, 201, 205, 206, 208
VLSI	very-large-scale integration 7
VMC	voltage-mode control 3, 4
VRM	voltage regulator module 2, 7, 9
VSS	variable structure system 5, 6
VT	verification theorem 30

Esta página ha sido intencionalmente dejada en blanco.

List of symbols related to the realistic buck converter control problem

Esta es la última página.
Compilado el lunes 7 septiembre, 2015.